2016

Synthesis of 1,2,3-triazole ligands, their metal complexes, and applications in catalysis; Gold (I) catalyzed 1,n-enyne ester cycloisomerization reactions

Sravan Kumar Thummanapelli

Synthesis of 1,2,3-triazole ligands, their metal complexes, and applications in catalysis; Gold (I) catalyzed 1,*n*-enyne ester cycloisomerization reactions.

Sravan Kumar Thummanapelli

Dissertation submitted to the
Eberly College of Arts and Sciences
at West Virginia University
in partial fulfillment of the requirements
for the degree of
Doctor of Philosophy
In
Chemistry

Björn C. G. Söderberg, Ph.D., Chair
John H. Penn, Ph.D.
Jeffrey L. Petersen, Ph.D.
Brian V. Popp, Ph.D.
Patrick S. Callery, Ph.D.

C. Eugene Bennett Department of Chemistry
Morgantown, West Virginia
2016

Key words: Enyne ester cycloisomerization, Gold(I) catalysis, Pincer ligands

Abstract

Synthesis of 1,2,3-triazole ligands, their metal complexes, and applications in catalysis; Gold (I) catalyzed 1,*n*-enyne ester cycloisomerization reactions.

Sravan Kumar Thummanapelli

Dihydronaphthalenes have been prepared from a ligand controlled gold catalyzed enyne cycloisomerization reaction by using water as an additive. Additionally, four membered rings were obtained in the absence of water under similar conditions. This method also provides excellent yields of substituted dihydroquinolines and dihydrobenzopyrans. Both aliphatic and aromatic terminal alkynes provide the cyclic products under the optimized conditions. The reaction represents a novel method for the synthesis of seven-membered rings with moderate yields.

1,2,3-Triazoles have been utilized as ligands in a number of synthetic transformations. In our attempt to mimicking the porphyrin with 1,2,3-triazole by macrocyclization was unsuccessful due to poor solubility. The intermediates, for both analogs were synthesized by using Click chemistry and a Mitsunobu reaction and are characterized by NMR.

In addition to porphyrin analogs, P,N,N pincer-type ligands featuring a 1,2,3-triazole were synthesized, characterized and used to prepare palladium, nickel and gold complexes. These complexes were characterized by homo and hetero nuclear 1D and 2D NMR spectroscopy and X-ray crystallography. Attempts to use the new pincer complexes in organic transformations were unsuccessful. However, several interesting crystal structures including four-coordinate nickel(II) square planar complexes and a k^1- benzoate gold(I) complex in which gold is bound to an oxygen atom of a benzoate were obtained.

Dedicated To

My Parents, my Wife

And my lovely

Daughter

ACKNOWLEDGEMENTS

Firstly, I would like to express my deepest gratitude to my advisor, Dr. Xiaodong Michael Shi, for his continuous support of my PhD study and related research. I have been so fortunate to have him as an advisor who gave an opportunity to explore myself in the science of organic chemistry and at the same time for the limitless support and guidance that he offered when required. His guidance helped me during times of research and writing of this thesis.

I would like to thank my chair: Dr. Björn Söderberg for his support in my academic development. I am highly indebted to him for accepting me in his group and allowing me to finish my work. His invaluable advice and suggestion throughout my year here in WVU are highly appreciated and acknowledged. I would like to thank Dr. Jeffrey L. Petersen, for performing several X-ray crystallographic analyses and guidance during my graduate studies. I am also thankful to Dr. Penn, Dr. Popp and Dr. Callery for their support in my academic development and for serving as research committee members. Moreover, I would also like to thank Dr. Novruz Akhmedov for his kind and friendly help with NMR experiments.

I thank my fellow lab mates with whom I've had the pleasure of working, mainly for the sleepless nights that we were working and stimulating discussions we have had in last five years with Dr. Dawei Wang, Dr. WumingYan, Dr. Qiaoyi Wang, Dr. Lekh Nath Gautam, Dr. Yijin Su, Dr. Haihui Peng, Dr. Rong Cai, Dr. Xiaohan Ye, Dr. Yanwei Zhang, Seyed Morteza Hosseyni, Steve Motika and Boliang Dong for all the assistance they have given me in the last five years. My special thanks goes to Mr. Ganesh Ghimire and Nurul Ansari for going through my manuscript.

Last but not least, I would like to express my heart-felt gratitude to my family for their unconditional love, support and guidance throughout my life. My parents, my wife and my daughter have been a constant source of love, concern, support and strength all these years.

Table of Contents

List of Schemes

List of Figures

List of Tables

Chapter 1 Gold catalyzed 1,n-enyne ester cycloisomerization reaction

1.1 Introduction

1.1.1 Introduction to cycloisomerization reactions

Cycloisomerization reactions generally take place using enyne,[1] diene, and allenyne substrates. A new carbon-carbon bond is formed during the cycloisomerization reactions of the polyunsaturated compounds and the resulting products are cyclic or bicyclic compounds with an ability to construct fused five-, six-, and seven membered ring systems.[2] Excellent stereochemistry transfer of chiral compounds is observed and in most instances a single enantiomer is isolated. Generally, cycloisomerization reactions are considered to be atom-economic[3] and efficient because in most of the circumstances no material loss is observed. These reactions occur under thermal conditions and also in the presence of transition metals such as palladium,[4] ruthenium,[5] rhodium,[6] iridium,[7] gold[8] and platinum.[9] These reactions with π-acidic metals like Au and Pt are considered to be a conventional method in complex organic synthesis. Some of the transition metal catalyzed reactions are outline below in Figure 1.

In recent years, gold catalyzed enyne cycloisomerization reactions gained a significant importance, facilitating the synthesis of complex molecules.[10] This is because gold(I) chemistry can allow for a rapid increase in molecular complexity from simple substrates. In general, gold(I) catalyzed reactions are highly chemoselective and can be performed under mild reaction conditions compared to other metal reactions. Among the reported systems of cycloisomerization reactions, those reactions involving an enyne containing propargyl ester exhibit special and excellent reactivity.[11]

Figure 1. Transition metal catalyzed cycloisomerization reactions.

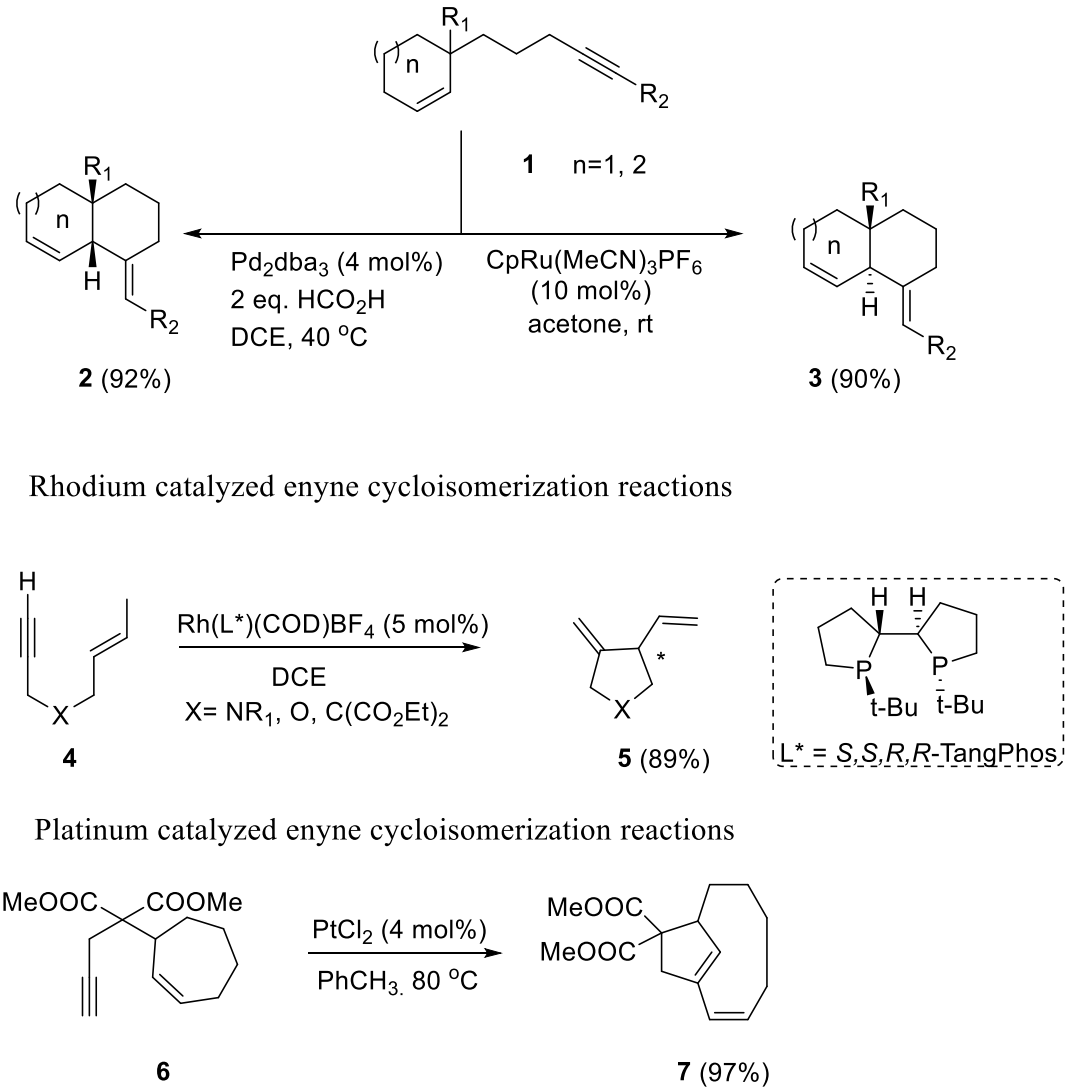

Gold catalyzed 1,n-enyne ester cycloisomerization reactions represent one of the most powerful and versatile methods for the efficient and atom economical synthesis of complex molecules in a single step.[12] 1,2- and 1,3-acyl rearrangement reactions have been more widely studied by gold(I) catalyst (Scheme 1). These rearrangements may involve activation of the alkyne

moiety by the gold catalyst, leading to either a gold carbene (Scheme 1a) or gold allene species (Scheme 1b), which are activated to do further chemistry such as hydroamination reactions.[13]

1.1.2 Transition metal catalyzed cycloisomerization reactions.

Scheme 1. Gold(I) catalyzed rearrangement reactions

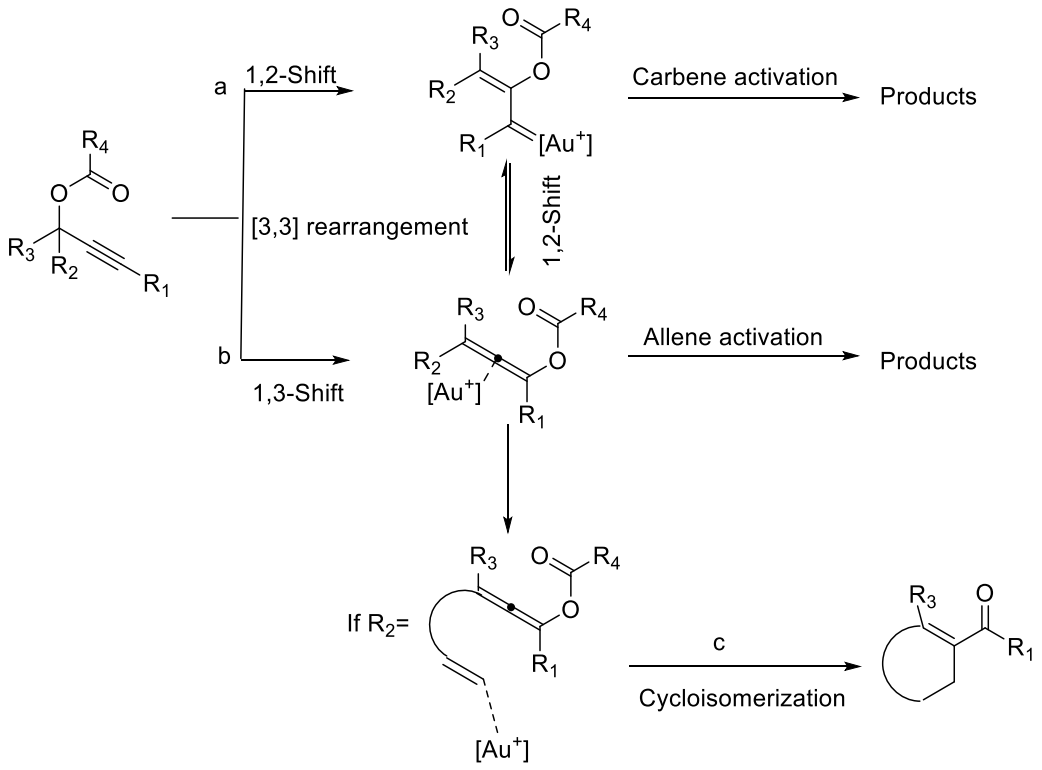

1.1.3 Chan's cycloisomerization.

Chan and coworkers reported several new gold catalyzed transformations of enyne esters using cycloisomerization strategy to form 4-and 6-membered bicycles with excellent synthetic efficiency. One well known method is a regioselective and stereoconvergent synthesis of azabicyclo[4.2.0]oct-5-enes with an efficient transfer of chirality from the enantiopure substrate.[14] In addition, the bicyclic adducts were obtained as single enantiomer with up to four stereogenic centers **8a**. A general reaction of 1,7-enyne ester to give bicyclic compound is shown in Scheme 2.

Scheme 2. Chan's cycloisomerization reaction of 1,7-enyne esters.

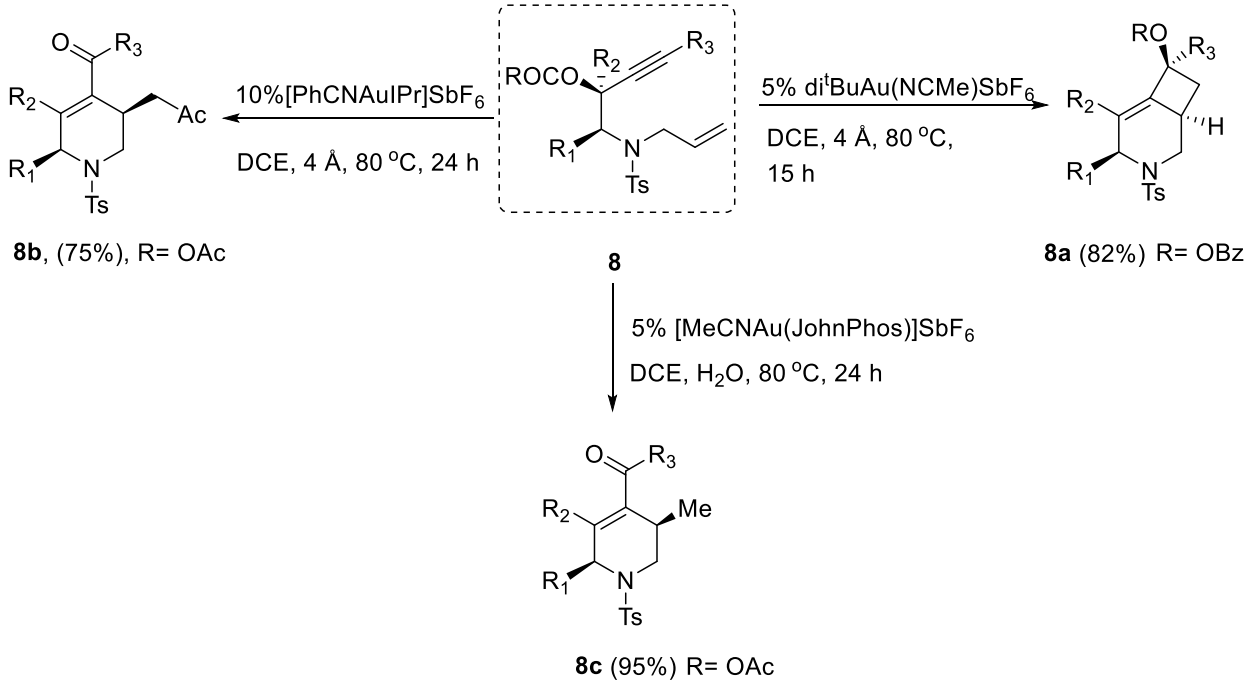

Figure 2. Examples of gold catalyst precursors.

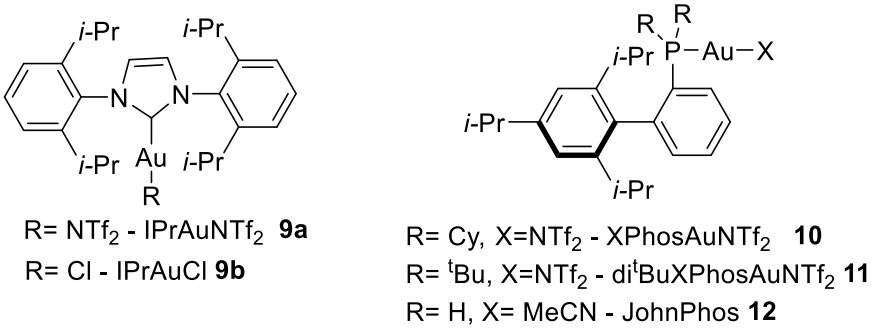

1.1.4 Nolan's gold catalyzed reactions

In 2006,[15] Nolan reported the chemoselective transformation of propargyl acetates to substituted indenes using a gold(I) catalyst (Scheme 3). Both reactions proceed through a tandem [3,3]-sigmatropic rearrangement followed by a nucleophilic addition from an aromatic ring furnishing an indene under anhydrous conditions. Enones were obtained in the presence of water.

Scheme 3. Examples of nucleophiles that lead to indene and enone formation.

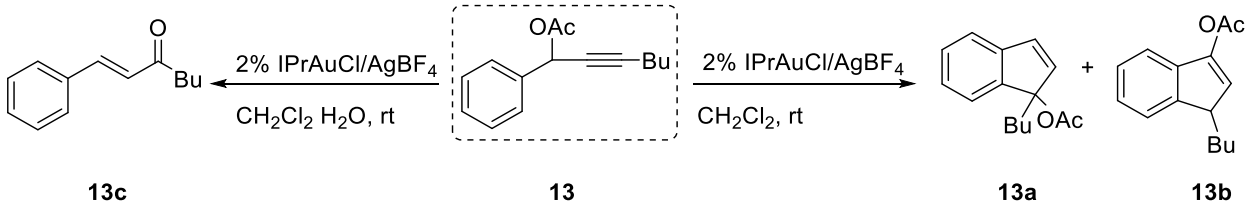

13c **13** **13a** **13b**

1.2 Research and design

Our initial research idea was to prepare aromatic bicyclic compounds by positioning the alkene ortho to the propargyl ester (Scheme 4). The expected products from the gold(I) catalyzed reactions should be aromatic bicyclic compounds. Although the proposed route is attractive for the construction of various aromatic bicyclic compounds, it has not been investigated. This is probably due to the addition of benzene to the gold activated allene intermediate that leads to formation of an undesired substituted indene derivatives reported by Nolan (Scheme 3). A typical gold catalyst will activate both alkyne and allene with approximately equal selectivity. Thus, the issue is how to achieve effective alkyne and alkene activation in the presence of an allene during the course of the cyclization process.

Scheme 4. Possible products from cycloisomerization of 1,7-enyne ester.[19]

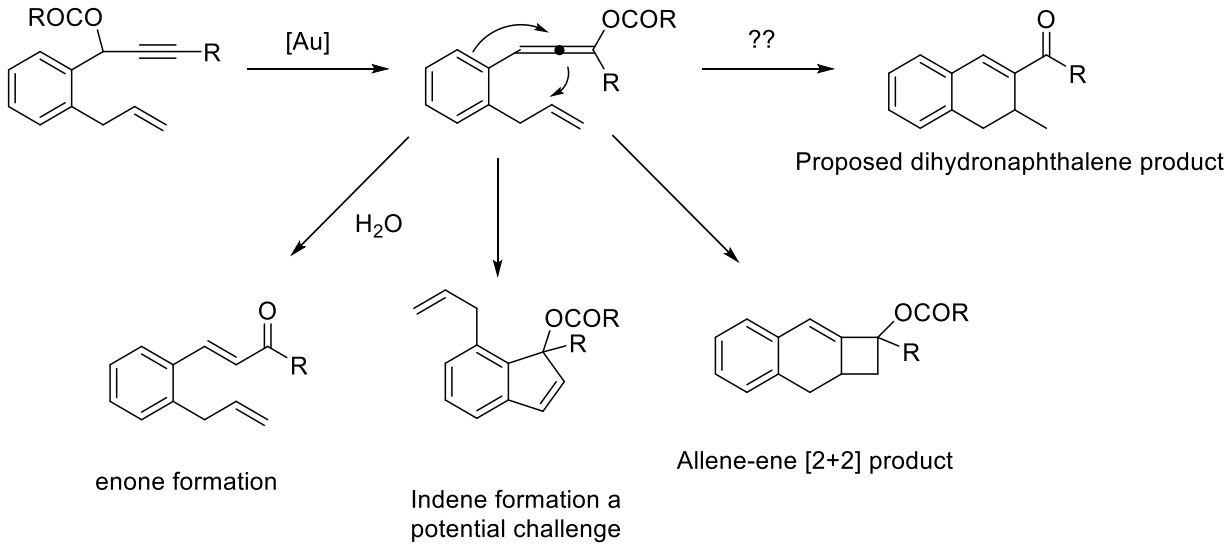

During the last several years, Shi and co-workers have explored 1,2,3-triazoles as new ligands for transition metal complexes. Their efforts led to the discovery of a triazole gold (TA-Au, **14**) complex, with significantly improved catalyst stability compared to N-heterocyclic carbene ligands.[16] One interesting discovery of the TA-Au (**14**) catalyst is its outstanding chemoselectivity of activating an alkyne over an allene. Thus, we speculated that the use of a TA-Au catalyst may promote the proposed cycloisomerization by avoiding allene activation.[21] To test this hypothesis, enyne ester **15** was prepared and subjected to the $PPh_3Au(TA)OTf$ (TA=benzotriazole, **14**) catalyst (Table 1a). Allene **16** was obtained in excellent yield (95%), while no cycloisomerization products were observed.

Similar to the previous report, the TA-Au catalyst exhibited excellent chemoselectivity for alkyne over allene activation (Table 1a).[17] It concludes that the TA-Au catalyst is not suitable for alkene activation. To evaluate the reactivity between the allene and the alkene, we have isolated allene **16** and treated it with various Lewis acids. As shown in Table 1b, typical Lewis acids,

including TfOH, $Sc(OTf)_3$ and $Bi(OTf)_3$, activated the allene over the alkene. However, the desired cyclization product **17** was not observesd. The allene double bond in **16** has a higher electron density than a simple alkene. Thus, differentiation between the two functional groups from pure electronic effect is apparently not viable. With this concern, we turned our attention to other factors that may cause different reactivity between the two functional groups.

Table 1. Screening study with other Lewis acids.

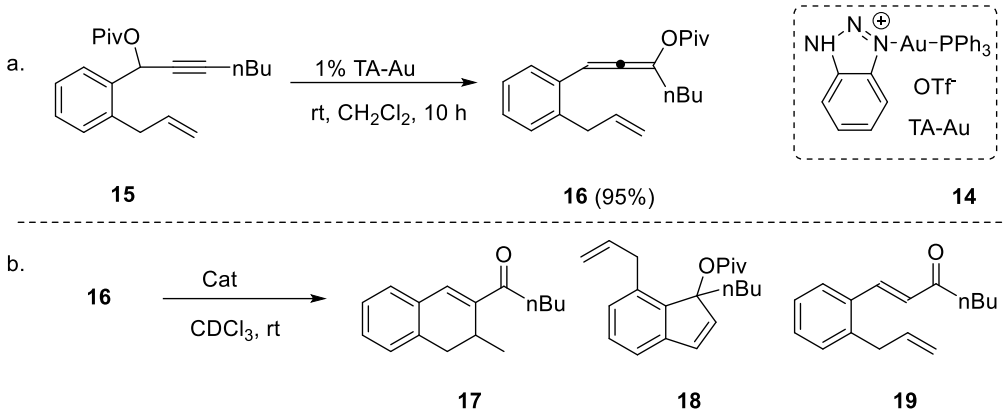

2% Cat.	Conver.	17	18	19
TfOH	100	ND	--	--
$Sc(OTf)_3$	60	0	20	40
$Bi(OTf)_3$	100	0	55	45
5% ditBuXPhosAuNTf$_2$	100	**65**	5	5

Compared to the alkene, the allene in **16** is sterically hindered having three substituents. Thus, it is plausible to obtain alkene activation if the catalyst is also sterically hindered. In practice, it would be better if a single gold catalyst could be used to achieve both alkyne and alkene activation with high efficiency. To explore this idea, we reacted **16** with di-^{t}BuXPhos-AuNTf$_2$ catalyst (5 mol%, at room temperature). The reaction was monitored by ^{1}H NMR spectroscopy and 65% of the desired cyclization product **17** was observed. Encouraged by this result, we

investigated the reactions of **15** with various gold complexes bearing bulky ligands. The results are summarized in Table 2.

Table 2. Screening studies for the cyclization of 1,7-enyne ester.[a]

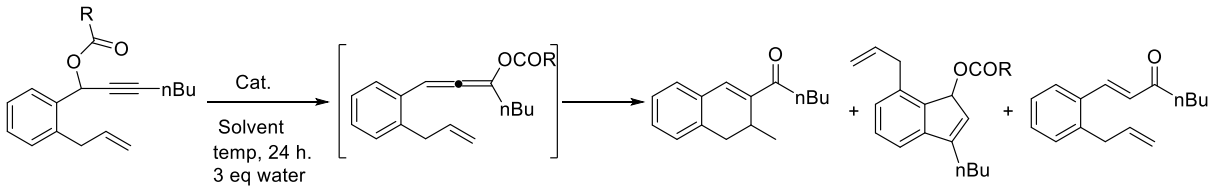

15 R=CH_3, ^{t}Bu **16** **17** **18** **19**

Entry	Cat.	migrating group	temp	sol	additive	relative yields(%)[b]			
						16	**17**	**18**	**19**
1	5% PPh_3AuNTf_2	Piv	rt	CH_2Cl_2	-	0	0	75	20
2[c]	5% $IPrAuNTf_2$	Piv	rt	CH_2Cl_2	-	27	11	35	8
3	5% XPhosAu(TA)OTf	Piv	rt	CH_2Cl_2	-	80	0	0	0
4	5% XPhosAu(ACN)OTf	Piv	rt	CH_2Cl_2	-	42	48	0	0
5	5% tri-^{t}BuPAuNTf$_2$	Piv	rt	CH_2Cl_2	-	52	10	23	6
6	5% di-^{t}BuXPhosAuNTf$_2$	Piv	rt	CH_2Cl_2	-	0	65	<5	<5
7	5% di-^{t}BuXPhosAuNTf$_2$	Piv	rt	DCE	-	0	50	<5	40
8	5% di-^{t}BuXPhosAuNTf$_2$	Piv	rt	THF	-	0	20	40	30
9	5% di-^{t}BuXPhosAuNTf$_2$	Piv	rt	Tol	-	0	74	10	10
10	5% di-^{t}BuXPhosAuNTf$_2$	Piv	rt	Tol	H_2O (3 eq)	0	83	tr	tr
11	2% di-^{t}BuXPhosAuNTf$_2$	OAc	rt	Tol.	H_2O (3 eq)	0	67	15	20
12	2% di-^{t}BuXPhosAuNTf$_2$	Piv	50 °C	Tol.	H_2O (3 eq)	0	89	tr	tr

[a]Reactions performed on a 0.2 mmol scale with R=^{t}Bu. [b] 1,3,5-Tribromobenzene was used as an internal standard for NMR analysis. [c]Unidentified products observed.

To establish optimal reaction conditions, we treated **15** with 5 mol% of PPh_3AuNTf_2 in dichloromethane at room temperature. In this case, the reaction afforded a mixture of the undesired products **18** and **19** (entry 1). Upon changing the catalyst to one containing an electron-rich carbene ligand IPr (entry 2), and using 5 mol% of $IPrAuNTf_2$, **17** was observed in 11% yield. Our studies

subsequently showed that using a sterically crowded and electron-rich gold(I) complex, such as XPhosAu(ACN)OTf, increased the yield of **17** to 48% (entry 4). These results suggest that the formation of the **17** may be directly related to the bulkiness of the ligand used. We then evaluated the catalytic performance of di^{t}BuXPhosAuNTf$_2$, which contains an even more bulky and electron rich di^{t}BuXPhos ligand, gave 65% of **17** (entry 5).[18] This is presumably due to the fact that the steric congestion of the bulky substituents helps stabilize the cationic gold center (gold cation stabilized by aromatic rings)[19] and inhibits allene activation as we predicted. Much better yields were obtained using pivaloyl as the migrating group instead of acetyl (75% entry 6). No significant improvement was observed upon changing the solvent from dichloromethane to 1,2-dichloroethane or THF (entries 7 and 8). To our delight, in toluene 75% of the cyclized product was obtained with a minimum amount of byproducts (entry 9). Using water as an additive increased the reaction efficiency in toluene resulting in 83% yield of **17** (entry 10) with minimum amount of byproducts**.** By reducing the catalyst loading to 2% and increasing the temperature of the reaction to 50 ^{o}C (entry 11) compound **17** was obtained in 89%. On the basis of above results, the optimum conditions for production of **17** from **15** are obtained when 2% loading of di-^{t}BuXPhosAuNTf$_2$ as the catalyst precursor in toluene at room temperature or at 50 ^{o}C for 12-24 h.

The substrate scope of the methodology was then assessed using a series of enyne-esters with the focus on alkyne substitution. The results are summarized below in Table 3. In general, the reaction scope proved to be broad and a variety of substituted dihydronapthalenes could be obtained. Aliphatic alkynes furnished products **17b-f** in 60-90% yield in toluene and substrates of aromatic alkynes gave products **17g-o** in 50-90% yield in dichloromethane. Substituents on the aromatic ring have some influence on the course of the reaction. Electron donating groups provided

excellent yields and electron withdrawing groups resulted in moderate yields of the cyclized products.

Table 3. Substrate scope for the formation of dihydronapthalenes.

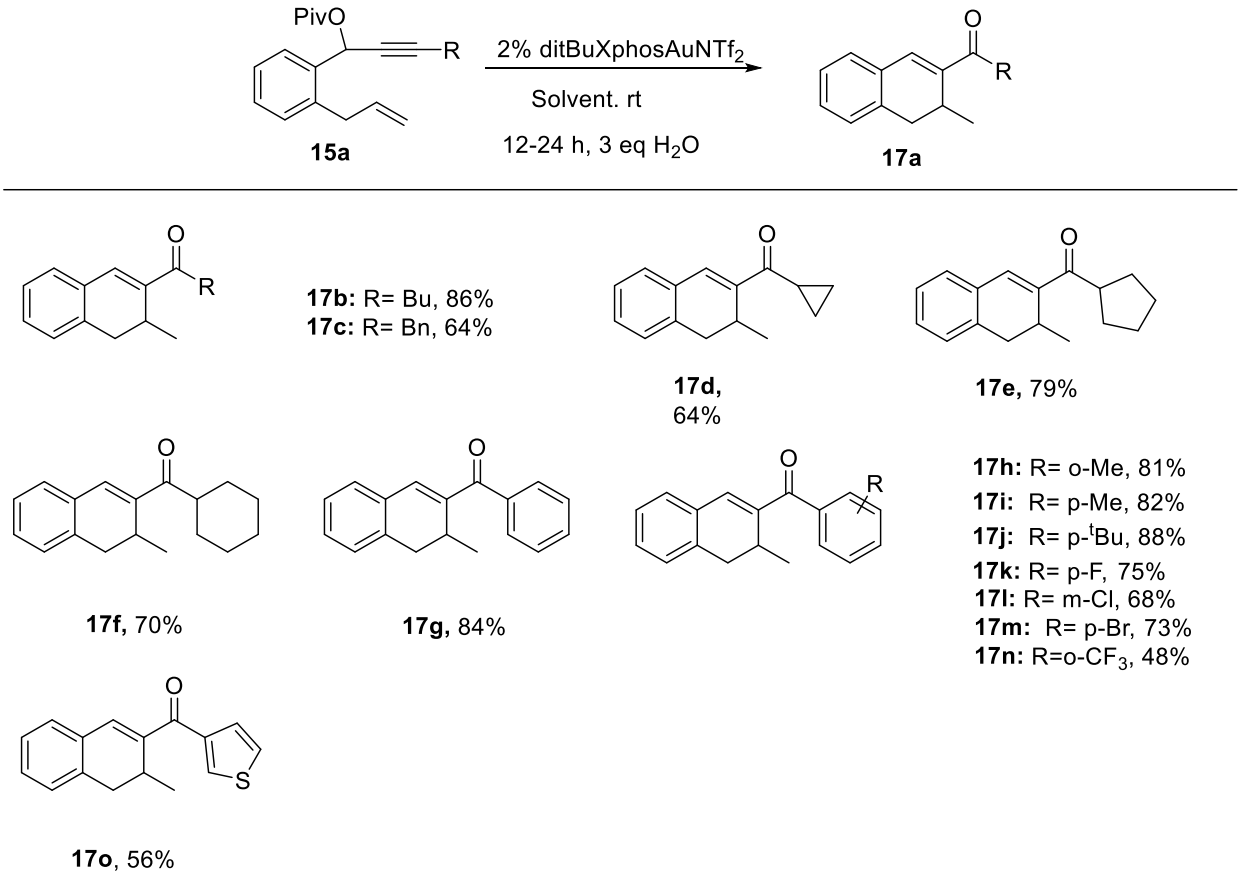

Reactions performed on 1-2 mmol scale level. 1,3,5-Tribromobenzene was used as internal standard for NMR analysis. Reported yields are isolated yields.**17b-f,** toluene as solvent. **17g-o** DCM as solvent.

To evaluate further the cycloisomerization reaction, we examined reactions of internal alkenes (Scheme 5, **18**) and of disubstituted terminal alkenes (Scheme 5, **19**). The starting materials (**18-21**) were prepared and subjected to gold catalysts under the optimized conditions. Based on ^{1}H NMR spectroscopy, the reactions were sluggish and only approximately 5% of the desired products were observed. No significant improvement in product yield was seen at higher temperatures (50 ^{o}C). This might be due to steric hindrance at the alkene center which may hinder

the ability of gold to activate it. We further tested the scope of the reaction with the homologated alkenes (Scheme 5, **20** and **21**), In this case, only unidentified products were obtained.

Scheme 5. Possibility of the internal, substituted alkenes and 1,8-enyne ester cycloisomerization.

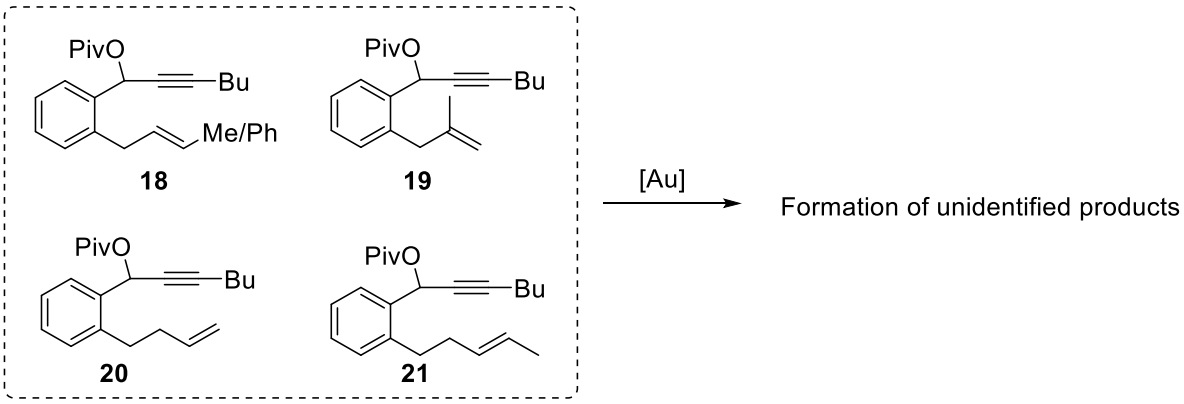

Encouraged by our success to perform cyclization through terminal alkenes activation with a gold catalyst bearing a bulky primary ligand such as di^{t}BuXPhos, we next focused on the evaluation of substrates containing O and N heteroatoms. The corresponding substrates, **22** and **23**, were prepared and studied using our optimized conditions. As expected, dihydrobenzopyran **24a** and dihydroquinoline **25a** derivatives were obtained. The reaction scope is shown below in Table 4.

This expanded methodology provided a new route to dihydrobenzopyran and dihydroquinolines. As compared to compound **15**, the cycloisomerization reactions of vinyl ethers (**22**) and vinyl amines (**23**) are much faster. Interestingly, with the vinyl ether as shown in the mechanism depicted in Scheme 6 (**36**), a pivalyl group migration was observed during the formation of the product by displacing the carbon-gold bond (Scheme 6, **34**). The electron rich carbon-gold bond attacks the carbonyl of pivaloyl moiety instead of undergoing protodeauration. The carbon-gold bond is synthetically very useful to incorporate other functional groups on to the

methyl group. Under anhydrous conditions, the reaction resulted in significant amount of unidentified products along with the [2+2] cyclic products that was observed in Chan's work (Scheme 2). In contrast, no such migration was observed with vinyl amines. We assumed that the steric hindrance from the tosyl group on the nitrogen atom helped promote protodeauration rather than pivaloyl migration.

Table 4. Substrate scope for vinylethers and vinylamines.

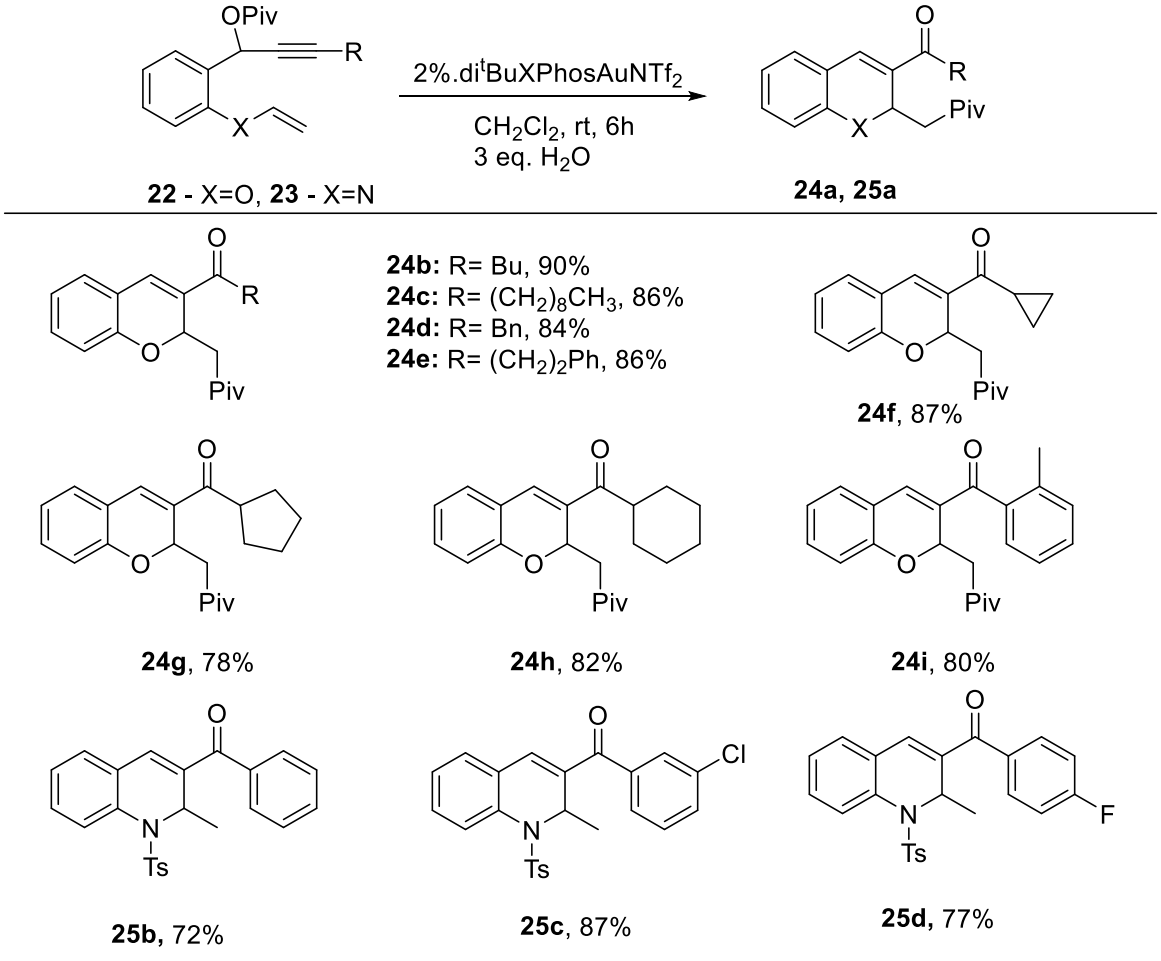

Reactions performed on 1-2 mmol scale level. 1,3,5-tribromobenzene used as internal standard for NMR analysis. Reported yeilds are isolated yields.

Considering that the double bonds of vinyl ethers are more nucleophilic due to the higher electron density, we questioned whether they could be used to facilitate the formation of the 7-

membered rings. The starting materials **26** were prepared according to literature procedure[19] and subjected to the optimized conditions (gold catalyst with 3 eq. H_2O). Initially, this reaction gave significant amounts of vinyl ether hydration products **28** (up to 30%). Thus, anhydrous conditions were used to avoid this side reaction. Under anhydrous conditions, the desired cyclization product **29a** was observed along with a trace amount of (~15% varies with substrate) of formal [2+2] cyclization product **29a′** (Table 5). Surprisingly, in contrast to the formation of dihydrobenzopyran, no pivaloyl migration was observed. The reactions of substrates containing an aromatic alkyne provided good yields, whereas substrates with an aliphatic alkyne resulted in unidentified products in addition to cyclic product in moderate yields.

Table 5. Substrate scope for the synthesis of seven membered ring.

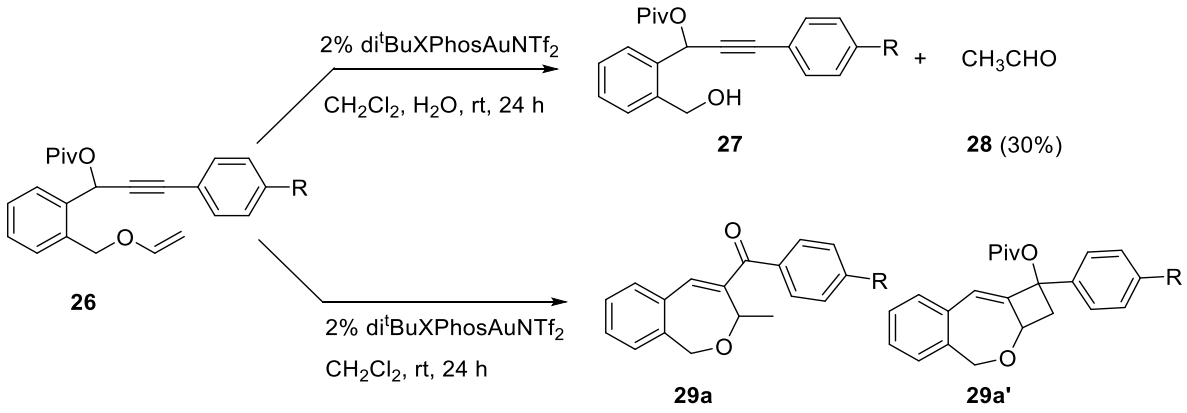

R=H	R=CH_3	R=^{t}Bu	R=F
29b 68%	**29c** 66%	**29d** 52%	**29e** 70%
29b' 7%	**29c'** 10%	**29d'** 15%	**29e'** 12%

1.3 Mechanism.

A tentative mechanism for the gold(I) catalyzed cycloisomerization reaction of 1,n-enyne esters (n = the number of atoms between the alkene and alkyne) to form the aromatic bicyclic compounds is outlined in Scheme 6. Initially it involves selective activation of the alkyne **30** by the gold catalyst to give an intermediate, gold coordinated species **31**. A 3,3-rearrangement of **32**

leads to an allenene intermediate **33**. Here the size of the catalyst plays a major role in selective activation of allene and alkene. If the size of the catalyst system is bulkier, the intermediate **34** gold cannot activate a tri- or tetra-substituted allene. Instead the bulky catalyst selectively coordinates to the alkene to give a gold-activated adduct **35**. Subsequent nucleophilic attack of the allene onto the gold coordinated alkene leads to a cyclized product **35**, a C-Au bond and also an oxonium intermediate. Protodeauration of the intermediate **36** leads to a hydrolyzed product **37** by eliminating the gold cation. Under anhydrous conditions the major formal [2+2] product **39** resulted with the nucleophilic attack of the C-Au bond on to the oxonium intermediate.[20]

Scheme 6. Tentative mechanism for cyclization catalyzed by gold cation.

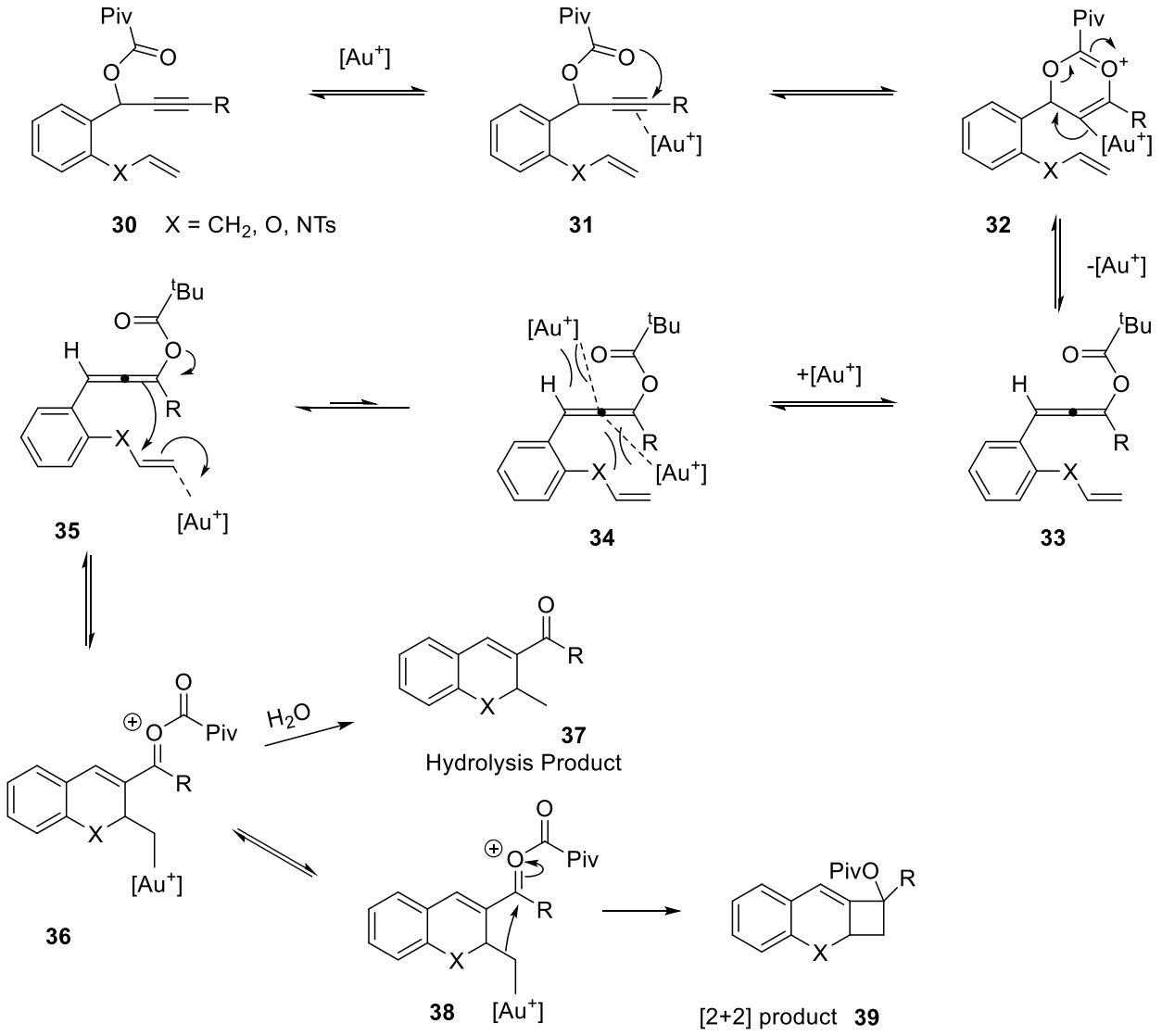

1.3.1 Deuterium labelling study of the proposed mechanism.

It was proposed that the reaction proceeds through electrophilic activation of the alkene by the gold catalyst. The alkyl-gold intermediate which presumably undergoes either protodeauration to provide a hydrolysis product or may be trapped by the acylium (Scheme 6) cation to afford a formal [2+2] product. In order to lend support to the proposed mechanism, we performed a reaction in the presence of 3.0 equivalents of D_2O (2% di^{t}BuXPhosAuNTf$_2$, dichloromethane, rt) to

determine whether or not deuterium is incorporated via deuterodeauration at the end of the reaction (Scheme 7).

Scheme 7. Deuterium labelling study of the proposed pathway.

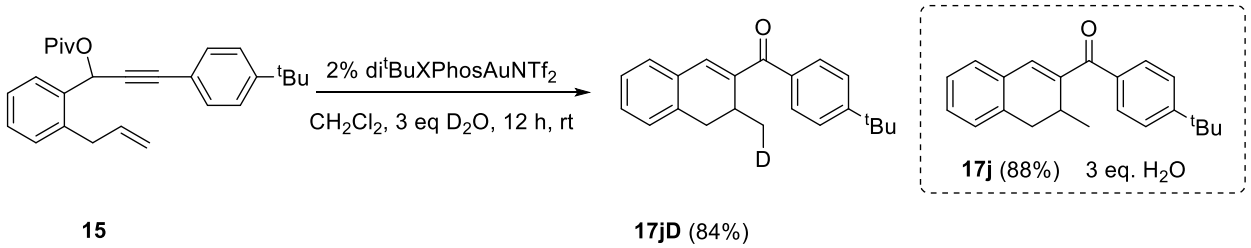

15 **17jD** (84%)

Based on ^{1}H NMR analysis of the reaction product (Figure 3), deuterium was incorporated successfully into the exo-methyl group. The exo methyl group of **17j** showed a doublet at δ 1.04 ppm due to splitting by ring proton with the integration of 3.0 protons. However, **17jD** showed an integration of 2.0 protons only. On the other hand, the ring proton in **17j** at around δ 3.25 ppm was a doublet of pentet. The same proton of the **17jD** gave a doublet of quartet clearly indicating deuterium incorporation or short of one proton (2 hydrogen atoms instead of 3). In the ^{13}C NMR spectrum of **17jD**, the deuterated carbon gave a triplet at δ 17.4 ppm with $^{13}J_{C\text{-}D}$ = 19.0 Hz consistent with the deuterium incorporation. Finally, the ^{2}H NMR further confirmed the incorporation of a deuterium on the methyl group.[20]

Figure 3. ^{1}H and ^{13}C NMR spectra of compound **17jD**.

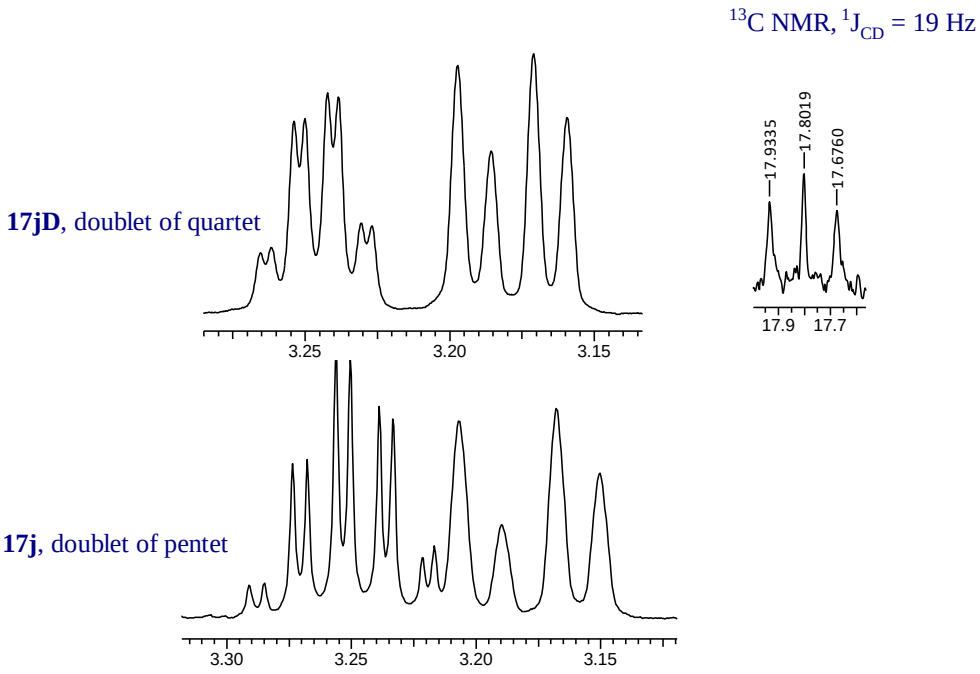

1.4 Conclusion.

In conclusion, we have developed a gold catalyzed synthesis of dihydronaphthalene, dihydrobenzopyran and dihydroquinoline derivatives. This method was applicable for both aliphatic and aromatic alkynes with good to excellent yields. This methodology can also be applied for the synthesis of 7-membered ring systems of 1,8-enyne ester vinyl ethers.

References

1. (a) Trost, B. M.; Krische, M. J. *Synlett* **1998**, 1–16. (b) Trost, B. M. *Acc. Chem. Res.* **1990**, *23*, 34–42. (c) Michelet, V.; Toullec, P. Y.; Genet, J.-P. *Angew. Chem., Int. Ed* **2008**, *47*, 4268–4315.
2. (a) Shiroodi, R.K.; Gevorgyan, V.; *Chem. Soc, Rev.*, **2013**, *42*, 4991; (b) Marion, N.; Fremont, P.; Lemiere, G.; Stevens, E. D.; Fensterbank, L.; Malacriab M.; Nolan, S. P. *Chem. Commun*., **2006**, 2048.
3. Trost, B. M. *Science* **1991**, *254*, 1471–1477.
4. a) Trost B. M.; *Acc. Chem. Res.* **1990**, *23*, 34; b) Goeke, A.; Kuwano, R.; Ito, Y.; Sawamura, M. *Angew. Chem. Int. Ed. Engl.* **1996**, 35, 662; c) Trost, B. M.; M. Lautens, *J. Am. Chem. Soc.* **1985**, *107*, 1781.
5. a) Trost, B. M.; Toste, F. D.; Pinkerton, A. B. *Chem. Rev.* **2001**, *101*, 2067; b) Kossler, D.; Cramer, N. *J. Am. Chem. Soc.* **2015**, *137*, 12478; c) Trost, B. M.; Gutierrez, A. C.; Ferreira. E. M. *J. Am. Chem. Soc.* **2010**, *132*, 9206; d) Trost, B. M.; Surivet, J.-P.; Toste, F. D. *J. Am. Chem. Soc.* **2004**, *126*, 15592; e) Trost, B. M.; Toste. F. D. *J. Am. Chem. Soc.* **2000**, *122*, 714.
6. a) Evans, P. A; Modern Rh catalyzed organic reactions (Ed.: P. A. Evans), Wiley-VCH, Weinheim, **2005**, 129–171; c) Li, J. J. Named Reactions, 5th ed., Springer, London, **2014**; 652–653.
7. Fan, B.-M.; Li, X.-J.; Peng, F.-Z.; Zhang, H.-B.; Chan, A. S. C.; Shao, Z.-H. *Org. Lett.* **2009**, *12*, 304–306.
8. a) Zhang, L.; J. Sun, Kozmin, S. A. *Adv. Synth. Catal*. **2006**, *348*, 2271; b) Fîrstner, A.; *Acc. Chem. Res.* **2014**, *47*, 925; c) Arumugam, K.; Varghese, B.; Brantley, J. N.; Konda, S. S. M.;

Lynch, V. M.; Bielawski C. W; *Eur. J. Org. Chem.* **2014**, 493; d) Fîrstner, A.; *Chem. Soc. Rev*. **2009**, *38*, 3208

9. (a) Bajracharya, G. B.; Nakamura, I.; Yamamoto, Y. *J. Org. Chem.* **2005**, *70*, 892–897. (b) Fürstner, A.; Davies, P. W.; Gress, T. *J. Am. Chem. Soc.* **2005**, *127*, 8244–8245. (c) Matsuda, T.; Kadowaki, S.; Goya, T.; Murakami, M. *Synlett* **2006**, 575–578.
10. (a) Flasterera D. P.; Hashmi, A. S. K. *Chem. Soc. Rev*., **2016**, *45*, 1331; (b) Dorel R.; Echavarren, A. M. *Chem. Rev*., **2015**, *115*, 9028; (c) Fensterbank, L.; Malacria. *Acc. Chem. Res*., **2014**, *47*, 953; (d) Rudolph M.; Hashmi, A. S. K. *Chem. Soc. Rev*., **2012**, *41*, 2448; (e) Krause N.; Winter, C. *Chem. Rev.*, **2011**, *111*, 1994.
11. (a) Marion, N.; De Fremont, P.; Lemiere, G.; Stevens, E. D.; Fensterbank, L.; Nolan, S. P. *Chem. Commun.*, **2006**, 2048; (c) Shi, X.; Gorin D. J.; Toste, F. D. *J. Am. Chem. Soc.*, **2005**, *127*, 5802; (d) Mamane, V.; Gress. T.; Krause H.; Furstner, A. *J. Am. Chem. Soc.*, **2004**, *126*, 8654.
12. Day, D. P.; Chan, P. W. H., *Adv. Syn. & Cat.* **2016,** *358* (9), 1368-1384.
13. Duan, H.; Sengupta, S.; Petersen, J. L.; Akhmedov, N.; Shi, X. *J. Am. Chem. Soc.* **2009,** *131*, 12100-12102.
14. a) Rao, W.; Koh, M. J.; Kothandaraman, P.; Chan, P. W. H. *J. Am. Chem. Soc*. **2012**, *134*, 10811. (b) Kothandaraman, P.; Huang, C.; Susanti, D.; Rao, W.; Chan, P. W. H. *Chem. Eur. J.* **2011**, *17*, 10081. (c) Sze, E. M. L.; Rao, W.; Koh, M. J.; Chan, P. W. H. *Chem. Eur. J.* **2011**, *17*, 1437. (d) Kothandaraman, P.; Rao, W.; Foo, S. J.; Chan, P. W. H. *Angew. Chem., Int. Ed*. **2010**, *49*, 4619. (e) Rao, W.; Chan, P. W. H. *Chem. Eur. J.* **2008**, *14*, 10486.

15. (a) Marion, N.; Dıez-Gonzalez. S.; Fremont, P.; Noble A. R.; Nolan, S. P. *Angew. Chem., Int. Ed.*, **2006**, *45*, 3647; (b) Marion, N.; Carlqvist, P.; Gealageas, R.; Fremont, P.; Maseras, F.; Nolan, S. P. *Chem. – Eur. J.*, **2007**, *13*, 6437.

16. (a) Hosseyni, S.; Su Y.; Shi, X. *Org. Lett.*, **2015**, *17*, 6010; (b) Cai, R.; Yan, W.; Bologna, M. G.; De Silva, K.; Finklea, H. O.; Petersen J. L.; Shi, X. *Org. Chem. Front*., **2015**, *2*, 141.

17. (a) Hosseyni, S.; Su, Y.; Akhmedov N. Shi, X. *Chem. Commun*., **2016**, *52*, 296; (b) Wang, Q.; Aparaj, S.; Akhmedov, N. G.; Petersen J. L.; Shi, X. *Org. Lett*., **2012**, *14*, 1334; (c) Wang, D.; Gautam, L. N. S.; Bollinger, C.; Harris, A.; Li, M.; Shi, X. *Org. Lett.*, **2011**, *13*, 2618; (d) Wang, D.; Ye X.; Shi, X. *Org. Lett*., **2010**, *12*, 2088–2091.

18. Hashmi, A. S. K.; Bechem, B.; Loos, A.; Hamzic, M.; Rominger F.; Rabaa, H. *Aust. J. Chem.*, **2014**, *67*, 481. (b). Jagdale, A. R.; Park J. H.; Youn, S. W. J. Org. Chem., 2011, 76, 7204–7215.

19. Nakamura, A.; Tokunaga, M., *Tetrahedron Lett.* **2008,** *49* (23), 3729-3732

20. Thummanapelli, S. K.; Hosseyni, S.; Su, Y. J.; Akhmedov, N. G.; Shi, X. *Chem. Comm.* **2016,** *52* (49), 7687-7690.

Chapter 2 Attempted synthesis of a 1,2,3-triazole analog of porphyrin

2.1 Introduction

2.1.1 Role of ligands in transition metal catalysis

Transition metal catalysis has revolutionized the synthesis of organic molecules over the past several decades.[1] Compared to traditional syntheses, transition metal catalysis provides new and efficient routes for the production of fine chemicals. The ligands play a crucial role in catalysis by binding to the metal centers and thus alter the chemical behavior of metals. Based on ligand field theory,[2] the ligand can control the metal reactivity by influencing the stereochemical and electronic environment around the metal center and provides spatial arrangement that leads to asymmetric synthesis.[2] The variation of the ligands as well as their steric and electronic properties provides a powerful tool to control the chemical reactivity, chemoselectivity and stability of transition metal complexes.[3] Numerous efforts have been put into the discovery and development of novel ligands for adjusting the chemical and stereoselective properties of metal complexes[4] that have been extensively applied in academic research and industrial synthesis.[5] Some of the very well-known examples are shown below in Figure 4 are pincer,[6] BINAP,[7] BOX,[8] DuPhos,[9] TADDOL,[10] and Salen[11].

Figure 4. Example ligands developed for transition metal mediated asymmetric catalysis.

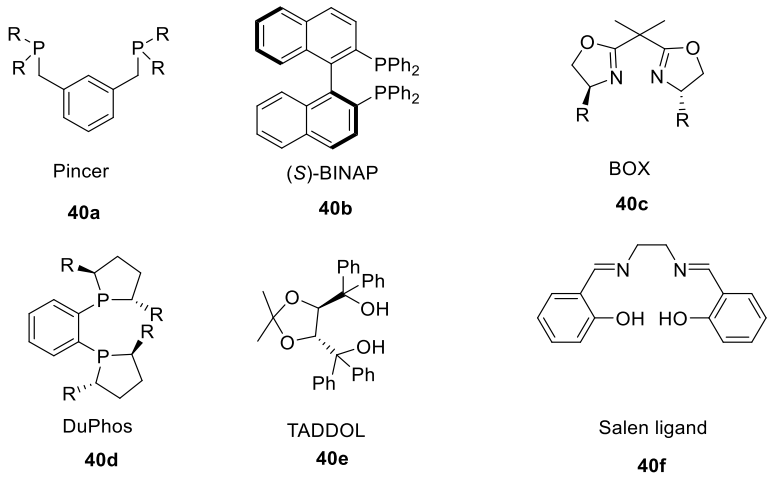

2.1.2 Introduction to porphyrins

Porphyrins are a group of heterocyclic macrocycles composed of four modified pyrrole subunits interconnected at their alpha carbon atoms via methine bridges. The porphyrin ring structure is aromatic with a total of 26 electrons (22 electrons from the double bonds and 4 from two NH groups) in the conjugated system.[12] The nitrogen atoms of the ring are involved differently in conjugation within the ring and the overall nature of the molecule is based on several smaller conjugated systems.[13-16] One prominent feature of this highly conjugated structure is that porphyrin molecules typically exhibit very intense absorption bands in the visible region and are deeply colored. The skeletal structure of porphyrin is shown in Figure 5.

Figure 5. Skeletal structure of porphyrin

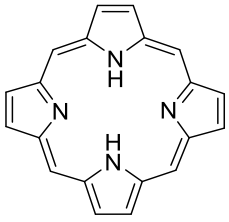

Many porphyrins are naturally occurring; two of the best known porphyrins are heme and chlorophyll. Heme provides the pigment in red blood cells and is a cofactor of the protein hemoglobin. It binds with iron, and is involved in the transportation of oxygen and carbon dioxide from lungs to internal organs and vice versa. Chlorophyll is another naturally occurring porphyrin present in plants. It binds with magnesium and is useful in the synthesis of carbohydrates via photosynthesis. The general structures of the heme, chlorophyll and examples of related porphyrins are shown in Figure 6.

Figure 6. Naturally occurring porphyrins.

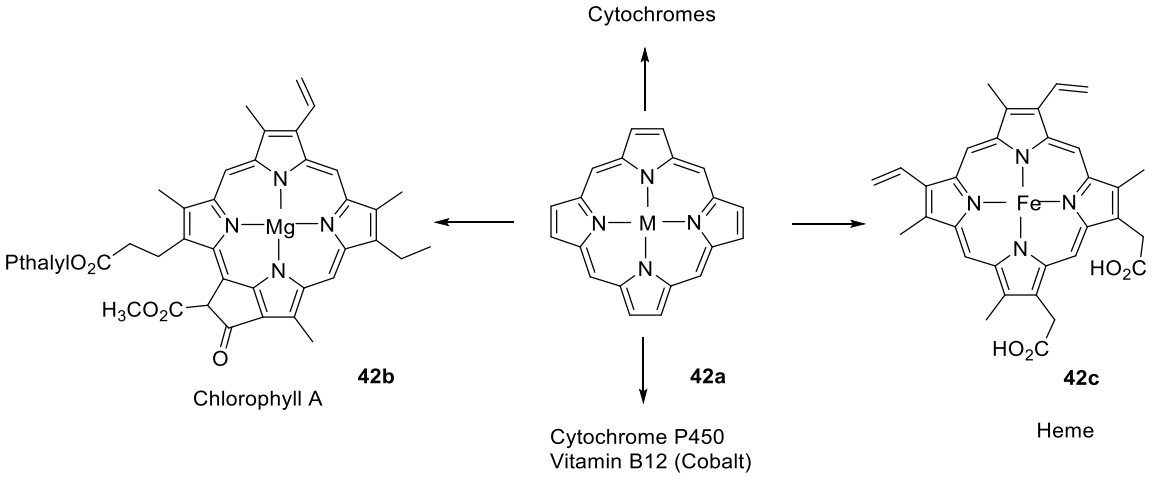

2.1.3 Introduction to Click Chemistry.

Click chemistry, involves a copper catalyzed azide alkyne 1,3-dipolar cycloaddition (abbreviated as CuAAC) that allows formation of 1,4-disubstituted 1,2,3-triazoles (Scheme 8).[17] Thereafter the importance of the 1,2,3-triazoles has been continuously demonstrated in organic synthesis,[18] pharmaceutical sciences[19] and medicinal chemistry.[20] The Click reaction proceeds smoothly under mild conditions with high yields. It involves a dinuclear CuAAC mechanism shown in Figure 7. The intermediate copper acetylide complex has been successfully isolated and analyzed by X-ray crystallography.

Scheme 8. A general Click reaction.

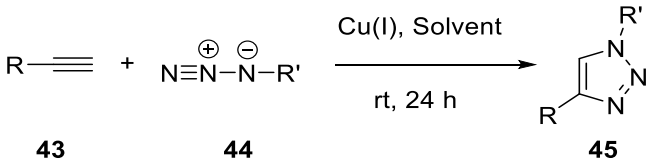

The reaction mechanism (Figure 7) has been investigated using Density Functional Theory calculations.[21] The copper (I) species that is generated in situ forms a complex with the triple bond. Initially the copper acetylide intermediate is formed by deprotonation of the acidic alkyne proton. DFT calculations suggest that this mechanism involves a dicopper species, one copper atom activates the alkyne and the second one activates the azide. At the end, protonation is affected by the solvent to complete cyclization. The active copper species is regenerated for further catalytic cycles.

Figure 7. Reaction mechanism for Click chemistry.

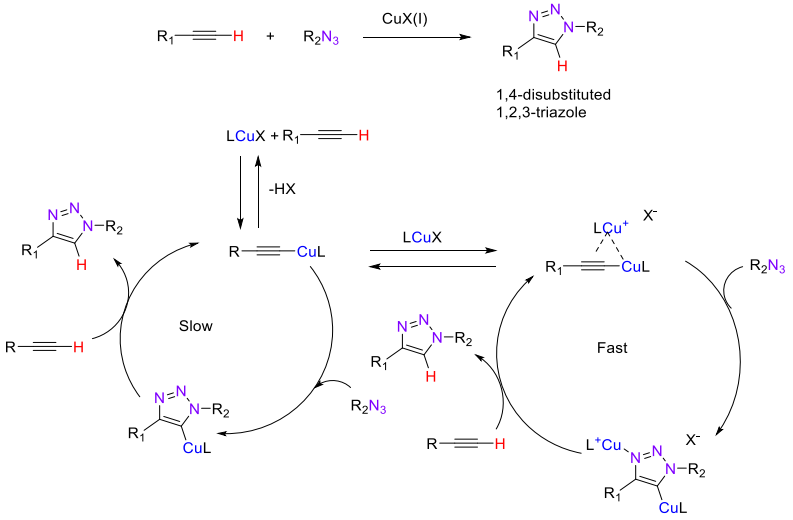

Professor Shi and his co-workers reported a Lewis base-catalyzed cascade nitro alkene-aldehyde-azide condensation for the synthesis of 4,5-disubstituted NH-1,2,3-triazoles (Scheme 9)[21] and introduced a different approach from Click chemistry for the synthesis of substituted 1,2,3-triazoles. A significant number of new triazoles have been synthesized in good to excellent yields under mild reaction conditions using this approach.

Scheme 9. Synthesis of 4,5-disubstituted-NH-1,2,3-triazole.

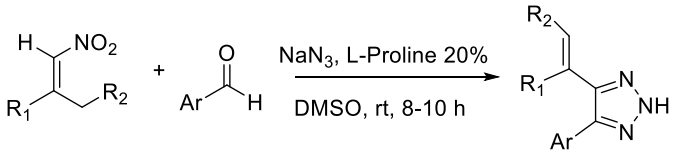

46 **47** **48**

2.1.4 Introduction to Mitsunobu reaction.

The Mitsunobu reaction converts an alcohol into a variety of functional groups with a range of nucleophiles. This reaction is mediated by the combination of a trialkyl or triarylphosphine and a dialkyl azodicarboxylate (If the alkyl is ethyl it is called DEAD or if the alkyl is isopropyl it is DIAD).[22-24] The reaction proceeds with inversion at the alcohol center of secondary and tertiary alcohols. The Mitsunobu reaction plays an important role in organic synthesis and medicinal chemistry[25] because of its scope, stereospecificity and mild reaction conditions. A wide range of compounds can be synthesized using a Mitsunobu protocol including esters,[26] amines,[27] azides,[28] ethers,[29] cyanides,[30] thiocyanides,[31] triazoles and benzotriazoles.[32] The mechanism of the Mitsunobu reaction is outlined in Scheme 10.

Scheme 10. A general Mitsunobu reaction and mechanism.

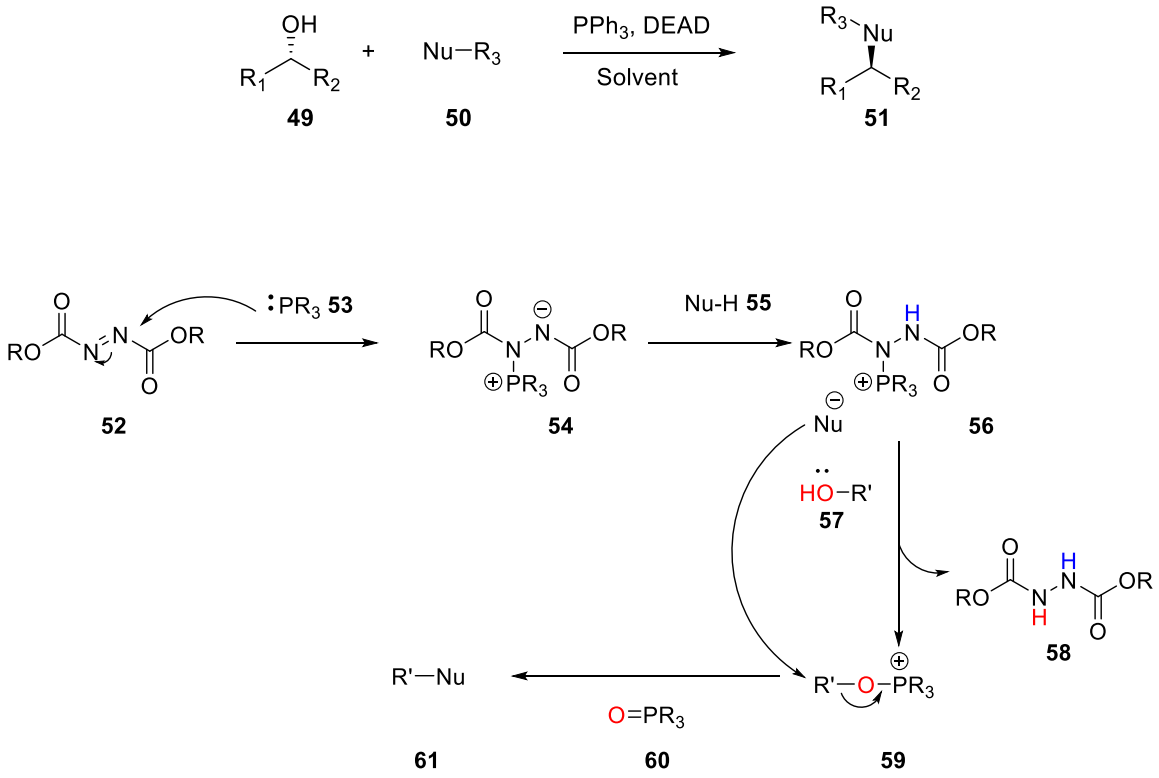

The first step of the Mitsunobu reaction is the irreversible formation of the intermediate betaine **54** from nucleophilic attack of phosphine (PR_3, **53**) on the dialkyl azodicarboxylate, **52**. This step has been confirmed by NMR and ESI-MS.[33] In the second step betaine **54** deprotonates the hydrogen of the nucleophile **55** to give intermediate **56**, which then reacts with the alcohol **57** to form the alkoxyphosphonium intermediate **59**. Finally, the desired product **61** is obtained by the attack of nucleophilic anion upon intermediate **59**. The byproducts of the Mitsunobu reaction are phosphine oxide **60** and dialkyl hydrazine-1,2 dicarboxylate **58**.[33]

The Click reaction conditions provides only N1 substituted products. To improve the N2 selectivity, Professor Shi and his co-workers developed a method for N2-substituted 1,2,3-triazoles using the Mitsunobu reaction (Scheme 11). [34] Good to excellent isolated yields of the N-2 isomers were obtained from different alcohols.

Scheme 11. Mitsunobu reaction of 1,2,3-triazole **62,** with an alcohol.

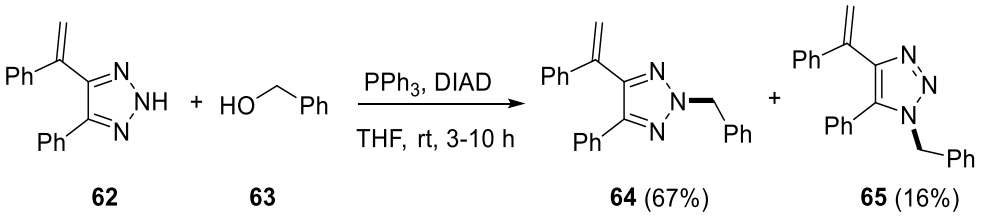

62 **63** **64** (67%) **65** (16%)

2.1.5 Introduction to porphyrin ligands in catalysis

Zhang reported cobalt catalyzed cyclopropanation and aziridination reactions (Scheme 12 and Scheme 13)[35] of olefins as a general approach for the synthesis of optically active cyclopropane[36] and aziridine derivatives. The cobalt metal was bound to a porphyrin ligand. These cobalt (II) porphyrin complexes have emerged as a new class of catalysts for asymmetric cyclopropanation with wide substrate scope.[37]

Scheme 12. Intra and intermolecular cyclopropanation reactions.

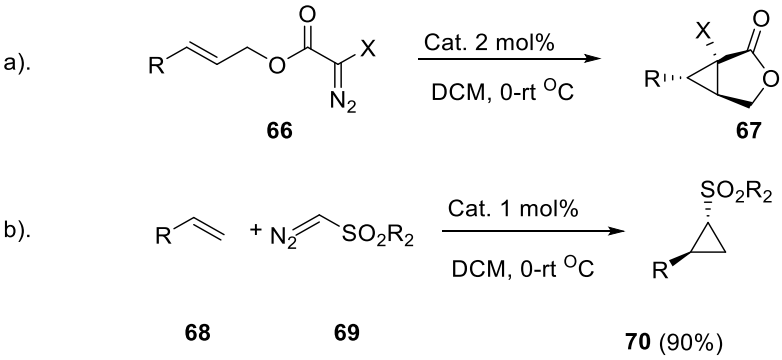

66 **67**

68 **69** **70** (90%)

Scheme 13. A cobalt porphyrin catalyzed asymmetric aziridination reaction.

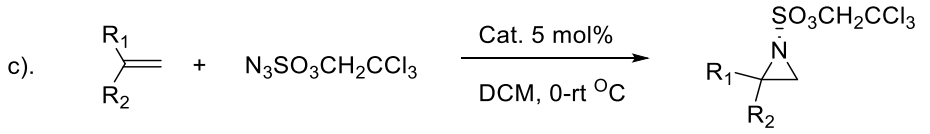

71 **72** **73** (>90%, ee >95%)

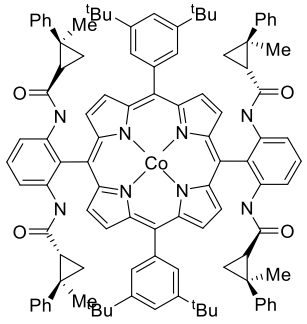

Cat for a and b

74

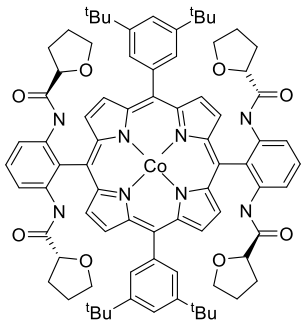

Cat for c

75

2.2 Research design

Porphyrins molecules, which consist of four pyrrole units with the nitrogen atoms facing the center, are capable of binding to transition metals to form very stable metal complexes. 1,2,3-Triazole is also a heterocycle having similar properties as that of the pyrrole ring. For example, the NH moiety of triazoles, just like pyrrole, has an ability of binding with metals, forming strong bonds by π back-bonding from metal ions. Most importantly the number of electrons in its cyclic form **76** are same as the porphyrin ring (26 electrons, 22 electrons from 11 double bonds and 4 electrons from 2 NH groups) and the mode of binding of nitrogen atom of the triazole is also expected to be similar that is shown below in Figure 8. With the successful synthesis of N-2 substituted triazoles in our earlier report,[34] we decided to synthesize the 1,2,3-triazole analog **76** however, the following issues needed to be evaluated.

- A Mitsunobu reaction between two triazoles and dimers of triazoles.
- Cyclization of a linear tetramer
- The conditions for oxidation/aromatization of the cyclic core and its coordination to metal ions.

Figure 8. Structures of porphyrin and 1,2,3-triazole analog of porphyrin.

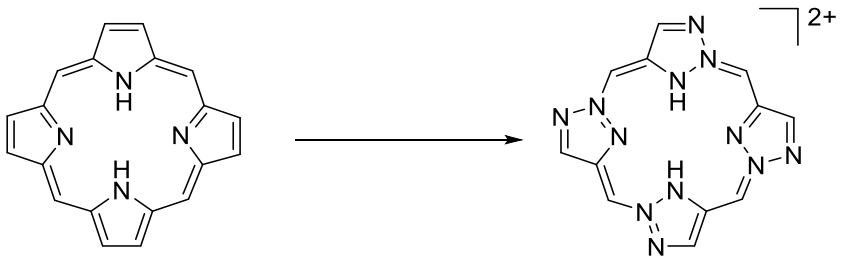

41
Porphyrin

76
Triazole porphyrin

2.2.1 Synthesis of 1,2,3-triazole analog of porphyrin

In our attempt to synthesize **76**, we hypothesized that the second triazole ring can easily be installed by a Click reaction given that the triazole ring (dimer) is at propargyl position as shown in Scheme 14. Once the dimer is obtained, synthesis of the tetramer may be possible using a Mitsunobu reaction. The cyclic tetramer would be obtained using a macrocyclization strategy. Macrocyclizations are performed under high dilution, typically submillimolar concentration, to minimize unwanted intermolecular processes such as oligomerization and polymerizations.[38]

The triazole monomer **77** was treated with an excess of propargyl bromide in the presence of potassium carbonate to afford **78** and **79**. Both N-1 and N-2 nitrogen act as a nucleophile resulting in a mixture of two isomeric products **78** and **79** in 80% overall yield. The two isomers were separated by column chromatography. Only **79** was used for further reactions.

Scheme 14. S_N2 reaction of triazole.[39]

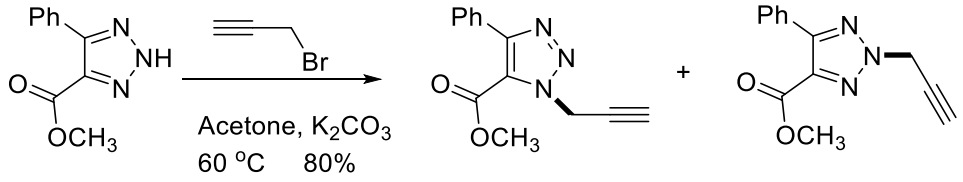

77 **78** (60%) **79** (40%)

The Click reaction of methyl pivaloyl azide and the terminal alkyne **79** provided triazole dimer 8**0**. This reaction, when performed in the presence of copper (II) salts and sodium ascorbate as a reducing agent in *t*-butanol/water as the solvent system,[40] resulted in N-1 protected 1,4-disubstituted triazole dimer **70** as a single product in 60% yield.

Scheme 15. Click reaction with compound **79.**

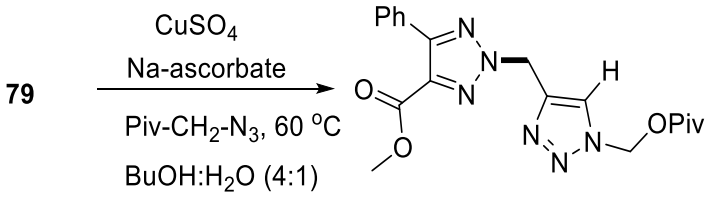

80 (60%)

Compound **80** was treated with lithium aluminum hydride to reduce the ester functional group. Unfortunately, the pivaloyl moiety was also reduced under the strong reducing conditions. Compound **81** was obtained in 52% yield as a white solid.

Scheme 16. Ester reduction.

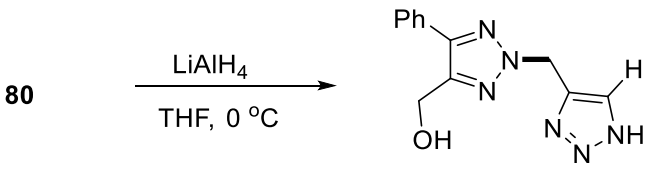

81 (52%)

In order to avoid the formation of multiple products in a later Mitsunobu reaction, it was necessary to protect one of the two functional groups of each dimer. Initially, product **81** was divided into two equal portions. The hydroxyl group of one portion was protected with TBDMS-Cl[41] to give **82,** and the NH group of the other portion was protected with methyl pivaloylchloride to give **83** and **84.** These two compounds were obtained in a 1:1 (90%) ratio of N-1 and N-2 isomers. These two isomers were successfully separated by column chromatography and compound **84** was used in further reactions.

Scheme 17. Protection of the alcohol and nitrogen of the triazole.

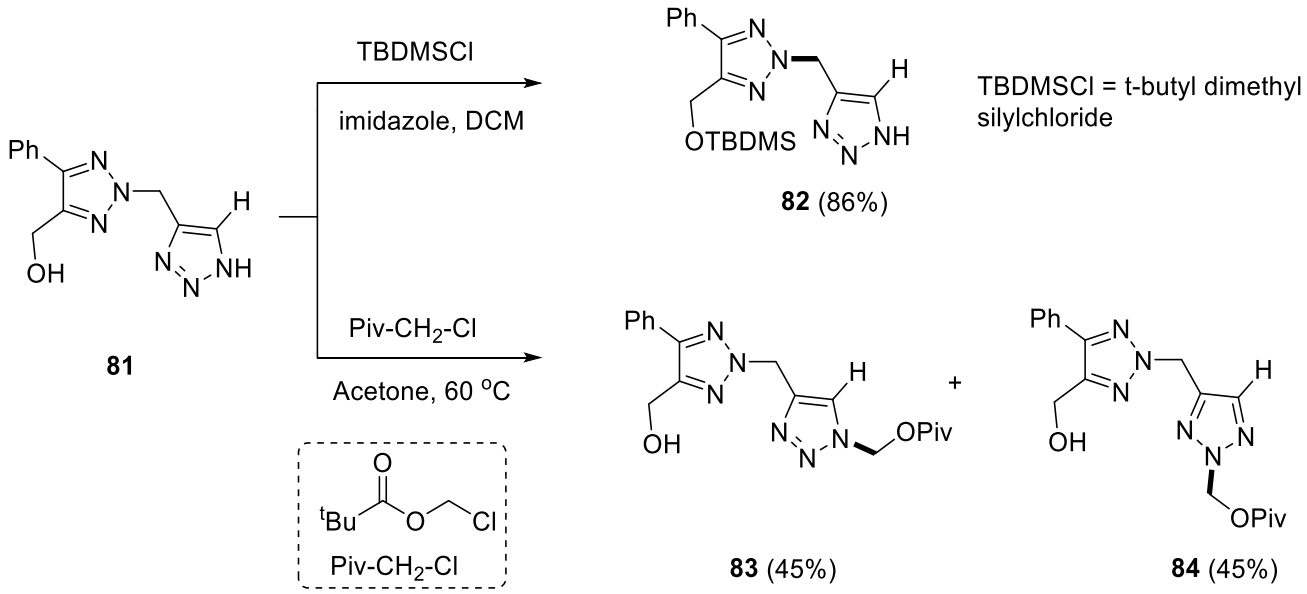

The protected forms of the dimer compounds **82** and **84** were subjected to Mitsunobu conditions[34] to link them together. The formation of two isomers was observed with an overall yield of 70%. Unexpectedly, the N-1 isomer **85,** was the major product based on ^{1}H NMR data. These isomers were separated by column chromatography and the N-2 isomer **86,** was used in further reactions.

Scheme 18. Coupling of **82** and **84** under Mitsunobu conditions.

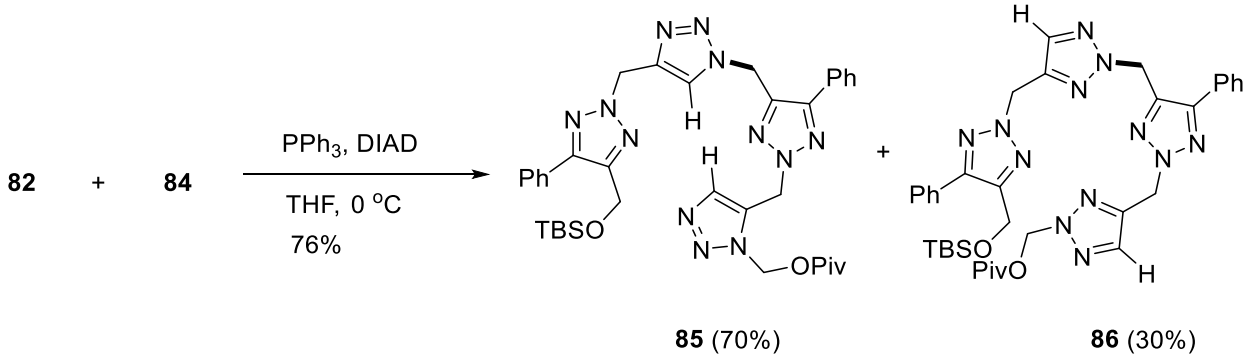

85 (70%) **86** (30%)

The N-2 isomer **86**, under the hydrolysis conditions[42] resulted in free hydroxy and NH groups with a yield of 60%. Unidentified products were also observed under these reaction conditions.

Scheme 19. Deprotection reactions of **86**.

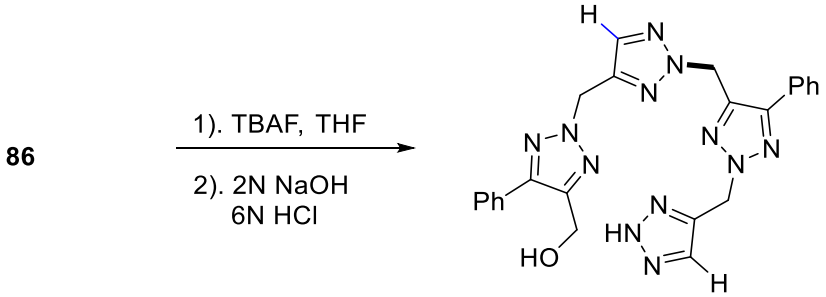

87 (60%)

Scheme 20. Cyclization of **87** by Mitsunobu reaction.

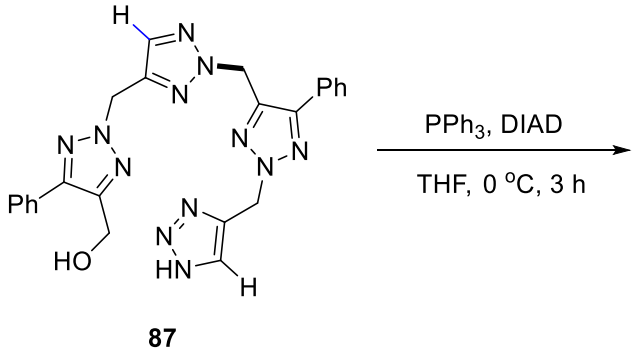

87

Cyclized product or straight chain

Figure 9

In view of the structure of **87**, there was a chance for the formation of cyclized product (**88, 89**) as well as a noncyclic octamer **90** (Figure 9)**.** We performed the crucial final cyclization by using a large amount of solvent since macrocyclization seemed to be the perfect condition for such intramolecular ring closure according to literature reports. To our delight, only two spots were observed by TLC. We are able to isolate only the bottom spot by column chromatography. The isolated compound was slightly soluble in organic solvents and the ^{1}H NMR spectrum is seen in Figure 10.

Figure 9. Possible products from macrocyclization (from Scheme 20).

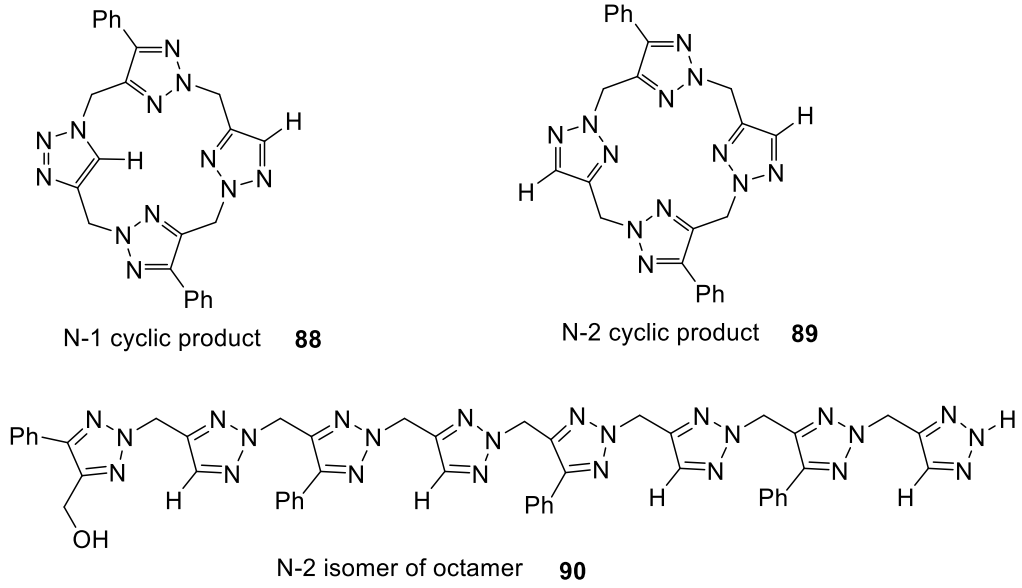

Figure 10. ^{1}H NMR spectrum of the isolated product.

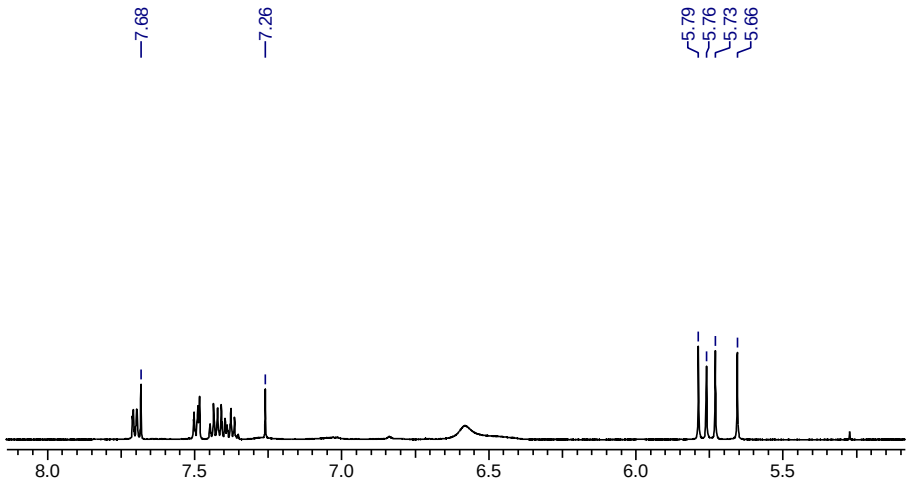

2.3 Results and discussion

Because there is a chance for octamer formation in the final step, we assumed that there would be free hydroxyl group on one side and NH group on the other side of the chain. As shown in Scheme 21, we treated the isolated product with TBDMSCl and pivaloylchloride separately. There was no reaction in both instances indicating the absence of free functional groups which excludes formation of the noncyclic octamer.

Scheme 21. Protection of the free functional groups of the noncyclic octamer.

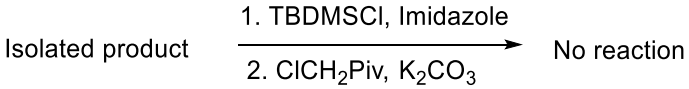

The ^{1}H NMR spectrum of the isolated product showed 4 CH_2 singlet peaks at δ 5.66-5.79 ppm. For the symmetric compound **89**, two sets of CH_2 singlets may be expected. However, 4 sets of CH_2 signals from proton NMR are consistent with the unsymmetrical nature of the product indicating the formation of **88** only. In order to prove that the isolated compound was a cyclic product, we performed NOE NMR experiment and the results are shown below.

Figure 11. NOE studies of the isolated product.

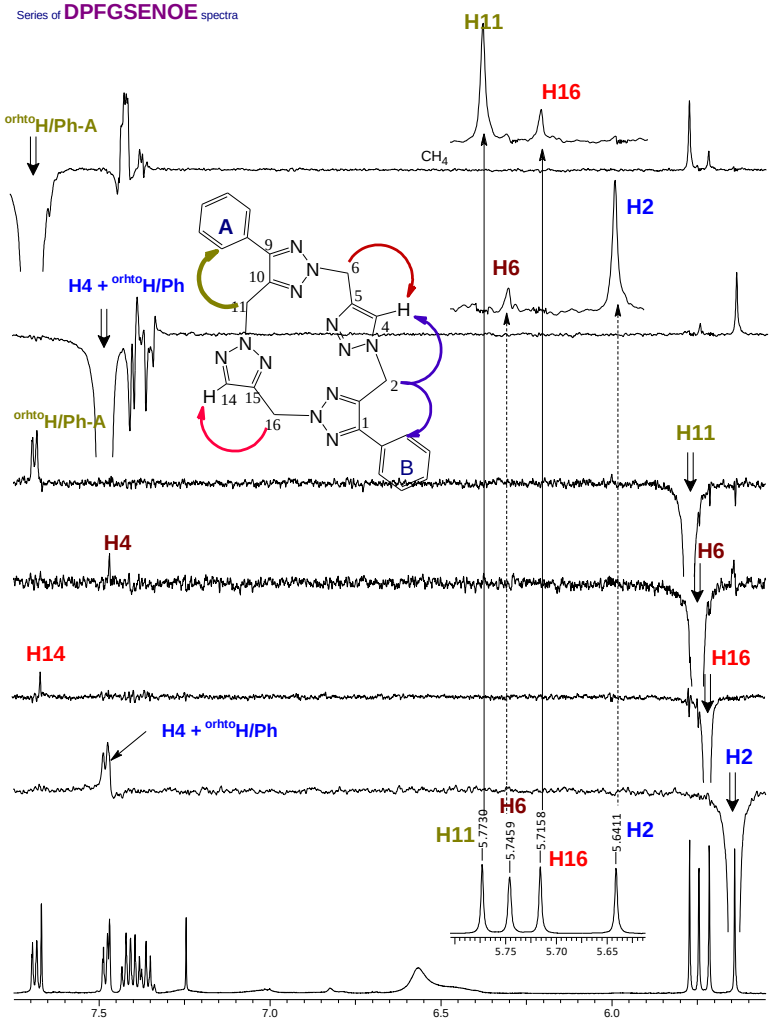

2.3.1 NOE results of the isolated product

As shown in Figures 11 and 12, in the cyclic structure of **88**, H6 (δ 5.76 ppm) and H16 (δ 5.73 ppm) have methylene protons that are opposite to each other and linked to a triazole ring with N-2 substitution. Selective decoupling of H6 shows a NOE only to H4 of the triazole. In the same manner, selective decoupling of H16 methylene protons has a NOE to H14 of another triazole. In these two positions the two methylene protons have similar environments and are not correlated with any phenyl ring protons since these are spatially far away to the phenyl group.

The remaining two methylene protons, H11 (δ 5.79 ppm) and H2 (δ 5.66 ppm) are opposite to each other. Selective excitation of the H11 methylene protons has a NOE only to the ortho hydrogens of the phenyl group (A). Interestingly, on the other hand selective excitation of H2 methylene protons shows a NOE to both H4 and the ortho hydrogens of phenyl group (B). In reality, the H2 methylene protons were expected to have a NOE only to the ortho hydrogens of phenyl group (B) similar to that of H11 if it was attached with the N-2 nitrogen atom. The extra NOE correlation for the H2 protons confirms that the ring closing took place with the N-1 nitrogen atom in the final cyclization reaction, leading to the loss of internal symmetry of the molecule.

2.3.2 Investigation of the major cyclized product

As evident from the NMR studies, 3 triazole rings of the major N-1 isomer were linked via the N-2 nitrogen atoms with one another but the fourth ring was linked by the N-1 atom. This was undesirable because it causes loss of symmetry of the entire ring which prevents a symmetrical binding of nitrogen atoms with metal ions.

As shown below in the Figure 12, Shi and co-workers previously reported that the N-1 nitrogen of a triazole[34] is usually high in electron density and is therefore is more basic than the N-2 nitrogen. The central N-2 nitrogen atom is sterically less hindered because there are no

substituents on its adjacent atoms and therefore kinetically favored. As a result, the highly stereosensitive Mitsunobu reactions could potentially favor the kinetic product which would in turn increase the N-2 selectivity.

Figure 12. Steric and electronic effects of the 1,2,3-triazoles.[43]

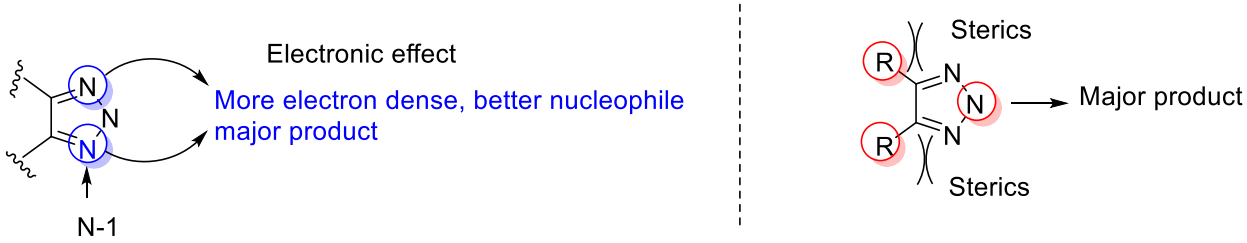

2.4 Designing 1,2,3-triazole version-2 porphyrin

In order to increase the N-2 selectivity in the final cyclization and to maintain the symmetry of the cyclized product, we hypothesized that introducing the phenyl group on the 4th position of the remaining two triazole rings would create sufficient steric hindrance to facilitate the formation of a symmetrical ring (Figure 13**)**.

Figure 13. Hypothesis for the formation of N-2 cyclized product.

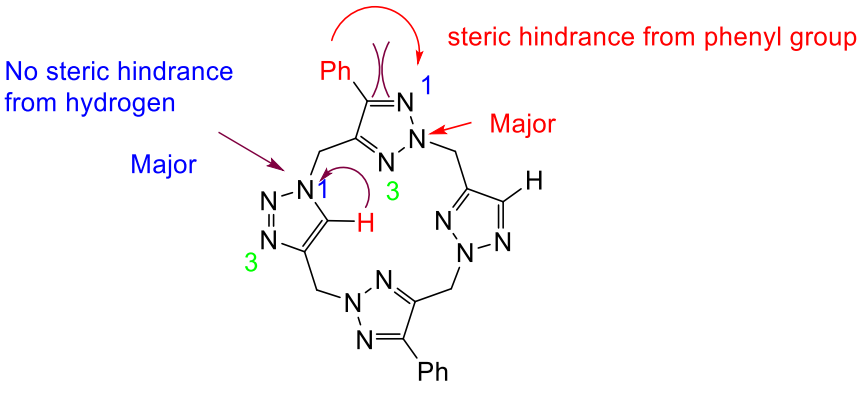

88

2.4.1 Attempted alternative synthesis of a 1,2,3-triazole analog of porphyrin

Scheme 22. Attempted Mitsunobu reaction.

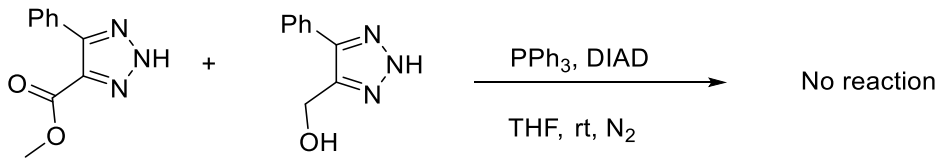

77 **91**

A Mitsunobu reaction[34] between **77** and **91** was unsuccessful even using excess of PPh_3 and DIAD reagents. Similar results were obtained in toluene as the solvent at 60 ^oC. Further investigation revealed that compound **91** was soluble only in methanol and water. It is also hygroscopic and melts at room temperature in an open container. We hypothesized that protection of hydroxyl and NH groups may increase the solubility in organic solvents, as mentioned earlier.

2.5 Synthetic Scheme for 1,2,3-triazole analog-2

Scheme 23. Protection of the alcohol with TBDMSCl.[41]

91 **92** (70%)

Scheme 24. Protection of the NH triazole and desilylation of the alcohol.[43]

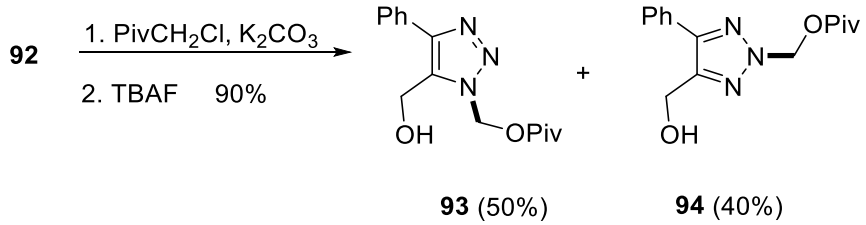

93 (50%) **94** (40%)

Scheme 25. Synthesis of dimer by Mitsunobu reaction.[34]

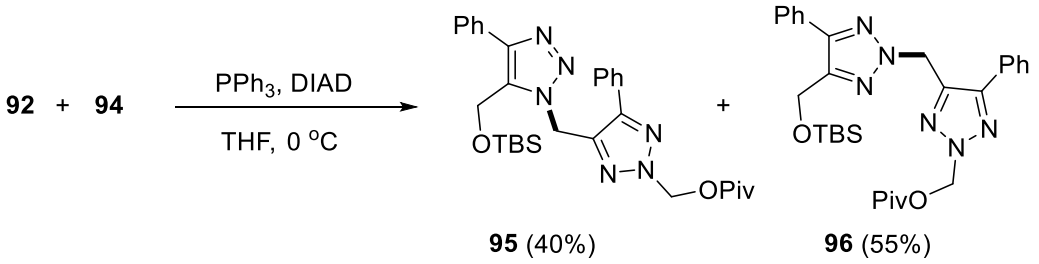

Scheme 26. Deprotection reactions of dimers and synthesis of tetramer by a Mitsunobu reaction.[42]

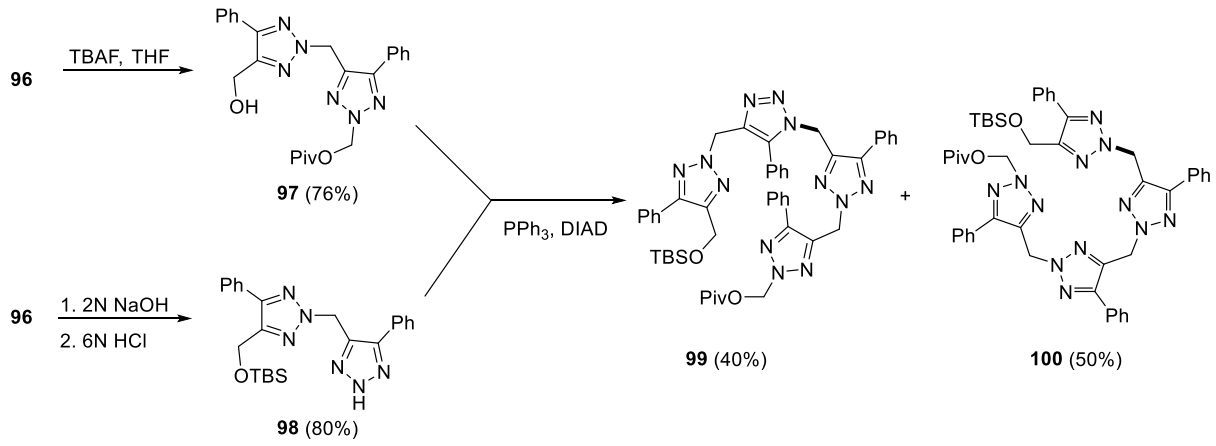

Scheme 27. Deprotection of tetramer

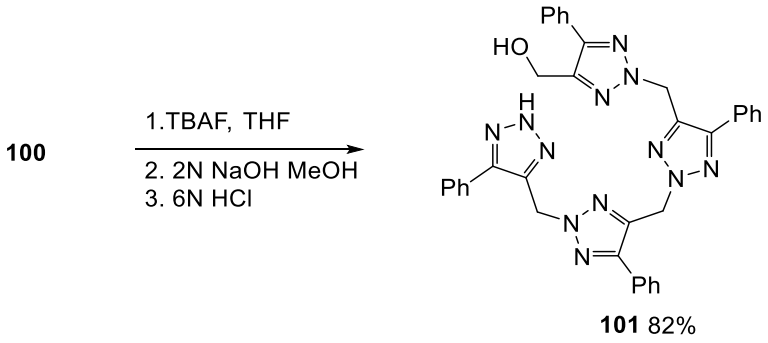

Scheme 28. Macrocyclization of tetramer **101**

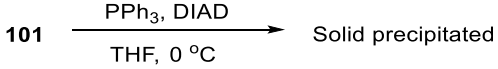

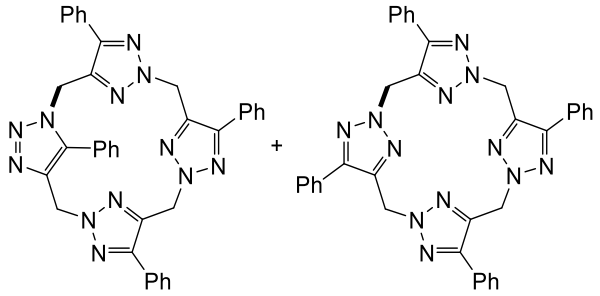

102 90% **103**

Initially, as shown in Scheme 23, compound **91** was suspended in dichloromethane followed by the addition of excess (2.5 eq) silyl chloride and imidazole reagents provided the silyl ether **92** as a yellow solid in 76% yield. After dividing compound **92** into two equal portions, one portion was treated with methylpivaloyl chloride to protect the NH group followed by desilylation of silyl ether to give **93** and **94** with the overall yield of 67%. Compound **94** and the remaining portion of **92** were mixed together and then subjected to similar conditions used for the synthesis of triazole analog-1 (compound **88**).

In the course of the final cyclization reaction, in contrast to other Mitsunobu reactions a white solid precipitated after the addition of DIAD. The solid was filtered off and the filtrate was analyzed by NMR. Surprisingly, neither starting materials nor the desired products were observed. Unfortunately, our attempts to characterize the products of cyclization reaction was unsuccessful because it was neither soluble in organic solvents nor in aqueous medium even at elevated temperatures (~120 ^{o}C).

2.6 Conclusion

Mimicking of the porphyrin with 1,2,3-triazole as building blocks was successful with both versions. In both cases the physical appearance of the final product was similar. However, in the earlier version N-1 isomer was the major product that was only slightly soluble in organic solvents, whereas in the second version, the final product does not show any degree of solubility in regular solvents.

References

1. (a) Ojima, I.; Tzamarioudaki, M.; Li, Z.; Donovan, R. J. *Chem. Rev.* **1996**, *96*, 635-662. (b) Tamaru, Y.; Kimura, M. *Synlett* **1997**, 749-757. (c) D'Souza, D. M.; Müller, T. J. J. *Chem. Soc. Rev***. 2007**, *36*, 1095-1108. (d) Ouchi, M.; Terashima, T.; Sawamoto, M. *Acc. Chem. Res.* **2008**, *41*, 1120-1132. (e) Díez-González, S.; Marion, N.; Nolan, S. P. *Chem. Rev.* **2009**, *109*, 3612-3676. (f) Zhong, C.; Shi, X. *Eur. J. Org. Chem.* **2010**, 2999-3025. (g) Dobereiner, G. E.; Crabtree, R. H. *Chem. Rev.* **2010**, *110*, 681-703.
2. (a) Schläfer, H. L.; Gliemann, G. *Basic Principles of Ligand Field Theory*, Wiley Interscience: New York, 1969. (b) Pearson, A. J. *Metallo-organic Chemistry*, Wiley, 1985. (c) Crabtree, R. H. *The Organometallic Chemistry of the Transition Metals*, 2nd ed.; Wiley, New York, 1994. (d) Spessard, G. O.; Miessler, G. L. *Organometallic Chemistry*, Prentice Hall, NJ, 1997.
3. Fu, G. C. *Acc. Chem. Res***. 2006**, *39*, 853-860.
4. (a) Gorin, D. J.; Sherry, B. D.; Toste, F. D. *Chem. Rev.* **2008**, *108*, 3351-3378. (b) Würtz, S.; Glorius, F. *Acc. Chem. Res.* **2008**, *41*, 1523-1533. (c) Daugulis, O.; Do, H. Q.; Shabashov, D. *Acc. Chem. Res.* **2009**, *42*, 1074-1086. (d) Shao, Z. H.; Zhang, H. B. *Chem. Soc. Rev.* **2009**, *38*, 2745-2755. (e) Teichert, J. F.; Feringa, B. L. *Angew. Chem. Int. Ed.* **2010**, *49*, 2486-2528. (f) van Leeuwen, W. N. M.; Kamer, P. C. J.; Claver, C.; Pamies, O.; Dieguez, M. *Chem. Rev.*,

2011, *111*, 2077-2118.

5. (a) Gomez Arrayas, R.; Adrio, J.; Carretero, J. C. *Angew. Chem. Int. Ed.* **2006**, *45*, 7674-7715. (b) Leuthäusser, S.; Schwarz, D.; Plenio, H. *Chem. Eur. J.* **2007**, *13*, 7195-7203. (c) Mellah, M.; Voituriez, A.; Schulz, E. *Chem. Rev*, **2007**, *107*, 5133-5209. (d) Hargaden, G. C.; Patrick, J. G. *Chem. Rev*, **2009**, *109*, 2505-2550. (e) Rasika Dias, H. V.; Lovely, C. J. *Chem. Rev.* **2008,** *108*, 3223-3238. (f) Nolan, S. P. *Acc. Chem. Res.* **2011**, *44*, 91-100.
6. (a) Pfaltz, A.; Drury, W. J. *Proc. Natl. Acad. Sci. U.S.A.* **2004**, *101*, 5723-5726. (b) Ohkuma, T.; Kitamura, M.; Noyori, R. *New Front. Asymmetric Catal.* **2007**, 1-32. (c) Lundgren, R. J.; Hesp, K. D.; Stradiotto, M. *Synlett* **2011**, 17, 2443-2458. (d) Weller, A. *Nat. Chem.* **2011**, *3*, 577-578. (d) Jin, S. S.; Wang, H.; Xu, M. H. *Chem. Commun.* **2011**, *47*, 7230-7232.
7. (a) Noyori, R.; Takaya, H. *Acc. Chem. Res.* **1990**, *23*, 345-350. (b) Kocovsky, P.; Vyskocil, S.; Smrcina, M. *Chem. Rev.* **2003,** *103*, 3213-3245. (c) Berthod, M.; Mignani, G.; Woodward, G.; Lemaire, M. *Chem. Rev.* **2005,** *105*, 1801-1836. (d) Tanaka, K. *Synlett* **2007**, *13*, 1977-1993. (e) Shimizu, H.; Nagasaki, I.; Matsumura, K.; Sayo, N.; Saito, T. *Acc. Chem. Res.* **2007**, *40*, 1385-1393. (f) Arshad, N.; Kappe, C. O. *Adv. Heterocycl. Chem.* **2010**, *99*, 33-59.
8. (a) Basak, R. *Synlett* **2003**, *8*, 1223-1224. (b) Sun, Z. K.; Yu, S. Y.; Ding, Z. D. Ma, D. W. *J. Am. Chem. Soc.* **2007**, *129*, 9300-9301. (c) Füerstner, A.; Schlecker, A. *Chem. Eur. J.* **2008**, *14*, 9181-9191. (d) Shu, W.; Ma, SS. M. *Chem. Commun.* **2009**, *41*, 6198-6200. (e) Poisson, T.; Yamashita, Y.; Kobayashi, S. *J. Am. Chem. Soc.* **2010**, *132*, 7890-7892. (f) Nakanishi, M.; Minard, C.; Retailleau, P.; Cariou, K.; Dodd, R. H. *Org. Lett.* **2011**, *13*, 5792-5795.
9. (a) Aikawa, K.; Akutagawa, S.; Mikami, K. *J. Am. Chem. Soc.* **2006**, *128*, 12648-12649. (b) Scriban, C.; Glueck, D. S. *J. Am. Chem. Soc.* **2006**, *128*, 2788-2789. (c) Cote, A.; Lindsay, V. N. G.; Charette, A. B. *Org. lett.* **2007**, 9, 85-87. (d) Shaikh, N. S.; Enthaler, S.; Junge, K.;

Beller, M. *Angew. Chem. Int. Ed.* **2008**, 47, 2497-2501. (e) Kanai, M.; Wada, R.; Shibuguchi, T.; Shibasaki, M. *Pure Appl. Chem.* **2008**, *80*, 1055-1062. (f) Campian, M. V.; Perutz, R. N.; Procacci, B.; Thatcher, R. J.; Torres, O.; Whitwood, A. C. *J. Am. Chem. Soc.* **2012**, *134*, 3480-3497.

10. (a) Moteki, S. A.; Wu, D.; Chandra, K. L.; Reddy, D. S.; Takacs, J. M. *Org. Lett.* **2006**, *8*, 3097-3100. (b) Robert, T.; Velder, J.; Schmalz, H. G. *Angew. Chem. Int. Ed.* **2008**, 47, 7718-7721. (c) Anderson, C. D.; Dudding, T.; Gordillo, R.; Houk, K. N. *Org. Lett.* **2008**, *10*, 2749-2752. (d) Teller, H.; Fluegge, S.; Goddard, R.; Füerstner, A. *Angew. Chem. Int. Ed.* **2010**, 49, 1949-1953. (e) Lam, H. W. *Synthesis* **2011**, *13*, 2011-2043. (f) Naeemi, Q.; Dindaroglu, M.; Kranz, D. P.; Velder, J.; Schmalz, H. G. *Eur. J. Org. Chem.* **2012**, 1179-1185.
11. (a) Jacobsen, E. N. *Acc. Chem. Res.* **2000**, *33*, 421-431. (b) Clever, G. H.; Soeltl, Y.; Burks, H.; Spahl, W.; Carell, T. *Chem. Eur. J.* **2006**, *12*, 8708-8718. (c) Kemper, S.; Hrobarik, P.; Kaupp, M.; Schlorer, N. E. *J. Am. Chem. Soc.* **2009**, *131*, 4172-4173. (d) Brown, M. K.; Blewett, M. M.; Colombe, J. R.; Corey, E. J. *J. Am. Chem. Soc.* **2010**, *132*, 11165-11170. (e) Clegg, W.; Harrington, R. W.; North, M.; Pasquale, R. *Chem. Eur. J.* **2010**, *16*, 6828-6843. (f) Kurahashi, T.; Fujii, H. *J. Am. Chem. Soc.* **2011**, *133*, 8307-8316.
12. Ivanov, A. S.; Boldyrev, A. I., *Org. & Bio. Che.* **2014,** *12* (32), 6145-6150.
13. Rothemund, P., *J. Am. Che. Society* **1935,** *57*, 2010-2011.
14. Rothemund, P., A new porphyrin synthesis. The synthesis of porphin. *J. Am. Chem. Soc.* **1936,** *58*, 625-627.
15. Sze But, T. Y.; Toy, P. H., *J. Am. Che. Soc.* **2006,** *128* (30), 9636-9637.
16. Zhang, B.; Lash, T. D., *Tet. Letts* **2003,** *44* (39), 7253-7256. b) Zucca, P.; Rescigno, A.; Rinaldi, A. C.; Sanjust, E., *J. Mol Cat.* **2014,** *388*, 2-34.

17. Huisgen, R. *Proc. Chem. Soc.* **1961**, 357-396. (b) Huisgen, R. Wiley, New York, **1984**, pp. 1-176. (c) Padwa, A. *Comp. Org. Syn*, Vol. 4 (Ed.: Trost, B. M.), Pergamon, Oxford, **1991**, pp. 1069-1109. (d) Gothelf, K. V.; Jorgensen, K. A. *Chem. Rev*. **1998**, *98*, 863-909. (e) Mulzer, J. *Org. Synth. Highlights* **1991**, 77-95.

18. (a) Nakamura, T.; Terashima, T.; Ogata, K.; Fukuzawa, S. *Org. Lett.* **2011**, *13*, 620-623. (b) Spiteri, C.; Moses, J. E. *Angew. Chem. Int. Ed.* **2010**, *49*, 31-33. (c) Kappe, C. O.; Van der Eycken, E. *Chem. Soc. Rev.* **2010**, *39*, 1280-1290. (d) Am-blard, F.; Cho, J. H.; Schinazi, R. F. *Chem. Rev.* **2009**, *109*, 4207-4220. (e) Shi, F.; Waldo, J. P.; Chen, Y.; Larock, R. C. *Org. Lett.* **2008**, *10*, 2409-2412. (f) Moses, J. E.; Moorhouse, A. D. *Chem. Soc. Rev.* **2007**, *36*, 1249-1262.

19. Moorhouse, A. D.; Santos, A. M.; Gunaratnam, M.; Moore, M.; Neidle, S.; Moses, J. E. *J. Am. Chem. Soc.* **2006**, *128*, 15972-15973 (b) Kumar, R.; El-Sagheer, A.; Tumpane, J.; Lincoln, P.; Wilhelmsson, L. M.; Brown, T. *J. Am. Chem. Soc.* **2007**, *129*, 6859-6864. (c) Mamidyala, S. K.; Finn, M. G. *Chem. Soc. Rev.* **2010**, *39*, 1252-1261. (d) Waengler, C.; Maschauer, S.; Prante, O.; Schaefer, M.; Schirrmacher, R.; Bartenstein, P.; Eisenhut, M.; Waengler, B. *Chembiochem* **2010**, *11*, 2168-2181. (e) Sharma, A.; Neibert, K.; Sharma, R.; Hourani, R.; Maysinger, D.; Kakkar, A. *Macromolecules* **2011**, *44*, 521-529.

20. (a) Whiting, M.; Muldoon, J.; Lin, Y. C.; Silverman, S. M.; Lindstrom, W.; Olson, A. J.; Kolb, H. C.; Finn, M. G.; Sharpless, K. B.; Elder, J. H.; Fokin, V. V. *Angew. Chem. Int. Ed.* **2006**, *45*, 1435-1439. (b) Moorhouse, A. D.; Moses, J. E. *Chemmedchem* **2008**, *3*, 715-723. (c) Tron, G. C.; Pirali, T.; Billington, R. A.; Canonico, P. L.; Sorba, G.; Genazzani, A. A. *Med. Res. Rev.* **2008**, *28*, 278-308. (d) 134 Gracia, S. R.; Gaus, K.; Sewald, N. *Future Med. Chem.* **2009**, *1*, 1289-1310. (e) Willand, N.; Desroses, M.; Toto, P.; Dirie, B.; Lens, Z.; Villeret, V.; Rucktooa,

P.; Locht, C.; Baulard, A.; Deprez, B. *ACS Chem. Biol.* **2010**, *5*, 1007-1013.

21. Sengupta, S.; Duan, H. F.; Lu, W. B.; Petersen, J. L.; Shi, X. D. *Org. Lett.* **2008**, *10*, 1493-1496.

22. Himo, F.; Lovell, T.; Hilgraf, R.; Rostovtsev, V. V.; Noodleman, L.; Sharpless, K. B.; Fokin, V. V. *J. Am. Chem. Soc.* **2005**, *127*: 210-216.

23.) Parenty, A.; Moreau, X.; Campagne, J. M. *Chem. Rev.* **2006**, *106*, 911-939.

24. (a) Mitsunobu, O.;Yamada, M. *Bull. Chem. Soc. Jpn.* **1967**, *40*, 2380-2382. (b) Mitsunobu, O.; Yamada, M.; Mukaiyama, T. *Bull. Chem. Soc. Jpn.* **1967**, *40*, 935-939. (c) Mitsunobu, O.; Kato, K.; Tomari, M. *Tetrahedron* **1970**, *26*, 5731-5736. (d) Mitsunobu, O.; Kimura, J.; Fujisawa, Y. *Bull. Chem. Soc. Jpn.* **1972**, *45*, 245-247. (e) Mitsunobu, O.; Wada, M.; Sano, T. *J. Am. Chem. Soc.* **1972**, *94*, 679-680. (f) Kurihara, T.; Nakajima, Y.; Mitsunobu, O. *Tet. Lett.* **1976**, *17*, 2455-2458. (g) Mitsunobu, O.; Kimura, J.; Iiizumi, K.; Yanagida, N. *Bull. Chem. Soc. Jpn.* **1976**, *49*, 510-513.

25. (a) Mitsunobu, O. *Synthesis* **1981**, *1*, 1-28. (b) Hughes, D. L. *Org. React.* **1992**, *42*, 335-656. (c) Lawrence, S. *PharmaChem* **2002**, *1*, 12-14. (d) Valentine, D. H. Jr.; Hillhouse, J. H. *Synthesis* **2003**, 317-334. (e) Dembinski, R. *Eur. J. Org. Chem.* **2004**, 2763-2772. (f) Dandapani, S.; Curran, D. P. *Chem. Eur. J.* **2004**, *10*, 3130-3138. (g) Parenty, A.; Moreau, X.; Campagne, J. M. *Chem. Rev.* **2006**, *106*, 911-939. (h) But, T. Y. S.; Toy, P. H. *Chem. Asian J.* **2007**, *2*, 1340-1355. (i) Kumara Swamy, K. C.; Bhuvan Kumar, N. N.; Balaraman, E.; Pavan Kumar, K. V. P. *Chem. Rev.* **2009**, *109*, 2551-2651.

26. (a) Wu, Y.; Esser, L.; De Brabander, J. K. *Angew. Chem. Int. Ed.* **2000**, *39*, 4308-4310. (b) Pungente, M. D.; Weiler, L. *Org. Lett.* **2001**, *3*, 643-646. (c) Wang, Y.; Janjic, J.; Kozmin, S. A. *J. Am. Chem. Soc.* **2002**, *124*, 13670-13671. (d) Grab, T.; Braese, S. *Adv. Synth. Catal.*

2005, *347*, 1765-1768. (e) Shirokawa, S. I.; 146 Shinoyama, M.; Ooi, I.; Hosokawa, S.; Nakazaki, A.; Kobayashi, S. *Org. Lett.* **2007**, *9*, 849-852. (f) Huang, J.; Wu, C.; Wulff, W. D. *J. Am. Chem. Soc.* **2007**, *129*, 13366-13367. (g) Deng, L.; Ma, Z.; Zhao, G. *Synlett* **2008**, 728-732.

27. (a) Koide, K.; Finkelstein, J. M.; Ball, Z.; Verdine, G. L. *J. Am. Chem. Soc.* **2001**, *123*, 398-408. (b) Kurosawa, W.; Kan, T.; Fukuyama, T. *J. Am. Chem. Soc.* **2003**, *125*, 8112-8113. (c) Yoon, U. C.; Kwon, H. C.; Hyung, T. G.; Choi, K. H.; Oh, S. W.; Yang, S.; Zhao, Z.; Mariano, P. S. *J. Am. Chem. Soc.* **2004**, *126*, 1110-1124. (d) Morita, N.; Krause, N. *Eur. J. Org. Chem.* **2006**, 4634-4641. (e) Wang, Y. G.; Takeyama, R.; Kobayashi, Y. *Angew. Chem. Int. Ed.* **2006**, *45*, 3320-3323. (f) Sakamoto, I.; Izumi, N.; Yamada, T.; Tsunoda, T. *Org. Lett.* **2006**, *8*, 71-74.

28. (a) Dong, L.; Roosenberg, J. M.; Miller, M. J. *J. Am. Chem. Soc.* **2002**, *124*, 15001-15005. (b) Chen, J.; Forsyth, C. J. *J. Am. Chem. Soc.* **2003**, *125*, 8734-8735. (c) Mergott, D. J.; Frank, S. A.; Roush, W. R. *Proc. Natl. Acad. Sci. U.S.A.* **2004**, *101*, 11955-11959. (d) Gagnon, D.; Lauzon, S.; Godbout, C.; Spino, C. *Org. Lett.* **2005**, *7*, 4769-4771. (e) Cohen, F.; Overman, L. E., *J. Am. Chem. Soc.* **2006**, *128*, 2594-2603. (f) Klepper, F.; Jahn, E. M.; Hickmann, V.; Carell, T. *Angew. Chem. Int. Ed.* **2007**, *46*, 2325-2327.

29. (a) Kemmler, M.; Bach, T. *Angew. Chem. Int. Ed.* **2003**, *42*, 4824-4826. (b) Krishnan, S.; Schreiber, S. L. *Org. Lett.* **2004**, *6*, 4021-4024. (c) Hodgetts, K. J. 147 *Tetrahedron* **2005**, *61*, 6860-6870. (d) Goundry, W. R. F.; Lee, V.; Baldwin, J. E. *Syn. Let.* **2006**, 2407-2410. (e) Jackson, T.; Woo, L. W. L.; Trusselle, M. N.; Chander, S. K.; Purohit, A.; Reed, M. J.; Potter, B. V. L. *Org. Biomol. Chem.* **2007**, *5*, 2940-2952.

30. (a) Aesa, M. C.; Baán, G.; Novák, L.; Szántay, C. *Synth. Commun.***1996**, *26*, 909-914. (b)

Tsunoda, T.; Uemoto, K.; Nagino, C.; Kawamura, M.; Kaku, H.; Ito, S. *Tetrahedron Lett.* **1999**, *40*, 7355-7358. (c) Bussiere, A.; Barragan-Montero, V.; Clavel, C.; Toupet, L.; Montero, J. L. *Lett. Org. Chem.* **2006**, *3*, 654-657. (d) Uchida, K.; Yokoshima, S.; Kan, T.; Fukuyama, T. *Org. Lett.* **2006**, *8*, 5311-5313. (e) Ghosh, A. K.; Moon, D. K. *Org. Lett.* **2007**, *9*, 2425-2427.

31. (a) Chaturvedi, D.; Ray, S. *Tetrahedron Lett.* **2006**, *47*, 1307-1309. (b) Chaturvedi, D.; Mishra, N.; Mishra, V. *Monatsh. Chem.* **2007**, *138*, 57-60. (c) Chaturvedi, D.; Mishra, N.; Mishra, V. *Syn.* **2008**, 355-357.
32. (a) McNulty, J.; Capretta, A.; Laritchev, V.; Dyck, J.; Robertson, A. J. *Angew. Chem. Int. Ed.* **2003**, *42*, 4051-4054. (b) Schenk, S.; Weston, J.; Anders, E. *J. Am. Chem. Soc.* **2005**, *127*, 12566-12576. (c) Kumara Swamy, K. C.; Praveen Kumar, K.; Bhuvan Kumar, N. N. *J. Org. Chem.* **2006**, *71*, 1002-1008. (d) Fitzjarrald, V. P.; Pongdee, R. *Tet. Lett.* **2007**, *48*, 3553-3557.
33. Tsunoda, T.; Nagino, C.; Oguri, M.; Ito, S., *Tet Lett*. ***1996***, *37 (14),* 2459-2462.
34. Yan, W.; Liao, T.; Tuguldur, O.; Zhong, C.; Petersen, J. L.; Shi, X. *Chem. Asian. J.* **2011**, *6*, 2720-2724.
35. Giedyk, M.; Goliszewska, K.; Proinsias, K. O.; Gryko, D., *Chem. Comm.* **2016,** *52* (7), 1389-1392.
36. Reddy, A. R.; Hao, F.; Wu, K.; Zhou, C.-Y.; Che, C.-M., *Angew. Chem., Int. Ed*. **2016,** *55* (5), 1810-1815.
37. Subbarayan, V.; Jin, L.-M.; Cui, X.; Zhang, X. P., *Tet. Lett.* **2015,** *56* (23), 3431-3434.
38. Marti-Centelles, V.; Pandey, M. D.; Isabel Burguete, M.; Luis, S. V., *Chem. Rev.* **2015,** *115* (16), 8736-8834.

39. Goyard, D.; Docsa, T.; Gergely, P.; Praly, J.-P.; Vidal, S., *Carb. Res.* **2015,** *402*, 245-251.

40. Xu, M.; Kuang, C.; Wang, Z.; Yang, Q.; Jiang, Y., *Synthesis-Stuttgart* **2011,** (2), 223-228.

41. Azumaya, I.; Uchida, D.; Kato, T.; Yokoyama, A.; Tanatani, A.; Takayanagi, H.;

42. Fouquet, T.; Fetzer, L.; Mertz, G.; Puchot, L.; Verge, P., *Rsc Advances* **2015,** *5* (68), 54899

43. Chen, Y.; Liu, Y.; Petersen, J. L.; Shi, X. *Chem. Commun.* **2008**, 3254-3256.

44. Lingamurthy, M.; Jagadeesh, Y.; Ramakrishna, K.; Rao, B. V., *J. Org. Chem.* **2016,** *81* (4), 1367-1377.

Chapter 3 Triazole as part of a pincer ligand, its complexations

3.1 Introduction

3.1.1 General introduction to pincer ligands and their metal complexes

Pincer ligands are in general uninegative, tridentate, 6-electron donor ligands that enforce meridional coordination geometry on the metal center (Figure 14). Ever since the first report of a pincer complex in the late 1970's,[1] there continues to be extensive interest in these complexes because of their desirable robust nature, generally simple synthesis and the remarkable transformations that they can mediate.[2] Due to their extraordinary thermal stability pincer complexes have been used in homogenous catalysis. Typically, the pincer complexes coordinate to the metal ion as the $[XYZ]^-$ form, where Y is the central atom, anchoring Lewis donor while X and Z are flanking Lewis donors. Most pincer ligands contain phosphines. At positions X and Z reactions of metal pincer complexes are localized at three site perpendicular to the plane of the pincer ligand.[3] Early examples of pincer ligands were anionic with a carbanion as the central donor site and flanking phosphine donors and are referred to as a PCP pincer.

Figure 14. Pincer ligand general structure.

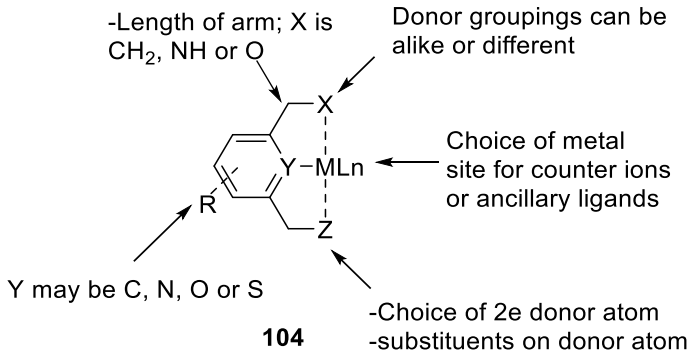

3.1.2 Introduction to P, N ligands

In 2010, Straditto and his group reported a structurally simple and air-stable P,N-ligand system.[4] The chelating mixed-donor P,N-ligands (Figure 15) are poised to exhibit hemi-labile behavior when coordinated to metal atoms. Phosphorous being a softer donor, serves to anchor the ligand to the metal, and the harder N-donor temporarily occupying a metal coordination site in the absence of substrate molecule. The P,N-ligand systems are useful in cross-couplings of aryl and heteroaryl chlorides to a diverse range of amine and related substrates,[5] including primary alkyl and aryl amines with low catalyst loadings and excellent functional group tolerance and chemoselectivity.

Figure 15. Bidentate P,N – ligand general structures.

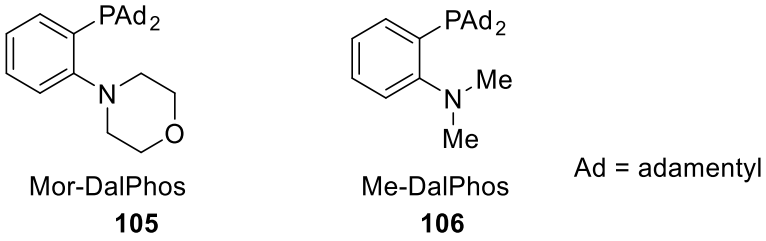

Mor-DalPhos **105**

Me-DalPhos **106**

3.1.3 1,2,3-Triazole as a ligand in transition metal catalysis

In 2007, Koten, Gebbink and co-workers[6] reported the first examples of 1,4-disubstituted 1,2,3-triazoles as monodentate Lewis-basic ligands for cationic Pd- and Pt-pincer complexes as indicated by the crystal structure, depicted in Scheme 29. The 1,2,3-triazole coordinated metal complexes were prepared by the addition of the triazole to the corresponding pincer Pd and Pt cations, which were generated in situ upon reaction of the bromide derivative **67**, with $AgBF_4$. The four coordinate M(II) ion displays a distorted square-planar ligand environment by virtue of the donor atoms of the tridentate pincer ligand and the N-3 nitrogen donor of the triazole.

Scheme 29. Example of a 1,2,3-triazole as a monodentate Lewis-basic ligand for a cationic Pt-pincer complexes.

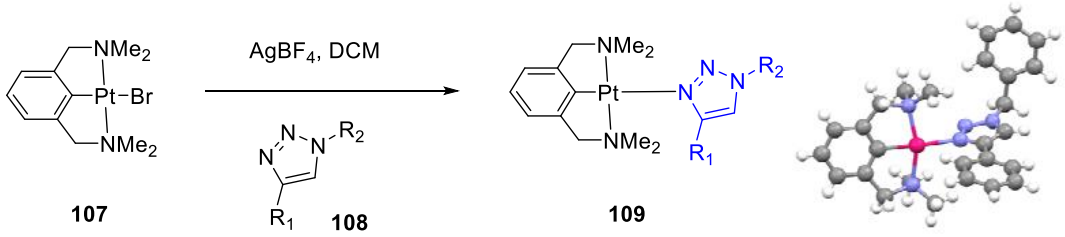

3.1.4 1,2,3-*NH*-Triazoles as anionic ligands.[7]

Compared to N-substituted triazoles, the NH-triazoles provide acidic N-H protons since the pKa of the NH of the triazole is ~10. Therefore, the acidic proton can easily be removed using a mild base. The negative charge evenly distributed on the ring can be applied as anionic ligands with multiple binding sites. Based on the literature reports, all efforts regarding triazole as an anionic ligand have only focused on benzotriazole.

3.2 Our group achievements with 1,2,3-triazole as ligand

Shi and his co-workers[55] have reported the synthesis and structural characterization of Rh(I) complexes featuring 4,5-disubstituted triazoles as an anionic ligand. To the best of our knowledge these are the first reported examples of X-ray structures of NH-triazoles-bound transition metal complexes. The complexes showed effective catalytic reactivity in Pauson-Khand reactions in excellent yield (~90%).

Scheme 30. First example of NH triazole as a bridging ligand with rhodium metal[55]

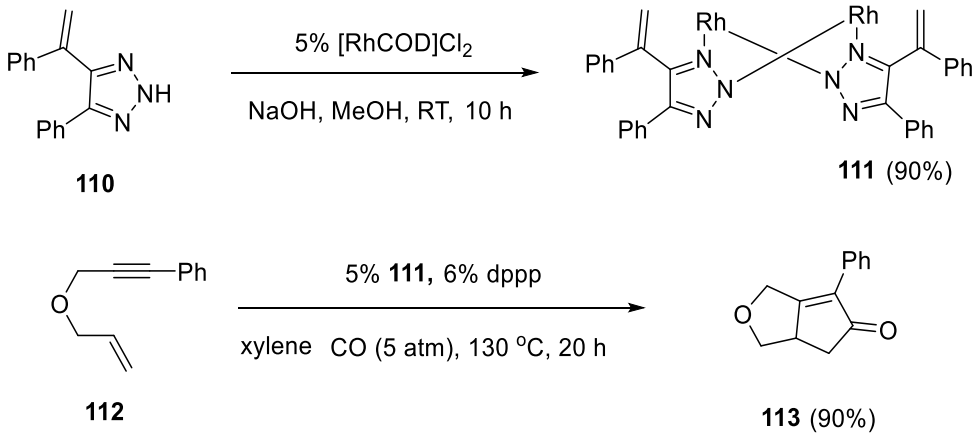

3.3 Research and design of the ligand

Push Pull system. The idea behind developing the P,N,N ligand system **114** shown in Figure 16, is to explore the triazole as a potential ligand for the coordination with transition metals. In general, the **t**riazole molecule is an electron deficient aromatic heterocycle with sigma donor and π acceptor abilities. It binds to metal atoms tightly with its strong π-backbonding nature. Usually electron deficient ligands such as triazoles are known to stabilize the low valent metal complexes in their low oxidation states. In addition, the phosphorous atom of the proposed structure **114** also donates electrons to the metal center. The anionic nitrogen[9] of **114** which is trans to the reactive site will play a crucial role in enhancing the reactivity of the metal by the trans effect, the lone pair of nitrogen atom can also occupy metal coordination site temporarily in the absence of substrate molecule.

Figure 16. Proposed ligand system.

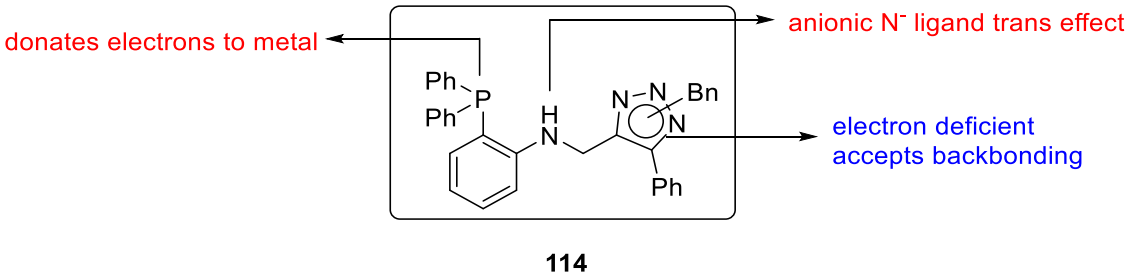

114

3.4 Synthesis of triazole containing pincer ligands

The P,N,N ligands **120** and **122** was synthesized following Scheme 31, Scheme 32, and Scheme 33 below. Initially, triazole **115** was treated with benzyl bromide to give the N-1 **(116)** and N-2 **(117)** protected triazole isomers in equal ratio with an overall yield of 80%. The isomers were successfully separated by chromatography and treated with compound **118**. The separate condensation reaction[10] of **116** and **117** with **118** resulted in an imine initially. This very stable compound which was further treated with sodium borohydride in MeOH:THF solvent system to give amines **119** and **121,** respectively. The resulting amines were recrystallized from methanol to give pure products. The iodides **119** and **121** were then converted to the corresponding phosphines **120** and **122** using Buchwald's phosphination procedure separately.[11] The N-1 protected isomer was a brown syrup whereas N-2 protected isomer was a white solid. Both are stable at room temperatures. The ^{31}P spectra of **122** displayed a singlet at δ -21.97 ppm.

Scheme 31. Synthesis of the N-protected triazole **116**, **117**.

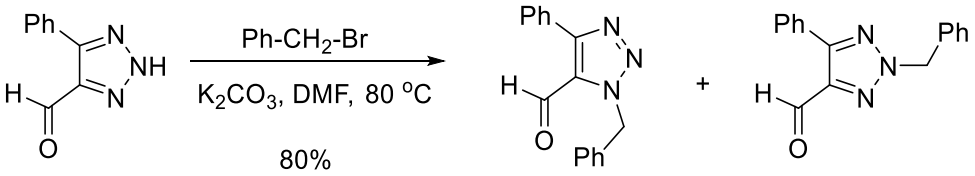

115 **116** (40%) **117** (40%)

Scheme 32. Synthesis of tridentate ligand **120**.

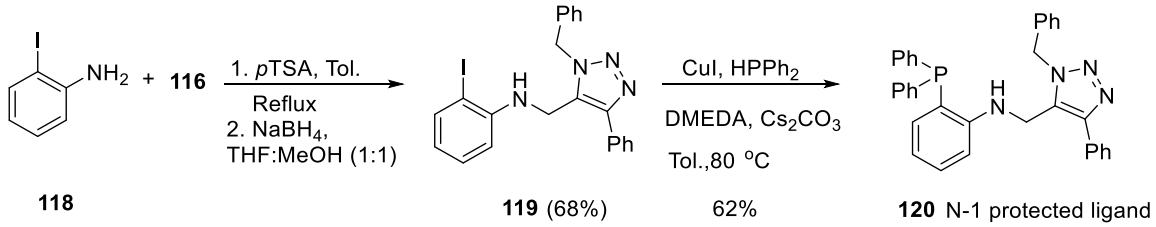

Scheme 33. Synthesis of tridentate ligand **122**.

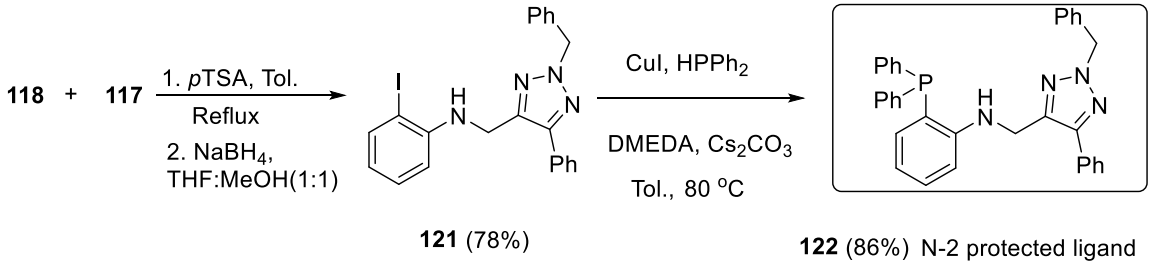

Figure 17. $^{31}P\ \{^{1}H\}$ NMR of **122**.

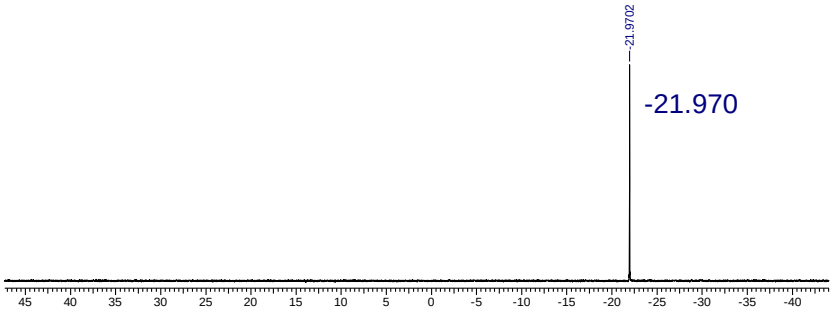

3.5 Crystal Structure

Figure 18. Crystal structure of the ligand **122**.

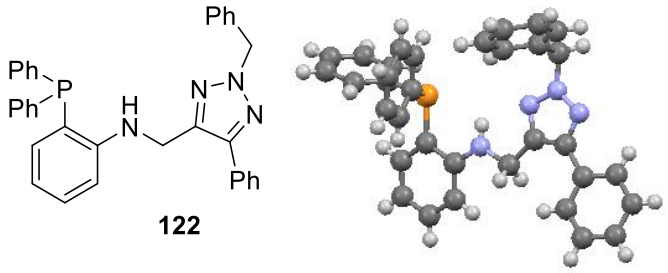

Crystal structure of the ligand with hydrogen atoms. The NH of the ligand is facing towards center of the ligand.

Crystals of **122** were grown from the pure fractions obtained after column chromatography of the phosphination product. The X-ray crystal structure of compound **122** verified that the NH group resides between the phosphorous and nitrogen of the triazole as expected. With the desired ligand in hand we attempted complexation with metals.

3.6 Complexation of the ligands 120 and 122

Scheme 34. Complexation with Ni^{+2} of **120**.

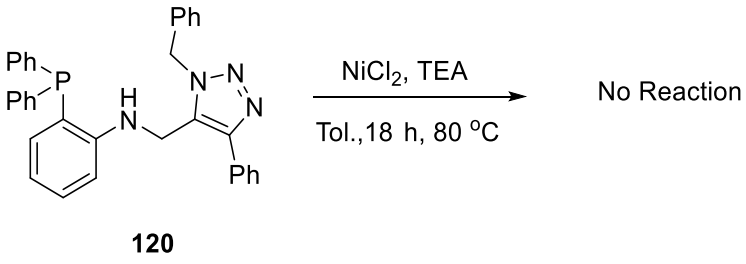

Scheme 35. Complexation with Ni^{+2} with ligand **122**.

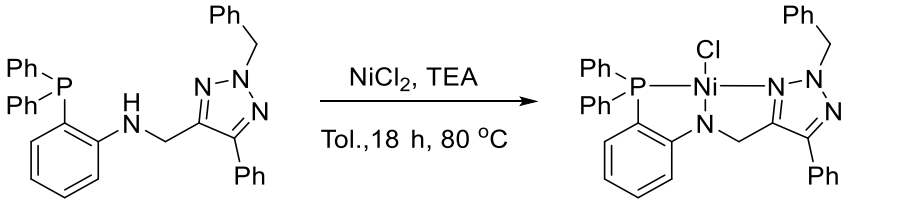

The four-coordinate nickel (II) complex **123** was prepared based on Guan's procedure.[12] Ligand **122**, when treated with nickel chloride in the presence of trimethylamine in toluene afforded a nickel complex with a dark green color. An attempt to synthesize the nickel complex of the N-1 ligand **120** was unsuccessful. This might be due to the steric hindrance from the benzyl group facing towards the amino group.

3.6.1 Crystal structure of nickel complex 123

Different solvents were tried in an effort to obtain a suitable crystal of the Ni complex for crystallographic analysis. Dichloromethane in heptane solvent system ultimately was used to obtain crystals of **123**. The molecular structure is depicted in Figure 19.

Figure 19. Crystal structure of the nickel complex **123** and its ^{31}P NMR.

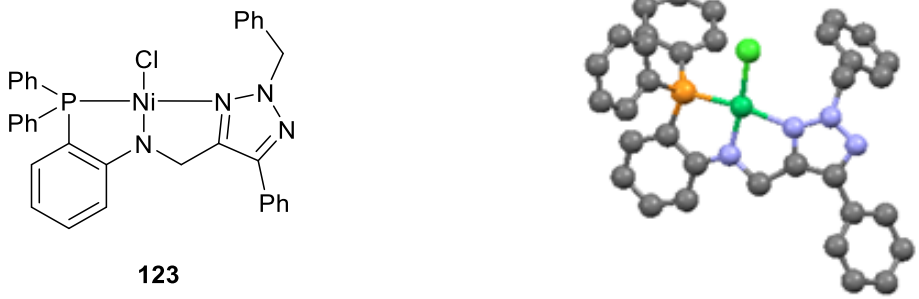

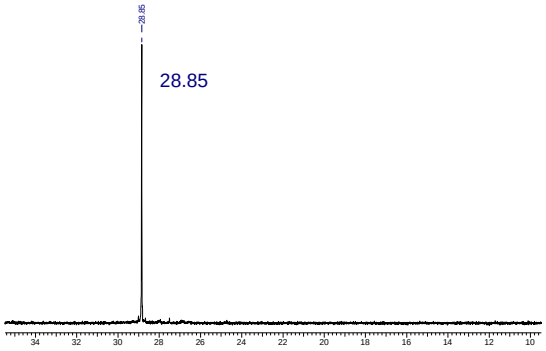

Molecular structure of complex **123**. Selected bond lengths (Å) Ni-P (2.135), Ni-N_1 (1.865), Ni-N_2 (1.960) and Ni-Cl (2.177)

The X-ray crystal structure shows that the triazole binds with nickel forming a square planar complex. To the best of our knowledge, such binding of triazole to nickel center has never been reported. We compared complex **123** with nickel diamino amido chloride complex **116** and bond lengths of both complexes are reported below. Complex **123** has similar bond lengths particularly the nitrogen atoms with **124.**[13]

Figure 20. Selected bond lengths (Å) of complex **123** in comparison with available literature nickel complexes.

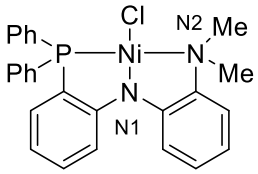

P,N,N nickel complex **125**

Ni-P - 2.1368 Å

Ni-N_1 - 1.858 Å

Ni-N_2 - 2.006 Å

Ni-Cl - 2.1636 Å

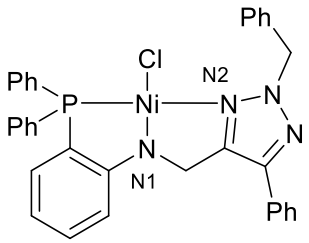

Nickel complex **123**

Ni-P - 2.135 Å

Ni-N_1 - 1.865 Å

Ni-N_2 - 1.960 Å

Ni-Cl - 2.177 Å

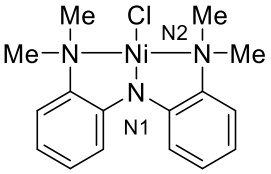

Nickamine chloride **124**

Ni1-N2 - 1.8907 Å

Ni-N_1 - 1.956 Å

Ni-N_3 - 1.982 Å

Ni-Cl - 2.210 Å

3.7 Cross coupling reactions with complex 123.[14]

To examine the catalytic activities of complex **123**, we initially focused on cross-coupling reactions. Particularly, cross coupling reactions of non-activated alkyl halides because of the potential problem with non-activated alkyl halides is ß-hydride elimination and they are reluctant to oxidative addition. The ß-hydride elimination can be suppressed and alkyl halide coupling can be achieved by choosing a suitable metal and ligand combination. In general, with the pincer ligands no such product formation is observed.

We performed similar cross coupling reactions that were already reported and catalyzed by complex **124,** with complex **123** shown below in Scheme 36. Unfortunately, the color of the reaction turned black using complex **123**, and no evidence of the desired cross coupled product was observed. The black color is indicative of nickel nanoparticle formation.

Scheme 36. Cross coupling reactions with complex **123**.

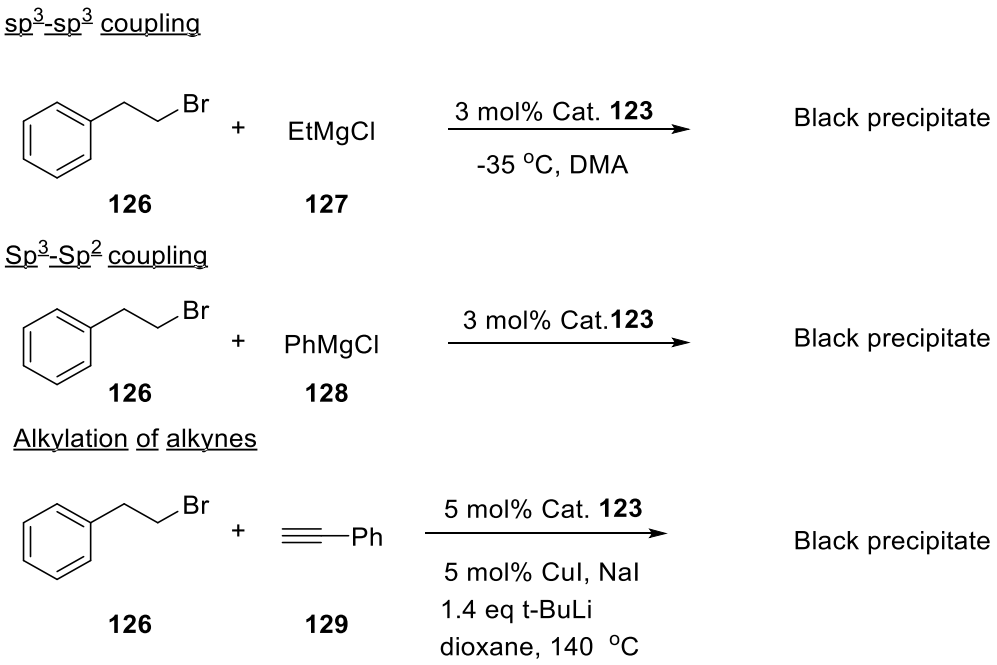

With the unsuccessful results from cross coupling reactions, we attempted to synthesize nickel hydride complexes since very few literature reports are available and their applications are not well studied. Based on the literature reports, we treated complex **123** with the reducing agents to obtain **130**, shown below in Scheme 37. Once again we observed formation of the nickel nanoparticles during the synthesis of nickel-hydride complex and no hydride peak observed in ^{1}H NMR in the negative chemical shift regions.

Scheme 37. Attempted synthesis of nickel hydride complex with reducing agents.[15, 16]

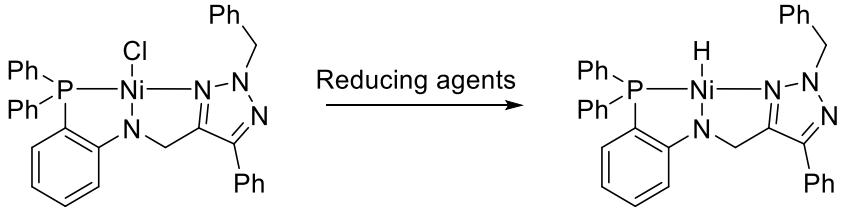

123 **130**

Reducing agents: $LiAlH_4$, $NaBH_4$, superhydride

Though the complex **123** binds tightly to the metal center comparable to complex **124** (Figure 18), with the formation of black nanoparticles, we questioned the stability of the complex **123** in solution because of the observed formation of black nanoparticles as noted previously and attempted to synthesize 1,2,3-benzotriazole stabilized nickel cationic complex, as shown below in the Scheme 38. Professor Shi and co-workers previously reported that benzotriazole stabilizes the gold(I) cation (TA-Au, **14**) in solution to avoid formation of gold nanoparticles shown in Figure 20. Unfortunately, from ^{31}P NMR, ligand **122** was obtained instead of compound **132**.

Scheme 38. Stability experiment for complex **123.**[17]

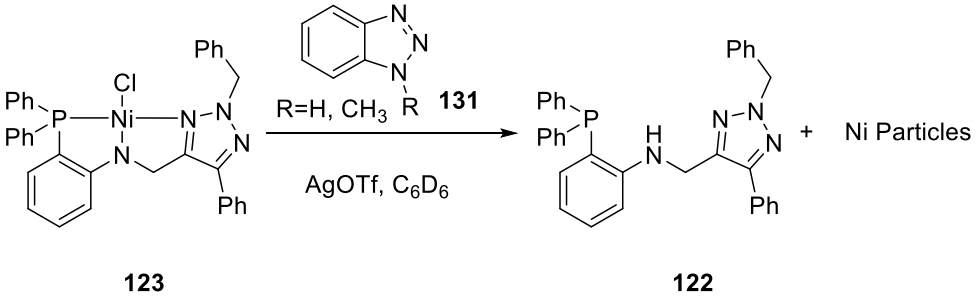

Figure 21. Expected 1,2,3-benzotriazole stabilized complex **132** and TA-Au complex **10**.

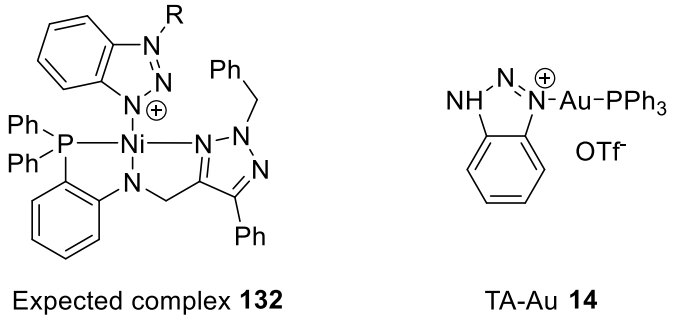

3.8 Modification of the ligand 122

We assumed that the possible intramolecular reductive elimination has occurred due to the strong basicity (anionic) of the NH nitrogen atom. To overcome the formation of **122** from the complex **123,** we predicted that decreasing the basicity of the nitrogen atom would increase the complex stability. With that in mind, we attempted to introduce an amide functional group shown in Figure 22 predicting that the basicity of nitrogen is reduced by resonance with the carbonyl group.

Figure 22. Predicted ligand **133** to reduce the basicity of amine.

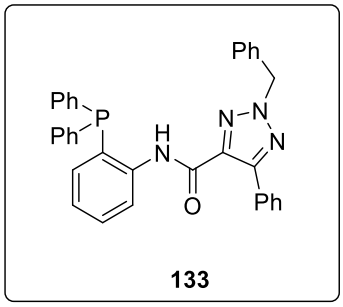

133

3.9 Synthesis of ligand 133

Based on the literature data, an amide group can easily be prepared using an acid and an amine coupling reaction for examples the Appel reaction. The synthetic scheme to **133** is shown below in Schemes 39 and 40.

3.9.1 Introduction to an Appel reaction

The Appel reaction is an organic reaction that converts an alcohol into an alkyl halide using triphenyl or trialkyl phosphines and carbon tetrahalides. The general reaction and mechanism are shown below (Scheme 39).

Scheme 39. General Appel reaction and its mechanism

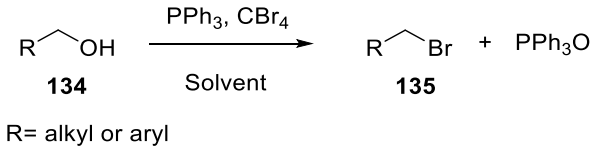

134 **135**

R= alkyl or aryl

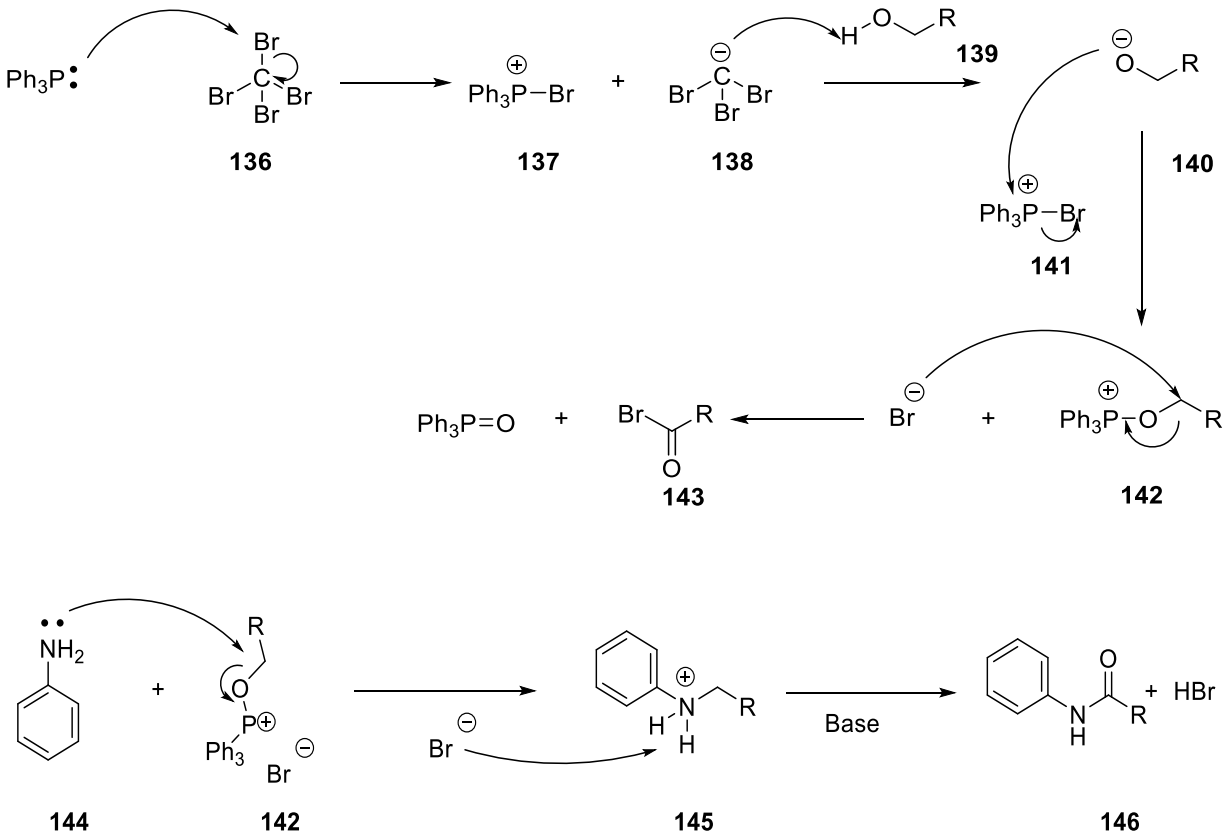

The Appel reaction begins with the nucleophilic attack of the phosphorous onto carbon tetrabromide **136** to form a phosphenium salt **137** and **138.** The anion is protonated by the acid, forming a yellow colored bromoform and alkoxide ion **140**. The nucleophilic displacement of the bromide by the alkoxide yields intermediate **142**.

If nucleophile **144** is available in the reaction instead of the bromide (Br^-) ion, the nucleophile will attack **142** to kick out the phosphorous oxide that results in an amine salt **141**. The bromide deprotonates **145** to form HBr, which is then neutralized by an inorganic base to give an amine **146**.

Reaction of **118** with **147** under Appel reaction conditions provided **148** as a white solid in 87% yield. The reaction was clean with no side products. The amide **148** was isolated by recrystallization from methanol.

Scheme 40. Synthesis **148** using an Appel reaction.

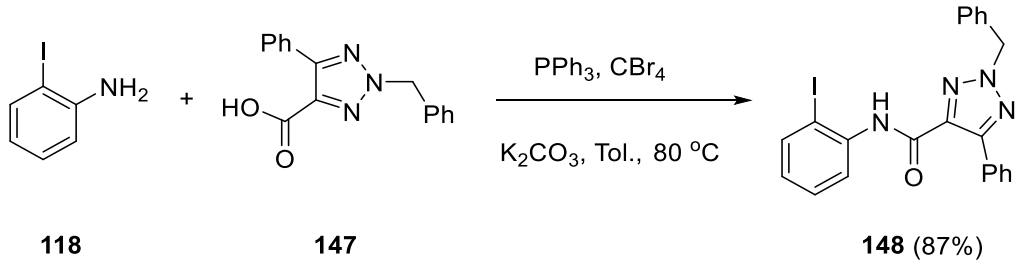

118 **147** **148** (87%)

Scheme 41. Phosphination of compound ligand **148**.

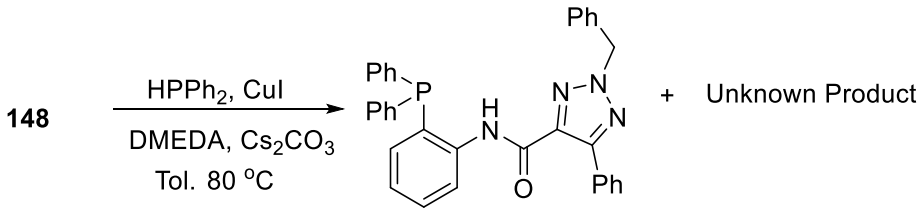

133 ^{31}P - -20.14 **149** ^{31}P - +31.36

With the successful isolation of the amide, we then attempted to introduce a phosphine group in place of the iodine in **148** using Buchwald's conditions (Scheme 41). Monitoring the reaction by $^{31}P\{^{1}H\}$ NMR showed two distinct peaks at δ -20.14 ppm and δ +34.68 ppm in a ratio of 10:90 shown in below Figure 22. Usually, as discussed during the synthesis of **122** and its nickel complexation **123**, the phosphine oxide and metal binding phosphorous both give positive values in ^{31}P NMR, at δ +36.0 ppm and δ +28.06 ppm respectively which indicates compound **133** was oxidized during the reaction. Other than ^{31}P NMR no spectroscopic data are available for the impurity **149** and no crystals for X-ray analysis were obtained. Interestingly, compound **133** was slowly converting to impurity **149**, when stored at room temperatures. Based on above given reasons it can be concluded that the impurity **149** is an oxidized product of **133**.

Figure 23. ^{31}P NMR of phosphination reaction.

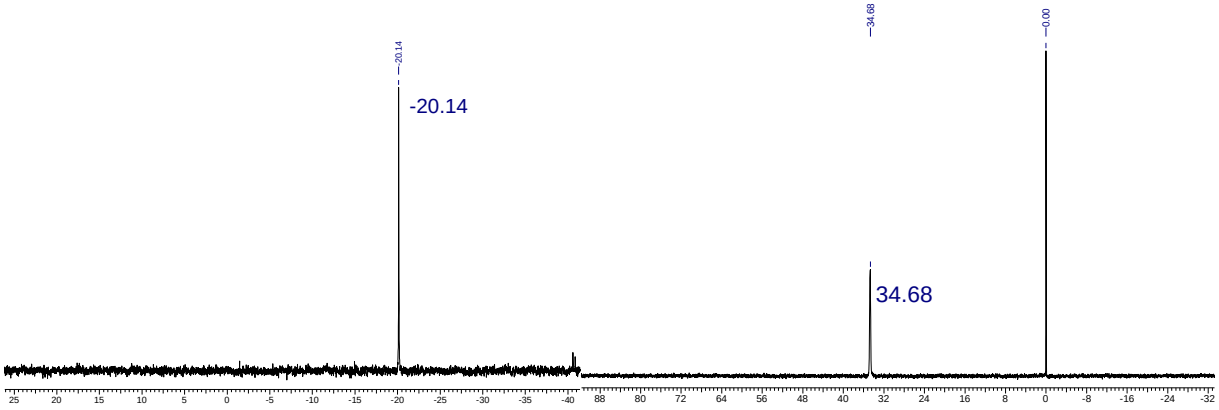

3.9.2 Nickel complex, 150 with 133

Compound **133** was reacted with nickel chloride under the similar conditions that was used for the synthesis of **123**. It also formed a nickel complex **150**. In contrast to **123**, complex **150** is a yellow solid and was isolated in 60% yields. Crystals of **150** were obtained from DCM:heptane and its molecular structure is shown in Figure 24.

Scheme 42. Complex formation of **149** with $NiCl_2$.

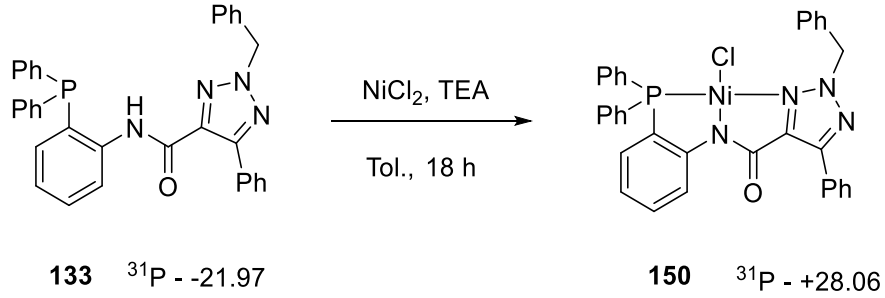

133 ^{31}P - -21.97 **150** ^{31}P - +28.06

Figure 24. X-ray crystal structure of **150** and its ^{31}P NMR.

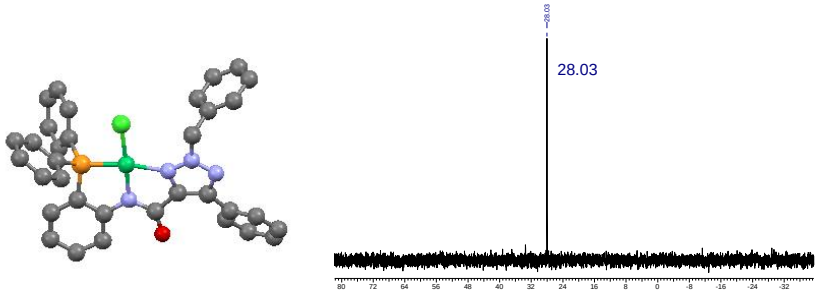

Figure 25. Bond length comparison of both complexes **123**, **125** and **150**.

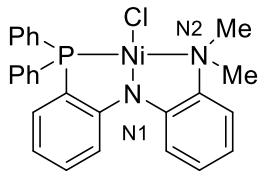

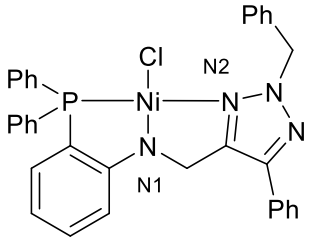

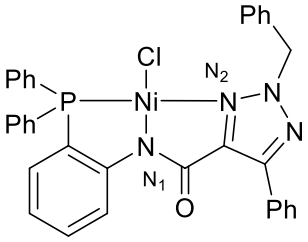

P,N,N nickel complex **125**	Nickel complex **123**	Nickel complex **150**
Ni-P - 2.1368 Å	Ni-P - 2.135 Å	Ni-P - 2.137 Å
Ni-N_1 - 1.858 Å	Ni-N_1 - 1.865 Å	Ni-N_1 - 1.919 Å
Ni-N_2 - 2.006 Å	Ni-N_2 - 1.960 Å	Ni-N_3 - 1.993 Å
Ni-Cl - 2.1636 Å	Ni-Cl - 2.177 Å	Ni-Cl - 2.162 Å

Based on the bond lengths shown above, a comparison of the Ni-N bond distance of **123** and **150** reveals the corresponding Ni-N bond distances are 0.03-0.05 Å longer. The only difference in between these two complexes is the carbonyl group in **150**.

3.10 Conclusion

We have successfully synthesized two P,N,N pincer type ligands (**122** and **133**) and their nickel complexes **(123** and **150**) and characterized them by NMR techniques. We also obtained crystal structures for both nickel chloride complexes (**123** and **150**). However, nickel complex **123** was not stable in its cationic form and also decomposed during the reaction. Nickel complex **150,** was isolated in trace amounts because of the undesired impurity formation of **149** during the synthesis of ligand **133**.

3.11 Tri-coordinated gold

2,4-Disubstituted oxazoles are structural motifs found in many bioactive natural products such as phorboxazoles[18] and hennoxazole.[19] Although several approaches to construct these important motifs are available, each has its own limitations. Zhang reported a synthesis of 2,4-

disubstituted oxazoles via a [3+2] annulation between readily available terminal alkynes and aromatic or alkenic carboxamides under the mild conditions in presence of the gold (I) shown in below Scheme 43.[20] A key intermediate involved in the catalytic cycle is a tricoordinated Au (I) complex which is rare in gold catalysis.

Scheme 43. 2, 4-Disubstituted oxazole's synthesis by gold catalyst.

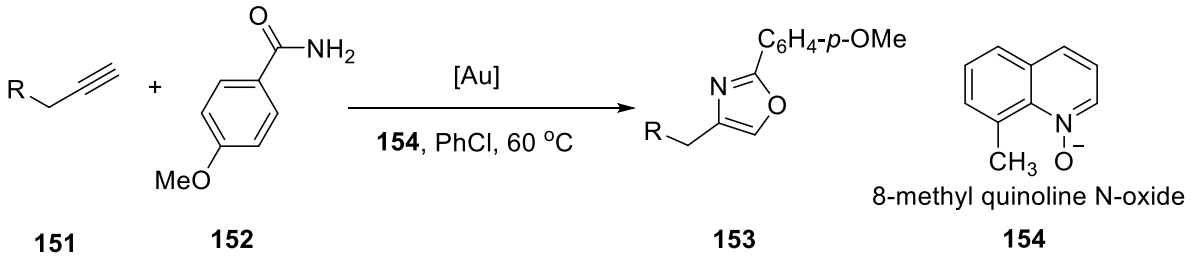

As shown below in Scheme 44, various typical gold catalyst precursors with a range of electronic and steric characteristics were screened during the course of our optimization of the reaction.[21] By expanding the types of ligands to a P,N bidentate ligand such as Mor-DalPhos,[84] and ligands related to the same family (Me-DalPhos and L1 (**158**), reaction yields were increased significantly.

Scheme 44. Optimized conditions.

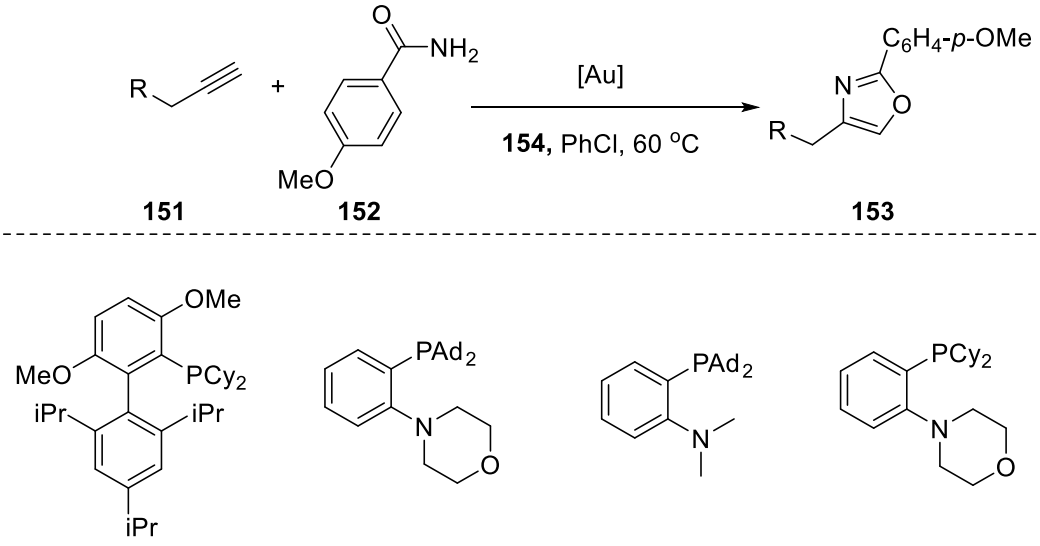

#	Cat.	Yield%
1	$Ph_3PAuNTf_2$ (5%)	0
2	Cy-JohnPhosAuNTf$_2$ (5%)	0
3	IPrAuNTf$_2$ (5%)	0
4	BrettPhosAuNTf2 (5%)	4
5	Mor-DalPhosPhosAuCl++NaBAr$_4$F)	87

To explain the effectiveness of Mor-DalPhos and the related Me-DalPhos and the role of neighboring amino group,[23] it was predicted that hydrogen bonding might be playing a role. However, during the inspection of the X-ray structure of Mor-DalPhosAuNTf$_2$ it was observed that the nitrogen atom with its lone pair was pointing toward and therefore shielded by the gold center. Under these circumstances the possibility of the H-bonding is literally impossible. Instead, the heteroatoms might be involved in coordination[24] with the formally cationic gold center.

3.12 Research Design

Since our ligand was similar to the Mar-DalPhos family of ligands, we decided to perform the same reaction to test the activity of our gold complex. We also predicted that the cationic gold

complex will be stabilized by the triazole ring to prevent the formation of gold nanoparticles, similar to TA-Au that is shown below in Figure 26.

Figure 26. TA-Au complex **14.**

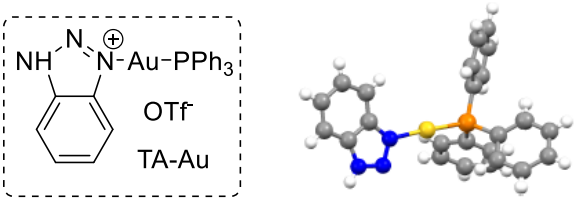

3.12.1 Complexation with gold chloride 159

Scheme 45. Complexation of the ligand with gold chloride.

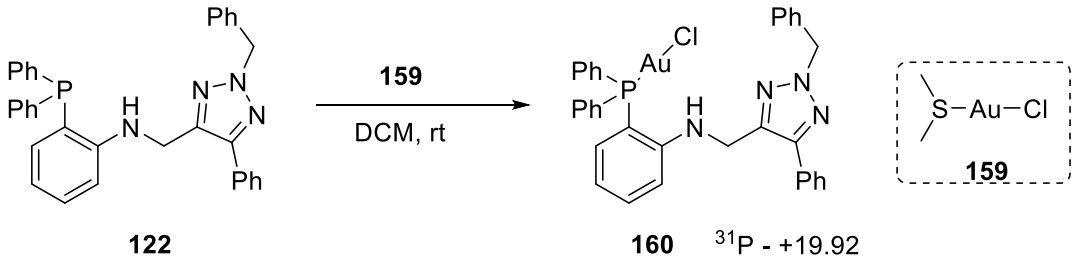

122 **160** ^{31}P - +19.92

Ligand **122** was treated with DMS-Au-Cl that afforded **160** as a white solid in 95% yield.

From the crystal structure of **160** that is shown below in Figure 26, the Au-N bond distances in Mar-DalPhos is 2.30 Å whereas it is 3.4 Å in complex **160** and the distance between Au and H of NH in the complex is 2.84 Å. These bond distances conclude that the gold is not involved in hydrogen bonding and the nitrogen is not bound to gold.

Figure 27. Crystal Structure of L-AuCl complex, **160**.

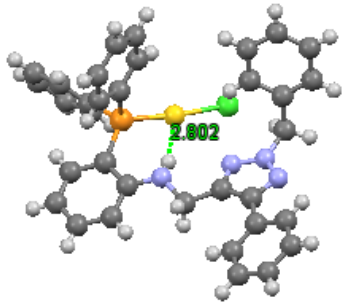

Table 6. Synthesis of different gold cation of complex **160**.

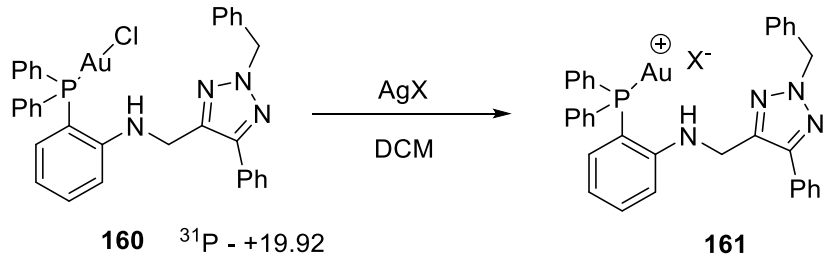

160 ^{31}P - +19.92 **161**

	Silver Salt	Results
160	$AgNTf_2$	multiple peaks in ^{31}P NMR
	$AgSbF_6$	multiple peaks in ^{31}P NMR
	AgOBz	Obtained fine crystals (^{31}P-+13.06)
	$AgPF_6$	multiple peaks in ^{31}P NMR

Figure 28. ^{31}P NMR of the gold-benzoate complex, **162**.

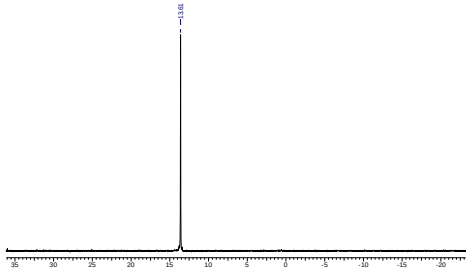

Scheme 46. Synthesis of 2,4-disubstituted oxazoles with complex **160**.

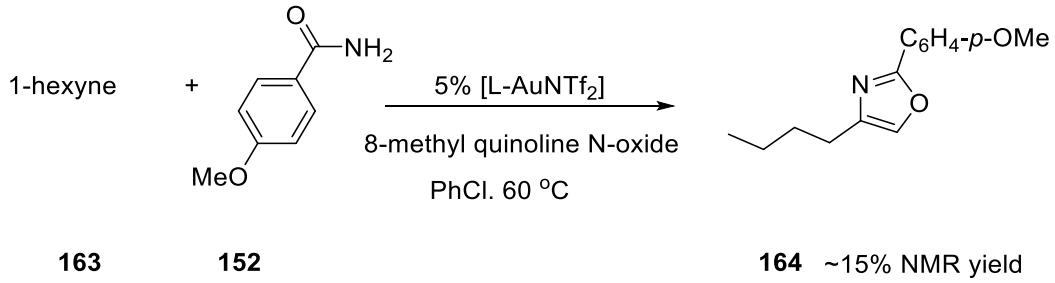

163 **152** **164** ~15% NMR yield

During optimization, (see in Scheme 44), various typical gold catalysts with a range of electronic and steric characteristics failed in the formation of the oxazole product. It was stated that, except MarDalPhos family ligands, other gold complexes were unable to form tricoordinated gold thereby providing no oxazole products. A minimum amount (15%) of product with complex **160** indicating that the gold atom may have been involved in tri-coordination during the reaction. However, at this point, it was not clear how the gold cation was involved in this process. No significant improvement in the product formation observed even after doubling the catalyst.

Figure 29. Crystal structure of k^1Au-OBz, **162**.

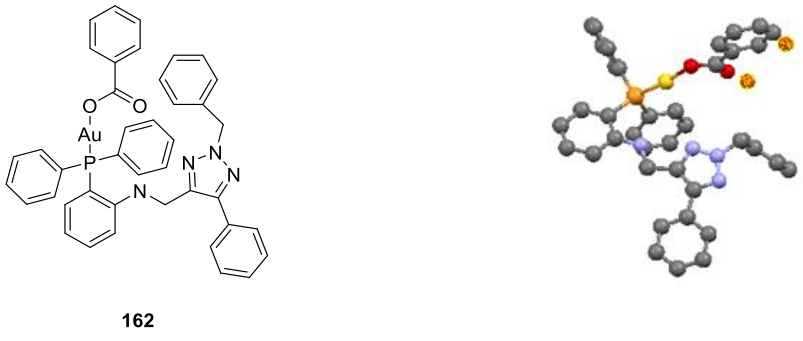

162

Crystal structure of the gold benzoate complex **162,** showing the formation of Au-O (benzoate) bond. For clarity purpose the hydrogen atoms are deleted.

Figure 30. Comparison of complexes **160** and **162**.

The crystal structures of gold chloride **160**, and gold-benzoate **162** are shown in Figure 27 and 29 respectively. Surprisingly, two interesting things were observed from these crystal structures. First, the structures of the gold chloride complex **160** and its benzoate complex **162** are not similar. In gold chloride complex **160**, two phenyl groups reside on the same side of the phosphorous atom and the position of the gold was towards the triazole ring. However, in its benzoate complex **162**, the phenyl groups are on either side of the phosphorous atom and the position of the gold was opposite to the aromatic ring that was attached to amine group at the ortho position of the phosphorous atom. Secondly, we were expecting a benzoate anion coordination to the gold cation. Surprisingly, a sigma bond between gold and oxygen atom was observed from the crystal structure.

3.13 Conclusion

We have successfully synthesized gold complex **160** and its benzoate complexes **162**. Based on the crystal structure **162,** as per Zhang's report, the formation of the gold-oxygen bond may be possible when the gold atom is an electron deficient.

References

1. Moulton, C. J.; Shaw, B. L. *J. Chem. Soc., Dalton Trans*. **1976**, 1020–1024.
2. Lundgren, R. J.; Hesp, K. D.; Stradiotto, M., *Synlett.,* **2011,** *17*, 2443-2458.
3. Rybtchinski, B.; Milstein, D. *Angew. Chem., Int. Ed.,* **1999**, *38*, 870-883. Jensen,M. *Chem. Comm*, **1999**, 2443-2449. C) Albrecht, M.; van Koten, G. *Angew. Chem., Int. Ed.,* **2001**, *40*, 3750-3781. d) Vigalok A.; Milstein, D. *Acc. Chem. Res.*, **2001**, *34*, 798-807. e). van der Boom M. E.; D. Milstein, *Chem. Rev.*, **2003**, *103*, 1759-1792. F). Singleton, J. T.; *Tetrahedron*, **2003**, *59*, 1837-1857. b) Milstein, D. *Pure and Appl. Chem.*, **2003**, 75, 445-460.
4. Lundgren, R. J.; Hesp, K. D.; Stradiotto, M., *Synlett* **2011,** 2443-2458.
5. Crawford, S. M.; Lavery, C. B.; Stradiotto, M., *Chem. Eur. J.* **2013,** *19* (49), 16760-16771. b) Tardiff, B. J.; Stradiotto, M., E. *J. Org. Chem.* **2012,** 3972-3977.
6. Suijkerbuijk, B. M. J. M.; Aerts, B. N. H.; Dijkstra, H. P.; Lutz, M.; Spek, A. L.; van Koten, G.; Klein Gebbink, R. J. M. *Dalton Trans.* **2007**, 1273-1276.
7. Suijkerbuijk, B. M. J. M.; Aerts, B. N. H.; Dijkstra, H. P.; Lutz, M.; Spek, A. L.; van Koten, G.; Klein Gebbink, R. J. M. *Dalton Trans.* **2007**, 1273-1276. B). Oro, L. A.; Pinillos, M. T.; Tejel, C.; *J. Organimet. Chem.* **1985**, *280*, 261-267.
8. Duan, H.; Sengupta, S.; Petersen, J. L.; Shi, X. *Organometallics* **2009**, *28*, 2352-2355.
9. Papo, T. R.; Jaganyi, D., *J. Coord. Chem.* **2015,** *68* (5), 794-807.
10. Dogan, H. N.; Duran, A.; Rollas, S., *Ind. J. Che.* **2005,** *44* (11), 2301-2307. b). Khalil, A. E.-G. M.; Berghot, M. A.; Gouda, M. A., *J. Saudi Chem. Soc.* **2016,** *20* (2), 165-172.
11. Gelman, D.; Jiang, L.; Buchwald, S. L., *Org. Lett.* **2003,** *5* (13), 2315-2318.
12. Chakraborty, S.; Krause, J. A.; Guan, H., *Abstracts of Papers of the Am. Chem. Soc.* **2009,** 237.

13. Csok, Z.; Vechorkin, O.; Harkins, S. B.; Scopelliti, R.; Hu, X., *J. A. Chem Soc.* **2008,** *130* (26), 8156

14. Vechorkin, O.; Csok, Z.; Scopelliti, R.; Hu, X., *Chem. Eur. J.* **2009,** *15* (15), 3889-3899.

15. Peuckert, M.; Keim, W. *Organometallics.*, **1983**, *2*, 594–597. (c) Muller, U.; Keim, W.; Kruger, C.; Betz, P. *Angew. Chem., Int. Ed. Engl.* **1989**, *28*, 1011–1013. (d) Keim, W. *Angew. Chem., Int. Ed. Engl.* **1990**, *29*, 235– 244. (e) Bertozzi, S.; Iannello, C.; Barretta, G. U.; Vitulli, G.; Lazzaroni,R.; Salvadori, P. *J. Mol. Catal.* **1992**, *77*, 1–6. (f) Fan, L.; Krzywicki, A.; Somogyvari, A.; Ziegler, T. *Inorg. Chem.* **1994**, *33*, 5287–5294. (g) Fan, L.; Krzywicki, A.; Somogyvari, A.; Ziegler, T. *Inorg. Chem.* **1996**, *35*, 4003–4006. (h) Brown, J. M.; Hughes, G. D. *Inorg. Chim. Acta* **1996**, *252*, 229–237. (i) Wiencko, H. L.; Kogut, E.; Warren, T. H. *Inorg. Chim. Acta* **2003**, *345*, 199–208. (j) Kogut, E.; Zeller, A.; Warren, T. H.; Strassner, T. *J. Am. Chem. Soc.* **2004**, *126*, 11984–11994. (k) Wang, K.; Patil, A. O.; Zushma, S.; McConnachie, J. M. *J. Inorg. Biochem.* **2007**, *101*, 1883–1890. (a) Sato, Y.; Takimoto, M.; Hayashi, K.; Katsuhara, T.; Takagi, K.; Mori, M.*J. Am. Chem. Soc.* **1994**, *116*, 9771–9772. (b) Sato, Y.; Takimoto, M.; Mori,M. *J. Am. Chem. Soc.* **2000**, *122*, 1624–1634.

16. Breitenfeld, J.; Scopelliti, R.; Hu, X., *Organometallics* **2012,** *31* (6), 2128-2136.

17. Duan, H.; Sengupta, S.; Petersen, J. L.; Shi, X. *Organometallics* **2009**, *28*, 2352-2355.

18. Ichiba, T.; Yoshida, W. Y.; Scheuer, P. J.; Higa, T.; Gravalos, D. G. *J. Am. Chem. Soc*. **1991**, *113*, 3173.

19. Searle, P. A.; Molinski, T. F. *J. Am. Chem. Soc*. **1995**, 117, 8126.

20. Luo, Y.; Ji, K.; Li, Y.; Zhang, L., *J. Am. Chem. Soc.* **2012,** *134* (42), 17412-17415

21. (a) Ye, L.; Cui, L.; Zhang, G.; Zhang, L. *J. Am. Chem. Soc.* **2010**, 132, 3258. (b) Ye, L.; He, W.; Zhang, L. *J. Am. Chem. Soc*. **2010**, 132, 8550. (c) Ye, L.; He, W.; Zhang, L. *Angew.*

Chem., Int. Ed. **2011**, *50*, 3236. (d) He, W.; Xie, L.; Xu, Y.; Xiang, J.; Zhang, L. *Org. Biomol. Chem*. **2012**, *10*, 3168. (e) Wang, Y.; Ji, K.; Lan, S.; Zhang, L. *Angew. Chem., Int. Ed.* **2012**, *51*, 1915.

22. Lundgren, R. J.; Peters, B. D.; Alsabeh, P. G.; Stradiotto, M. *Angew. Chem., Int. Ed*. **2010**, *49*, 4071. (b) Hesp, K. D.; Stradiotto, M. *J. Am. Chem. Soc.* **2010**, *132*, 18026.
23. He, W.; Li, C.; Zhang, L. *J. Am. Chem. Soc*. **2011**, *133*, 8482., b). He, W.; Xie, L.; Xu, Y.; Xiang, J.; Zhang, L. *Org. Biomol. Chem.* **2012**, 10, 3168., c). Ye, L.; He, W.; Zhang, L. Angew. *Chem., Int. Ed.* **2011**, *50*, 3236., d) Lundgren, R. J.; Peters, B. D.; Alsabeh, P. G.; Stradiotto, M. *Angew. Chem., Int. Ed.* **2010**, *49*, 4071., e). Hesp, K. D.; Stradiotto, M. *J. Am. Chem. Soc.* **2010**, *132*, 18026.
24. Pérez-Galán, P.; Delpont, N.; Herrero-Gómez, E.; Maseras, F.; Echavarren, A. M. *Chem. Eur. J.* **2010**, *16*, 5324.

Experimental Section

General Remarks

All NMR spectra were recorded in $CDCl_3$ at 400 MHz (^{1}H NMR) and 100 MHz (^{13}C NMR, ^{1}H-broadband decoupled) at ambient temperature unless otherwise stated. Chemical shifts are expressed in δ values relative to Me_4Si (0.0 ppm, ^{1}H and ^{13}C) or $CDCl_3$ (77.0 ppm, ^{13}C) internal standards. HRMS data were obtained via electrospray ionization (ESI) with an ion trap mass analyzer. THF was purified and dried via two consecutive columns composed of activated alumina and Q5 catalyst on a Glass Contours solvent purification system. Dichloromethane and toluene were purified and dried via two consecutive columns composed of activated alumina on a Glass Contours solvent purification system. Hexanes and ethyl acetate were distilled from calcium hydride. Chemicals prepared according to literature procedures are referenced the first time they are used in the Experimental Section; all other reagents were obtained from commercial sources and used as received. All reactions were performed under a nitrogen atmosphere in oven-dried glassware unless otherwise stated. Solvents were removed from reaction mixtures and products on a rotary evaporator at water aspirator pressure.

Chapter 1. Gold catalyzed 1,n-enyne ester cycloisomerization reaction

Procedure for the synthesis of 2-formyl styrene.

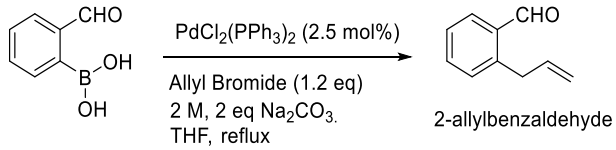

To a solution of the 2-formylphenylboronic acid (1.50 g, 10.0 mmol) in THF (50 mL) in a round bottom flask were added allyl bromide (1.45 g, 12.0 mmol), $PdCl_2(PPh_3)_2$ (0.175 g, 0.25 mmol). The reaction mixture was heated to 60 °C, and then aq. Na_2CO_3 (2.12 g, 20.0 mmol) solution was added over a period of 2 h and the heating continued for 3-4 h. The reaction mixture was quenched with H_2O and extracted with CH2Cl2 (3x100 mL). The combined organic layers washed with brine, dried (Na_2SO_4), and concentrated in vacuum. The residue was purified by column chromatography on silica gel with pure n-hexanes; to afford the desired product as yellow syrup (1.32 g, 9.0 mmol, 90%).

Procedure for the synthesis of O-(2-Bromoethoxy) benzaldehyde.

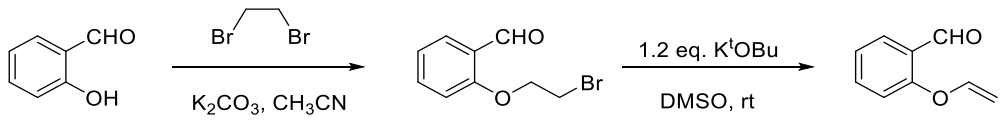

In a 250 mL two-necked flask equipped with a magnetic stir bar and reflux condenser salicylaldhyde (1.22 g, 10.0 mmol), 1,2-dibromoethane (9.40 g, 50.0 mmol) and anhydrous K_2CO_3 (2.76 g, 20.0 mmol) were mixed with anhydrous CH_3CN (50 mL). The mixture was refluxed for 30 h and then cooled to room temperature, filtered and the solid was washed with CH_3CN. The filtrate was evaporated to dryness. The crude product was purified by column chromatography on

silica gel using diethylether:n-hexane (8:1) to give as a white crystalline solid (1.52 g, 6.69 mmol, 67%).

Procedure for the synthesis of 2-(vinyloxy)benzaldehyde.

To a solution of *O*-(2-Bromoethoxy) benzaldehyde (2.30 g, 10.0 mmol) in DMSO (25 mL) was added potassium ter-butoxide (1.35 g, 12.0 mmol) at room temperature and stirred for 1 h. After the completion of the reaction (TLC), 2N HCl (50 mL) was added followed by 40 mL of water to saturate the DMSO and extracted with diethylether (3 x 50 mL). Combined the organic layers, dried (Na_2SO_4), and evaporated under vacuum at room temperature to afford the desired product as yellow liquid. (1.01 g, 6.82 mmol, 68%).

Spectral data: ^{1}H NMR ($CDCl_3$, 400 MHz) δ 10.45 (s, 1H), 7.88-7.86 (dd, *J* = 2.0, 7.6 Hz, 1H), 7.57 (m, 1H), 7.16 (m, 1H), 7.09-7.07 (dd, *J* = 1.0, 8.2 Hz, 1H), 6.73-6.68 (dd, *J* = 6.0, 13.7 Hz, 1H), 4.87-4.84 (dd, *J* = 2.0, 13.7 Hz, 1H), 4.61-4.59 (dd, *J* = 2.2, 6.2 Hz, 1H); ^{13}C NMR ($CDCl_3$, 100 MHz) δ 188.96, 158.77, 147.47, 135.71, 128.31, 125.89, 123.31, 116.82, 97.22; HRMS (ESI) calculated for $C_9H_8O_2$ $[M]^+$. 148.0524, Found: 148.0524.

Procedure for Au-catalyzed transfer vinylation of alcohols.

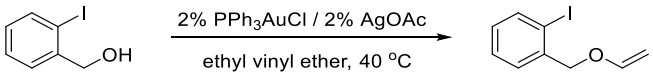

To a screw cap tube was added $AuClPPh_3$ (0.099 g, 0.02 mmol) and silver acetate (0.033 g, 0.02 mmol), ethyl vinyl ether (10 mL). The mixture was stirred at room temperature for 10 mins. 2-iodo benzylalcohol was added (2.34 g, 10.0 mmol) and the mixture was stirred at 50 °C for 6 h. After the completion of the reaction (TLC), the product was isolated by column chromatography (diethyl ether :n-hexanes;1:20) as a colorless liquid (1.58 g, 6.1 mmol, 61%).

Procedure for the synthesis of 2-((vinyloxy)methyl) benzaldehyde.

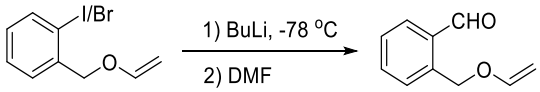

Under Nitrogen atmosphere, to a solution of 1-bromo or iodo aryl compound (2.60 g, 10.0 mmol) in anhydrous diethyl ether (40 mL) at -78 ºC was slowly added *n*-butyl lithium (4.4 mL, 11.0 mmol). The reaction was stirred at the same temperature for 40 min and DMF (3.7 g, 5 mmol) was added dropwise manner. The reaction allowed to warm to room temperature over 1 h before it was quenched by saturated aqueous NH_4Cl (10 mL) at 0 ºC. The reaction mixture was diluted by Et_2O (30 mL), washed with saturated NH_4Cl (10 mL) and brine (10 mL), dried over Na_2SO_4, and concentrated. The residue was purified by silica gel chromatography (ethyl acetate:hexanes = 1:5) to afford the pure product as a colorless oil (1.25 g, 7.7 mmol, 77%).

Spectral data. ^{1}H NMR ($CDCl_3$, 400 MHz) δ 10.15 (s, 1H), 7.87-7.85 (d, *J* = 7.1 Hz, 1H), 7.68-7.67 (d, J = 8.4 Hz, 1H), 7.64-7.61 (t, J = 7.1 Hz, 1H), 7.51-7.49 (t, J = 8.4 Hz, 1H), 6.60-6.57 (dd, J = 8.5, 13.8 Hz, 1H), 5.21 (s, 2H), 4.39-4.37 (dd, J = 2.5, 11.8 Hz, 1H), 4.14-4.12 (dd, J = 2.5, 7.5 Hz, 1H); ^{13}C NMR ($CDCl_3$, 100 MHz) δ 192.66, 151.06, 19.08, 133.69, 133.22, 132.80, 127.62, 127.49, 87.68, 67.28; HRMS (ESI) calculated for $C_{10}H_{10}O_2$ $[M]^+$.162.0680, Found: 162.0681.

Procedure for synthesis of N-(2-formylpphenyl)-4-methyl-N-vinylbenzenesulfonamide

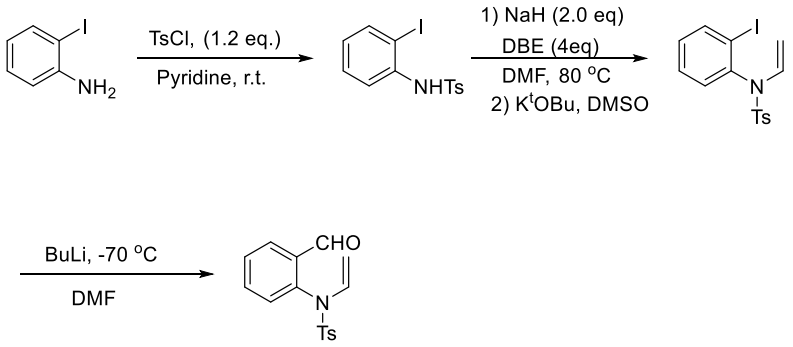

To a solution of 2-iodo aniline (2.19 g, 10.0 mmol,) in pyridine (40 mL) was added TsCl (2.29 g, 12.0 mmol) at room temperature. The mixture was stirred for 5 h and monitored the reaction by TLC. Remove the pyridine under the vacuum. The product was extracted with ethyl acetate (50 mL x 3), and the combined organic extracts were washed with brine and dried over Na_2SO_4. After removal of the solvents under reduced pressure, the products were purified by column to give N-tosyl-2-iodo aniline. Then to a solution of NaH (60% oil dispersion) (2.0 g, 50.0 mmol) in DMF (30 mL), N-tosyl-2-iodo aniline (3.73 g, 10.0 mmol) in DMF (10.0 mL) was added dropwise. After stirred for 30 min, 1,2-dibromoethane (9.40 g, 50.0 mmol,) was added. The mixture was heated to 80 ^oC for 8 h. When N-toyl-2-iodo aniline was disappeared, quench the reaction with saturated NH_4Cl and extract with ethyl acetate (50 mL x 3). The combined organic extracts were washed with brine and dried over Na_2SO_4. The final product was isolated as a yellow syrup (1.67 g, 42%).

Spectral data. ^1H NMR ($CDCl_3$, 400 MHz) δ 9.89 (s, 1H), 8.05 (m, 1H), 7.59-7.53 (m, 4H), 7.35-7.29 (dd, *J* = 1.5, 6.4 Hz, 3H), 6.85-6.83 (m, 1H), 4.36-4.34 (dd, *J* = 1.5, 9.0 Hz, 1H), 3.79-3.75 (dd, *J* = 1.7, 15.3 Hz, 1H), 2.45 (s, 3H); ^{13}C NMR ($CDCl_3$, 100 MHz) δ 189.15, 144.72, 138.03,

135.32, 135.11, 135.10, 134.69, 130.91, 129.94, 129.87, 128.76, 127.50, 95.04, 21.64; HRMS (ESI) calculated for $C_{16}H_{15}O_3S$ $[M]^+$. 301.0772, Found: 301.0773.

Procedure for the synthesis of propargyl esters from propargyl alcohols.

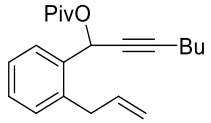

15b

1-(2-allylphenyl)hept-2-yn-1-yl pivalate

To a solution of 1-(2-allylphenyl) hept-2-yn-1-ol (0.230 g, 1.0 mmol) in CH2Cl2 (5 mL) was added triethylamine (0.28 mL, 2.0 mmol) and DMAP (0.012 g, 0.10 mmol) at room temperature. The reaction mixture was cooled to 0 ^oC, and added trimethylacetyl chloride (0.132 mL, 1.1 mmol) over a period of 5 mins. The resulting mixture was stirred for 2 h at room temperature. After completion of the reaction (TLC), the reaction mixture was quenched with 1N HCl (3 mL). The organic layer was separated, washed with saturated sodium bicarbonate solution (2 x 3 mL), brine (3 mL), dried (Na_2SO_4), concentrated under reduced pressure, and purified by flash column chromatography (ethyl acetate:n-hexanes; 1:6) on silica gel to get **15b** as a colorless liquid (0.265 g, 8.5 mmol, 85%).

Spectral data. ^1H NMR ($CDCl_3$, 400 MHz) δ 7.61(dd, *J* = 2.4, 7.0 Hz, 1H), 7.27-7.18 (m, 3H), 6.54 (t, *J* = 2.2 Hz, 1H), 5.96 (m, 1H), 5.09-4.99 (m, 2H), 3.53 (m, 2H), 2.21 (dt, *J* = 1.8, 7.1 Hz, 2H), 1.51-1.34 (m, 4H), 1.20 (s, 9H), 0.89 (t, *J* = 7.5 Hz, 3H); ^{13}C NMR ($CDCl_3$, 100 MHz) δ 176.87, 137.57, 136.49, 135.94, 129.77, 128.49, 127.90, 126.42, 116.06, 87.56, 76.92, 63.48, 38.59, 36.43 30.32, 26.88, 21.70, 18.37, 13.39; HRMS (ESI) calculated for $C_{21}H_{28}O_2$ $[M]^+$. 312.2089, Found: 312.2089.

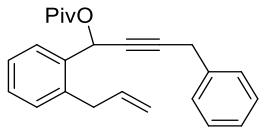

15c

1-(2-allylphenyl)-4-phenylbut-2-yn-1-yl pivalate

To a solution of 1-(2-allylphenyl)-4-phenylbut-2-yn-1-ol (0.260 g, 1.0 mmol) in CH2Cl2 (5 mL) was added triethylamine (0.28 mL, 2.0 mmol) and DMAP (0.012 g, 0.10 mmol) at room temperature. The reaction mixture was cooled to 0 ^{o}C, and added trimethylacetyl chloride (0.132 mL, 1.1 mmol) over a period of 5 mins. The resulting mixture was stirred for 2 h at room temperature. After completion of the reaction (TLC), the reaction mixture was quenched with 1N HCl (3 mL). The organic layer was separated, washed with saturated sodium bicarbonate solution (2 x 3 mL), brine (3 mL), dried (Na_2SO_4), concentrated under reduced pressure, and purified by flash column chromatography (ethyl acetate:n-hexanes; 1:6) on silica gel to get **15c** as a colorless liquid (0.295 g, 8.5 mmol, 85%).

Spectral data. ^{1}H NMR ($CDCl_3$, 400 MHz) δ 7.66-7.64 (dd, *J* = 1.4, 7.0 Hz, 1H), 7.30-7.18 (m, 8H), 6.62 (t, *J* = 2.0 Hz, 1H), 5.01 (m, 1H), 3.64 (d, 2H), 3.53 (d, *J* = 7.6 Hz, 2H), 1.21 (s, 9H); ^{13}C NMR ($CDCl_3$, 100 MHz) δ 177.01, 137.67, 136.52, 136.12, 135.76, 135.41 129.94, 128.72, 128.39, 128.06, 127.77, 126.61, 116.25, 84.92, 79.47, 63.48, 38.74, 36.58, 26.99, 25.10; HRMS (ESI) calculated for $C_{24}H_{26}O_2$ $[M]^+$ 346.1932, Found: 346.1933.

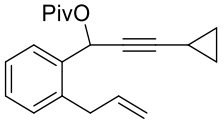

15d

1-(2-allylphenyl)-3-cyclopropylprop-2-yn-1-yl pivalate

To a solution of 1-(2-allylphenyl)-3-cyclopropylprop-2-yn-1-ol (0.210 g, 1.0 mmol) in CH2Cl2 (5 mL) was added triethylamine (0.28 mL, 2.0 mmol) and DMAP (0.012 g, 0.10 mmol) at room temperature. The reaction mixture was cooled to 0 ^{o}C, and added trimethylacetyl chloride (0.132 mL, 1.1 mmol) over a period of 5 mins. The resulting mixture was stirred for 2 h at room

temperature. After completion of the reaction (TLC), the reaction mixture was quenched with 1N HCl (3 mL). The organic layer was separated, washed with saturated sodium bicarbonate solution (2 x 3 mL), brine (3 mL), dried (Na_2SO_4), concentrated under reduced pressure, and purified by flash column chromatography (ethyl acetate:n-hexanes; 1:6) on silica gel to get **15d** as a colorless liquid (0.192 g, 6.5 mmol, 65%).

Spectral data. ^{1}H NMR ($CDCl_3$, 400 MHz) δ 7.56 (dd, *J* = 2.0 Hz, 7.2 Hz, 1H), 7.28-7.17 (m, 3H), 6.49 (d, *J* = 2.0 Hz, 1H), 5.95 (m, 1H), 5.09-5.00 (m, 2H), 3.50 (dt, *J* = 1.6, 6.6 Hz, 2H), 1.23 (m, 1H), 1.19 (s, 9H), 0.07-0.65 (m, 4H); ^{13}C NMR ($CDCl_3$, 100 MHz) δ 177.02, 137.67, 136.61, 136.05, 129.93, 128.60, 127.99, 126.55, 116.20, 90.73, 72.22, 63.65, 38.72, 36.54, 27.01, 26.50, 8.32, -0.37; HRMS (ESI) calculated for $C_{20}H_{24}O_2$ $[M]^+$ 296.1176, Found. 296.1175.

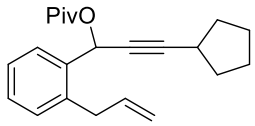

15e

1-(2-allylphenyl)-3-cyclopentylprop-2-yn-1-yl pivalate

To a solution of 1-(2-allylphenyl)-3-cyclopentylprop-2-yn-1-ol (0.240 g, 1.0 mmol) in CH2Cl2 (5 mL) was added triethylamine (0.28 mL, 2.0 mmol) and DMAP (0.012 g, 0.10 mmol) at room temperature. The reaction mixture was cooled to 0 ^{o}C, and added trimethylacetyl chloride (0.132 mL, 1.1 mmol) over a period of 5 mins. The resulting mixture was stirred for 2 h at room temperature. After completion of the reaction (TLC), the reaction mixture was quenched with 1N HCl (3 mL). The organic layer was separated, washed with saturated sodium bicarbonate solution (2 x 3 mL), brine (3 mL), dried (Na_2SO_4), concentrated under reduced pressure, and purified by flash column chromatography (ethyl acetate:n-hexanes; 1:6) on silica gel to get **15e** as a colorless liquid (0.256 g, 7.9 mmol, 79%).

Spectral data. ^{1}H NMR ($CDCl_3$, 400 MHz) δ 7.60 (dd, *J* = 1.6, 7.2 Hz, 1H), 7.30-7.22 (m, 2H), 7.20-7.18 (dd, J = 1.9, 7.2 Hz, 2H), 6.54 (d, *J* = 1.9 Hz, 1H), 6.02-5.92 (m, 1H), 5.09-5.02 (m, 2H), 3.52 (dt, *J* = 1.6 Hz, 6.3 Hz, 2H), 2.69-2.62 (dp, *J* = 1.9, 7.2 Hz, 1H), 1.91-1.85 (m, 8H), 1.71-1.51 (m, 8H), 1.20 (s, 9H); ^{13}C NMR ($CDCl_3$, 100 MHz) δ 177.02, 137.79, 136.65, 136.07, 129.89, 128.57, 128.10, 126.50, 116.15, 91.94, 76.57, 63.73, 38.71, 36.52, 33.60, 30.19, 26.99, 24.89. HRMS (ESI) calculated for $C_{22}H_{28}O_2$ $[M]^+$ 324.2089, Found. 324.2089.

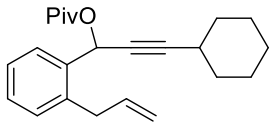

15f

1-(2-allylphenyl)-3-cyclohexylprop-2-yn-1-yl pivalate

To a solution of 1-(2-allylphenyl)-3-cyclohexylprop-2-yn-1-ol (0.250 g, 1.0 mmol) in CH2Cl2 (5 mL) was added triethylamine (0.28 mL, 2.0 mmol) and DMAP (0.012 g, 0.10 mmol) at room temperature. The reaction mixture was cooled to 0 ^{o}C, and added trimethylacetyl chloride (0.132 mL, 1.1 mmol) over a period of 5 mins. The resulting mixture was stirred for 2 h at room temperature. After completion of the reaction (TLC), the reaction mixture was quenched with 1N HCl (3 mL). The organic layer was separated, washed with saturated sodium bicarbonate solution (2 x 3 mL), brine (3 mL), dried (Na_2SO_4), concentrated under reduced pressure, and purified by flash column chromatography (ethyl acetate:n-hexanes; 1:6) on silica gel to get **15f** as a colorless liquid (0.230 g, 6.8 mmol, 68%).

Spectral data. ^{1}H NMR ($CDCl_3$, 400 MHz) δ 8.20-8.18 (dd, *J* = 1.8, 8.0 Hz, 1H), 7.30-7.18 (m, 3H), 6.56 (d, J = 7.8 Hz, 1H), 6.00 (m, 1H), 5.11 (m, 1H), 3.81 (dt, *J* = 1.6, 6.3 Hz, 1H), 3.53 (dt, *J* = 6.5 Hz, 2H), 2.65 (m, 1H), 2.43 (m, 1H), 1.91-1.28 (m, 16H), 1.20 (s, 9H); ^{13}C NMR ($CDCl_3$, 100 MHz) δ 204.08, 141.69, 136.05, 134019, 132.12, 129.79, 128.79, 128.43, 126.58, 44.49,

35.01, 29.89, 29.83, 25.96, 25.91, 25.84, 20.98, 17.94, -0.01**.** HRMS (ESI) calculated for $C_{23}H_{30}O_2$ $[M]^+$ 338.2245, Found: 338.2246

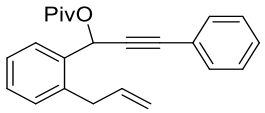

15g

1-(2-allylphenyl)-3-phenylprop-2-yn-1-yl pivalate

To a solution of 1-(2-allylphenyl)-3-phenylprop-2-yn-1-ol (0.250 g, 1.0 mmol) in CH2Cl2 (5 mL) was added triethylamine (0.28 mL, 2.0 mmol) and DMAP (0.012 g, 0.10 mmol) at room temperature. The reaction mixture was cooled to 0 ^oC, and added trimethylacetyl chloride (0.132 mL, 1.1 mmol) over a period of 5 mins. The resulting mixture was stirred for 2 h at room temperature. After completion of the reaction (TLC), the reaction mixture was quenched with 1N HCl (3 mL). The organic layer was separated, washed with saturated sodium bicarbonate solution (2 x 3 mL), brine (3 mL), dried (Na_2SO_4), concentrated under reduced pressure, and purified by flash column chromatography (ethyl acetate:n-hexanes; 1:6) on silica gel to get **15g** as a colorless liquid (0.295 g, 88%).

Spectral data. ^1H NMR ($CDCl_3$, 400 MHz) δ 7.70-7.68 (dd, *J* = 2.20 Hz, 7.16 Hz, 1H), 7.43-7.41 (m, 2H), 7.31-7.21 (m, 6H), 6.79 (s, 1H), 6.04-5.96 (m, 1H), 5.12-5.05 (m, 2H), 3.61-3.59 (dt, *J* = 1.2, 6.3 Hz, 2H), 1.23 (s, 9H); ^{13}C NMR ($CDCl_3$, 100 MHz) δ 176.96, 137.80, 136.53, 135.53, 131.78, 130.07, 128.84, 128.20, 128.16, 127.58, 126.68, 122.32, 116.34, 86.54, 86.02, 63.67, 38.78, 36.64, 27.01; HRMS (ESI) calculated for $C_{23}H_{24}O_2$ $[M]^+$ 332.1776, Found: 332.1777.

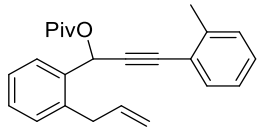

15h

1-(2-allylphenyl)-3-(*o*-tolyl)prop-2-yn-1-yl pivalate

To a solution of 1-(2-allylphenyl)-3-(o-tolyl)prop-2-yn-1-ol (0.260 g, 1.0 mmol) in CH2Cl2 (5 mL) was added triethylamine (0.28 mL, 2.0 mmol) and DMAP (0.012 g, 0.10 mmol) at room temperature. The reaction mixture was cooled to 0 ^{o}C, and added trimethylacetyl chloride (0.132 mL, 1.10 mmol) over a period of 5 mins. The resulting mixture was stirred for 2 h at room temperature. After completion of the reaction (TLC), the reaction mixture was quenched with 1N HCl (3 mL). The organic layer was separated, washed with saturated sodium bicarbonate solution (2 x 3 mL), brine (3 mL), dried (Na_2SO_4), concentrated under reduced pressure, and purified by flash column chromatography (ethyl acetate:n-hexanes; 1:6) on silica gel to get **15h** as a colorless liquid (0.310 g, 9.0 mmol, 90%).

Spectral data. ^{1}H NMR ($CDCl_3$, 400 MHz) δ 7.70 (d, *J* = 1.6, 7.1 Hz, 1H), 7.33-7.22 (dd, *J* = 2.1 Hz, 7.1 Hz, 1H), 7.11 (m, 5H), 7.09 (dt, J = 1.6, 7.3 Hz, 2H), 6.77 (s, 1H), 6.06-5.96 (m, 1H), 5.12-5.05 (m, 2H), 3.60 (dt, *J* = 1.6 Hz, 6.3 Hz, 2H), 2.34 (s, 3H), 1.23 (s, 9H); ^{13}C NMR ($CDCl_3$, 100 MHz) δ 177.04, 138.73, 137.85, 136.59, 135.67, 130.05, 129.14, 128.94, 128.79, 128.22, 127.68, 126.67, 119.29, 116.33, 86.72, 85.33, 63.79, 38.81, 36.64, 27.03, 21.46; HRMS (ESI) calculated for $C_{24}H_{26}O_2$ $[M]^+$.346.1932, Found: 346.1933.

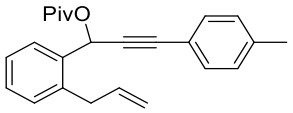

15i

1-(2-allylphenyl)-3-(*p*-tolyl)prop-2-yn-1-yl pivalate

To a solution of 1-(2-allylphenyl)-3-(p-tolyl)prop-2-yn-1-ol (0.260 g, 1.0 mmol) in CH2Cl2 (5 mL) was added triethylamine (0.28 mL, 2.0 mmol) and DMAP (0.012 g, 0.10 mmol) at room temperature. The reaction mixture was cooled to 0 ^{o}C, and added trimethylacetyl chloride

(0.132 mL, 1.10 mmol) over a period of 5 mins. The resulting mixture was stirred for 2 h at room temperature. After completion of the reaction (TLC), the reaction mixture was quenched with 1N HCl (3 mL). The organic layer was separated, washed with saturated sodium bicarbonate solution (2 x 3 mL), brine (3 mL), dried (Na_2SO_4), concentrated under reduced pressure, and purified by flash column chromatography (ethyl acetate:n-hexanes; 1:6) on silica gel to get **15i** as a yellow liquid (0.320 g, 9.2 mmol, 92%).

Spectral data. ^{1}H NMR ($CDCl_3$, 400 MHz) δ 7.70 (dd, *J* = 2.1 Hz, 7.2 Hz, 1H) 7.33-7.22(dd, *J* = 1.0 Hz, 7.2 Hz, 1H), 7.11 (m, 5H), 7.09 (d, J = 2.4 Hz, 2H), 6.77 (s, 1H), 6.06-5.96 (m, 1H), 5.12-5.05 (m, 2H), 3.60 (dt, *J* = 1.6 Hz, 6.3 Hz, 2H), 2.34 (s, 3H), 1.23 (s, 9H); ^{13}C NMR ($CDCl_3$, 100 MHz) δ 177.04, 138.73, 137.85, 136.59, 135.67, 131.73, 130.05, 128.94, 128.79, 128.22, 126.67, 119.29, 116.33, 86.72, 85.33, 63.79, 38.81, 36.64, 27.03, 21.46; HRMS (ESI) calculated for $C_{24}H_{26}O_2$ $[M]^+$. 346.1932, Found: 346.1933

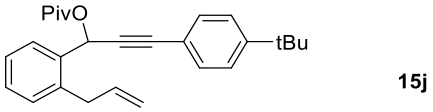

15j

1-(2-allylphenyl)-3-(4-(*tert*-butyl)phenyl)prop-2-yn-1-yl pivalate

To a solution of 1-(2-allylphenyl)-3-(4-(tert-butyl)phenyl)prop-2-yn-1-ol (0.300 g, 1.0 mmol) in CH2Cl2 (5 mL) was added triethylamine (0.28 mL, 2.0 mmol) and DMAP (0.012 g, 0.10 mmol) at room temperature. The reaction mixture was cooled to 0 ^{o}C, and added trimethylacetyl chloride (0.132 mL, 1.10 mmol) over a period of 5 mins. The resulting mixture was stirred for 2 h at room temperature. After completion of the reaction (TLC), the reaction mixture was quenched with 1N HCl (3 mL). The organic layer was separated, washed with saturated sodium bicarbonate solution (2 x 3 mL), brine (3 mL), dried (Na_2SO_4), concentrated under reduced pressure, and purified by flash column chromatography (ethyl acetate:n-hexanes; 1:6) on silica gel to get **15j** as a colorless liquid (0.330 g, 8.5 mmol, 85%).

Spectral data. ^{1}H NMR ($CDCl_3$, 400 MHz) δ 7.70-7.68 (d, *J* = 1.7, 6.8 Hz, 1H) 7.37-7.21 (m, 7H), 6.77 (s, 1H), 6.04-5.96 (m, 1H), 5.12-5.05 (m, 2H), 3.60 (dt, *J* = 1.5, 6.5 Hz, 2H), 1.29 (s, 9H), 1.23 (s, 9H); ^{13}C NMR ($CDCl_3$, 100 MHz) δ 177.02, 152.60, 127.60, 137.86, 136.60, 135.66, 131.58, 130.05, 126.66, 125.19, 119.35, 116.35, 86.71, 85.38, 63.81, 38.80, 36.65, 34.76, 31.12, 27.04; HRMS (ESI) calculated for $C_{24}H_{26}O_2$ $[M]^+$. 388.5510, Found: 388.5511.

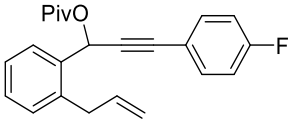

15k

1-(2-allylphenyl)-3-(4-fluorophenyl)prop-2-yn-1-yl pivalate

To a solution of 1-(2-allylphenyl)-3-(4-fluorophenyl)prop-2-yn-1-ol (0.265 g, 1.0 mmol) in CH2Cl2 (5 mL) was added triethylamine (0.28 mL, 2.0 mmol) and DMAP (0.012 g, 0.10 mmol) at room temperature. The reaction mixture was cooled to 0 ºC, and added trimethylacetyl chloride (0.132 mL, 1.10 mmol) over a period of 5 mins. The resulting mixture was stirred for 2 h at room temperature. After completion of the reaction (TLC), the reaction mixture was quenched with 1N HCl (3 mL). The organic layer was separated, washed with saturated sodium bicarbonate solution (2 x 3 mL), brine (3 mL), dried (Na_2SO_4), concentrated under reduced pressure, and purified by flash column chromatography (ethyl acetate:n-hexanes; 1:6) on silica gel to get **15k** as a colorless liquid (0.273 g, 7.8 mmol, 78%).

Spectral data. ^{1}H NMR ($CDCl_3$, 400 MHz) δ 7.67 (dd, *J* = 2.0, 7.1 Hz, 1H), 7.42-7.37 (m, 2H), 7.30-7.27 (dt, *J* = 1.8, 6.6 Hz, 2H), 7.23-7.21 (dd, *J* = 2.6, 8.0 Hz, 1H), 6.98 (t, *J* = 8.6 Hz, 2H), 6.76 (s, 1H), 6.06-5.96 (m, 1H), 5.12-5.04 (m, 2H), 3.59 (dt, *J* = 1.6 Hz, 6.3 Hz, 2H), 1.23 (s, 9H); ^{13}C NMR ($CDCl_3$, 100 MHz**)** δ 177.01, 137.60, 136.53, 133.81, 133.73, 130.13, 128.91, 128.16, 126.73, 118.43, 116.37, 115.61, 115.39, 85.79, 85.47, 63.60, 38.81, 36.65, 27.01; HRMS (ESI) calculated for $C_{23}H_{23}FO_2$ $[M]^+$ 350.1682, Found: 350.1682.

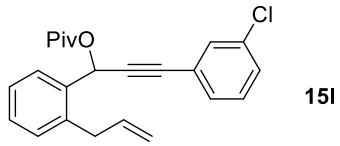

15l

1-(2-allylphenyl)-3-(3-chlorophenyl)prop-2-yn-1-yl pivalate

To a solution of 1-(2-allylphenyl)-3-(3-chlorophenyl)prop-2-yn-1-ol (0.280 g, 1.0 mmol) in CH2Cl2 (5 mL) was added triethylamine (0.28 mL, 2.0 mmol) and DMAP (0.012 g, 0.10 mmol) at room temperature. The reaction mixture was cooled to 0 ^{o}C, and added trimethylacetyl chloride (0.132 mL, 1.10 mmol) over a period of 5 mins. The resulting mixture was stirred for 2 h at room temperature. After completion of the reaction (TLC), the reaction mixture was quenched with 1N HCl (3 mL). The organic layer was separated, washed with saturated sodium bicarbonate solution (2 x 3 mL), brine (3 mL), dried (Na_2SO_4), concentrated under reduced pressure, and purified by flash column chromatography (ethyl acetate:n-hexanes; 1:6) on silica gel to get **15l** as a colorless liquid (0.293 g, 8.0 mmol, 80%).

Spectral data. ^{1}H NMR ($CDCl_3$, 400 MHz) δ 7.68-7.65 (dd, *J* = 2.0 Hz, 7.5 Hz, 1H), 7.41 (dt, *J* = 2.8 Hz, 7.4 Hz, 1H), 7.34-7.19 (m, 6H), 6.76 (s, 1H), 6.05-5.95(m, 1H), 5.13-5.04 (m, 2H), 3.59 (dt, *J* = 1.6, 6.3 Hz, 1H), 1.23 (s, 9H); ^{13}C NMR ($CDCl_3$, 100 MHz) δ 176.97, 17.77, 136.48, 135.25, 134.05, 131.65, 130.16, 129.92, 129.43, 128.98, 128.88, 128.16, 126.77, 124.01, 116.40, 87.28, 85.05, 83.45, 38.80, 36.65, 27.01. HRMS (ESI) calculated for $C_{23}H_{23}ClO_2$ $[M]^+$ 366.1386, Found: 366.1387.

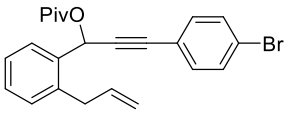

15m

1-(2-allylphenyl)-3-(4-bromophenyl)prop-2-yn-1-yl pivalate

To a solution of 1-(2-allylphenyl)-3-(4-bromophenyl)prop-2-yn-1-ol (0.325 g, 1.0 mmol) in CH2Cl2 (5 mL) was added triethylamine (0.28 mL, 2.0 mmol) and DMAP (0.012 g, 0.10 mmol) at room temperature. The reaction mixture was cooled to 0 ^{o}C, and added trimethylacetyl chloride

(0.132 mL, 1.10 mmol) over a period of 5 mins. The resulting mixture was stirred for 2 h at room temperature. After completion of the reaction (TLC), the reaction mixture was quenched with 1N HCl (3 mL). The organic layer was separated, washed with saturated sodium bicarbonate solution (2 x 3 mL), brine (3 mL), dried (Na_2SO_4), concentrated under reduced pressure, and purified by flash column chromatography (ethyl acetate:n-hexanes; 1:6) on silica gel to get **15m** as a colorless liquid (0.295 g, 7.2 mmol, 72%).

Spectral data. ^{1}H NMR ($CDCl_3$, 400 MHz) δ 7.65 (dd, *J* = 1.5 Hz, 7.5 Hz, 1H), 7.43-7.41 (d, *J* = 7.9 Hz, 2H), 7.34-7.22 (m, 5H), 6.75 (s, 1H), 6.03-5.95 (m, 1H), 5.12-5.04 (m, 2H), 3.58 (d, *J* = 6.3 Hz, 1H), 1.22 (s, 9H); ^{13}C NMR ($CDCl_3$, 100 MHz) δ 177.00, 137.80, 136.52, 135.30, 133.24, 131.48, 130.16, 128.17, 126.75, 122.92, 121.28, 87.22, 85.44, 63.58, 63.55, 38.81, 36.65, 27.03, 27.01; HRMS (ESI) calculated for $C_{23}H_{23}BrO_2$ $[M]^+$ 410.0881, Found: 410.0881

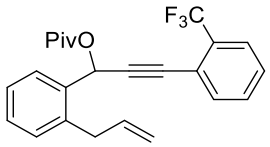

15n

1-(2-allylphenyl)-3-(2-(trifluoromethyl)phenyl)prop-2-yn-1-yl pivalate

To a solution of 1-(2-allylphenyl)-3-(2-(trifluoromethyl)phenyl)prop-2-yn-1-ol (0.310 g, 1.0 mmol) in CH2Cl2 (5 mL) was added triethylamine (0.28 mL, 2.0 mmol) and DMAP (0.012 g, 0.10 mmol) at room temperature. The reaction mixture was cooled to 0 ^{o}C, and added trimethylacetyl chloride (0.132 mL, 1.10 mmol) over a period of 5 mins. The resulting mixture was stirred for 2 h at room temperature. After completion of the reaction (TLC), the reaction mixture was quenched with 1N HCl (3 mL). The organic layer was separated, washed with saturated sodium bicarbonate solution (2 x 3 mL), brine (3 mL), dried (Na_2SO_4), concentrated under reduced pressure, and purified by flash column chromatography (ethyl acetate:n-hexanes; 1:6) on silica gel to get **15n** as a yellow liquid (0.264 g, 6.6 mmol, 66%).

Spectral data. ^{1}H NMR ($CDCl_3$, 400 MHz) δ 7.10 (dd, *J* = 2.9 Hz, 7.6 Hz, 1H), 7.61-7.53 (dd, *J* = 1.0 Hz, 6.8 Hz, 2H), 7.45-7.36 (tt, *J* = 1.0 Hz, 7.6 Hz, 2H), 7.30-7.24 (m, 3H), 6.80 (s, 1H), 6.01 (m, 1H), 5.12-5.03 (m, 2H), 3.58 (d, *J* = 7.68 Hz, 2H), 1.24 (s, 9H); ^{13}C NMR ($CDCl_3$, 100 MHz) δ 176.97, 137.83, 136.50, 134.94, 133.97, 131.28, 130.04, 129.03, 128.44, 128.31, 126.77, 125.76, 125.71, 122.01, 120.59, 116.38, 91.72, 82.42, 63.38, 38.81, 36.64, 26.98; HRMS (ESI) calculated for $C_{24}H_{23}F_3O_2$ $[M]^+$. 400.1650, Found: 400.1651.

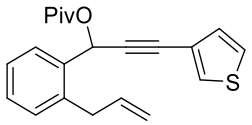

15o

1-(2-allylphenyl)-3-(thiophen-3-yl)prop-2-yn-1-yl pivalate

To a solution of 1-(2-allylphenyl)-3-(thiophen-3-yl)prop-2-yn-1-ol (0.250 g, 1.0 mmol) in CH2Cl2 (5 mL) was added triethylamine (0.28 mL, 2.0 mmol) and DMAP (0.012 g, 0.10 mmol) at room temperature. The reaction mixture was cooled to 0 ^{o}C, and added trimethylacetyl chloride (0.132 mL, 1.10 mmol) over a period of 5 mins. The resulting mixture was stirred for 2 h at room temperature. After completion of the reaction (TLC), the reaction mixture was quenched with 1N HCl (3 mL). The organic layer was separated, washed with saturated sodium bicarbonate solution (2 x 3 mL), brine (3 mL), dried (Na_2SO_4), concentrated under reduced pressure, and purified by flash column chromatography (ethyl acetate:n-hexanes; 1:6) on silica gel to get **15o** as a yellow liquid (0.287 g, 8.5 mmol, 85%).

Spectral data. ^{1}H NMR ($CDCl_3$, 400 MHz) δ 7.68-7.67 (dd, *J* = 1.9 Hz, 7.3 Hz, 1H), 7.45-7.44 (dd, *J* = 1.0 Hz, 3.0 Hz, 1H), 7.33-7.22 (m, 4H), 7.10 (dd, *J* = 1.3, 5.0 Hz, 1H), 6.76 (s, 1H), 6.06-5.96 (m, 1H), 5.12-5.04 (m, 2H), 3.60 (d, *J* = 7.0 Hz, 2H), 1.23 (s, 9H); ^{13}C NMR ($CDCl_3$, 100 MHz) δ 177.02, 137.80, 136.55, 135.54, 130.09, 129.93, 129.48, 128.85, 128.17, 126.70, 125.22, 121.38, 116.35, 85.63, 81.73, 63.71, 38.80, 36.64, 27.03; HRMS (ESI) calculated for $C_{21}H_{22}O_2S$ $[M]^+$ 338.1340, Found: 338.1341

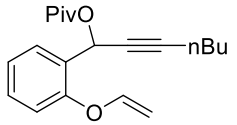

22b

1-(2-(vinyloxy)phenyl)hept-2-yn-1-yl pivalate

To a solution of 1-(2-allylphenyl)-3-(thiophen-3-yl)prop-2-yn-1-ol (0.230 g, 1.0 mmol) in CH2Cl2 (5 mL) was added triethylamine (0.28 mL, 2.0 mmol) and DMAP (0.012 g, 0.10 mmol) at room temperature. The reaction mixture was cooled to 0 ^{o}C, and added trimethylacetyl chloride (0.132 mL, 1.10 mmol) over a period of 5 mins. The resulting mixture was stirred for 2 h at room temperature. After completion of the reaction (TLC), the reaction mixture was quenched with 1N HCl (3 mL). The organic layer was separated, washed with saturated sodium bicarbonate solution (2 x 3 mL), brine (3 mL), dried (Na_2SO_4), concentrated under reduced pressure, and purified by flash column chromatography (ethyl acetate:n-hexanes; 1:6) on silica gel to get **22b** as a yellow liquid (0.276 g, 8.8 mmol, 88%).

Spectral data. ^{1}H NMR ($CDCl_3$, 400 MHz) δ 7.66-7.64 (dd, *J* = 2.4 Hz, 7.6 Hz, 1H), 7.32-7.28 (dt, *J* = 1.8 Hz, 7.4 Hz, 1H), 7.14 (dt, *J* = 2.2 Hz, 8.0 Hz, 1H), 7.00-6.97 (dd, *J* = 1.5 Hz, 9.8 Hz, 1H), 6.66-6.61 (dd, *J* = 5.7 Hz, 13.2 Hz, 1H), 4.79-7.75 (dd, *J* = 1.9 Hz, 13.9 Hz, 1H), 4.49-4.47 (dd, *J* = 1.3 Hz, 5.4 Hz, 1H), 2.29-2.24 (dt, *J* = 1.6 Hz, 6.3 Hz, 2H), 1.54-1.37 (m, 4H), 0.91(t, 3H); ^{13}C NMR ($CDCl_3$, 100 MHz) δ 176.86, 153.90, 148.24, 131.14, 129.50, 128.19, 123.58, 116.68, 95.63, 87.30, 79.13, 60.47, 30.62, 21.92, 18.51, 13.56; HRMS (ESI) calculated for $C_{20}H_{26}O_3$ $[M]^+$ 314.1881, Found 314.1882.

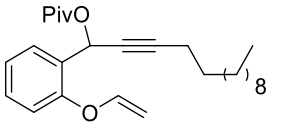

22c

1-(2-(vinyloxy)phenyl)hept-2-yn-1-yl pivalate

To a solution of 1-(2-(vinyloxy)phenyl)hept-2-yn-1-ol (0.310 g, 1.0 mmol) in CH2Cl2 (5 mL) was added triethylamine (0.28 mL, 2.0 mmol) and DMAP (0.012 g, 0.10 mmol) at room temperature. The reaction mixture was cooled to 0 ^{o}C, and added trimethylacetyl chloride (0.132 mL, 1.10 mmol) over a period of 5 mins. The resulting mixture was stirred for 2 h at room temperature. After completion of the reaction (TLC), the reaction mixture was quenched with 1N HCl (3 mL). The organic layer was separated, washed with saturated sodium bicarbonate solution (2 x 3 mL), brine (3 mL), dried (Na_2SO_4), concentrated under reduced pressure, and purified by flash column chromatography (ethyl acetate:n-hexanes; 1:6) on silica gel to get **22c** as a yellow liquid (0.350, 8.8 mmol, 88%).

Spectral data. ^{1}H NMR ($CDCl_3$, 400 MHz) δ 7.72-7.70 (dd, *J* = 2.4 Hz, 7.6 Hz, 1H), 7.33-7.29 (dt, *J* = 2.0, 7.9 Hz, 1H), 7.13-7.10 (dt, *J* = 1.9 Hz, 7.9 Hz, 1H), 6.98-6.95 (dd, *J* = 1.0, 8.0 Hz, 1H), 6.70 (t, *J* = 2.5 Hz, 1H), 6.60-6.55 (dd, *J* = 6.4, 13.9 Hz, 1H), 4.72-4.68 (dd, *J* = 1.6, 13.9 Hz, 1H), 4.42-4.40 (dd, *J* = 2.0 Hz, 6.4 Hz, 1H), 2.26 (dt, *J* = 1.6 Hz, 6.3 Hz, 2H), 1.55-1.26 (m, 18H), 1.19 (s, 9H), 0.87 (t, *J* = 8.2 Hz, 3H); ^{13}C NMR ($CDCl_3$, 100 MHz) δ 176.80, 153.92, 148.14, 129.83, 128.93, 127.81, 123.22, 116.48, 95.27, 87.72, 76.47, 60.77, 38.61, 31.85, 29.46, 29.23, 29.07, 29.06, 28.74, 28.68, 28.43, 27.02, 22.62, 18.79, 14.06; HRMS (ESI) calculated for $C_{26}H_{28}O_3$ $[M]^+$ 398.2821, Found 398.2822.

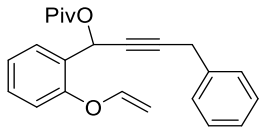

22d

4-phenyl-1-(2-(vinyloxy)phenyl)but-2-yn-1-yl pivalate

To a solution of 4-phenyl-1-(2-(vinyloxy)phenyl)but-2-yn-1-ol (0.260 g, 1.0 mmol) in CH2Cl2 (5 mL) was added triethylamine (0.28 mL, 2.0 mmol) and DMAP (0.012 g, 0.10 mmol) at room temperature. The reaction mixture was cooled to 0 ^{o}C, and added trimethylacetyl chloride (0.132 mL, 1.10 mmol) over a period of 5 mins. The resulting mixture was stirred for 2 h at room temperature. After completion of the reaction (TLC), the reaction mixture was quenched with 1N HCl (3 mL). The organic layer was separated, washed with saturated sodium bicarbonate solution (2 x 3 mL), brine (3 mL), dried (Na_2SO_4), concentrated under reduced pressure, and purified by flash column chromatography (ethyl acetate:n-hexanes; 1:6) on silica gel to get **22d** as a yellow liquid (0.265 g, 7.6 mmol, 76%).

Spectral data. ^{1}H NMR ($CDCl_3$, 400 MHz) δ 7.73-7.71 (dd, J = 1.8, 7.2 Hz, 1H), 7.29 (m, 6H), 7.21 (d, J = 8.1 Hz, 1H), 7.11 (t, J = 7.3 Hz, 1H), 6.97 (d, J = 7.3 Hz, 1H), 6.78 (t, J = 2.2 Hz, 1H) ,6.58 (dd, J = 5.0, 13.1 Hz, 1H), 4.70 (dd, J = 1.4, 13.6 Hz, 1H), 4.43 (dd, J = 1.4, 6.0 Hz, 1H), 1.23 (s, 9H); ^{13}C NMR ($CDCl_3$, 100 MHz) δ 176.87, 153.92, 148.09, 136.19, 129.97, 129.34, 128.91, 128.40, 127.81, 127.49, 126.54, 123.28, 116.50, 95.44, 84.81, 78.91, 60.77, 38.69, 27.04; HRMS (ESI) calculated for $C_{23}H_{24}O_3$ $[M]^+$ 348.1725, Found 348.1724

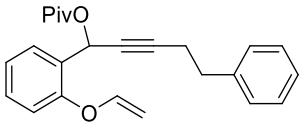

22e

5-phenyl-1-(2-(vinyloxy)phenyl)pent-2-yn-1-yl pivalate

To a solution of 5-phenyl-1-(2-(vinyloxy)phenyl)pent-2-yn-1-ol (0.280 g, 1.0 mmol) in CH2Cl2 (5 mL) was added triethylamine (0.28 mL, 2.0 mmol) and DMAP (0.012 g, 0.10 mmol) at room temperature. The reaction mixture was cooled to 0 ^{o}C, and added trimethylacetyl chloride

(0.132 mL, 1.10 mmol) over a period of 5 mins. The resulting mixture was stirred for 2 h at room temperature. After completion of the reaction (TLC), the reaction mixture was quenched with 1N HCl (3 mL). The organic layer was separated, washed with saturated sodium bicarbonate solution (2 x 3 mL), brine (3 mL), dried (Na_2SO_4), concentrated under reduced pressure, and purified by flash column chromatography (ethyl acetate:n-hexanes; 1:6) on silica gel to get **22e** as a yellow liquid (0.254 g, 7.0 mmol, 70%).

Spectral data. ^{1}H NMR ($CDCl_3$, 400 MHz) δ 7.58-7.56 (dd, J = 1.8, 7.2 Hz, 1H), 7.33-7.19 (m, 6 H), 7.08 (dt, J = 1.0 Hz, 7.2 Hz, 1H), 6.97 (dd, J = 1.0, 8.4 Hz, 1H), 6.68 (t, J = 2.1 Hz, 1H), 6.57 (dd, J = 2.0, 13.6 Hz, 1H), 4.71-4.67 (dd, J = 2.0, 13.6 Hz, 1H), 4.42-4.40 (dd, J = 2.0, 6.0

Hz, 1H), 2.83 (t, J = 7.0 Hz, 2H), 2.56-2.52 (dt, J = 3.0, 7.5 Hz, 2H), 1.19 (s, 9H); ^{13}C NMR ($CDCl_3$, 100 MHz) δ 176.83, 153.86, 148.11, 140.43, 129.86, 128.96, 128.48, 128.29, 127.60, 127.45, 126.20, 123.24, 116.44, 95.34, 86.74, 60.67, 38.63, 34.74, 27.04, 21.02; HRMS (ESI) calculated for $C_{24}H_{26}O_3$ $[M]^+$ 362.1881, Found 362.1882

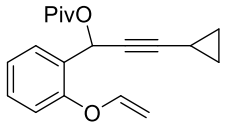

22f

3-cyclopropyl-1-(2-(vinyloxy)phenyl)prop-2-yn-1-yl pivalate

To a solution of 3-cyclopropyl-1-(2-(vinyloxy)phenyl)prop-2-yn-1-ol (0.210 g, 1.0 mmol) in CH2Cl2 (5 mL) was added triethylamine (0.28 mL, 2.0 mmol) and DMAP (0.012 g, 0.10 mmol) at room temperature. The reaction mixture was cooled to 0 ^{o}C, and added trimethylacetyl chloride (0.132 mL, 1.10 mmol) over a period of 5 mins. The resulting mixture was stirred for 2 h at room temperature. After completion of the reaction (TLC), the reaction mixture was quenched with 1N HCl (3 mL). The organic layer was separated, washed with saturated sodium bicarbonate solution (2 x 3 mL), brine (3 mL), dried (Na_2SO_4), concentrated under reduced pressure, and purified by

flash column chromatography (ethyl acetate:n-hexanes; 1:6) on silica gel to get **22f** as a yellow liquid (0.215 g, 7.2 mmol, 72%).

Spectral data. ^{1}H NMR ($CDCl_3$, 400 MHz) δ 7.67 (dd, *J* = 2.4 Hz, 7.6 Hz, 1H), 7.31 (dt, *J* = 1.0 Hz, 6.6 Hz, 1H), 7.10 (t, *J* = 2.0 Hz, 1H), 6.95 (d, *J* = 2.1 Hz, 1H), 6.66 (d, *J* =8.0 Hz, 1H), 6.59 (dd, *J* = 5.7 Hz, 13.2 Hz, 1H), 4.68 (dd, *J* = 2.0 Hz, 13.2 Hz, 1H), 4.41 (dd, *J* = 2.0 Hz, 6.2 Hz, 1H), 1.29 (m, 1H), 1.18 (s, 9H), 0.76(m, 4H); ^{13}C NMR ($CDCl_3$, 100 MHz) δ 176.81, 153.86, 148.15, 129.83, 129.33, 128.86, 127.80, 123.25, 116.53, 95.32, 90.65, 71.58, 60.75, 38.61, 27.02, 8.35, -0.39; HRMS (ESI) calculated for $C_{19}H_{22}O_3$ $[M]^+$. 298.1568, Found 298.1569.

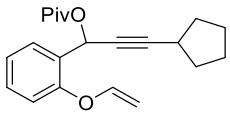

22g

3-cyclopentyl-1-(2-(vinyloxy)phenyl)prop-2-yn-1-yl pivalate

To a solution of 3-cyclopentyl-1-(2-(vinyloxy)phenyl)prop-2-yn-1-ol (0.240 g, 1.0 mmol) in CH2Cl2 (5 mL) was added triethylamine (0.28 mL, 2.0 mmol) and DMAP (0.012 g, 0.10 mmol) at room temperature. The reaction mixture was cooled to 0 ^{o}C, and added trimethylacetyl chloride (0.132 mL, 1.10 mmol) over a period of 5 mins. The resulting mixture was stirred for 2 h at room temperature. After completion of the reaction (TLC), the reaction mixture was quenched with 1N HCl (3 mL). The organic layer was separated, washed with saturated sodium bicarbonate solution (2 x 3 mL), brine (3 mL), dried (Na_2SO_4), concentrated under reduced pressure, and purified by flash column chromatography (ethyl acetate:n-hexanes; 1:6) on silica gel to get **22g** as a yellow liquid (0.235 g, 0.72 mmol, 72%).

Spectral data. ^{1}H NMR ($CDCl_3$, 400 MHz) δ 7.72 (d, *J* = 9.5 Hz, 1H), 7.31 (t, *J* = 8.9 Hz, 1H), 7.12(t, *J* = 8.9 Hz, 1H), 6.96 (d, *J* = 8.2 Hz, 1H), 6.71 (d, *J* = 2.1 Hz, 1H), 6.60-6.55(dd, *J* = 6.0, 13.6 Hz, 1H), 4.71-4.67 (dd, *J* = 2.0, 13.6 Hz, 1H), 4.42-4.40 (dd, *J* = 2.0, 5.7 Hz, 1H), 2.68 (dp, *J* = 1.6 Hz, 7.5 Hz, 1H), 1.89 (m, 2H), 1.72-1.52 (m, 8 H), 1.19 (s, 9H); ^{13}C NMR ($CDCl_3$, 100 MHz) δ 176.79, 153.98, 148.18, 129.84, 129.00, 127.85, 123.22, 116.52, 95.21, 91.94, 75.91, 60.82, 38.60, 33.66, 30.18, 27.01, 24.89. HRMS (ESI) calculated for $C_{21}H_{26}O_3$ $[M]^+$ 326.1881, Found 326.1882

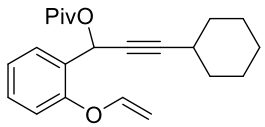

22h

3-cyclohexyl-1-(2-(vinyloxy)phenyl)prop-2-yn-1-yl pivalate

To a solution of 3-cyclohexyl-1-(2-(vinyloxy)phenyl)prop-2-yn-1-ol (0.260 g, 1.0 mmol) in CH2Cl2 (5 mL) was added triethylamine (0.28 mL, 2.0 mmol) and DMAP (0.012 g, 0.10 mmol) at room temperature. The reaction mixture was cooled to 0 ^{o}C, and added trimethylacetyl chloride (0.132 mL, 1.10 mmol) over a period of 5 mins. The resulting mixture was stirred for 2 h at room temperature. After completion of the reaction (TLC), the reaction mixture was quenched with 1N HCl (3 mL). The organic layer was separated, washed with saturated sodium bicarbonate solution (2 x 3 mL), brine (3 mL), dried (Na_2SO_4), concentrated under reduced pressure, and purified by flash column chromatography (ethyl acetate:n-hexanes; 1:6) on silica gel to get **22h** as a yellow liquid (0.230 g, 6.8 mmol, 68%).

Spectral data. ^{1}H NMR ($CDCl_3$, 400 MHz) δ 7.74 (d, *J* = 9.9 Hz, 1H), 7.32 (m, 1H), 7.12 (d, *J* = 8.2 Hz, 1H), 6.98 (d, *J* = 9.0 Hz, 1H), 6.72 (d, *J* = 2.2 Hz, 1H), 6.59 (dd, *J* = 5.7, 13.2 Hz, 1H), 4.71-4.67, (dd, *J* = 2.0, 13.6 Hz, 1H), 4.41 (dd, *J* = 2.0, 6.0 Hz, 1H), 2.46 (m, 2H), 1.76-1.67 (m, 4H), 1.47-1.30 (m, 4H), 1.20 (s, 9H); ^{13}C NMR ($CDCl_3$, 100 MHz) δ 176.76, 154.00, 148.17, 129.84, 129.04, 127.81, 123.21, 116.49, 95.21, 91.65, 76.51, 60.80, 38.60, 32.35, 28.95, 27.01, 25.84, 24.58; HRMS (ESI) calculated for $C_{22}H_{28}O_3$ $[M]^+$ 340.2038, Found 340.2038.

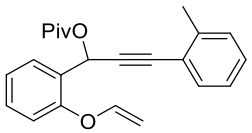

22i

3-(*o*-tolyl)-1-(2-(vinyloxy)phenyl)prop-2-yn-1-yl pivalate

To a solution of 3-(o-tolyl)-1-(2-(vinyloxy)phenyl)prop-2-yn-1-ol (0.270 g, 1.0 mmol) in CH2Cl2 (5 mL) was added triethylamine (0.28 mL, 2.0 mmol) and DMAP (0.012 g, 0.10 mmol) at room temperature. The reaction mixture was cooled to 0 ^{o}C, and added trimethylacetyl chloride (0.132 mL, 1.10 mmol) over a period of 5 mins. The resulting mixture was stirred for 2 h at room temperature. After completion of the reaction (TLC), the reaction mixture was quenched with 1N HCl (3 mL). The organic layer was separated, washed with saturated sodium bicarbonate solution (2 x 3 mL), brine (3 mL), dried (Na_2SO_4), concentrated under reduced pressure, and purified by flash column chromatography (ethyl acetate:n-hexanes; 1:6) on silica gel to get **22i** as a yellow liquid (0.272 g, 7.8 mmol, 78%).

Spectral data. ^{1}H NMR ($CDCl_3$, 400 MHz) δ 7.79-7.77 (dd, J = 1.4, 7.7 Hz, 1H), 7.37-6.99 (m, 7H), 6.93 (s, 1H), 6.64-6.60 (dd, J = 5.9, 13.6 Hz, 1H), 4.76-4.72 (dd, J = 2.0, 13.7 Hz, 1H), 4.45-4.44 (dd, J = 2.0, 6.0 Hz, 1H), 2.34 (s, 3H), 1.22 (s, 9H); ^{13}C NMR ($CDCl_3$, 100 MHz) δ 176.88, 153.97, 148.14, 138.71, 131.79, 130.06, 129.02, 128.94, 128.68, 127.38, 123.35, 119.36, 116.57, 95.50, 86.64, 84.75, 60.93, 38.73, 27.07, 21.48; HRMS (ESI) calculated for $C_{23}H_{24}O_3$ $[M]^+$ 348.1725, Found 348.1725

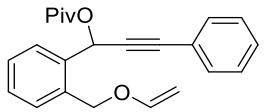

26b

3-phenyl-1-(2-((vinyloxy)methyl)phenyl)prop-2-yn-1-yl pivalate

To a solution of 3-phenyl-1-(2-((vinyloxy)methyl)phenyl)prop-2-yn-1-ol (0.250 g, 1.0 mmol) in CH2Cl2 (5 mL) was added triethylamine (0.28 mL, 2.0 mmol) and DMAP (0.012 g, 0.10 mmol) at room temperature. The reaction mixture was cooled to 0 ^{o}C, and added trimethylacetyl chloride (0.13 mL, 1.10 mmol) over a period of 10 mins. The resulting mixture was stirred for 2 h at room temperature. After completion of the reaction (TLC), the reaction mixture was quenched with 1N HCl (3 mL). The organic layer was separated, washed with saturated sodium bicarbonate solution (2 x 3 mL), brine (3 mL), dried (Na_2SO_4), concentrated under reduced pressure, and purified by flash column chromatography (ethyl acetate:n-hexanes; 1:6) on silica gel to get **26b** as a yellow liquid (0.250 g, 7.2 mmol, 72%).

Spectral data. ^{1}H NMR ($CDCl_3$, 400 MHz) δ 7.67 (d, *J* = 9.9 Hz, 1H), 7.48-7.29 (m, 9H), 6.76 (s, 1H), 6.60-6.56 (m, 1H), 5.05 (m, 2H), 4.36-4.34 (dt, *J* = 2.2, 13.0 Hz, 1H), 4.11 (m, 1H), 1.23 (s, 3H); ^{13}C NMR ($CDCl_3$, 100 MHz) δ 176.91, 151.43, 135.33, 134.99, 131.84, 129.18, 128.94, 128.87, 128.36, 128.29, 128.22, 122.18, 87.66, 86.89, 85.48, 67.26, 63.87, 38.83, 27.02; HRMS (ESI) calculated for $C_{23}H_{24}O_3$ $[M]^+$. 348.1725, Found 348.1725

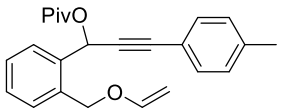

26c

3-(*p*-tolyl)-1-(2-((vinyloxy)methyl)phenyl)prop-2-yn-1-yl pivalate

To a solution of 3-(p-tolyl)-1-(2-((vinyloxy)methyl)phenyl)prop-2-yn-1-ol (0.260 g, 1.0 mmol) in CH2Cl2 (5 mL) was added triethylamine (0.28 mL, 2.0 mmol) and DMAP (0.012 g, 0.10 mmol) at room temperature. The reaction mixture was cooled to 0 ^{o}C, and added trimethylacetyl chloride (0.132 mL, 1.10 mmol) over a period of 5 mins. The resulting mixture was stirred for 2 h

at room temperature. After completion of the reaction (TLC), the reaction mixture was quenched with 1N HCl (3 mL). The organic layer was separated, washed with saturated sodium bicarbonate solution (2 x 3 mL), brine (3 mL), dried (Na_2SO_4), concentrated under reduced pressure, and purified by flash column chromatography (ethyl acetate:n-hexanes; 1:6) on silica gel to get **26c** as a yellow liquid (0.311 g, 8.6 mmol, 86%).

Spectral data. ^{1}H NMR ($CDCl_3$, 400 MHz) δ 7.67 (dd, *J* = 2.6, 7.9 Hz, 1H), 7.48 (m, 1H), 7.37-7.33 (m, 4H), 7.10 (m, 2H), 6.76 (s, 1H), 6.60 (m, 1H), 5.05 (m, 2H), 4.36-4.34 (dt, *J* = 2.2, 13.0 Hz, 1H), 4.11-4.10 (m, 1H), 2.33 (s, 3H), 1.23 (s, 9H); ^{13}C NMR ($CDCl_3$, 100 MHz) δ 176.89, 151.43, 138.86, 135.39, 134.99, 131.73, 128.96, 128.62, 128.34, 128.22, 119.06, 87.63, 87.08, 84.77, 67.22, 63.96, 38.80, 27.00, 21.45; HRMS (ESI) calculated for $C_{24}H_{26}O_3$ $[M]^+$. 362.1881, Found 362.1882.

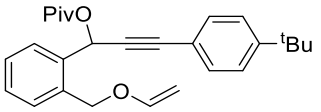

26d

3-(4-(*tert*-butyl)phenyl)-1-(2-((vinyloxy)methyl)phenyl)prop-2-yn-1-yl pivalate

To a solution of 3-(4-(tert-butyl)phenyl)-1-(2-((vinyloxy)methyl)phenyl)prop-2-yn-1-ol (0.320 g, 1.0 mmol) in CH2Cl2 (5 mL) was added triethylamine (0.28 mL, 2.0 mmol) and DMAP (0.012 g, 0.10 mmol) at room temperature. The reaction mixture was cooled to 0 ^{o}C, and added trimethylacetyl chloride (0.132 mL, 1.10 mmol) over a period of 5 mins. The resulting mixture was stirred for 2 h at room temperature. After completion of the reaction (TLC), the reaction mixture was quenched with 1N HCl (3 mL). The organic layer was separated, washed with saturated sodium bicarbonate solution (2 x 3 mL), brine (3 mL), dried (Na_2SO_4), concentrated under reduced pressure, and purified by flash column chromatography (ethyl acetate:n-hexanes; 1:6) on silica gel to get **26d** as a yellow liquid (0.320 g, 7.9 mmol, 79%).

Spectral data. ^{1}H NMR ($CDCl_3$, 400 MHz) δ 7.68 (m, 1H), 7.46-7.30 (m, 6H), 6.77 (s, 1H), 6.57 (m, 1H), 5.05 (m, 2H), 4.36 (dt, *J* = 2.2, 13.0 Hz, 1H) 4.11 (m, 1H), 1.28 (s, 9H), -1.22 (s, 9H), ^{13}C NMR ($CDCl_3$, 100 MHz) δ 176.78, 151.98, 151.39, 135.33, 134.99, 131.55, 128.84, 128.58, 128.33, 128.17, 125.18, 119.12, 87.60, 87.03, 84.79, 67.17, 63.95, 38.76, 34.70, 31.07, 26.98; HRMS (ESI) calculated for $C_{27}H_{32}O_3$ $[M]^+$. 404.2351, Found 404.2351.

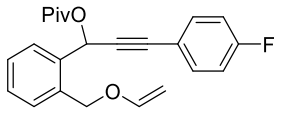

26e

3-(4-fluorophenyl)-1-(2-((vinyloxy)methyl)phenyl)prop-2-yn-1-yl pivalate

To a solution of 3-(4-fluorophenyl)-1-(2-((vinyloxy)methyl)phenyl)prop-2-yn-1-ol (0.280 g, 1.0 mmol) in CH2Cl2 (5 mL) was added triethylamine (0.28 mL, 2.0 mmol) and DMAP (0.012 g, 0.10 mmol) at room temperature. The reaction mixture was cooled to 0 ^{o}C, and added trimethylacetyl chloride (0.132 mL, 1.10 mmol) over a period of 5 mins. The resulting mixture was stirred for 2 h at room temperature. After completion of the reaction (TLC), the reaction mixture was quenched with 1N HCl (3 mL). The organic layer was separated, washed with saturated sodium bicarbonate solution (2 x 3 mL), brine (3 mL), dried (Na_2SO_4), concentrated under reduced pressure, and purified by flash column chromatography (ethyl acetate:n-hexanes; 1:6) on silica gel to get **26e** as a yellow liquid (0.315 g, 8.6 mmol, 86%).

Spectral data. ^{1}H NMR ($CDCl_3$, 400 MHz) δ 7.67-7.65 (dd, *J* = 2.4, 7.6 Hz, 1H), 7.47-7.36 (m, 5H), 6.79 (dt, *J* = 3.3, 9.2 Hz, 2H), 6.73 (s, 1H), 6.57 (m, 1H), 5.03 (dq, *J* = 3.1, 12.1 2H), 4.32 (dt, *J* = 2.2, 12.0 Hz, 1H), 4.10 (m, 1H), 1.22 (s, 9H); ^{13}C NMR ($CDCl_3$, 100 MHz) δ 176.90, 151.43, 135.32, 134.93, 133.85, 133.79, 128.98, 128.80, 128.35, 118.27, 115.62, 115.48, 87.66, 85.80, 85.26, 67.27, 63.79, 38.83, 27.02; HRMS (ESI) calculated for $C_{23}H_{23}O_3$ $[M]^+$ 366.1631, Found 366.1631.

Procedure for gold transformation reactions.

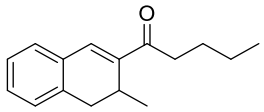

17b

1-(3-methyl-3,4-dihydronaphthalen-2-yl)pentan-1-one

To a solution of **15b** (0.265 g, 0.85 mmol) in toluene (4.3 mL) was added water (0.047 mL, 2.60 mmol) and di^{t}BuXPhosAuNTf$_2$ (0.015 g, 0.02 mmol). The reaction mixture was stirred for 12 h at room temperature and was monitored by TLC. After completion of the reaction, solvent was evaporated to get a crude mass. Purified on silica gel (CH2Cl2:n-hexanes; 1:5) to give **17b** as a colorless liquid (0.167 g, 7.3 mmol, 86%).

Spectral data. ^{1}H NMR ($CDCl_3$, 400 MHz) δ 7.34 (s, 1H), 7.29-7.17 (m, 4H), 3.19 (dp, *J* = 2.0, 7.2 Hz, 1H), 3.06-3.00 (dd, *J* = 7.8, 16.8 Hz, 1H), 2.78 (t, *J* = 6.8 Hz, 2H), 2.68-2.63 (dd, *J* = 2.4, 16.8 Hz, 1H), 1.71-1.63 (m, 2H), 1.44-1.33 (m, 2H), 0.95 (t, *J* = 6.4 Hz, 3H), 0.89-0.87 (d, *J* = 5.4 Hz, 3H); ^{13}C NMR ($CDCl_3$, 100 MHz) δ 200.60, 142.63, 135.97, 134.83, 132.01, 129.81, 128.77, 128.38, 126.57, 37.05, 34.99, 27.13, 25.77, 22.52, 17.91, 13.94; HRMS (ESI) calculated for $C_{16}H_{20}O$ $[M]^+$ 228.1514, Found 228.1514.

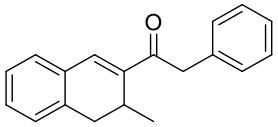

17c

1-(3-methyl-3,4-dihydronaphthalen-2-yl)-2-phenylethan-1-one

To a solution of **15c** (0.250 g, 0.72 mmol) in toluene (3.6 mL) was added water (0.040 mL, 2.20 mmol) and di^{t}BuXPhosAuNTf$_2$ (0.013 g, 0.02 mmol). The reaction mixture was stirred for 12 h at room temperature and was monitored by TLC. After completion of the reaction, solvent was evaporated under reduced pressure to get a crude mass. Purified on silica gel (CH2Cl2:hexanes, 1:5) to give **17c** as a yellow liquid (0.121 g, 4.6 mmol, 64%).

Spectral data. ^{1}H NMR ($CDCl_3$, 400 MHz) δ 7.45 (s, 1H), 7.34 -7.17 (m, 9H), 4.11 (s, 2H), 3.19 -3.12 (dp, *J* = 2.0, 7.2 Hz, 1H), 3.06-3.00 (dd, *J* = 16.2, 7.4 Hz, 1H), 2.6-2.63 (d, *J* = 2.0, 16.2 Hz, 1H), 0.87 (d, *J* = 7.0 Hz, 3H); ^{13}C NMR ($CDCl_3$, 100 MHz) δ 197.62, 142.35, 136.28, 136.08, 135.35, 132.06, 131.87, 130.11, 129.26, 128.85, 128.59, 127.19, 126.67, 44.29, 34.95, 25.95, 17.82; HRMS (ESI) calculated for $C_{19}H_{18}O$ $[M]^+$ 262.1357, Found 262.1358.

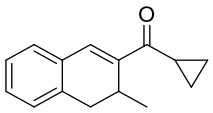

17d

cyclopropyl(3-methyl-3,4-dihydronaphthalen-2-yl)methanone

To a solution of **17d** (0.180 g, 0.60 mmol) in toluene (3 mL) was added water (0.032 mL, 1.80 mmol) and di^{t}BuXPhosAuNTf$_2$ (0.011 g, 0.02 mmol). The reaction mixture was stirred for 12 h at room temperature and was monitored by TLC. After completion of the reaction, solvent was evaporated under reduced pressure to get a crude mass. Purified on silica gel (CH2Cl2:n-hexanes; 1:6) to give **17d** as a yellow liquid (0.082 g, 3.9 mmol, 64%).

Spectral data. ^{1}H NMR ($CDCl_3$, 400 MHz) δ 7.51 (s, 1H), 7.28-7.18 (m, 4H), 3.18-3.11 (dp, *J* = 2.0, 7.5 Hz, 1H), 3.09-3.04 (dd, *J* = 6.7, 16.0 Hz, 1H), 2.69-2.65 (dd, *J* = 2.0, 16.0 Hz, 1H), 2.57-2.51 (s, 1H), 1.14-1.10 (m, 2H), 0.96-0.93 (m, 2H), 0.92-0.90 (d, *J* = 6.9 Hz, 3H); ^{13}C NMR ($CDCl_3$, 100 MHz) δ 203.9, 142.5, 136.0, 134.8, 132.1, 129.7, 128.7, 128.3, 126.5, 45.0, 35.0, 30.4, 26.3, 25.9, 17.9; HRMS (ESI) calculated for $C_{15}H_{16}O$ $[M]^+$ 212.1201, Found 212.1201.

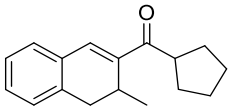

17e

cyclopentyl(3-methyl-3,4-dihydronaphthalen-2-yl)methanone

To a solution of **15e** (0.260 g, 0.80 mmol) in toluene (4 mL) was added water (0.043 mL, 2.40 mmol) and di^{t}BuXPhosAuNTf$_2$ (0.014 g, 0.02 mmol). The reaction mixture was stirred at room temperature for 12 h and was monitored by TLC. After completion of the reaction, solvent

was evaporated under reduced pressure to get a crude mass. Purified on silica gel (CH2Cl2:n-hexanes; 1:5) to give **17e** as a colorless liquid (0.152 g, 6.3 mmol, 79%).

Spectral data. ^{1}H NMR ($CDCl_3$, 400 MHz) δ 7.34 (s, 1H), 7.30-7.18 (m, 4H), 3.63-3.55 (p, *J* = 8.0 Hz, 1H), 3.20-3.12 (dp, *J* = 1.4, 7.0 Hz, 1H), 3.07-3.02 (dd, *J* = 7.0, 15.9 Hz, 1H), 2.68-2.64 (dd, *J* = 1.4, 15.9 Hz, 1H), 1.91-1.59 (m, 8H), 0.89-0.87 (d, *J* = 7.0 Hz, 3H); ^{13}C NMR ($CDCl_3$, 100 MHz) δ 202.94, 142.55, 136.00, 134.83, 132.15, 129.75, 128.78, 128.39, 126.56, 45.04, 35.02, 30.50, 26.34, 25.97, 17.92; HRMS (ESI) calculated for $C_{17}H_{20}O$ $[M]^+$ 240.1514, Found 240.1513

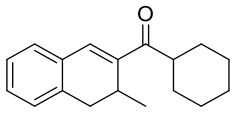

17f

cyclohexyl(3-methyl-3,4-dihydronaphthalen-2-yl)methanone

To a solution of **15f** (0.240 g, 0.70 mmol) in toluene (3.5 mL) was added water (0.038 mL, 2.10 mmol) and di^{t}BuXPhosAuNTf$_2$ (0.012 g, 0.02 mmol) The reaction stirred at room temperature for 12 h and was monitored by TLC. After completion of the reaction, solvent was evaporated under reduced pressure to get a crude mass. Purified on silica gel (CH2Cl2:n-hexanes; 1:8) to give **17f** as a colorless liquid (0.125 g, 4.9 mmol, 70%).

Spectral data. ^{1}H NMR ($CDCl_3$, 400 MHz) δ 7.34 (s, 1H), 7.30-7.18 (m, 4H), 3.63-3.55 (q, *J* = 8.5 Hz, 1H), 3.20-3.12 (dp, *J* = 1.7 Hz, 7.0 Hz, 1H), 3.07-3.02 (dd, *J* = 7.0 Hz, 15.0 Hz, 1H), 2.68-2.64 (dd, *J* = 1.0 Hz, 15.5 Hz, 1H), 1.91-1.59 (m, 10H), 0.89-0.87 (d, *J* = 7.9 Hz, 3H); ^{13}C NMR ($CDCl_3$, 100 MHz) δ 204.07, 141.68, 136.04, 134.06, 129.74, 128.67, 128.42, 126.57, 44.32, 35.00, 29.88, 29.82, 25.95, 25.90, 25.84, 17.93; HRMS (ESI) calculated for $C_{18}H_{22}O$ $[M]^+$ 254.1670, Found 254.1671.

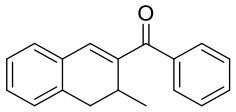

17g

(3-methyl-3,4-dihydronaphthalen-2-yl)(phenyl)methanone

To a solution of **15g** (0.200 g, 0.60 mmol) in CH2Cl2 (3 mL) was added water (0.032 mL,1.80 mmol) and di^{t}BuXPhosAuNTf$_2$ (0.011 g, 0.02 mmol). The reaction mixture was stirred at room temperature for 12 h and was monitored by TLC. After completion of the reaction, solvent was evaporated under reduced pressure to get a crude reaction mass. Purified on silica gel (CH2Cl2:n-hexanes; 1:5) to give **17g** as a yellow liquid (0.125 g, 5.0 mmol, 84%).

Spectral data. ^{1}H NMR ($CDCl_3$, 400 MHz) δ 7.72 (m, 1H), 7.57-7.53 (m, 1H), 7.47(m, 1H), 7.31-7.12(m, 4H), 7.04 (s, 1H), 3.27 (dp, *J* = 2.0, 7.2 Hz, 1H), 3.18 (dd, *J* = 16.7, 6.79 Hz, 1H), 2.74 (dd, *J* = 16.7, 2.4 Hz, 1H), 1.06 (d, *J* = 6.8 Hz, 3H); ^{13}C NMR ($CDCl_3$, 100 MHz) δ 197.2, 142.08, 139.0, 131.9, 131.5, 130.01, 129.1, 128.8, 128.5, 128.19, 126.6, 125.60, 35.2, 27.3, 18.0; HRMS (ESI) calculated for $C_{18}H_{16}O$ $[M]^+$ 248.1201, Found 248.1201.

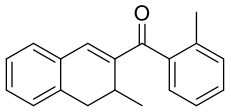

17h

(3-methyl-3,4-dihydronaphthalen-2-yl)(*o*-tolyl)methanone

To a solution of **15h** (0.210 g, 0.60 mmol) in CH2Cl2 (3 mL) was added water (0.032 mL, 1.80 mmol) and di^{t}BuXPhosAuNTf$_2$ (0.011 g, 0.02 mmol). The reaction stirred at room temperature for 12 h and was monitored by TLC. After completion of the reaction, solvent was evaporated under reduced pressure to get a crude reaction mass. Purified on silica gel (CH2Cl2:n-hexanes; 1:5) to give **17h** as a yellow liquid (0.127 g, 4.9 mmol, 81%).

Spectral data. ^{1}H NMR ($CDCl_3$, 400 MHz) δ 7.35 (m, 1H), 7.30-7.15 (m, 6H), 7.08-7.06 (dd, *J* = 1.1, 7.5 Hz, 1H), 6.90 (s, 1H), 3.38-3.31 (dp, *J* =2.0, 7.2 Hz, 1H), 3.18-3.12 (dd, *J* = 7.0, 15.9 Hz, 1H), 2.75 (dd, *J* = 1.8, 15.9 Hz, 1H), 2.32 (s, 3H), 1.04 (d, *J* = 6.8 Hz, 3H); ^{13}C NMR ($CDCl_3$, 100

MHz) δ 199.08, 143.14, 140.49, 139.46, 136.12, 135.69, 132.03, 130.65, 130.27, 129.82, 129.37, 128.79, 127.49, 126.62, 125.10, 35.04, 25.79, 19.49, 17.99; HRMS (ESI) calculated for $C_{19}H_{18}O$ $[M]^+$ 262.1357, Found 262.1358.

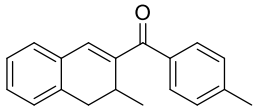

17i

(3-methyl-3,4-dihydronaphthalen-2-yl)(*p*-tolyl)methanone

To a solution of **15i** (0.242 g, 0.70 mmol) in CH2Cl2 (3.5 mL) was added water (0.038 mL, 2.10 mmol) and di^{t}BuXPhosAuNTf$_2$ (0.013 g, 0.02 mmol). The reaction stirred at room temperature for 12 h and was monitored by TLC. After completion of the reaction, solvent was evaporated under reduced pressure to get a crude mass. Purified on silica gel (CH2Cl2:n-hexanes; 1:5) to give **17i** as a yellow liquid (0.150 g, 5.7 mmol, 82%).

Spectral data. ^{1}H NMR ($CDCl_3$, 400 MHz) δ 7.35 (m, 1H), 7.30-7.15 (m, 6H), 7.08-7.06 (dd, *J* = 2.4 7.2 Hz, 1H), 6.90 (s, 1H), 3.38-3.31 (dp, *J* = 2.4, 7.28 Hz, 1H), 3.18-3.12 (dd, *J* = 16.7, 6.7 Hz, 1H), 2.75 (dd, *J* = 16.6 Hz, 1H), 2.32 (s, 3H), 1.04 (d, *J* = 6.8 Hz, 3H); ^{13}C NMR ($CDCl_3$, 100 MHz) δ 197.09, 142.16, 138.27, 136.04, 135.85, 132.03, 129.82, 129.35, 128.85, 128.42, 127.64, 126.62, 125.50, 35.28, 27.52, 21.55, 18.06; HRMS (ESI) calculated for $C_{19}H_{18}O$ $[M]^+$ 262.1357, Found 262.1357.

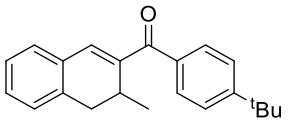

17j

(4-(*tert*-butyl)phenyl)(3-methyl-3,4-dihydronaphthalen-2-yl)methanone

To a solution of **15j** (0.272 g, 0.70 mmol) in CH2Cl2 (3.5 mL) was added water (0.038 mL, 2.10 mmol) and di^{t}BuXPhosAuNTf$_2$ (0.012 g, 0.02 mmol) The reaction stirred at room temperature for 12 h and was monitored by TLC. After completion of the reaction, the solvent was evaporated under reduced pressure to get a crude reaction mass. Purified on silica gel (CH2Cl2:n-hexanes; 1:5) to give **17j** as a colorless liquid (0.187 g, 6.2 mmol, 88%).

Spectral data. ^{1}H NMR ($CDCl_3$, 400 MHz) δ 7.69-7.68 (d, *J* = 7.6 Hz, 2H), 7.49-7.47 (d, *J* = 7.6 Hz, 2H), 7.28-7.14 (m, 4H), 7.06 (s, 1H), 3.26-3.23 (dq, *J* =6.8, 2.0 Hz, 1H), 3.20-3.16 (dd, *J* = 15.2, 6.9 Hz, 1H), 2.76-2.73 (dd, *J* = 15.2, 2.0 Hz, 1H), 1.37 (s, 9H), 1.05-1.04 (d, *J* = 7.3 Hz, 2H); ^{13}C NMR ($CDCl_3$, 100 MHz) δ 197.05, 155.21, 142.17, 138.29, 135.98, 135.87, 132.08, 129.81, 129.18, 128.77, 128.44, 126.61, 125.14, 35.29, 35.00, 31.18, 27.47, 18.08; HRMS (ESI) calculated for $C_{22}H_{24}O$ $[M]^+$ 304.1827, Found 304.1827

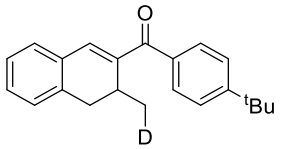

17jD

(4-(*tert*-butyl)phenyl)(3-(methyl-*d*)-3,4-dihydronaphthalen-2-yl)methanone

To a solution of **15j** (0.155 g, 0.4 mmol) in CH2Cl2 (2 mL) was added deuterated water (0.025 mL, 1.20 mmol) and di^{t}BuXPhosAuNTf$_2$ (0.007 g, 0.02 mmol). The reaction mixture was stirred for 14 h at room temperature, and was monitored by TLC. After completion of the reaction, solvent was evaporated under reduced pressure to get a crude reaction mass. Purified on silica gel (CH2Cl2:n-hexanes; 1:5) to give **17jD** as a colorless liquid (0.103 g, 3.4 mmol, 84%).

Spectral data. ^{1}H NMR ($CDCl_3$, 400 MHz) δ 7.69-7.68 (d, *J* = 9.7 Hz, 2H), 7.49-7.47 (d, *J* = 9.7 Hz, 2H), 7.28 (t, *J* = 8.6 Hz, 1H), 7.22-7.19 (dd, *J* = 7.5 Hz, 13.8 Hz, 2H), 7.16-7.15 (d, *J* = 8.0 Hz, 1H), 7.06 (s, 1H), 3.26-3.23 (dq, *J* =7.8 Hz, 2.24 Hz, 1H), 3.20-3.16 (dd, *J* = 16.0 Hz, 6.9 Hz, 1H), 2.76-2.73 (dd, *J* = 15.1, 2.0 Hz, 1H), 1.37 (s, 9H), 1.05-1.04 (d, *J* = 7.3 Hz, 2H); ^{13}C NMR ($CDCl_3$, 100 MHz) δ 197.07, 155.22, 142.19, 138.30, 136.00, 135.89, 132.09, 129.82, 129.19, 128.79, 128.45, 126.662, 125.16, 35.27, 35.01, 31.19, 27.42, 17.80 (t, *J* =17.50Hz); HRMS (ESI) calculated for $C_{22}H_{23}DO$ $[M]^+$ 306.1827, Found 306.1827.

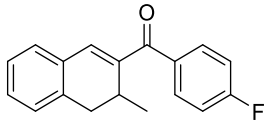

17k

(4-fluorophenyl)(3-methyl-3,4-dihydronaphthalen-2-yl)methanone

To a solution of **15k** (0.245 g, 0.70 mmol) in CH2Cl2 (3.5 mL) was added water (0.038 mL, 2.10 mmol) and di^{t}BuXPhosAuNTf$_2$ (0.013 g, 0.02 mmol). The reaction mixture was stirred at room temperature for 12 h and was monitored by TLC. After completion of the reaction, solvent was evaporated under reduced pressure to get a crude reaction mass. Purified on silica gel (CH2Cl2:n-hexanes; 1:5) to give **17k** as a yellow liquid (0.142 g, 5.3 mmol, 75%).

Spectral data. ^{1}H NMR ($CDCl_3$, 400 MHz) δ 7.75 (m, 1H), 7.31-7.13 (m, 6H), 7.01 (s, 1H), 3.28-3.14 (m, 2H), 2.77-2.73 (dd, *J* = 2.4, 16.0 Hz, 1H), 1.07-1.04 (d, *J* = 6.8 Hz, 3H); ^{13}C NMR ($CDCl_3$, 100 MHz) δ 195.84, 141.98, 138.74, 135.88, 134.92, 131.81, 131.54, 130.09, 128.84, 128.56, 126.70, 115.40, 115.19, 35.22, 27.55, 18.04; HRMS (ESI) calculated for $C_{18}H_{15}OF$ $[M]^+$ 266.1106, Found 266.1107; ^{19}F NMR ($CDCl_3$, 376 MHz) δ -109.46.

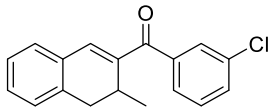

17l

(3-chlorophenyl)(3-methyl-3,4-dihydronaphthalen-2-yl)methanone

To a solution **15l** (0.257 g, 0.70 mmol) in CH2Cl2 (3.5 mL) was added water (0.038 mL, 2.10 mmol) and di^{t}BuXPhosAuNTf$_2$ (0.013 g, 0.02 mmol). The reaction mixture was stirred at room temperature for 12 h and was monitored by TLC. After completion of the reaction, solvent was evaporated under reduced pressure to get a crude mass. Purified on silica gel (CH2Cl2:n-hexanes; 1:5) to give **17l** colorless liquid (0.134 g, 4.8 mmol, 68%).

Spectral data. ^{1}H NMR ($CDCl_3$, 400 MHz) δ 7.68 (dt, *J* = 0.9, 2.4 Hz, 1H), 7.5-7.56 (tt, *J* = 1.3, 5.0 Hz, 2H), 7.53- 7.50 (m, 1H), 7.42-7.38 (t, *J* = 7.4 Hz, 1H), 7.21-7.19 (m, 3H), 7.04 (s, 1H), 3.28-3.21 (dp, *J* = 2.3, 7.1 Hz, 1H), 3.20-3.16 (dd, *J* = 7.2, 15.7 Hz, 1H), 2.76-2.73 (dd, *J* = 2.4, 15.7 Hz, 1H), 1.06-105 (d, *J* = 7.2 Hz, 3H); ^{13}C NMR ($CDCl_3$, 100 MHz) δ 195.66, 141.69, 140.50, 139.72, 135.97, 134.38, 131.67, 131.39, 130.31, 129.51, 129.00, 128.86, 128.76, 127.11, 126.73, 35.12, 27.26, 17.99; HRMS (ESI) calculated for $C_{18}H_{15}OCl$ $[M]^+$ 282.0811, Found 282.0812.

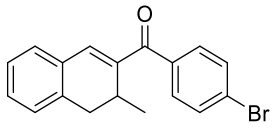

17m

(4-bromophenyl)(3-methyl-3,4-dihydronaphthalen-2-yl)methanone

To a solution of **15m** (0.245 g, 0.60 mmol) in CH2Cl2 (3 mL) was added water (0.032 mL, 1.80 mmol) and di^{t}BuXPhosAuNTf$_2$ (0.011 g, 0.02 mmol). The reaction mixture was stirred at room temperature for 12 h and was monitored by TLC. After completion of the reaction, solvent was evaporated under reduced pressure to get a crude mass. Purified on silica gel (CH2Cl2:n-hexanes;1:5) to give **17m** as a white solid (0.143 g, 4.4 mmol, 73%).

Spectral data. ^{1}H NMR ($CDCl_3$, 400 MHz) δ 7.60 (dd, *J* = 1.69, 7.2 Hz, 4H), 7.31-7.13 (m, 4H), 7.01 (s, 1H), 3.28 - 3.13 (m, 2H), 2.74 (dd, *J* = 2.4, 15.0 Hz, 1H), 1.06 (d, *J* = 6.5 Hz, 3H); ^{13}C

NMR ($CDCl_3$, 100 MHz) δ 196.08, 141.98, 138.74, 137.5, 135.9, 131.7, 131.4, 130.6, 130.2, 128.85, 128.6, 126.7, 126.2, 35.22, 27.55, 18.04; HRMS (ESI) calculated for $C_{18}H_{15}OBr$ $[M]^+$ 326.0306, Found 326.0307.

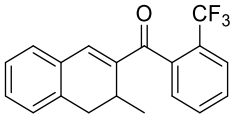

17n

(3-methyl-3,4-dihydronaphthalen-2-yl)(2-(trifluoromethyl)phenyl)methanone

To a solution of **15n** (0.200 g, 0.50 mmol) in CH2Cl2 (2.5 mL) was added water (0.027 mL, 1.50 mmol) and di^{t}BuXPhosAuNTf$_2$ (0.010 g, 0.02 mmol) The reaction stirred at room temperature for 12 h and was monitored by TLC. After completion of the reaction, solvent was evaporated under reduced pressure to get a crude reaction mass. Purified on silica gel (CH2Cl2:n-hexanes; 1:5) to give **17n** as a yellow liquid (0.076 g, 2.4 mmol, 48%).

Spectral data. ^{1}H NMR ($CDCl_3$, 400 MHz) δ 7.75 (dd, *J* = 1.6, 7.5 Hz, 1H), 7.61 (m, 2H), 7.39 (d, *J* = 6.8 Hz, 1H), 7.17-7.15 (m, 4 H), 7.07-7.05 (d, *J* = 6.8 Hz, 1H), 6.78 (s, 1H), 3.35 (dp, *J* = 1.6, 7.4 Hz, 1H), 3.18-3.13 (dd, *J* = 7.0, 16.0 Hz, 1H), 2.77 (dd, *J* = 1.6, 16.0 Hz, 1H), 1.03 (d, *J* = 7.1 Hz, 3H); ^{13}C NMR ($CDCl_3$, 100 MHz) δ 195.69, 142.79, 141.75, 136.29, 131.56, 131.28, 130.62, 129.32, 128.97, 128.90, 128.22, 126.67, 126.54, 126.55, 126.50, 126.46, 34.91, 25.88, 17.52; HRMS (ESI) calculated for $C_{19}H_{15}OF_3$ $[M]^+$ 316.1075, Found 316.1075. ^{19}F NMR ($CDCl_3$, 376 MHz) δ -61.09

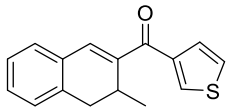

17o

(3-methyl-3,4-dihydronaphthalen-2-yl)(thiophen-3-yl)methanone

To a solution of **15o** (0.237 g, 0.70 mmol) in CH2Cl2 (3.5 mL) was added water (0.038 mL, 2.10 mmol) and di^{t}BuXPhosAuNTf$_2$ (0.013 g, 0.02 mmol) The reaction stirred at room temperature for 12 h and was monitored by TLC. After completion of the reaction, solvent was evaporated under reduced pressure to get a crude reaction mass. Purified on silica gel (CH2Cl2:n-hexanes; 1:5) to give **17o** as a yellow liquid (0.100 g, 3.9 mmol, 56%).

Spectral data. ^{1}H NMR ($CDCl_3$, 400 MHz) δ 7.88-7.87 (dd, *J* = 2.0, 4.0 Hz, 1H), 7.50 (dd, *J* = 1.4, 5.1 Hz, 1H), 7.37 (m, 1H), 7.30-7.17 (m, 5H), 3.25-3.13 (dp, *J* = 2.6, 7.0 Hz, 1H), 3.15-3.13 (d, *J* = 6.5, 15.7 Hz, 1H), 2.74-2.71 (dd, *J* = 1.6, 13.8 Hz, 1H), 1.06 (d, *J* = 1.6 Hz, 3H); ^{13}C NMR ($CDCl_3$, 100 MHz) δ 187.61, 143.09, 141.63, 137.31, 135.87, 131.94, 131.33, 129.86, 128.78, 128.44, 128.34, 126.64, 125.96, 35.25, 27.71, 18.11; HRMS (ESI) calculated for $C_{16}H_{14}OS$ $[M]^+$ 254.0765, Found 254.0764.

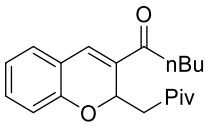

24b

1-(2-(3,3-dimethyl-2-oxobutyl)-2*H*-chromen-3-yl)pentan-1-one

To a solution of **22b** (0.252 g, 0.80 mmol) in CH2Cl2 (4 mL) was added water (0.043 mL, 2.40 mmol) and di^{t}BuXPhosAuNTf$_2$ (0.014 g, 0.02 mmol). The reaction mixture was stirred at room temperature for 5 h, and was monitored by TLC. After completion of the reaction, solvent was evaporated under reduced pressure to get a crude reaction mass. Purified on silica gel (CH2Cl2:n-hexanes; 1:5) to give **24b** as a yellow liquid (0.226 g, 7.2 mmol, 90%).

Spectral data. ^{1}H NMR ($CDCl_3$, 400 MHz) δ 7.34 (s,1H), 7.27-7.23 (m, 1H), 7.20-7.18 (dd, J = 7.7, 7.5 Hz, 1H), 6.96-6.92 (dt, *J* = 1.2, 7.5 Hz, 1H), 6.81-6.79 (d, *J* = 8.0 Hz, 1H), 5.95-5.93 (dd,

J = 2.5, 9.6 Hz, 1H), 3.20-3.13 (dd, *J* = 8.8 , 15.0 Hz, 1H), 2.74 (dt, *J* = 7.6 Hz, 2H), 2.33-2.29 (dd, *J* = 2.5, 16.0 Hz, 1H), 1.69 (m, 2H), 1.39 (m, 2H), 1.07 (s, 9H), 0.95 (t, 7.4 Hz, 3H); ^{13}C NMR ($CDCl_3$, 100 MHz) δ 210.95, 198.31, 153.26, 132.82, 132.53, 132.41, 128.96, 121.68, 120.19, 117.31, 70.12, 44.45, 39.52, 36.82, 26.67, 25.89, 22.43, 13.87; HRMS (ESI) calculated for $C_{20}H_{26}O_3$ $[M]^+$. 314.1881, Found 314.1882

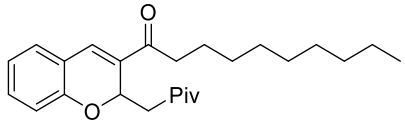

24c

1-(2-(3,3-dimethyl-2-oxobutyl)-2*H*-chromen-3-yl)decan-1-one

To a solution of **22c** (0.277 g, 0.70 mmol) in CH2Cl2 (3.5 mL) was added water (0.038 mL, 2.10 mmol) and di^{t}BuXPhosAuNTf$_2$ (0.013 g, 0.02 mmol). The reaction mixture was stirred at room temperature for 6 h, and was monitored by TLC. After completion of the reaction, solvent was evaporated under reduced pressure to get a crude reaction mass. Purified on silica gel (CH2Cl2:n-hexanes; 1:5) to give **24c** as a yellow liquid (0.232 g, 6.0 mmol, 86%).

Spectral data. ^{1}H NMR ($CDCl_3$, 400 MHz) δ 7.34 (s, 1H), 7.25-7.18 (m, 2H), 6.95-6.91 (dt, *J* = 1.7, 7.1 Hz, 1H), 6.79 (d, *J* = 8.5 Hz, 1H), 5.95 (dd, *J* = 2.5, 9.6 Hz, 1H), 3.20-3.13 (dd, *J* = 8.8, 15.0 Hz, 1H), 2.74 (dt, *J* = 7.6 Hz, 2H), 2.30 (dd, *J* = 2.5, 16.0 Hz,, 1H), 1.66 (m, 2H), 1.27 (m, 12H), 1.07 (s, 9H), 0.88 (t, *J* = 7.4 Hz, 3H); ^{13}C NMR ($CDCl_3$, 100 MHz) δ 210.91, 198.31, 153.26, 132.81, 132.51, 132.39, 128.95, 121.66, 120.19, 117.28, 70.11, 44.43, 39.50, 37.10, 31.81, 29.40, 29.30, 29.22, 25.87, 24.86, 24.56, 22.50, 14.05; HRMS (ESI) calculated for $C_{25}H_{36}O_3$ $[M]^+$. 384.2664, Found 384.2665.

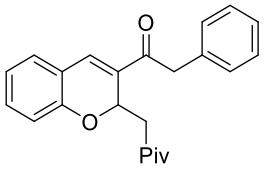

24d

3,3-dimethyl-1-(3-(2-phenylacetyl)-2*H*-chromen-2-yl)butan-2-one

To a solution of **22d** (0.209 g, 0.60 mmol) in CH2Cl2 (3 mL) was added water (0.032 mL, 1.80 mmol) and di^{t}BuXPhosAuNTf$_2$ (0.010 g, 0.02 mmol). The reaction mixture was stirred at room temperature for 8 h, and was monitored by TLC. After completion of the reaction, solvent was evaporated under reduced pressure to get a crude reaction mass. Purified on silica gel (CH2Cl2:n-hexanes; 1:5) to give **24d** as a yellow liquid (0.176 g, 5.0 mmol, 84%).

Spectral data. ^{1}H NMR ($CDCl_3$, 400 MHz) δ 7.46 (s, 1H) 7.35-7.18 (m, 6H), 7.20-7.18 (dd, *J* = 2.6, 8.0 Hz, 1H), 6.96-6.92 (dt, *J* = 1.0, 8.0 Hz, 1H), 6.80-6.78 (d, *J* = 8.0 Hz, 1H), 5.96-5.93 (dd, *J* = 2.8, 9.4 Hz, 1H), 4.07 (s, 2H), 3.18-3.11 (dd, *J* = 7.4, 16.0 Hz, 1H), 2.30-2.25 (dd, *J* = 2.4, 16.4 Hz, 1H), 1.04 (s, 9H); ^{13}C NMR ($CDCl_3$, 100 MHz) δ 210.68, 195.35, 153.32, 134.39, 133.67, 132.84, 132.46, 129.24, 129.16, 128.69, 126.94, 121.74, 120.06, 117.36, 70.15, 44.42, 44.12, 39.39, 25.88; HRMS (ESI) calculated for $C_{23}H_{24}O_3$ $[M]^+$ 348.1725, Found 348.1725.

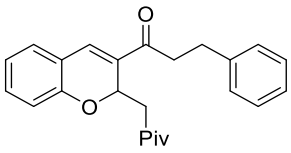

24e

3,3-dimethyl-1-(3-(3-phenylpropanoyl)-2*H*-chromen-2-yl)butan-2-one

To a solution of **22e** (0.217 g, 0.60 mmol) in CH2Cl2 (3 mL) was added water (0.032 mL, 1.80 mmol) and di^{t}BuXPhosAuNTf$_2$ (0.011 g, 0.02 mmol). The reaction mixture was stirred at room temperature for 8 h, and was monitored by TLC. After completion of the reaction, solvent was evaporated under reduced pressure to get a crude reaction mass. Purified on silica gel (CH2Cl2:n-hexanes;1:5) to give **24e** as a yellow liquid (0.187 g, 5.2 mmol, 86%).

Spectral data. ^{1}H NMR ($CDCl_3$, 400 MHz) δ 7.31-7.12 (m, 8H), 6.93 (t, *J* = 7.7 Hz, 1H), 6.79 (d, *J* = 8.0 Hz, 1H), 5.95 (dd, *J* = 2.0, 10.0 Hz, 1H), 3.17-2.96 (m, 5H), 2.27 (dd, *J* = 2.7, 16.0 Hz, 1H), 1.06 (s, 9H); ^{13}C NMR ($CDCl_3$, 100 MHz) δ 210.90, 196.95, 153.27, 140.98, 132.73, 132.68, 132.65, 129.0, 128.48, 128.36, 126.16, 121.70, 120.06, 117.30, 70.04, 44.4, 39.47, 38.86, 30.29, 25.87; HRMS (ESI) calculated for $C_{24}H_{26}O_3$ $[M]^+$ 362.1881, Found 362.1882.

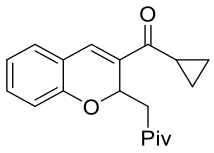

24f

1-(3-(cyclopropanecarbonyl)-2*H*-chromen-2-yl)-3,3-dimethylbutan-2-one

To a solution of **22f** (0.210 g, 0.70 mmol) in CH2Cl2 (3.5 mL) was added water (0.038 mL, 2.10 mmol) and di^{t}BuXPhosAuNTf$_2$ (0.013 g, 0.02 mmol). The reaction mixture was stirred at room temperature for 6 h, and was monitored by TLC. After completion of the reaction, solvent was evaporated under reduced pressure to get a crude reaction mass. Purified on silica gel (CH2Cl2:n-hexanes; 1:5) to give **24f** as a yellow liquid (0.182 g, 6.1 mmol, 87%).

Spectral data. ^{1}H NMR ($CDCl_3$, 400 MHz) δ 7.48 (s, 1H), 7.26-7.18 (m, 2H), 6.93 (t, *J* = 7.0, Hz, 1H), 6.80 (d, *J* = 3.5, 10.0 Hz, 1H), 5.94-5.92 (dd, *J* = 2.3, 10.1 Hz, 1H), 3.20-3.14 (dd, *J* = 10.4, 16.0 Hz, 1H), 2.46 (m, 1H), 2.34-2.29 (dd, *J* = 3.0, 16.2 Hz, 1H), 1.11 (m, 2H), 1.04 (s, 9H), 0.95 (m, 2H); ^{13}C NMR ($CDCl_3$, 100 MHz) δ 211.02, 197.34, 153.31, 133.54, 132.47, 132.31, 128.97, 121.68, 120.40, 117.35, 70.38, 44.47, 39.58, 25.91, 15.86, 11.13, 10.95; HRMS (ESI) calculated for $C_{19}H_{22}O_3$ $[M]^+$. 298.1568, Found 298.1569.

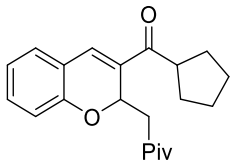

24g

1-(3-(cyclopentanecarbonyl)-2*H*-chromen-2-yl)-3,3-dimethylbutan-2-one

To a solution of **22g** (0.196 g, 0.60 mmol) in CH2Cl2 (3 mL) was added water (0.032 mL, 1.80 mmol) and di^{t}BuXPhosAuNTf$_2$ (0.011 g, 0.02 mmol). The reaction mixture was stirred at room temperature for 8 h, and was monitored by TLC. After completion of the reaction, solvent was evaporated under reduced pressure to get a crude reaction mass. Purified on silica gel (CH2Cl2:n-hexanes;1:5) to give **24g** as a colorless liquid (0.153 g, 0.47 mmol, 78%).

Spectral data. ^{1}H NMR ($CDCl_3$, 400 MHz) δ 7.35 (s, 1H), 7.27-7.18 (m, 2H), 6.94 (t, *J* = 7.7 Hz, 1H), 6.80-6.78 (d, *J* = 7.7 Hz, 1H), 5.97-5.93 (dd, *J* = 2.0, 10.0 Hz, 1H), 3.56-8.48 (p, 1H), 3.20-3.14 (dd, *J* = 10.0, 16.0 Hz, 1H), 2.32 (dd, *J* = 2.7, 16.0 Hz, 1H), 1.87-1.62 (m, 8H), 1.07 (s, 9H); ^{13}C NMR ($CDCl_3$, 100 MHz) δ 210.93, 200.72, 153.23, 132.59, 132.47, 128.97, 121.65, 120.31, 17.29, 70.33, 44.96, 44.44, 39.50, 30.53, 29.98, 26.23, 25.89; HRMS (ESI) calculated for $C_{21}H_{26}O_3$ $[M]^+$ 326.1881, Found 326.1882.

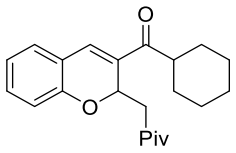

24h

1-(3-(cyclohexanecarbonyl)-2*H*-chromen-2-yl)-3,3-dimethylbutan-2-one

To a solution of **22h** (0.205 g, 0.60 mmol) in CH2Cl2 (3 mL) was added water (0.032 mL, 1.80 mmol) and di^{t}BuXPhosAuNTf$_2$ (0.012 g, 0.02 mmol). The reaction mixture was stirred at room temperature for 8 h, and was monitored by TLC. After completion of the reaction, solvent was evaporated under reduced pressure to get a crude reaction mass. Purified on silica gel (CH2Cl2:n-hexanes; 1:5) to give **24h** as a yellow liquid (0.167 g, 4.9 mmol, 82%).

Spectral data. ^{1}H NMR ($CDCl_3$, 400 MHz) δ 7.33 (s, 1H), 7.26-7.17 (m, 2H), 6.93 (t, *J* = 7.7 Hz, 1H), 6.80 (dd, *J* = 7.1, 2.0 Hz, 1H), 5.90 (dd, *J* = 2.0, 10.2 Hz, 1H), 3.14 (dd, *J* = 1.2, 16.0 Hz, 1H), 3.06 (m, 1H), 2.30 (dd, *J* = 2.7, 16.0 Hz, 1H), 1.85-1.69 (m, 5H), 1.47-1.20 (m, 6H), 1.05 (s, 9H); 13C NMR ($CDCl_3$, 100 MHz) δ 210.92, 210.66, 153.26, 132.50, 131.93, 131.69, 128.97, 121.65, 120.25, 117.29, 70.23, 44.44, 44.39, 39.52, 29.78, 29.38, 25.90, 25.77; HRMS (ESI) calculated for $C_{22}H_{28}O_3$ $[M]^+$. 340.2038, Found 340.2038.

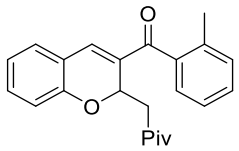

24i

3,3-dimethyl-1-(3-(2-methylbenzoyl)-2*H*-chromen-2-yl)butan-2-one

To a solution of **22i** (0.245 g, 0.70 mmol) in CH2Cl2 (3.5 mL) was added water (0.038 mL, 2.10 mmol) and di^{t}BuXPhosAuNTf$_2$ (0.013 g, 0.02 mmol). The reaction mixture was stirred at room temperature for 8 h, and was monitored by TLC. After completion of the reaction, solvent was evaporated under reduced pressure to get a crude mass. Purified on silica gel (CH2Cl2:n-hexanes; 1:5) to give **24i** as a yellow liquid (0.195 g, 5.6 mmol, 80%).

Spectral data. ^{1}H NMR ($CDCl_3$, 400 MHz) δ 7.41 (t, *J* = 7.3 Hz, 1H), 7.34-7.24 (m, 5H), 7.07-7.04 (d, *J* = 7.3 Hz, 1H), 6.93 (s, 1H), 6.91-6.89 (d, *J* = 7.3 Hz, 1H), 6.84-6.82 (d, *J* = 9.1 Hz, 1H), 6.15-6.11 (dd, *J* = 2.8, 9.9 Hz, 1H), 3.55-3.28 (dd, *J* = 1.2, 16.0 Hz, 1H), 2.55-2.50 (dd, *J* = 2.8, 16.0 Hz, 1H), 2.34 (s, 3H), 1.11 (s, 9H); ^{13}C NMR ($CDCl_3$, 100 MHz) δ 211.07, 196.30, 153.35, 137.89, 137.64, 136.21, 133.22, 133.03, 130.96, 130.00, 129.32, 127.82, 125.19, 121.74, 120.19, 117.35, 70.38, 44.58, 39.54, 25.94, 19.61; HRMS (ESI) calculated for $C_{23}H_{24}O_3$ $[M]^+$ 348.1725, Found 348.1725.

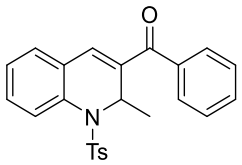

25b

(2-methyl-1-tosyl-1,2-dihydroquinolin-3-yl)(phenyl)methanone

To a solution of **23b** (0.150 g, 0.31mmol) in CH2Cl2 (1.6 mL) was added water (0.022 mL, 1.20 mmol) and di^{t}BuXPhosAuNTf$_2$ (0.007 g, 0.02 mmol). The reaction mixture was stirred at room temperature for 8 h, and was monitored by TLC. After completion of the reaction, solvent was evaporated under reduced pressure to get a crude reaction mass. Purified on silica gel (CH2Cl2:n-hexanes; 1:8) to give **25b** as a yellow liquid (0.090 g, 2.2 mmol, 72%).

Spectral data. ^{1}H NMR ($CDCl_3$, 400 MHz) δ 7.79-7.77 (d, *J* = 8.0 Hz, 1H), 7.46-7.38 (m, 2H), 7.32-6.98 (m, 10H), 6.52 (s, 1H), 5.53 (q, *J* = 7.5 Hz, 1H), 2.25 (s, 3H), 1.20-1.18 (d, *J* = 11.8 Hz, 3H); ^{13}C NMR ($CDCl_3$, 100 MHz) δ 193.54, 143.50, 137.39, 137.21, 136.22, 135.48, 134.15, 131.80, 131.11, 129.34, 128.78, 128.71, 128.52, 128.14, 127.01, 126.91, 126.74, 50.08, 21.43, 19.43; HRMS (ESI) calculated for $C_{24}H_{21}SNO_3$ $[M]^+$. 403.1242, Found 403.1242.

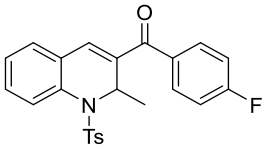

25c

(4-fluorophenyl)(2-methyl-1-tosyl-1,2-dihydroquinolin-3-yl)methanone

To a solution of **23c** (0.205 g, 0.40 mmol) in CH2Cl2 (2 mL) was added water (0.027 mL, 1.50 mmol) and di^{t}BuXPhosAuNTf$_2$ (0.009 g, 0.02 mmol). The reaction mixture was stirred at room temperature for 8 h, and was monitored by TLC. After completion of the reaction, solvent was evaporated under reduced pressure to get a crude reaction mass. Purified on silica gel (CH2Cl2:n-hexanes; 1:8) to give **25c** as a yellow liquid (0.130 g, 3.1 mmol, 77%).

Spectral data. ^{1}H NMR ($CDCl_3$, 400 MHz) δ 7.86 (d, 9.0 Hz, 1H), 7.48 (dt, *J* = 2.4, 7.2 Hz, 1H), 7.30-7.21 (m, 5H), 7.12-7.03 (m, 5H), 6.57 (s, 1H), 5.56 (q, *J* = 7.5 Hz, 1H), 2.32 (s, 3H), 1.27-1.25 (d, *J* = 11.8 Hz, 3H); ^{13}C NMR ($CDCl_3$, 100 MHz) 192.04, 143.49, 137.07, 136.26, 135.24, 134.12, 133.48, 131.32, 131.22, 129.32, 128.73, 128.50, 128.93, 18.49, 126.92, 126.80, 115.42, 50.19, 21.44, 19.44; HRMS (ESI) calculated for $C_{24}H_{20}FNSO_3$ $[M]^+$. 421.1147, Found 421.1148.

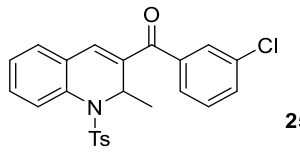

25d

(3-chlorophenyl)(2-methyl-1-tosyl-1,2-dihydroquinolin-3-yl)methanone

To a solution of **23d** (0.210 g, 0.38 mmol) in CH2Cl2 (2 mL) was added water (0.027 mL, 1.50 mmol) and di^{t}BuXPhosAuNTf$_2$ (0.010 g, 0.02 mmol). The reaction mixture was stirred at room temperature for 8 h, and was monitored by TLC. After completion of the reaction, solvent was evaporated under reduced pressure to get a crude reaction mass. Purified on silica gel (CH2Cl2:n-hexanes; 1:5) to give **25d** as a color less liquid (0.136 g, 3.1 mmol, 82%).

Spectral data. ^{1}H NMR ($CDCl_3$, 400 MHz) δ 7.85 (d, *J* = 8.4 Hz, 1H), 7.49 (dt, *J* = 2.4, 7.2 Hz, 2H), 7.33-7.26 (m, 4H), 7.12-7.06 (m, 5H), 6.59 (s, 1H), 5.58 (q, *J* = 7.5 Hz, 1H), 2.35 (s, 3H), 1.26 (d, *J* = 11.8, 3H); ^{13}C NMR ($CDCl_3$, 100 MHz) δ 192.01, 139.05, 136.82, 136.21, 136.17, 134.28, 134.20, 131.70, 131.47, 129.66, 129.41, 128.93, 128.57, 127.60, 126.92, 126.83, 126.80, 126.77, 49.99, 21.53, 19.37; HRMS (ESI) calculated for $C_{24}H_{20}ClNSO_3$ $[M]^+$. 437.0852, Found 437.0852.

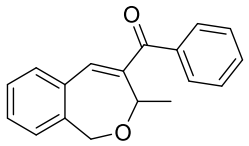

29b

(3-methyl-1,3-dihydrobenzo[*c*]oxepin-4-yl)(phenyl)methanone

To a solution of **26b** (0.245 g, 0.70 mmol) in CH2Cl2 (3.5 mL) was added di^{t}BuXPhosAuNTf$_2$ (0.013 g, 0.02 mmol). The reaction mixture was stirred at room temperature for 8 h, and was monitored by TLC. After completion of the reaction, solvent was evaporated under reduced pressure to get a crude reaction mass. Purified on silica gel (CH2Cl2:n-hexanes; 1:5) to give **29b** as a yellow liquid (0.126 g, 4.8 mmol, 68%).

Spectral data. ^{1}H NMR ($CDCl_3$, 400 MHz) δ 7.12 (dd, *J* = 1.8, 8.8 Hz, 2H), 7.23-7.10 (m, 7H), 6.84 (d, *J* = 1.8 Hz, 1H), 5.36-5.33 (dq, *J* = 1.8, 6.5 Hz, 1H), 4.73-4.63 (q, 2H), 1.33 (d, *J* = 8.0 Hz, 3H); ^{13}C NMR ($CDCl_3$, 100 MHz) δ 197.99, 147.02, 143.39, 140.95, 135.87, 134.87, 133.54, 132.49, 129.76, 129.08, 128.68, 127.80, 127.03, 79.27, 70.81, 19.98; HRMS (ESI) calculated for $C_{18}H_{16}O_2$ $[M]^+$. 264.1150, Found 264.1150.

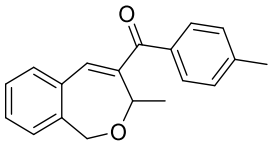

29c

(3-methyl-1,3-dihydrobenzo[*c*]oxepin-4-yl)(*p*-tolyl)methanone

To a solution of **26c** (0.217 g, 0.60 mmol) in CH2Cl2 (3 mL) was added di^{t}BuXPhosAuNTf$_2$ (0.010 g, 0.02 mmol). The reaction mixture was stirred at room temperature for 8 h, and was monitored by TLC. After completion of the reaction, solvent was evaporated under reduced pressure to get a crude reaction mass. Purified on silica gel (CH2Cl2:n-hexanes; 1:6) to give **29c** as a yellow liquid (0.110 g, 4.0 mmol, 66%).

Spectral data. ^{1}H NMR ($CDCl_3$, 400 MHz) δ 7.71 (d, *J* = 7.9 Hz, 1H), 7.29-7.18 (m, 7H), 6.84 (d, *J* = 1.8 Hz, 1H), 5.33 (dq, *J* = 1.8, 6.5 Hz, 1H), 4.70-4.63 (q, J = 11.0, 14.0 Hz, 2H), 2.38 (s,

3H), 1.33 (d, *J* = 8.0 Hz, 3H); ^{13}C NMR ($CDCl_3$, 100 MHz) δ 198.09**,** 147.12, 143.49, 141.05, 135.97, 134.97, 133.64, 132.59, 129.86, 129.18, 128.78, 127.90, 127.13, 79.37, 70.91, 21.60, 20.08; HRMS (ESI) calculated for $C_{19}H_{18}O_2$ [M]$^+$. 278.1306, Found 278.1307.

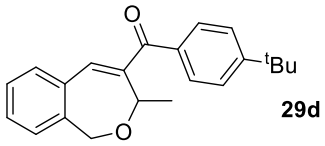

29d

(4-(*tert*-butyl)phenyl)(3-methyl-1,3-dihydrobenzo[*c*]oxepin-4-yl)methanone

To a solution of **26d** (0.245 g, 0.60 mmol) in CH2Cl2 (3 mL) was added di^{t}BuXPhosAuNTf$_2$ (0.012 g, 0.02 mmol). The reaction mixture was stirred at room temperature for 8 h, and was monitored by TLC. After completion of the reaction, solvent was evaporated under reduced pressure to get a crude reaction mass. Purified on silica gel (CH2Cl2:n-hexanes; 1:6) to give **29d** color less liquid (0.100 g, 3.1 mmol, 52%).

Spectral data. ^{1}H NMR ($CDCl_3$, 400 MHz) δ 7.3-7.81 (m, 2H), 7.52-7.50 (m, 2H), 7.29-7.18 (m, 4H), 6.95 (d, *J* = 1.8 Hz, 1H), 5.44-5.39 (dq, *J* = 1.8, 6.57 Hz, 1H), 4.81-4.71 (dd, *J* = 12.0, 15.0 Hz, 2H), 1.41 (d, *J* = 8 Hz, 3H), 1.38 (s, 9H); ^{13}C NMR ($CDCl_3$, 100 MHz) δ 197.98, 156.42, 147.00, 140.97, 135.89, 134.78, 133.59, 132.57, 129.65, 128.72, 127.82, 127.06, 125.40, 79.35, 70.87, 31.07, 26.94, 20.01; HRMS (ESI) calculated for $C_{22}H_{24}O_2$ [M]$^+$. 320.1776, Found 320.1775.

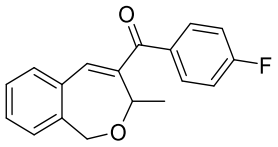

29e

(4-fluorophenyl)(3-methyl-1,3-dihydrobenzo[*c*]oxepin-4-yl)methanone

To a solution of **26e** (0.220 g, 0.60 mmol) in CH2Cl2 (3 mL) was added di^{t}BuXPhosAuNTf$_2$ (0.012 g, 0.02 mmol). The reaction mixture was stirred at room temperature for 8 h, and was monitored by TLC. After completion of the reaction, solvent was evaporated

under reduced pressure to get a crude reaction mass. Purified on silica gel (CH2Cl2:n-hexanes; 1:5) to give **29e** as a yellow liquid (0.118 g, 4.2 mmol, 70%).

Spectral data. ^{1}H NMR ($CDCl_3$, 400 MHz) δ 7.86 (m, 1H), 7.26-7.14 (m, 6H), 6.89 (d, *J* = 1.89 Hz, 1H), 5.39 (dq, *J* = 1.8, 6.5 Hz, 1H), 4.76-4.69 (q, 2H), 1.38 (d, *J* = 8.0 Hz, 3H); ^{13}C NMR ($CDCl_3$, 100 MHz) δ 196.84, 146.82, 141.13, 136.55, 133.36, 132.72, 132.24, 132.15, 129.04, 127.96, 127.19, 115.79, 115.57, 79.23, 70.89, 20.06; HRMS (ESI) calculated for $C_{18}H_{15}O_2$ $[M]^+$. 282.1056, Found 282.1056. ^{19}F NMR ($CDCl_3$, 376 MHz) δ -66.36

Chapter 2. Attempted synthesis of a 1,2,3-triazole analog of porphyrin

Procedure for the preparation of methyl 5-phenyl-2-(prop-2-yn-1-yl)-2H-1,2,3-triazole-4-carboxylate.

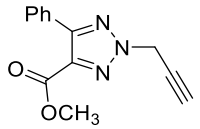

79

methyl 5-phenyl-2-(prop-2-yn-1-yl)-2*H*-1,2,3-triazole-4-carboxylate

To a 50 mL round-bottom flask was added methyl 5-phenyl-2H-1,2,3-triazole-4-carboxylate (2.03 g, 10.0 mmol), potassium carbonate (2.76 g, 20.0 mmol) acetone (50 mL) and propargyl bromide (1.78 g, 15.0 mmol) at room temperature. The reaction mixture was heated up to 60 ^{o}C and stirred for 6 h at the same temperature. After the completion of the reaction (TLC), the solvent was evaporated under reduced pressure and water (50 mL) was added. The mixture was extracted with ethyl acetate (3 x 30 mL). The combined organic layers were washed with brine, dried (Na_2SO_4) and the solvent was removed under reduced pressure to get a residue. The residue was purified by column chromatography (ethyl acetate:n-hexanes; 1:4) to give **79** as colorless liquids (1.45 g, 6.0 mmol, 60%).

Spectral data. ^{1}H NMR ($CDCl_3$, 400 MHz) δ 7.86 (d, *J* = 6.0 Hz, 2H), 7.46 (m, 3H), 5.30 (d, *J* = 6.8 Hz, 2H), 3.93 (s, 3H), 2.56 (t, *J* = 6.5 Hz, 1H); 13C NMR ($CDCl_3$, 100 MHz) δ 184.03, 161.30, 150.65, 136.11, 129.37, 129.27, 129.16, 128.16, 128.09, 75.72, 52.38, 45.27, 40.94.

Procedure for Click chemistry reaction.

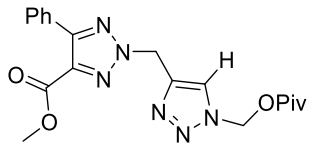

80

methyl 5-phenyl-2-((1-((pivaloyloxy)methyl)-1*H*-1,2,3-triazol-4-yl)methyl)-2*H*-1,2,3-triazole-4-carboxylate

To a 100 mL round-bottom flask was added methyl 5-phenyl-2-(prop-2-yn-1-yl)-2H-1,2,3-triazole-4-carboxylate (2.41 g, 10.0 mmol), copper sulfate (0.080 g, 0.50 mmol), sodium ascorbate (0.198 g, 1.0 mmol), azidomethyl pivalate (1.89 g, 12.0 mmol) and t-butanol:water (1:4, 50 mL) at room temperature and the reaction mixture was stirred at 60 ^{o}C for 6 h. After completion of the reaction (TLC), water (50 mL) was added. The mixture was extracted with ethyl acetate (3 x 30 mL). The combined organic layers were washed with brine, dried (Na_2SO_4) and the solvent was removed under reduced pressure to get a residue. The residue was purified by column chromatography (ethyl acetate:n-hexanes; 1:4) to give **80** as colorless liquids (2.39 g, 6.0 mmol, 60%).

Spectral data. ^{1}H NMR ($CDCl_3$, 400 MHz) δ 7.80 (s, 1H), 7.52-7.44 (dd, *J* = 4.8, 6.0 Hz, 5H), 6.18 (s, 2H), 5.52 (s, 2H), 3.83 (s, 3H), 1.17 (s, 9H); ^{13}C NMR ($CDCl_3$, 100 MHz) δ 177.54, 176.14, 162.98, 161.19, 142.09, 141.53, 136.37, 130.39, 130.01, 128.72, 125.10, 124.78, 69.67, 51.98, 43.47, 38.73, 26.74.

Procedure for N-pivaloylation NH triazoles.

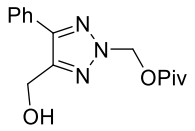

94

(4-(hydroxymethyl)-5-phenyl-2*H*-1,2,3-triazol-2-yl)methyl pivalate

To a 50 mL round-bottom flask was added (5-phenyl-2H-1,2,3-triazol-4-yl)methanol (0.525 g, 3.0 mmol), potassium carbonate (0.829 g, 6.0 mmol) and acetone (15 mL) followed by chloromethyl pivolate (0.680 g, 4. 52 mmol) at room temperature. The reaction mixture was stirred at 60 ^{o}C for 6 h. After completion of the reaction (TLC), the solvent was evaporated under the reduced pressure and water (20 mL) was added. The mixture was extracted with ethyl acetate (3 x 30 mL). The combined organic layers were washed with brine, dried (Na_2SO_4) and the solvent was removed under reduced pressure to get a residue. The residue was purified by column chromatography (ethyl acetate:n-hexanes; 1:4) to give **94** as colorless liquids (0.405 g, 1.40 mmol, 47%).

Spectral data. ^{1}H NMR ($CDCl_3$, 400 MHz) δ 7.82-7.80 (d, *J* = 7.5 Hz, 2H), 7.43 (m, 3H), 6.26 (s, 2H), 4.88 (s, 2H), 1.19 (s, 9H); ^{13}C NMR ($CDCl_3$, 100 MHz) δ 178.01, 146.08, 132.54, 129.94, 128.79, 128.51, 127.74, 68.84, 52.31, 38.89, 26.80.

Procedure for N-pivaloylation of dimer compounds.

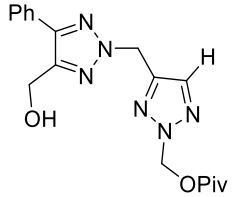

84

(4-((4-(hydroxymethyl)-5-phenyl-2*H*-1,2,3-triazol-2-yl)methyl)-2*H*-1,2,3-triazol-2-yl)methyl pivalate

To a 100 mL round-bottom flask was added (2-((1H-1,2,3-triazol-4-yl)methyl)-5-phenyl-2H-1,2,3-triazol-4-yl)methanol (0.256 g, 1.0 mmol), potassium carbonate (0.276 g, 2.0 mmol) and acetone (10 mL) followed by chloromethyl pivolate (0.226 g, 1.5 mmol) at room temperature. The

reaction mixture was heated up to 60 ^{o}C, stirred for 6 h. After completion of the reaction TLC, the solvent was evaporated under reduced pressure and water (20 mL) was added. The mixture was extracted with ethyl acetate (3 x 30 mL). The combined organic layers were washed with brine, dried (Na_2SO_4) and the solvent was removed under reduced pressure to get a residue; the residue was purified by column chromatography (ethyl acetate:n-hexanes; 1:6) to give **84** as a colorless liquid product (0.170 g, 0.46 mmol, 46%).

Spectral data. ^{1}H NMR ($CDCl_3$, 400 MHz) δ 7.90 (s, 1H), 7.75-7.73 (dd, *J* = 2.6, 7.5 Hz, 2H), 7.45 (m, 3H), 6.21 (s, 2H), 5.75 (s, 2H), 4.75 (s, 2H), 1.17 (s, 9H); 13C NMR ($CDCl_3$, 100 MHz) δ 140.36, 129.27, 129.04, 128.91, 128.81, 128.20, 127.66, 74.70, 57.66, 49.93, 27.29, 27.09

General procedure for depivaloylation.

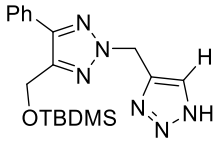

82

4-((4-(((*tert*-butyldimethylsilyl)oxy)methyl)-5-phenyl-2*H*-1,2,3-triazol-2-yl)methyl)-1*H*-1,2,3-triazole

To a 50 mL round-bottom flask was added (4-((4-(((tert-butyldimethylsilyl)oxy)methyl)-5-phenyl-2H-1,2,3-triazol-2-yl)methyl)-1H-1,2,3-triazol-1-yl)methyl pivalate (0.486 g, 1.0 mmol) and methanol (5 mL) and sodium hydroxide (0.080 g, 2.0 mmol) solution at room temperature. The reaction mixture was stirred at same temperature for 2 h. After the reaction was completed (TLC), 6N hydrochloric acid (10 mL) was added followed by water (10 mL). The mixture was extracted with ethyl acetate (3 x 30 mL). The combined organic phases were washed with brine, dried (Na_2SO_4) and the solvent was removed under reduced pressure to get a residue; the residue was purified by column chromatography (ethyl acetate:n-hexanes; 1:4) to get **82** as a yellow liquid (0.282 g, 0.76 mmol, 76%).

Spectral data. ^{1}H NMR ($CDCl_3$, 400 MHz) δ 7.86-7.85 (d, *J* = 8.9 Hz, 2H), 7.75 (s, 1H), 7.42-7.40 (m, 3H), 5.77 (s, 2H), 4.84 (s, 2H), 0.87 (s, 9H), 0.06 (s, 6H); 13C NMR ($CDCl_3$, 100 MHz) δ 146.76, 144.45, 130.72, 129.00, 128.83, 128.81, 128.51, 128.29, 127.94, 127.75, 56.48, 49.17, 25.76, 18.21.

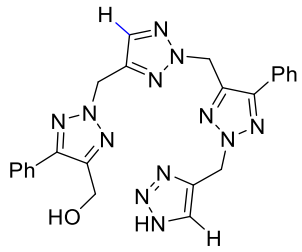

87

(2-((2-((2-((1*H*-1,2,3-triazol-4-yl)methyl)-5-phenyl-2*H*-1,2,3-triazol-4-yl)methyl)-2*H*-1,2,3-triazol-4-yl)methyl)-5-phenyl-2*H*-1,2,3-triazol-4-yl)methanol

To a 50 mL round-bottom flask was added (4-((4-((4-((4-(((tert-butyldimethylsilyl)oxy)methyl)-5-phenyl-2H-1,2,3-triazol-2-yl)methyl)-2H-1,2,3-triazol-2-yl)methyl)-5-phenyl-2H-1,2,3-triazol-2-yl)methyl)-1H-1,2,3-triazol-1-yl)methyl pivalate (0.723 g, 1.0 mmol), methanol (5 mL) and sodium hydroxide (0.080 g, 2.0 mmol) solution at room temperature. The reaction mixture was stirred at same temperature for 2 h. After the reaction was completed (TLC), 6N hydrochloric acid (10 mL) was added followed by water (10 mL). The mixture was extracted with ethyl acetate (3 x 30 mL). The combined organic phases were washed with brine, dried (Na_2SO_4). The solvent was removed under reduced pressure to get a residue; the residue was purified by column chromatography (ethyl acetate:n-hexanes; 1:5) to give **87** as a color less liquid (0.375 g, 0.76 mmol, 76%).

Spectral data. ^{1}H NMR ($CDCl_3$, 400 MHz) δ 7.73 (d, *J* = 8.0 Hz, 2H), 7.72-7.63 (m, 4H), 7.41-7.26 (m, 6H), 5.75 (s, 2H), 5.74 (s, 2H), 5.65 (s, 2H), 4.85 (s, 2H); ^{13}C NMR ($CDCl_3$, 100 MHz) δ 146.98, 146.17, 144.56, 142.64, 138.91, 134.19, 130.01, 129.28, 128.82, 128.53, 127.77, 127.50, 55.95, 49.90, 49.71, 49.55.

General procedure for hydroxy protection with TBDMSCl.

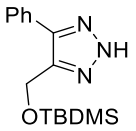

92

4-(((*tert*-butyldimethylsilyl)oxy)methyl)-5-phenyl-2*H*-1,2,3-triazole

To a 250 mL round-bottom flask was added (5-phenyl-2H-1,2,3-triazol-4-yl) methanol (1.75 g, 10.0 mmol), imidazole (3.40 g, 50.0 mmol), CH2Cl2 (100 mL) and TBDMSCl (4.52 g, 30.0 mmol) at room temperature. The reaction mixture was stirred at the same temperature for 4 h. After the reaction was completed (TLC), the mixture was washed with brine, dried (Na_2SO_4) and the solvent was removed under reduced pressure to get a residue; the residue was purified by column chromatography (ethyl acetate:n-hexanes; 1:4) to give **92** as yellow solid (2.37 g, 8.2 mmol, 82%).

Spectral data. ^{1}H NMR ($CDCl_3$, 400 MHz) δ 7.87-7.85 (d, *J* = 6.5 Hz, 2H), 7.47-7.45 (t, *J* = 7.4 Hz, 2H), 7.40 (m, 1H), 4.95 (s, 2H), 0.91(s, 9H), 0.12 (s, 6H); ^{13}C NMR ($CDCl_3$, 100 MHz) δ 130.0, 128.71, 128.43, 128.03, 127.85, 127.65, 56.48, 25.78, 18.23, -5.28.

Procedure for the silylation reactions.

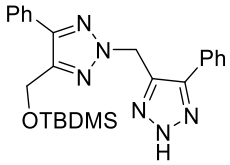

98

4-(((*tert*-butyldimethylsilyl)oxy)methyl)-5-phenyl-2-((5-phenyl-2*H*-1,2,3-triazol-4-yl)methyl)-2*H*-1,2,3-triazole

To a 250 mL round-bottom flask was added **81** (1.50 g, 4.5 mmol), imidazole (0.613 g, 9.0 mmol), CH2Cl2 (15 mL) followed by TBDMSCl (1.02 g, 6.75 mmol) at room temperature. The reaction mixture was stirred at the same temperature for 4 h. After the reaction was completed (TLC), the reaction mixture was washed with 1N hydrochloric acid, brine, dried (Na_2SO_4) and the

solvent was removed under reduced pressure to get a residue; the residue was purified by column chromatography (ethyl acetate:n-hexanes; 1:4) to give **98** as a color less liquid (1.80 g, 4.03 mmol, 90%).

Spectral data. ^{1}H NMR ($CDCl_3$, 400 MHz) δ 7.80-7.79 (d, *J* = 6.5 Hz, 2H), 7.66+72 (dd, *J* = 2.3, 7.4 Hz, 2H), 7.38-7.29 (m, 6H), 5.80 s, 2H), 4.78 (s, 2H), 0.81 (s, 9H), 0.01 (s, 6H); ^{13}C NMR ($CDCl_3$, 100 MHz) δ 162.96, 148.34, 145.99, 141.66, 129.85, 129.49, 128.88, 128.78, 128.66, 128.52, 127.96, 127.88, 127.80, 127.56, 127.38, 57.34, 56.47, 25.71, 18.14, -5.28.

Procedure for desilylation reactions.

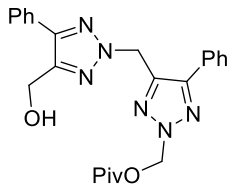

97

(4-((4-(hydroxymethyl)-5-phenyl-2*H*-1,2,3-triazol-2-yl)methyl)-5-phenyl-2*H*-1,2,3-triazol-2-yl)methyl pivalate

To a 50 mL round-bottom flask was added **96** (0.561 g, 1.0 mmol), THF (5 mL) followed by TBAF (0.52 g, 2 mmol) at room temperature. The reaction mixture was stirred at room temperature for 10 h. After the reaction was completed (TLC), water (20 mL) was added. The mixture was extracted with ethyl acetate (3 x 30 mL). The combined organic phases were washed with brine, dried (Na_2SO_4) and the solvent was removed under reduced pressure to get a residue; the residue was purified by column chromatography (ethyl acetate:n-hexanes; 1:4) to give **97** as a yellow liquid (0.390 g, 0.87 mmol, 87%).

Spectral data. ^{1}H NMR ($CDCl_3$, 400 MHz) δ 7.81-7.80 (d, *J* = 6.5 Hz, 2H), 7.68 (dd, *J* = 2.3, 7.4 Hz, 2H), 7.44-7.37 (m, 6H), 6.82 (s, 2H), 5.27 (s, 2H), 4.87 (s, 2H), 1.13 (s, 9H); ^{13}C NMR ($CDCl_3$, 100 MHz) δ 186.94, 178.9, 177.85, 162.96, 148.34, 145.99, 141.66, 129.85, 129.49, 129.49, 128.88, 128.78, 128.66, 128.52, 127.88, 127.56, 68.91, 57.34, 38.73, 26.99.

Procedure for Mitsunobu reaction of 1,2,3-NH-triazole with alcohol.

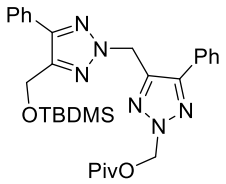

96

(4-((4-(((*tert*-butyldimethylsilyl)oxy)methyl)-5-phenyl-2*H*-1,2,3-triazol-2-yl)methyl)-5-phenyl-2*H*-1,2,3-triazol-2-yl)methyl pivalate

To a 50 mL round-bottomed flask is equipped with a stirring bar, nitrogen inlet, rubber septum. The flask is charged with **92** (1.45 g, 4.4 mmol), **94** (1.45 g, 4.4 mmol), triphenyl phosphine (2.31 g, 8.8 mmol) and distilled THF (25 mL). The flask is immersed in an ice bath, and added dropwise addition diisopropyl azodicarboxylate (1.78 g, 8.8 mmol). Upon completion of the addition, the flask is removed from the ice bath and the solution was allowed to stir at room temperature for 3 h, and monitored by TLC. After completion of the reaction, solvent was evaporated under the reduced pressure to get a residue. The residue was applied to a flash silica gel chromatography column (hexane:ethyl acetate = 10:1) to give **96** as a yellow liquid (1.54 g, 2.75 mmol, 62%).

Spectral data. ^{1}H NMR ($CDCl_3$, 400 MHz) δ 7.95-7.93 (dd, *J* = 2.3, 6.5 Hz, 2H), 7.70 (dd, *J* = 2.3, 7.2 Hz, 2H), 7.44-7.38 (m, 6H), 6.83 (s, 2H), 5.29 (s, 2H), 4.87 (s, 2H), 1.14 (s, 9H), 0.87 (s, 9H), 0.05 (s, 6H); ^{13}C NMR ($CDCl_3$, 100 MHz) δ 177.85, 148.34, 148.27, 145.99, 141.66, 129.85, 129.49, 128.88, 128.66, 128.56, 128.52, 128.47, 127.96, 127.88, 127.56, 68.91, 57.34, 56.47, 38.73, 26.99, 25.71, 18.14, -5.28.

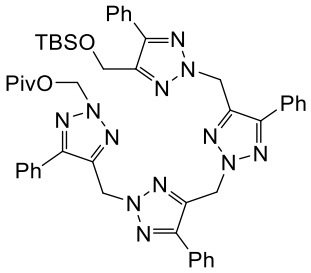

100

To a 50 mL round-bottomed flask is equipped with a stirring bar, nitrogen inlet, rubber septum. The flask is charged with **97** (0.450 g, 1.0 mmol), **98** (0.450 g, 1.0 mmol), triphenylphosphine (0.530 g, 2.0 mmol), and distilled THF (25 mL). The flask was immersed in an ice bath, and added drop wise addition of diisopropyl azodicarboxylate (0.40 g, 2.0 mmol). Upon completion of the addition, the flask is removed from the ice bath and the solution was allowed to stir at room temperature for 3 h, and monitored by TLC. After completion of the reaction, solvent was evaporated under the reduced pressure to get a residue. The residue is applied to a flash silica gel chromatography column (hexane:ethyl acetate = 10:1) to give **100** (0.49 g, 0.60 mmol, 56%).

Spectral data. ^{1}H NMR ($CDCl_3$, 400 MHz) δ 7.83-7.80 (dd, *J* = 6.5 Hz, 2.3 Hz, 2H), 7.70-7.66 (m, 4H), 7.63-7.61 (m, 2H), 7.39-7.26 (m, 10H), 6.25 (s, 2H), 5.80 (s, 2H), 5.74 (s, 2H), 5.69 (s, 2H), 4.76 (s, 2H), 1.15 (s, 9H), 0.81 (s, 9H), 0.01 (s, 6H); ^{13}C NMR ($CDCl_3$, 100 MHz) δ 177.83, 162.96, 154.79, 151.79, 148.49, 148.41, 146.99, 146.57, 144.20, 141.79, 140.29, 138.81, 130.48, 129.81, 128.90, 128.67, 128.60, 128.59, 128.56, 128.42, 127.93, 127.88, 127.68, 127.55, 72.16, 70.14, 69.89, 69.06, 57.32, 56.46, 49.83, 49.31, 38.71, 26.96, 25.73, 22.02, 21.87, 21.63, 18.15, -5.28.

Procedure for macrocyclization reactions.

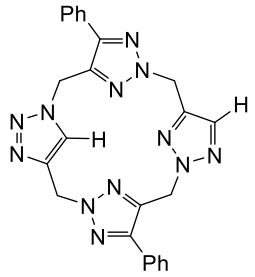

88

(4*Z*,9*Z*,14*Z*,19*Z*)-8,18-diphenyl-21,23-didehydro-5*H*,10*H*,15*H*,20*H*-1,2,3,6,7,11,12,16,17-nonaazaporphyrin

To a 50 mL round-bottomed flask is equipped with a stirring bar, nitrogen inlet, rubber septum. The flask is charged with **87** (0.395 g, 0.80 mmol), triphenylphosphine (0.420 g, 1.6 mmol), and added distilled THF (40 mL). The flask is immersed in an ice bath, and was added drop wise addition of diisopropyl azodicarboxylate (0.324 g, 1.6 mmol). The reaction was monitored by TLC and after completion of the addition, the flask is removed from the ice bath and the solution is allowed to stir at room temperature for 3 h. Solvent was evaporated under the reduced pressure to get a residue. The residue was applied to a flash silica gel chromatography column (methanol:ethyl acetate = 1:10) to give **88** as a white solid (0.150 g, 0.31 mmol, 39%).

Spectral data. ^{1}H NMR ($CDCl_3$, 400 MHz) δ 7.74-7.72 (m, 2H), 7.70 (s, 1H), 7.53-7.51 (m, 2H), 7.50 (s, 1H), 7.48-7.39 (m, 6H), 5.81 (s, 2H), 5.79 (s, 2H), 5.75 (s, 2H), 5.68 (s, 2H); ^{13}C NMR ($CDCl_3$, 100 MHz) δ 146.27, 146.20, 143.54, 142.68, 139.56, 138.96, 133.55, 129.42, 129.08, 128.94, 128.85, 127.85, 127.75, 123.29, 51.28, 49.93, 49.80, 44.66.

Chapter 3. Triazole as part of a pincer ligand, its complexations

Procedure for N-benzylation of NH triazoles.

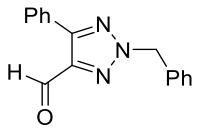

117

2-benzyl-5-phenyl-2*H*-1,2,3-triazole-4-carbaldehyde

To a 50 mL round-bottom flask was added 5-phenyl-2H-1,2,3-triazole-4-carbaldehyde, **115** (1.73 g, 10.0 mmol), potassium carbonate (2.76 g, 20.0 mmol), DMF (20 mL) followed by drop wise addition of benzyl bromide (2.05 g, 12.0 mmol) at room temperature over a period of 5 mins. The temperature of the reaction mixture was raised to 80 ^{o}C for 6h. After the reaction was completed (TLC), allow it to cool down to room temperature and water (100 mL) was added. The mixture was extracted with ethyl acetate (3 x 30 mL). The combined organic phases were washed with brine, dried (Na_2SO_4) and the solvent was removed under reduced pressure to get a residue; the residue was purified by column chromatography to give **117** as a brown syrup (1.60 g, 6.1 mmol, 61%).

Spectral data. ^{1}H NMR ($CDCl_3$, 400 MHz) δ 9.99 (s, 1H), 7.73 (d, *J* = 7.5 Hz, 2H), 7.51-7.31 (m, 8H), 5.93 (s, 2H); ^{13}C NMR ($CDCl_3$, 100 MHz) δ 165.43, 151.02, 134.93, 133.87, 129.61, 129.39, 129.31, 129.23, 128.90, 128.76, 128.46, 128.35, 128.17, 128.08, 127.97, 59.66.

Procedure for condensation followed by reductive amination reaction.

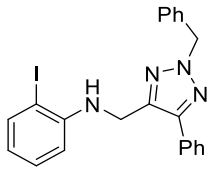

121

N-((2-benzyl-5-phenyl-2*H*-1,2,3-triazol-4-yl)methyl)-2-iodoaniline

To a 100 mL round-bottom flask was equipped with a stirring bar, nitrogen inlet, rubber septum and dean stark apparatus. The flask was charged with **117** (2.63 g, 10.0 mmol), 2-iodo aniline (2.30 g, 10.5 mmol) and toluene (50 mL). pTSA (0.190 g, 1.0 mmol) was added and stirred the reaction mixture at reflux temperature for 6 h. The reaction was monitored by TLC, was cooled to room temperature and added triethylamine (0.2 mL, 2.7 mmol) was added and washed with water (100 mL). Organic layer was separated, dried (Na_2SO_4) and the solvent was evaporated under reduced pressure to get a thick syrup. Methanol and THF were added to the crude syrup and cooled the solution to 0 ^oC. Sodium borohydride (0.757 g, 20.0 mmol) was added and stirred at room temperature for 15 h. The reaction was quenched with water and solvent was removed under reduced pressure to get a residue. The residue was purified by recrystallization in methanol to get **121** as a white solid (3.73 g, 8.0 mmol, 80%).

Spectral data. ^1H NMR ($CDCl_3$, 400 MHz) δ 7.69-7.64 (m, 3H), 7.45-7.30 (m, 8H), 7.21 (dt, *J* = 1.6, 7.7 Hz, 1H), 6.69-6.66 (dd, *J* = 1.5, 7.6 Hz, 1H), 6.49-6.45 (dt, *J* = 1.5, 7.6 Hz, 1H), 5.62 (s, 2H), 4.75 (t, *J* = 4.9 Hz, 1H), 4.53 (d, *J* = 4.9 Hz, 2H); ^{13}C NMR ($CDCl_3$, 100 MHz) δ 146.70, 145.61, 141.76, 139.02, 135.14, 130.37, 129.34, 128.92, 128.89, 128.85, 128.73, 128.41, 128.28, 128.06, 128.01, 127.49, 119.20, 110.29, 85.58, 58.72, 40.18.

Procedure for an Appel reaction for the synthesis of 148.

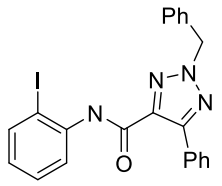

148

(2-benzyl-5-phenyl-2*H*-1,2,3-triazol-4-yl)((2-iodophenyl)-λ^2-azaneyl)methanone

To a 250 mL round-bottom flask containing toluene (50 mL) was added **147** (2.79 g, 10.0 mmol), 2-iodo aniline (2.30 g, 10.5 mmol), triphenylphosphine (5.25 g, 20.0 mmol), potassium carbonate (2.76 g, 20.0 mmol) and carbon tetrabromide (6.63 g, 20.0 mmol) at room temperature. The reaction mixture was heated to 80 ^{o}C and stirred for 6 h. The reaction was monitored by TLC and was cooled to room temperature. Washed with water (3x100 mL) and the organic layer was separated, dried (Na_2SO_4) and the solvent was evaporated under reduced pressure to get a thick syrup. Methanol was added to the syrup to get **148** as a white powder (4.20 g, 8.7 mmol, 87%).

Spectral data. ^{1}H NMR ($CDCl_3$, 400 MHz) δ 9.15 (s, 1H), 8.39-8.36 (dd, *J* = 1.7, 8.4 Hz, 1H), 8.04-8.02 (dd, *J* = 1.7, 8.4 Hz, 2H) 7.83-7.80 (dd, *J* = 1.6, 7.8 Hz, 1H), 7.48-7.33 (m, 9H), 6.88-6.83 (dt, *J* = 1.6, 7.4 Hz, 1H), 5.68 (s, 2H); ^{13}C NMR ($CDCl_3$, 100 MHz) δ 187.40, 158.44, 149.24, 146.73, 138.94, 138.26, 134.08, 129.33, 129.30, 129.19, 128.92, 128.75, 128.51, 128.20, 128.13, 128.09, 125.88, 121.73, 119.93, 114.70, 89.76, 59.43.

Procedure for phosphination of aryl iodides with diarylphosphines.

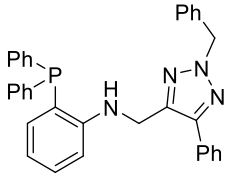

122

N-((2-benzyl-5-phenyl-2*H*-1,2,3-triazol-4-yl)methyl)-2-(diphenylphosphaneyl)aniline

An oven dried Schlenk tube was evacuated and refilled with argon three times and then charged with CuI (0.010 g, 0.053 mmol), diphenyl phosphine (0.195 g, 1.05 mmol) and *N, N'* -

dimethylethylenediamine (0.031 g, 0.35 mmol). The colorless solution was stirred for 5-10 min. Then N-((2-benzyl-5-phenyl-2H-1,2,3-triazol-4-yl) methyl)-2-iodoaniline, **121** (0.466 g, 1.0 mmol) and Cs_2CO_3 (0.652 g, 2.0 mmol) were added at once followed by anhydrous toluene (10 mL). The Schlenk tube was sealed with a Teflon valve and the reaction mixture was stirred at 110 °C until the complete conversion of **121** (TLC). The resulting suspension allowed to reach room temperature, diluted with water (20 mL) and extracted with diethyl ether (4 × 10 mL). The combined organic phases were dried (Na_2SO_4), concentrated under reduced pressure, and the residue was purified by flash chromatography on silica with (ethyl acetate:n-hexanes; 1:4) to get **122** as white powder (0.325 g, 0.62 mmol, 62%).

Spectral data. ^{1}H NMR ($CDCl_3$, 400 MHz) δ 7.56-7.33 (d, *J* = 4.8 Hz, 2H), 7.27 (m, 19H), 6.82 (d, *J* = 7.2 Hz, 1H), 6.77 (dt, *J* = 3.6, 7.2 Hz, 1H), 6.67 (s, *J* = 9.6 Hz, 1H), 5.55 (s, 2H), 5.31 (t, *J* = 6.0 Hz, 1H), 4.45 (s, 2H); ^{13}C NMR ($CDCl_3$, 100 MHz) δ 145.75, 142.10, 135.28, 134.63, 133.69, 133.50, 128.66, 128.49, 128.42, 128.21, 127.99, 127.45, 119.68, 117.79, 110.58, 58.60, 39.88. ^{31}P{^{1}H} NMR (162 MHz, $CDCl_3$) δ -21.68.

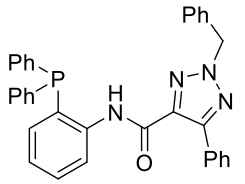

133

2-benzyl-*N*-(2-(diphenylphosphaneyl)phenyl)-5-phenyl-2*H*-1,2,3-triazole-4-carboxamide

An oven dried Schlenk tube was evacuated and refilled with argon three times and then charged with CuI (0.010 g, 0.05 mmol), diphenylphosphine (0.195 g, 1.05 mmol) and *N, N'* -dimethylethylenediamine (0.031 g, 0.35 mmol). The colorless solution was stirred for 5-10 min. Then 2-benzyl-N-(2-iodophenyl)-5-phenyl-2H-1,2,3-triazole-4-carboxamide, **148** (0.480 g, 1.0 mmol) and Cs_2CO_3 (0.650 g, 2.0 mmol) were added at once followed by anhydrous toluene (10 mL). The Schlenk tube was sealed with a Teflon valve and the reaction mixture was stirred at 110

°C until the complete conversion of aryl halide. The resulting suspension allowed to reach room temperature, diluted with water (10 mL) and extracted with diethyl ether (4 × 10 mL). The combined organic phases were dried (Na_2SO_4), concentrated, and the residue was purified by flash chromatography (ethyl acetate:n-hexanes; 1:5) to get **133** as white powder (0.102 g, 0.19 mmol, 19%).

Spectral data. ^{1}H NMR ($CDCl_3$, 400 MHz) δ 8.61 (s, 1H), 8.04-8.03 (d, *J* = 4.0 Hz, 2H), 7.65-7.63 (d, *J* = 2.4 Hz, 2H), 7.46-7.32 (m, 8H), 7.14-7.10 (t, *J* = 7.4 Hz, 1H), 5.65 (s, 2H); ^{13}C NMR ($CDCl_3$, 100 MHz) δ 183.60, 158.27, 149.10, 138.46, 137.48, 134.22, 129.38, 129.26, 129.09, 128.95, 128.87, 128.65, 128.11, 128.02, 124.35, 119.94, 119.84, 59.23; ^{31}P{^{1}H} NMR (162 MHz, $CDCl_3$) δ -21.68.

Procedure for Complexation reactions with nickel chloride.

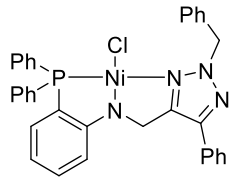

123

Under argon atmosphere 10 mL of toluene was added to a round bottom flask containing **122** (0.525 g, 1.0 mmol) and anhydrous $NiCl_2$ (0.136 g, 1.05 mmol.), giving a brown suspension. While the solution was being boiled for 18 h, the mixture was cooled to room temperature. The reaction volume was reduced to 5 mL, and then hexanes was added to cause precipitation. The product was collected by filtration, washed with hexanes, and dried under vacuum to give **123** as a green powder (0.370 g, 0.60 mmol, 60%). X-ray-quality crystals were grown by allowing a layer of pentane to slowly diffuse into a saturated CH2Cl2 solution of **123**.

Spectral data. ^{1}H NMR ($CDCl_3$, 400 MHz) δ 7.56-7.55 (dd, *J* = 3.8, 2.4 Hz, 2H), 7.33-7.25 (m, 19H), 6.85-6.82 (dt, *J* = 1.6, 7.7 Hz, 1H), 6.79-6.75 (dd, *J* = 4.9, 7.7 Hz, 1H), 6.69-6.65 (t, *J* = 6.6

Hz, 1H), 5.55 (s, 2H), 4.47 (d, *J* = 4.77 Hz, 2H); ^{13}C NMR ($CDCl_3$, 100 MHz) δ 145.69, 142.05, 134.58, 133.63, 133.44, 130.58, 130.34, 128.66, 128.59, 128.44, 128.37, 128.15, 128.12, 127.94, 127.40, 117.75, 110.54, 110.52, 67.90, 58.56.

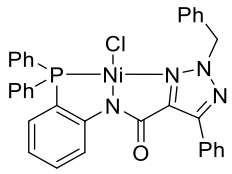

150

Under argon atmosphere toluene (10 mL) was added to a round bottom flask containing **133** (0.102 g, 0.19 mmol) and anhydrous $NiCl_2$ (0.026 g, 0.20 mmol), giving a yellow suspension. While the solution was being boiled for 18 h, the mixture was cooled to room temperature. The reaction volume was reduced to 5 mL, and then hexanes was added to cause precipitation. The product was collected by filtration, washed with hexanes, and dried under vacuum to give **150** as a yellow powder (0.034 g, 0.054 mmol, 29%). X-ray-quality crystals were grown by allowing a layer of heptane to slowly diffuse into a saturated CH2Cl2 solution of **150**.

Spectral data. ^{1}H NMR ($CDCl_3$, 400 MHz) δ 7.56-7.55 (dd, *J* = 3.8, 2.40 Hz, 2H), 7.33-7.25 (m, 19H), 6.85-6.82 (dt, *J* = 1.6, 7.7 Hz, 1H), 6.79-6.75 (dd, *J* = 4.9, 7.7 Hz, 1H), 6.69-6.65 (t, *J* = 6.6 Hz, 1H), 5.55 (s, 2H); ^{13}C NMR ($CDCl_3$, 100 MHz) δ 145.76, 142.10, 135.55, 135.27, 135.64, 134.61, 133.70, 133.51, 130.63, 128.72, 128.67, 128.64, 128.50, 128.42, 128.22, 128.17, 128.00, 127.46, 117.81, 117.78, 110.59, 110.56, 58.60, 39.89; ^{31}P{^{1}H} NMR (162 MHz, $CDCl_3$) δ +28.06.

Procedure for complexation with gold chloride.

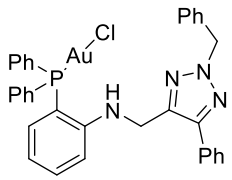

160

Under argon atmosphere CH2Cl2 (10 mL) was added to a round bottom flask containing **122** (0.525 g, 1.0 mmol) and dimethylsulfide-gold(I) chloride (0.561 g, 1.0 mmol) to give a clear solution. The solution was stirred at room temperature for 2 h. Hexanes was added to the reaction mass to get a precipitation. Filtered the solid and dried under vacuum to give **160** as a white powder (0.728 g, 0.96 mmol, 96%). X-ray-quality crystals were grown by allowing a layer of heptane to slowly diffuse into a saturated CH2Cl2 solution of **160**.

Spectral data. ^{1}H NMR ($CDCl_3$, 400 MHz) δ 7.55-7.31 (m, 21H), 6.84-6.80 (t, *J* = 6.2 Hz, 1H), 6.74-6.69 (m, 2H), 5.65 (s, 2H), 5.50 (br, 1H), 4.46 (s, 2H); ^{13}C NMR ($CDCl_3$, 100 MHz) δ 141.11, 141.03, 135.53, 134.48, 134.33, 134.02, 133.47, 132.03, 131.99, 129.48, 129.29, 129.17, 128.77, 128.67, 128.27, 128.20, 128.09, 127.24, 58.63, 40.05; ^{31}P{^{1}H} NMR (162 MHz, $CDCl_3$) δ +18.77

Appendix

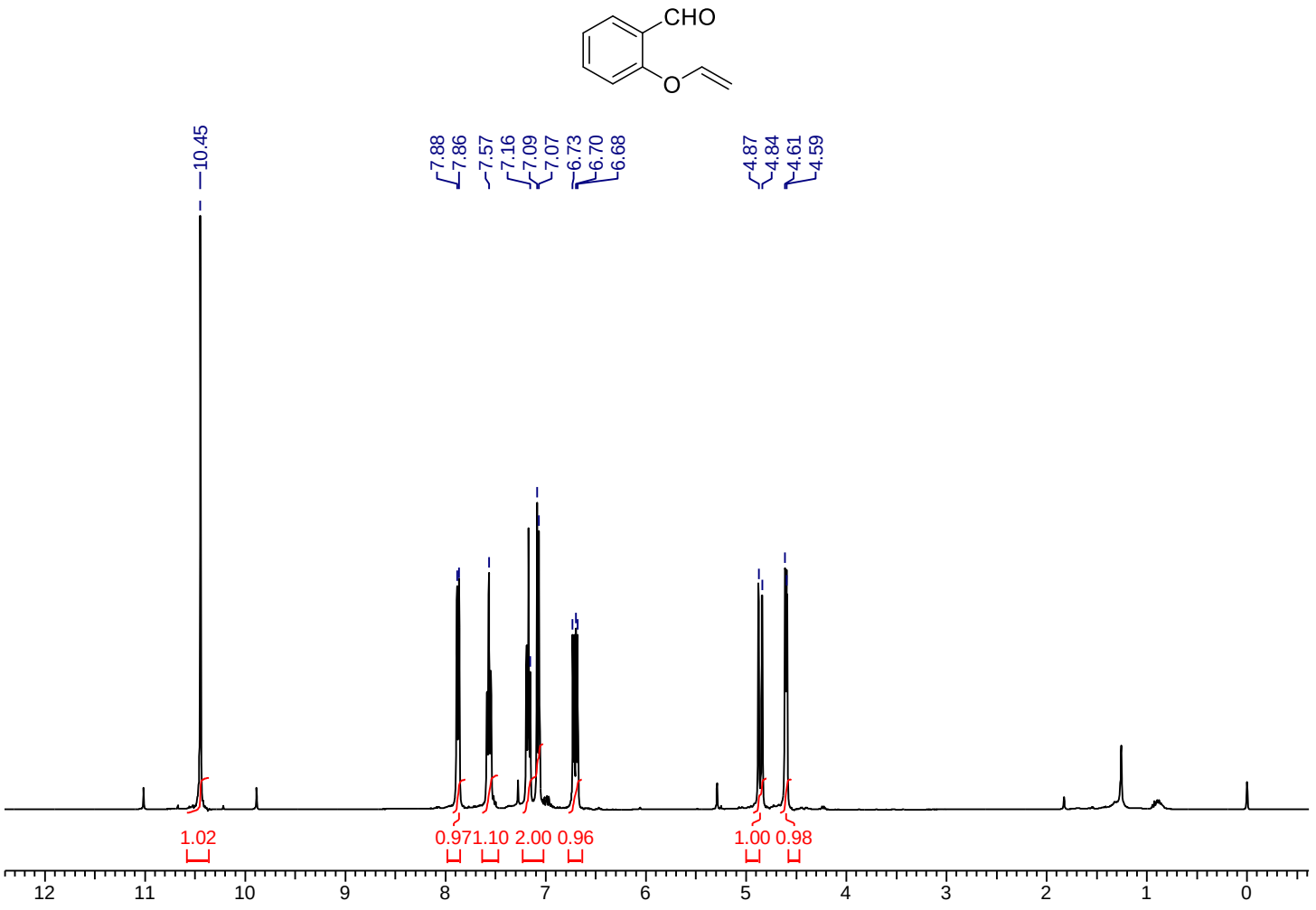
CHO
O
10.45
7.88
7.86
7.57
7.16
7.09
7.07
6.73
6.70
6.68
4.87
4.84
4.61
4.59
1.02
0.97
1.10
2.00
0.96
1.00
0.98
12
11
10
9
8
7
6
5
4
3
2
1
0

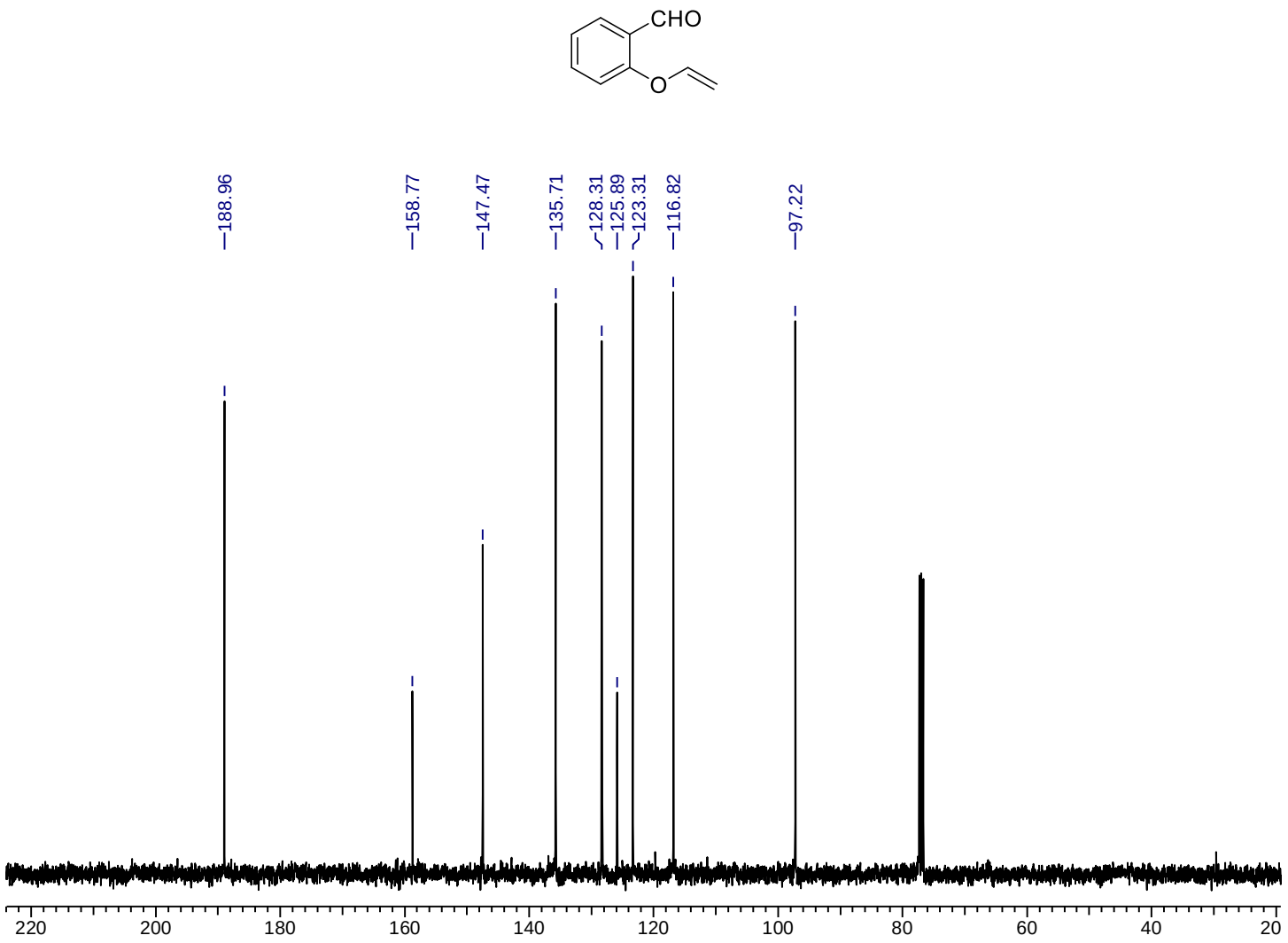
CHO
O
188.96
158.77
147.47
135.71
128.31
125.89
123.31
116.82
97.22
220
200
180
160
140
120
100
80
60
40
20

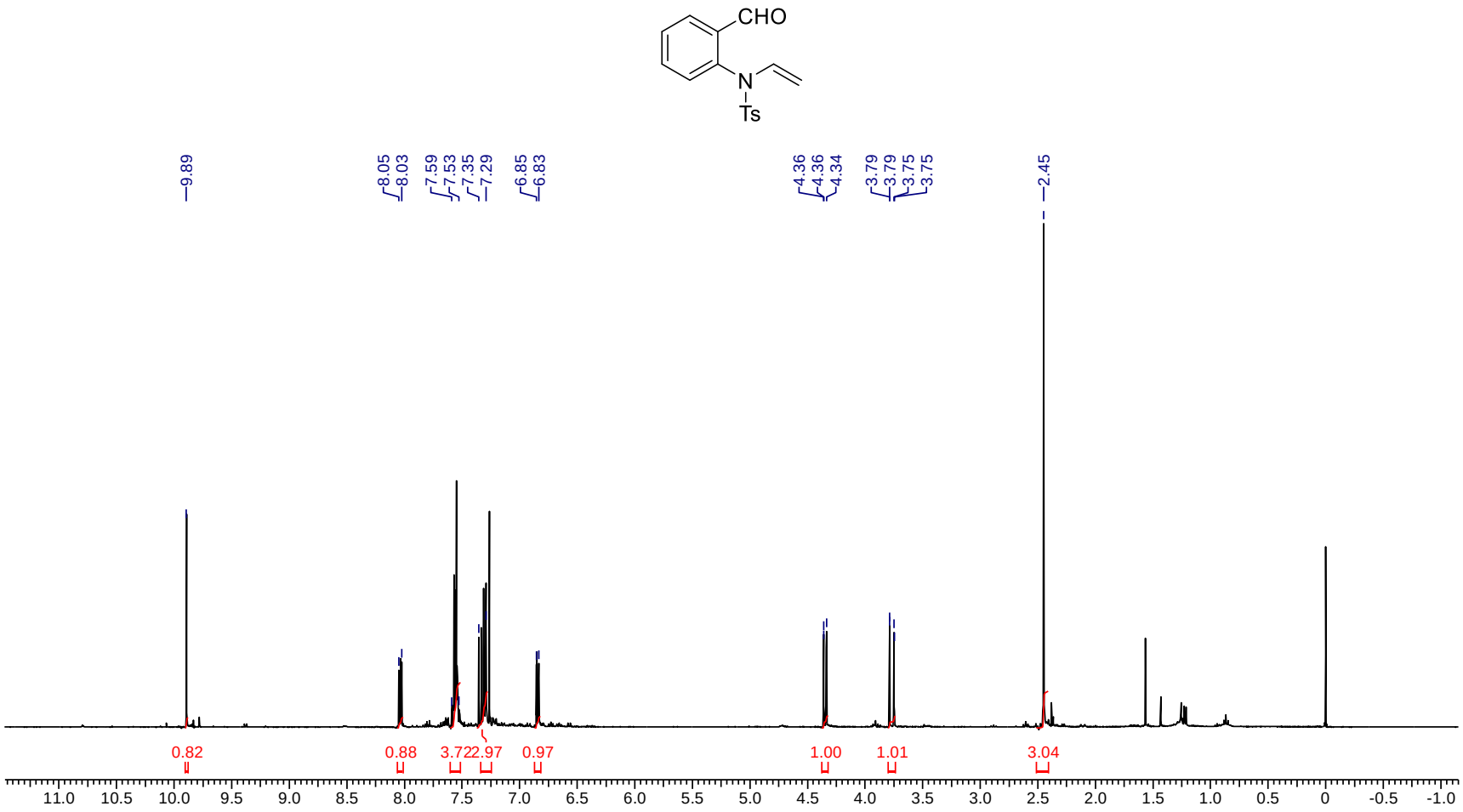
CHO
N
Ts
9.89
8.05
8.03
7.59
7.53
7.35
7.29
6.85
6.83
4.36
4.36
4.34
3.79
3.79
3.75
3.75
2.45
0.82
0.88
3.72
2.97
0.97
1.00
1.01
3.04
11.0
10.5
10.0
9.5
9.0
8.5
8.0
7.5
7.0
6.5
6.0
5.5
5.0
4.5
4.0
3.5
3.0
2.5
2.0
1.5
1.0
0.5
0
-0.5
-1.0

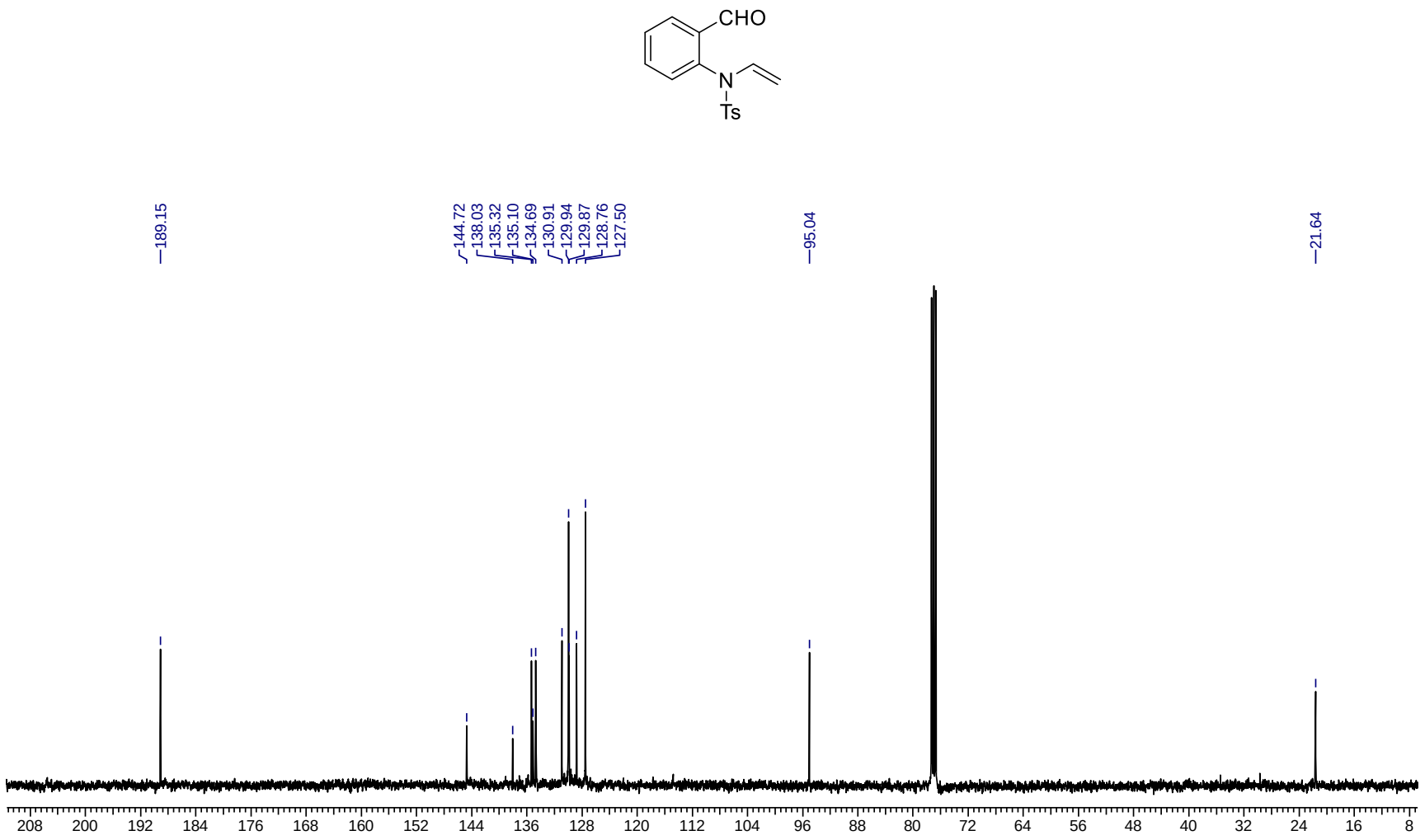
CHO
N
Ts
189.15
144.72
138.03
135.32
135.10
134.69
130.91
129.94
129.87
128.76
127.50
95.04
21.64
208
200
192
184
176
168
160
152
144
136
128
120
112
104
96
88
80
72
64
56
48
40
32
24
16
8

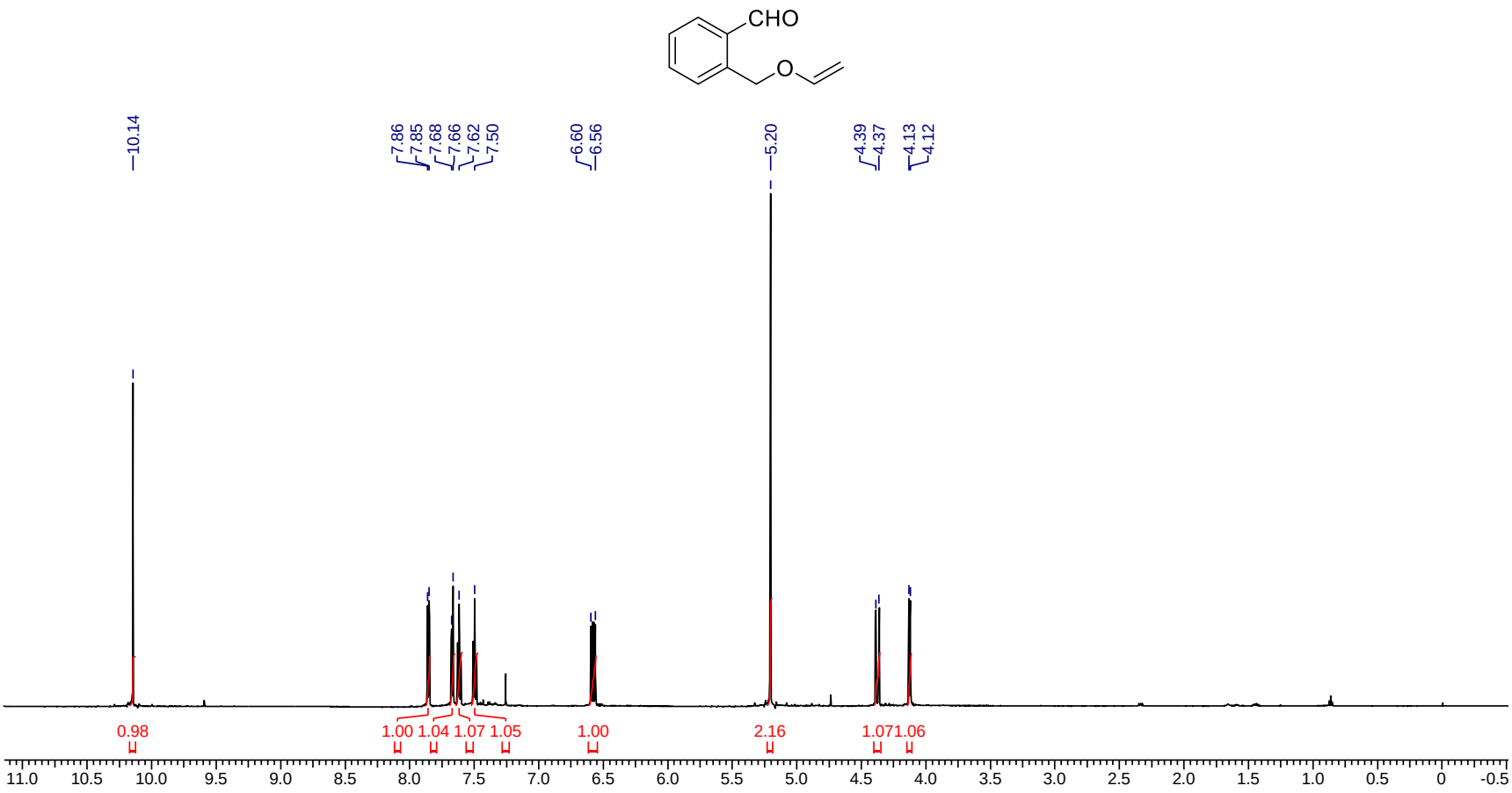
CHO
O
10.14
7.86
7.85
7.68
7.66
7.62
7.50
6.60
6.56
5.20
4.39
4.37
4.13
4.12
0.98
1.00
1.04
1.07
1.05
1.00
2.16
1.07
1.06
11.0
10.5
10.0
9.5
9.0
8.5
8.0
7.5
7.0
6.5
6.0
5.5
5.0
4.5
4.0
3.5
3.0
2.5
2.0
1.5
1.0
0.5
0
-0.5

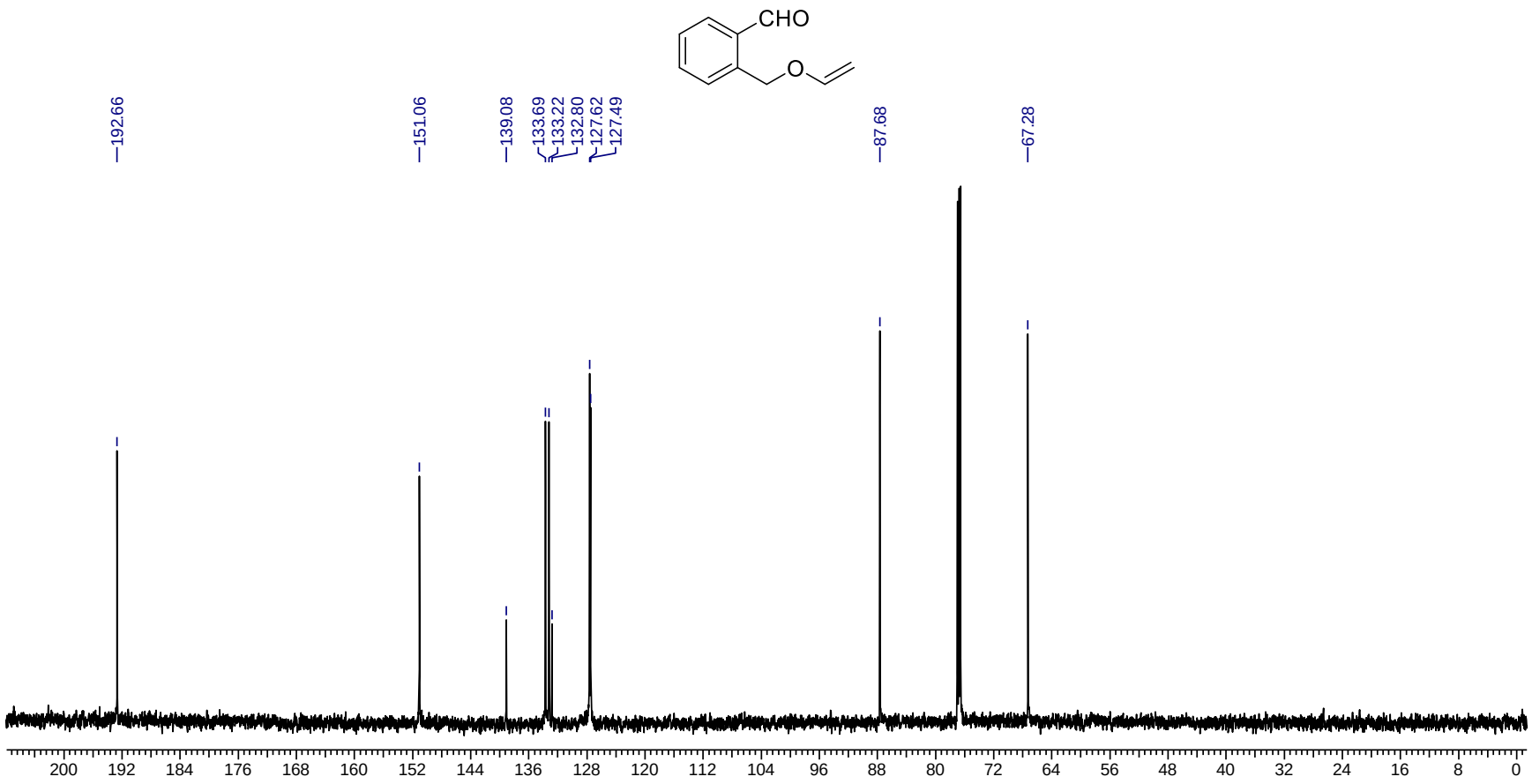
CHO
O
192.66
151.06
139.08
133.69
133.22
132.80
127.62
127.49
87.68
67.28
200
192
184
176
168
160
152
144
136
128
120
112
104
96
88
80
72
64
56
48
40
32
24
16
8
0

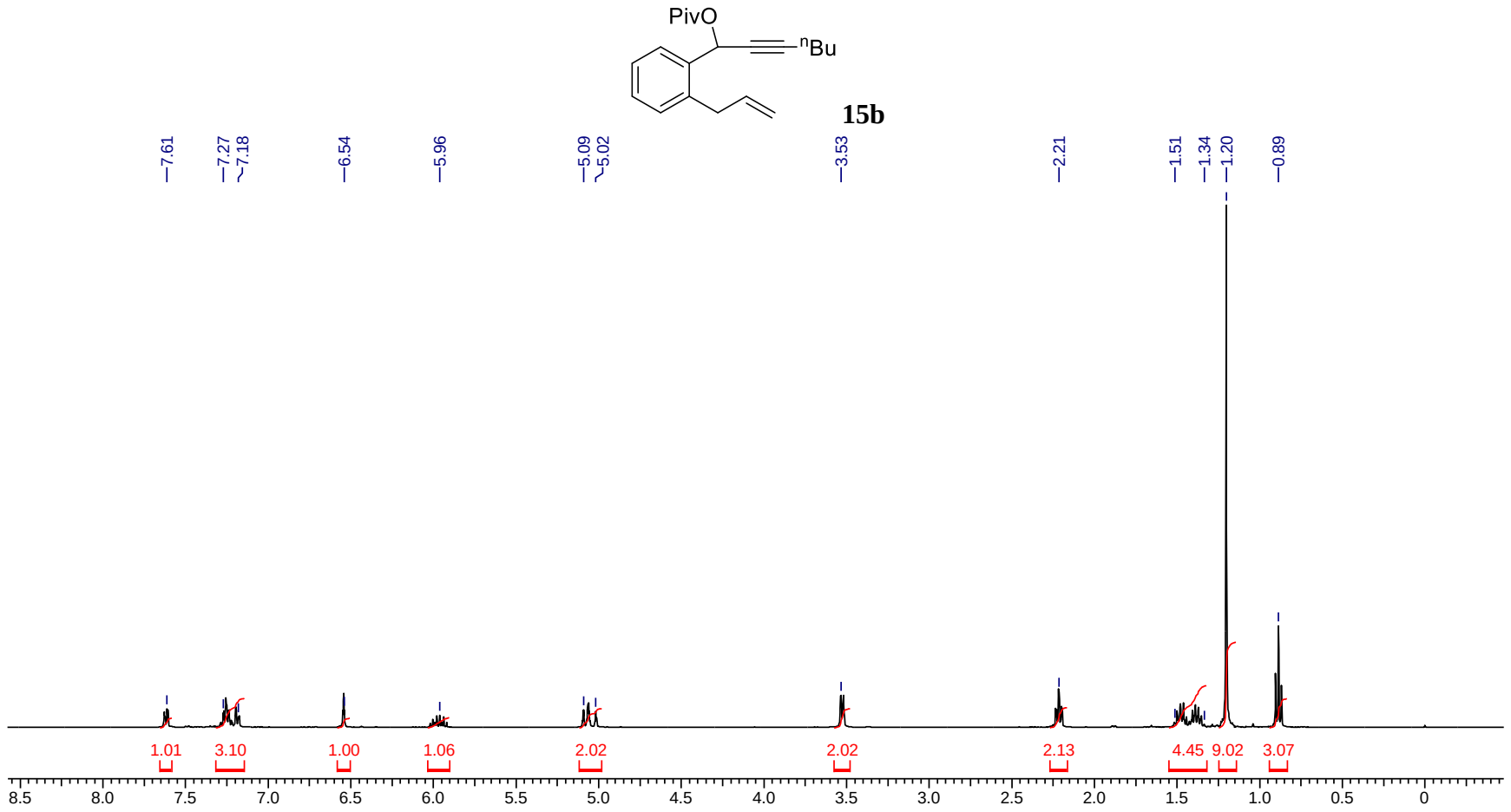
PivO
nBu
15b
7.61
7.27
7.18
6.54
5.96
5.09
5.02
3.53
2.21
1.51
1.34
1.20
0.89
1.01
3.10
1.00
1.06
2.02
2.02
2.13
4.45
9.02
3.07
8.5
8.0
7.5
7.0
6.5
6.0
5.5
5.0
4.5
4.0
3.5
3.0
2.5
2.0
1.5
1.0
0.5
0

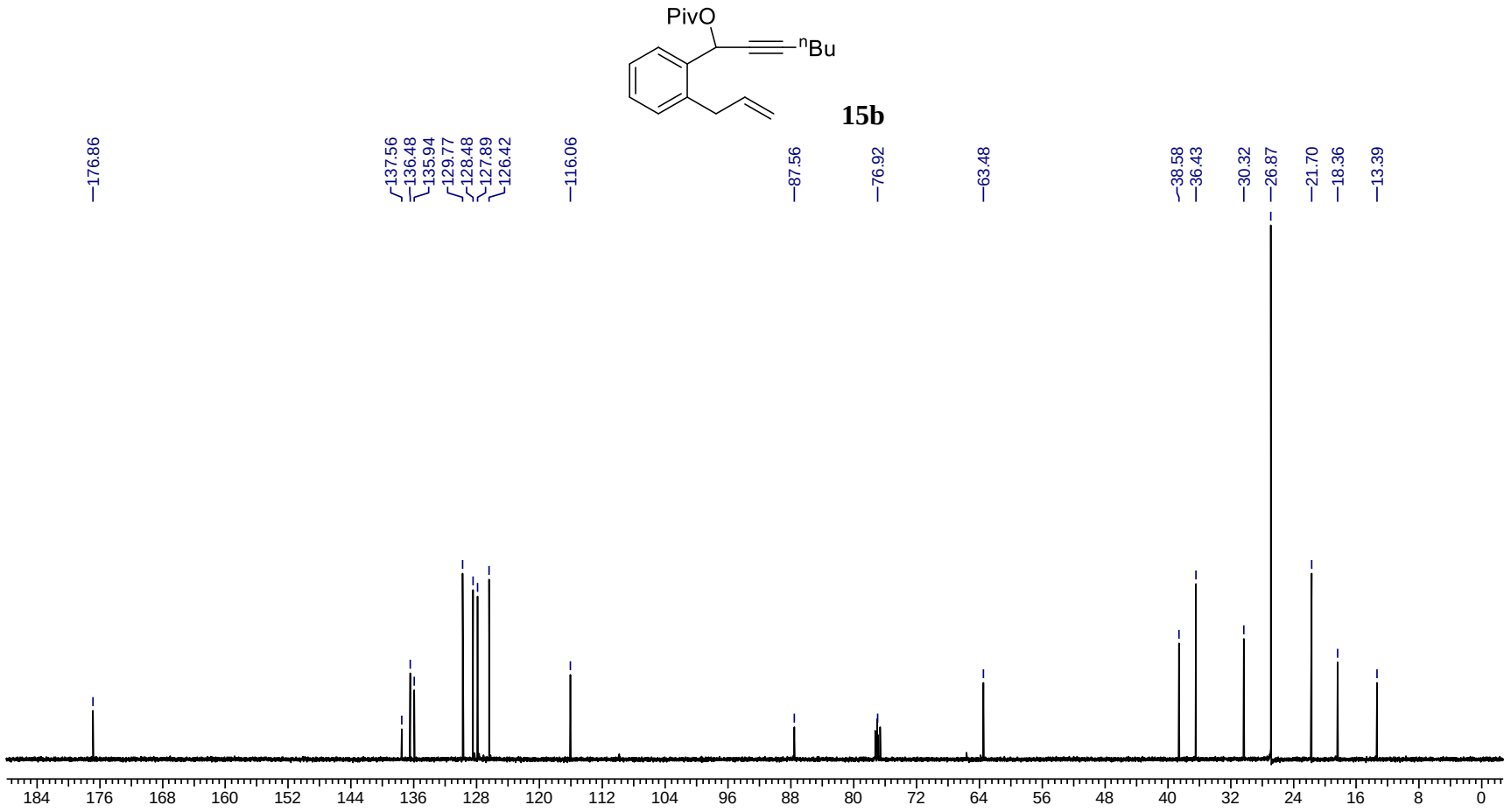
PivO
nBu
15b
176.86
137.56
136.48
135.94
129.77
128.48
127.89
126.42
116.06
87.56
76.92
63.48
38.58
36.43
30.32
26.87
21.70
18.36
13.39
184 176 168 160 152 144 136 128 120 112 104 96 88 80 72 64 56 48 40 32 24 16 8 0

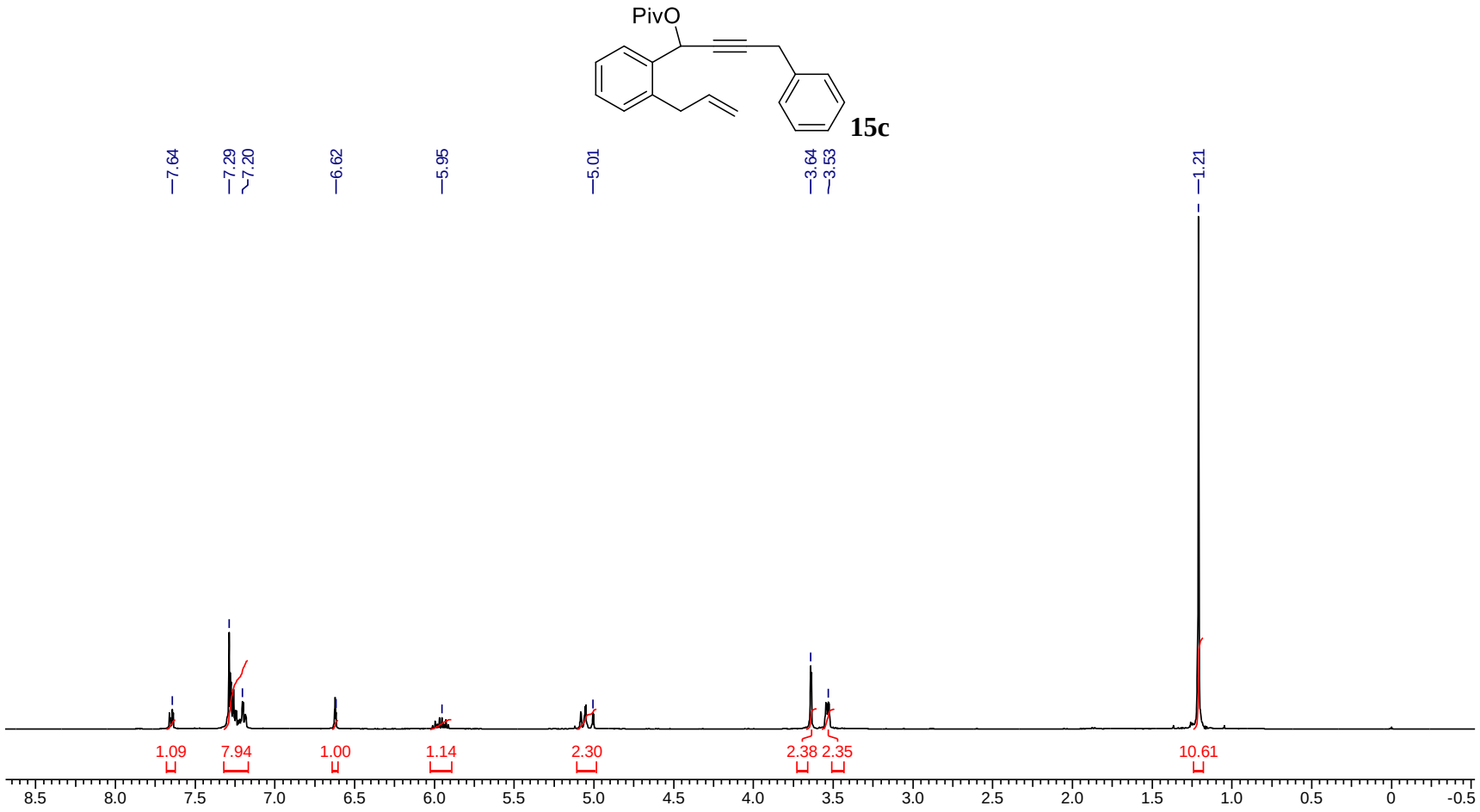
PivO
15c
7.64
7.29
7.20
6.62
5.95
5.01
3.64
3.53
1.21
1.09
7.94
1.00
1.14
2.30
2.38
2.35
10.61
8.5
8.0
7.5
7.0
6.5
6.0
5.5
5.0
4.5
4.0
3.5
3.0
2.5
2.0
1.5
1.0
0.5
0
-0.5

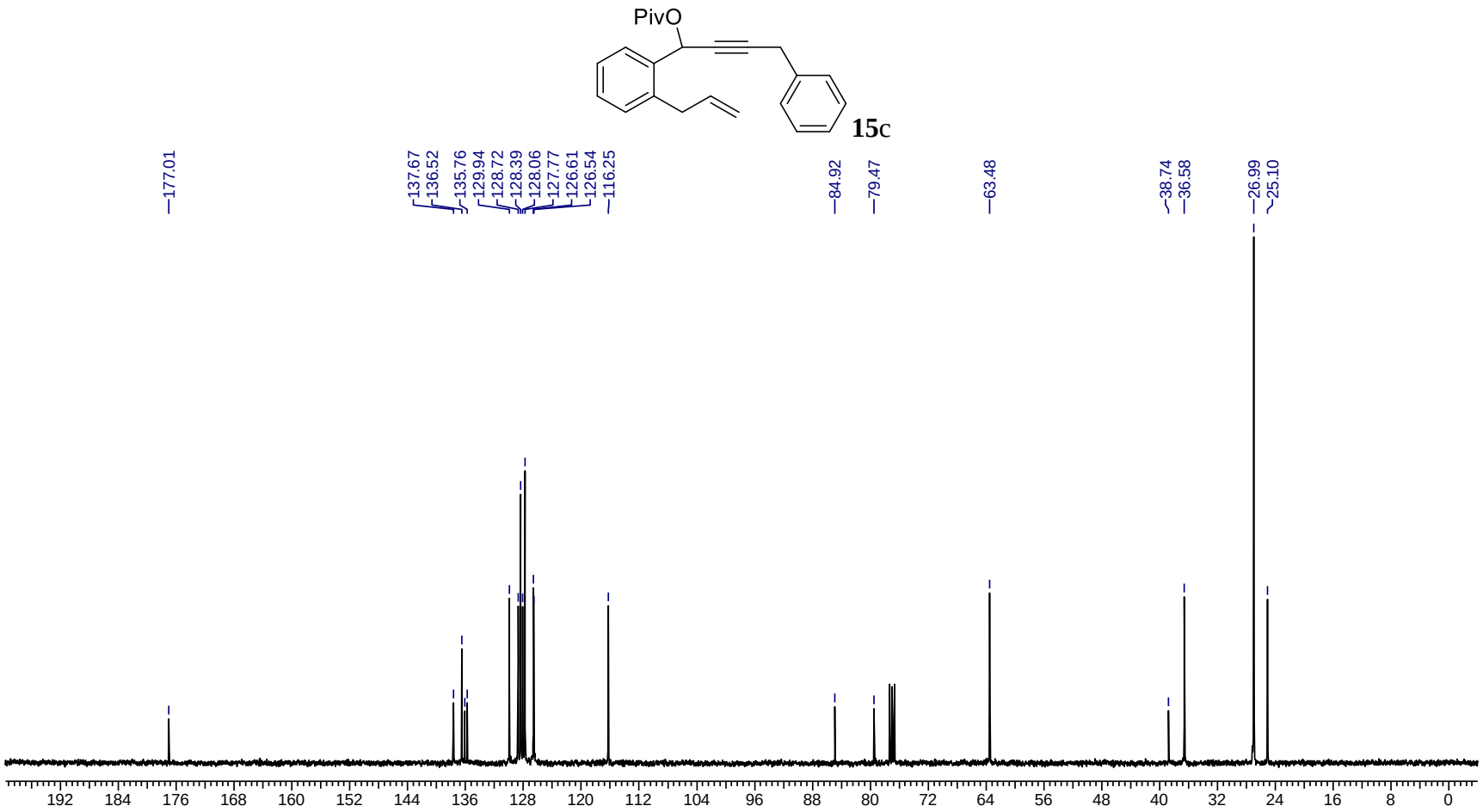
PivO
15c
177.01
137.67
136.52
135.76
129.94
128.72
128.39
128.06
127.77
126.61
126.54
116.25
84.92
79.47
63.48
38.74
36.58
26.99
25.10
192
184
176
168
160
152
144
136
128
120
112
104
96
88
80
72
64
56
48
40
32
24
16
8
0

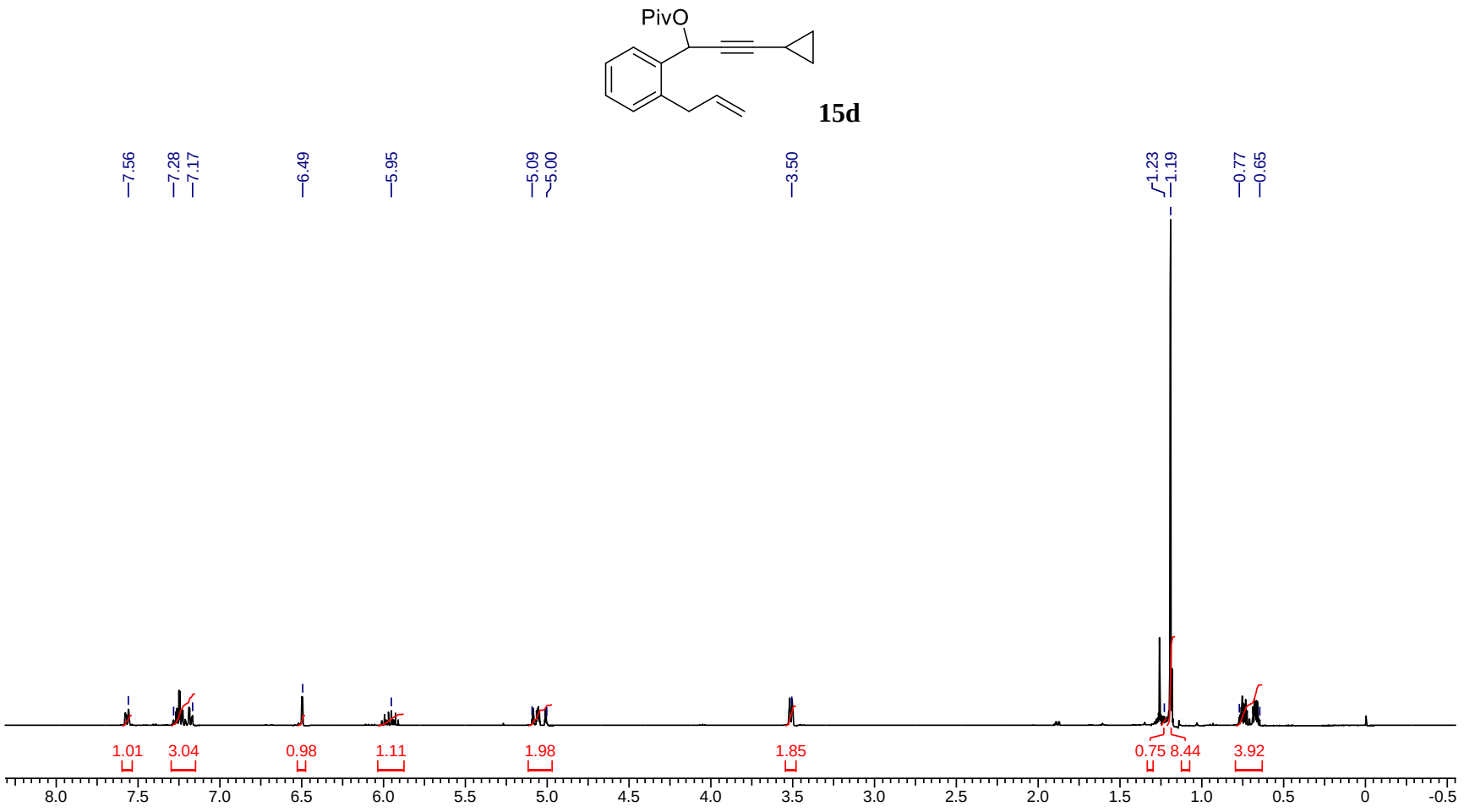
PivO
15d
7.56
7.28
7.17
6.49
5.95
5.09
5.00
3.50
1.23
1.19
0.77
0.65
1.01
3.04
0.98
1.11
1.98
1.85
0.75
8.44
3.92
8.0
7.5
7.0
6.5
6.0
5.5
5.0
4.5
4.0
3.5
3.0
2.5
2.0
1.5
1.0
0.5
0
-0.5

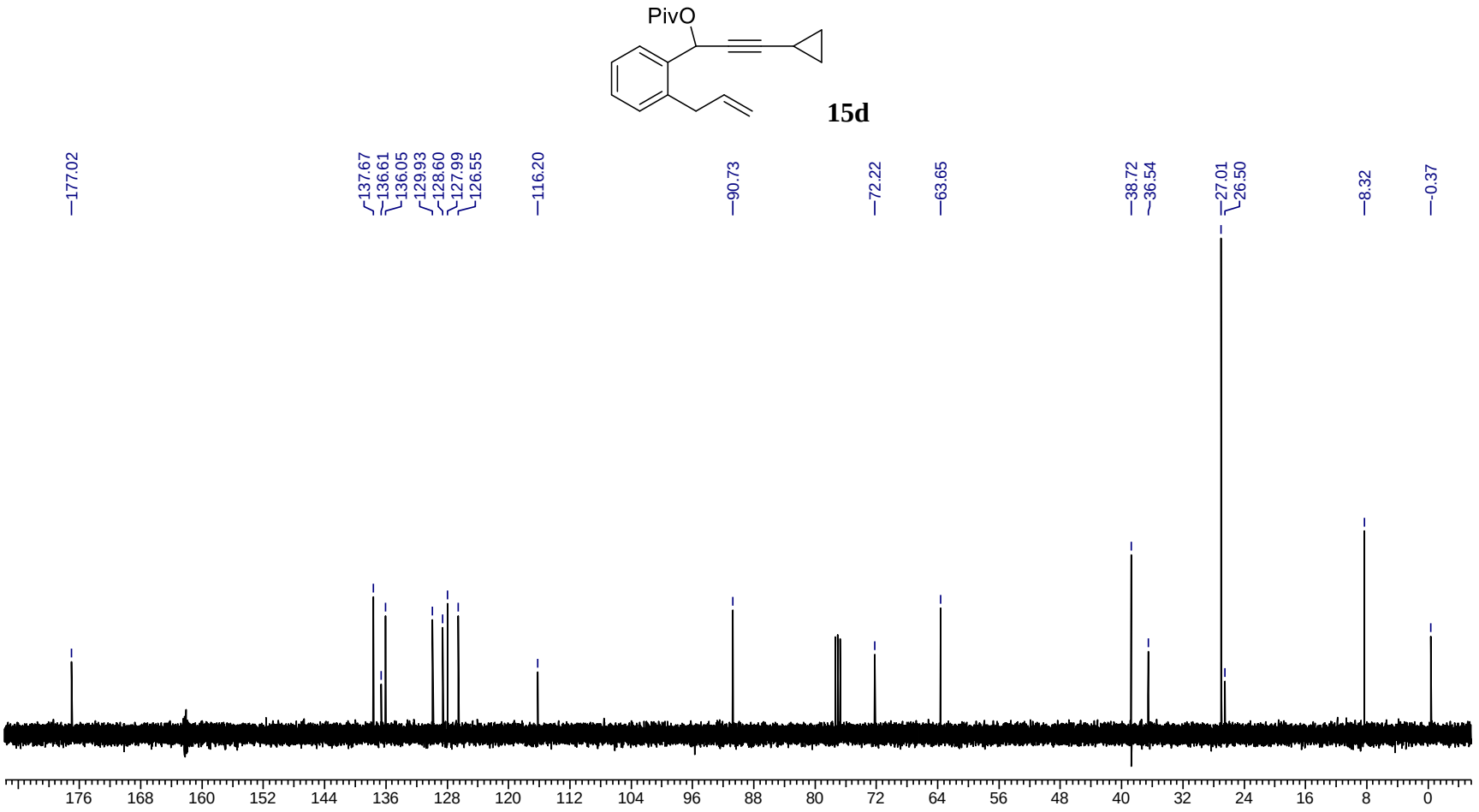
PivO
15d
177.02
137.67
136.61
136.05
129.93
128.60
127.99
126.55
116.20
90.73
72.22
63.65
38.72
36.54
27.01
26.50
8.32
-0.37
176
168
160
152
144
136
128
120
112
104
96
88
80
72
64
56
48
40
32
24
16
8
0

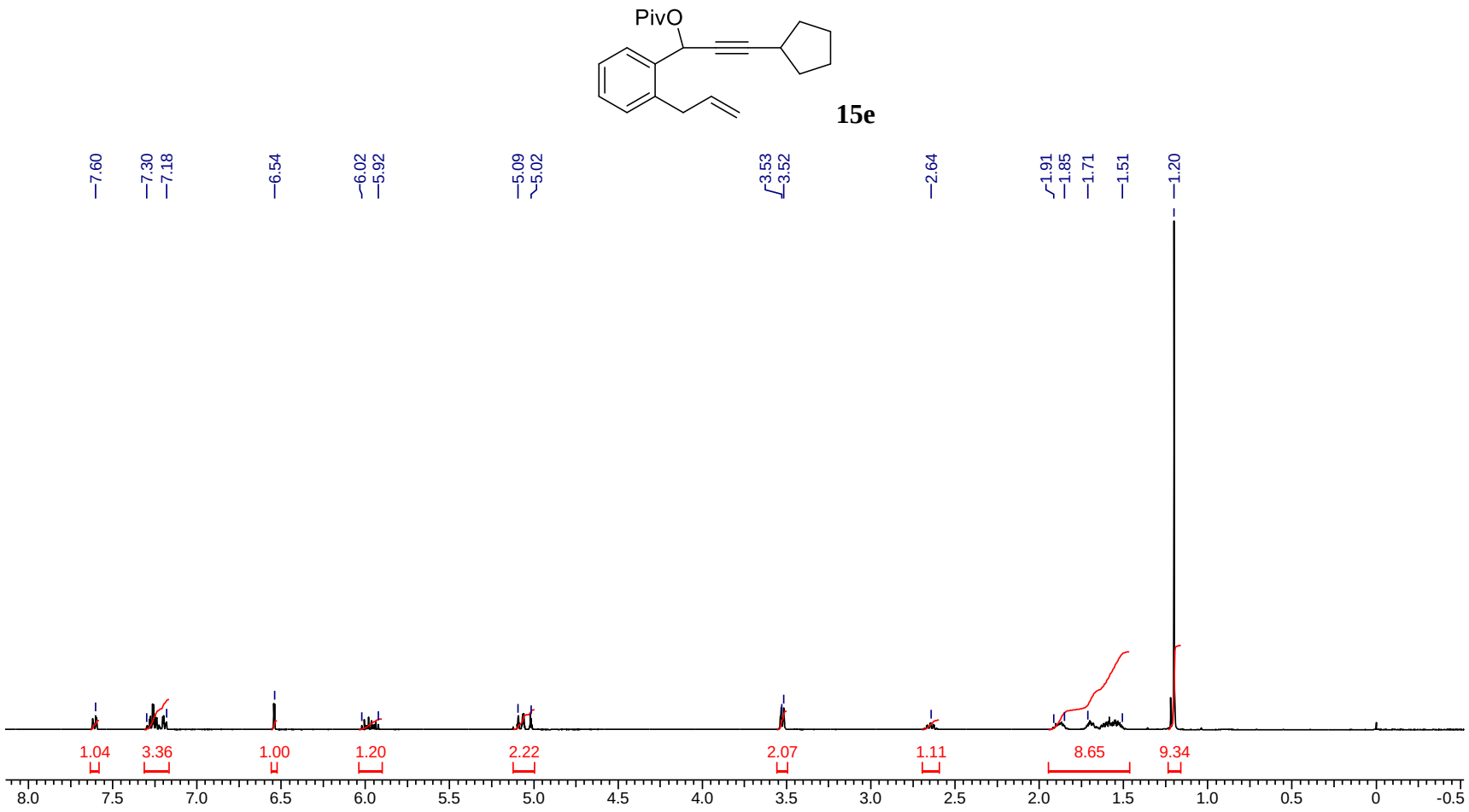
PivO
15e
7.60
7.30
7.18
6.54
6.02
5.92
5.09
5.02
3.53
3.52
2.64
1.91
1.85
1.71
1.51
1.20
1.04
3.36
1.00
1.20
2.22
2.07
1.11
8.65
9.34
8.0
7.5
7.0
6.5
6.0
5.5
5.0
4.5
4.0
3.5
3.0
2.5
2.0
1.5
1.0
0.5
0
-0.5

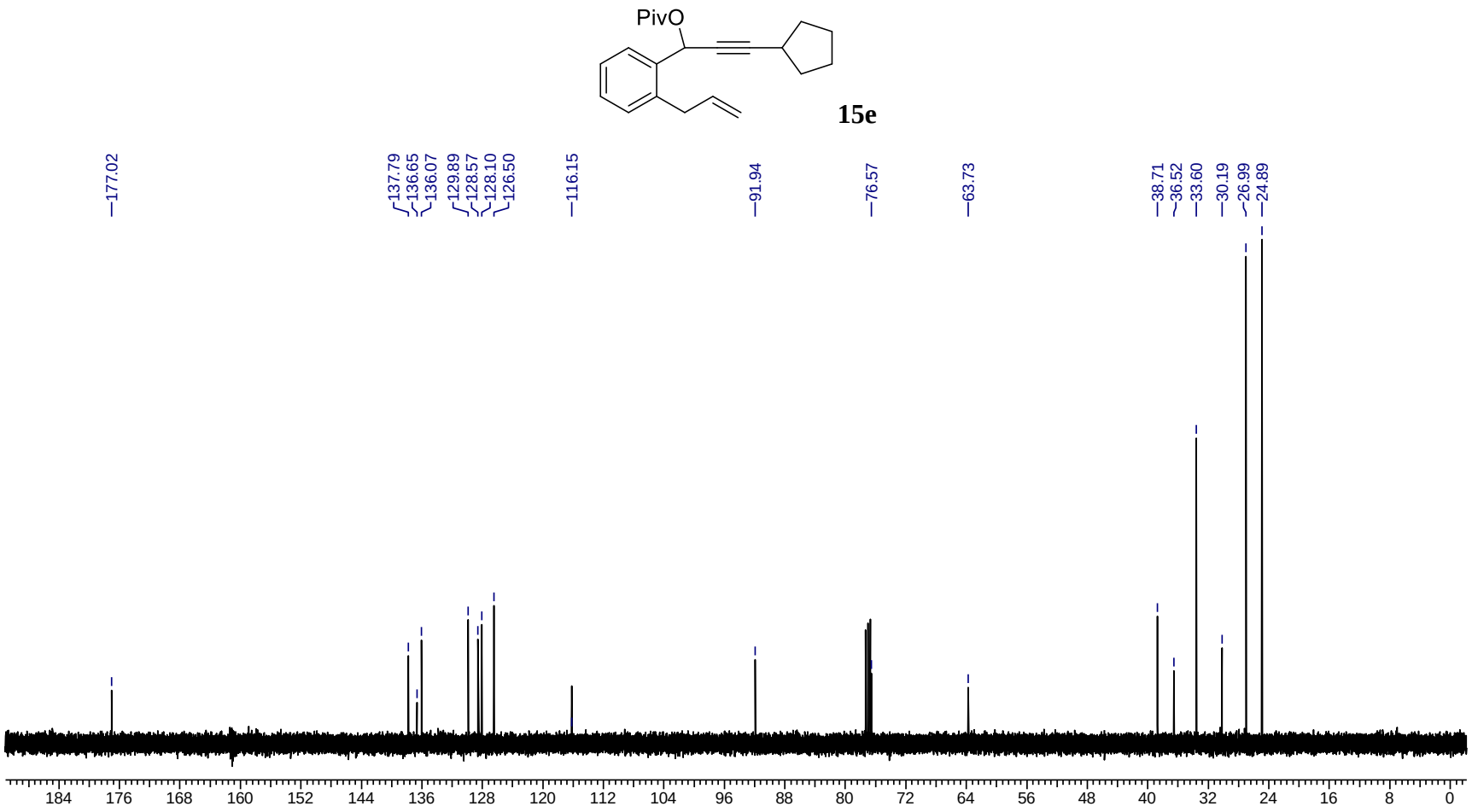
PivO
15e
177.02
137.79
136.65
136.07
129.89
128.57
128.10
126.50
116.15
91.94
76.57
63.73
38.71
36.52
33.60
30.19
26.99
24.89
184
176
168
160
152
144
136
128
120
112
104
96
88
80
72
64
56
48
40
32
24
16
8
0

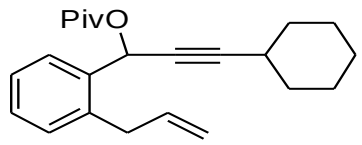
PivO

15f

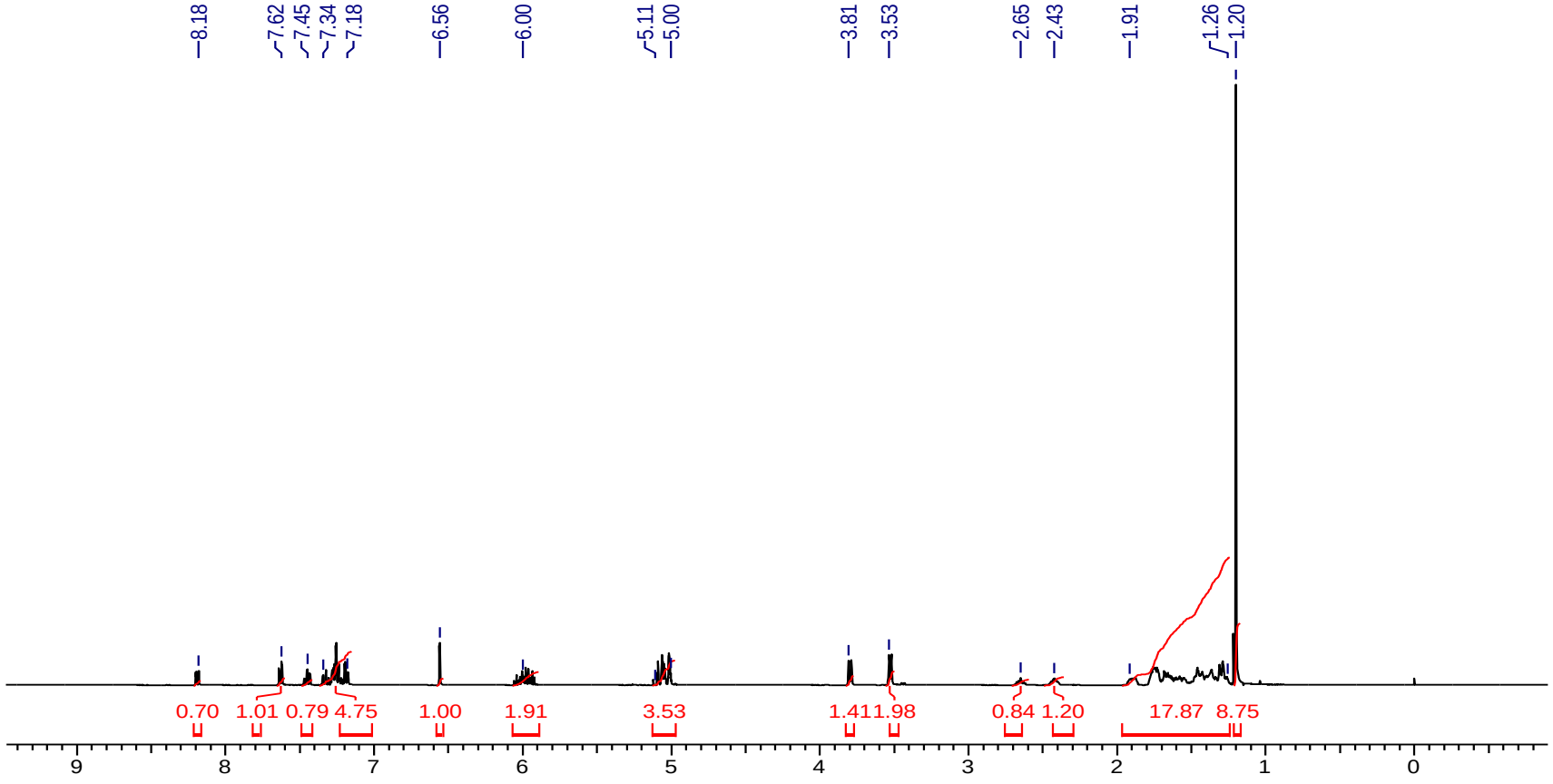
8.18
7.62
7.45
7.34
7.18
6.56
6.00
5.11
5.00
3.81
3.53
2.65
2.43
1.91
1.26
1.20
0.70
1.01
0.79
4.75
1.00
1.91
3.53
1.41
1.98
0.84
1.20
17.87
8.75
9
8
7
6
5
4
3
2
1
0

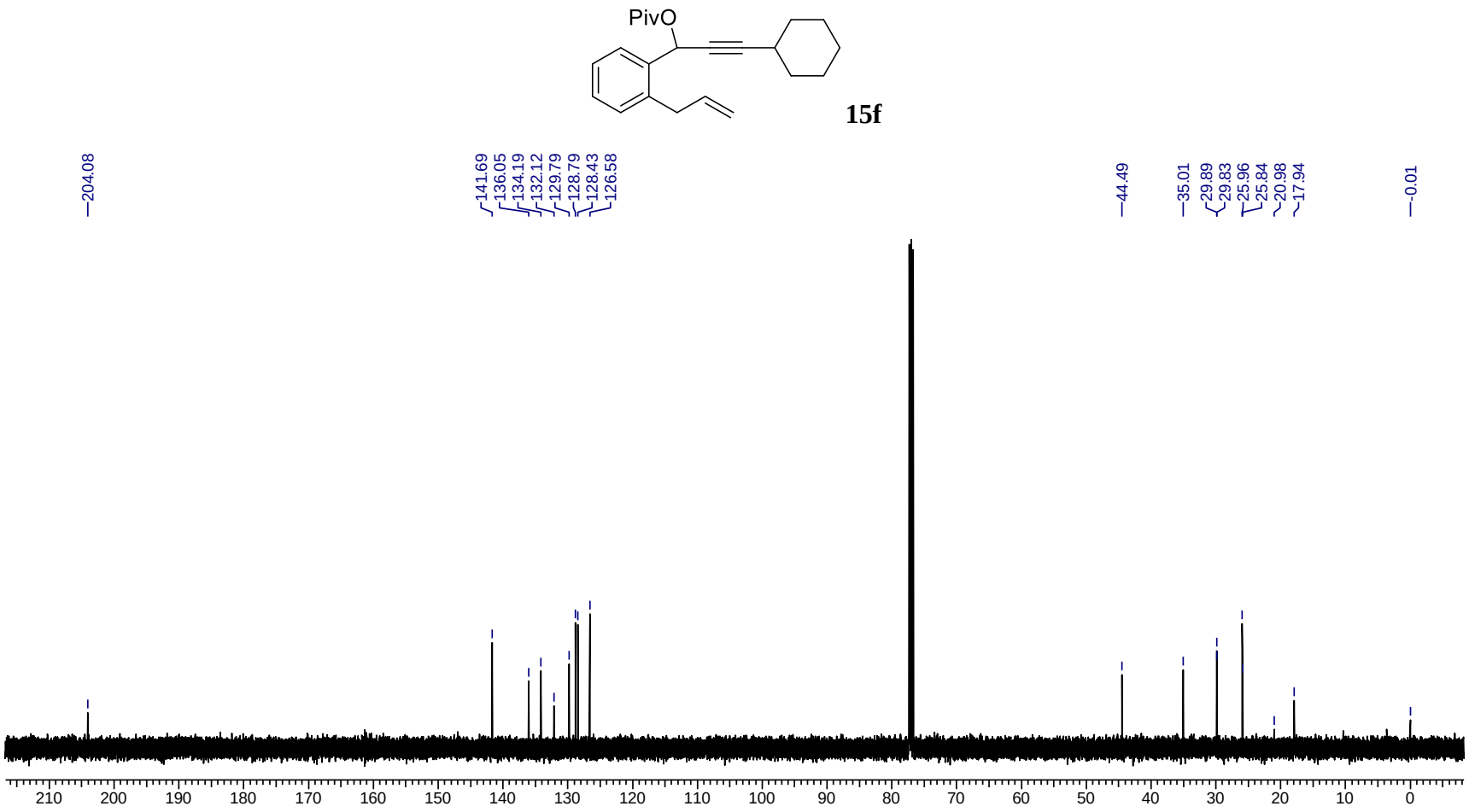
PivO
15f
204.08
141.69
136.05
134.19
132.12
129.79
128.79
128.43
126.58
44.49
35.01
29.89
29.83
25.96
25.84
20.98
17.94
0.01
210
200
190
180
170
160
150
140
130
120
110
100
90
80
70
60
50
40
30
20
10
0

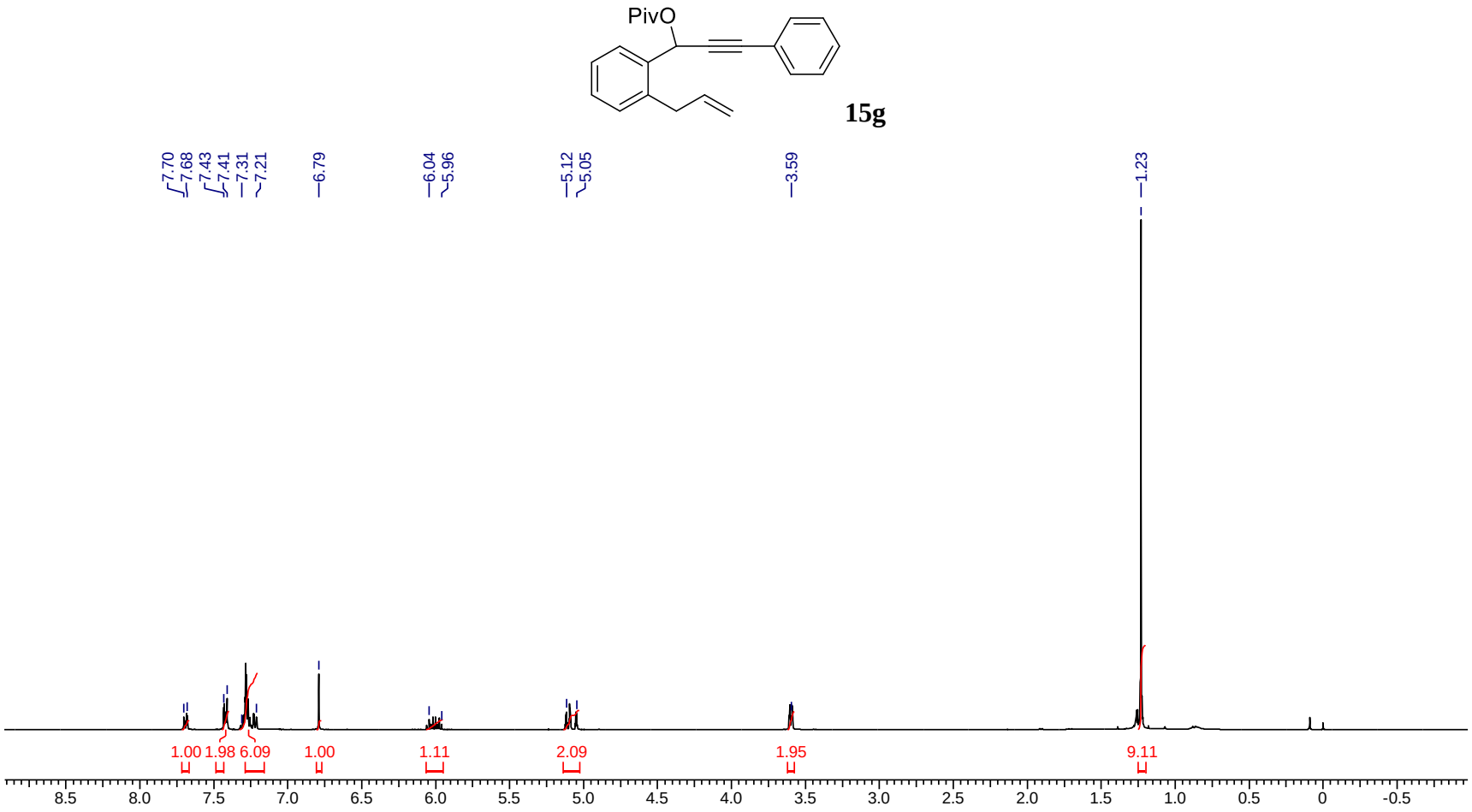
PivO
15g
7.70
7.68
7.43
7.41
7.31
7.21
6.79
6.04
5.96
5.12
5.05
3.59
1.23
1.00
1.98
6.09
1.00
1.11
2.09
1.95
9.11
8.5
8.0
7.5
7.0
6.5
6.0
5.5
5.0
4.5
4.0
3.5
3.0
2.5
2.0
1.5
1.0
0.5
0
-0.5

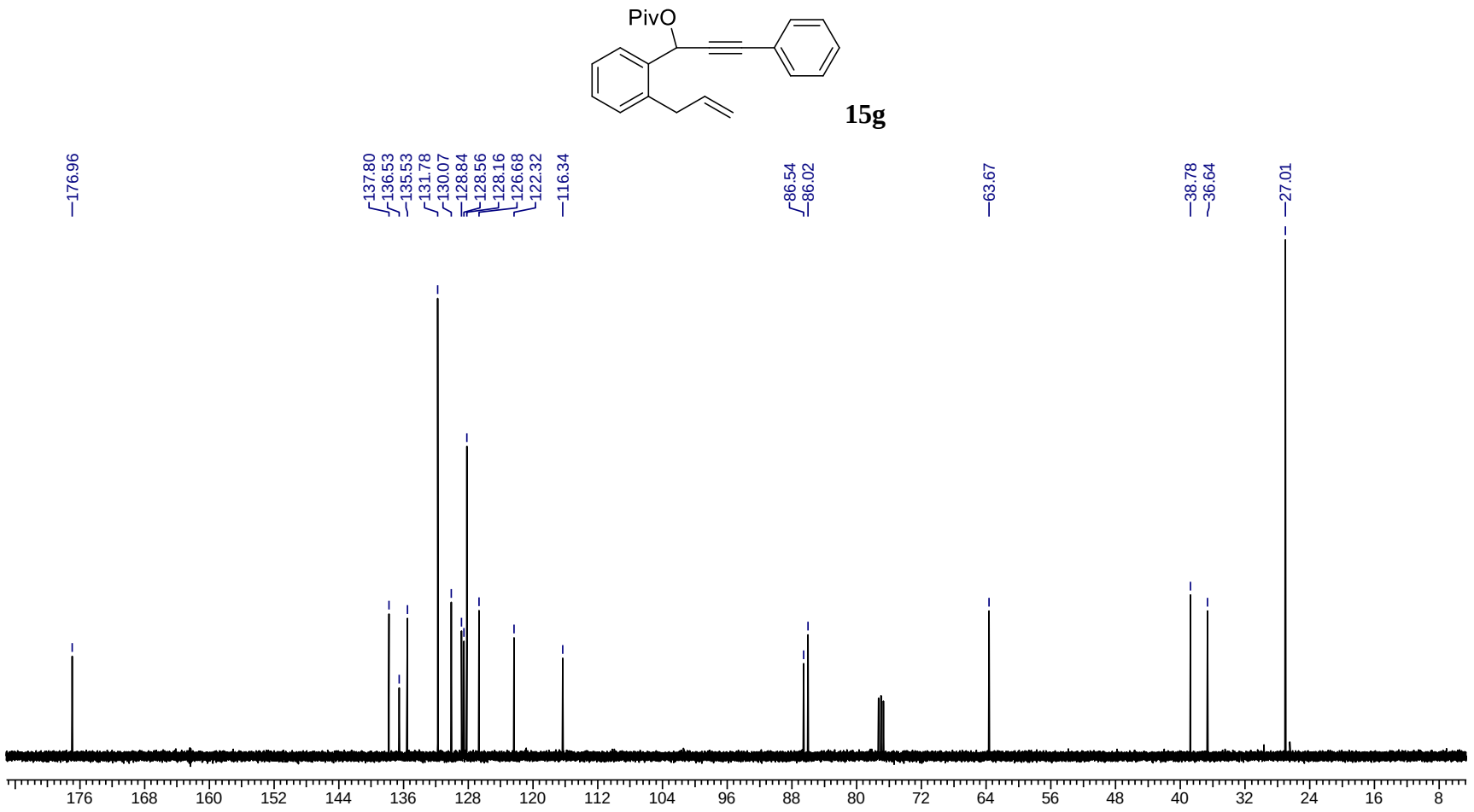
PivO
15g
176.96
137.80
136.53
135.53
131.78
130.07
128.84
128.56
128.16
126.68
122.32
116.34
86.54
86.02
63.67
38.78
36.64
27.01
176
168
160
152
144
136
128
120
112
104
96
88
80
72
64
56
48
40
32
24
16
8

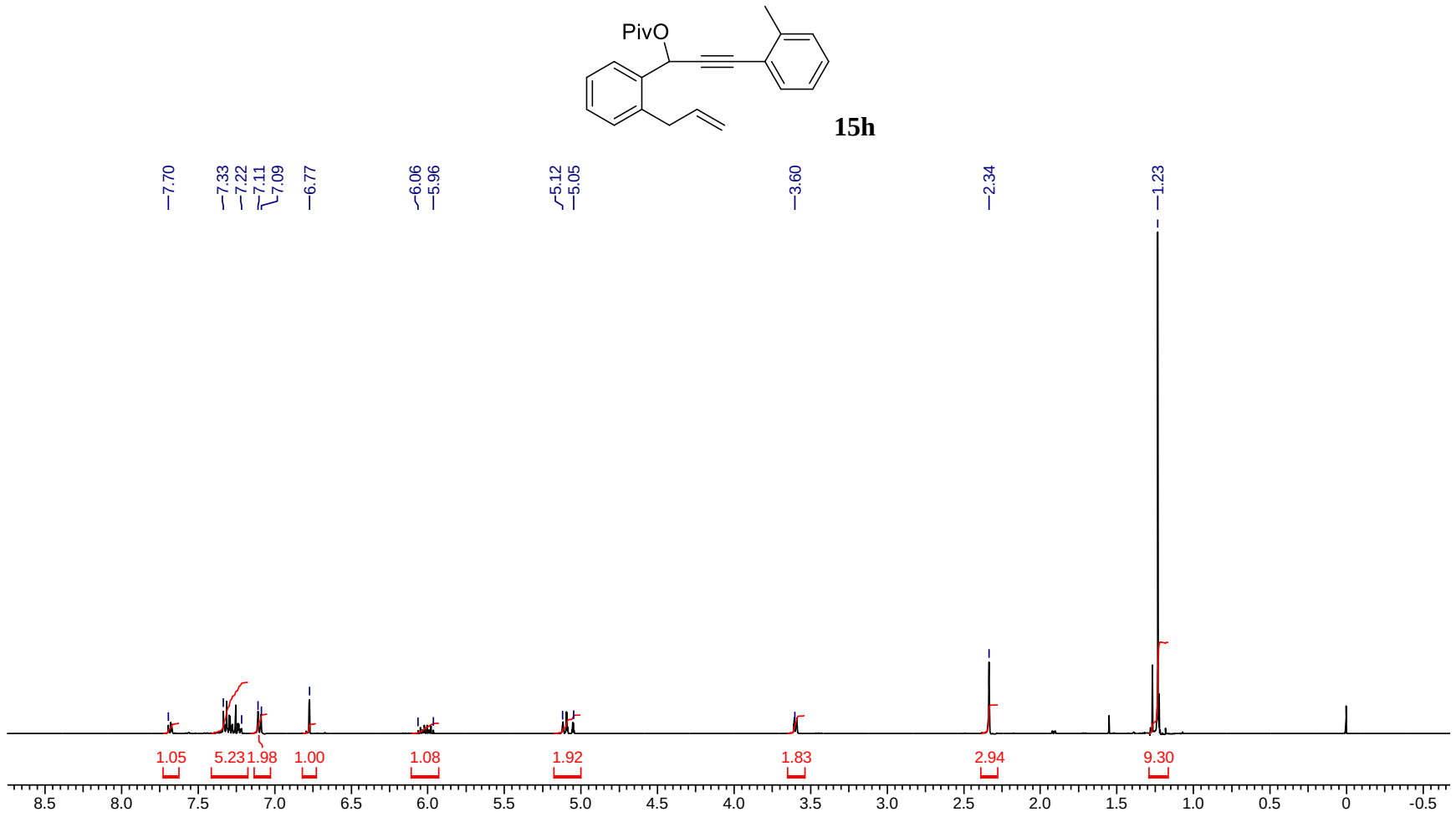
PivO
15h
7.70
7.33
7.22
7.11
7.09
6.77
6.06
5.96
5.12
5.05
3.60
2.34
1.23
1.05
5.23
1.98
1.00
1.08
1.92
1.83
2.94
9.30
8.5
8.0
7.5
7.0
6.5
6.0
5.5
5.0
4.5
4.0
3.5
3.0
2.5
2.0
1.5
1.0
0.5
0
-0.5

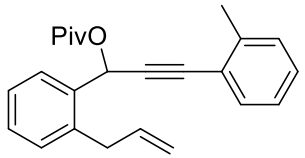
PivO

15h

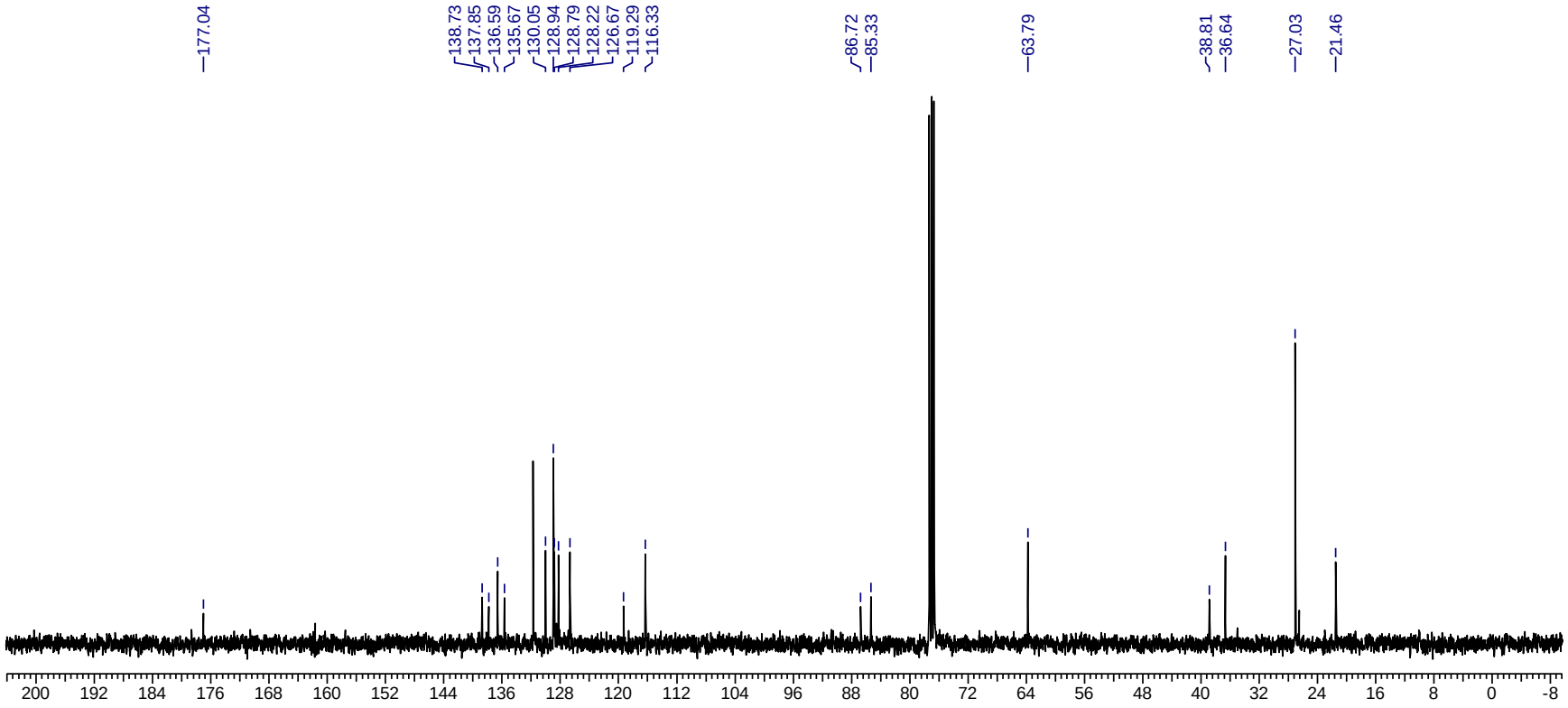
177.04
138.73
137.85
136.59
135.67
130.05
128.94
128.79
128.22
126.67
119.29
116.33
86.72
85.33
63.79
38.81
36.64
27.03
21.46
200
192
184
176
168
160
152
144
136
128
120
112
104
96
88
80
72
64
56
48
40
32
24
16
8
0
-8

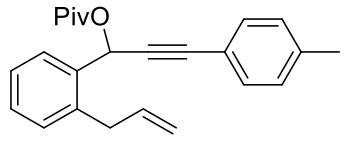
PivO

15i

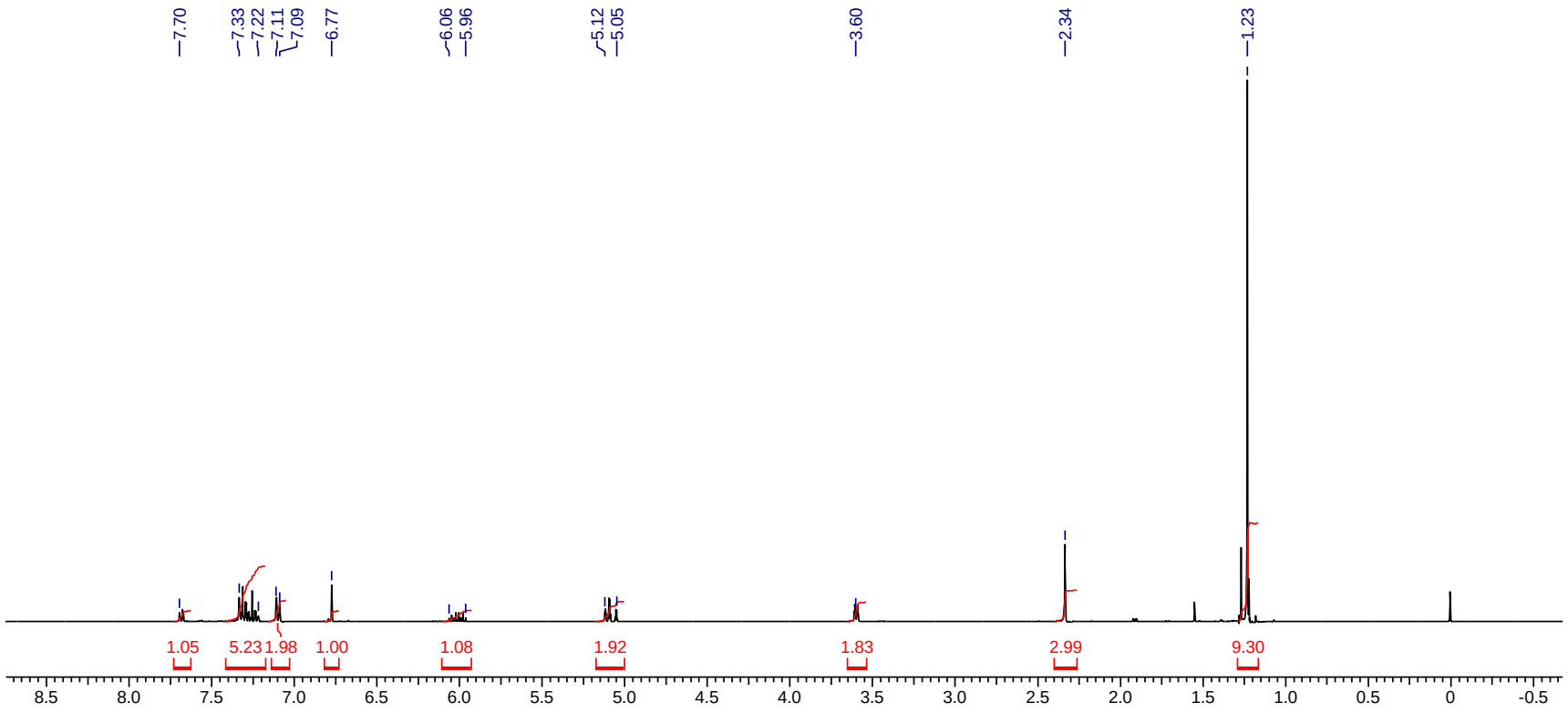
7.70
7.33
7.22
7.11
7.09
6.77
6.06
5.96
5.12
5.05
3.60
2.34
1.23
1.05
5.23
1.98
1.00
1.08
1.92
1.83
2.99
9.30
8.5
8.0
7.5
7.0
6.5
6.0
5.5
5.0
4.5
4.0
3.5
3.0
2.5
2.0
1.5
1.0
0.5
0
-0.5

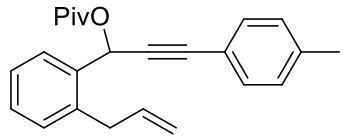
PivO

15i

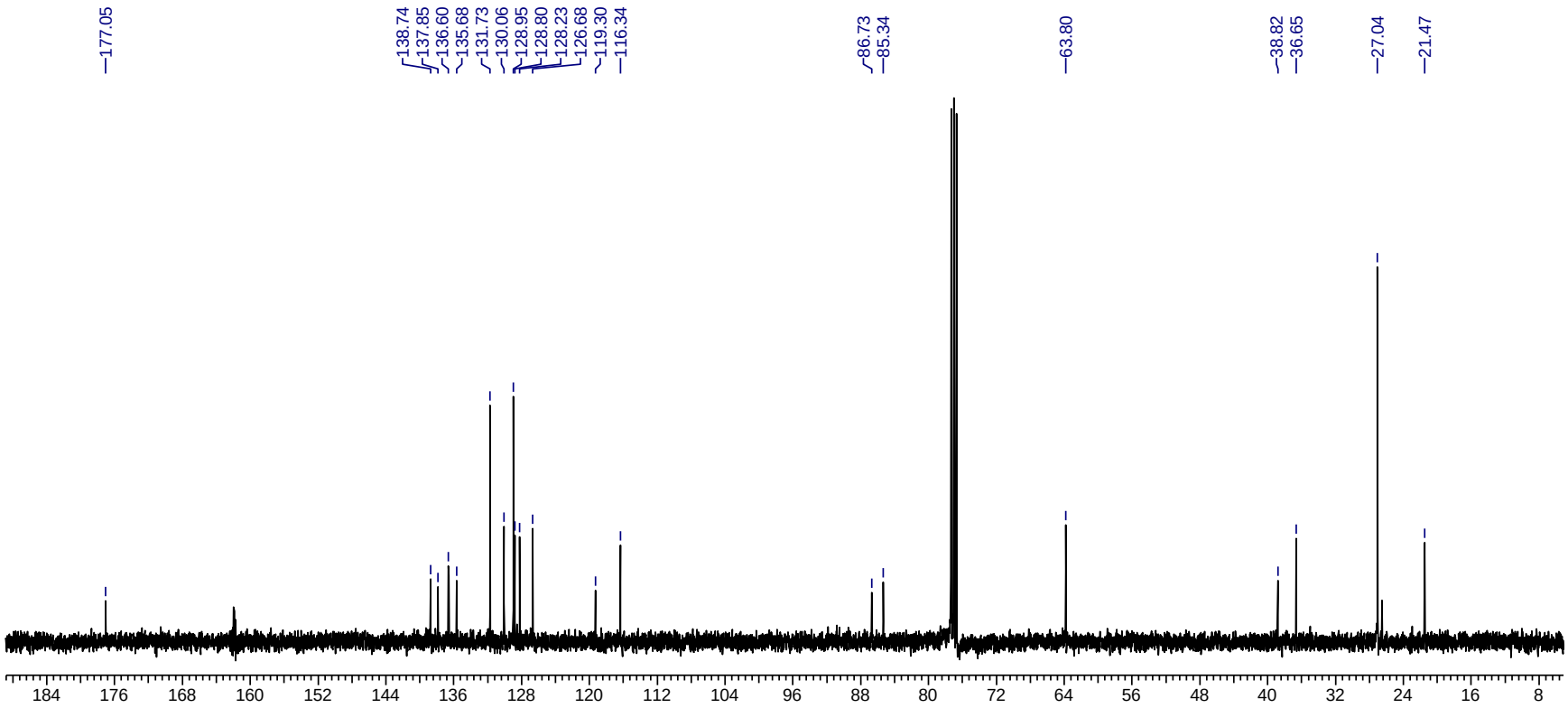
177.05
138.74
137.85
136.60
135.68
131.73
130.06
128.95
128.80
128.23
126.68
119.30
116.34
86.73
85.34
63.80
38.82
36.65
27.04
21.47
184
176
168
160
152
144
136
128
120
112
104
96
88
80
72
64
56
48
40
32
24
16
8

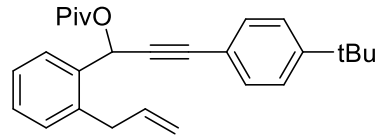
PivO
tBu

15j

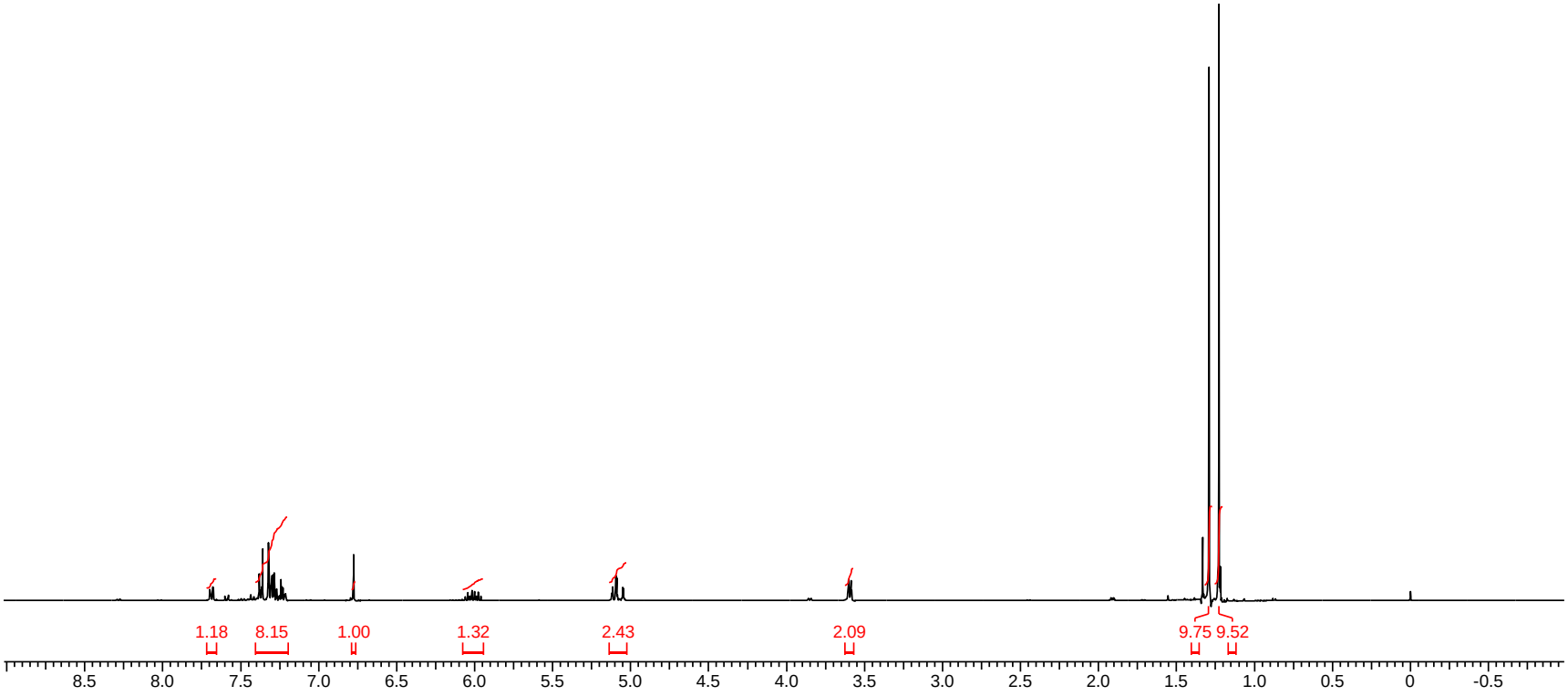
1.18
8.15
1.00
1.32
2.43
2.09
9.75
9.52
8.5
8.0
7.5
7.0
6.5
6.0
5.5
5.0
4.5
4.0
3.5
3.0
2.5
2.0
1.5
1.0
0.5
0
-0.5

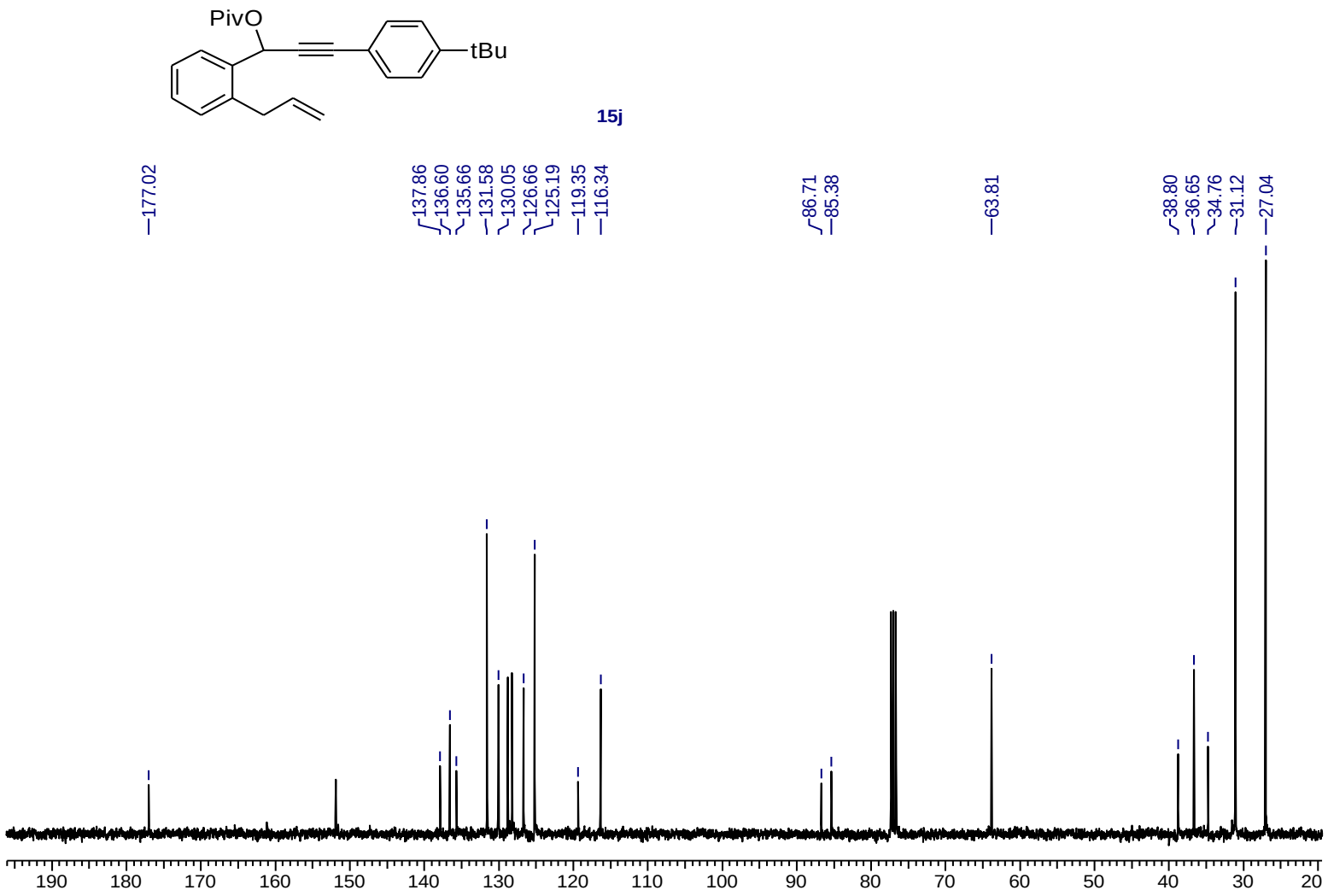
PivO
tBu
15j
177.02
137.86
136.60
135.66
131.58
130.05
126.66
125.19
119.35
116.34
86.71
85.38
63.81
38.80
36.65
34.76
31.12
27.04
190
180
170
160
150
140
130
120
110
100
90
80
70
60
50
40
30
20

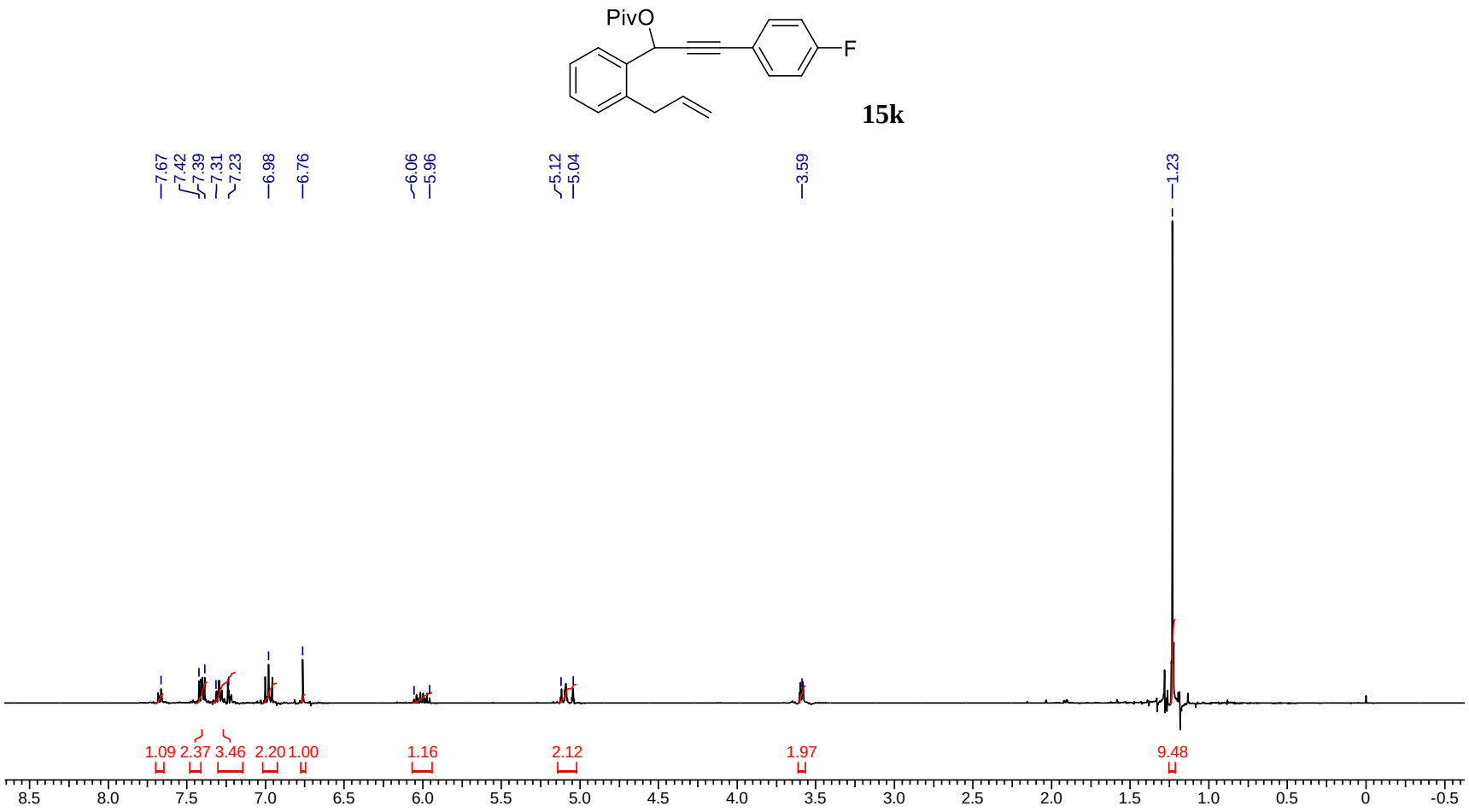
PivO
F
15k
7.67
7.42
7.39
7.31
7.23
6.98
6.76
6.06
5.96
5.12
5.04
3.59
1.23
1.09
2.37
3.46
2.20
1.00
1.16
2.12
1.97
9.48
8.5
8.0
7.5
7.0
6.5
6.0
5.5
5.0
4.5
4.0
3.5
3.0
2.5
2.0
1.5
1.0
0.5
0
-0.5

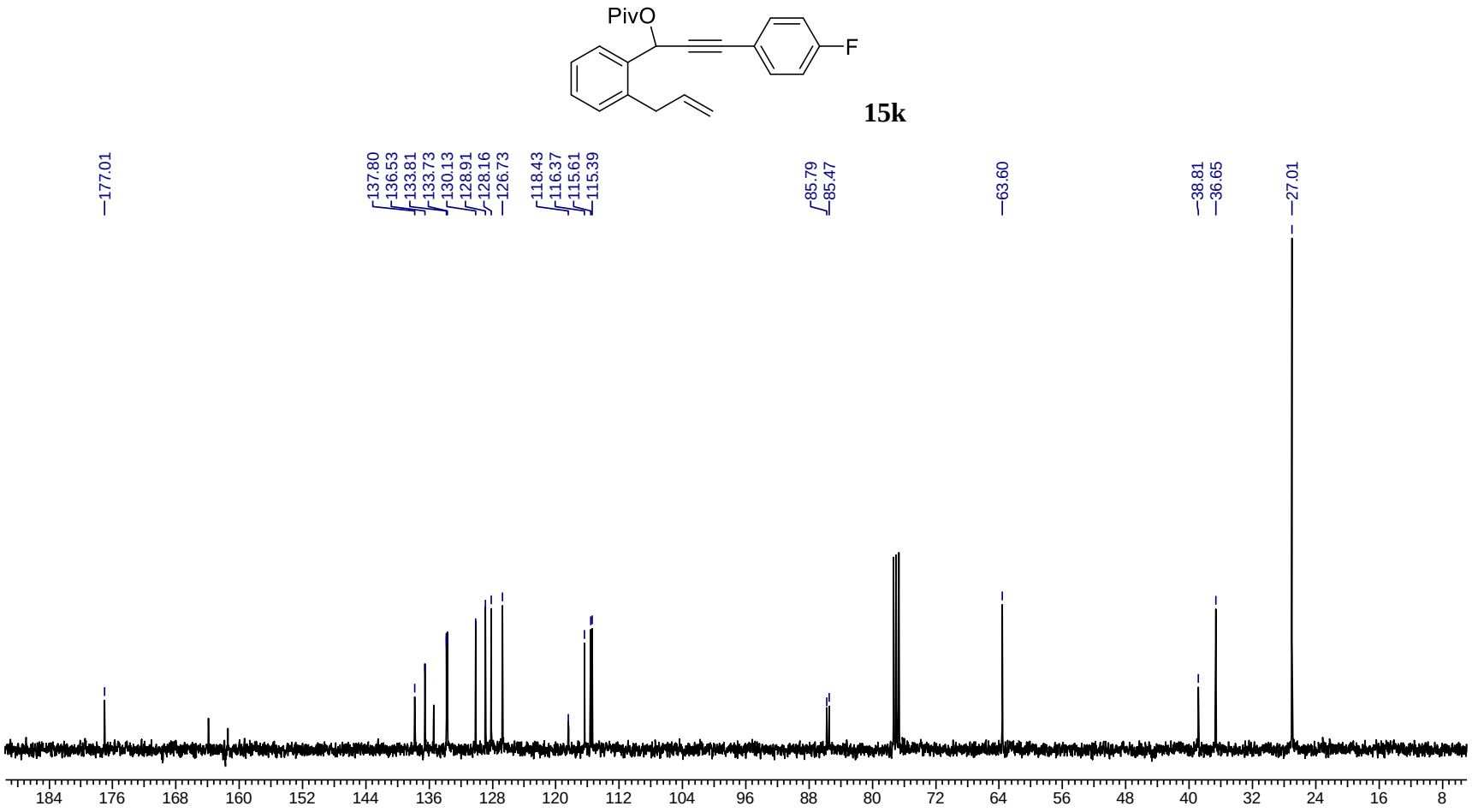
PivO
F
15k
177.01
137.80
136.53
133.81
133.73
130.13
128.91
128.16
126.73
118.43
116.37
115.61
115.39
85.79
85.47
63.60
38.81
36.65
27.01
184
176
168
160
152
144
136
128
120
112
104
96
88
80
72
64
56
48
40
32
24
16
8

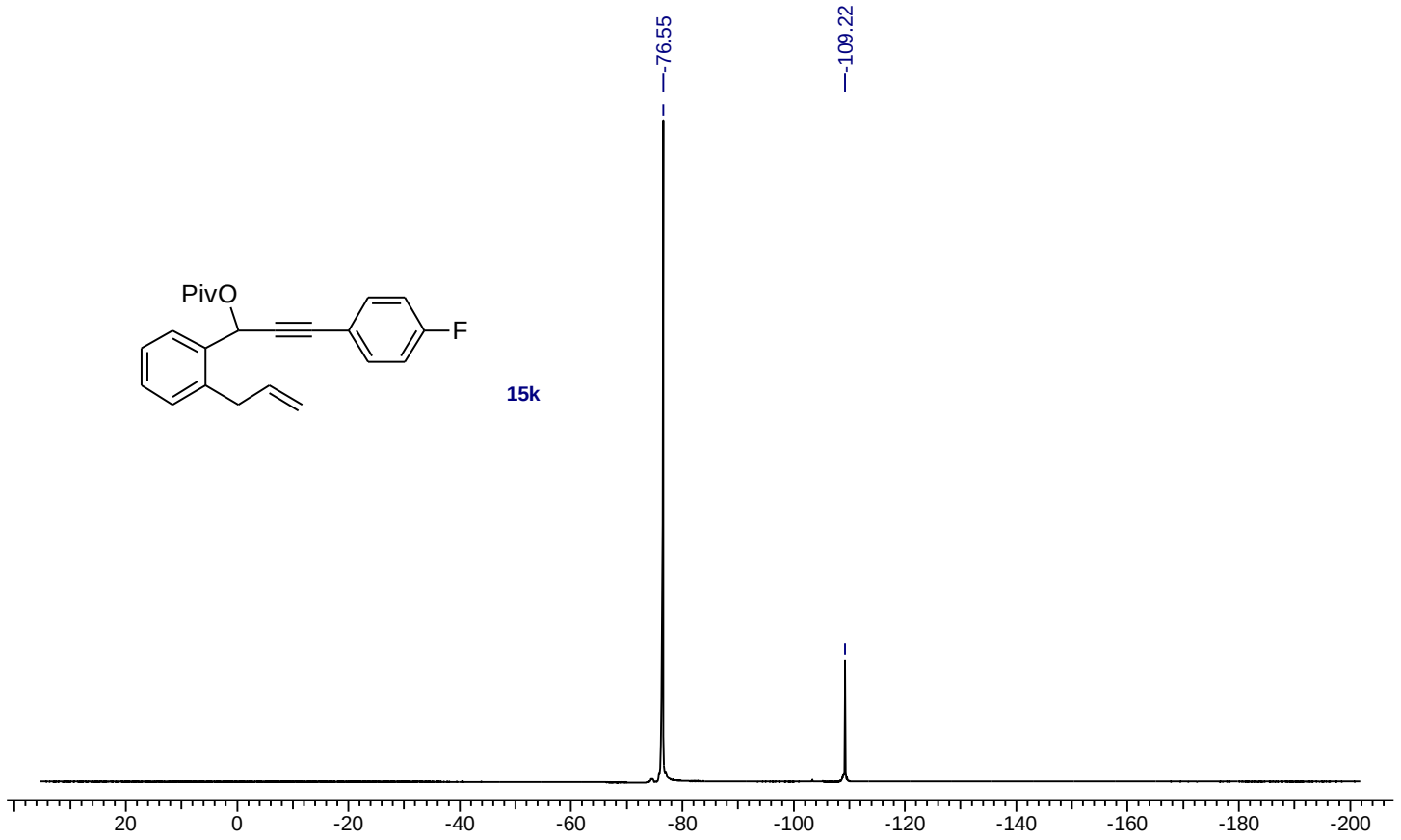
PivO
F
15k
-76.55
-109.22
20
0
-20
-40
-60
-80
-100
-120
-140
-160
-180
-200

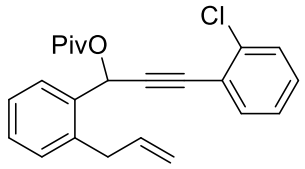
Cl
PivO

15l

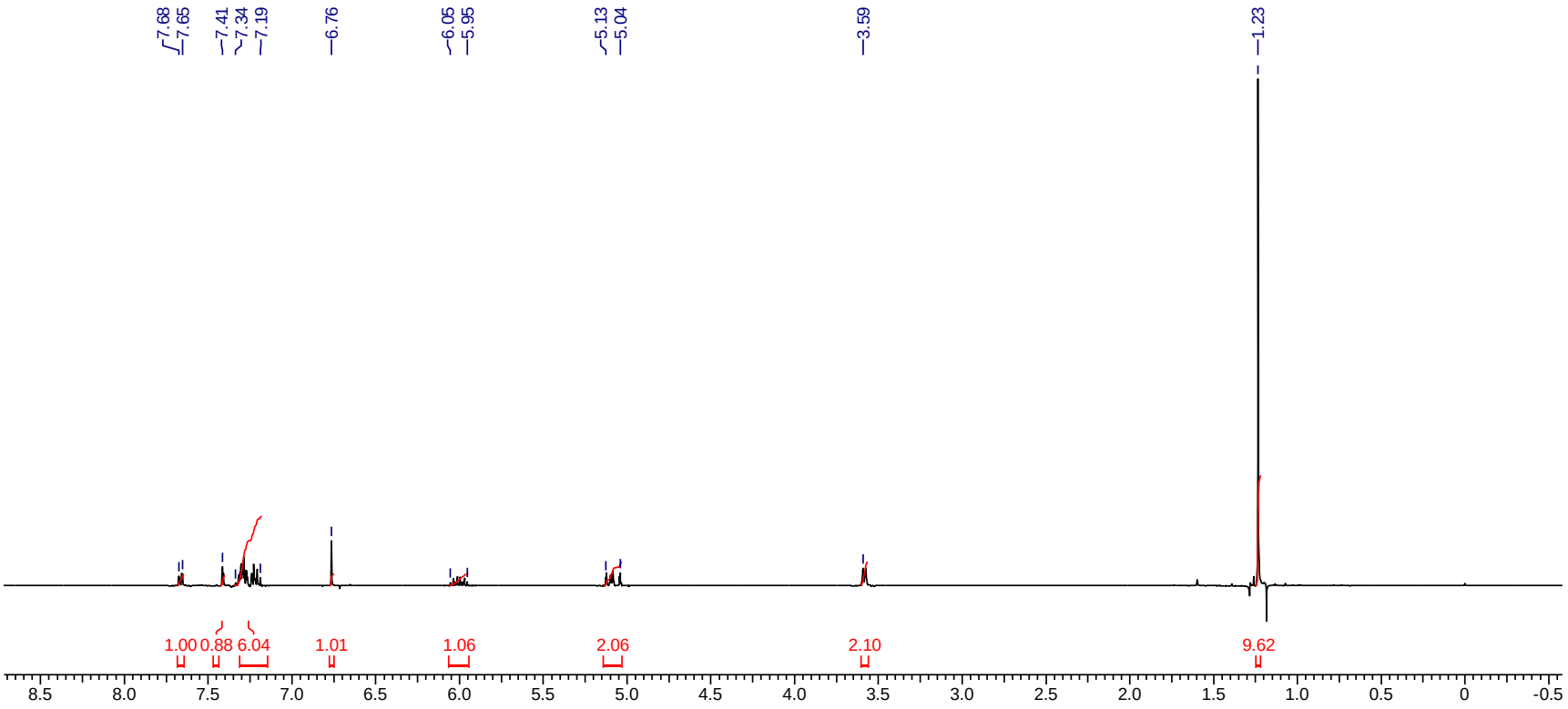
7.68
7.65
7.41
7.34
7.19
6.76
6.05
5.95
5.13
5.04
3.59
1.23
1.00
0.88
6.04
1.01
1.06
2.06
2.10
9.62
8.5
8.0
7.5
7.0
6.5
6.0
5.5
5.0
4.5
4.0
3.5
3.0
2.5
2.0
1.5
1.0
0.5
0
-0.5

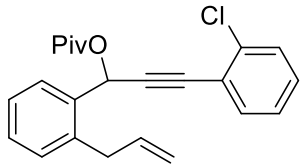
Cl
PivO

15l

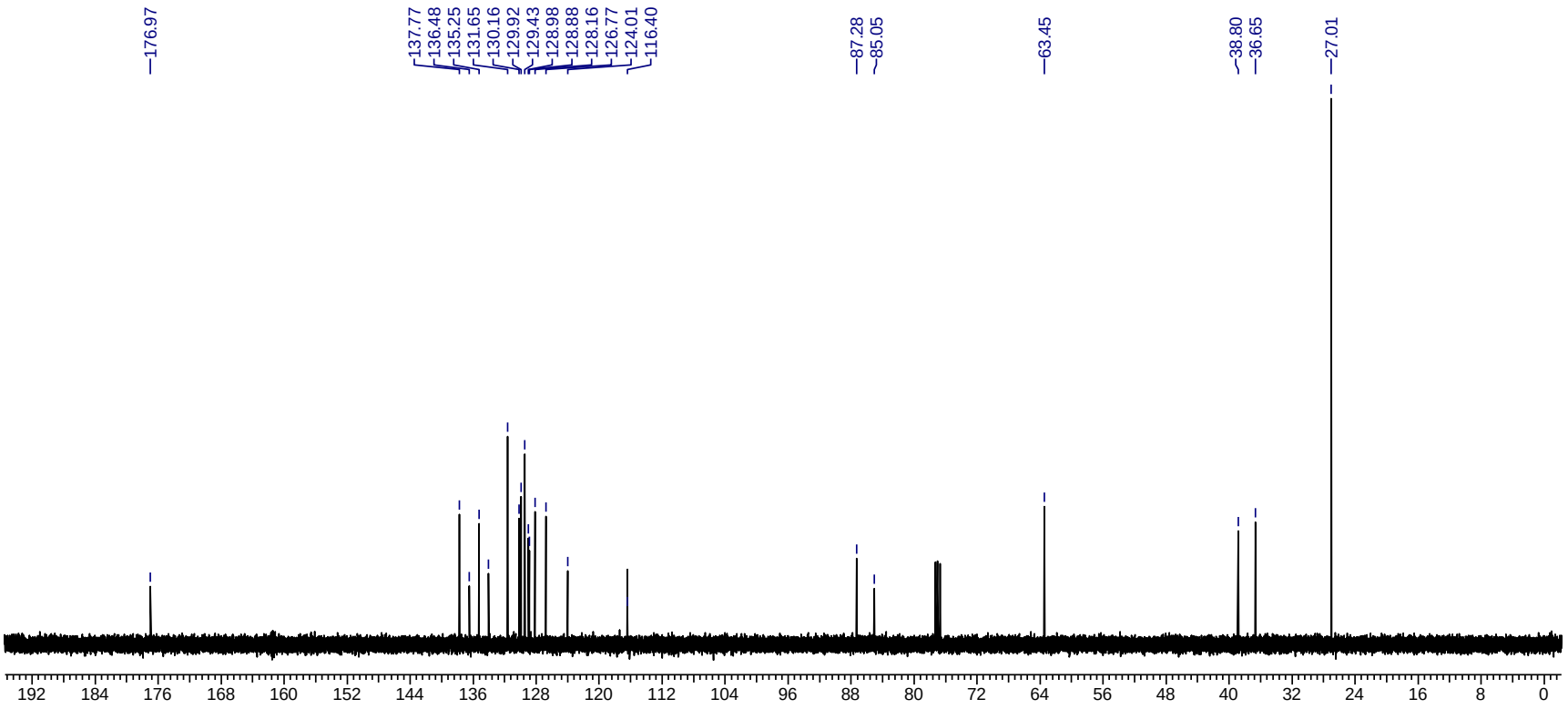
176.97
137.77
136.48
135.25
131.65
130.16
129.92
129.43
128.98
128.88
128.16
126.77
124.01
116.40
87.28
85.05
63.45
38.80
36.65
27.01
192
184
176
168
160
152
144
136
128
120
112
104
96
88
80
72
64
56
48
40
32
24
16
8
0

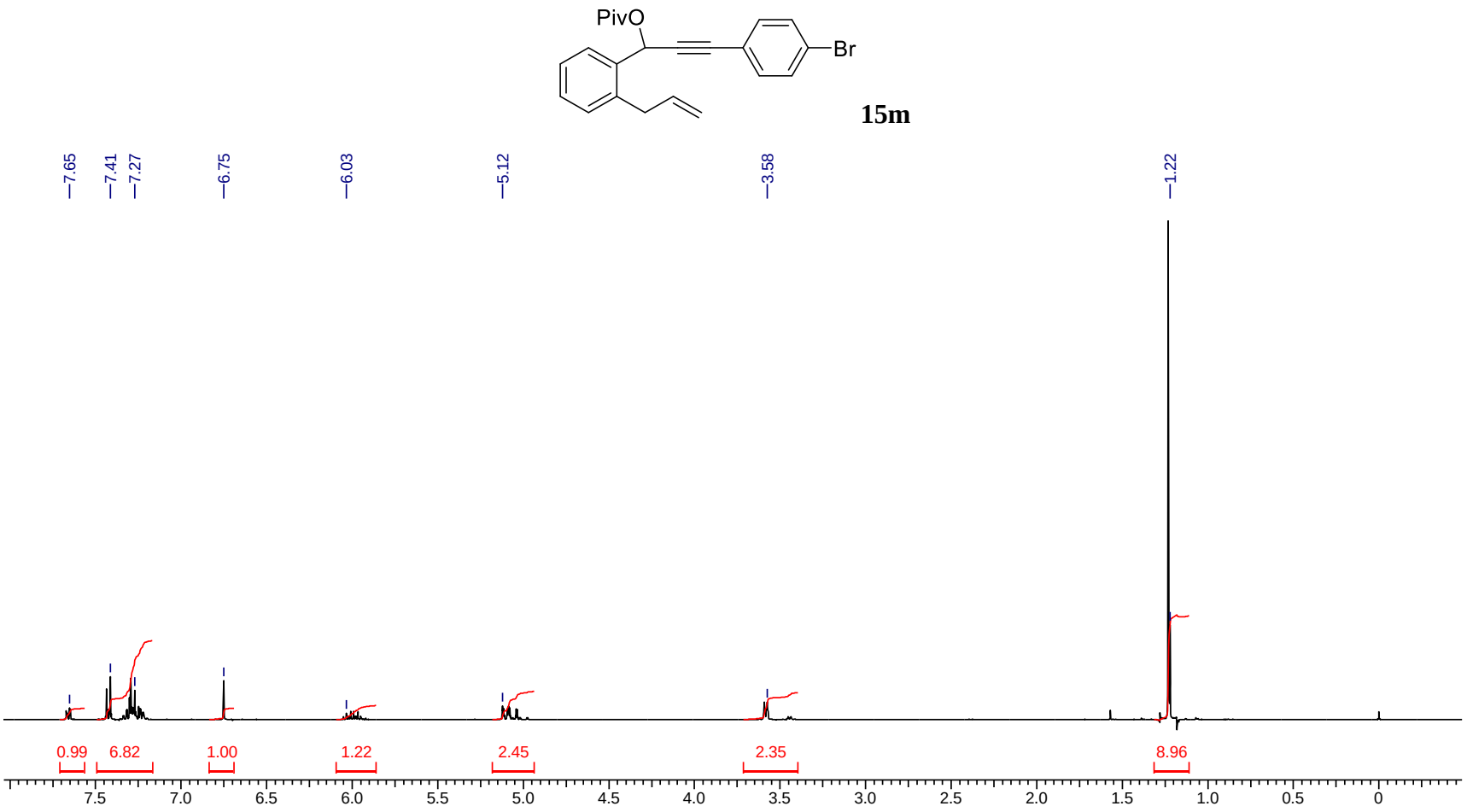
PivO
Br
15m
7.65
7.41
7.27
6.75
6.03
5.12
3.58
1.22
0.99
6.82
1.00
1.22
2.45
2.35
8.96
7.5
7.0
6.5
6.0
5.5
5.0
4.5
4.0
3.5
3.0
2.5
2.0
1.5
1.0
0.5
0

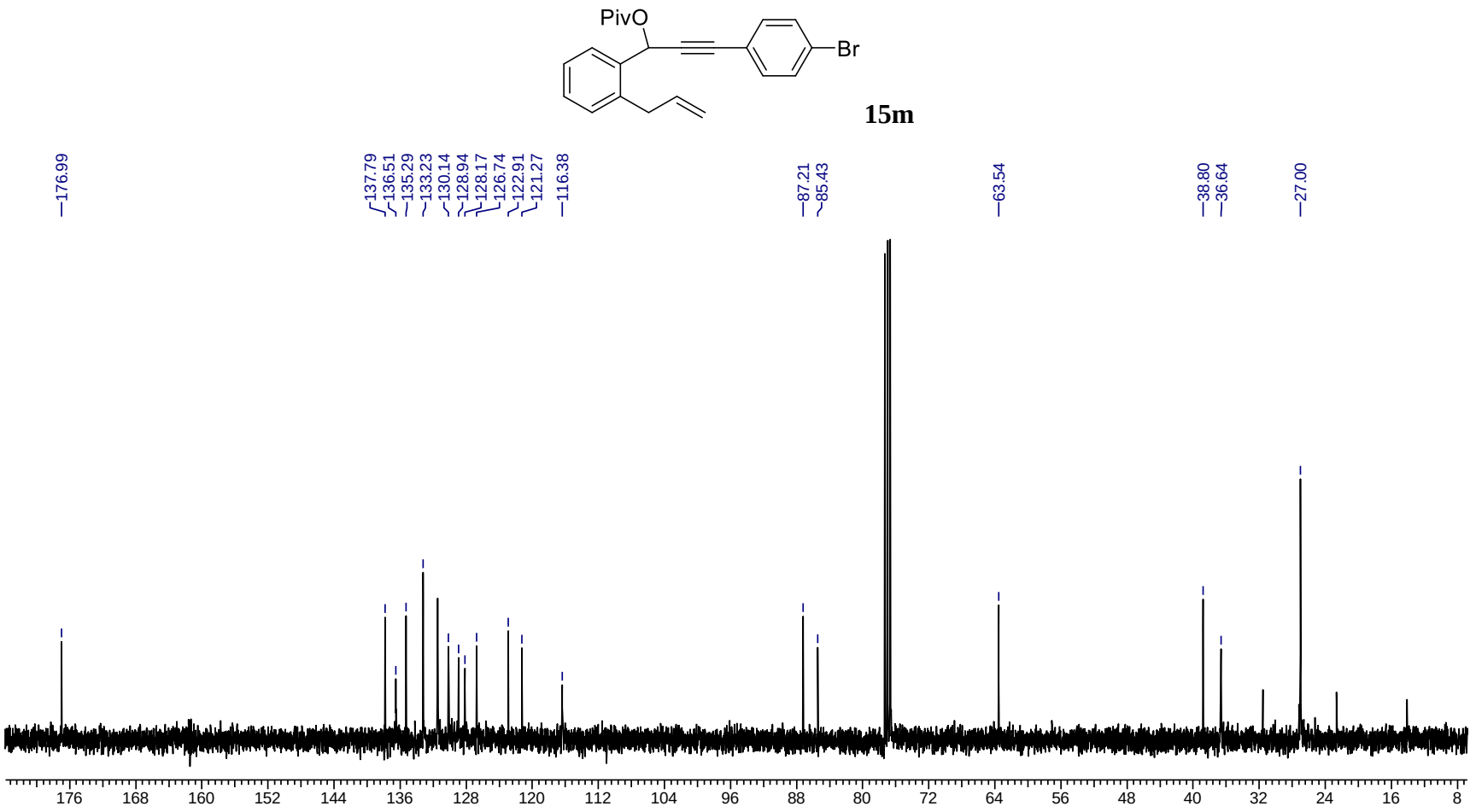
PivO
Br
15m
176.99
137.79
136.51
135.29
133.23
130.14
128.94
128.17
126.74
122.91
121.27
116.38
87.21
85.43
63.54
38.80
36.64
27.00
176
168
160
152
144
136
128
120
112
104
96
88
80
72
64
56
48
40
32
24
16
8

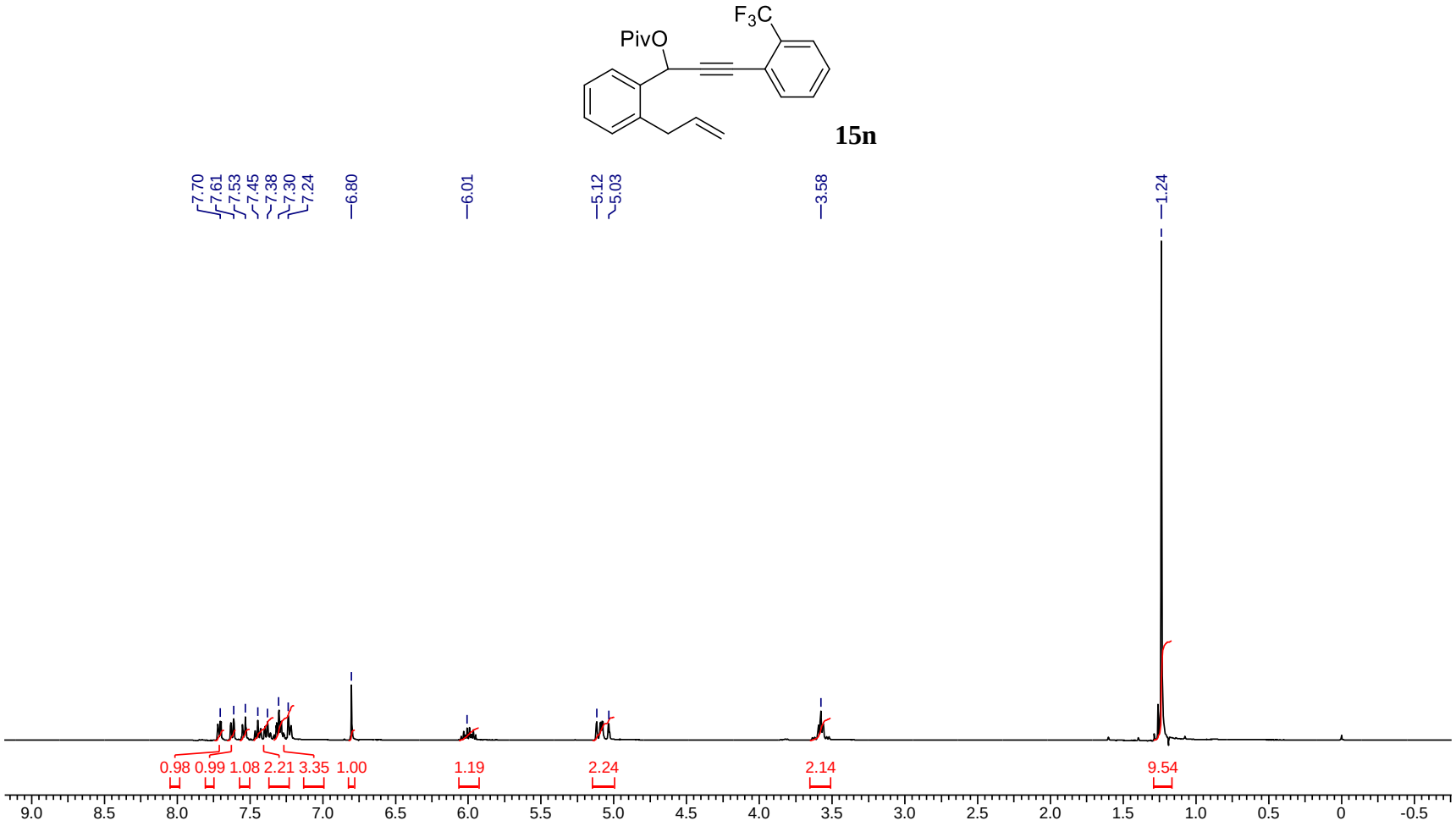
F3C
PivO
15n
7.70
7.61
7.53
7.45
7.38
7.30
7.24
6.80
6.01
5.12
5.03
3.58
1.24
0.98 0.99 1.08 2.21 3.35 1.00
1.19
2.24
2.14
9.54
9.0 8.5 8.0 7.5 7.0 6.5 6.0 5.5 5.0 4.5 4.0 3.5 3.0 2.5 2.0 1.5 1.0 0.5 0 -0.5

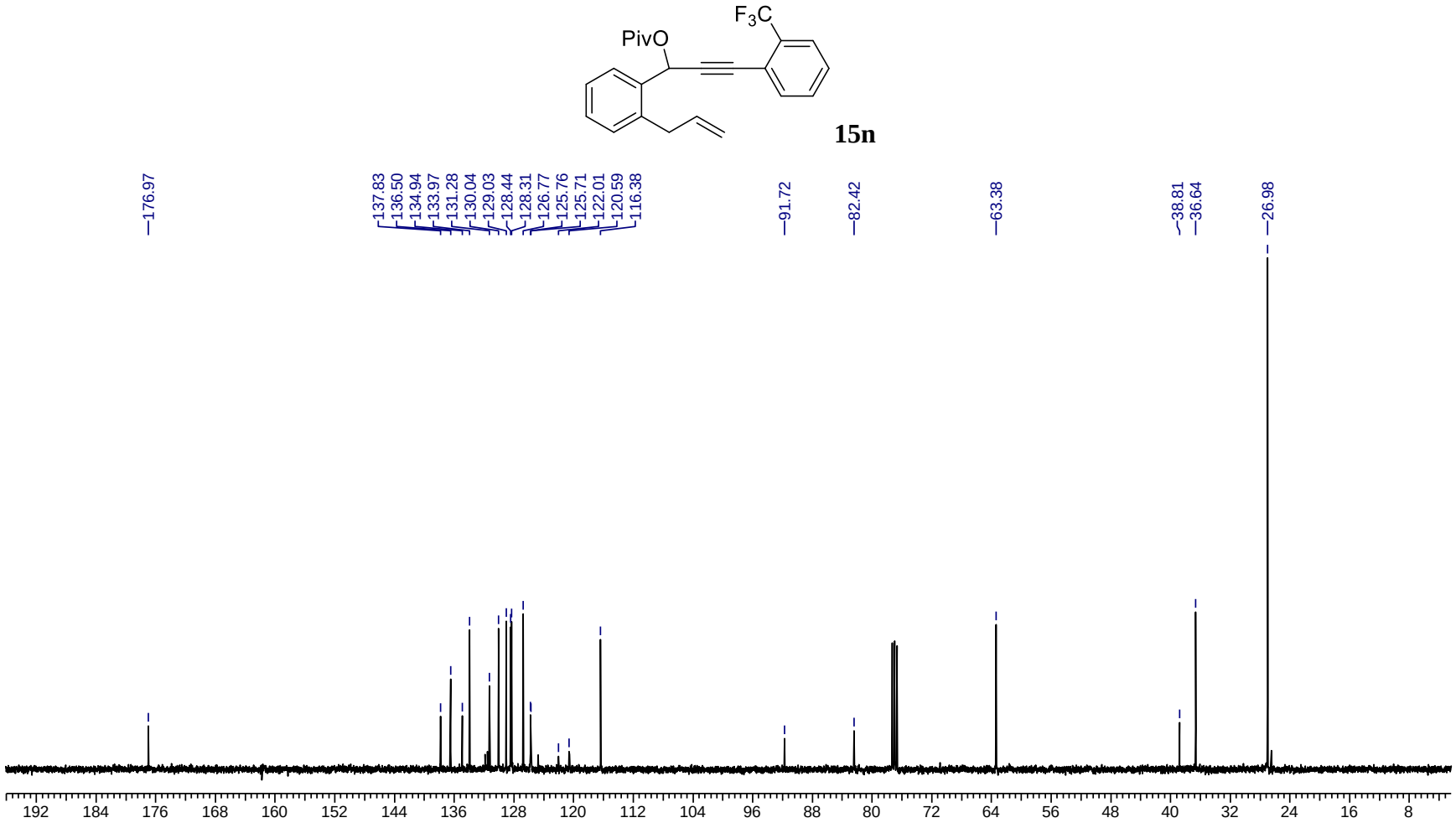
F3C
PivO
15n
176.97
137.83
136.50
134.94
133.97
131.28
130.04
129.03
128.44
128.31
126.77
125.76
125.71
122.01
120.59
116.38
91.72
82.42
63.38
38.81
36.64
26.98
192
184
176
168
160
152
144
136
128
120
112
104
96
88
80
72
64
56
48
40
32
24
16
8

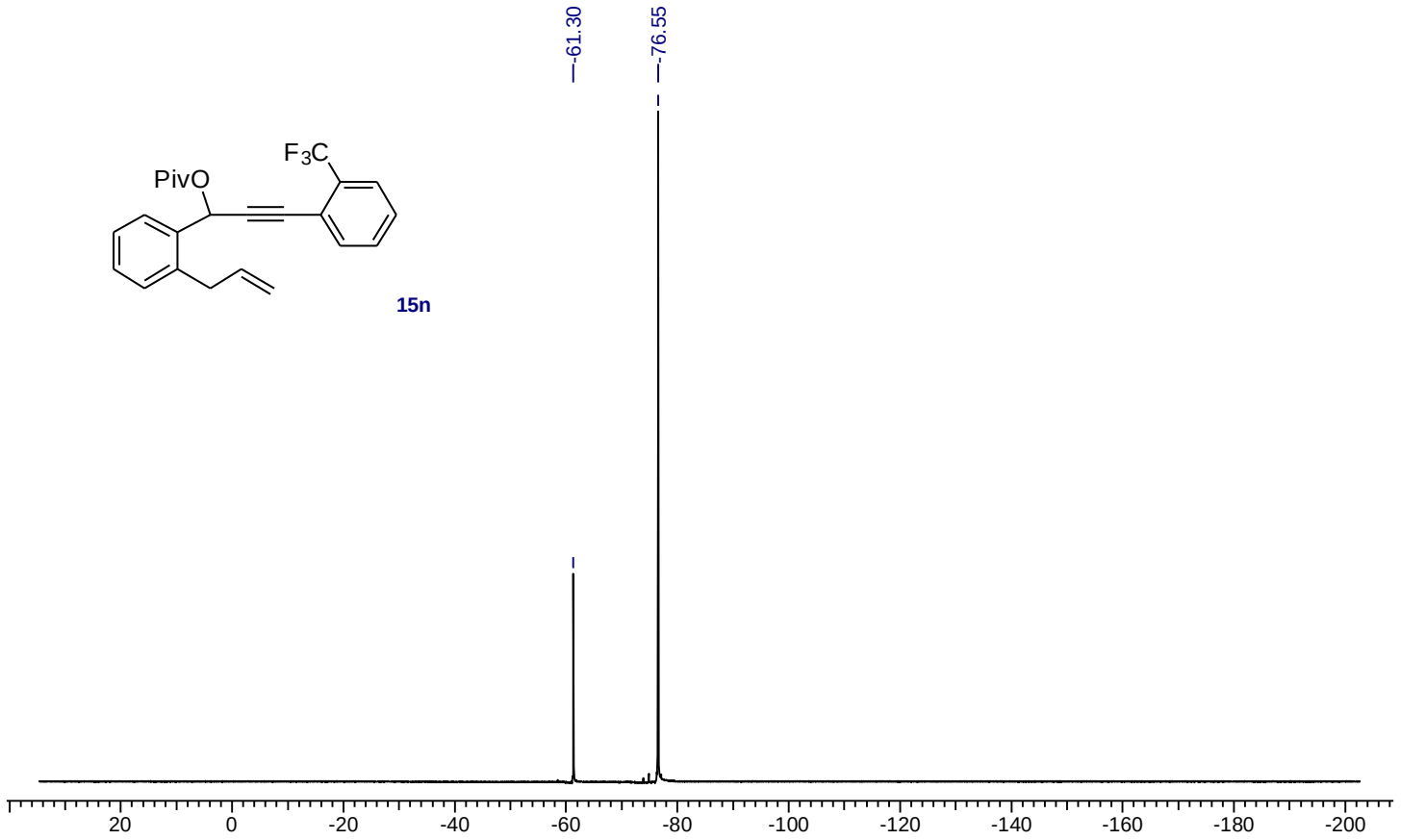
-61.30
-76.55
F3C
PivO
15n
20
0
-20
-40
-60
-80
-100
-120
-140
-160
-180
-200

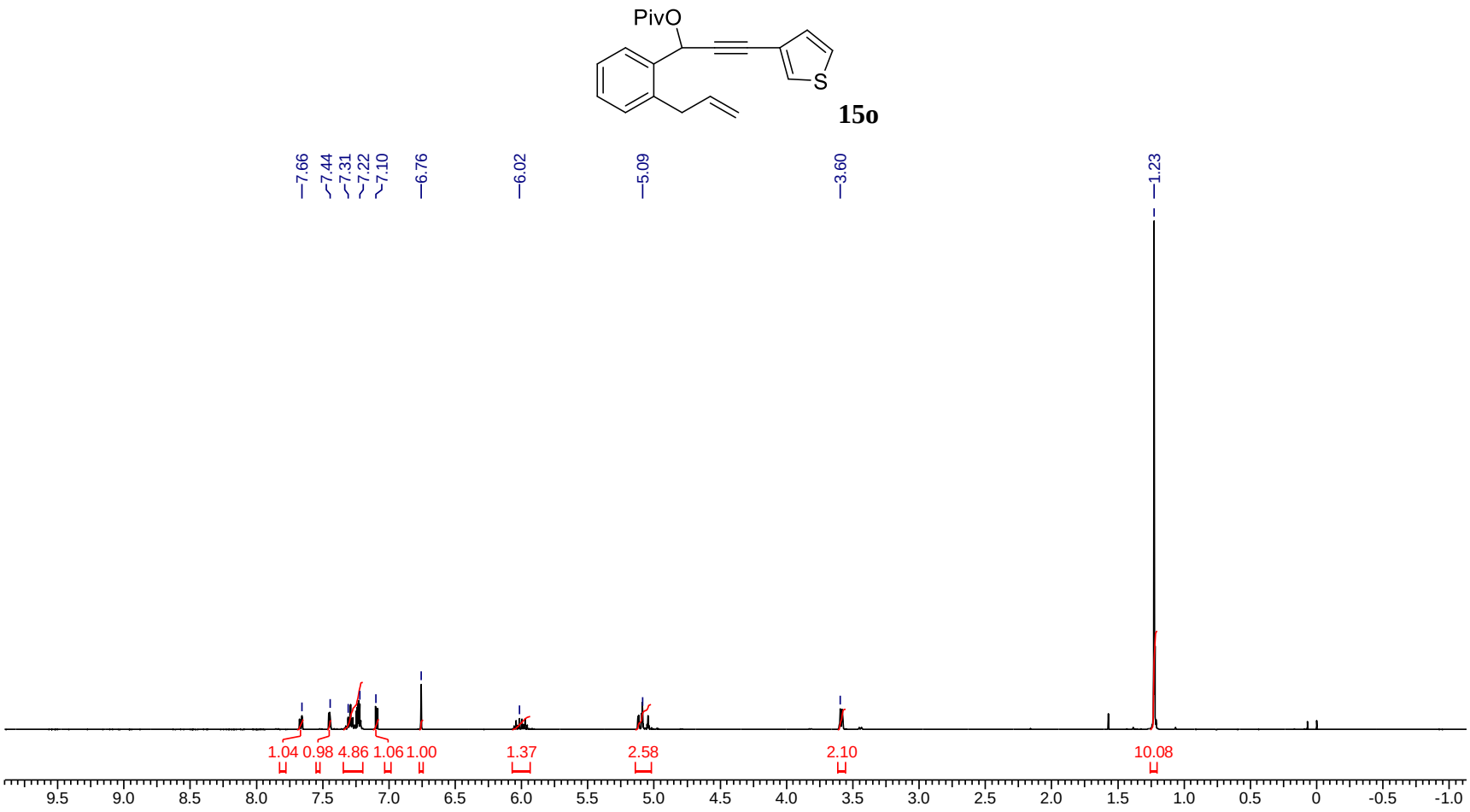
PivO
S
15o
7.66
7.44
7.31
7.22
7.10
6.76
6.02
5.09
3.60
1.23
1.04
0.98
4.86
1.06
1.00
1.37
2.58
2.10
10.08
9.5
9.0
8.5
8.0
7.5
7.0
6.5
6.0
5.5
5.0
4.5
4.0
3.5
3.0
2.5
2.0
1.5
1.0
0.5
0
-0.5
-1.0

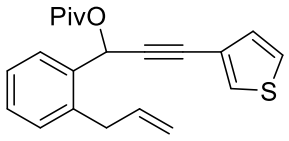
PivO
S

15o

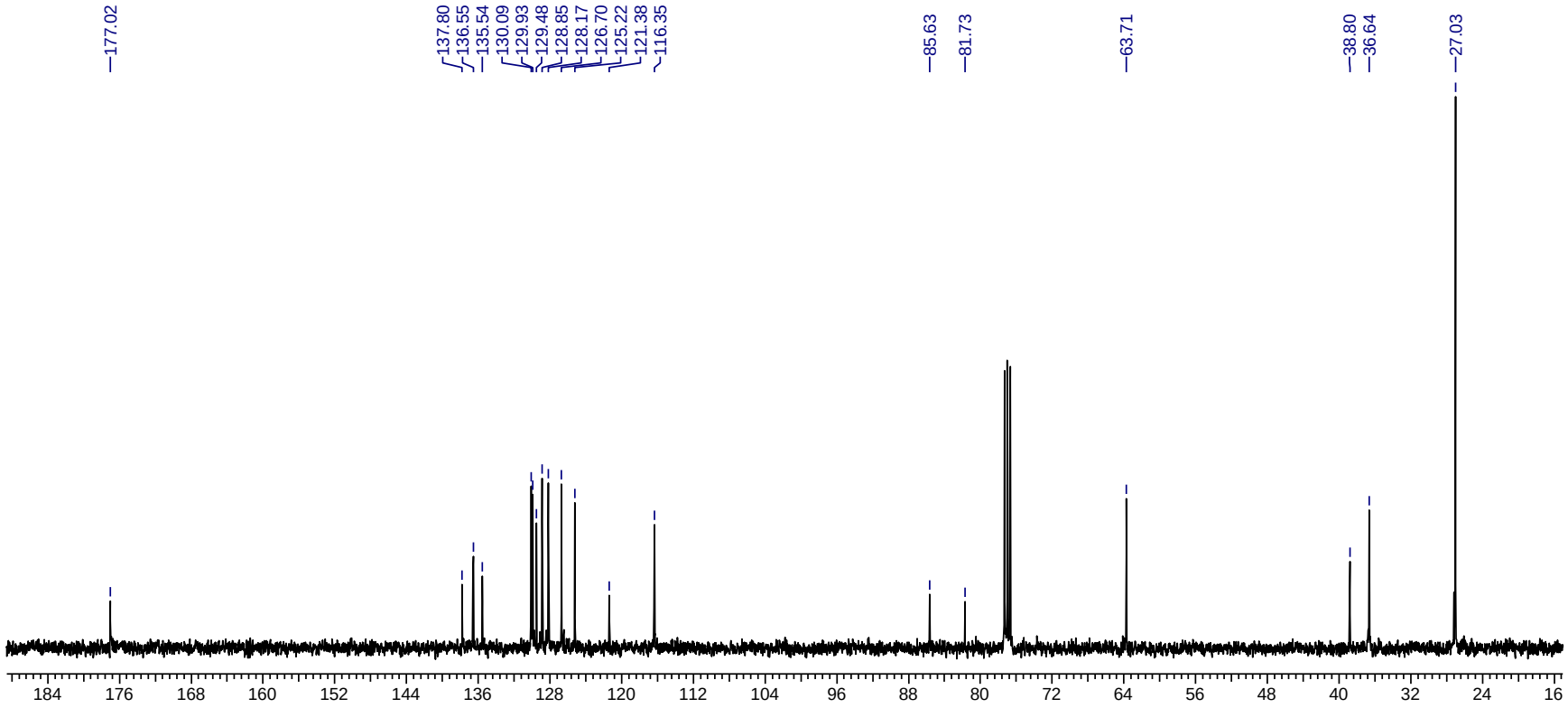
177.02
137.80
136.55
135.54
130.09
129.93
129.48
128.85
128.17
126.70
125.22
121.38
116.35
85.63
81.73
63.71
38.80
36.64
27.03
184
176
168
160
152
144
136
128
120
112
104
96
88
80
72
64
56
48
40
32
24
16

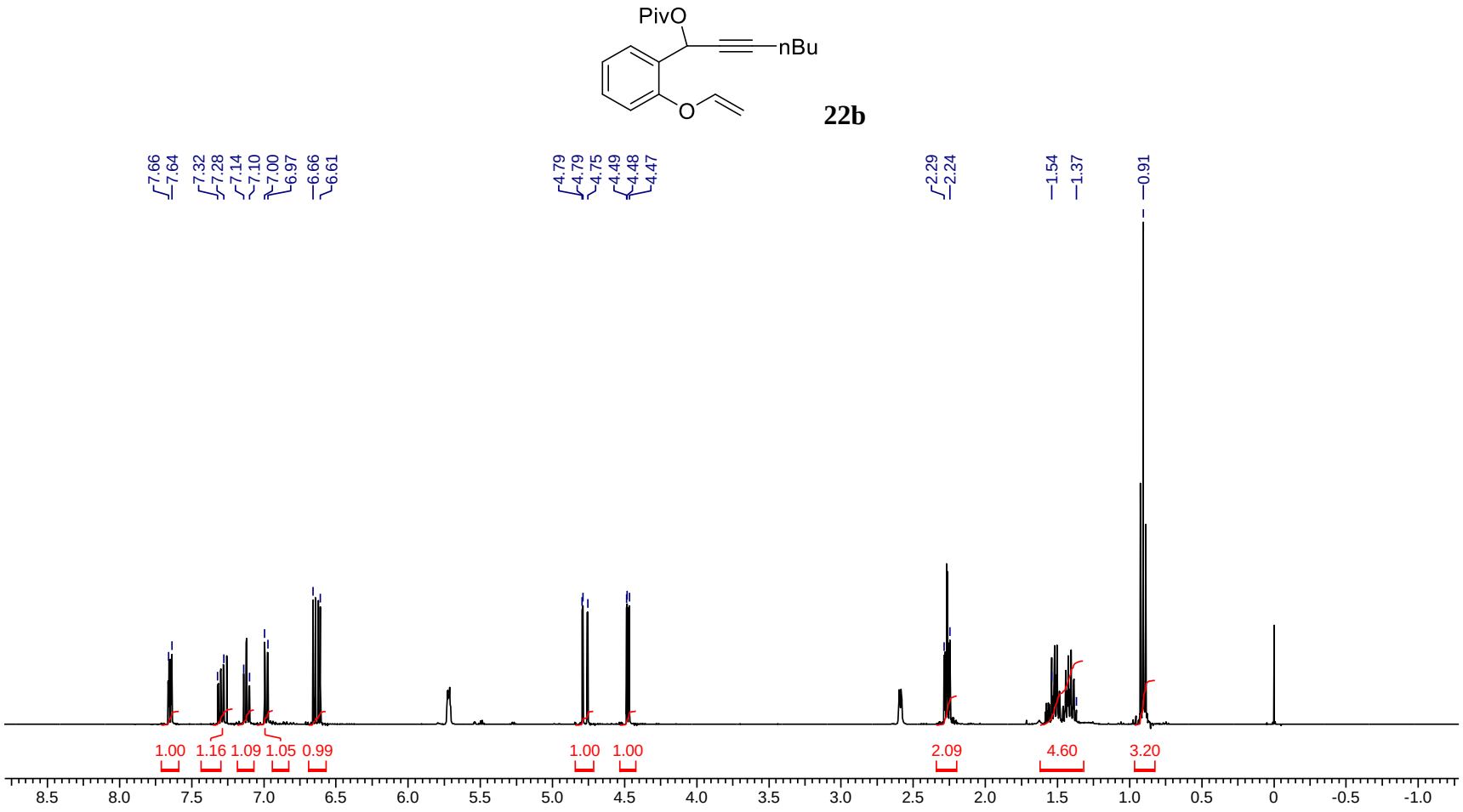
PivO
nBu
O
22b
7.66
7.64
7.32
7.28
7.14
7.10
7.00
6.97
6.66
6.61
4.79
4.79
4.75
4.49
4.48
4.47
2.29
2.24
1.54
1.37
0.91
1.00
1.16
1.09
1.05
0.99
1.00
1.00
2.09
4.60
3.20
8.5
8.0
7.5
7.0
6.5
6.0
5.5
5.0
4.5
4.0
3.5
3.0
2.5
2.0
1.5
1.0
0.5
0
-0.5
-1.0

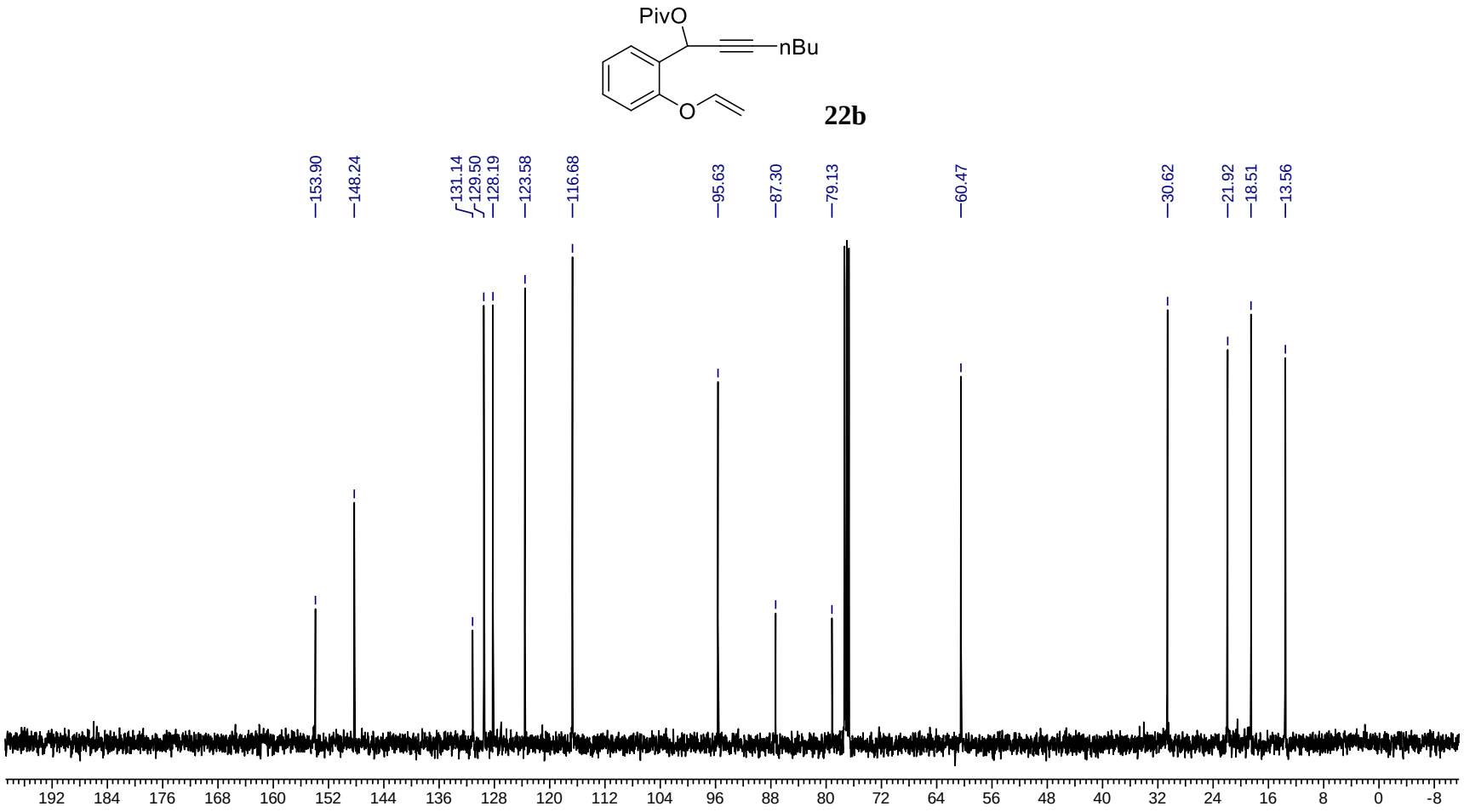
PivO
nBu
O
153.90
148.24
131.14
129.50
128.19
123.58
116.68
95.63
87.30
79.13
60.47
30.62
21.92
18.51
13.56
192 184 176 168 160 152 144 136 128 120 112 104 96 88 80 72 64 56 48 40 32 24 16 8 0 -8

22b

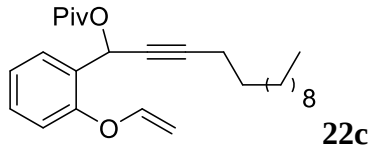
PivO
8
O

22c

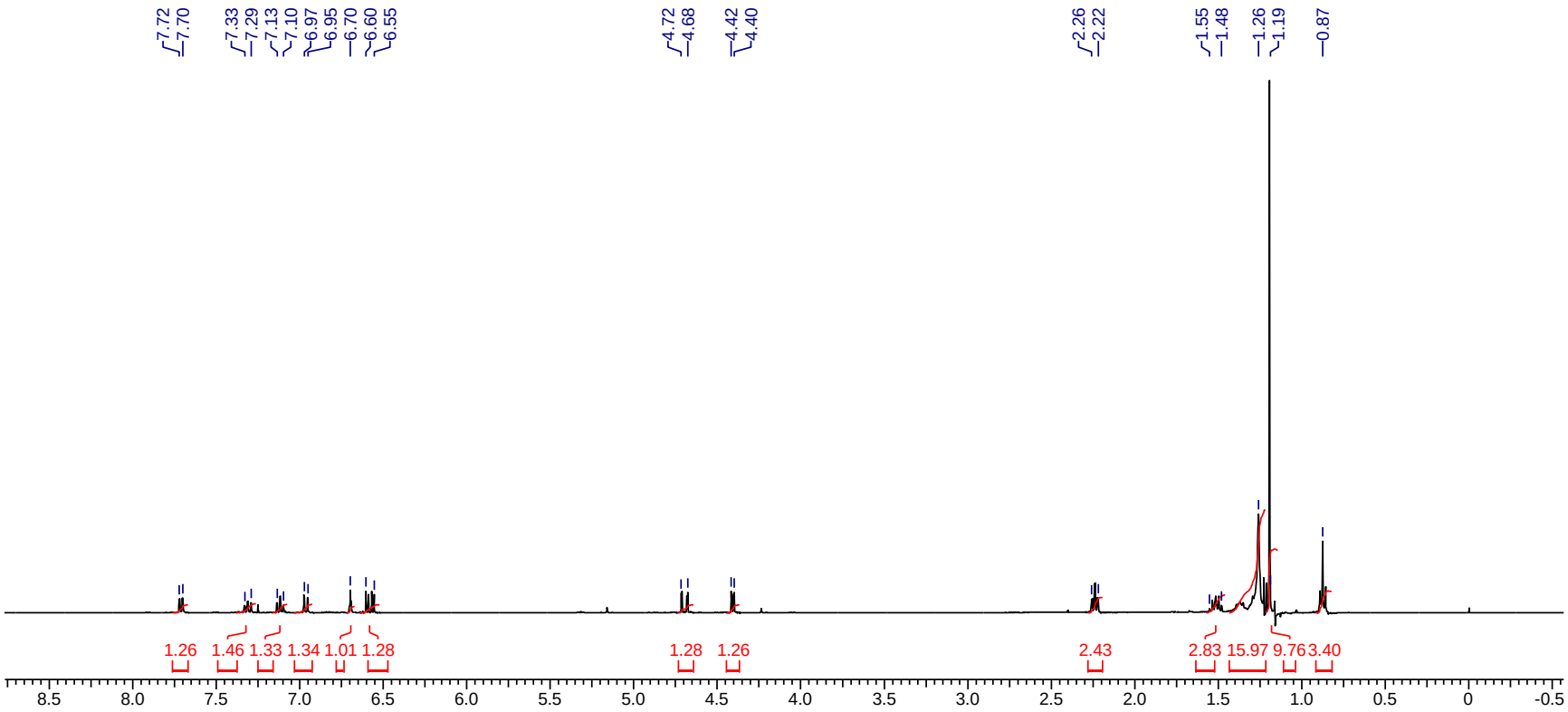
7.72
7.70
7.33
7.29
7.13
7.10
6.97
6.95
6.70
6.60
6.55
4.72
4.68
4.42
4.40
2.26
2.22
1.55
1.48
1.26
1.19
0.87
1.26
1.46
1.33
1.34
1.01
1.28
1.28
1.26
2.43
2.83
15.97
9.76
3.40
8.5
8.0
7.5
7.0
6.5
6.0
5.5
5.0
4.5
4.0
3.5
3.0
2.5
2.0
1.5
1.0
0.5
0
-0.5

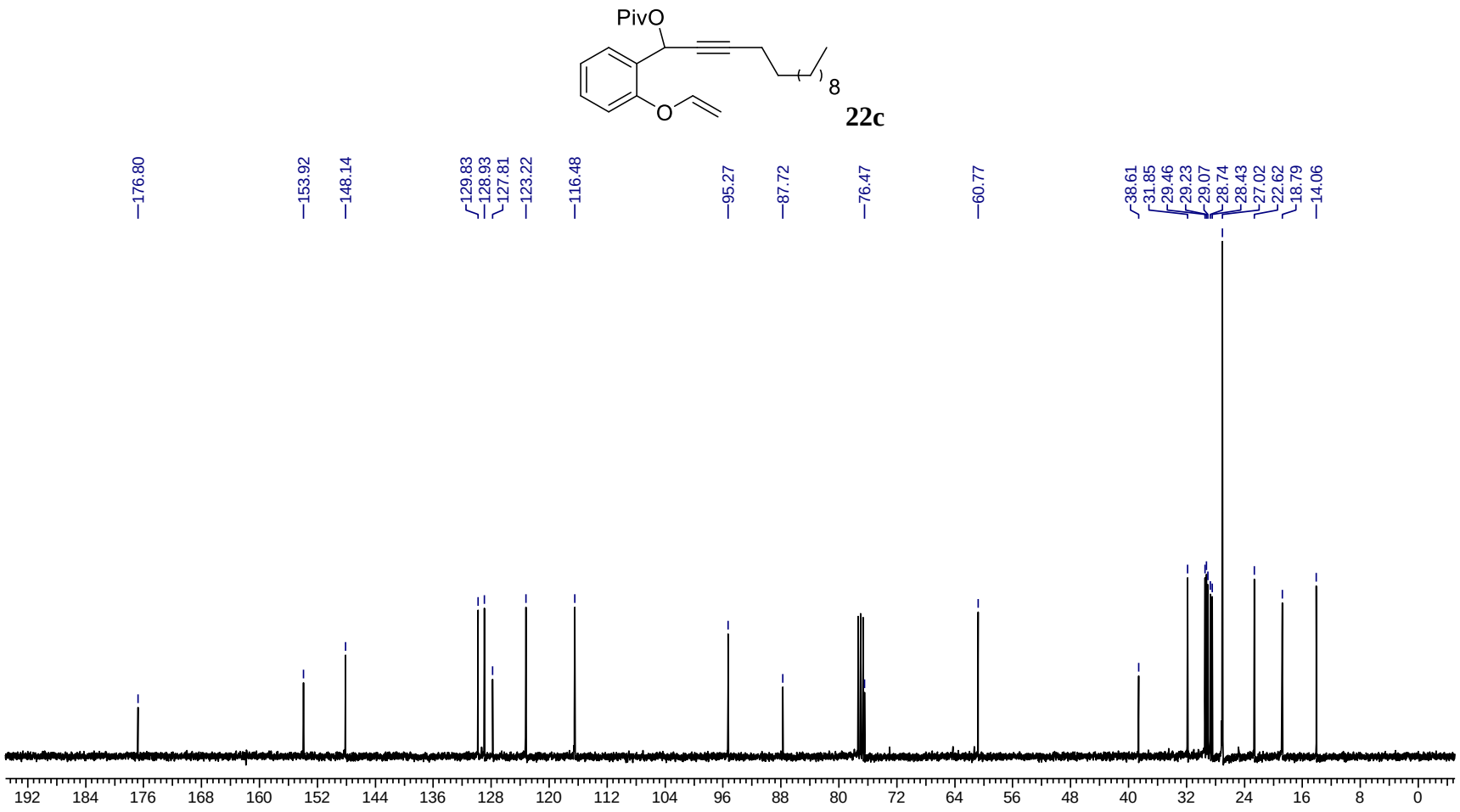
PivO
O
8
22c
176.80
153.92
148.14
129.83
128.93
127.81
123.22
116.48
95.27
87.72
76.47
60.77
38.61
31.85
29.46
29.23
29.07
28.74
28.43
27.02
22.62
18.79
14.06
192 184 176 168 160 152 144 136 128 120 112 104 96 88 80 72 64 56 48 40 32 24 16 8 0

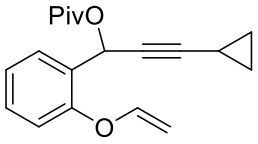
PivO
O

22f

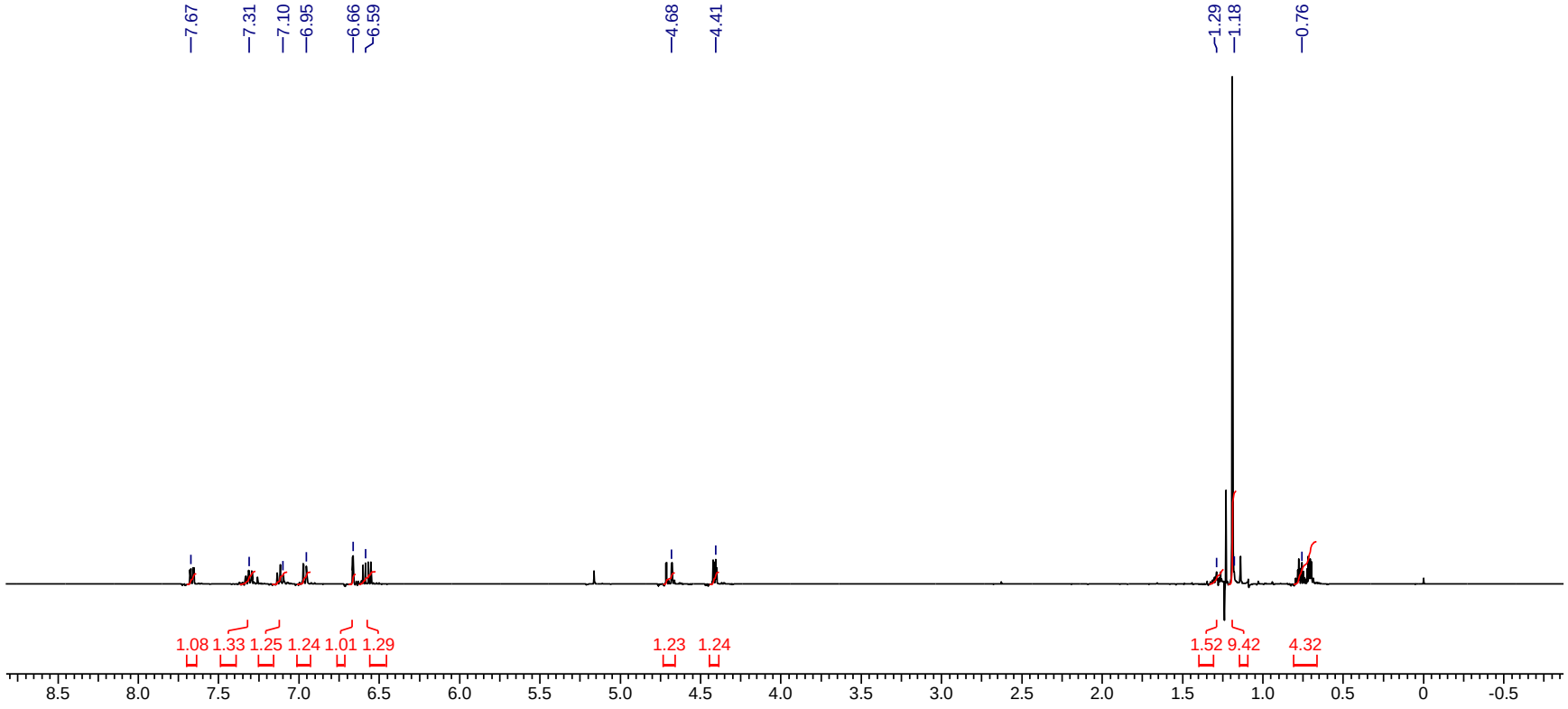
7.67
7.31
7.10
6.95
6.66
6.59
4.68
4.41
1.29
1.18
0.76
1.08 1.33 1.25 1.24 1.01 1.29
1.23 1.24
1.52 9.42 4.32
8.5 8.0 7.5 7.0 6.5 6.0 5.5 5.0 4.5 4.0 3.5 3.0 2.5 2.0 1.5 1.0 0.5 0 -0.5

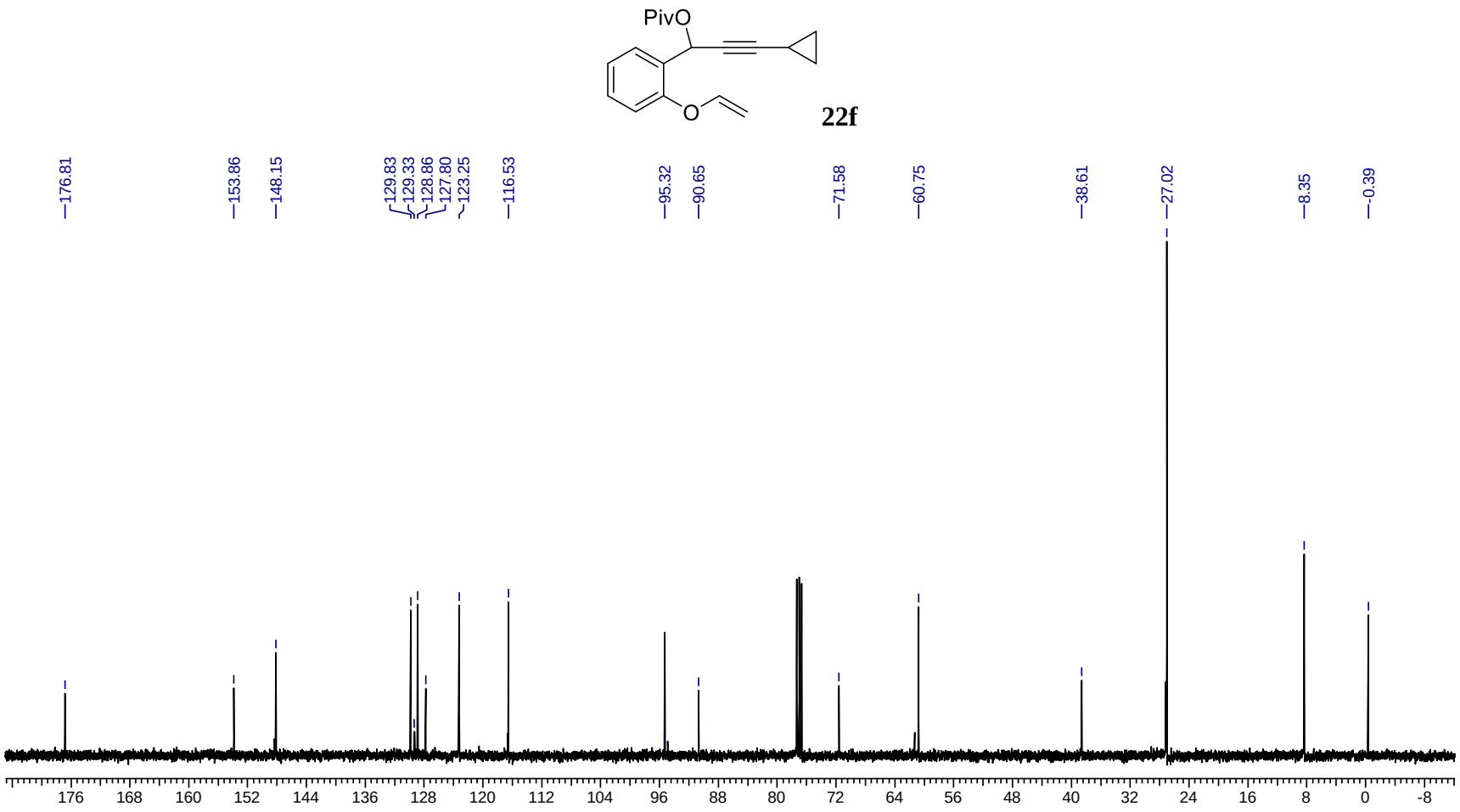
PivO
O
22f
176.81
153.86
148.15
129.83
129.33
128.86
127.80
123.25
116.53
95.32
90.65
71.58
60.75
38.61
27.02
8.35
-0.39
176
168
160
152
144
136
128
120
112
104
96
88
80
72
64
56
48
40
32
24
16
8
0
-8

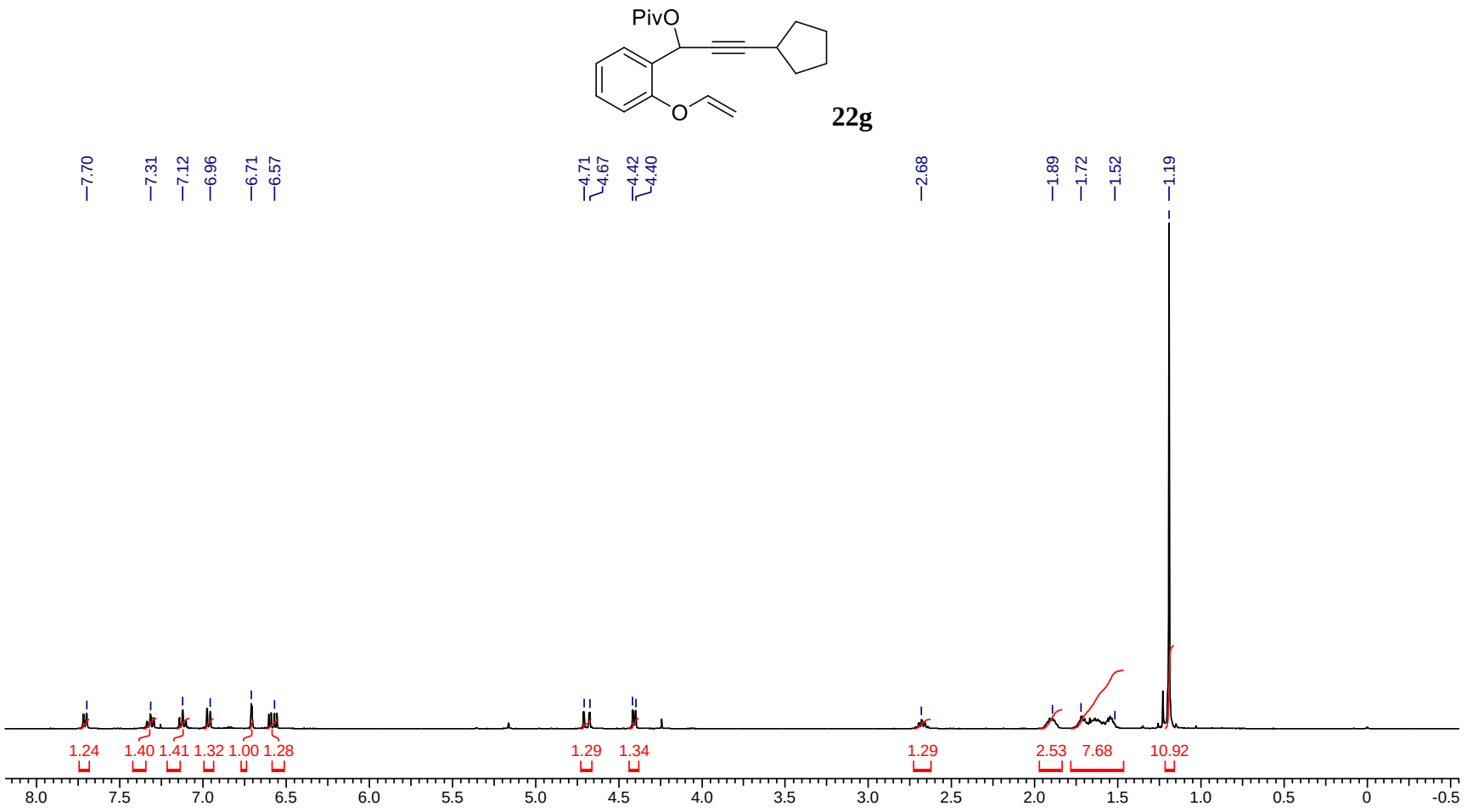
PivO
O
22g
7.70
7.31
7.12
6.96
6.71
6.57
4.71
4.67
4.42
4.40
2.68
1.89
1.72
1.52
1.19
1.24
1.40
1.41
1.32
1.00
1.28
1.29
1.34
1.29
2.53
7.68
10.92
8.0
7.5
7.0
6.5
6.0
5.5
5.0
4.5
4.0
3.5
3.0
2.5
2.0
1.5
1.0
0.5
0
-0.5

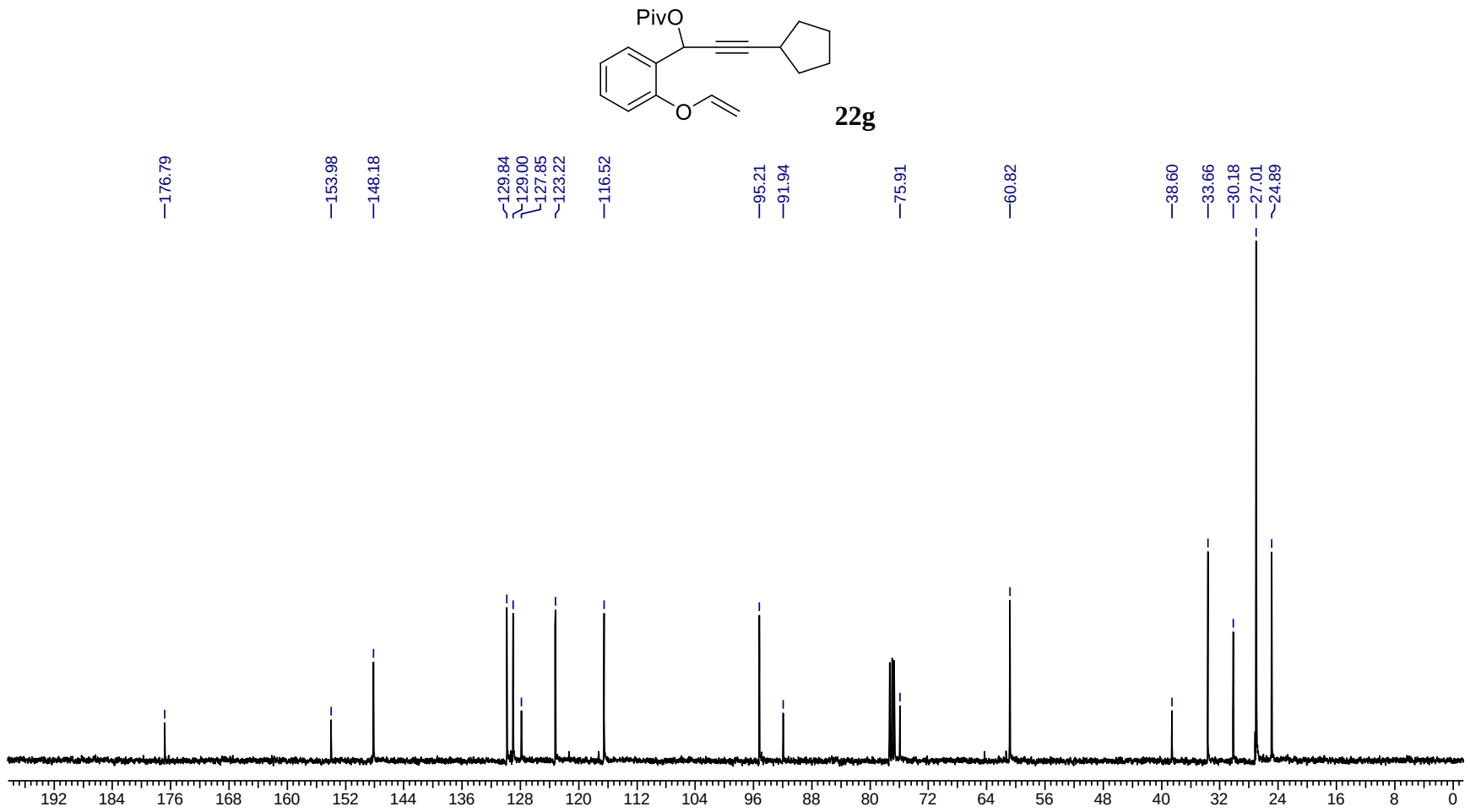
PivO
O
22g
176.79
153.98
148.18
129.84
129.00
127.85
123.22
116.52
95.21
91.94
75.91
60.82
38.60
33.66
30.18
27.01
24.89
192
184
176
168
160
152
144
136
128
120
112
104
96
88
80
72
64
56
48
40
32
24
16
8
0

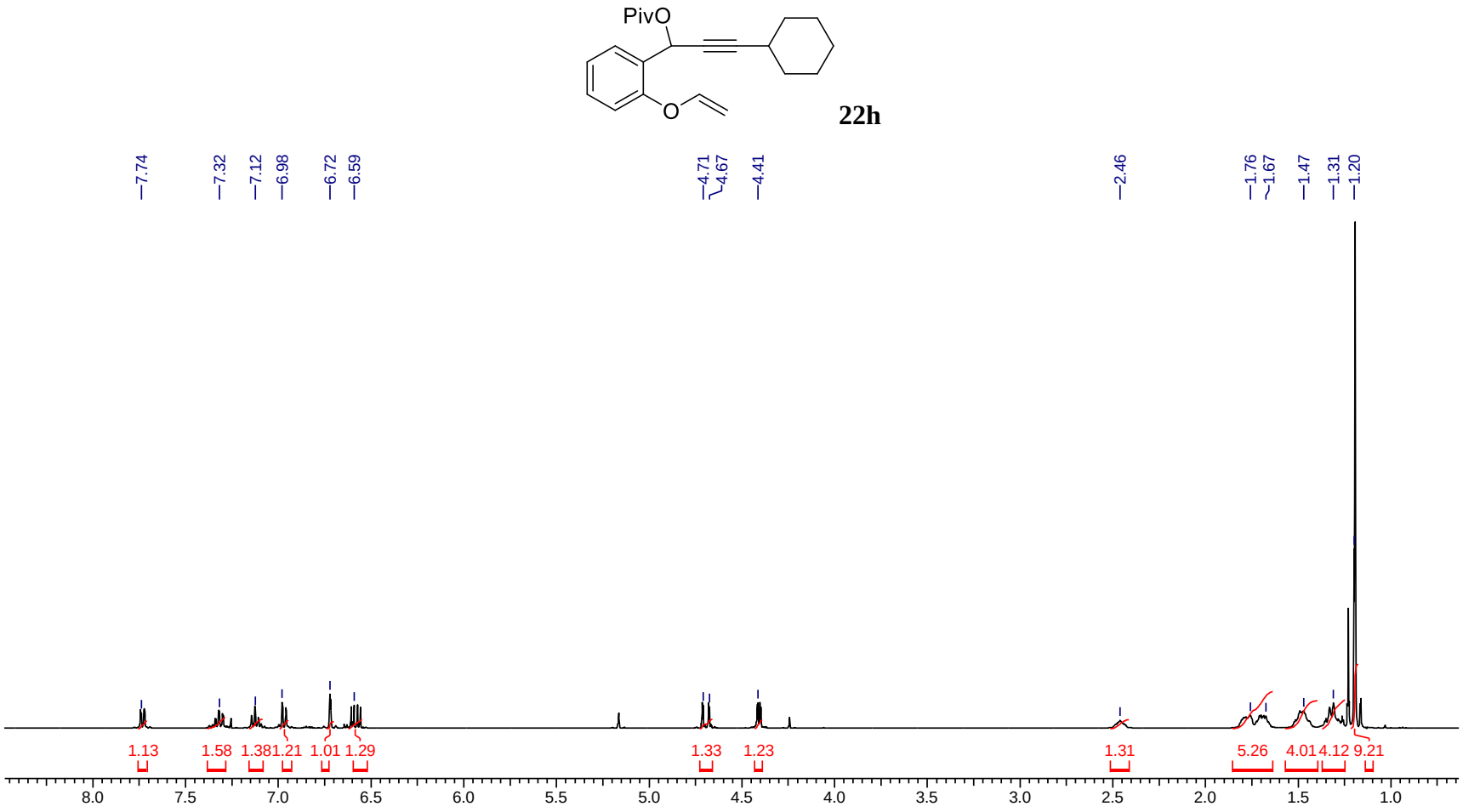
PivO
O
22h
7.74
7.32
7.12
6.98
6.72
6.59
4.71
4.67
4.41
2.46
1.76
1.67
1.47
1.31
1.20
1.13
1.58
1.38
1.21
1.01
1.29
1.33
1.23
1.31
5.26
4.01
4.12
9.21
8.0
7.5
7.0
6.5
6.0
5.5
5.0
4.5
4.0
3.5
3.0
2.5
2.0
1.5
1.0

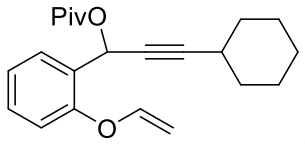
PivO
O

22h

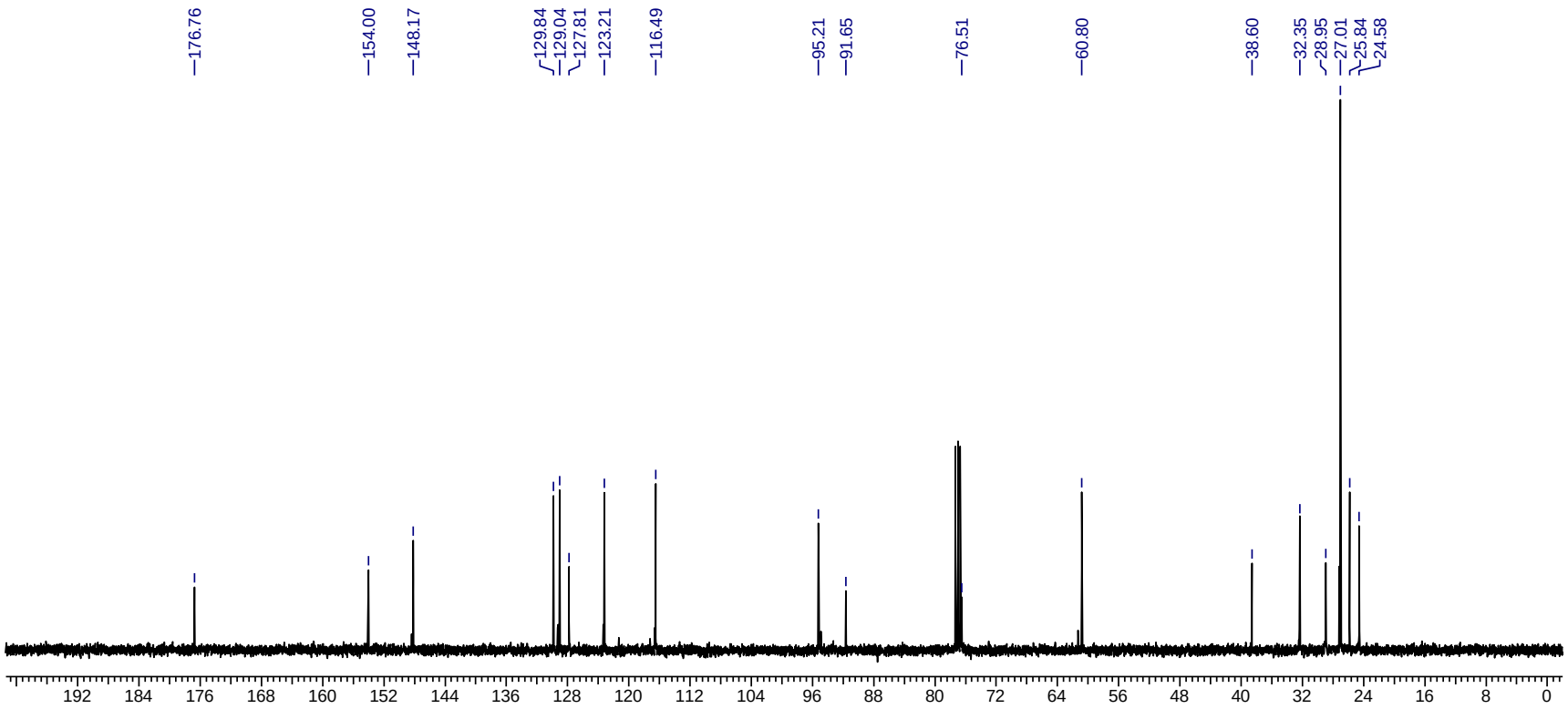
176.76
154.00
148.17
129.84
129.04
127.81
123.21
116.49
95.21
91.65
76.51
60.80
38.60
32.35
28.95
27.01
25.84
24.58
192 184 176 168 160 152 144 136 128 120 112 104 96 88 80 72 64 56 48 40 32 24 16 8 0

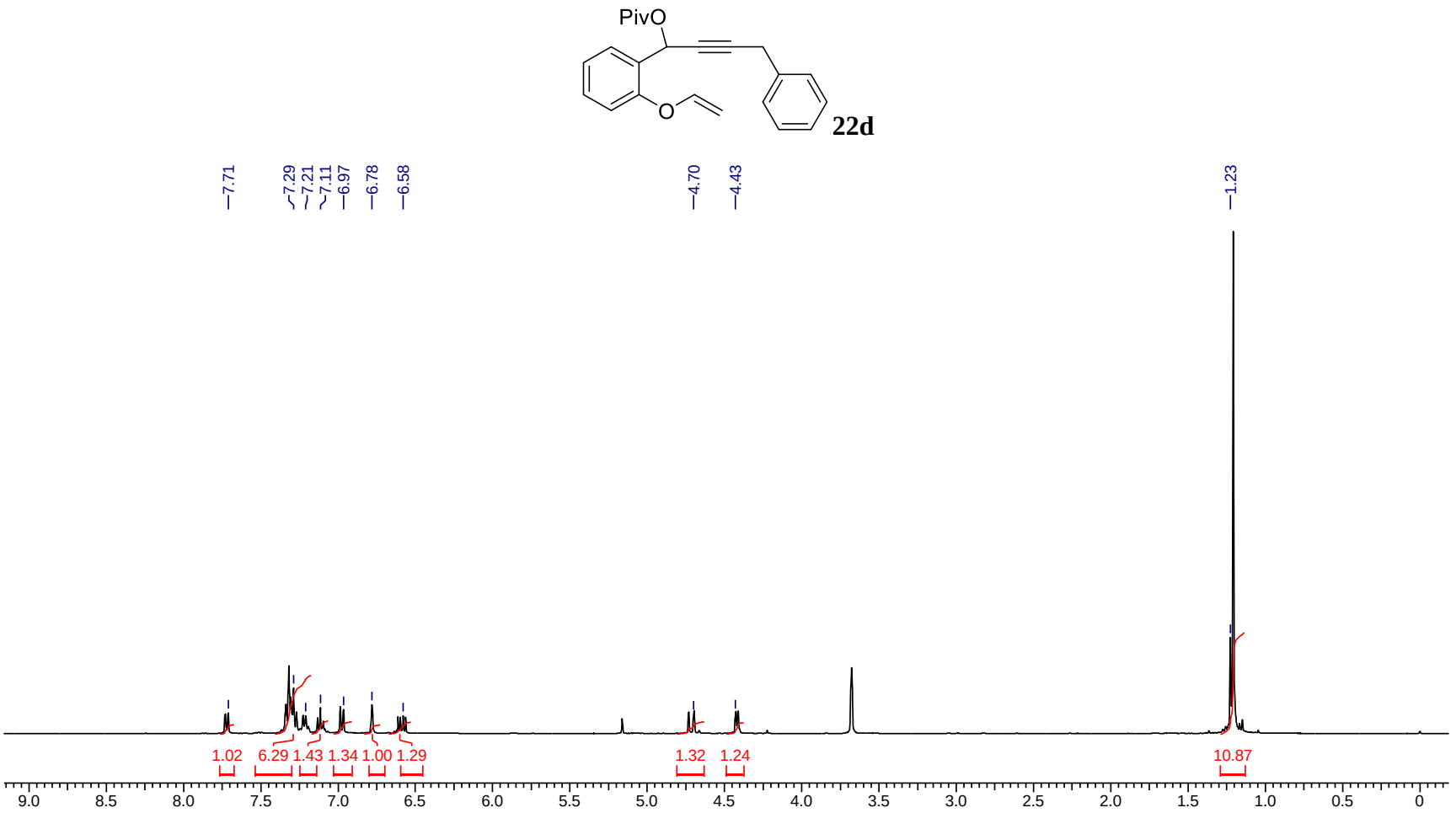
PivO
O
22d
7.71
7.29
7.21
7.11
6.97
6.78
6.58
4.70
4.43
1.23
1.02
6.29
1.43
1.34
1.00
1.29
1.32
1.24
10.87
9.0
8.5
8.0
7.5
7.0
6.5
6.0
5.5
5.0
4.5
4.0
3.5
3.0
2.5
2.0
1.5
1.0
0.5
0

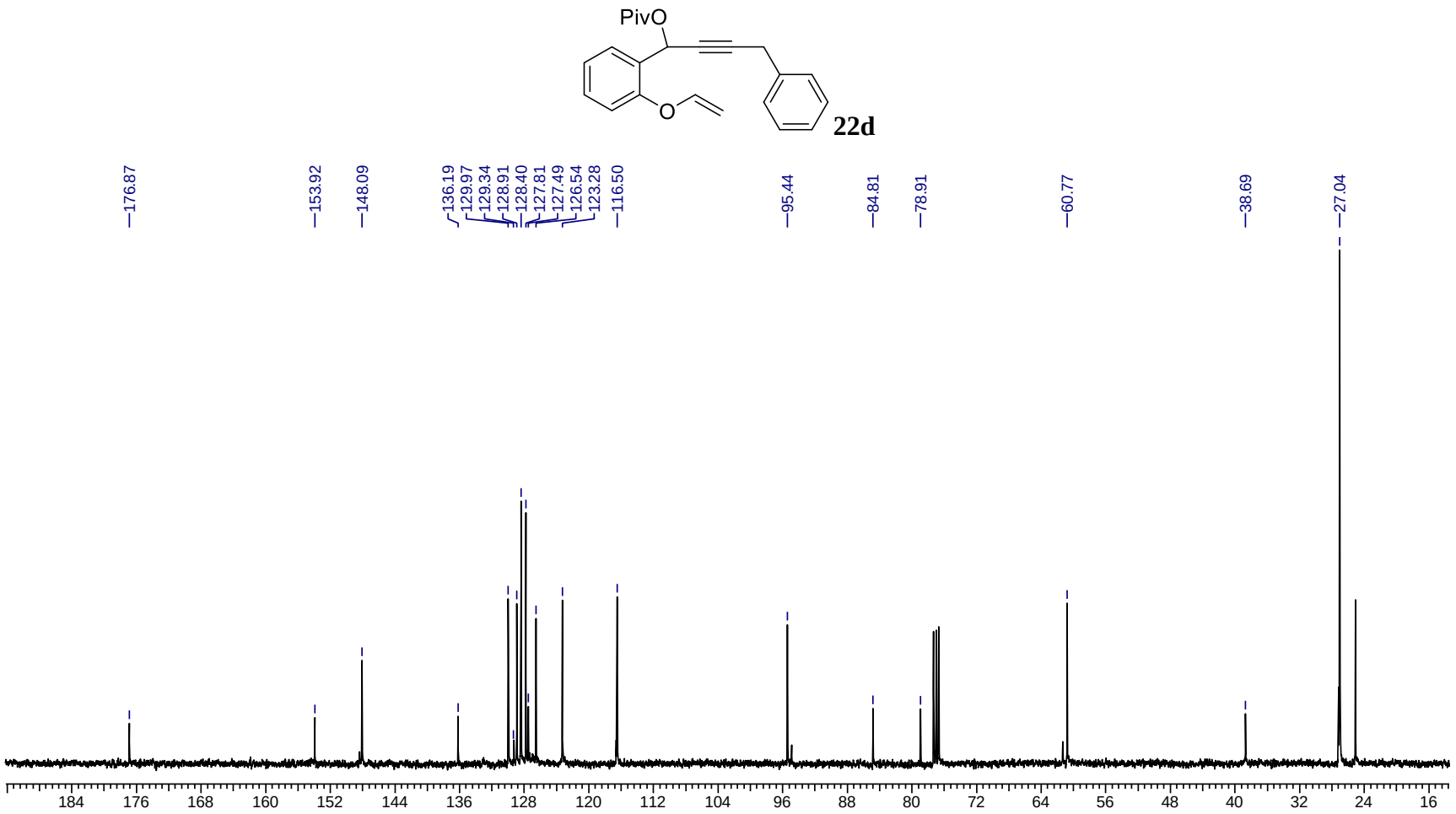
PivO
O
22d
176.87
153.92
148.09
136.19
129.97
129.34
128.91
128.40
127.81
127.49
126.54
123.28
116.50
95.44
84.81
78.91
60.77
38.69
27.04
184
176
168
160
152
144
136
128
120
112
104
96
88
80
72
64
56
48
40
32
24
16

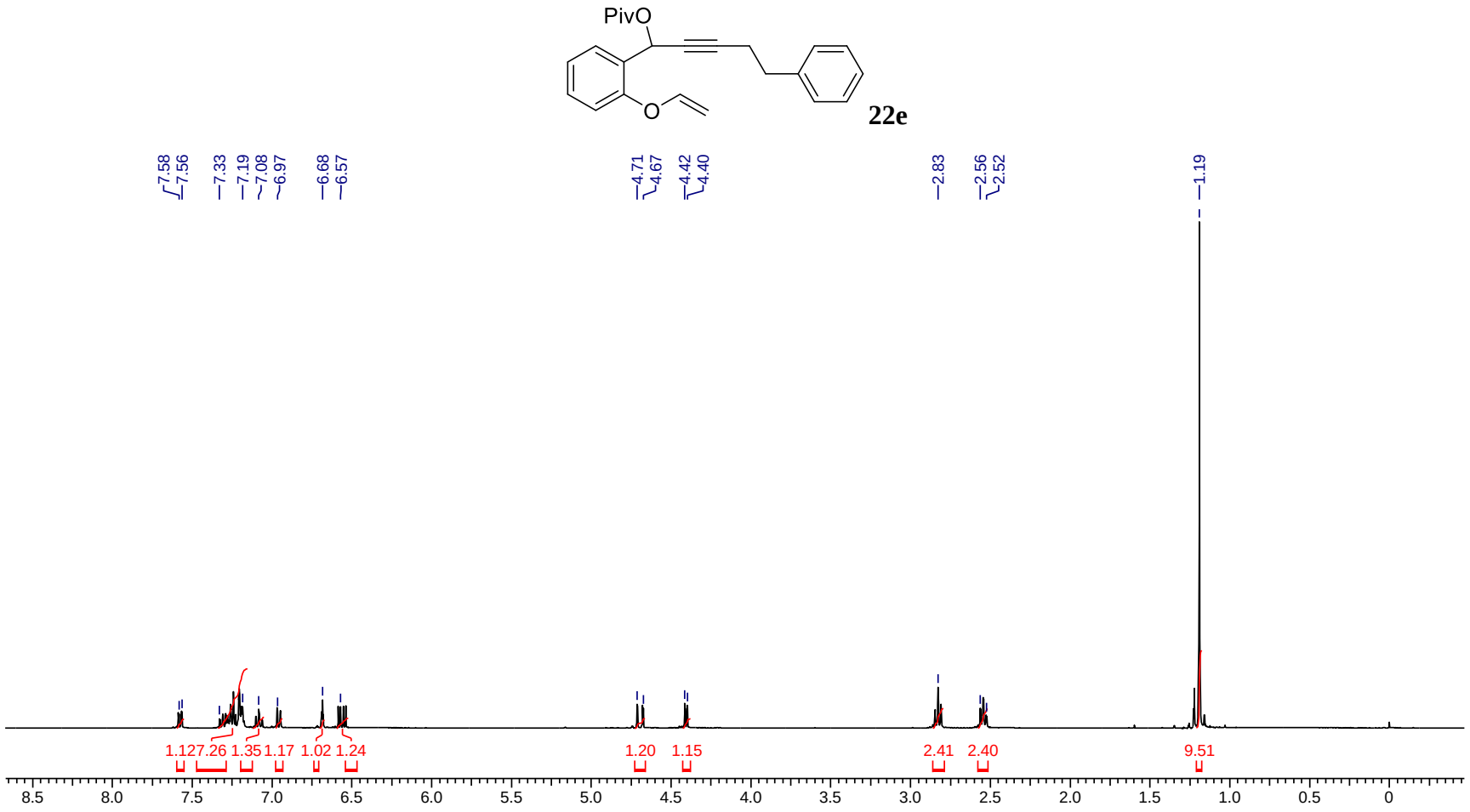
PivO
O
22e
7.58
7.56
7.33
7.19
7.08
6.97
6.68
6.57
4.71
4.67
4.42
4.40
2.83
2.56
2.52
1.19
1.12
7.26
1.35
1.17
1.02
1.24
1.20
1.15
2.41
2.40
9.51
8.5
8.0
7.5
7.0
6.5
6.0
5.5
5.0
4.5
4.0
3.5
3.0
2.5
2.0
1.5
1.0
0.5
0

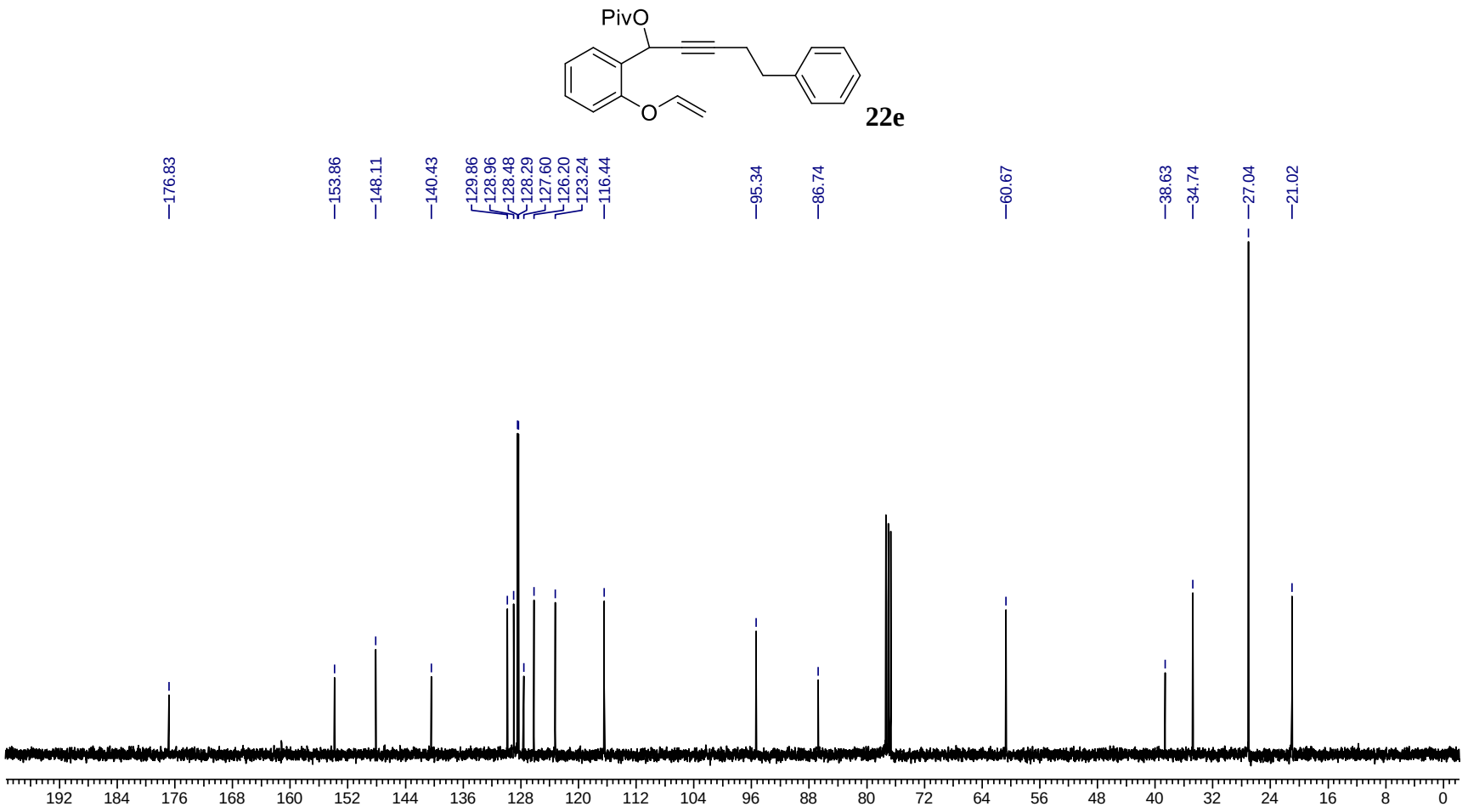
PivO
O
22e
176.83
153.86
148.11
140.43
129.86
128.96
128.48
128.29
127.60
126.20
123.24
116.44
95.34
86.74
60.67
38.63
34.74
27.04
21.02
192
184
176
168
160
152
144
136
128
120
112
104
96
88
80
72
64
56
48
40
32
24
16
8
0

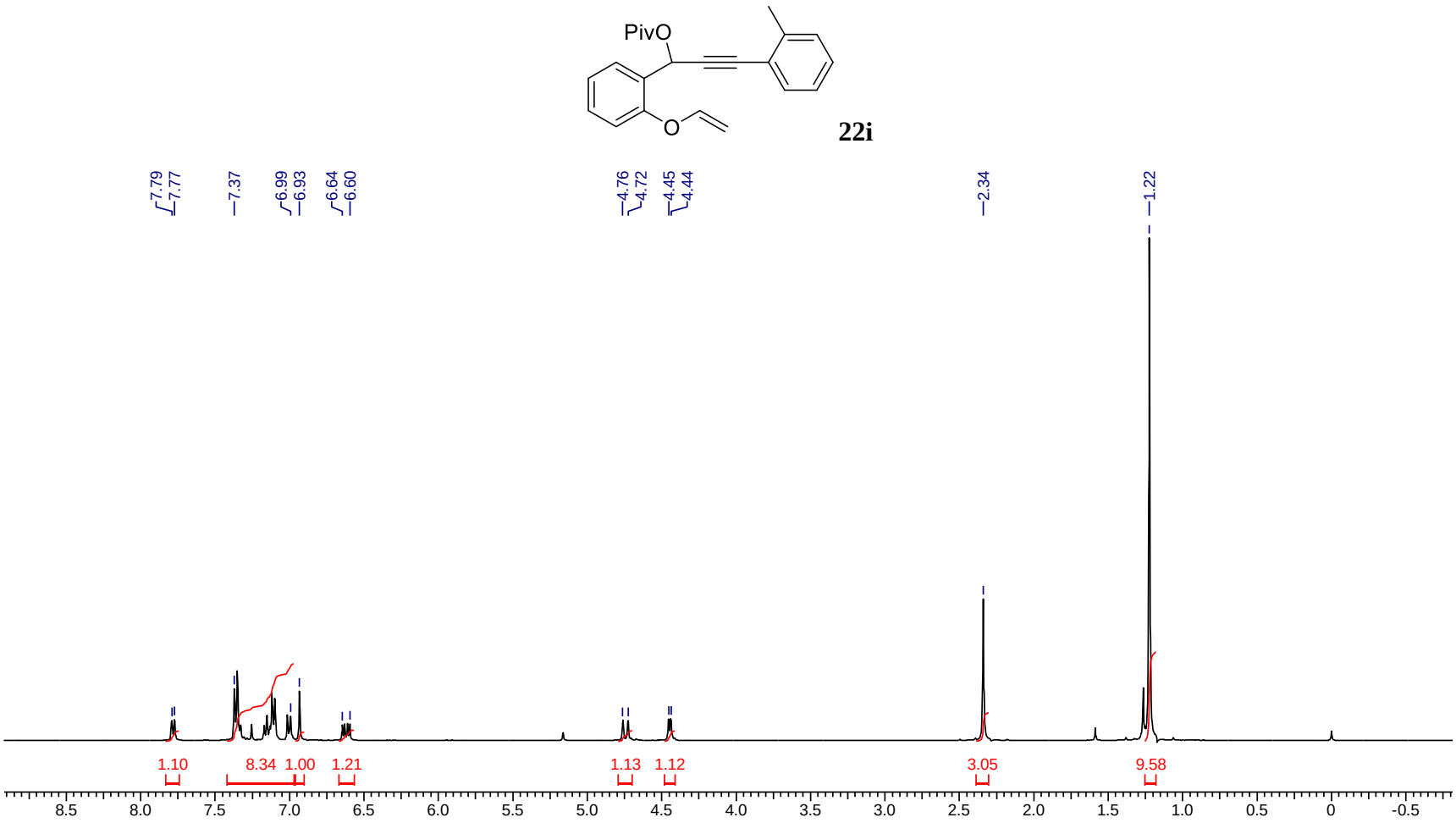
PivO
O
22i
7.79
7.77
7.37
6.99
6.93
6.64
6.60
4.76
4.72
4.45
4.44
2.34
1.22
1.10
8.34
1.00
1.21
1.13
1.12
3.05
9.58
8.5
8.0
7.5
7.0
6.5
6.0
5.5
5.0
4.5
4.0
3.5
3.0
2.5
2.0
1.5
1.0
0.5
0
-0.5

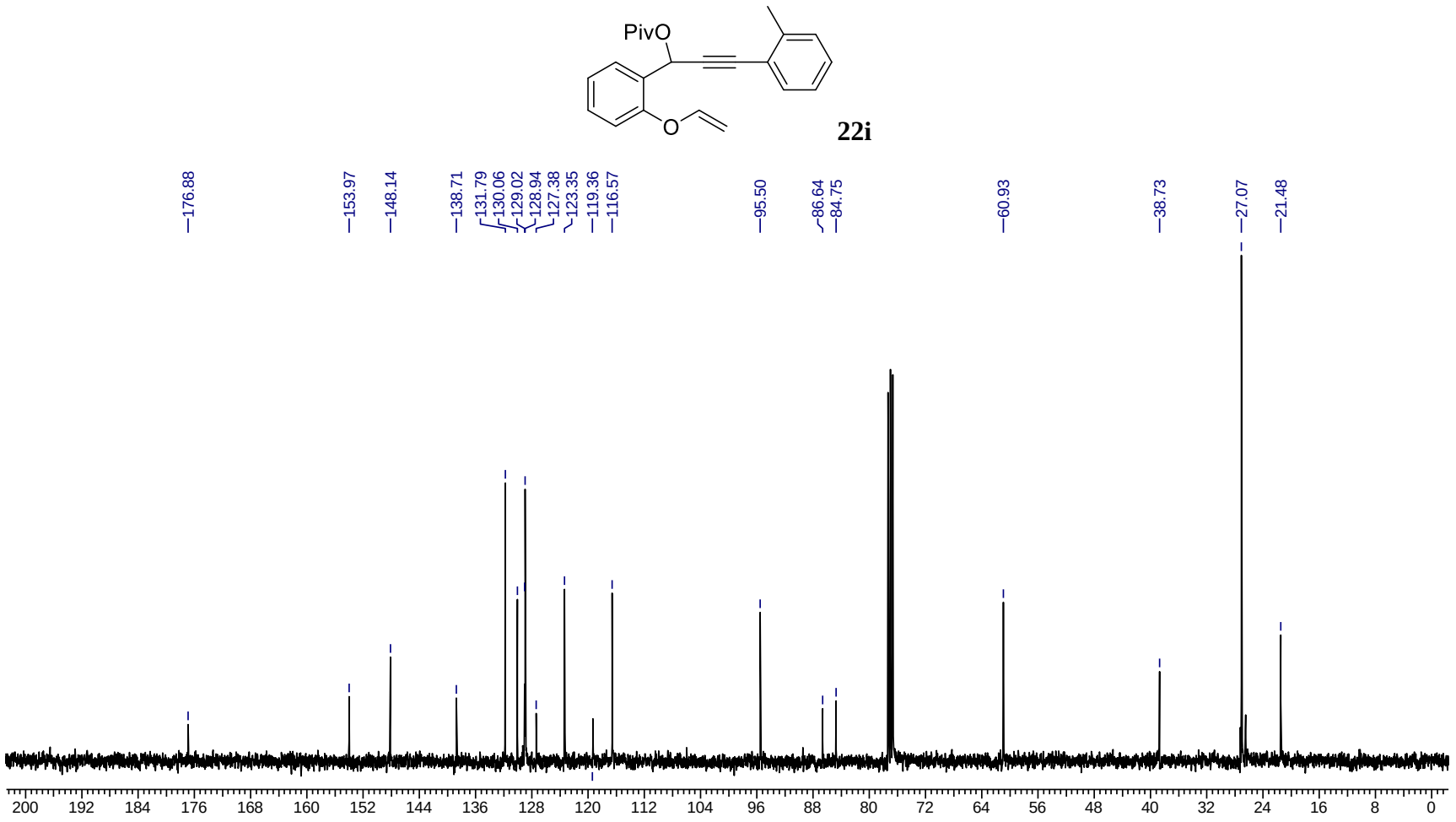
PivO
O
22i
176.88
153.97
148.14
138.71
131.79
130.06
129.02
128.94
127.38
123.35
119.36
116.57
95.50
86.64
84.75
60.93
38.73
27.07
21.48
200
192
184
176
168
160
152
144
136
128
120
112
104
96
88
80
72
64
56
48
40
32
24
16
8
0

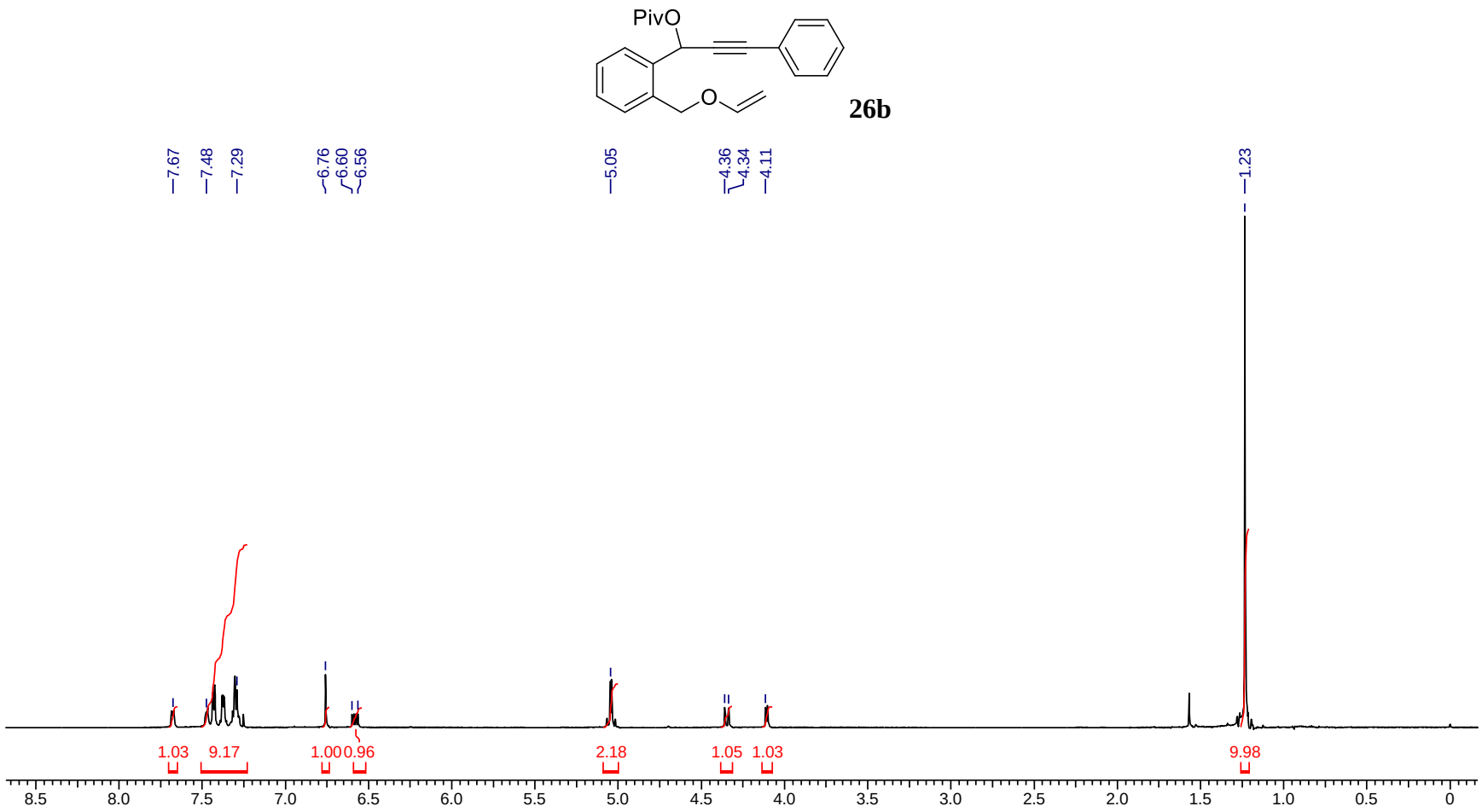
PivO
O
26b
7.67
7.48
7.29
6.76
6.60
6.56
5.05
4.36
4.34
4.11
1.23
1.03
9.17
1.00
0.96
2.18
1.05
1.03
9.98
8.5
8.0
7.5
7.0
6.5
6.0
5.5
5.0
4.5
4.0
3.5
3.0
2.5
2.0
1.5
1.0
0.5
0

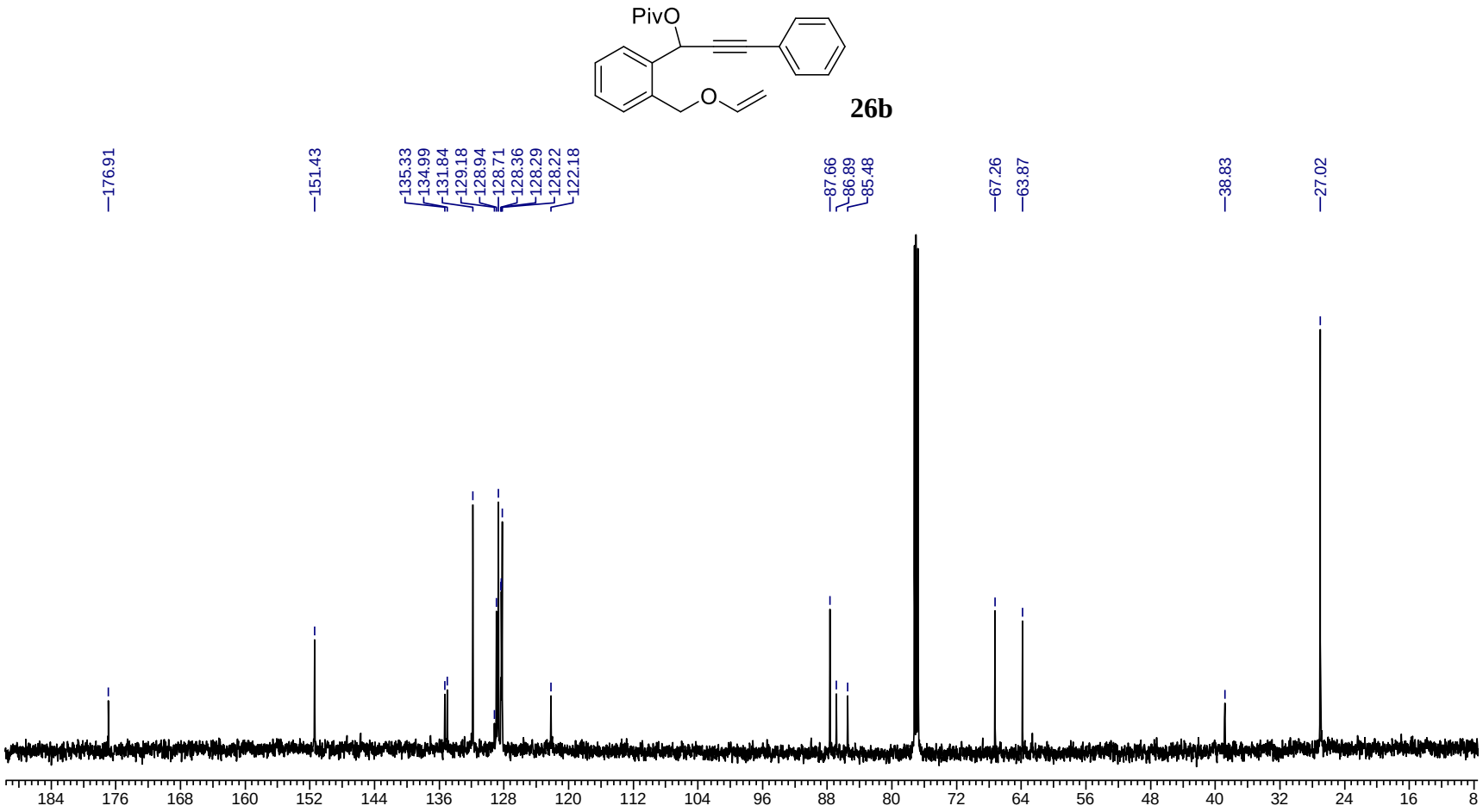
PivO
O
26b
176.91
151.43
135.33
134.99
131.84
129.18
128.94
128.71
128.36
128.29
128.22
122.18
87.66
86.89
85.48
67.26
63.87
38.83
27.02
184
176
168
160
152
144
136
128
120
112
104
96
88
80
72
64
56
48
40
32
24
16
8

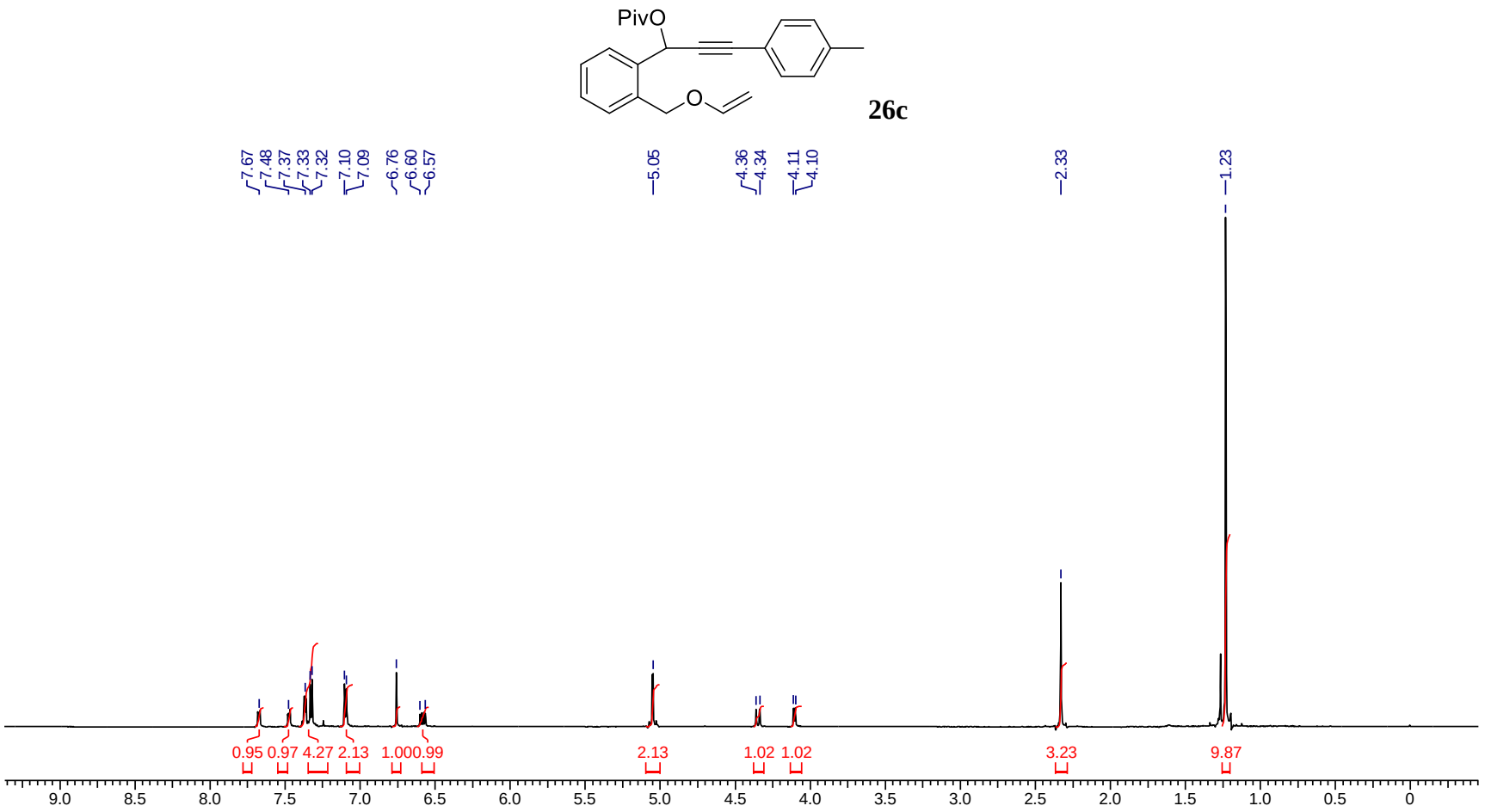
PivO
O
26c
7.67
7.48
7.37
7.33
7.32
7.10
7.09
6.76
6.60
6.57
5.05
4.36
4.34
4.11
4.10
2.33
1.23
0.95 0.97 4.27 2.13 1.00 0.99
2.13
1.02 1.02
3.23
9.87
9.0 8.5 8.0 7.5 7.0 6.5 6.0 5.5 5.0 4.5 4.0 3.5 3.0 2.5 2.0 1.5 1.0 0.5 0

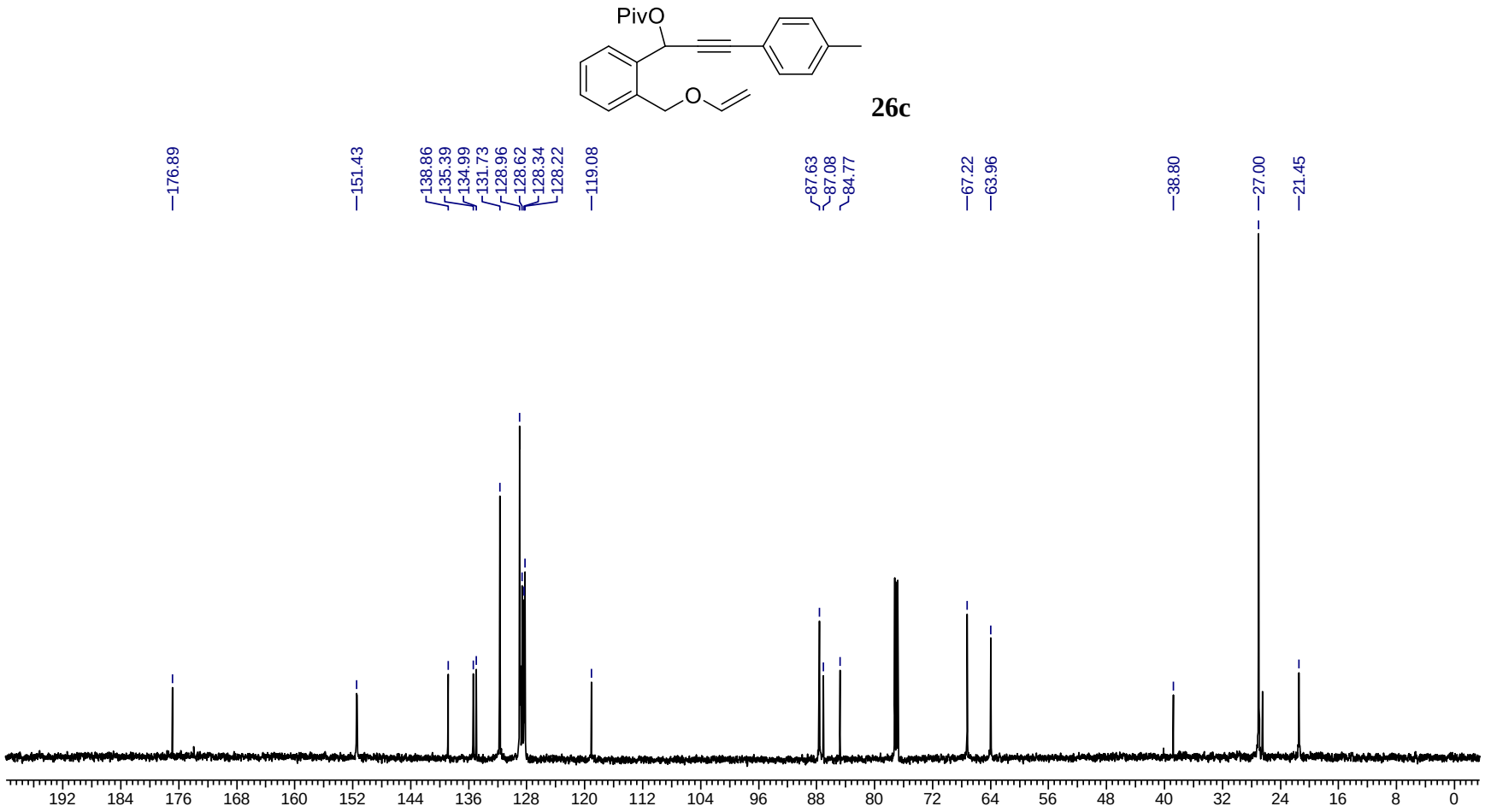
PivO
O
26c
176.89
151.43
138.86
135.39
134.99
131.73
128.96
128.62
128.34
128.22
119.08
87.63
87.08
84.77
67.22
63.96
38.80
27.00
21.45
192
184
176
168
160
152
144
136
128
120
112
104
96
88
80
72
64
56
48
40
32
24
16
8
0

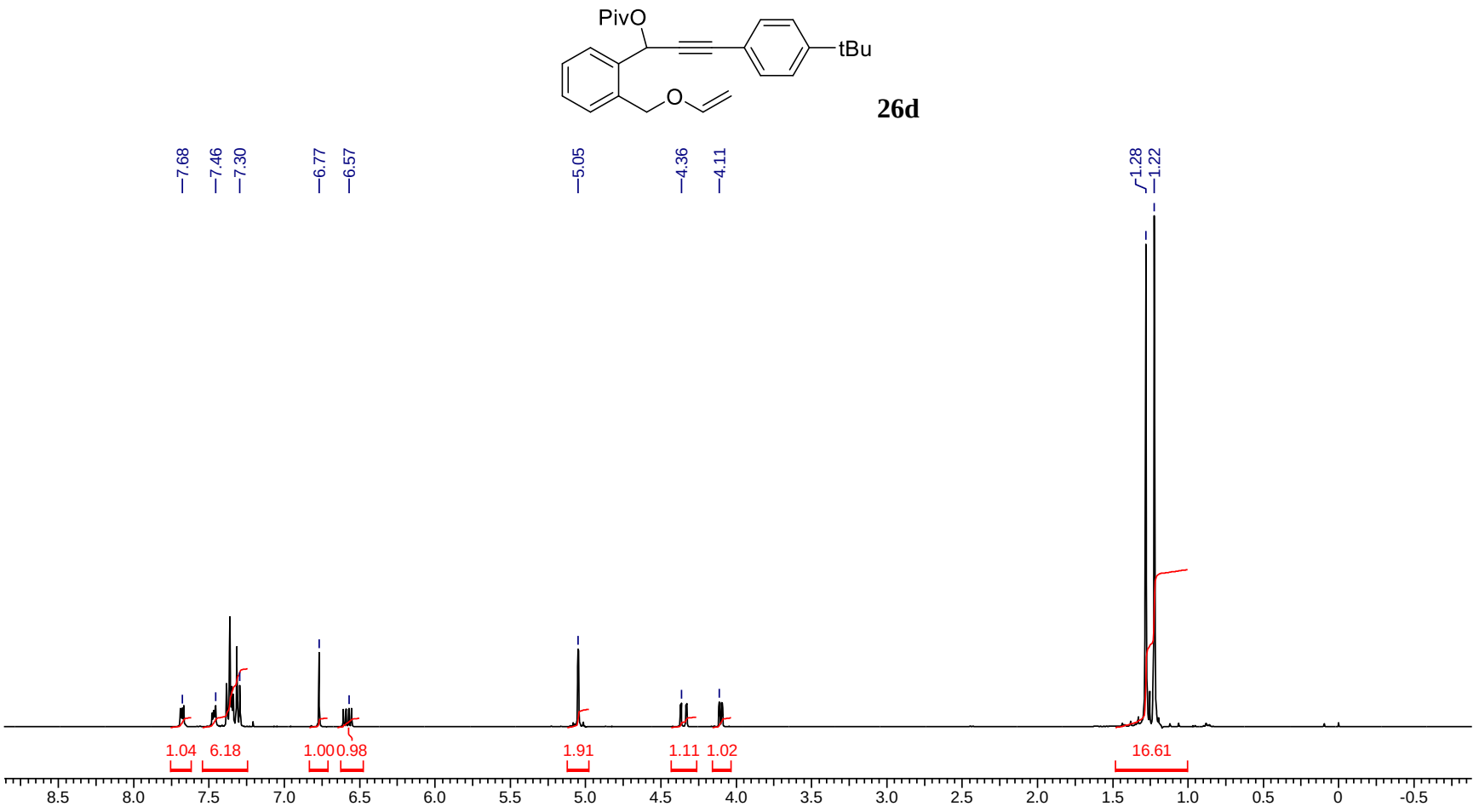
PivO
tBu
O
26d
7.68
7.46
7.30
6.77
6.57
5.05
4.36
4.11
1.28
1.22
1.04
6.18
1.00
0.98
1.91
1.11
1.02
16.61
8.5
8.0
7.5
7.0
6.5
6.0
5.5
5.0
4.5
4.0
3.5
3.0
2.5
2.0
1.5
1.0
0.5
0
-0.5

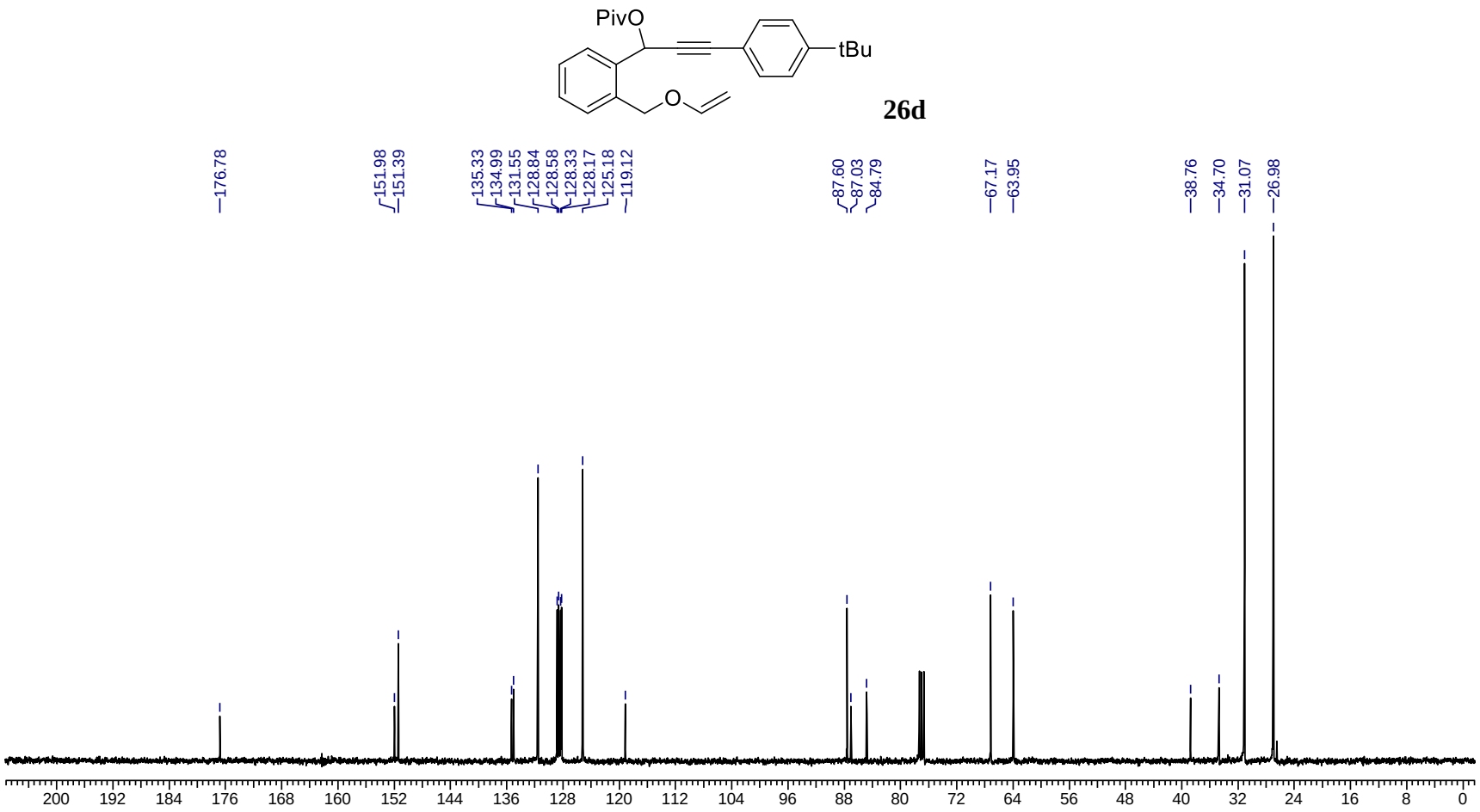
PivO
tBu
O
176.78
151.98
151.39
135.33
134.99
131.55
128.84
128.58
128.33
128.17
125.18
119.12
87.60
87.03
84.79
67.17
63.95
38.76
34.70
31.07
26.98
200
192
184
176
168
160
152
144
136
128
120
112
104
96
88
80
72
64
56
48
40
32
24
16
8
0

26d

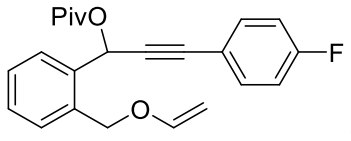
PivO
F
O

26e

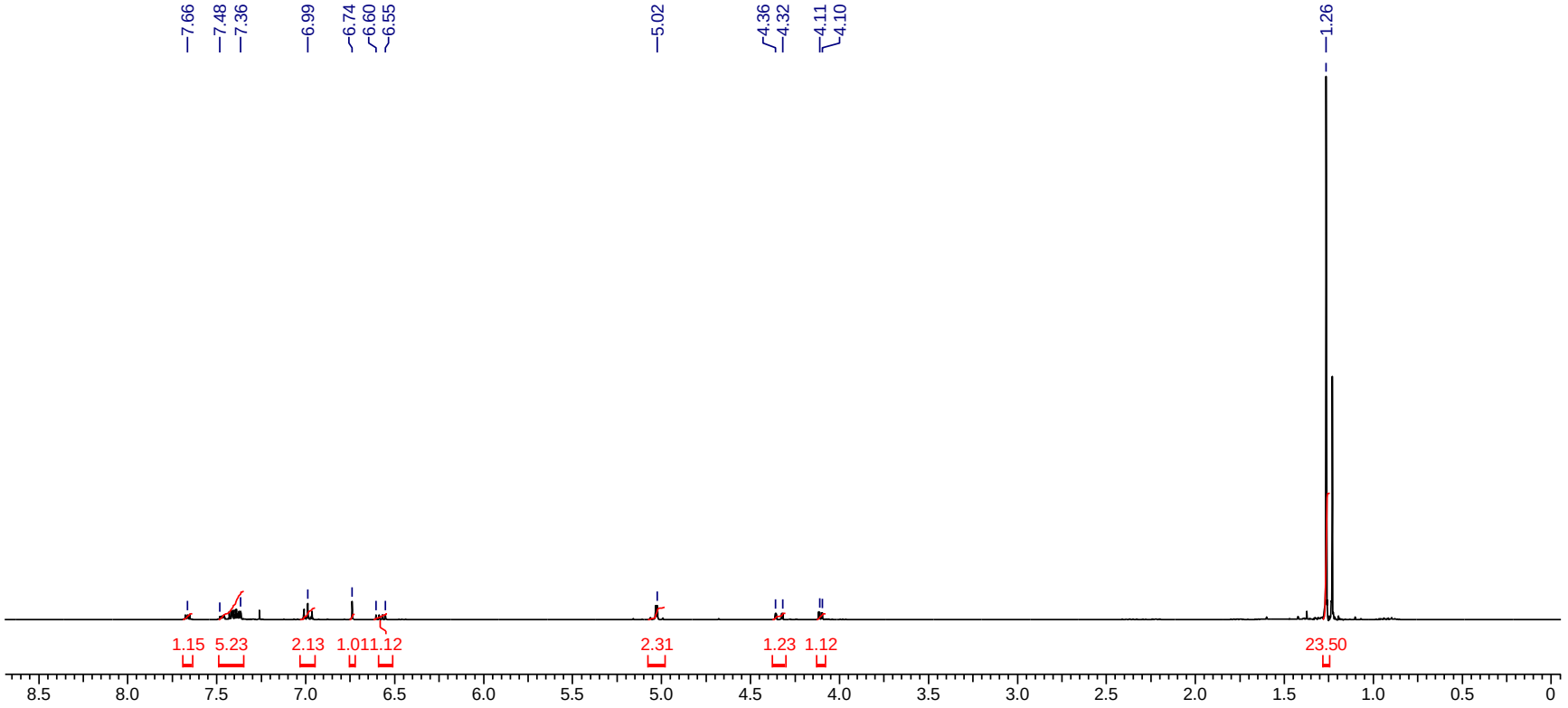
7.66
7.48
7.36
6.99
6.74
6.60
6.55
5.02
4.36
4.32
4.11
4.10
1.26
1.15
5.23
2.13
1.01
1.12
2.31
1.23
1.12
23.50
8.5
8.0
7.5
7.0
6.5
6.0
5.5
5.0
4.5
4.0
3.5
3.0
2.5
2.0
1.5
1.0
0.5
0

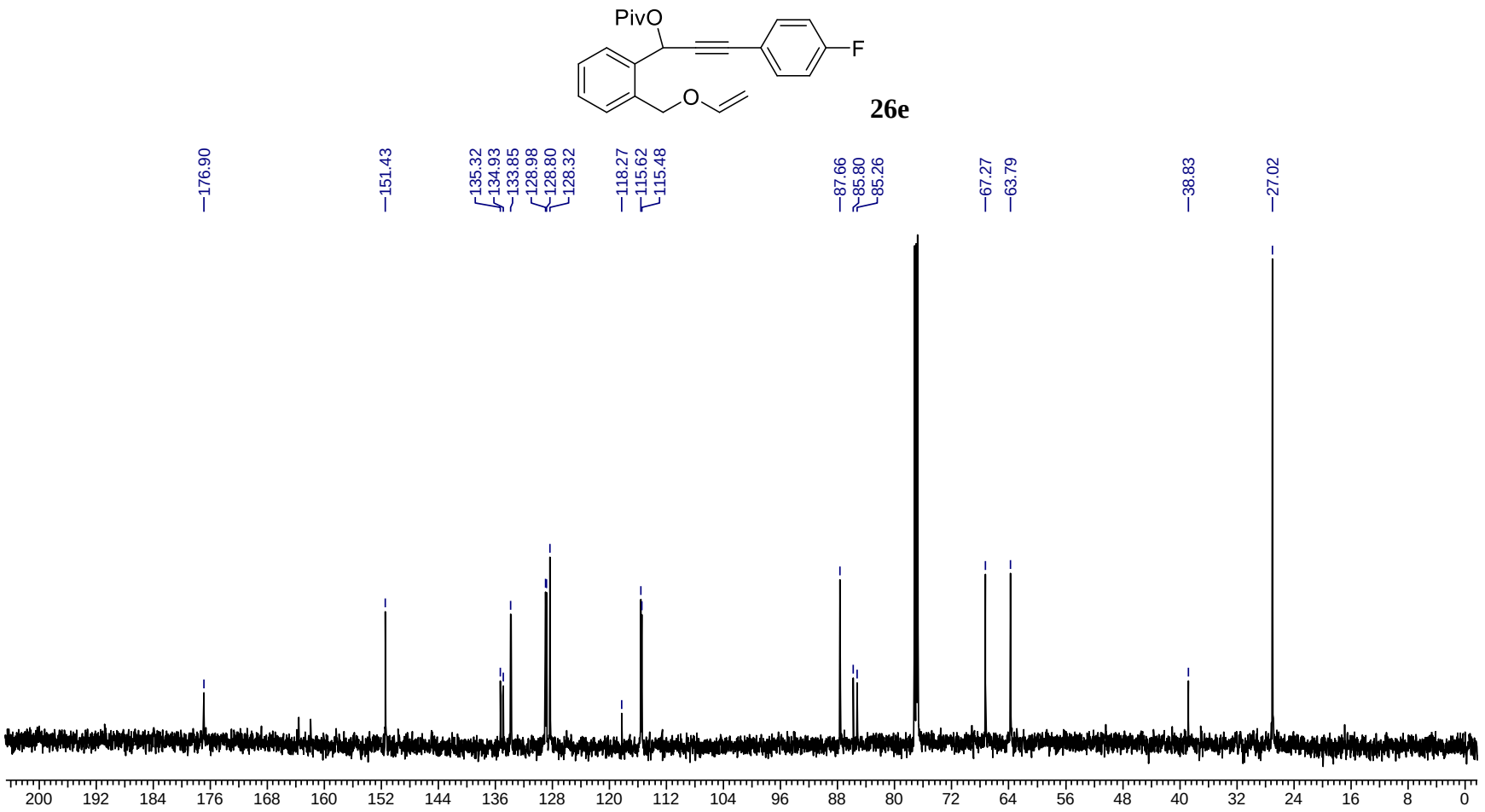
PivO
F
O
26e
176.90
151.43
135.32
134.93
133.85
128.98
128.80
128.32
118.27
115.62
115.48
87.66
85.80
85.26
67.27
63.79
38.83
27.02
200
192
184
176
168
160
152
144
136
128
120
112
104
96
88
80
72
64
56
48
40
32
24
16
8
0

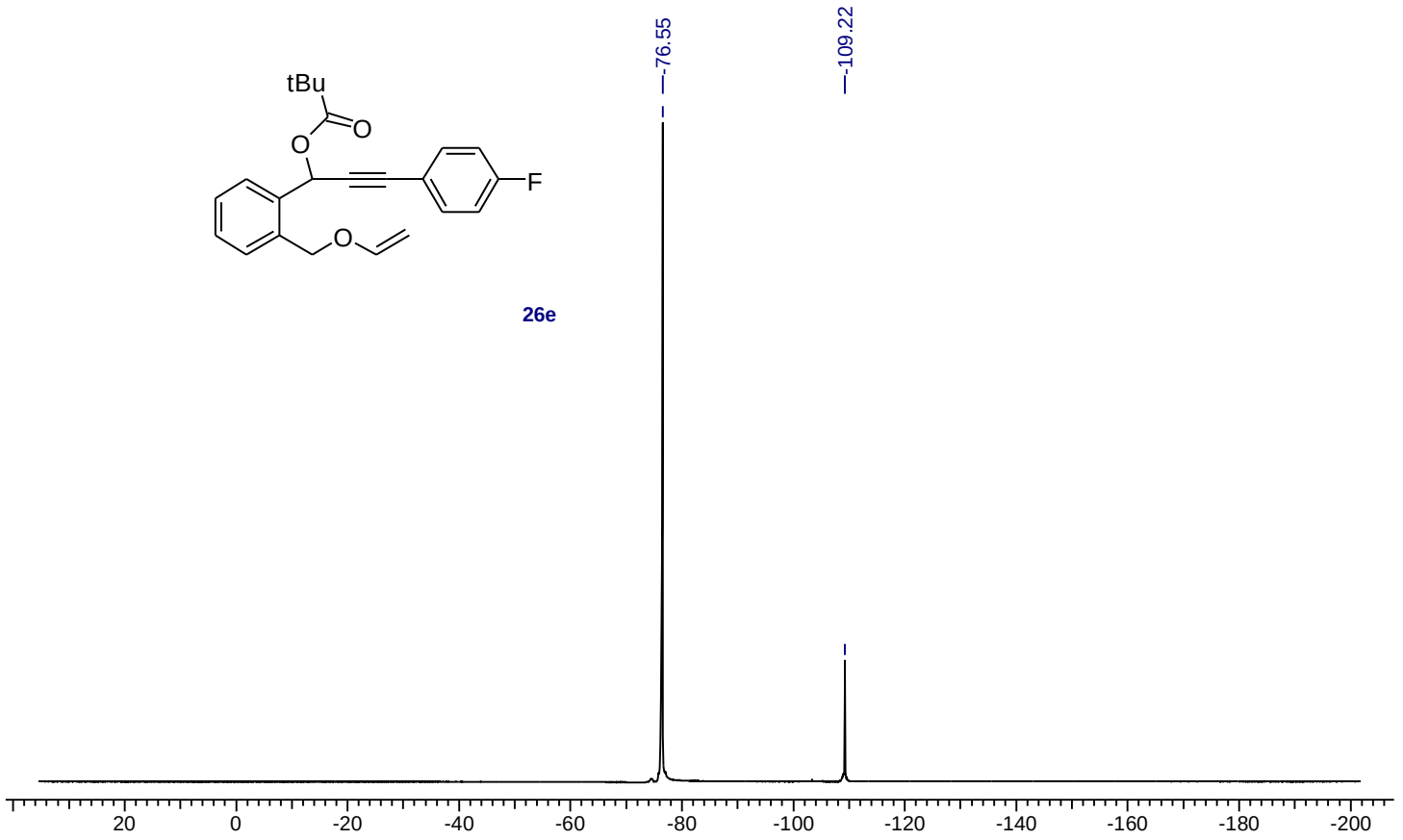
tBu
O
O
O
F
O
26e
-76.55
-109.22
20
0
-20
-40
-60
-80
-100
-120
-140
-160
-180
-200

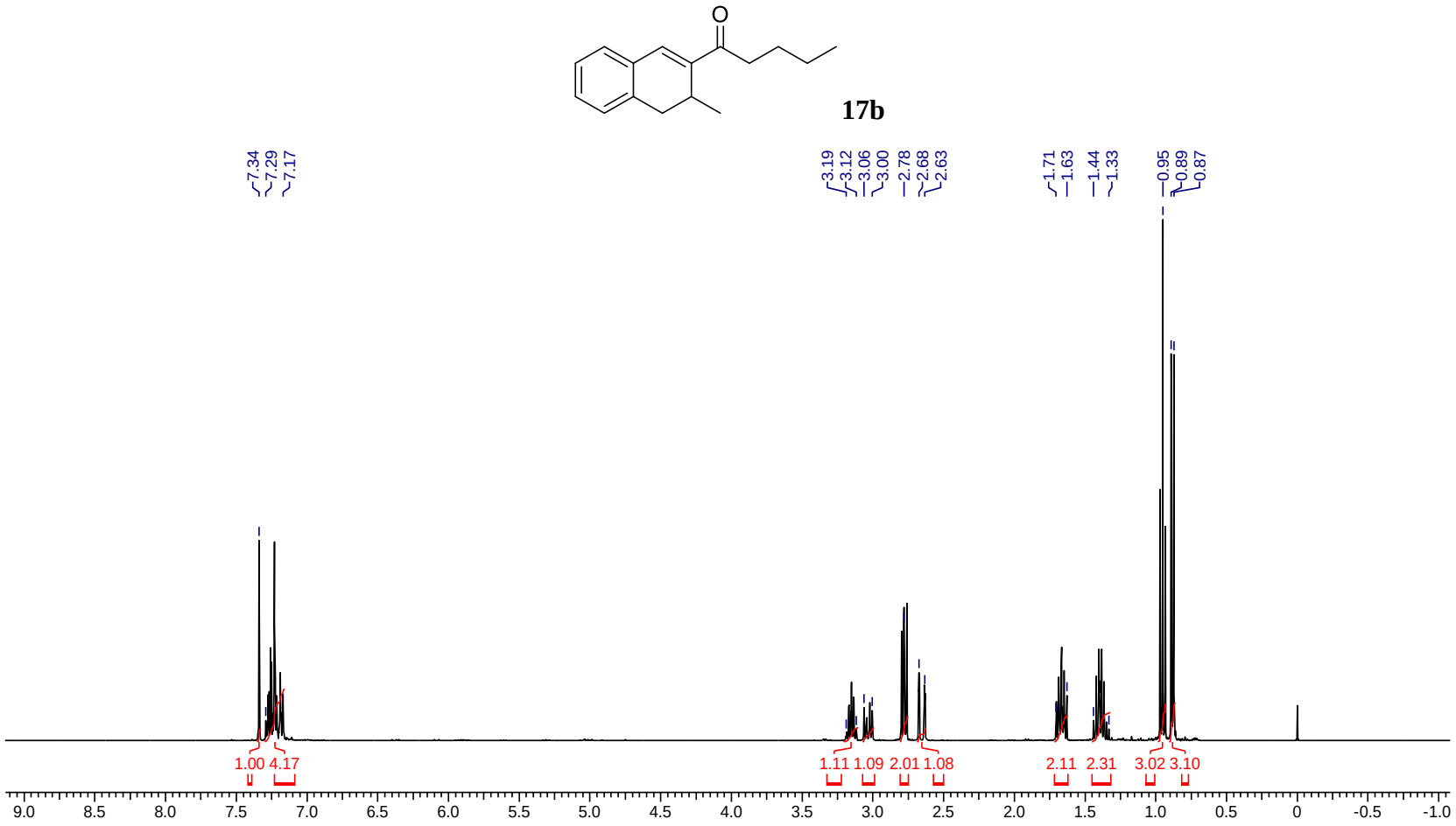
O
17b
7.34
7.29
7.17
3.19
3.12
3.06
3.00
2.78
2.68
2.63
1.71
1.63
1.44
1.33
0.95
0.89
0.87
1.00 4.17
1.11 1.09 2.01 1.08
2.11 2.31 3.02 3.10
9.0 8.5 8.0 7.5 7.0 6.5 6.0 5.5 5.0 4.5 4.0 3.5 3.0 2.5 2.0 1.5 1.0 0.5 0 -0.5 -1.0

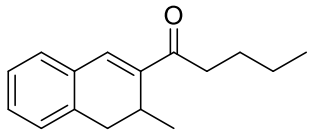
O

17b

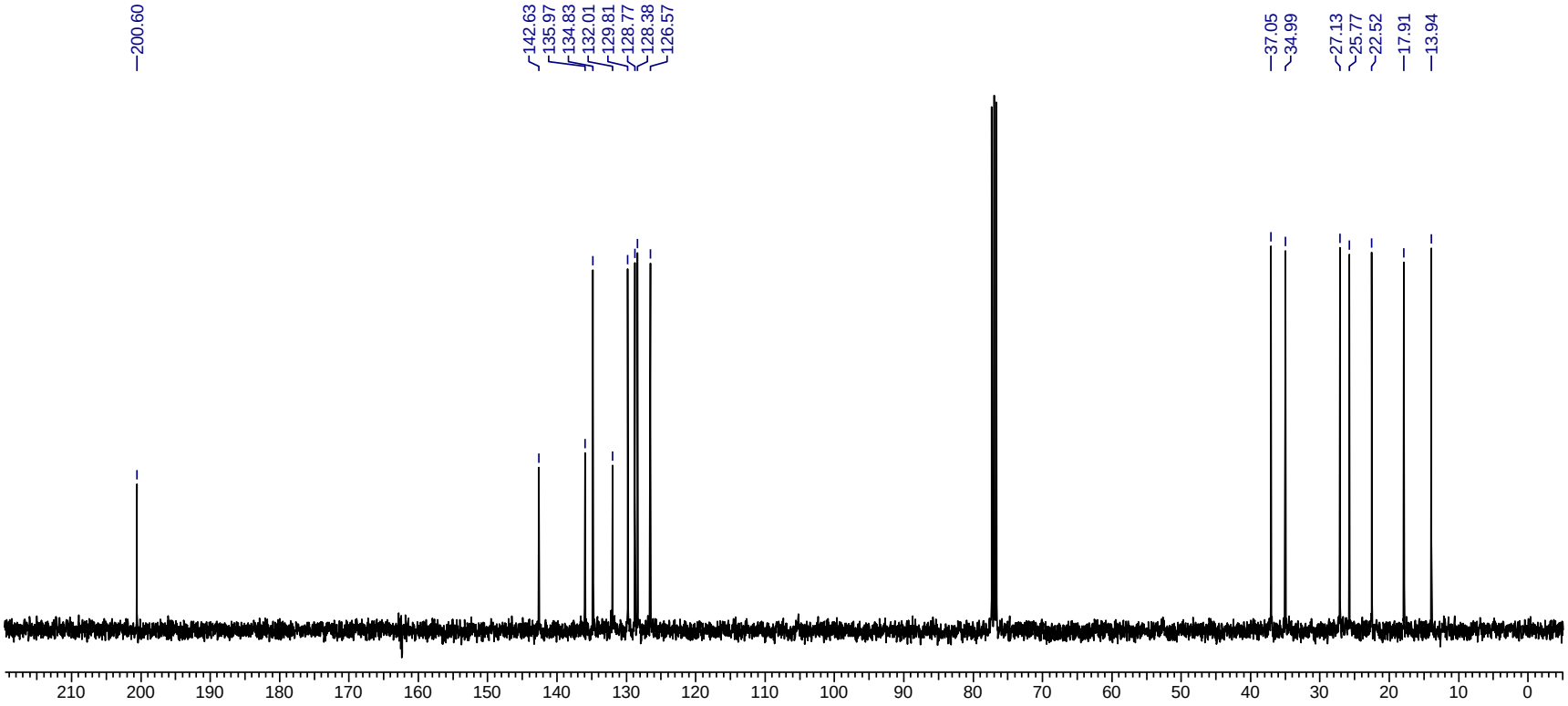
200.60
142.63
135.97
134.83
132.01
129.81
128.77
128.38
126.57
37.05
34.99
27.13
25.77
22.52
17.91
13.94
210
200
190
180
170
160
150
140
130
120
110
100
90
80
70
60
50
40
30
20
10
0

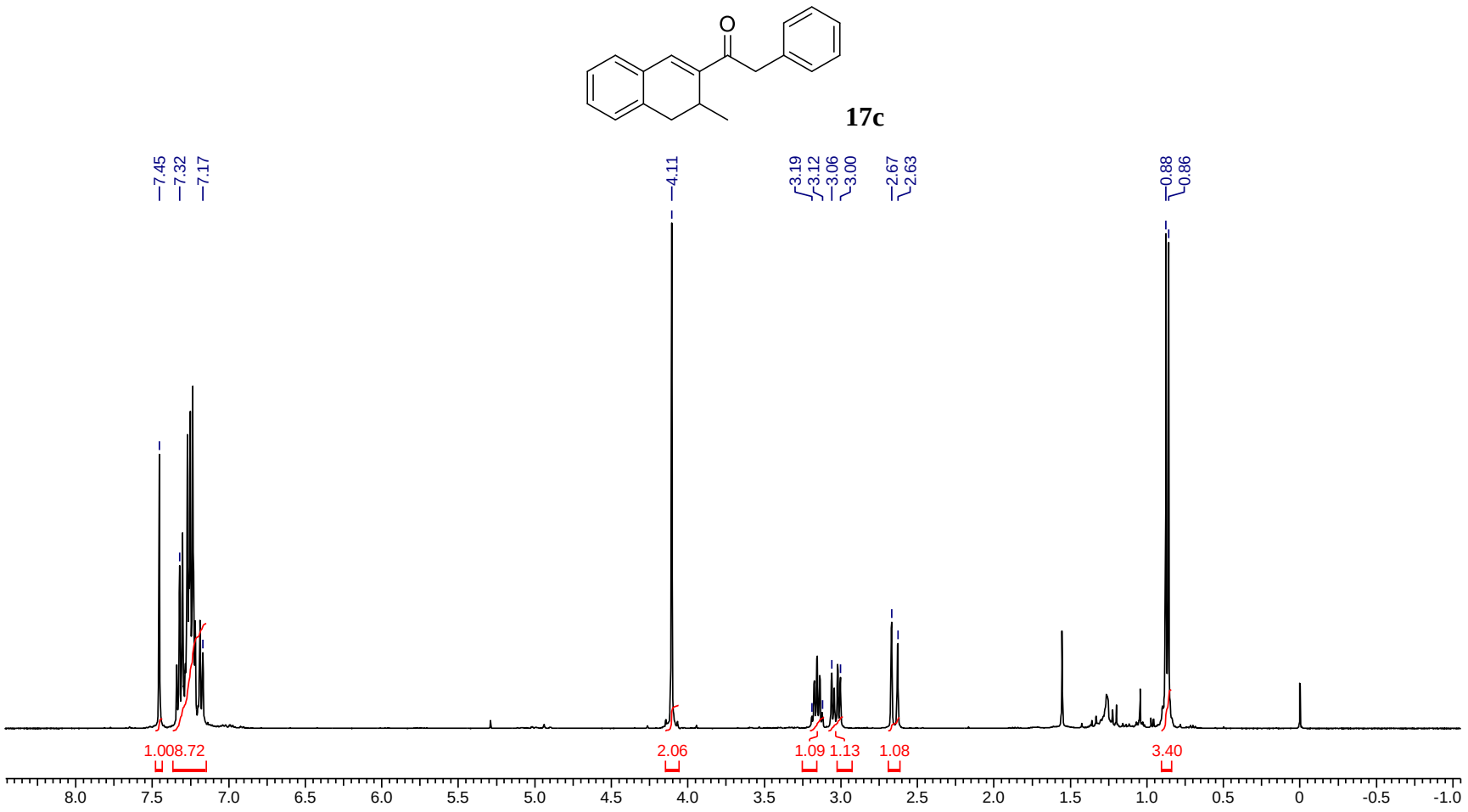
O
17c
7.45
7.32
7.17
4.11
3.19
3.12
3.06
3.00
2.67
2.63
0.88
0.86
1.00
8.72
2.06
1.09
1.13
1.08
3.40
8.0
7.5
7.0
6.5
6.0
5.5
5.0
4.5
4.0
3.5
3.0
2.5
2.0
1.5
1.0
0.5
0
-0.5
-1.0

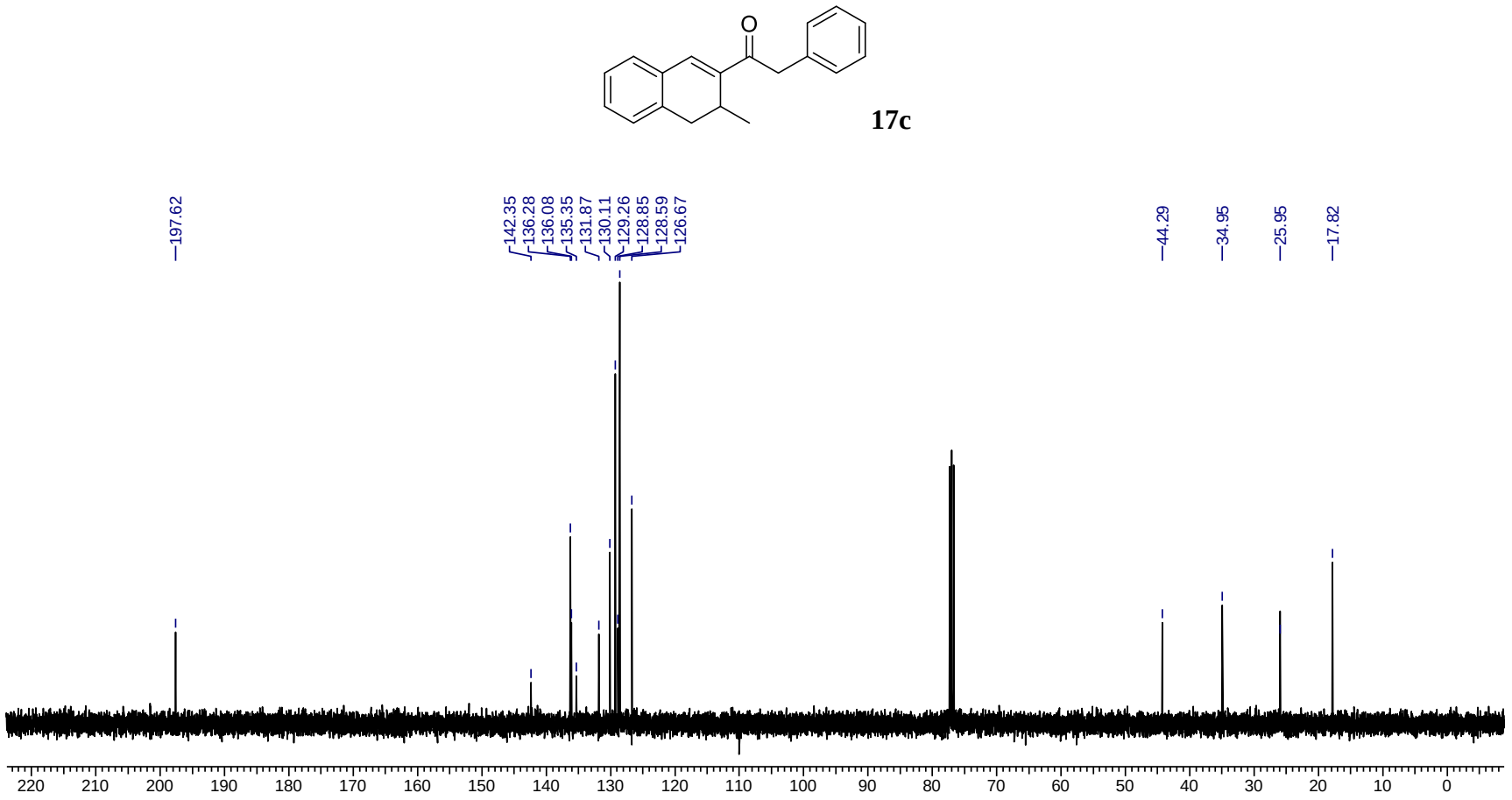
O
17c
197.62
142.35
136.28
136.08
135.35
131.87
130.11
129.26
128.85
128.59
126.67
44.29
34.95
25.95
17.82
220
210
200
190
180
170
160
150
140
130
120
110
100
90
80
70
60
50
40
30
20
10
0

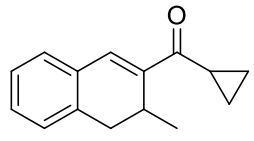
O

17d

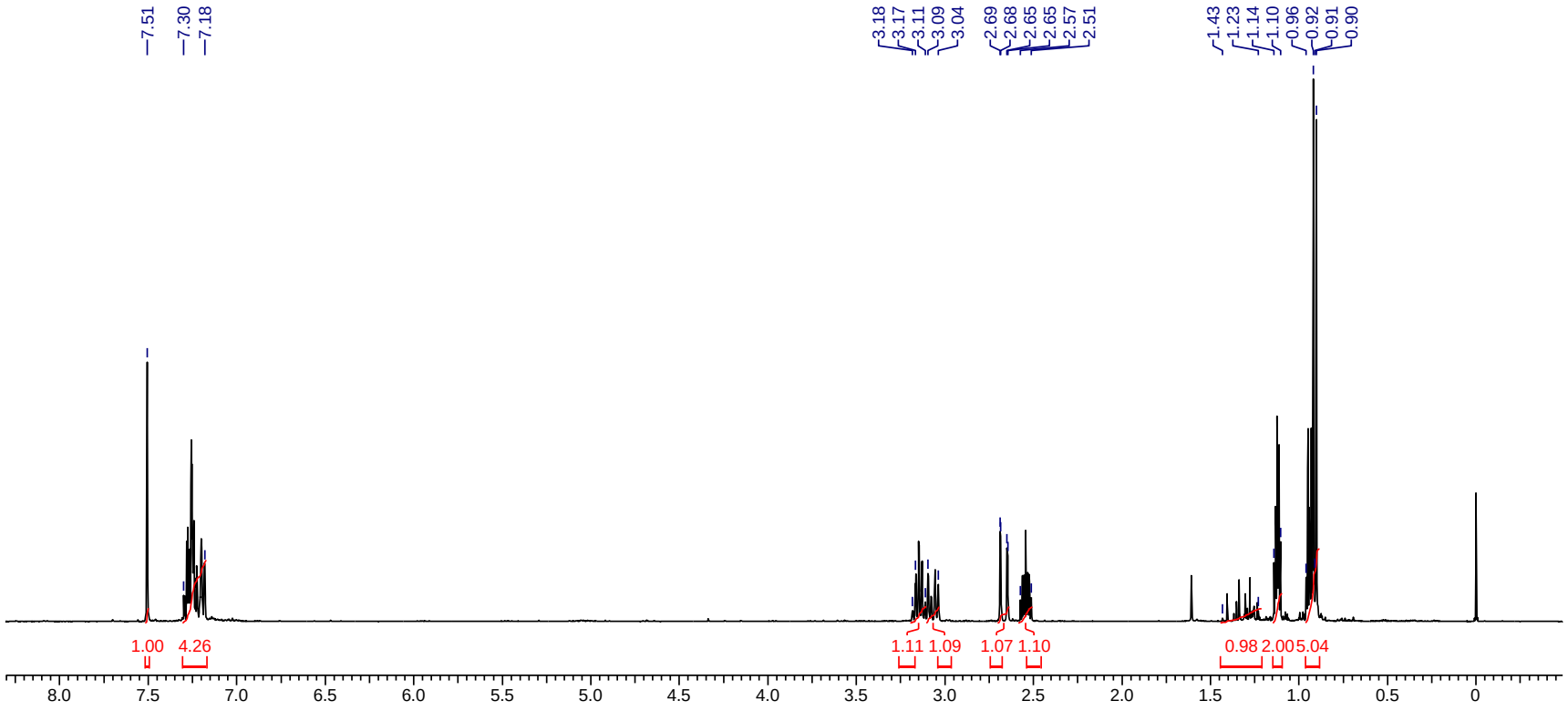
7.51
7.30
7.18
3.18
3.17
3.11
3.09
3.04
2.69
2.68
2.65
2.57
2.51
1.43
1.23
1.14
1.10
0.96
0.92
0.91
0.90
1.00
4.26
1.11
1.09
1.07
1.10
0.98
2.00
5.04
8.0
7.5
7.0
6.5
6.0
5.5
5.0
4.5
4.0
3.5
3.0
2.5
2.0
1.5
1.0
0.5
0

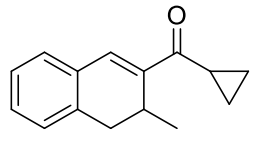
O

17d

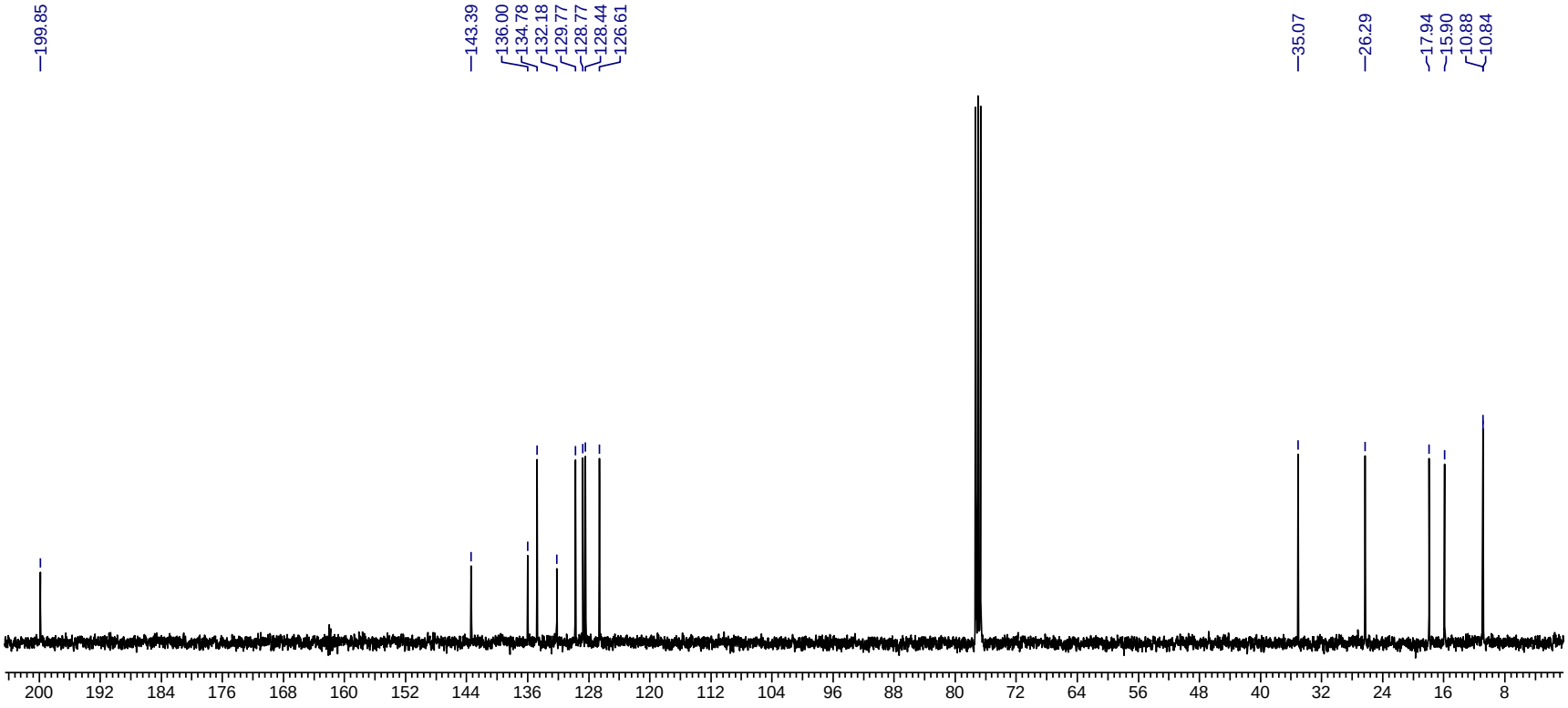
199.85
143.39
136.00
134.78
132.18
129.77
128.77
128.44
126.61
35.07
26.29
17.94
15.90
10.88
10.84
200
192
184
176
168
160
152
144
136
128
120
112
104
96
88
80
72
64
56
48
40
32
24
16
8

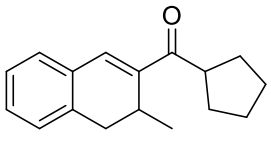

17e

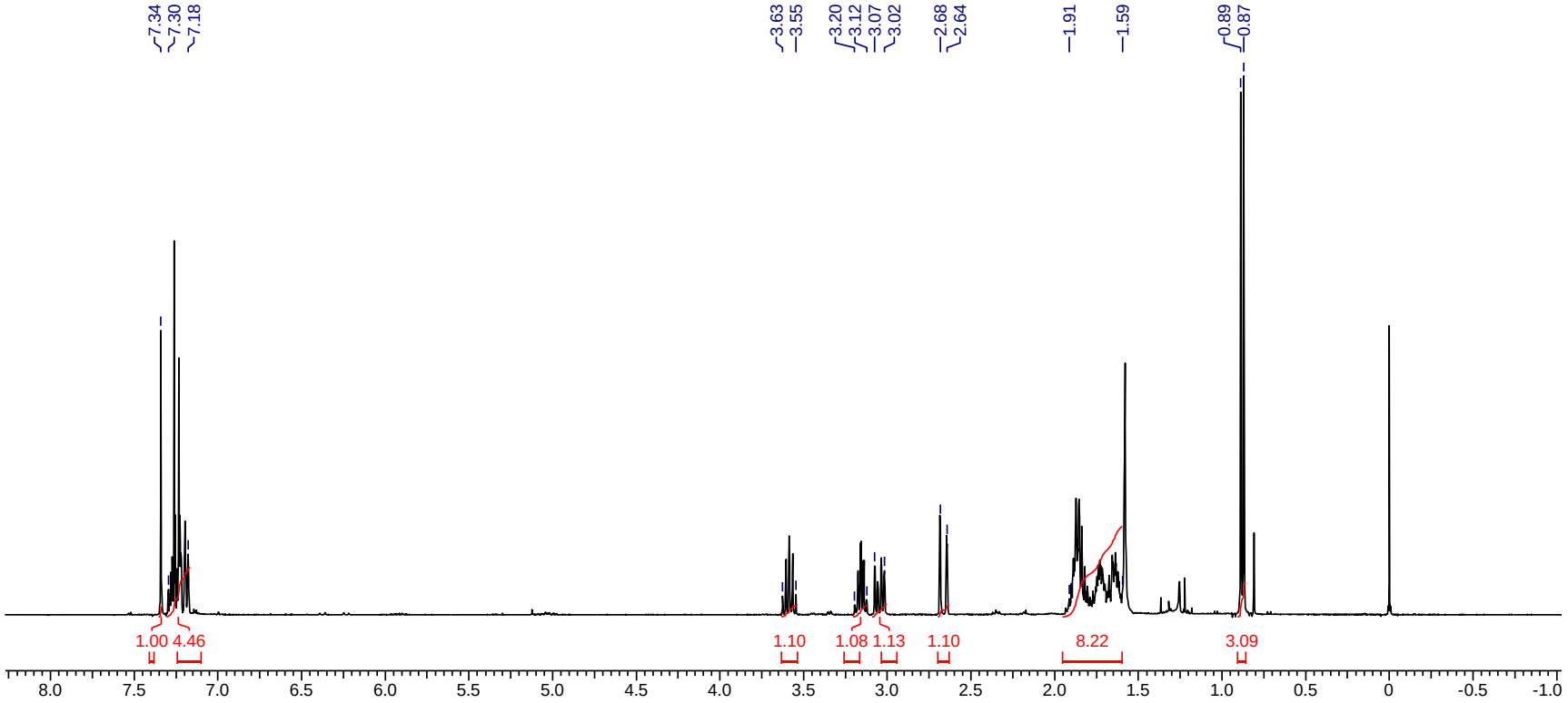
7.34
7.30
7.18
3.63
3.55
3.20
3.12
3.07
3.02
2.68
2.64
1.91
1.59
0.89
0.87
1.00
4.46
1.10
1.08
1.13
1.10
8.22
3.09
8.0
7.5
7.0
6.5
6.0
5.5
5.0
4.5
4.0
3.5
3.0
2.5
2.0
1.5
1.0
0.5
0
-0.5
-1.0

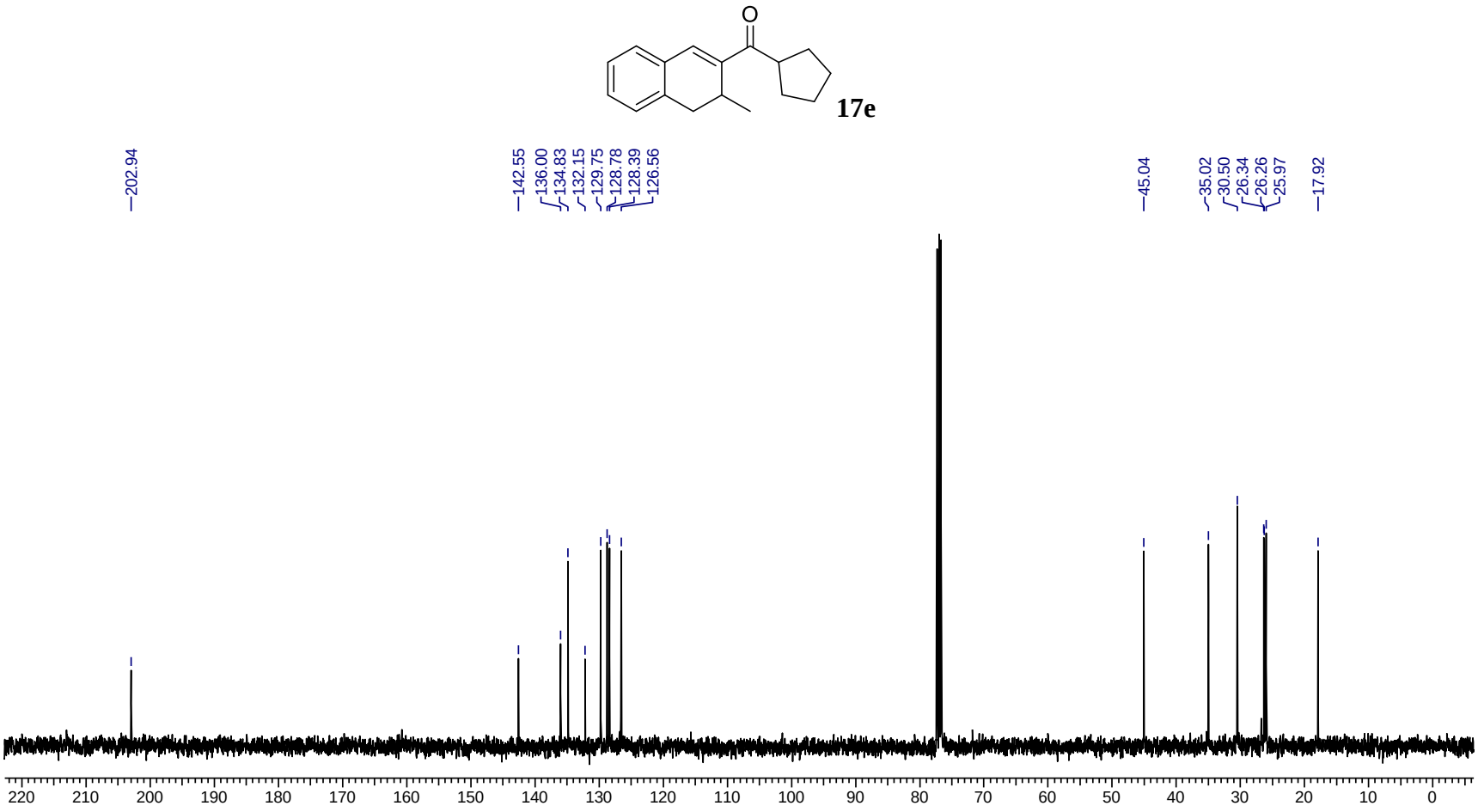
O
17e
202.94
142.55
136.00
134.83
132.15
129.75
128.78
128.39
126.56
45.04
35.02
30.50
26.34
26.26
25.97
17.92
220
210
200
190
180
170
160
150
140
130
120
110
100
90
80
70
60
50
40
30
20
10
0

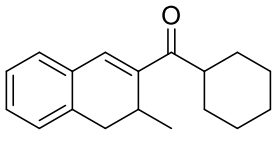
O

17f

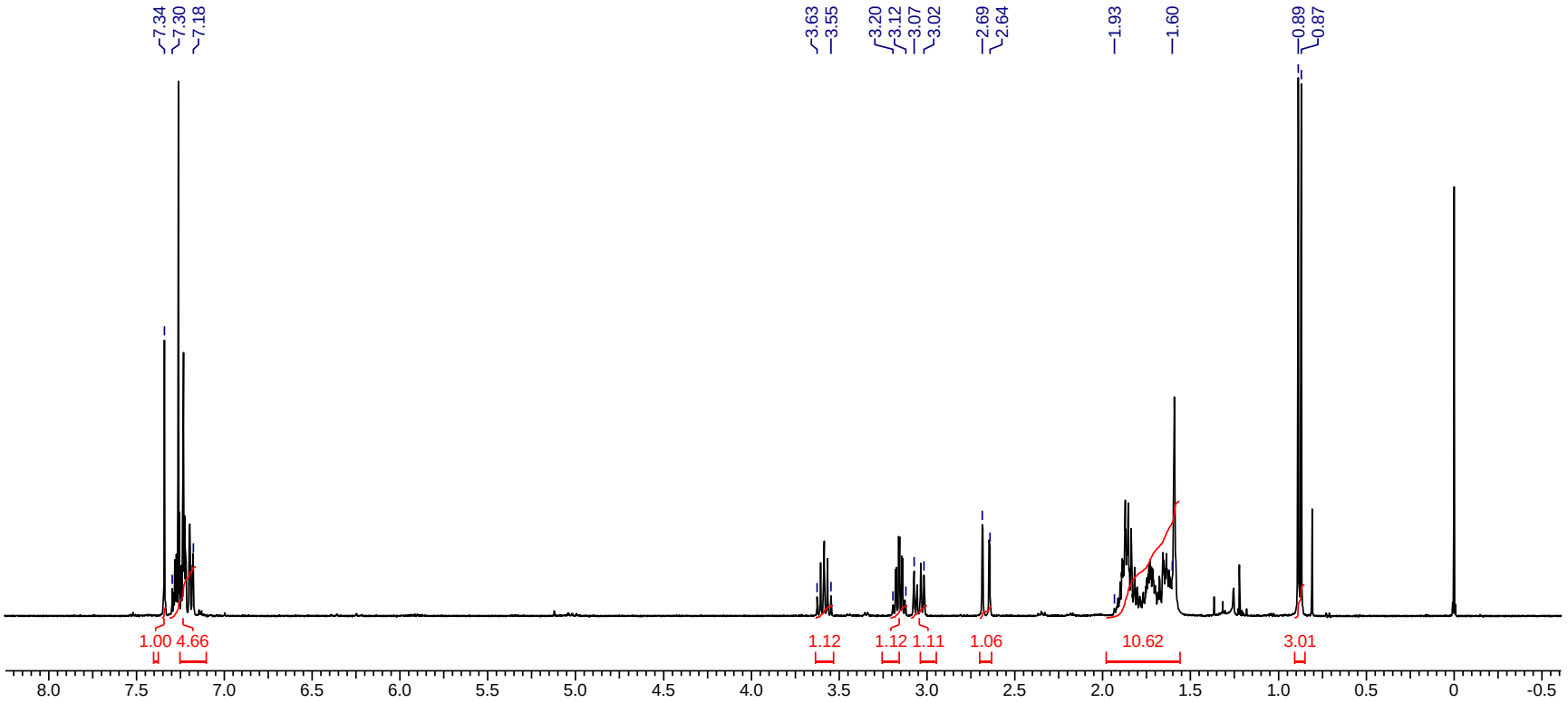
7.34
7.30
7.18
3.63
3.55
3.20
3.12
3.07
3.02
2.69
2.64
1.93
1.60
0.89
0.87
1.00
4.66
1.12
1.12
1.11
1.06
10.62
3.01
8.0
7.5
7.0
6.5
6.0
5.5
5.0
4.5
4.0
3.5
3.0
2.5
2.0
1.5
1.0
0.5
0
-0.5

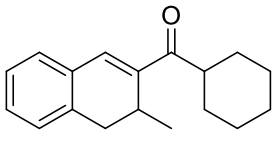
O

17f

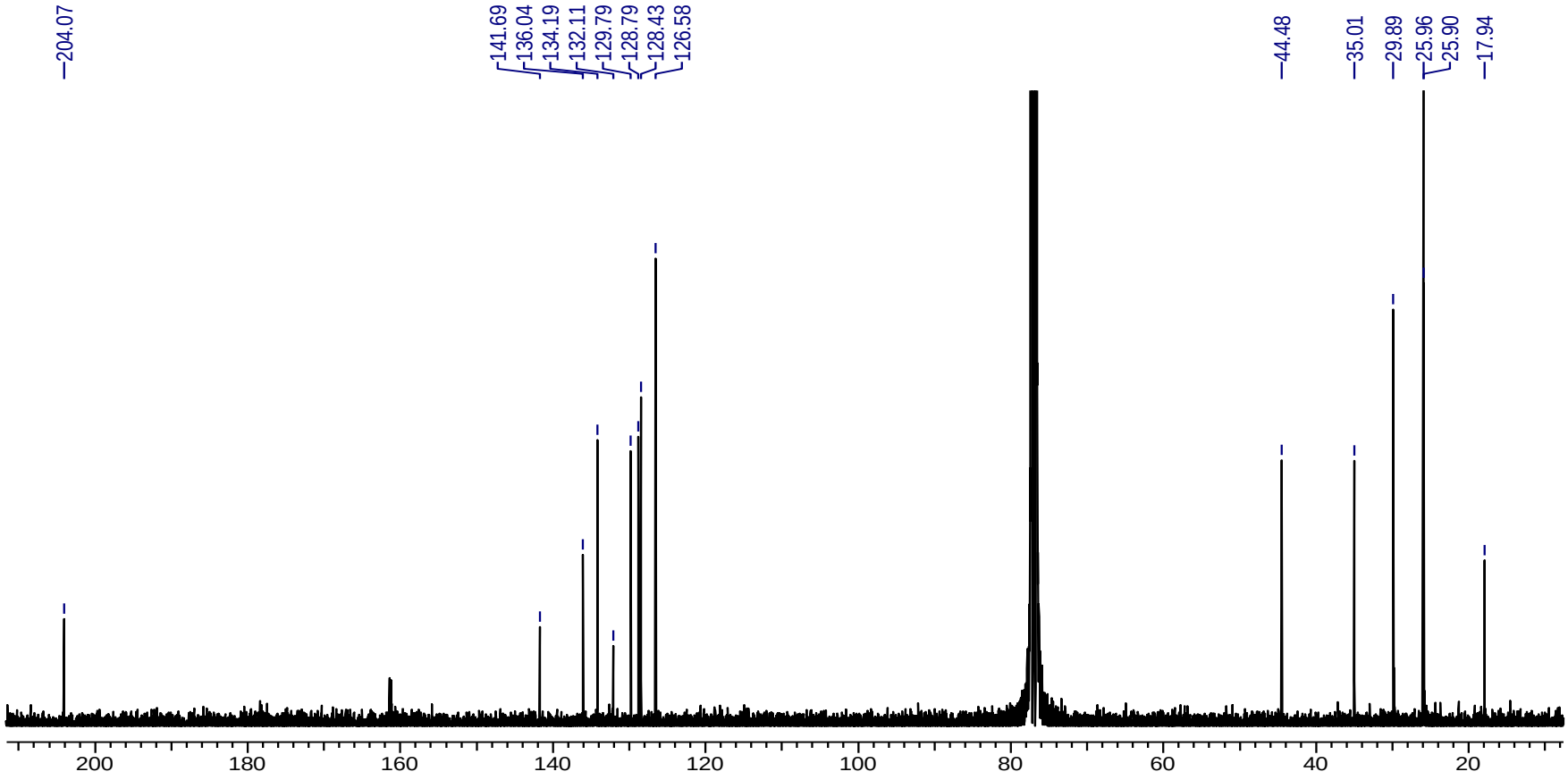
204.07
141.69
136.04
134.19
132.11
129.79
128.79
128.43
126.58
44.48
35.01
29.89
25.96
25.90
17.94
200
180
160
140
120
100
80
60
40
20

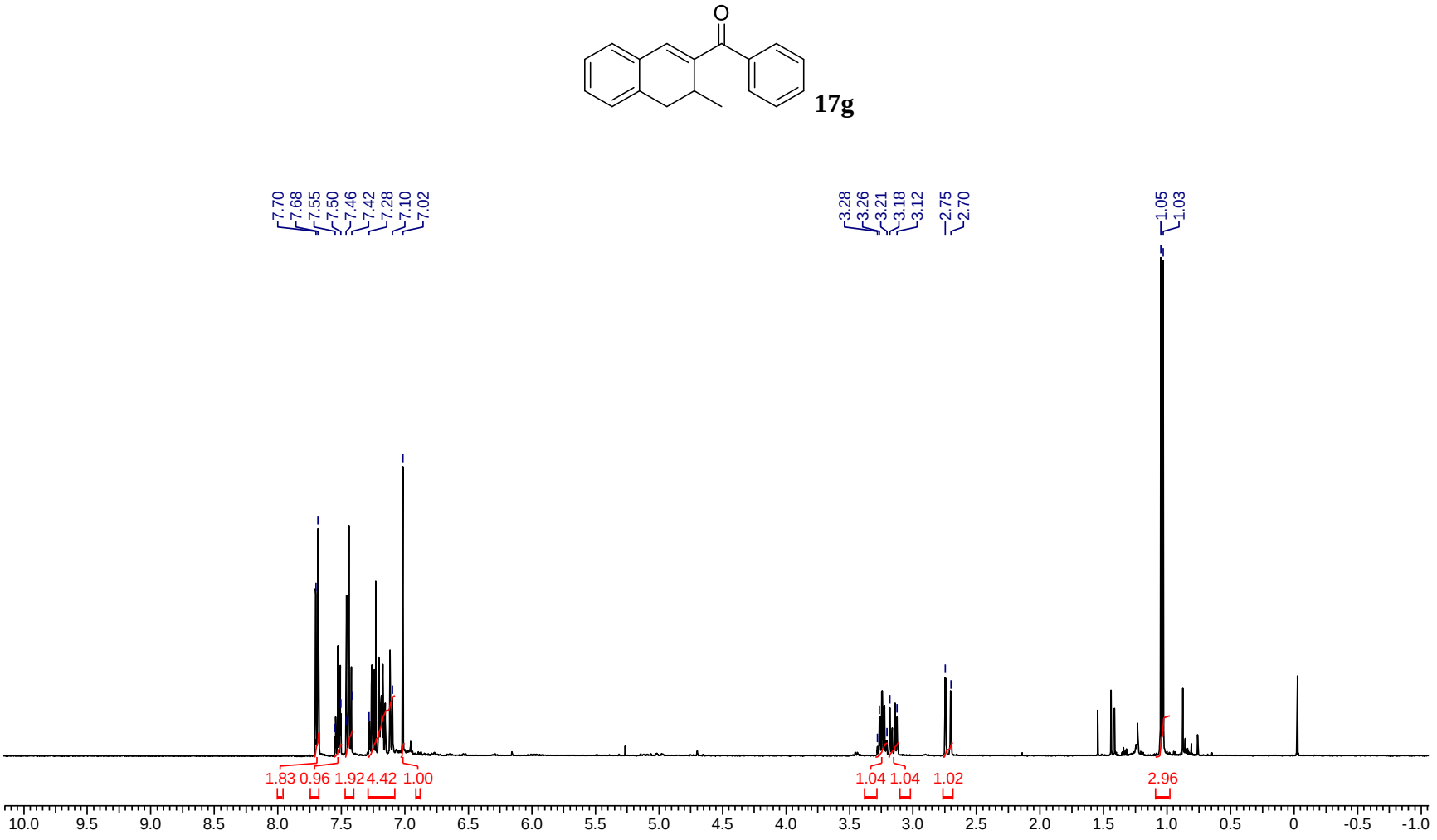
O
17g
7.70
7.68
7.55
7.50
7.46
7.42
7.28
7.10
7.02
3.28
3.26
3.21
3.18
3.12
2.75
2.70
1.05
1.03
1.83
0.96
1.92
4.42
1.00
1.04
1.04
1.02
2.96
10.0
9.5
9.0
8.5
8.0
7.5
7.0
6.5
6.0
5.5
5.0
4.5
4.0
3.5
3.0
2.5
2.0
1.5
1.0
0.5
0
-0.5
-1.0

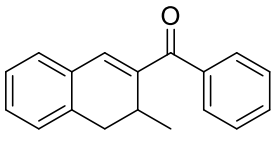
O

17g

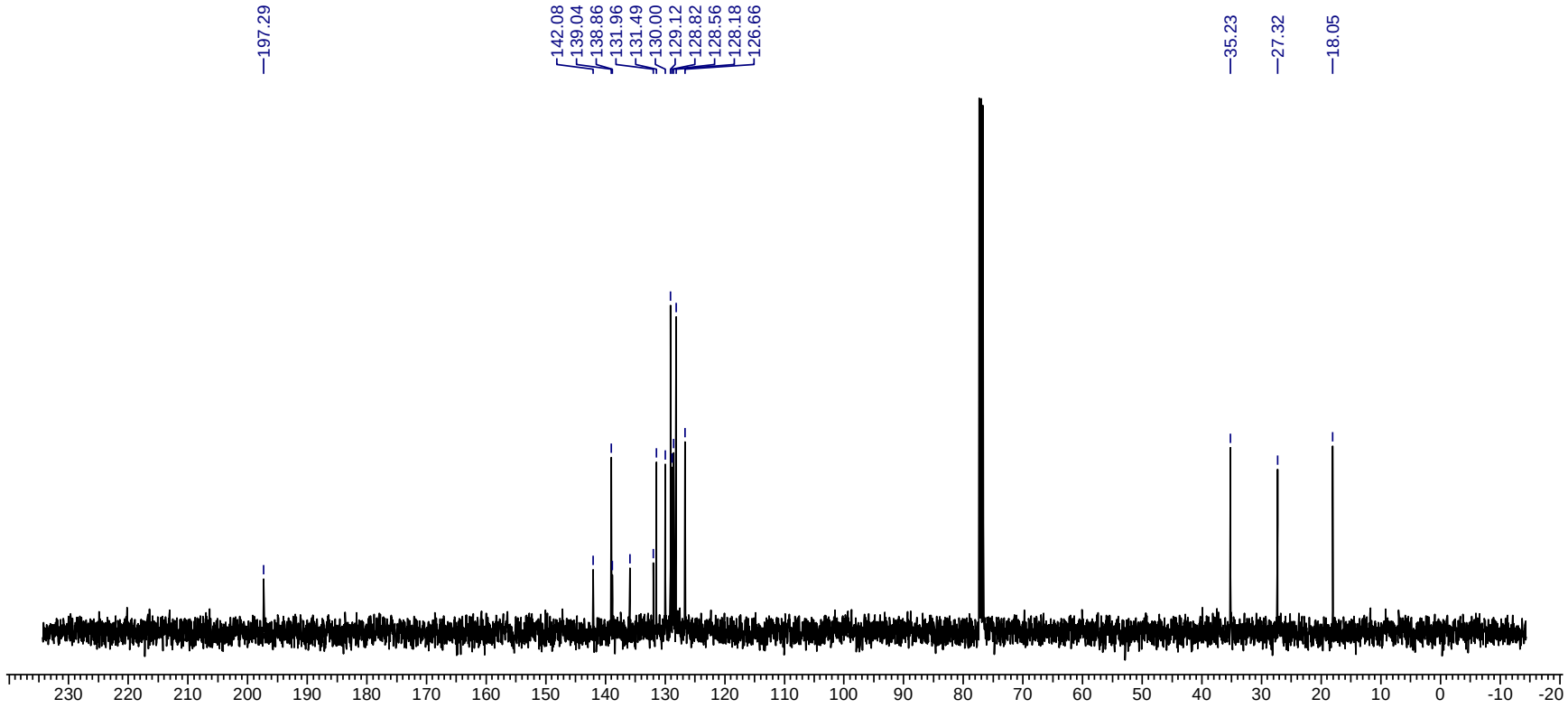
197.29
142.08
139.04
138.86
131.96
131.49
130.00
129.12
128.82
128.56
128.18
126.66
35.23
27.32
18.05
230
220
210
200
190
180
170
160
150
140
130
120
110
100
90
80
70
60
50
40
30
20
10
0
-10
-20

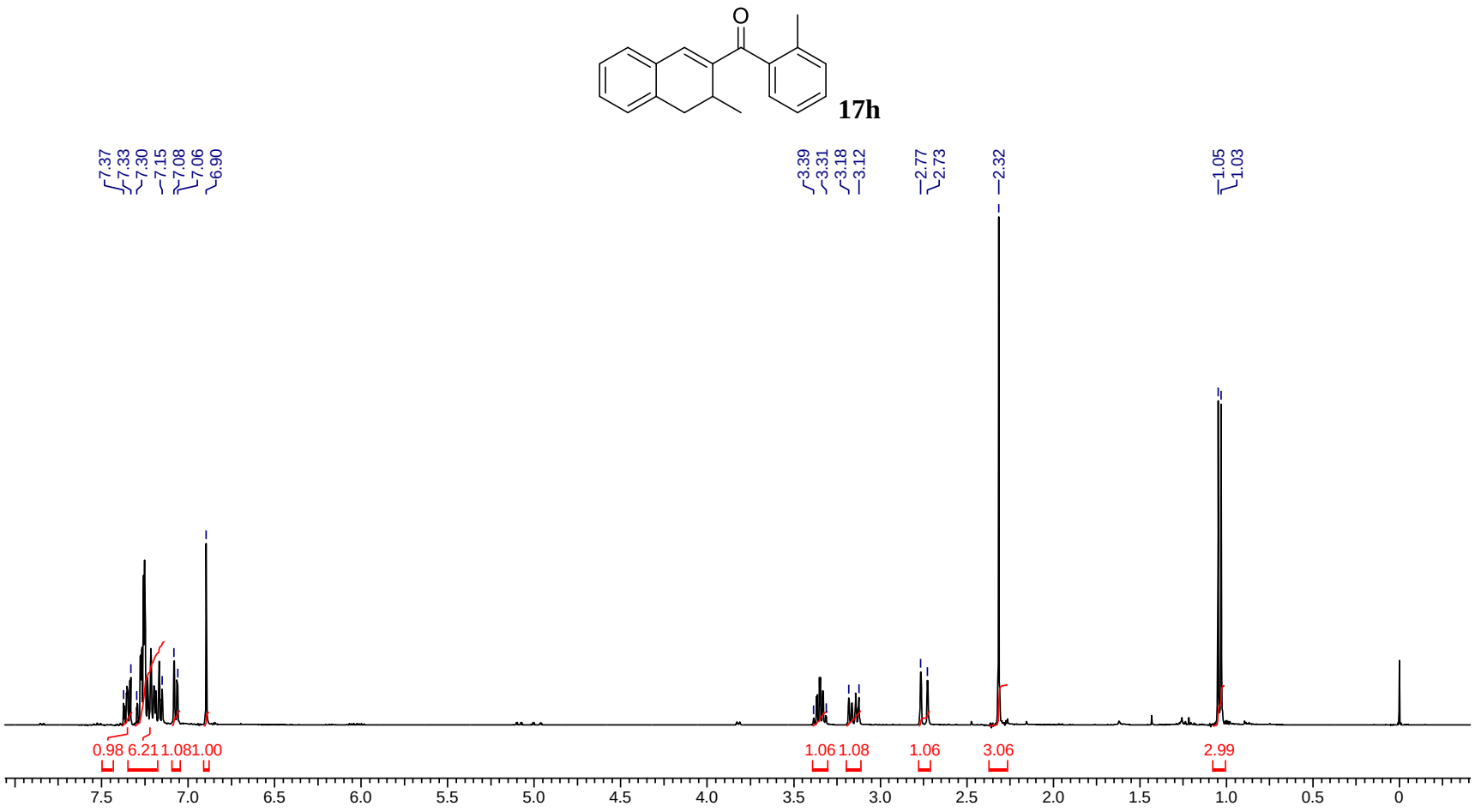
O
17h
7.37
7.33
7.30
7.15
7.08
7.06
6.90
3.39
3.31
3.18
3.12
2.77
2.73
2.32
1.05
1.03
0.98
6.21
1.08
1.00
1.06
1.08
1.06
3.06
2.99
7.5
7.0
6.5
6.0
5.5
5.0
4.5
4.0
3.5
3.0
2.5
2.0
1.5
1.0
0.5
0

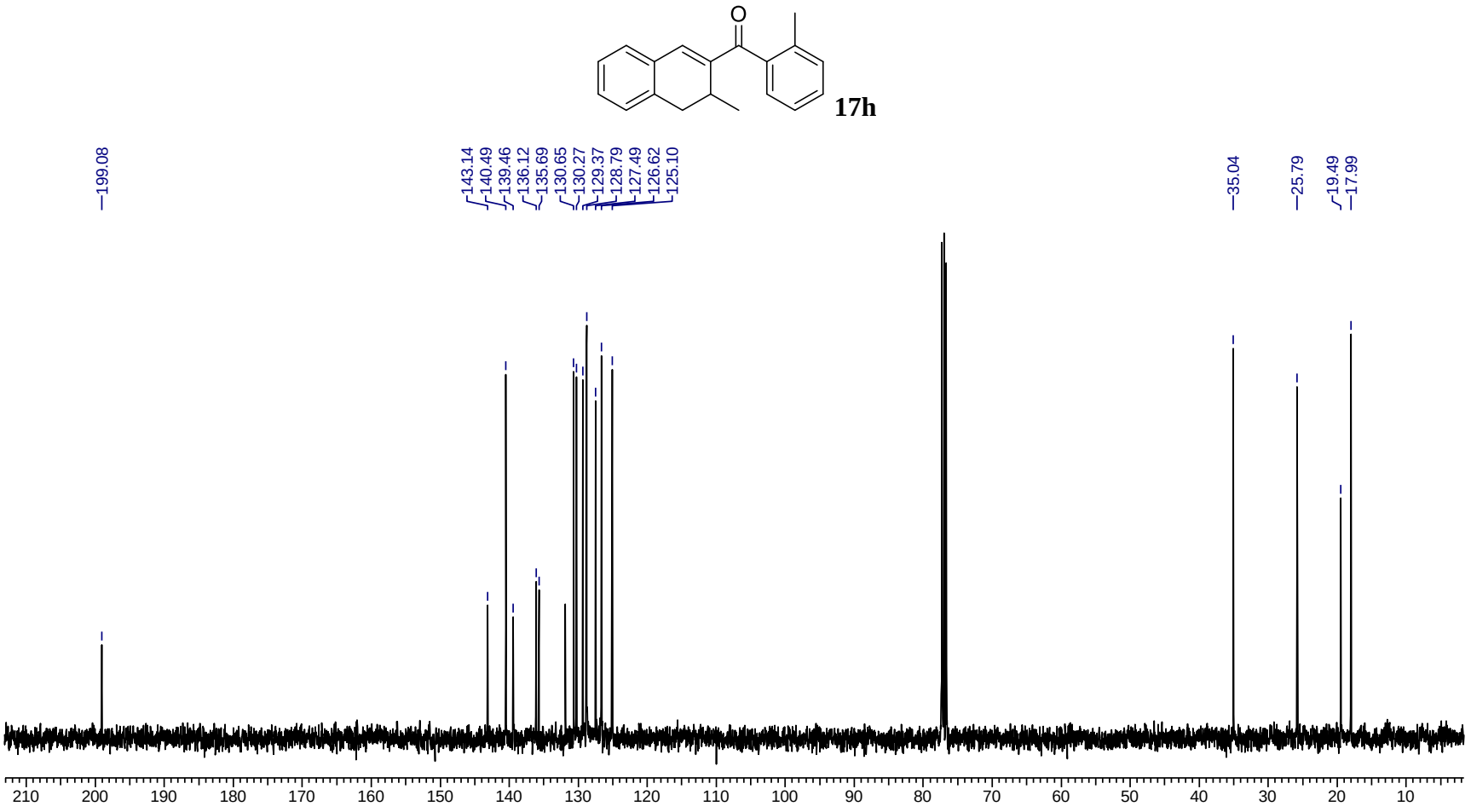
O
17h
199.08
143.14
140.49
139.46
136.12
135.69
130.65
130.27
129.37
128.79
127.49
126.62
125.10
35.04
25.79
19.49
17.99
210
200
190
180
170
160
150
140
130
120
110
100
90
80
70
60
50
40
30
20
10

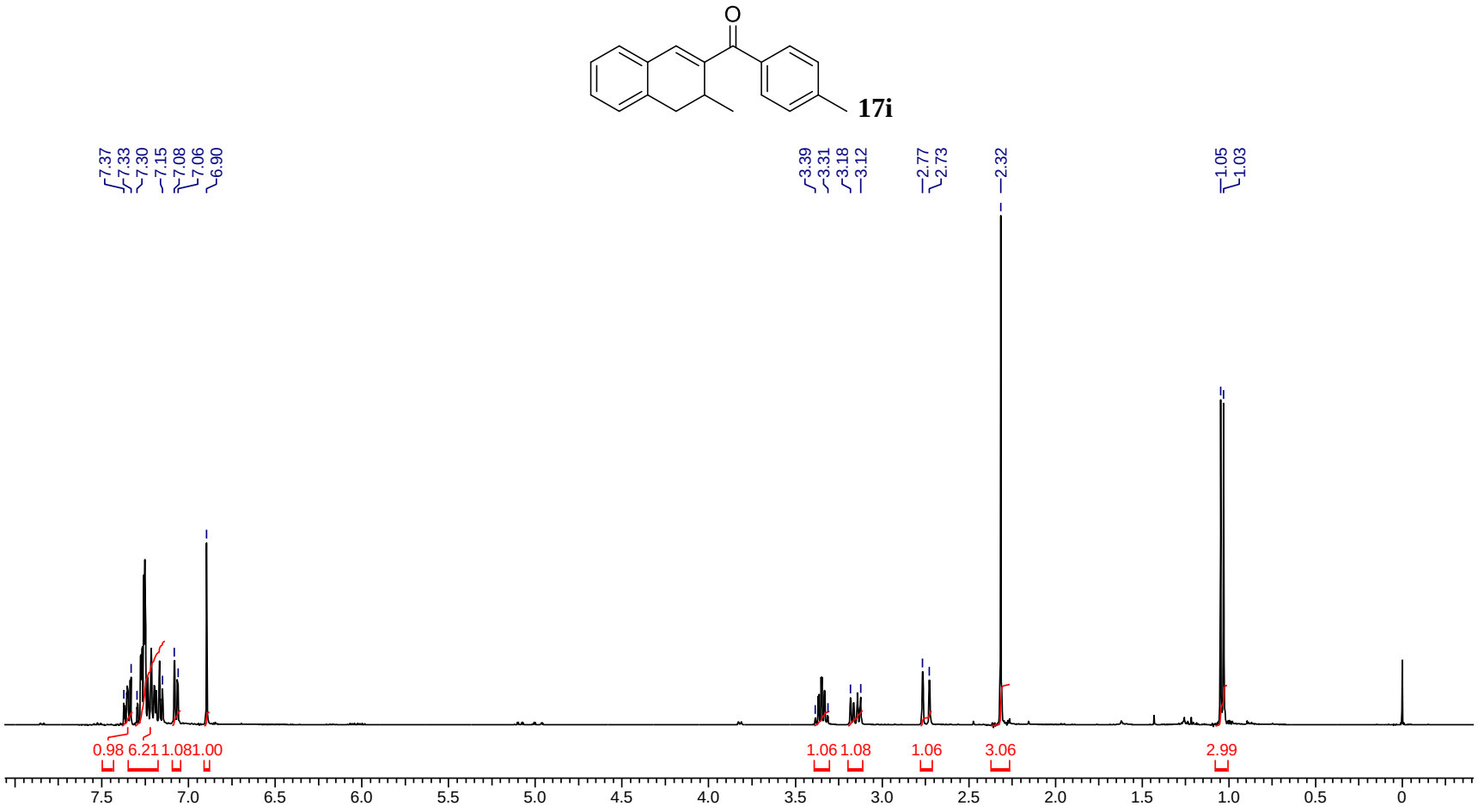
O
17i
7.37
7.33
7.30
7.15
7.08
7.06
6.90
3.39
3.31
3.18
3.12
2.77
2.73
2.32
1.05
1.03
0.98
6.21
1.08
1.00
1.06
1.08
1.06
3.06
2.99
7.5
7.0
6.5
6.0
5.5
5.0
4.5
4.0
3.5
3.0
2.5
2.0
1.5
1.0
0.5
0

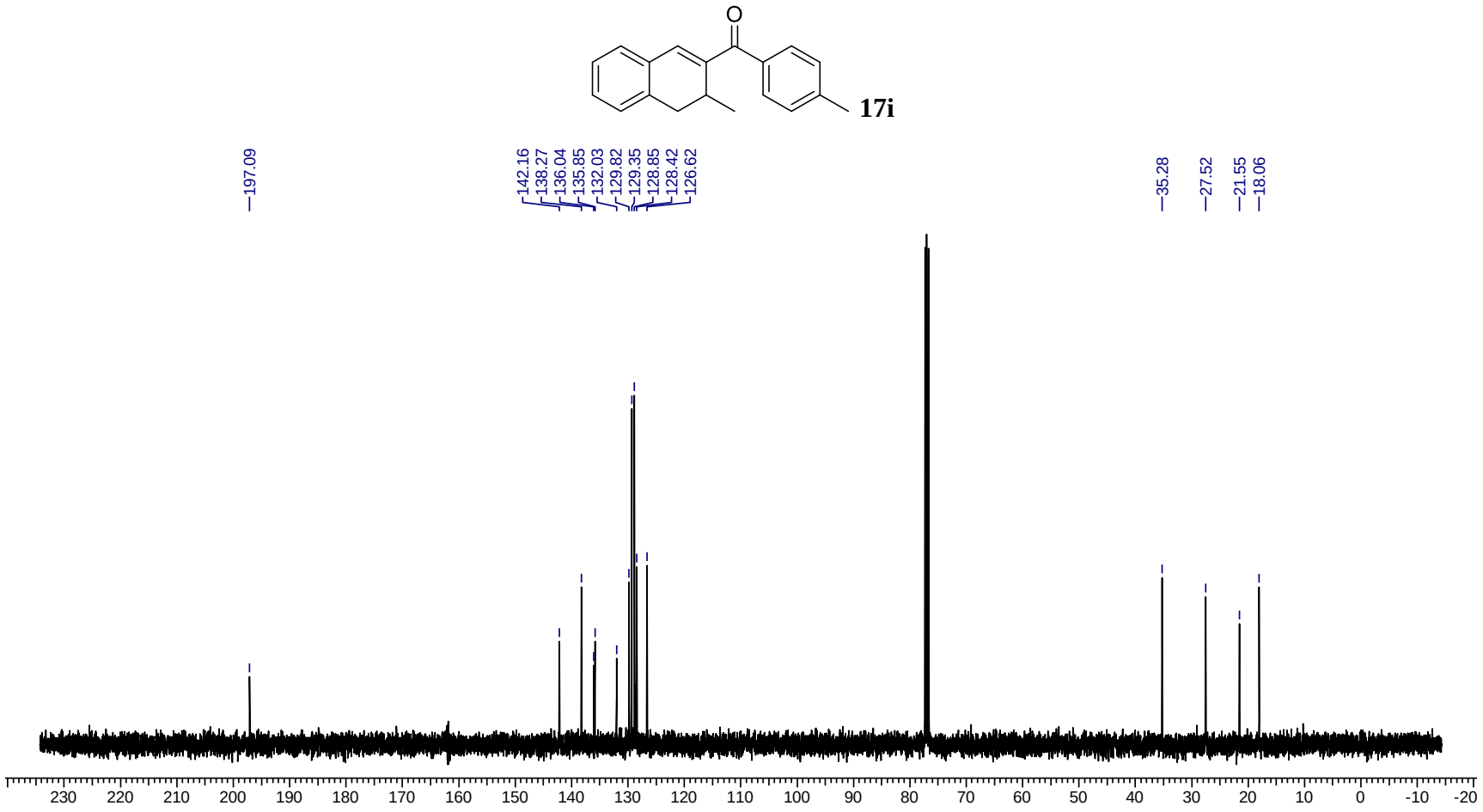
O
17i
197.09
142.16
138.27
136.04
135.85
132.03
129.82
129.35
128.85
128.42
126.62
35.28
27.52
21.55
18.06
230 220 210 200 190 180 170 160 150 140 130 120 110 100 90 80 70 60 50 40 30 20 10 0 -10 -20

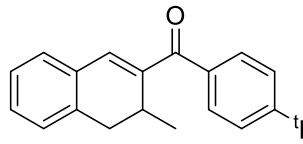
O
tBu

17j

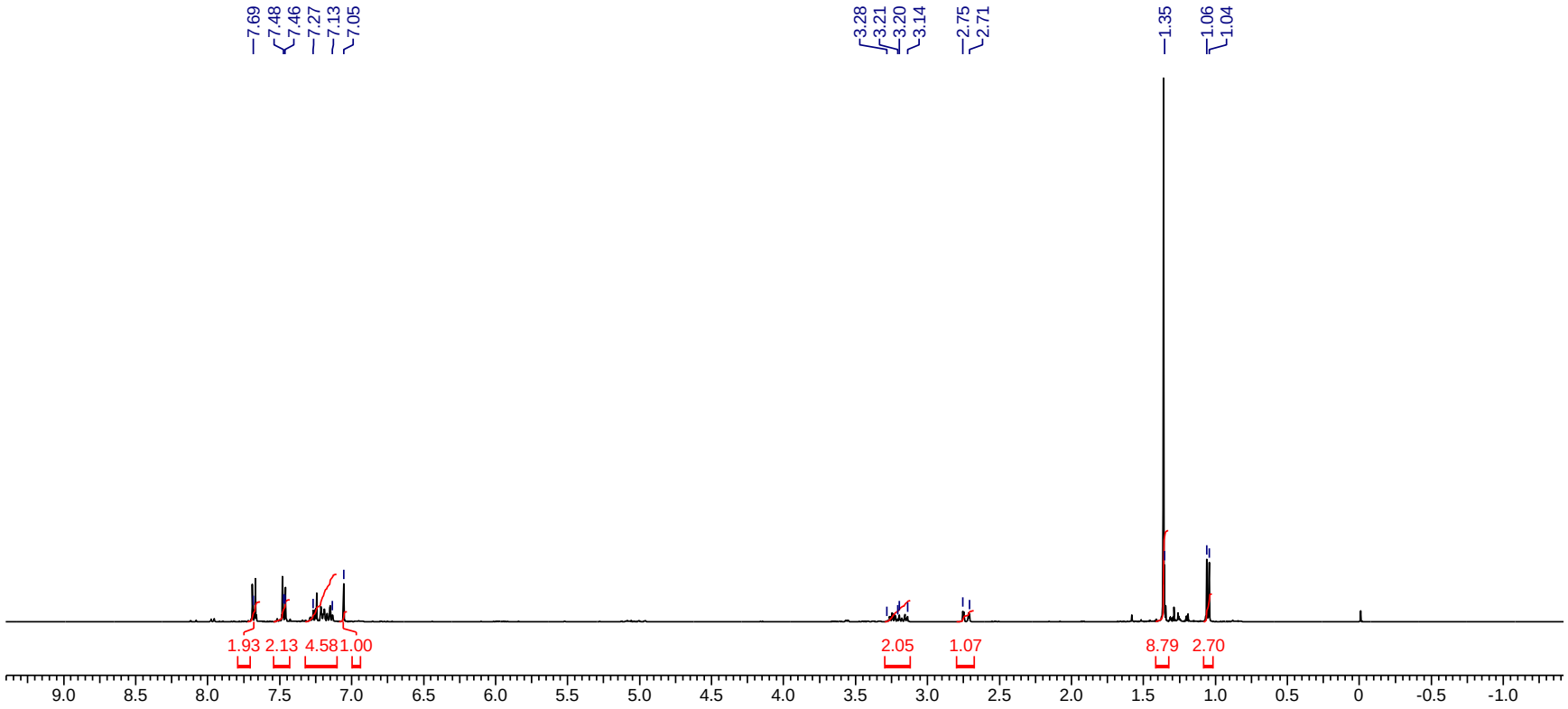
7.69
7.48
7.46
7.27
7.13
7.05
3.28
3.21
3.20
3.14
2.75
2.71
1.35
1.06
1.04
1.93
2.13
4.58
1.00
2.05
1.07
8.79
2.70
9.0
8.5
8.0
7.5
7.0
6.5
6.0
5.5
5.0
4.5
4.0
3.5
3.0
2.5
2.0
1.5
1.0
0.5
0
-0.5
-1.0

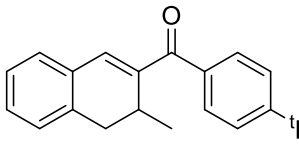
O
tBu

17j

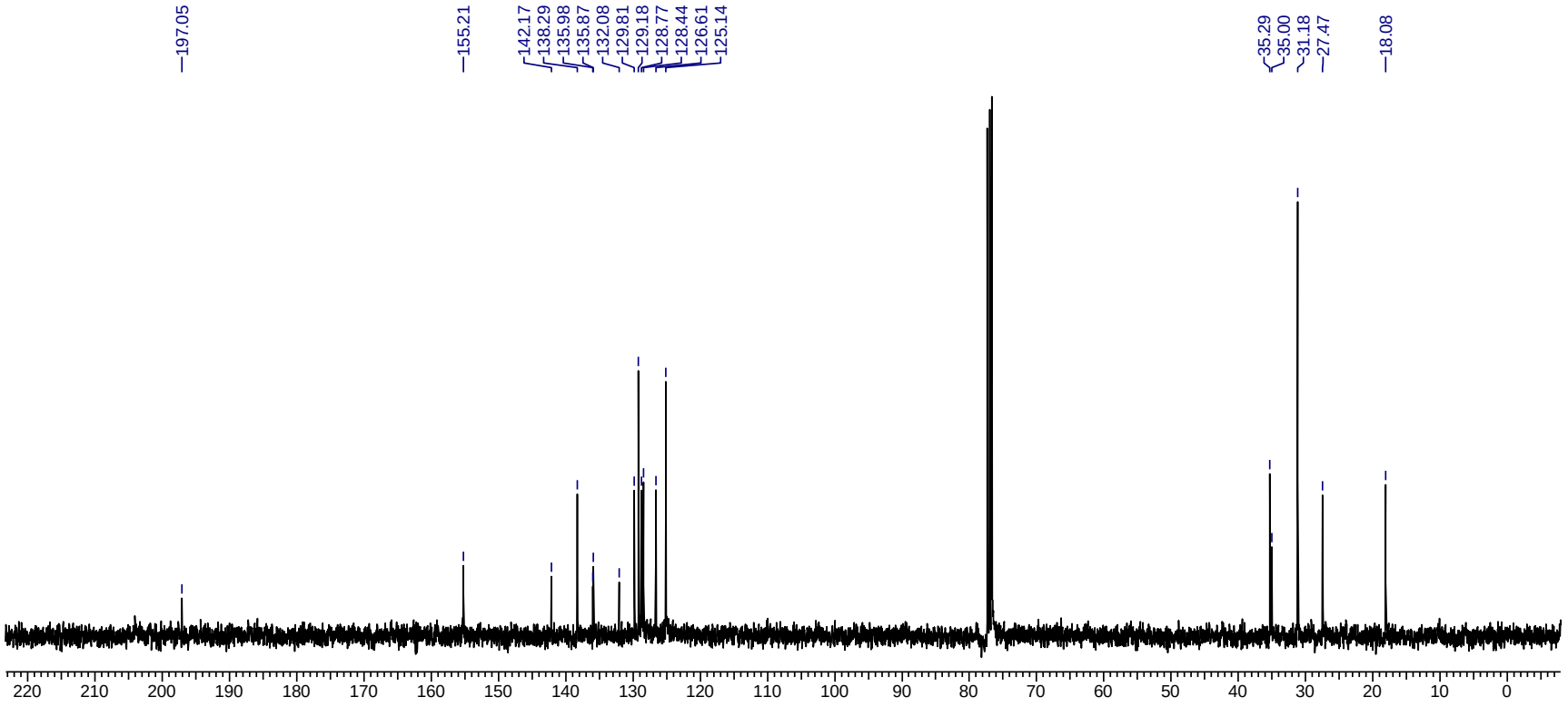
197.05
155.21
142.17
138.29
135.98
135.87
132.08
129.81
129.18
128.77
128.44
126.61
125.14
35.29
35.00
31.18
27.47
18.08
220
210
200
190
180
170
160
150
140
130
120
110
100
90
80
70
60
50
40
30
20
10
0

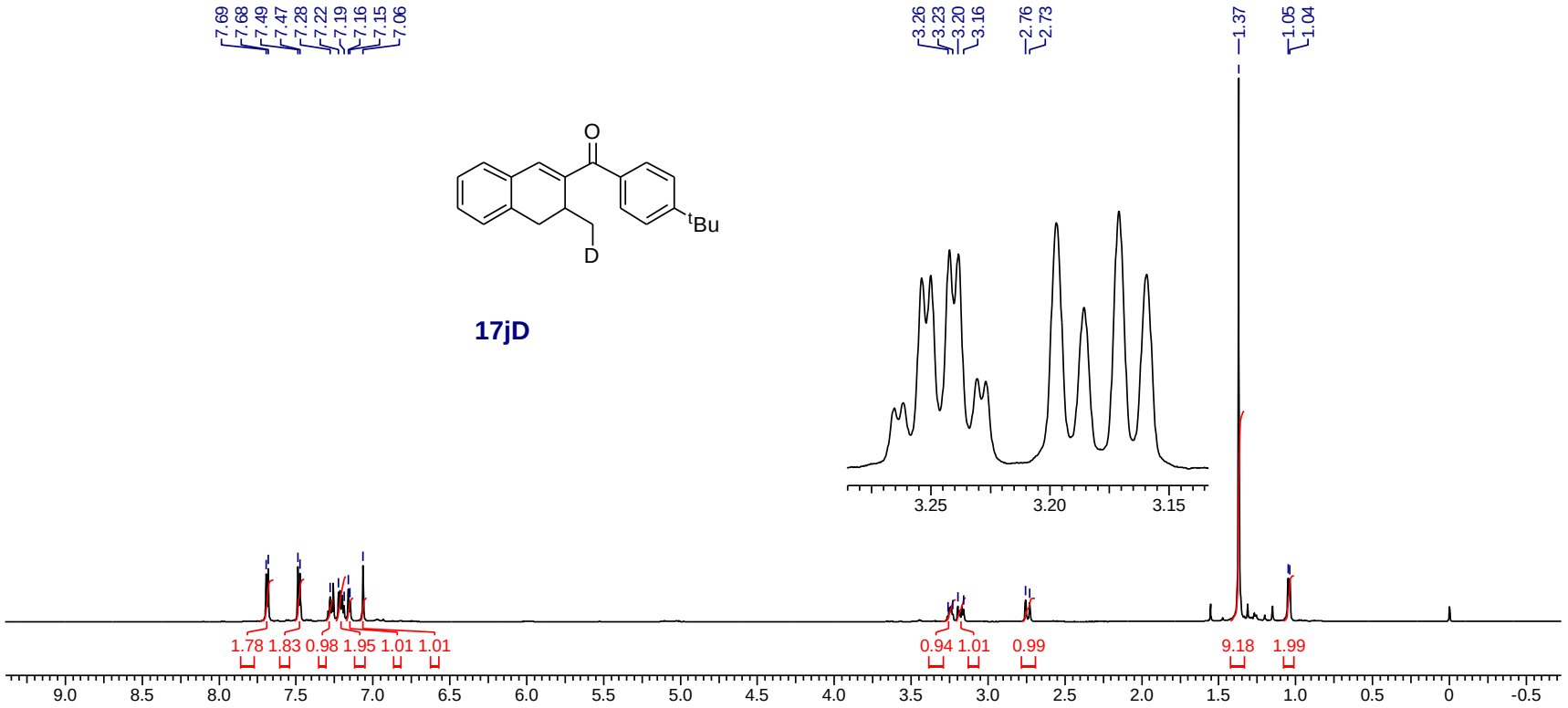
7.69
7.68
7.49
7.47
7.28
7.22
7.19
7.16
7.15
7.06
3.26
3.23
3.20
3.16
2.76
2.73
1.37
1.05
1.04
O
tBu
D
17jD
3.25
3.20
3.15
1.78 1.83 0.98 1.95 1.01 1.01
0.94 1.01 0.99
9.18 1.99
9.0 8.5 8.0 7.5 7.0 6.5 6.0 5.5 5.0 4.5 4.0 3.5 3.0 2.5 2.0 1.5 1.0 0.5 0 -0.5

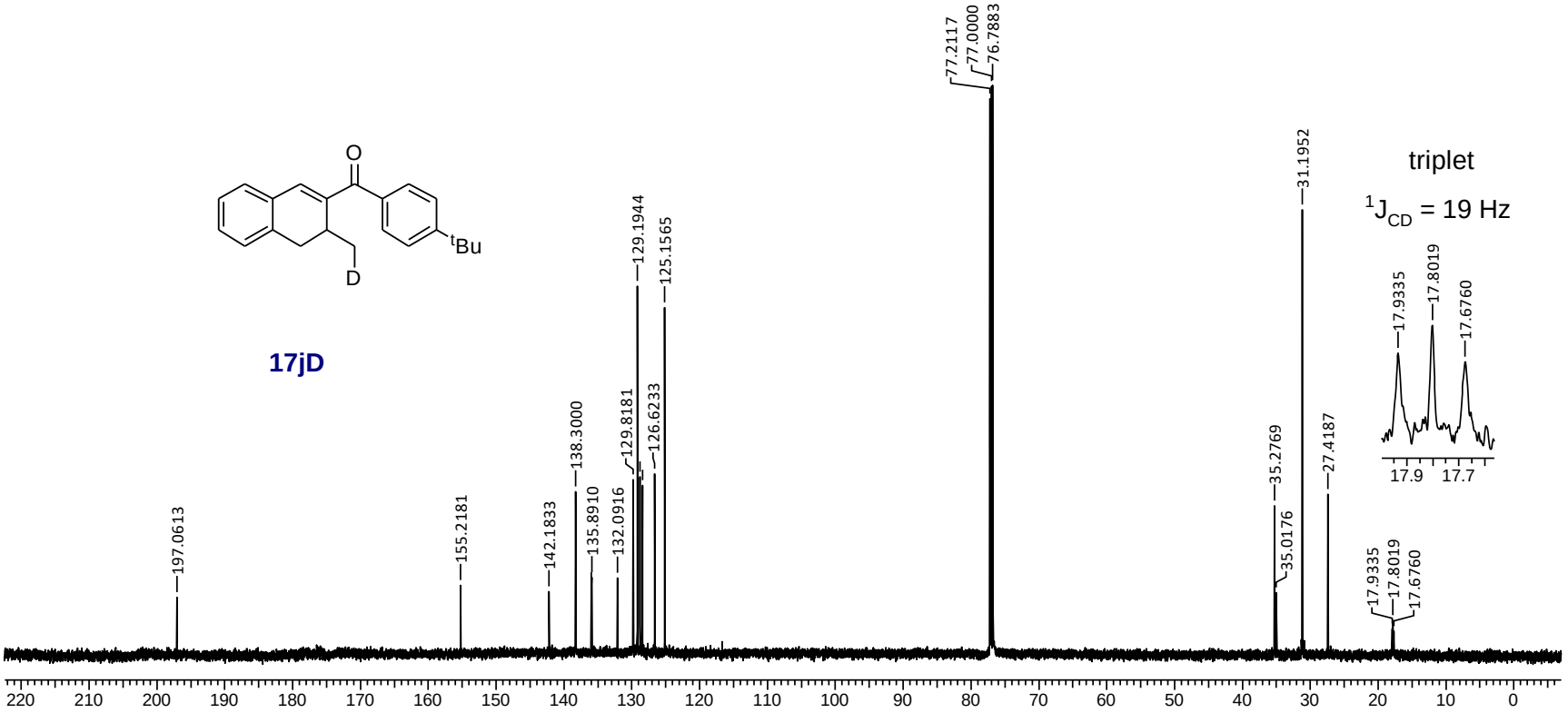
O
tBu
D
17jD
triplet
1JCD = 19 Hz
77.2117
77.0000
76.7883
31.1952
129.1944
125.1565
138.3000
129.8181
126.6233
197.0613
155.2181
142.1833
135.8910
132.0916
35.2769
35.0176
27.4187
17.9335
17.8019
17.6760
17.9
17.7
220
210
200
190
180
170
160
150
140
130
120
110
100
90
80
70
60
50
40
30
20
10
0

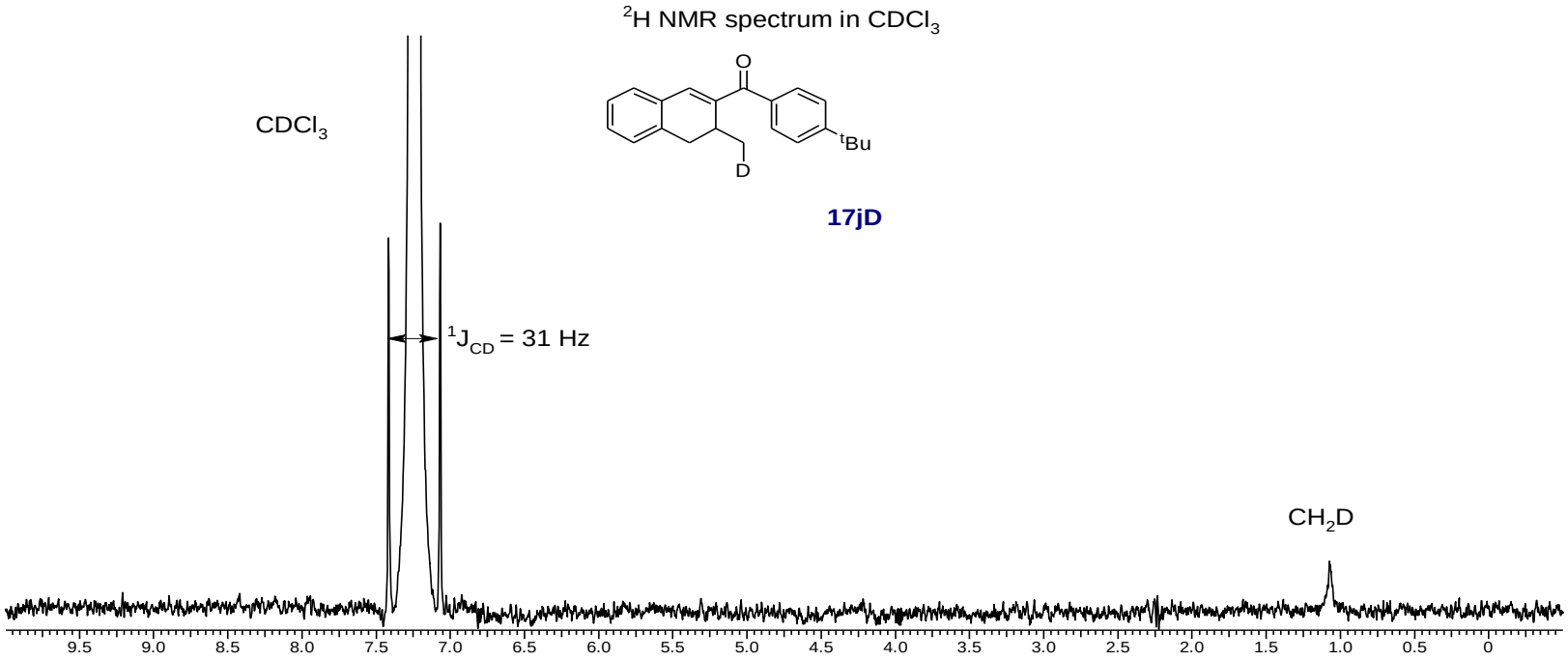
^{2}H NMR spectrum in $CDCl_3$
O
^{t}Bu
D
17jD
$CDCl_3$
$^1J_{CD}$ = 31 Hz
CH_2D
9.5
9.0
8.5
8.0
7.5
7.0
6.5
6.0
5.5
5.0
4.5
4.0
3.5
3.0
2.5
2.0
1.5
1.0
0.5
0

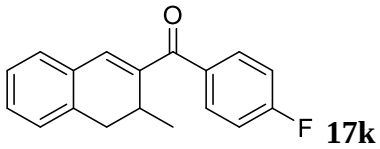
O
F

17k

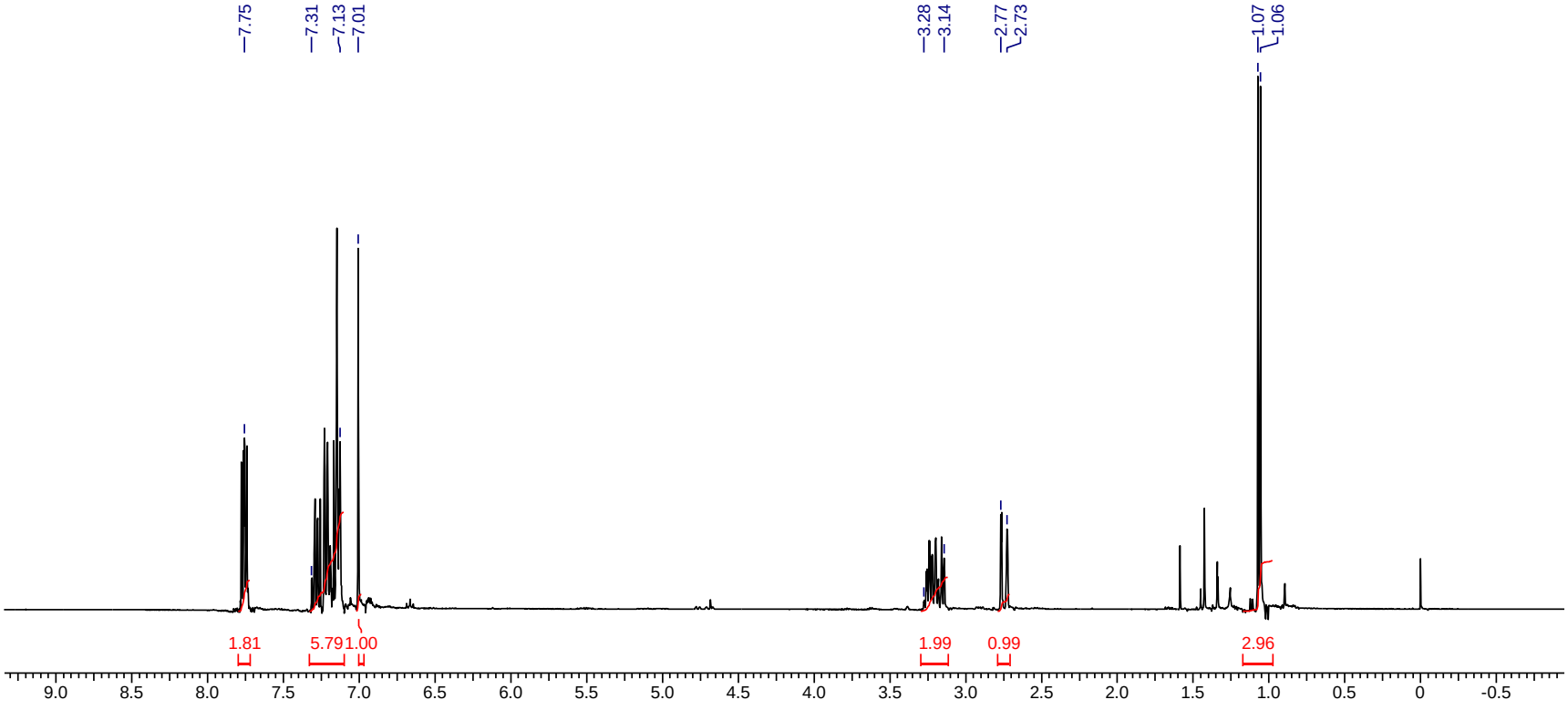
7.75
7.31
7.13
7.01
3.28
3.14
2.77
2.73
1.07
1.06
1.81
5.79
1.00
1.99
0.99
2.96
9.0
8.5
8.0
7.5
7.0
6.5
6.0
5.5
5.0
4.5
4.0
3.5
3.0
2.5
2.0
1.5
1.0
0.5
0
-0.5

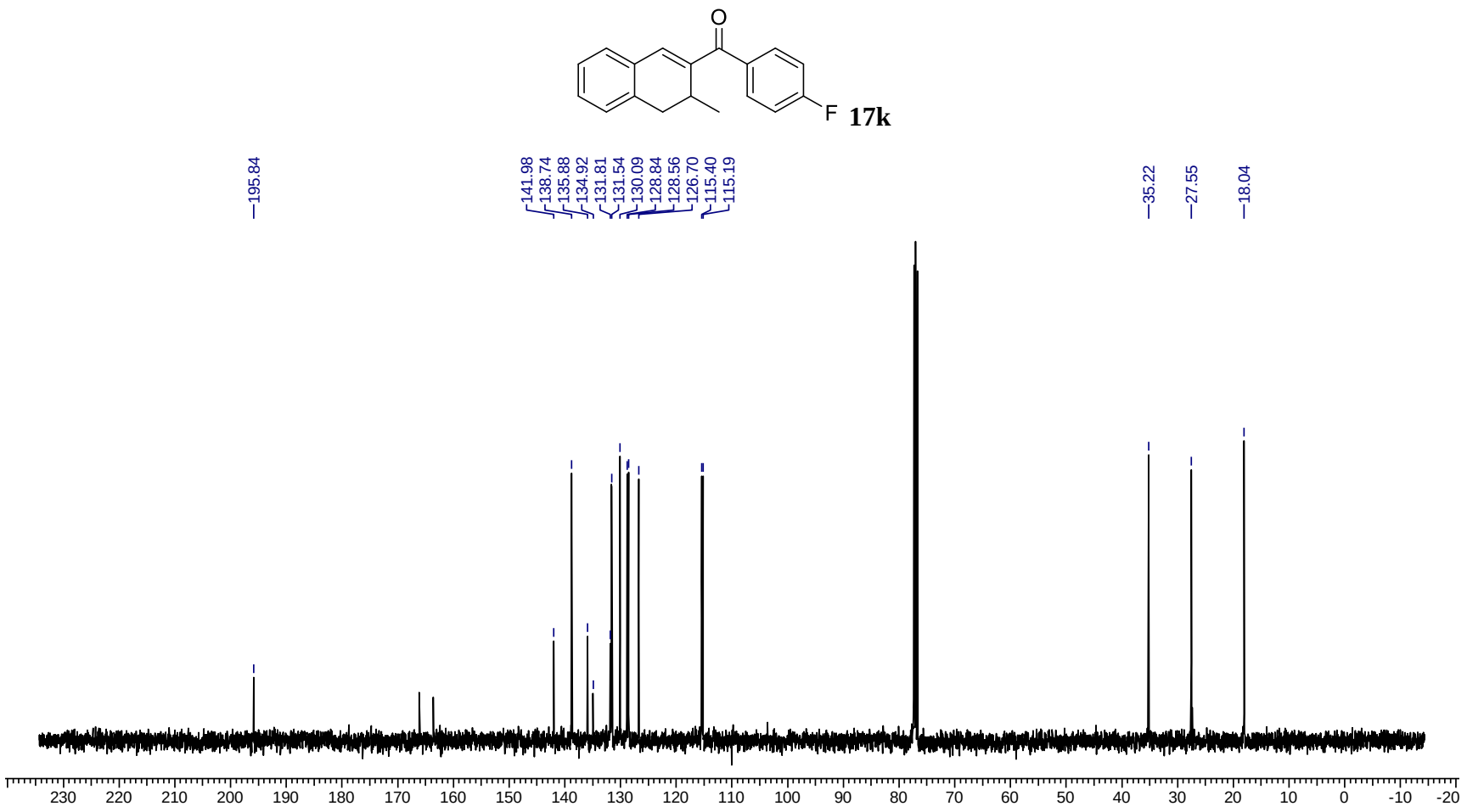
O
F
17k
195.84
141.98
138.74
135.88
134.92
131.81
131.54
130.09
128.84
128.56
126.70
115.40
115.19
35.22
27.55
18.04
230 220 210 200 190 180 170 160 150 140 130 120 110 100 90 80 70 60 50 40 30 20 10 0 -10 -20

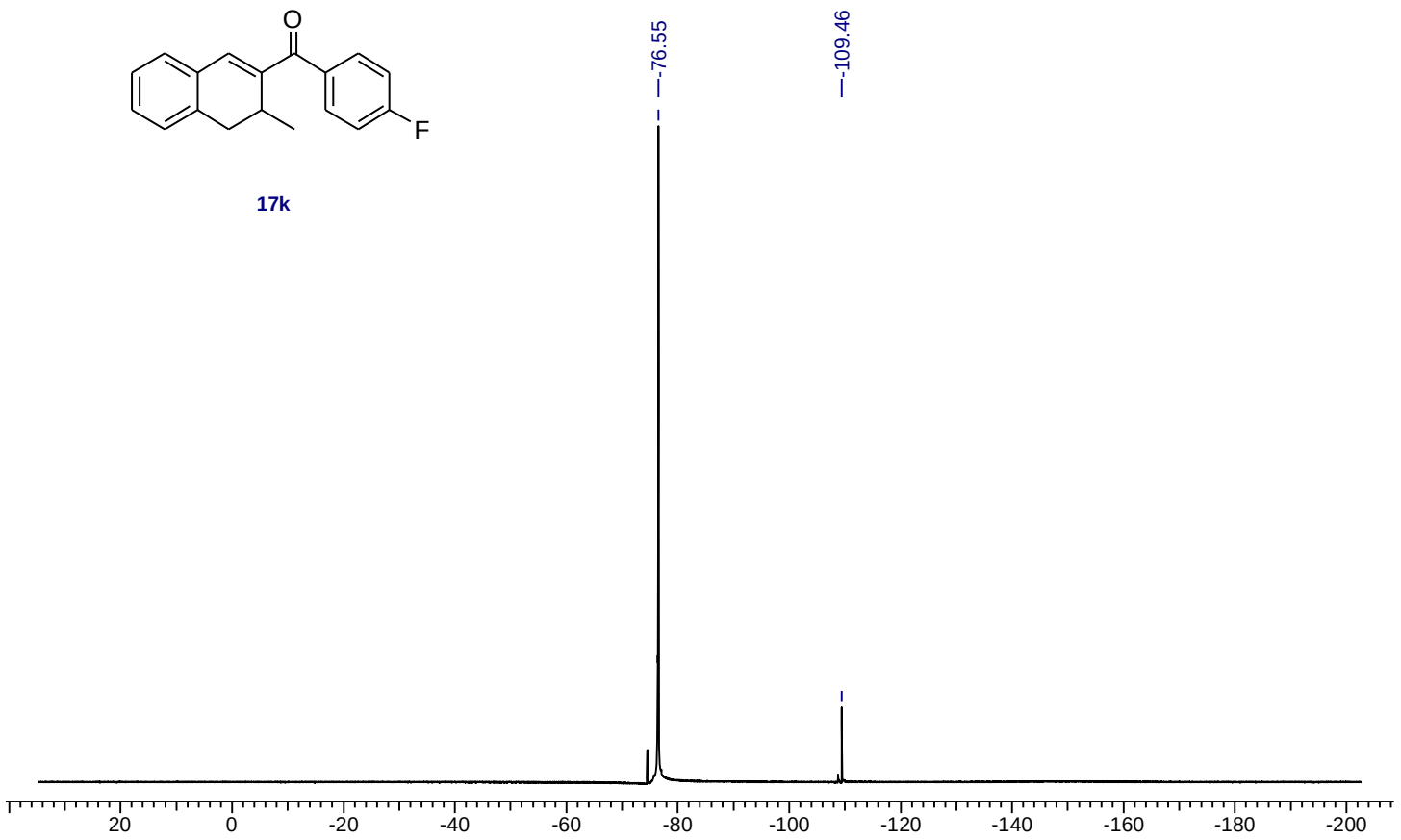
O
F
17k
-76.55
-109.46
20
0
-20
-40
-60
-80
-100
-120
-140
-160
-180
-200

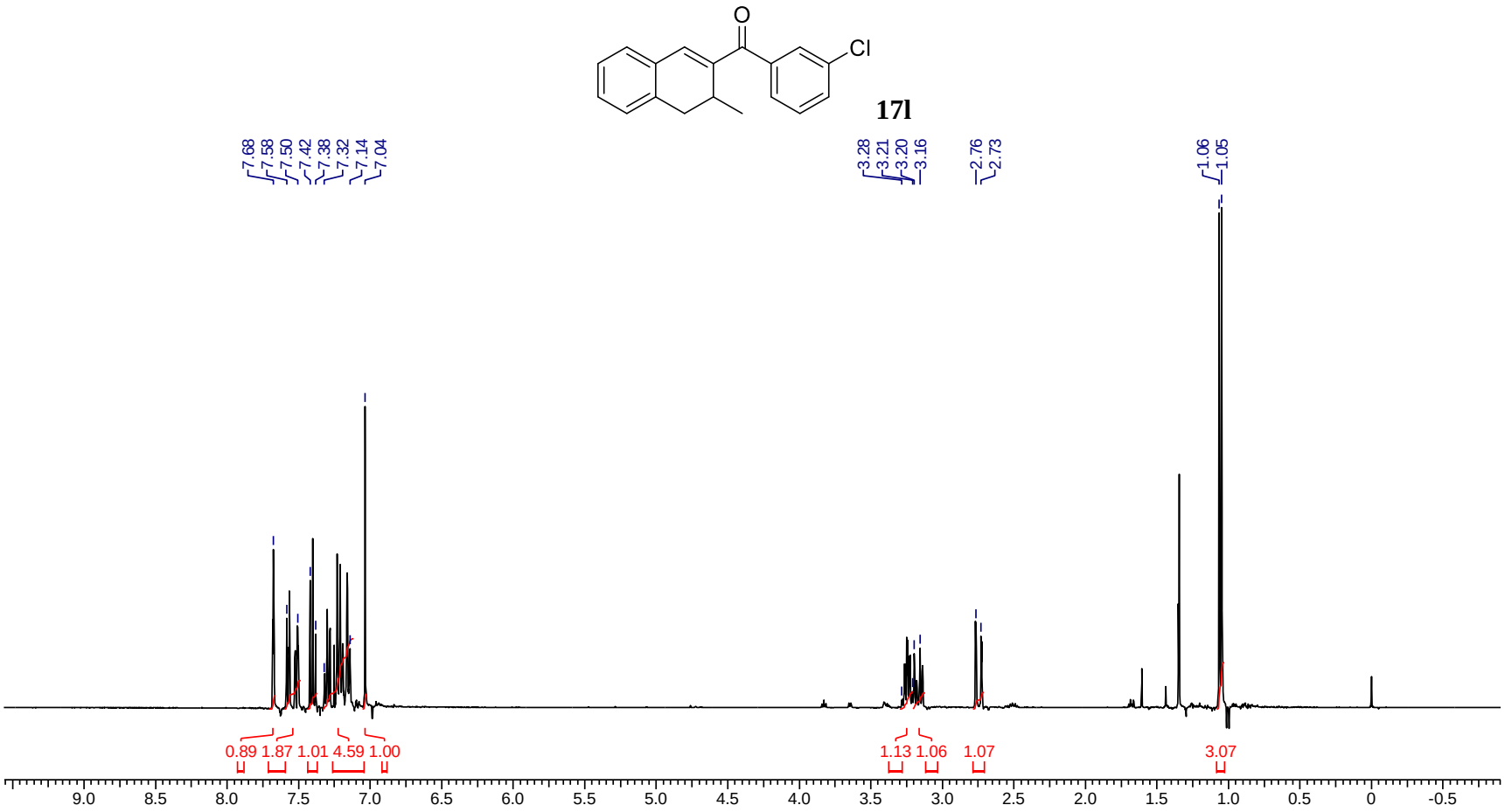
O
Cl
17l
7.68
7.58
7.50
7.42
7.38
7.32
7.14
7.04
3.28
3.21
3.20
3.16
2.76
2.73
1.06
1.05
0.89
1.87
1.01
4.59
1.00
1.13
1.06
1.07
3.07
9.0
8.5
8.0
7.5
7.0
6.5
6.0
5.5
5.0
4.5
4.0
3.5
3.0
2.5
2.0
1.5
1.0
0.5
0
-0.5

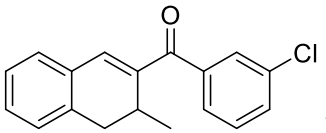
O
Cl

17l

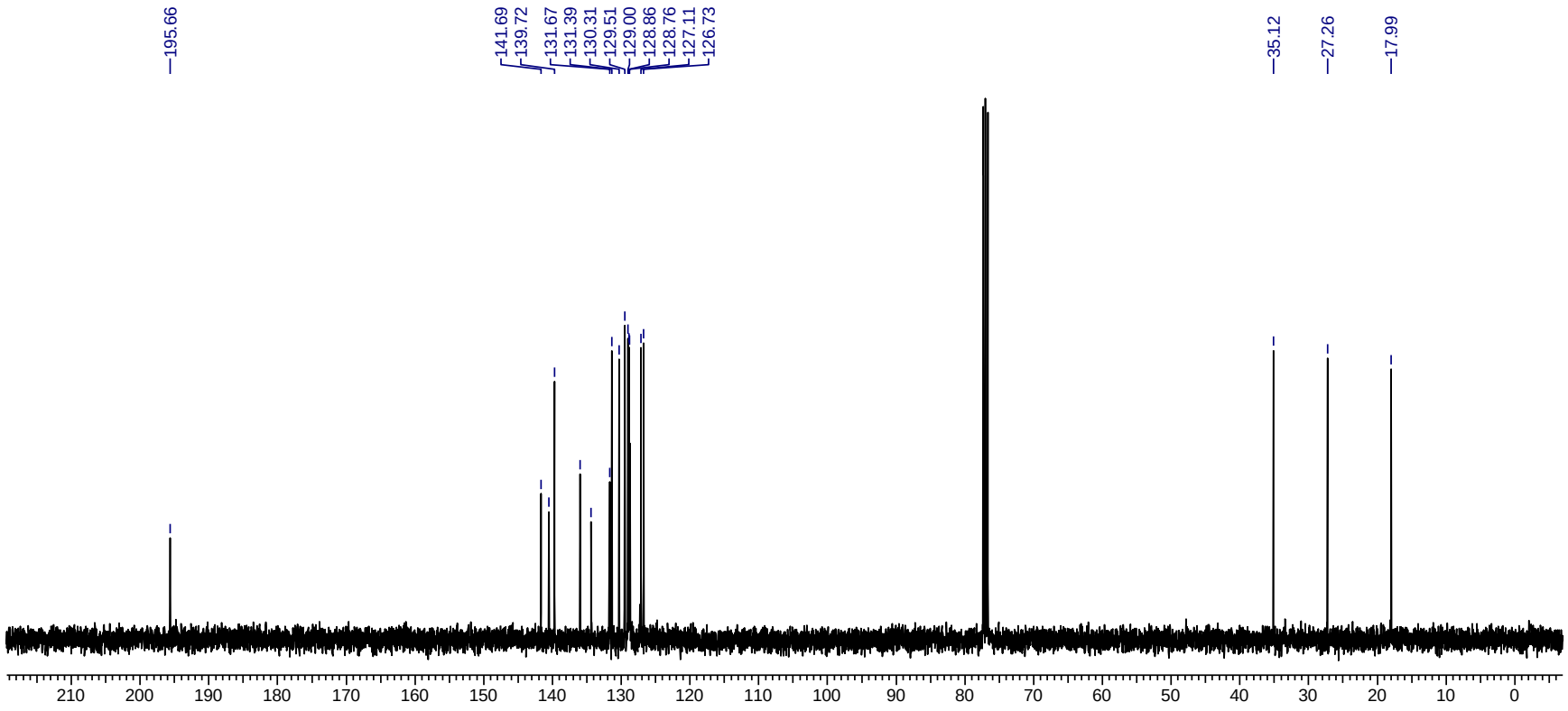
195.66
141.69
139.72
131.67
131.39
130.31
129.51
129.00
128.86
128.76
127.11
126.73
35.12
27.26
17.99
210
200
190
180
170
160
150
140
130
120
110
100
90
80
70
60
50
40
30
20
10
0

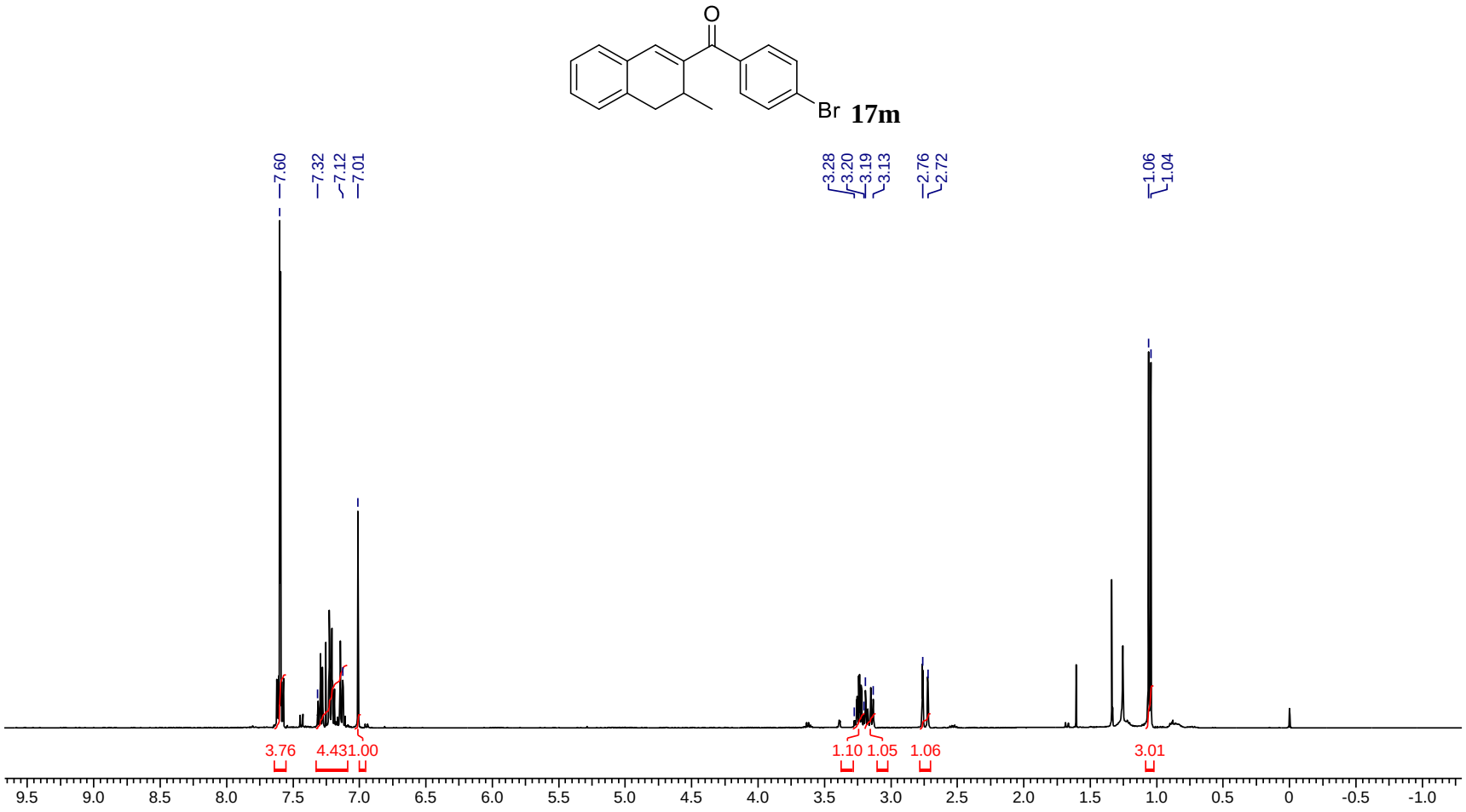
O
Br
17m
7.60
7.32
7.12
7.01
3.28
3.20
3.19
3.13
2.76
2.72
1.06
1.04
3.76
4.43
1.00
1.10
1.05
1.06
3.01
9.5
9.0
8.5
8.0
7.5
7.0
6.5
6.0
5.5
5.0
4.5
4.0
3.5
3.0
2.5
2.0
1.5
1.0
0.5
0
-0.5
-1.0

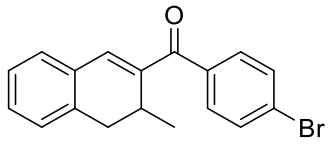
O
Br

17m

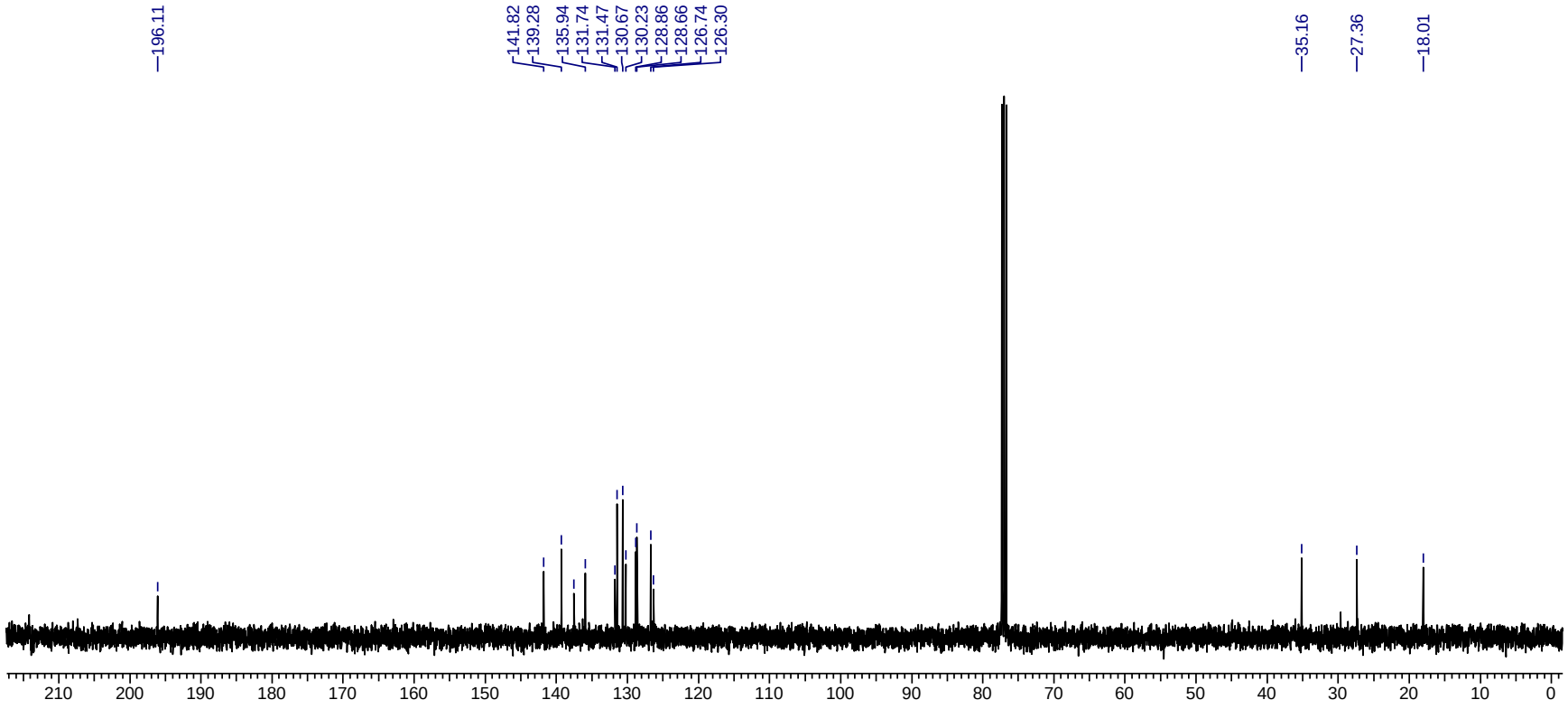
196.11
141.82
139.28
135.94
131.74
131.47
130.67
130.23
128.86
128.66
126.74
126.30
35.16
27.36
18.01
210
200
190
180
170
160
150
140
130
120
110
100
90
80
70
60
50
40
30
20
10
0

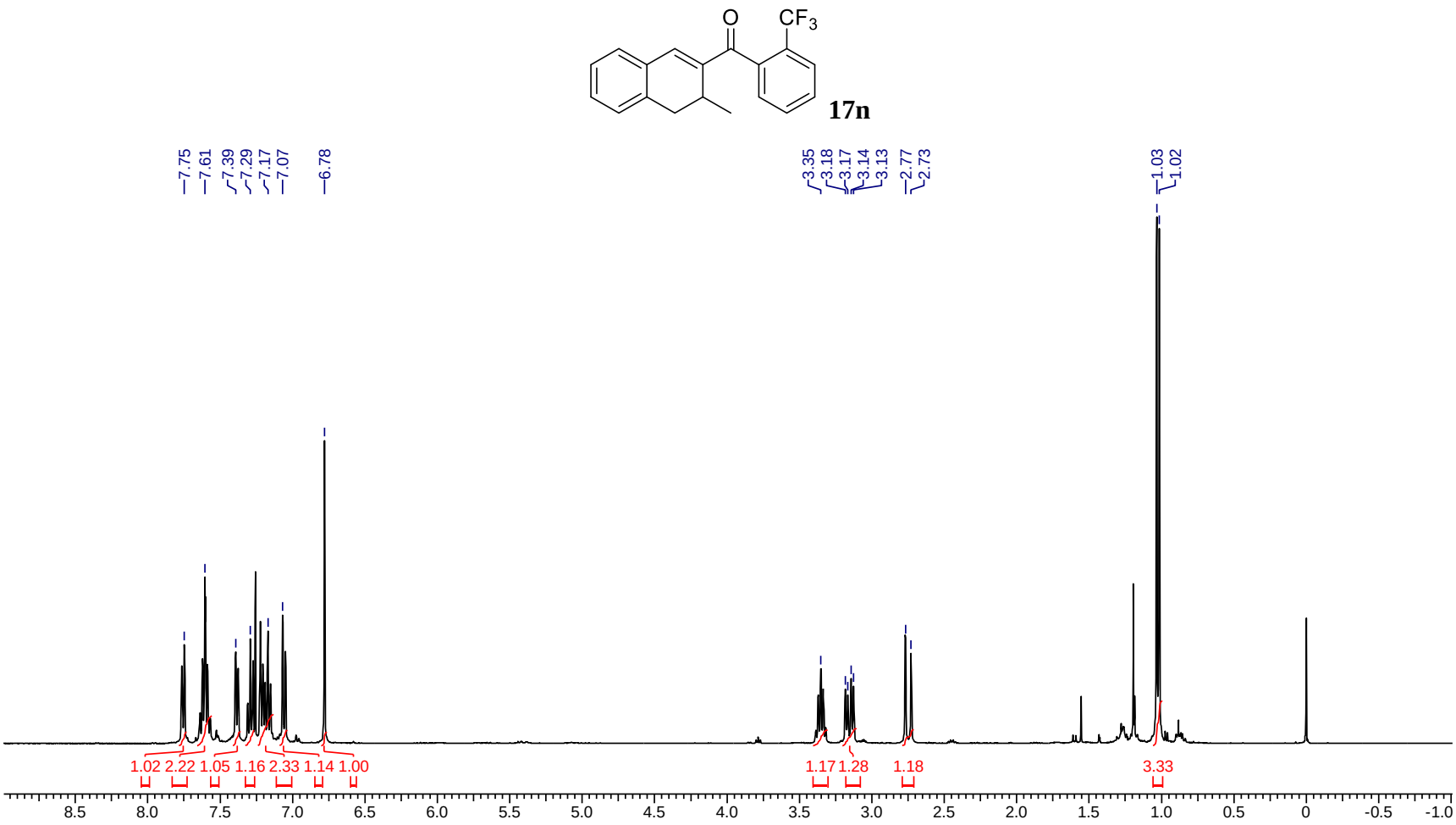
O
CF3
17n
7.75
7.61
7.39
7.29
7.17
7.07
6.78
3.35
3.18
3.17
3.14
3.13
2.77
2.73
1.03
1.02
1.02 2.22 1.05 1.16 2.33 1.14 1.00
1.17 1.28
1.18
3.33
8.5 8.0 7.5 7.0 6.5 6.0 5.5 5.0 4.5 4.0 3.5 3.0 2.5 2.0 1.5 1.0 0.5 0 -0.5 -1.0

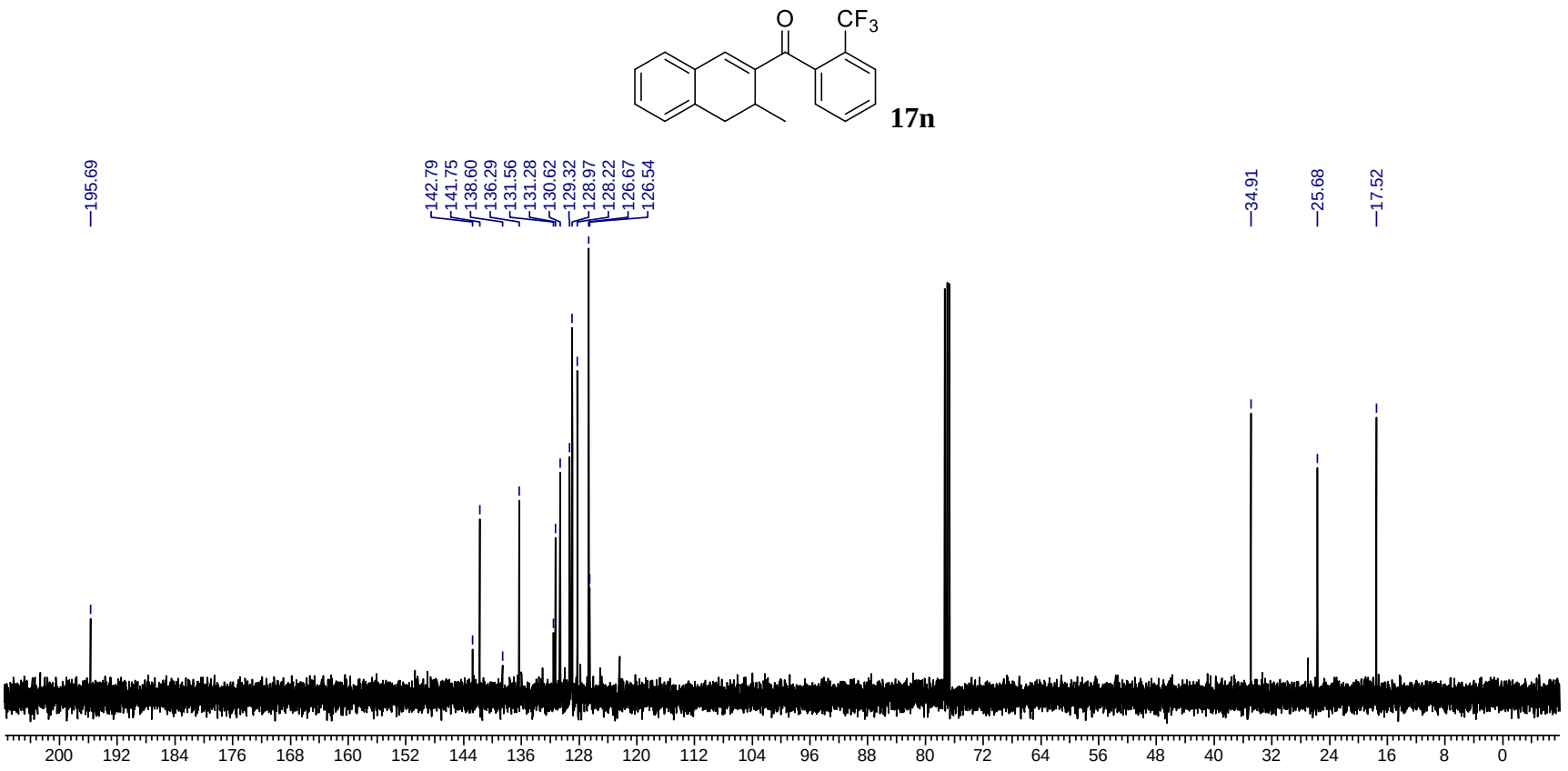
O
CF3
17n
195.69
142.79
141.75
138.60
136.29
131.56
131.28
130.62
129.32
128.97
128.22
126.67
126.54
34.91
25.68
17.52
200
192
184
176
168
160
152
144
136
128
120
112
104
96
88
80
72
64
56
48
40
32
24
16
8
0

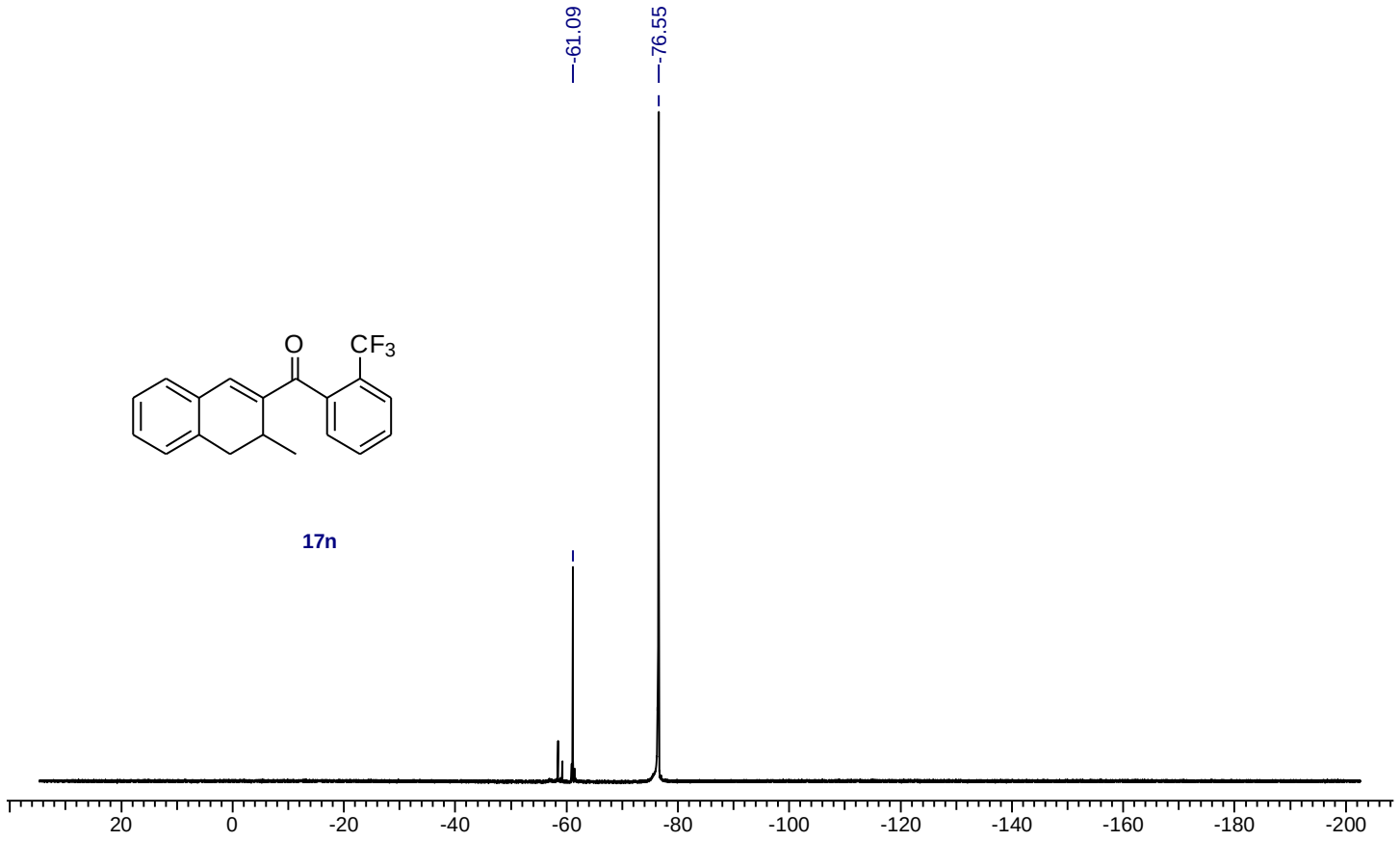
-61.09
-76.55
O
CF3
17n
20
0
-20
-40
-60
-80
-100
-120
-140
-160
-180
-200

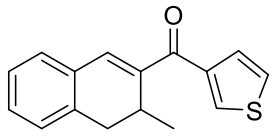
O
S

17o

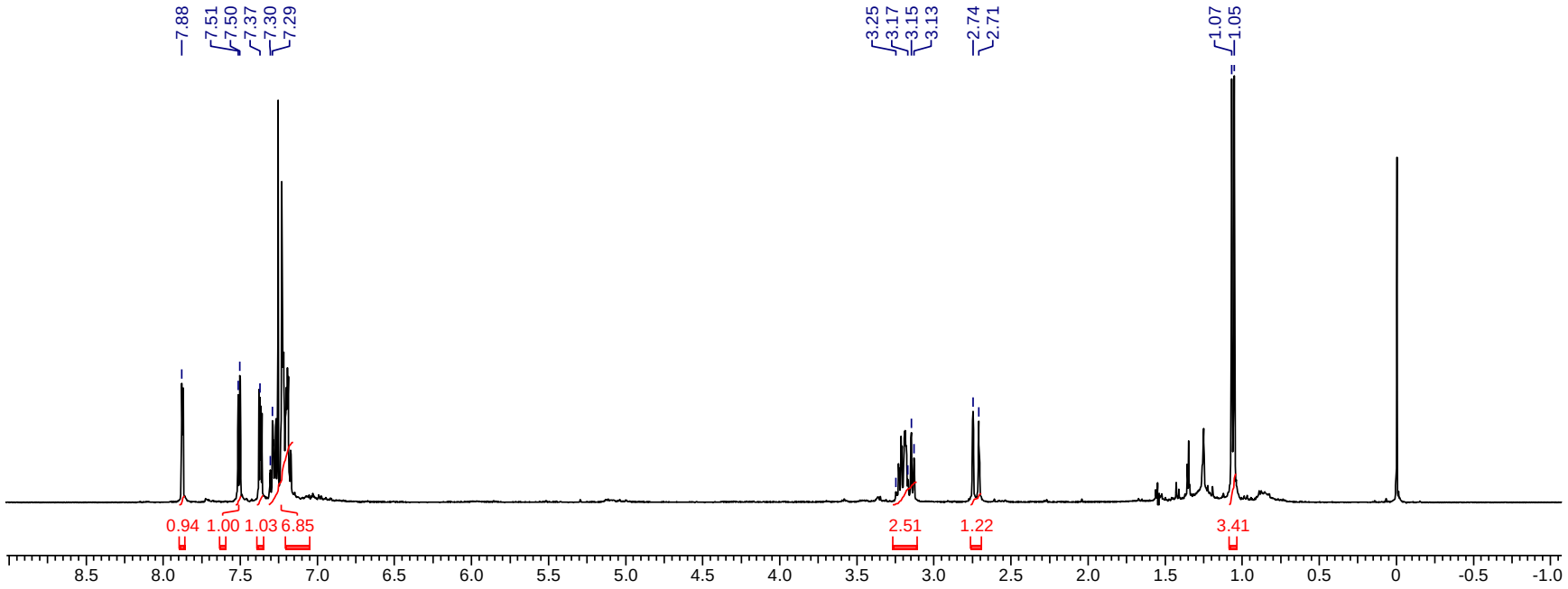
7.88
7.51
7.50
7.37
7.30
7.29
3.25
3.17
3.15
3.13
2.74
2.71
1.07
1.05
0.94
1.00
1.03
6.85
2.51
1.22
3.41
8.5
8.0
7.5
7.0
6.5
6.0
5.5
5.0
4.5
4.0
3.5
3.0
2.5
2.0
1.5
1.0
0.5
0
-0.5
-1.0

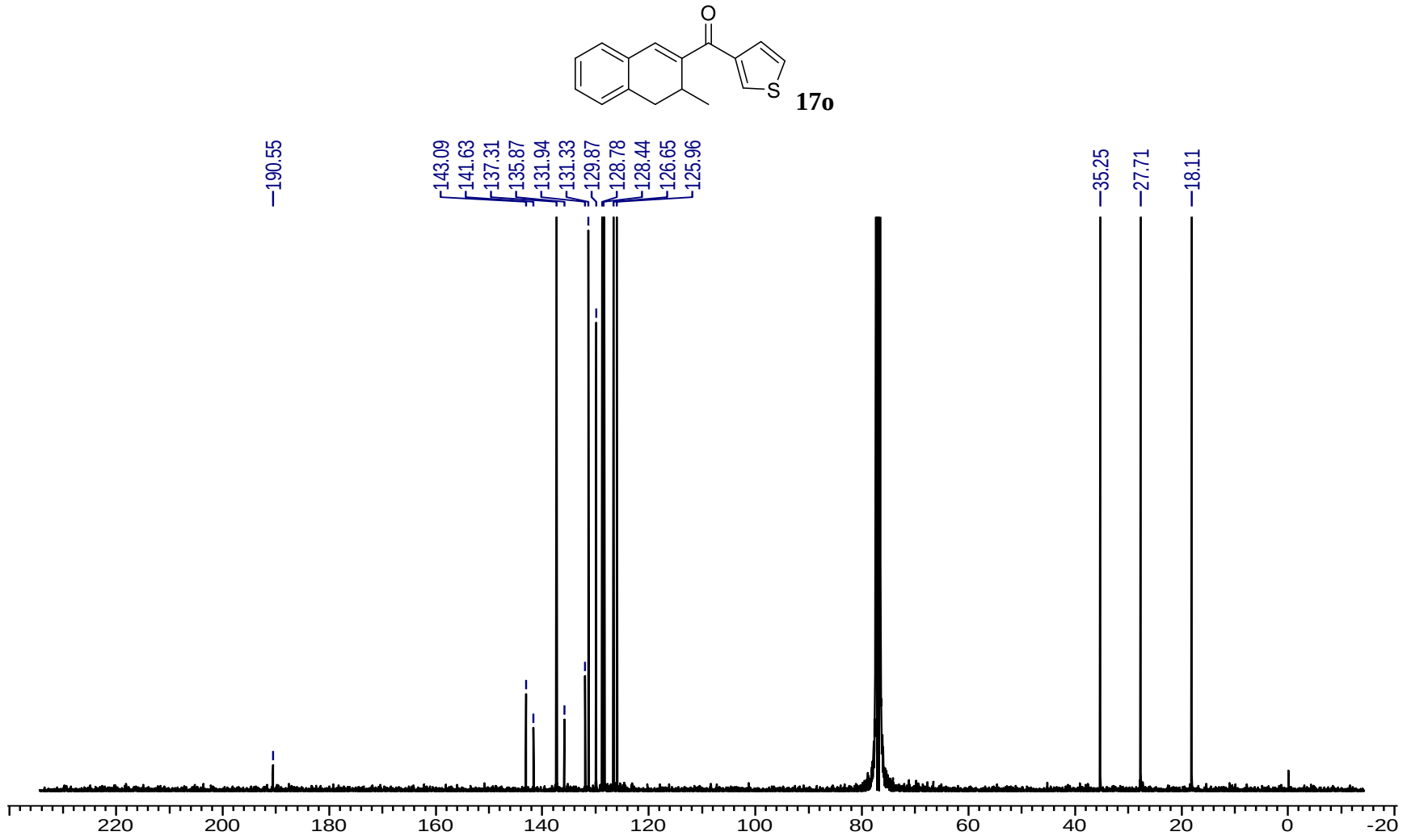
O
S
17o
190.55
143.09
141.63
137.31
135.87
131.94
131.33
129.87
128.78
128.44
126.65
125.96
35.25
27.71
18.11
220
200
180
160
140
120
100
80
60
40
20
0
-20

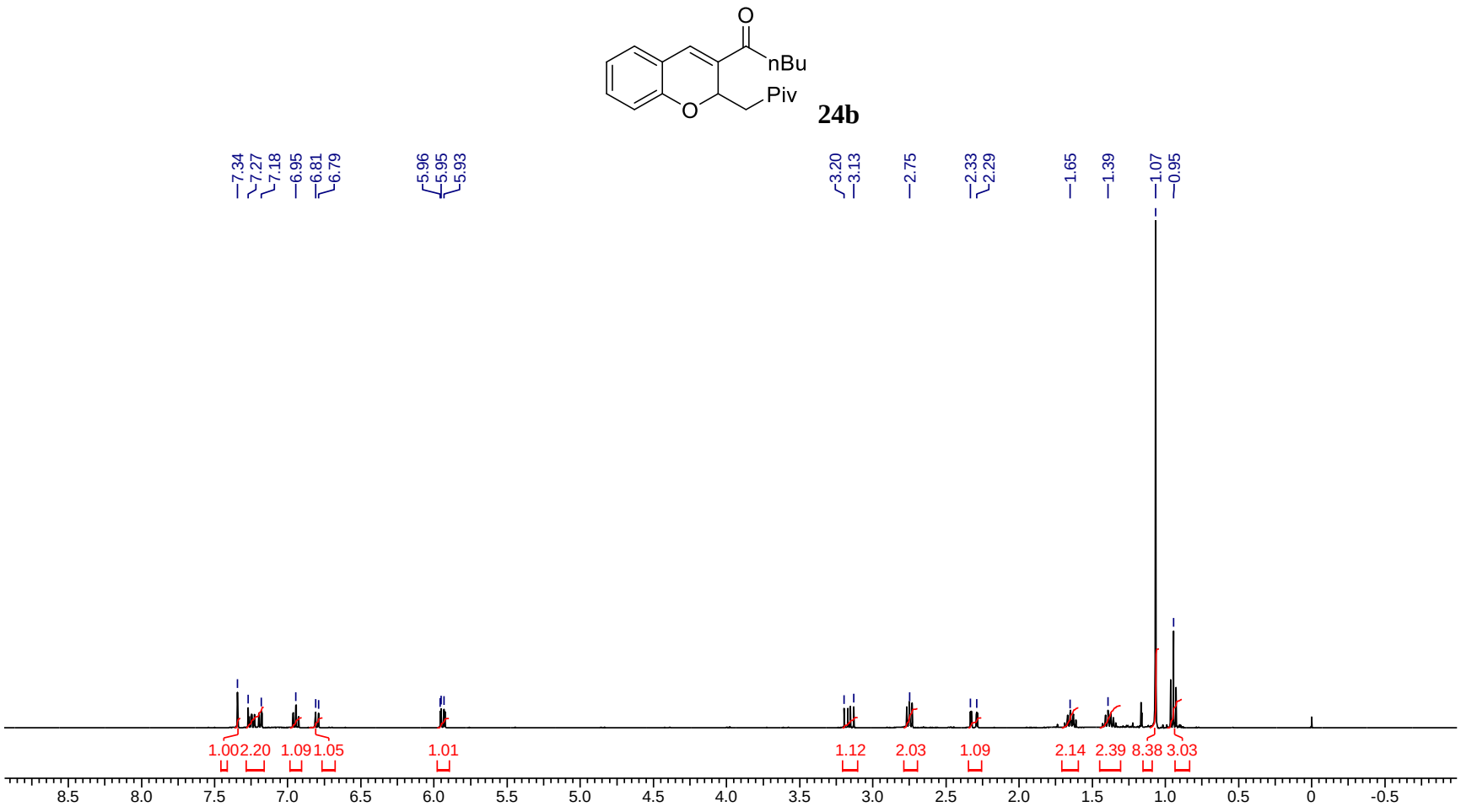
O
nBu
Piv
O
24b
7.34
7.27
7.18
6.95
6.81
6.79
5.96
5.95
5.93
3.20
3.13
2.75
2.33
2.29
1.65
1.39
1.07
0.95
1.00
2.20
1.09
1.05
1.01
1.12
2.03
1.09
2.14
2.39
8.38
3.03
8.5
8.0
7.5
7.0
6.5
6.0
5.5
5.0
4.5
4.0
3.5
3.0
2.5
2.0
1.5
1.0
0.5
0
-0.5

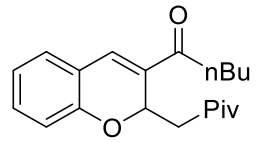
O
nBu
Piv
O

24b

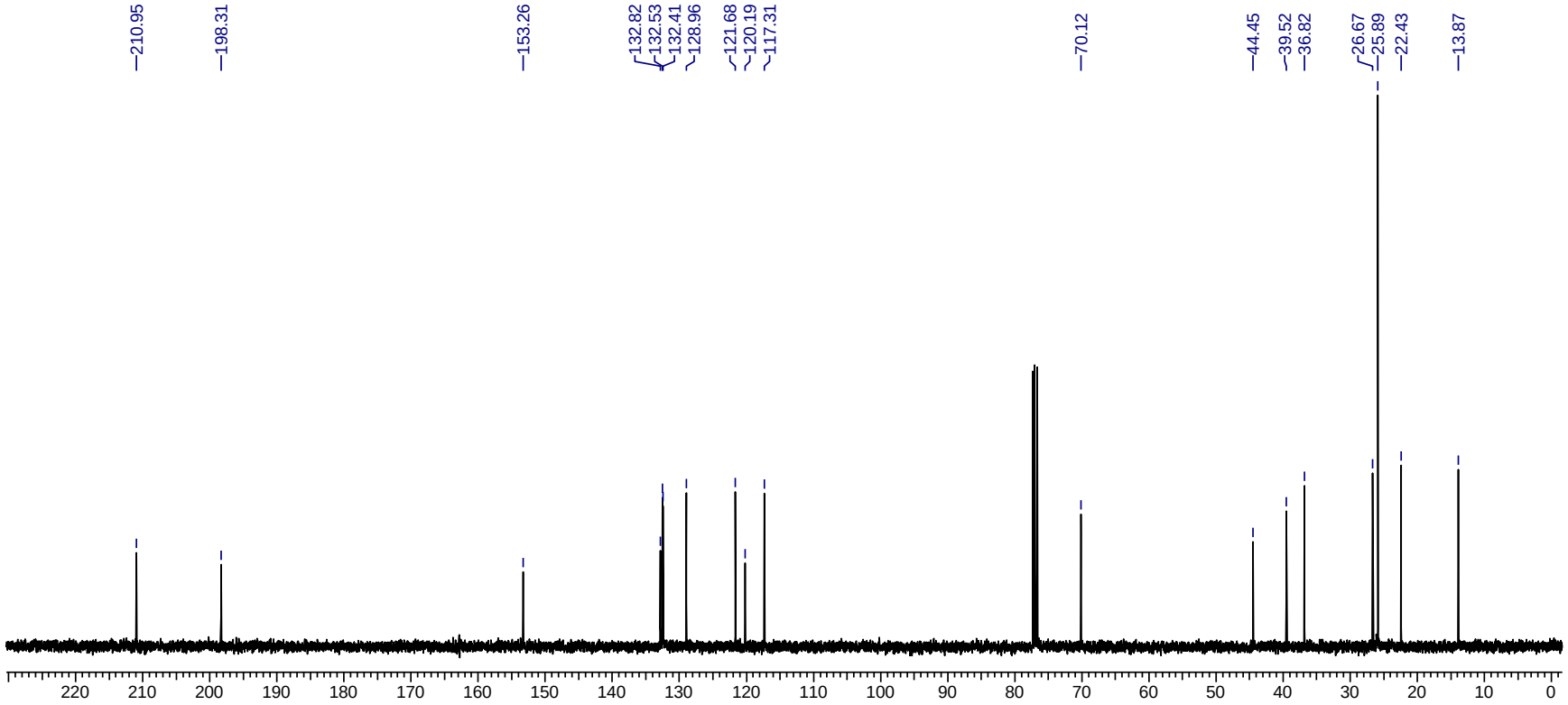
210.95
198.31
153.26
132.82
132.53
132.41
128.96
121.68
120.19
117.31
70.12
44.45
39.52
36.82
26.67
25.89
22.43
13.87
220
210
200
190
180
170
160
150
140
130
120
110
100
90
80
70
60
50
40
30
20
10
0

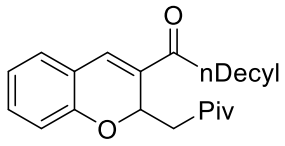
O
nDecyl
Piv
O

24c

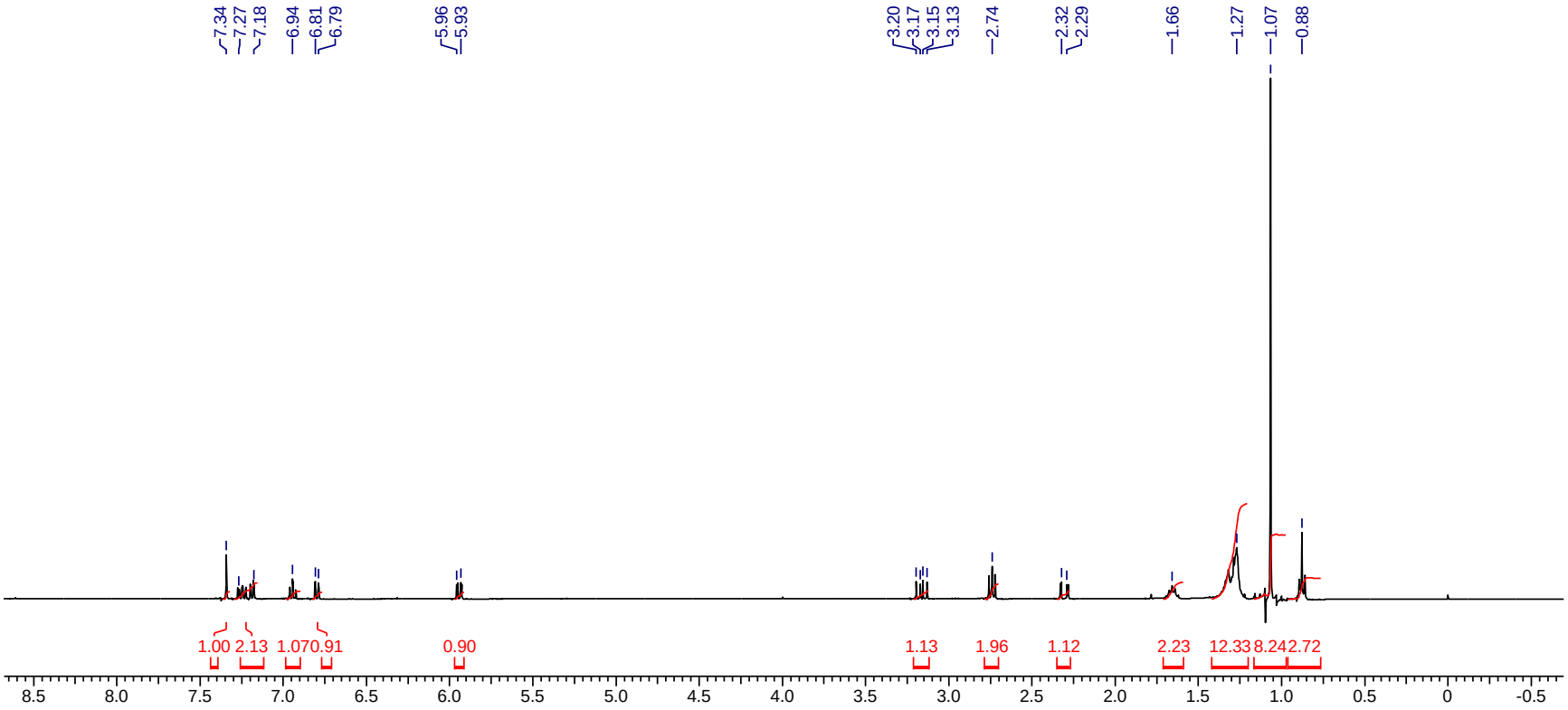
7.34
7.27
7.18
6.94
6.81
6.79
5.96
5.93
3.20
3.17
3.15
3.13
2.74
2.32
2.29
1.66
1.27
1.07
0.88
1.00
2.13
1.07
0.91
0.90
1.13
1.96
1.12
2.23
12.33
8.24
2.72
8.5
8.0
7.5
7.0
6.5
6.0
5.5
5.0
4.5
4.0
3.5
3.0
2.5
2.0
1.5
1.0
0.5
0
-0.5

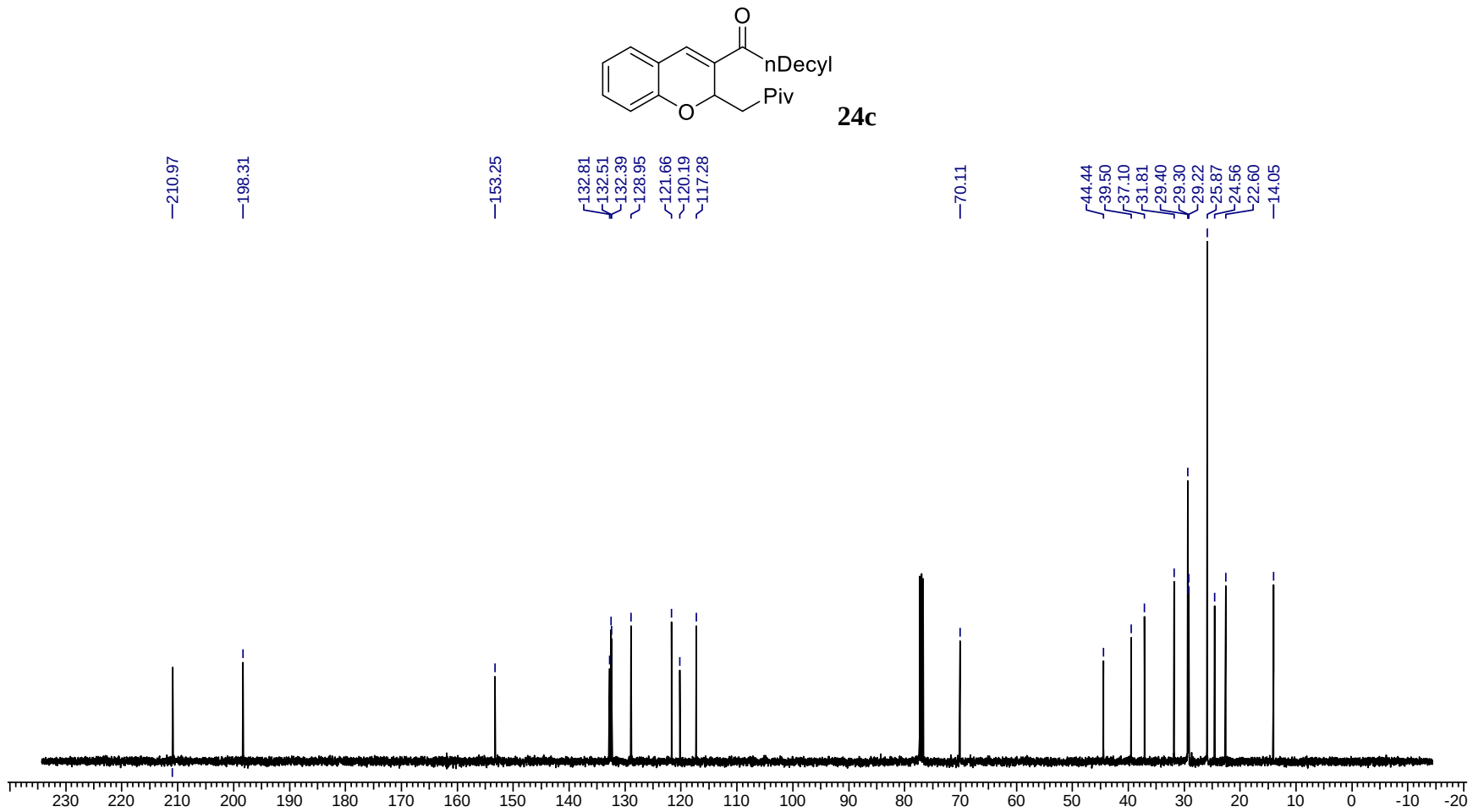
O
nDecyl
Piv
O
24c
210.97
198.31
153.25
132.81
132.51
132.39
128.95
121.66
120.19
117.28
70.11
44.44
39.50
37.10
31.81
29.40
29.30
29.22
25.87
24.56
22.60
14.05
230 220 210 200 190 180 170 160 150 140 130 120 110 100 90 80 70 60 50 40 30 20 10 0 -10 -20

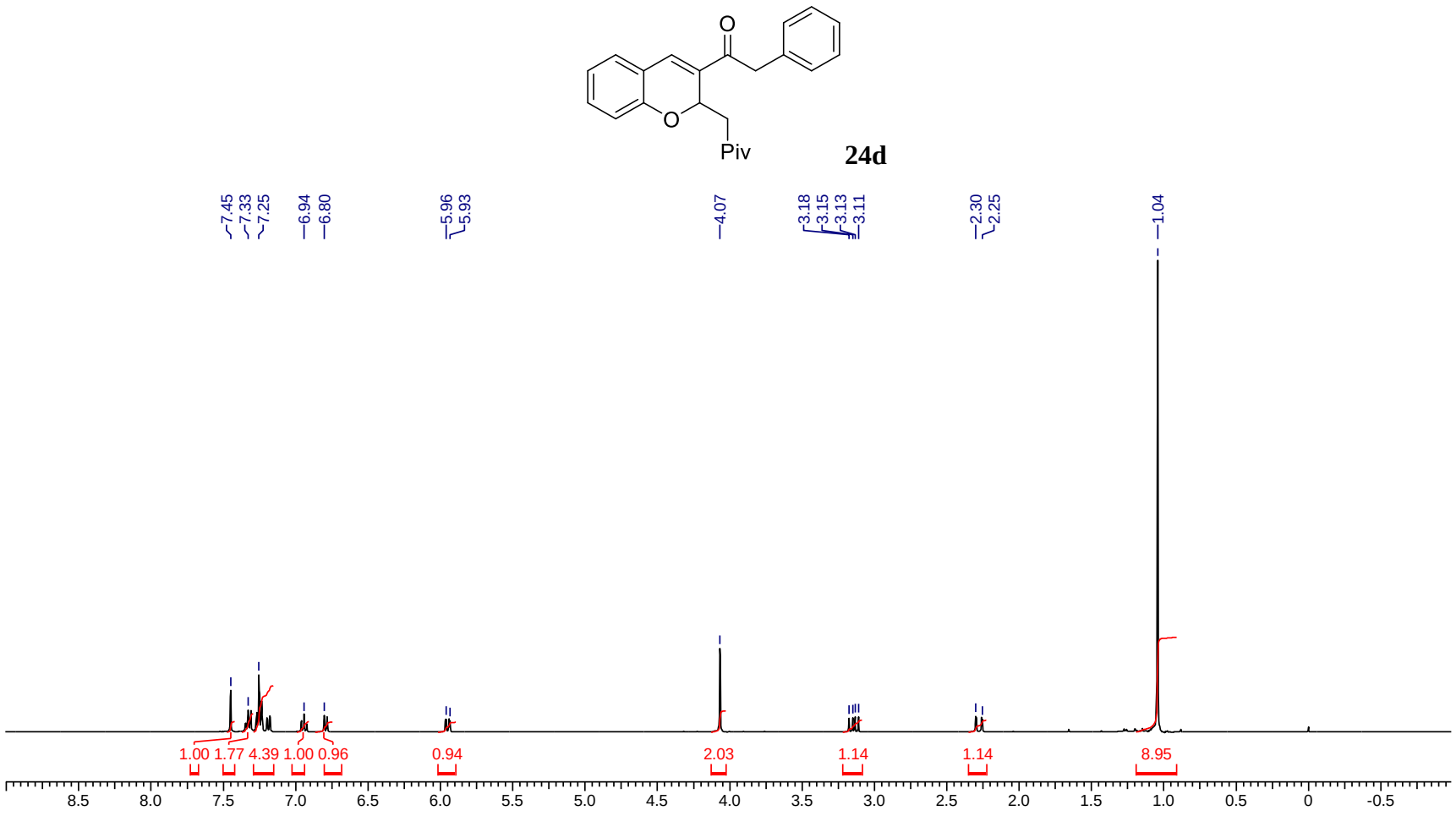
O
O
Piv
24d
7.45
7.33
7.25
6.94
6.80
5.96
5.93
4.07
3.18
3.15
3.13
3.11
2.30
2.25
1.04
1.00 1.77 4.39 1.00 0.96
0.94
2.03
1.14
1.14
8.95
8.5 8.0 7.5 7.0 6.5 6.0 5.5 5.0 4.5 4.0 3.5 3.0 2.5 2.0 1.5 1.0 0.5 0 -0.5

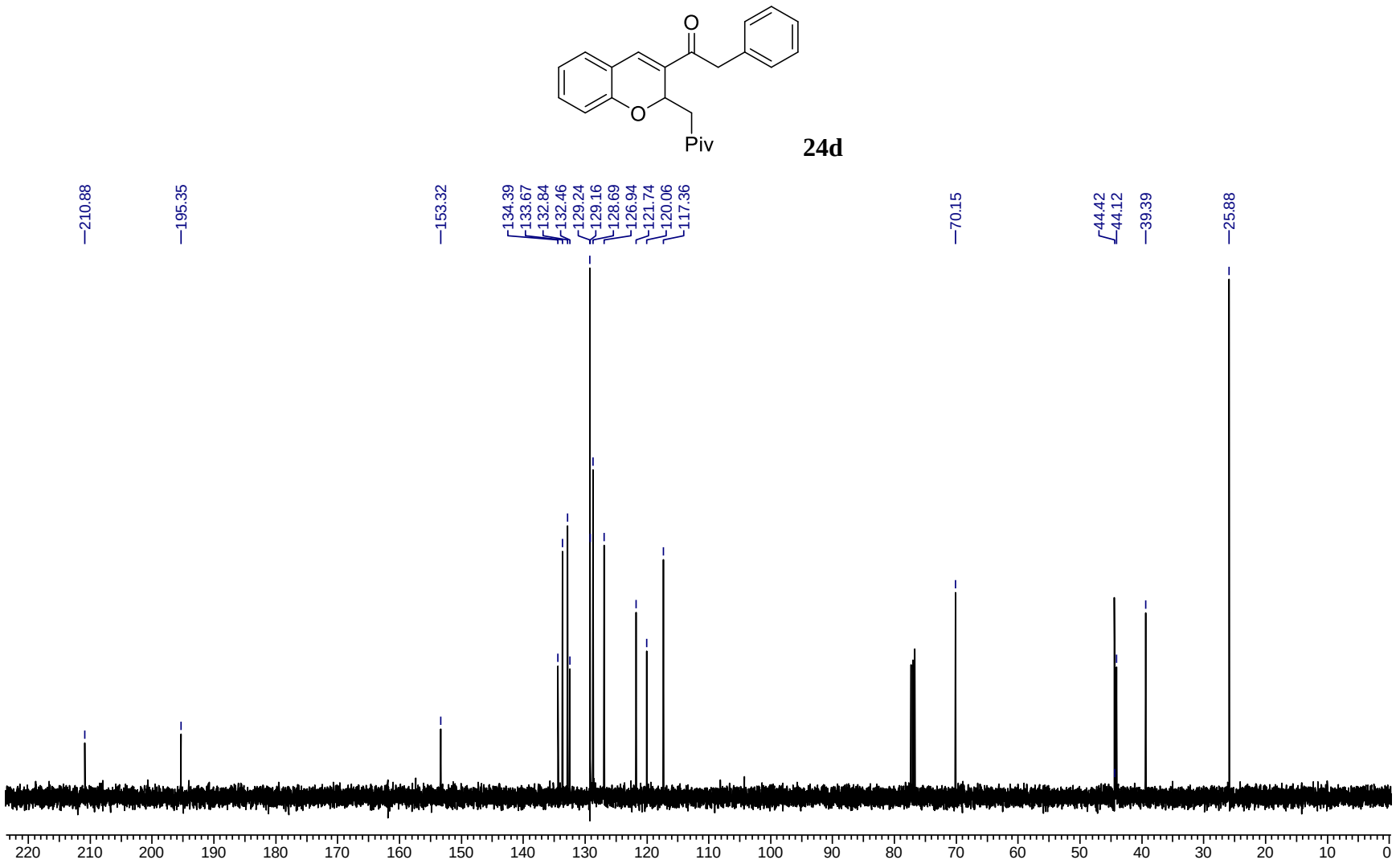
O
O
Piv
24d
210.88
195.35
153.32
134.39
133.67
132.84
132.46
129.24
129.16
128.69
126.94
121.74
120.06
117.36
70.15
44.42
44.12
39.39
25.88
220
210
200
190
180
170
160
150
140
130
120
110
100
90
80
70
60
50
40
30
20
10
0

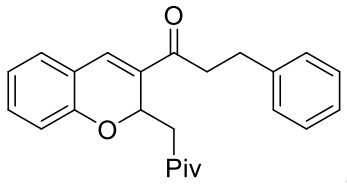
O
O
Piv

24e

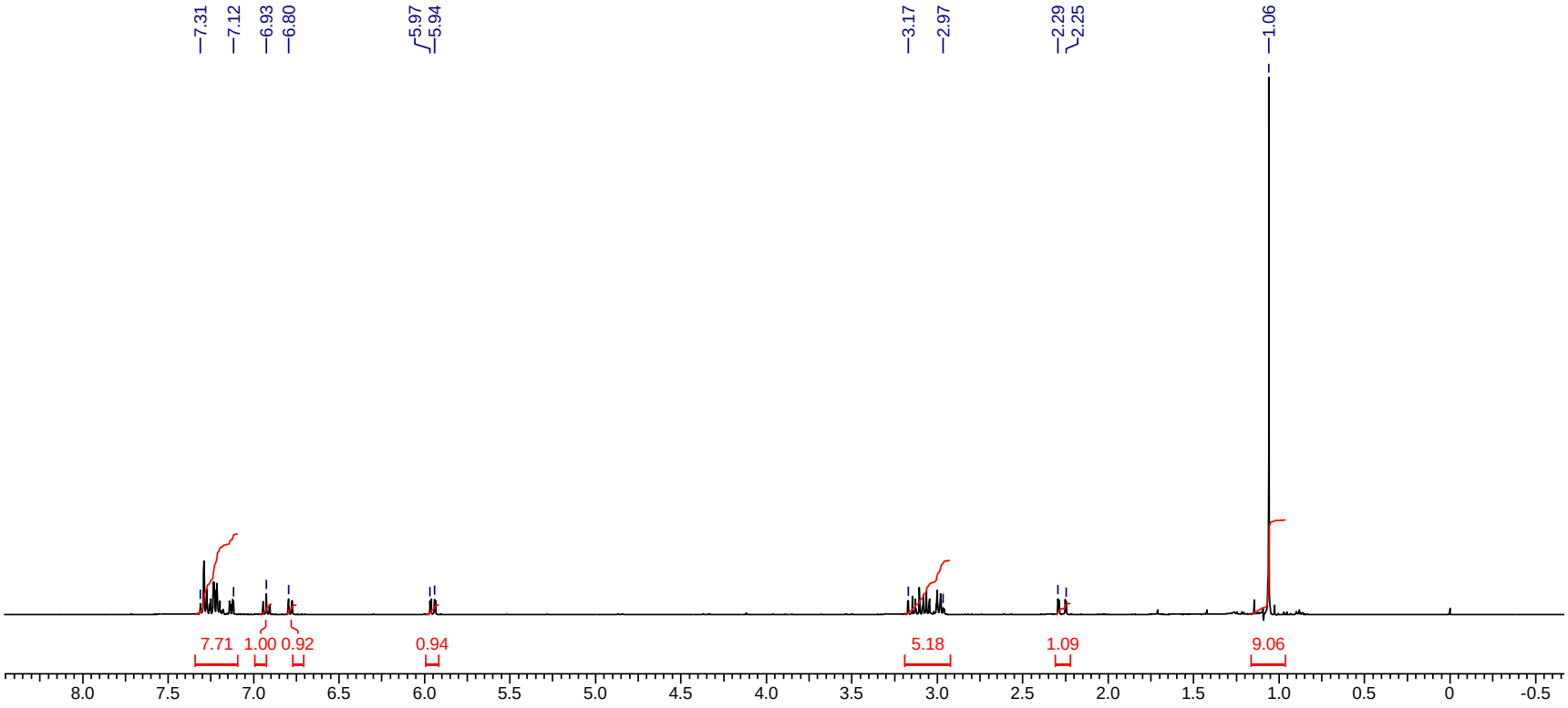
7.31
7.12
6.93
6.80
5.97
5.94
3.17
2.97
2.29
2.25
1.06
7.71
1.00
0.92
0.94
5.18
1.09
9.06
8.0
7.5
7.0
6.5
6.0
5.5
5.0
4.5
4.0
3.5
3.0
2.5
2.0
1.5
1.0
0.5
0
-0.5

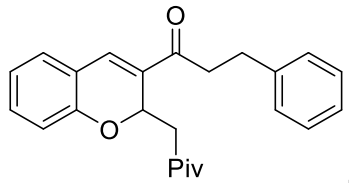
O
O
Piv

24e

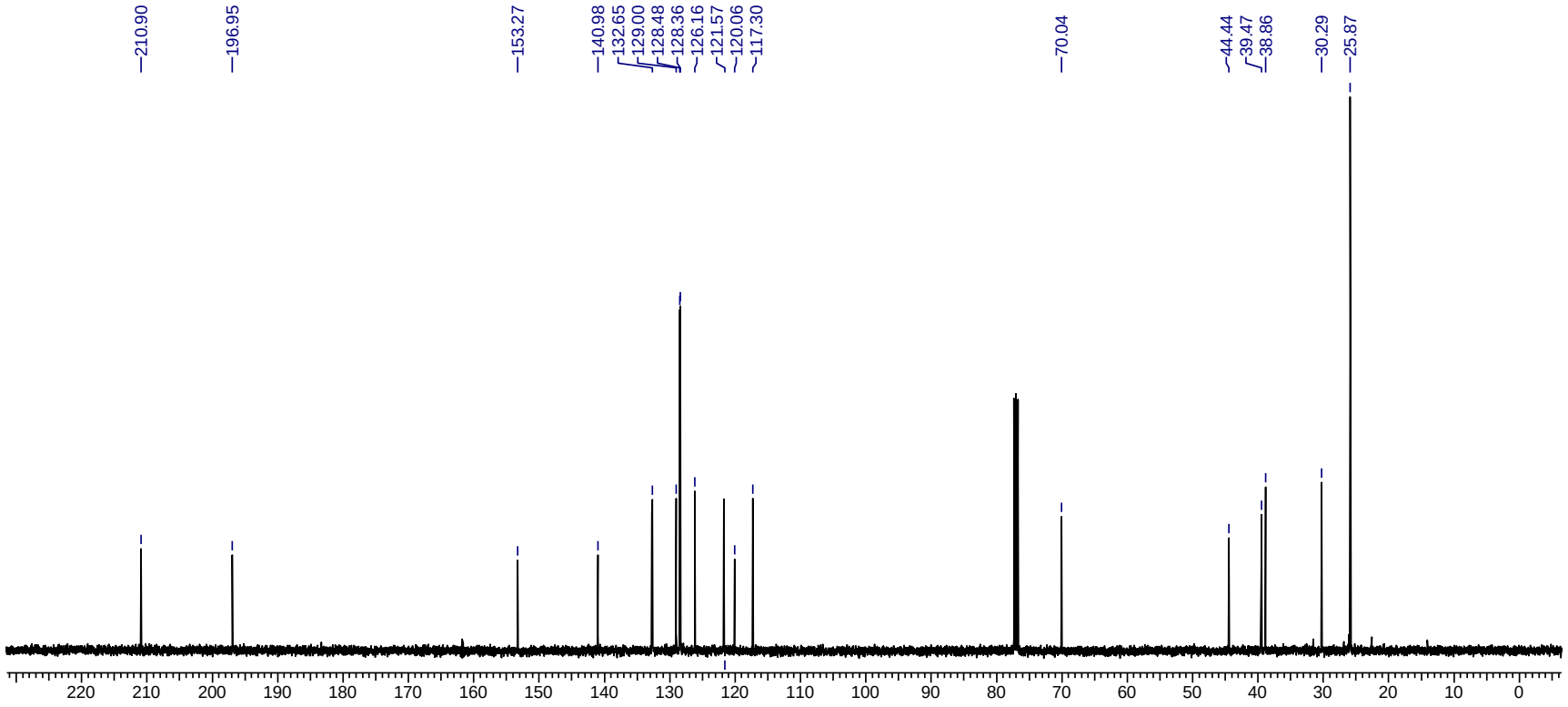
210.90
196.95
153.27
140.98
132.65
129.00
128.48
128.36
126.16
121.57
120.06
117.30
70.04
44.44
39.47
38.86
30.29
25.87
220
210
200
190
180
170
160
150
140
130
120
110
100
90
80
70
60
50
40
30
20
10
0

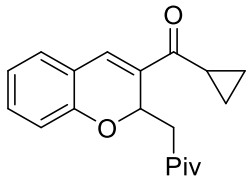
O
O
Piv

24f

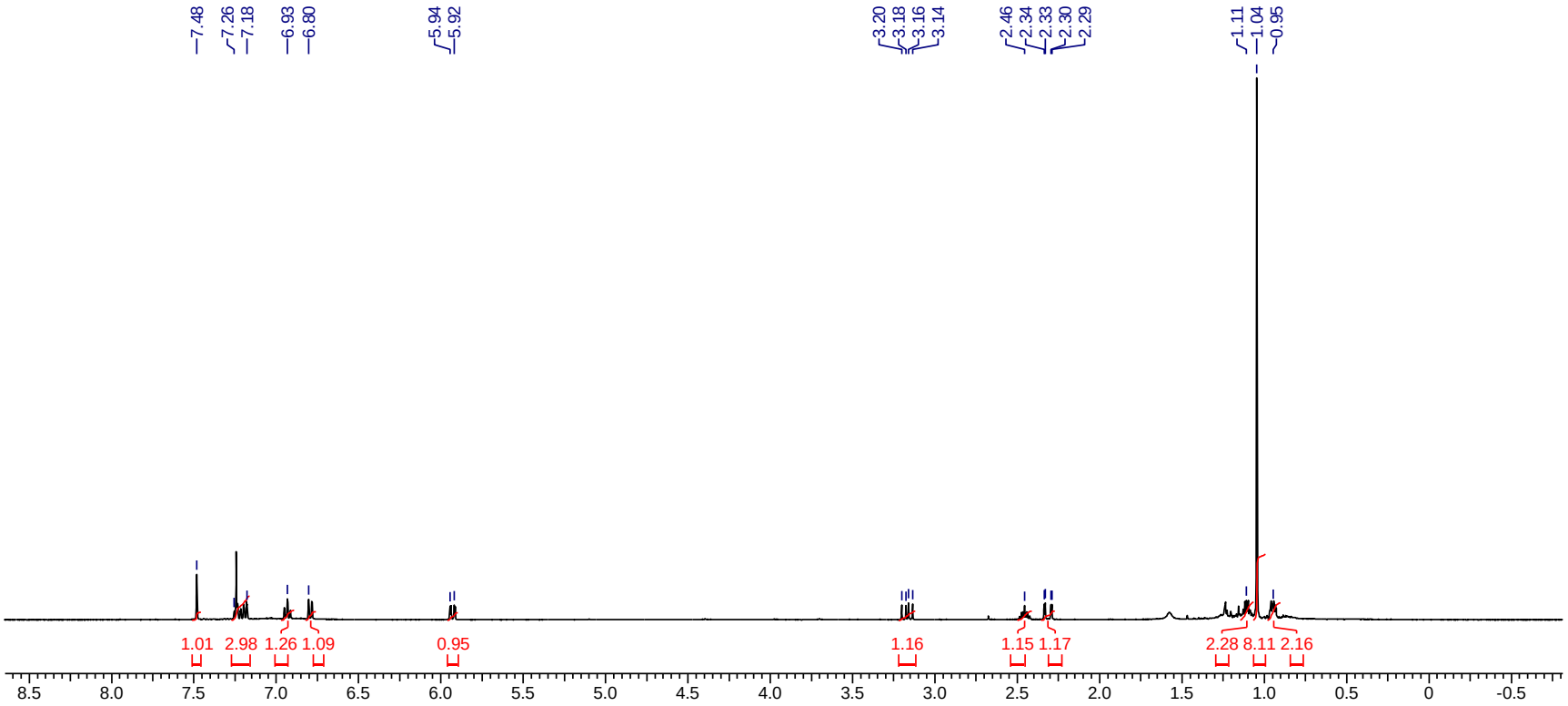
7.48
7.26
7.18
6.93
6.80
5.94
5.92
3.20
3.18
3.16
3.14
2.46
2.34
2.33
2.30
2.29
1.11
1.04
0.95
1.01
2.98
1.26
1.09
0.95
1.16
1.15
1.17
2.28
8.11
2.16
8.5
8.0
7.5
7.0
6.5
6.0
5.5
5.0
4.5
4.0
3.5
3.0
2.5
2.0
1.5
1.0
0.5
0
-0.5

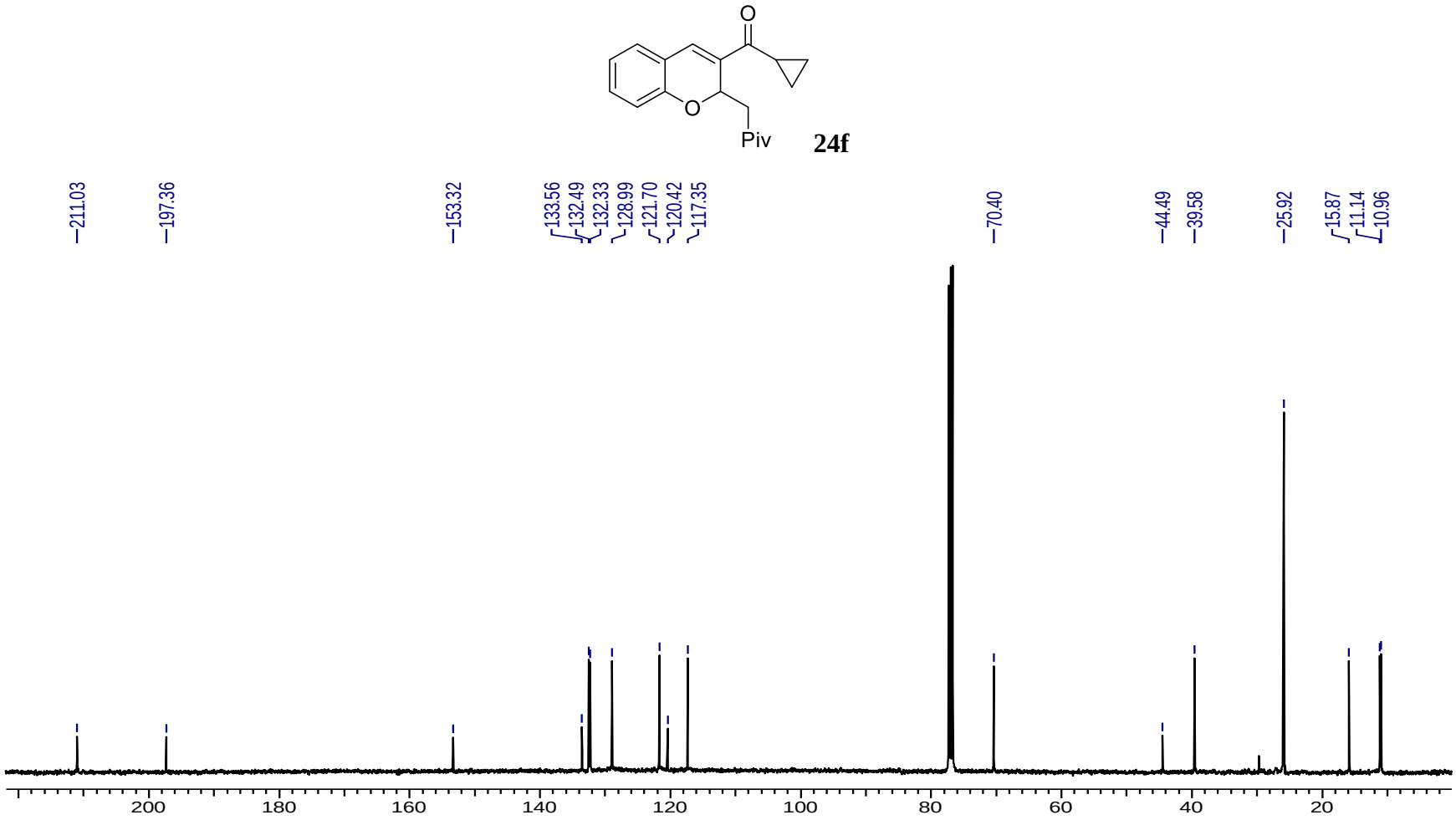
O
O
Piv
24f
211.03
197.36
153.32
133.56
132.49
132.33
128.99
121.70
120.42
117.35
70.40
44.49
39.58
25.92
15.87
11.14
10.96
200
180
160
140
120
100
80
60
40
20

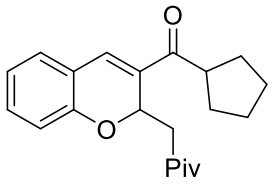
O
O
Piv

24g

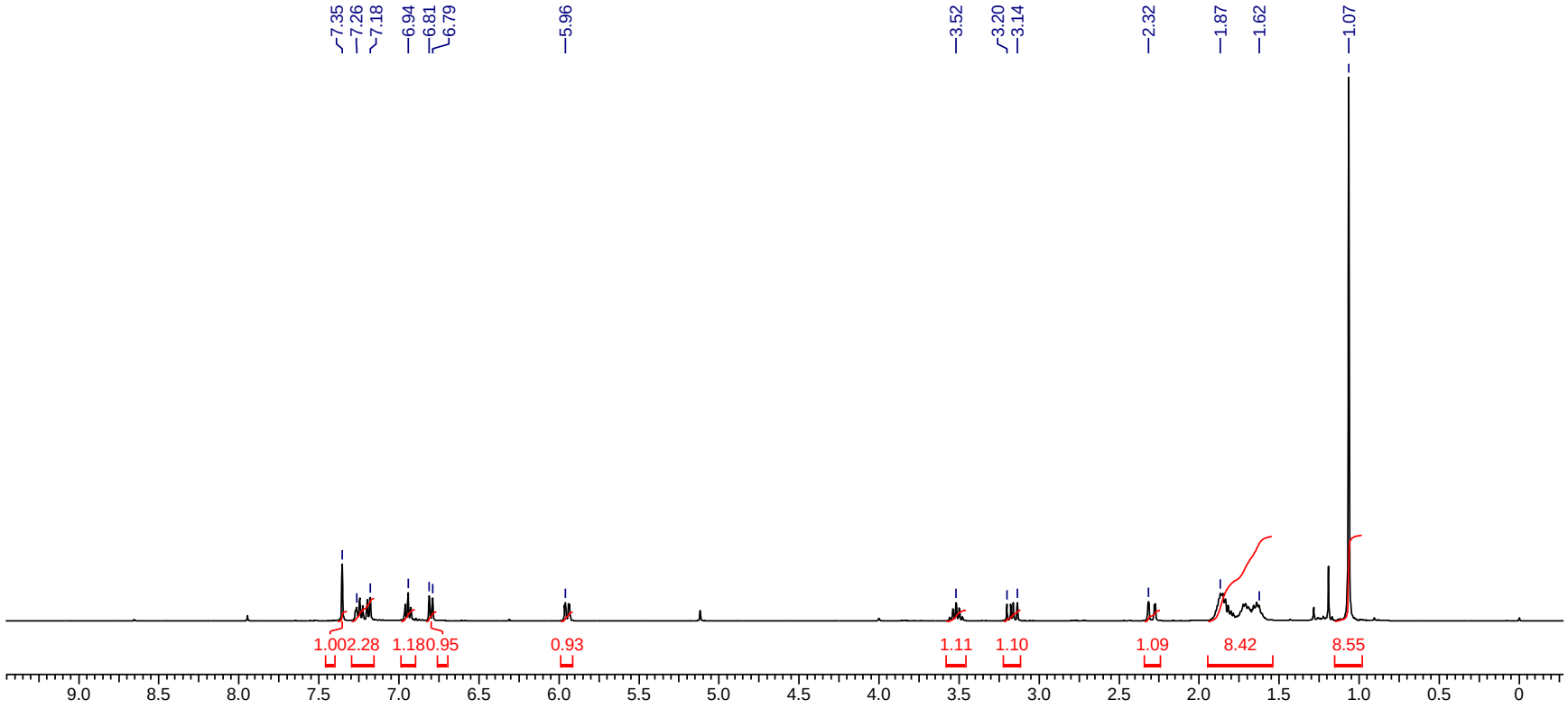
7.35
7.26
7.18
6.94
6.81
6.79
5.96
3.52
3.20
3.14
2.32
1.87
1.62
1.07
1.00
2.28
1.18
0.95
0.93
1.11
1.10
1.09
8.42
8.55
9.0
8.5
8.0
7.5
7.0
6.5
6.0
5.5
5.0
4.5
4.0
3.5
3.0
2.5
2.0
1.5
1.0
0.5
0

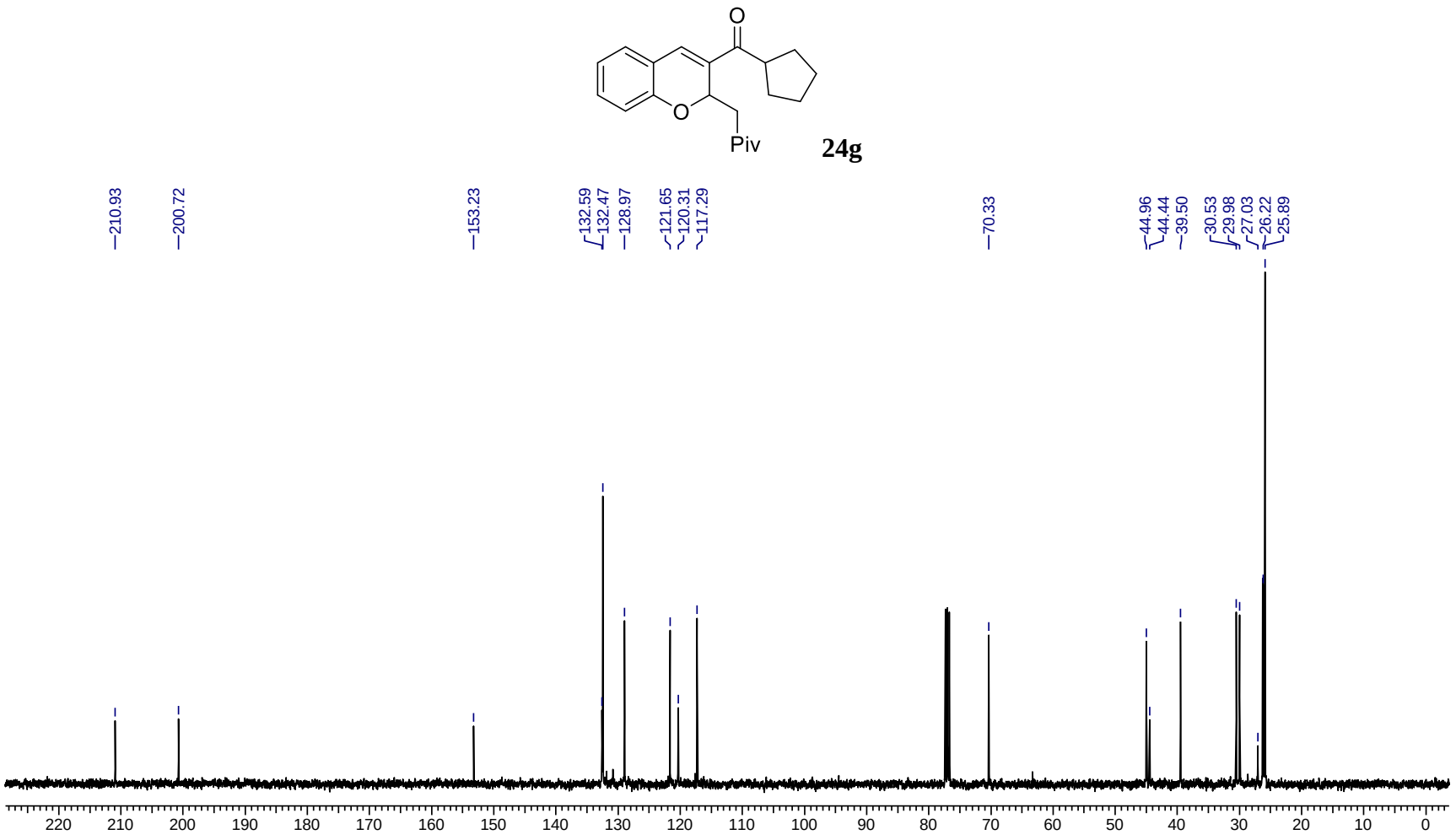
O
O
Piv
24g
210.93
200.72
153.23
132.59
132.47
128.97
121.65
120.31
117.29
70.33
44.96
44.44
39.50
30.53
29.98
27.03
26.22
25.89
220
210
200
190
180
170
160
150
140
130
120
110
100
90
80
70
60
50
40
30
20
10
0

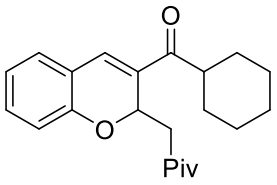
O
O
Piv

24h

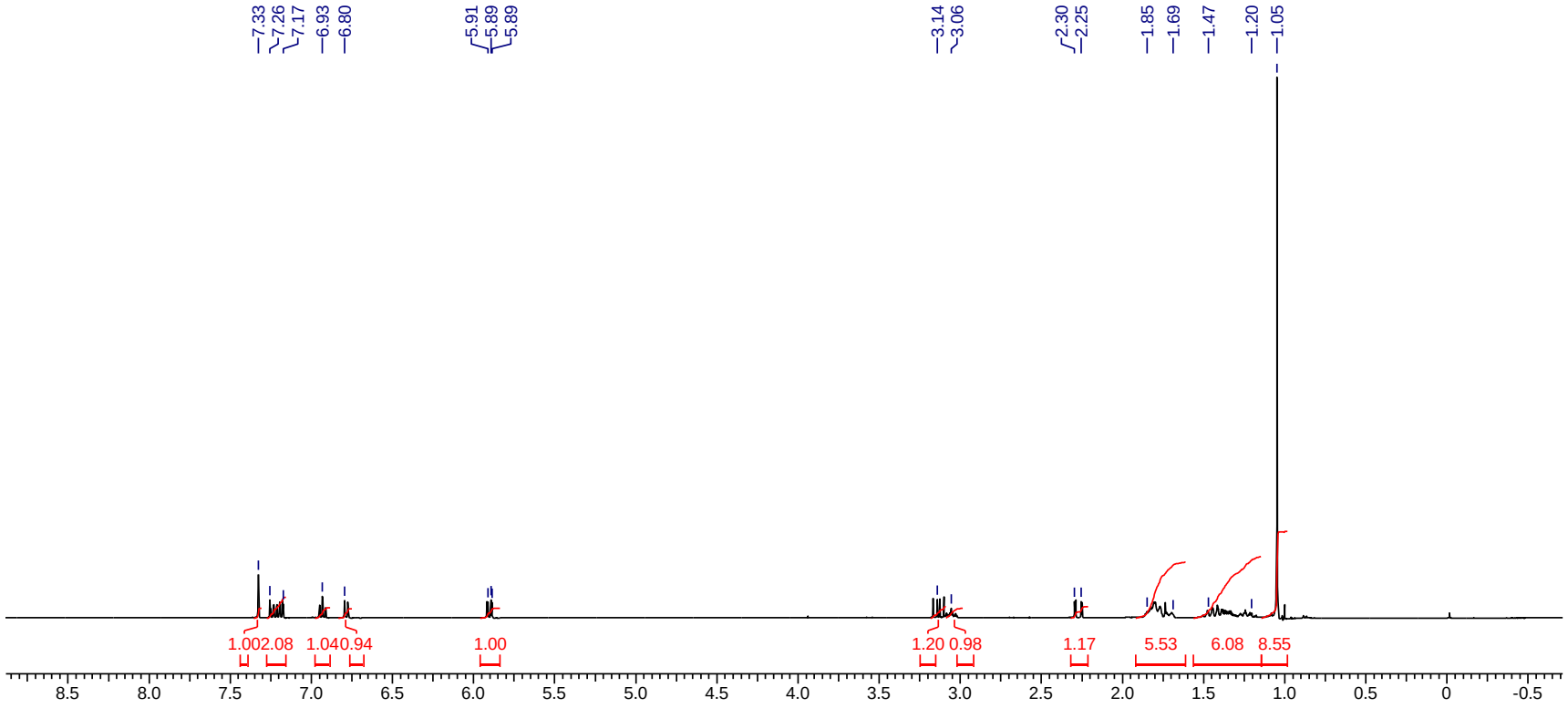
7.33
7.26
7.17
6.93
6.80
5.91
5.89
5.89
3.14
3.06
2.30
2.25
1.85
1.69
1.47
1.20
1.05
1.00
2.08
1.04
0.94
1.00
1.20
0.98
1.17
5.53
6.08
8.55
8.5
8.0
7.5
7.0
6.5
6.0
5.5
5.0
4.5
4.0
3.5
3.0
2.5
2.0
1.5
1.0
0.5
0
-0.5

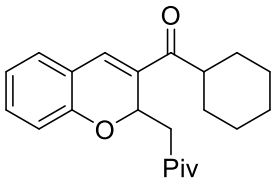
O
O
Piv

24h

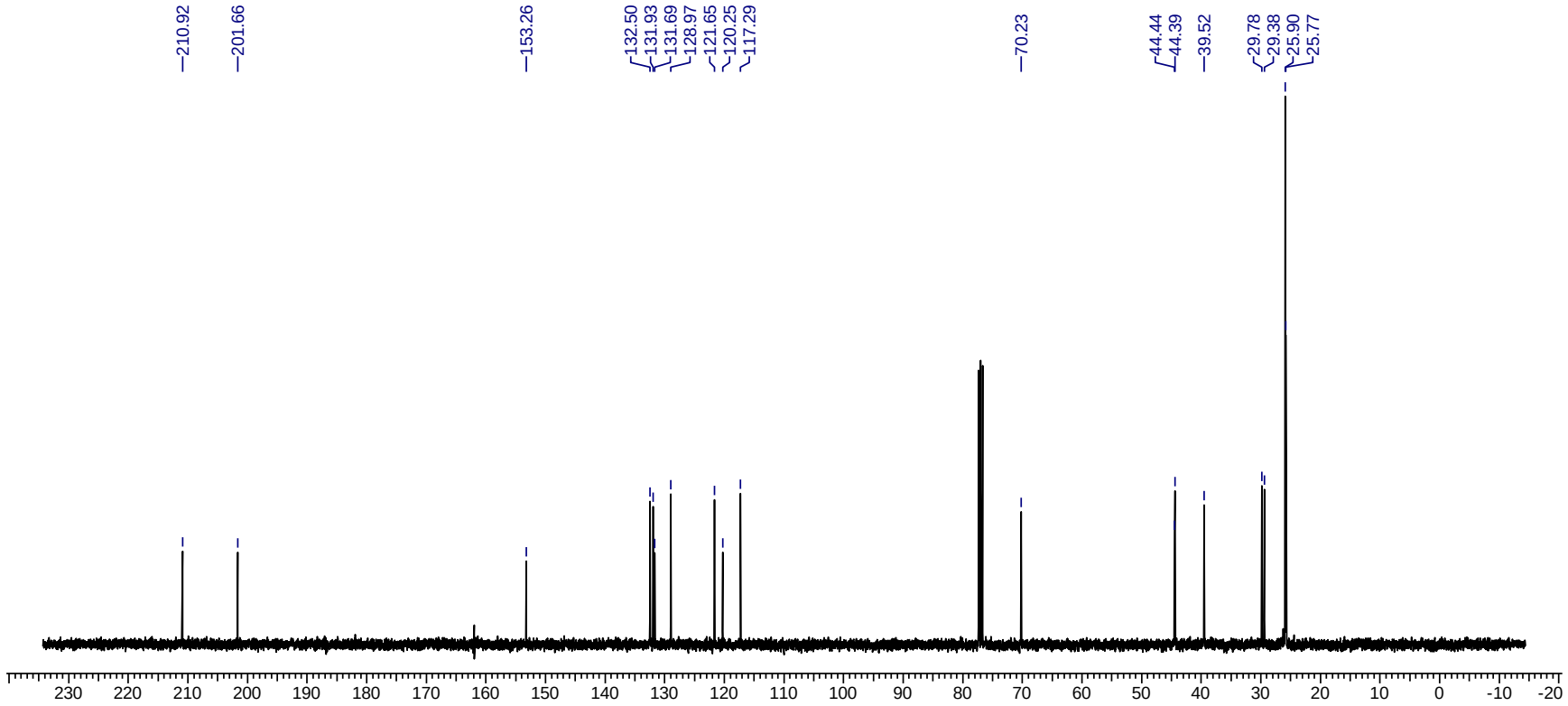
210.92
201.66
153.26
132.50
131.93
131.69
128.97
121.65
120.25
117.29
70.23
44.44
44.39
39.52
29.78
29.38
25.90
25.77
230 220 210 200 190 180 170 160 150 140 130 120 110 100 90 80 70 60 50 40 30 20 10 0 -10 -20

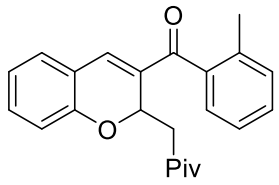
O
O
Piv

24i

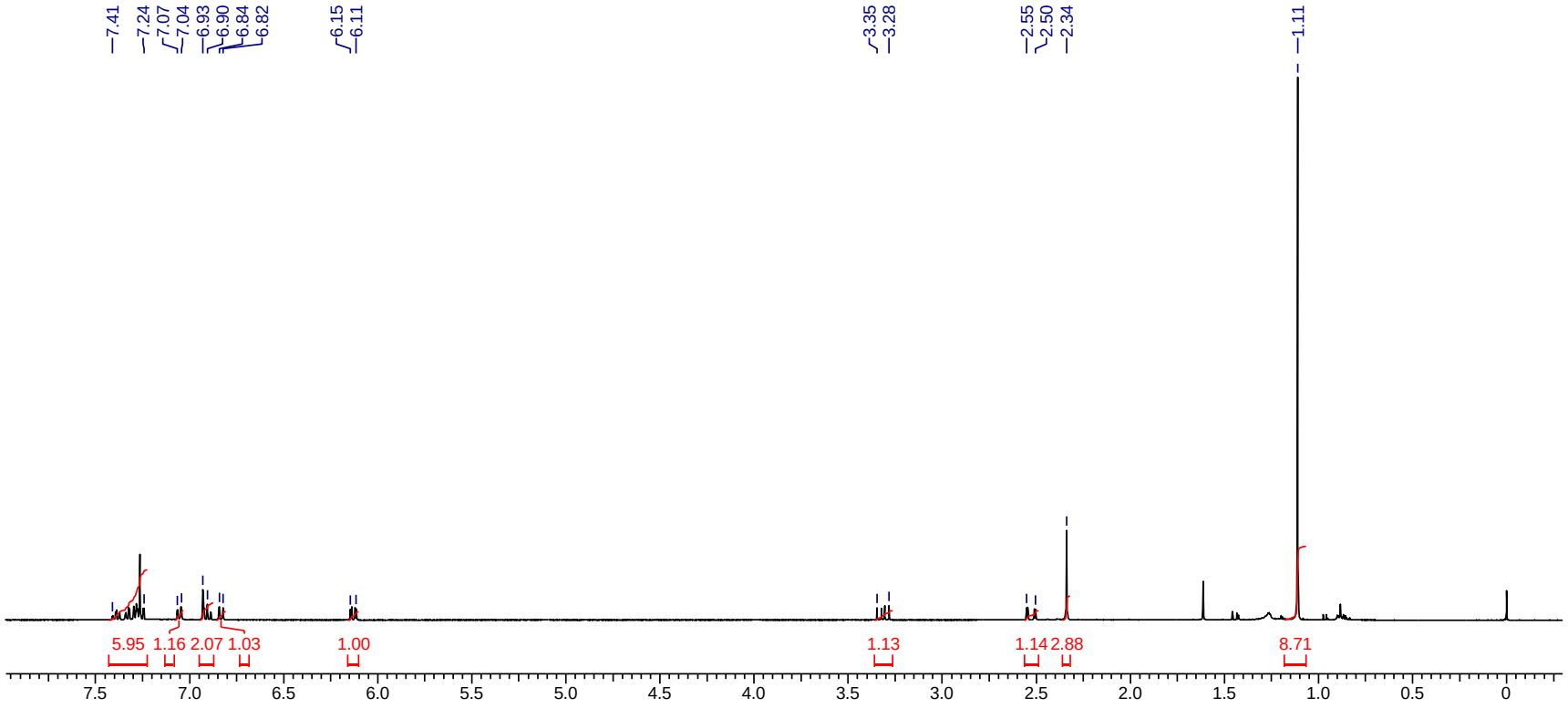
7.41
7.24
7.07
7.04
6.93
6.90
6.84
6.82
6.15
6.11
3.35
3.28
2.55
2.50
2.34
1.11
5.95
1.16
2.07
1.03
1.00
1.13
1.14
2.88
8.71
7.5
7.0
6.5
6.0
5.5
5.0
4.5
4.0
3.5
3.0
2.5
2.0
1.5
1.0
0.5
0

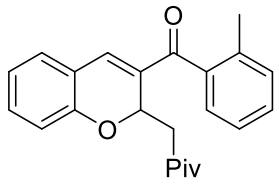
O
O
Piv

24i

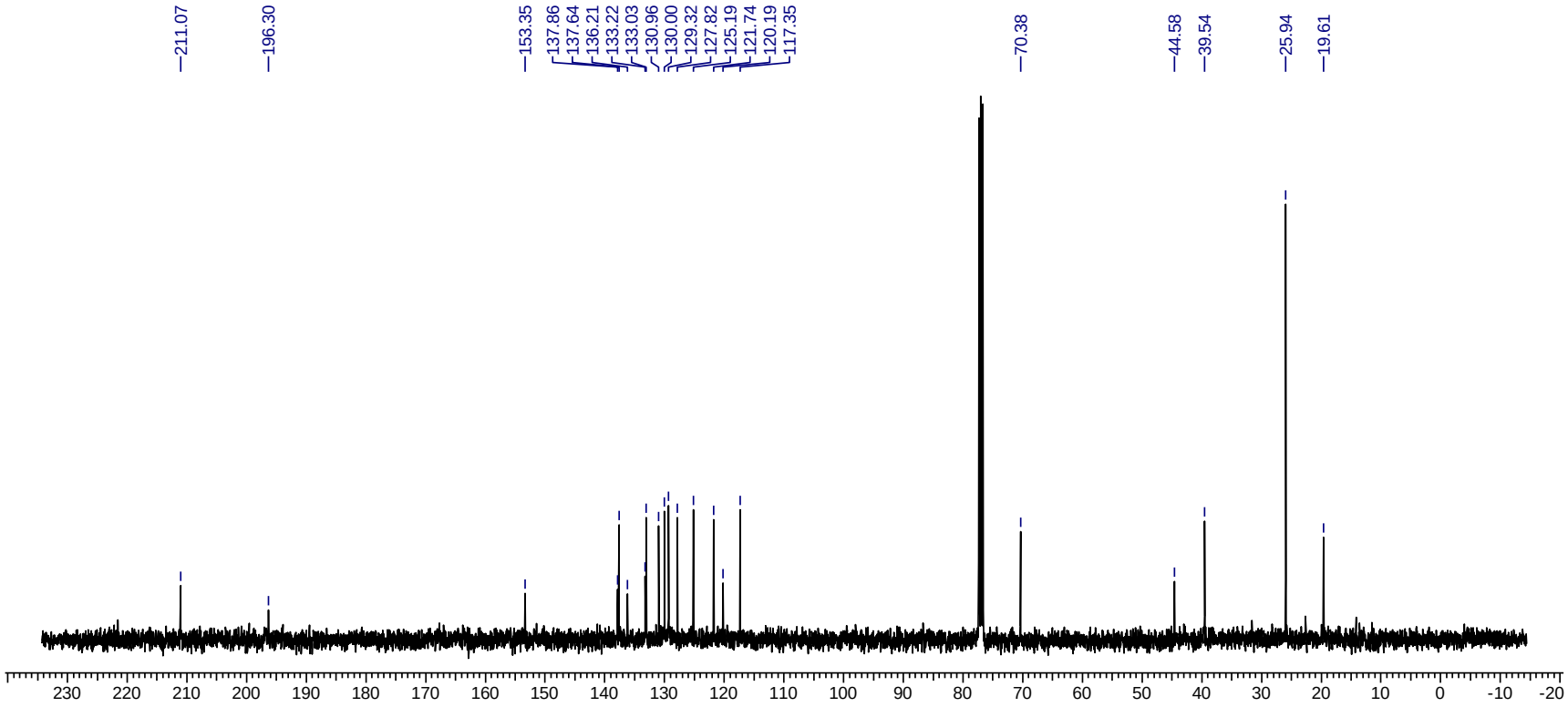
211.07
196.30
153.35
137.86
137.64
136.21
133.22
133.03
130.96
130.00
129.32
127.82
125.19
121.74
120.19
117.35
70.38
44.58
39.54
25.94
19.61
230 220 210 200 190 180 170 160 150 140 130 120 110 100 90 80 70 60 50 40 30 20 10 0 -10 -20

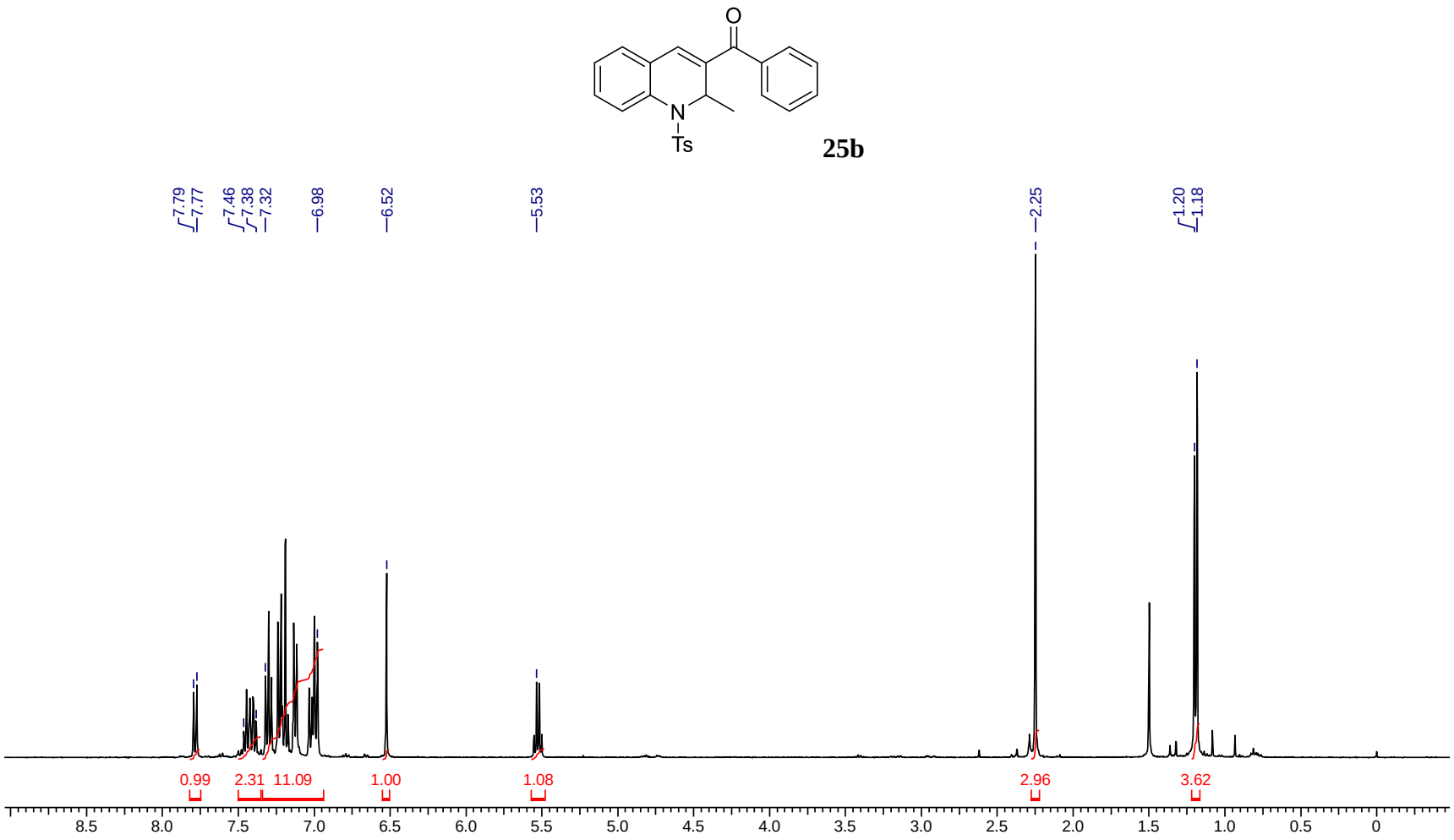
O
N
Ts
25b
7.79
7.77
7.46
7.38
7.32
6.98
6.52
5.53
2.25
1.20
1.18
0.99
2.31
11.09
1.00
1.08
2.96
3.62
8.5
8.0
7.5
7.0
6.5
6.0
5.5
5.0
4.5
4.0
3.5
3.0
2.5
2.0
1.5
1.0
0.5
0

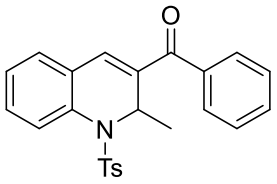
O
N
Ts

25b

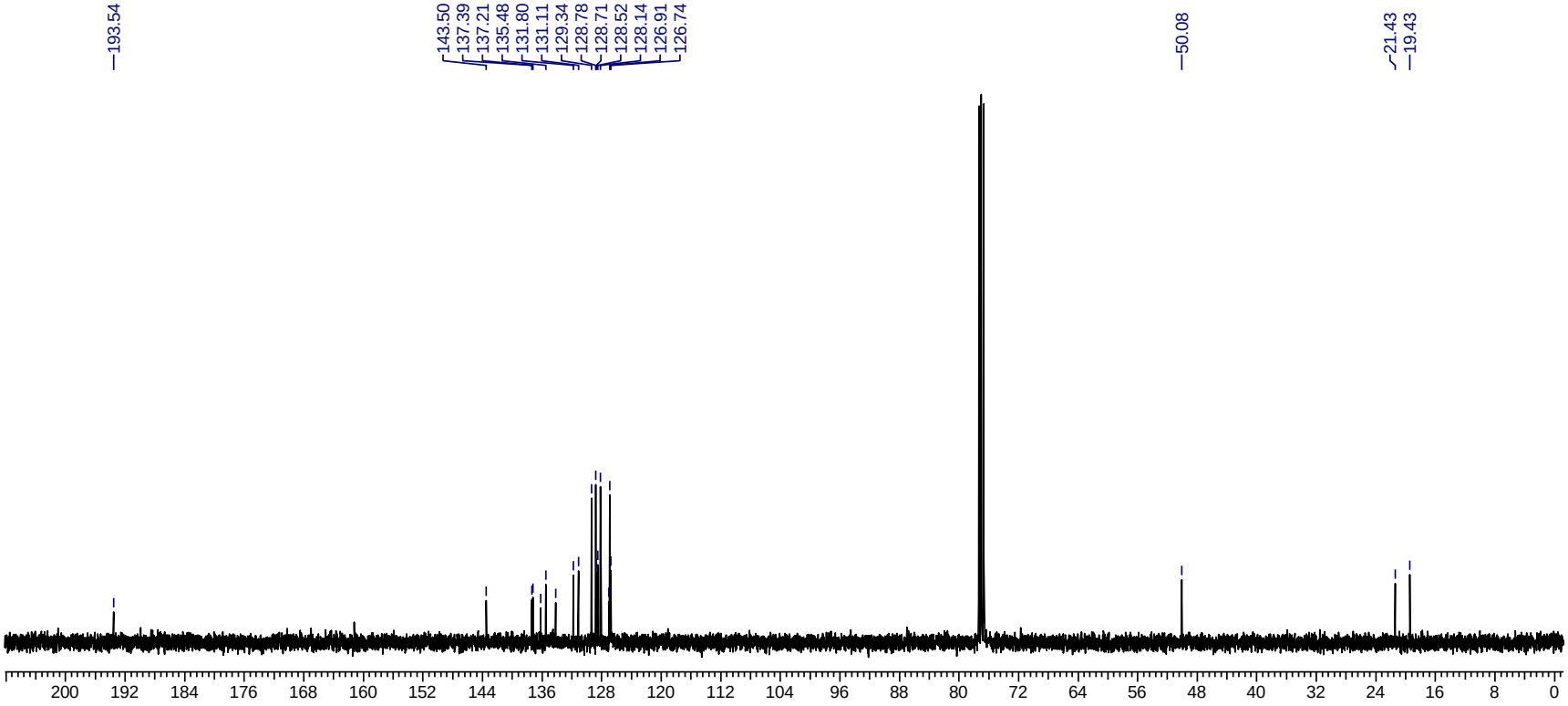
193.54
143.50
137.39
137.21
135.48
131.80
131.11
129.34
128.78
128.71
128.52
128.14
126.91
126.74
50.08
21.43
19.43
200
192
184
176
168
160
152
144
136
128
120
112
104
96
88
80
72
64
56
48
40
32
24
16
8
0

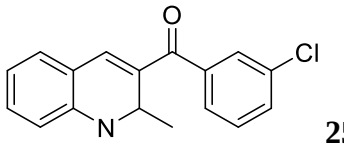
O
Cl
N

25c

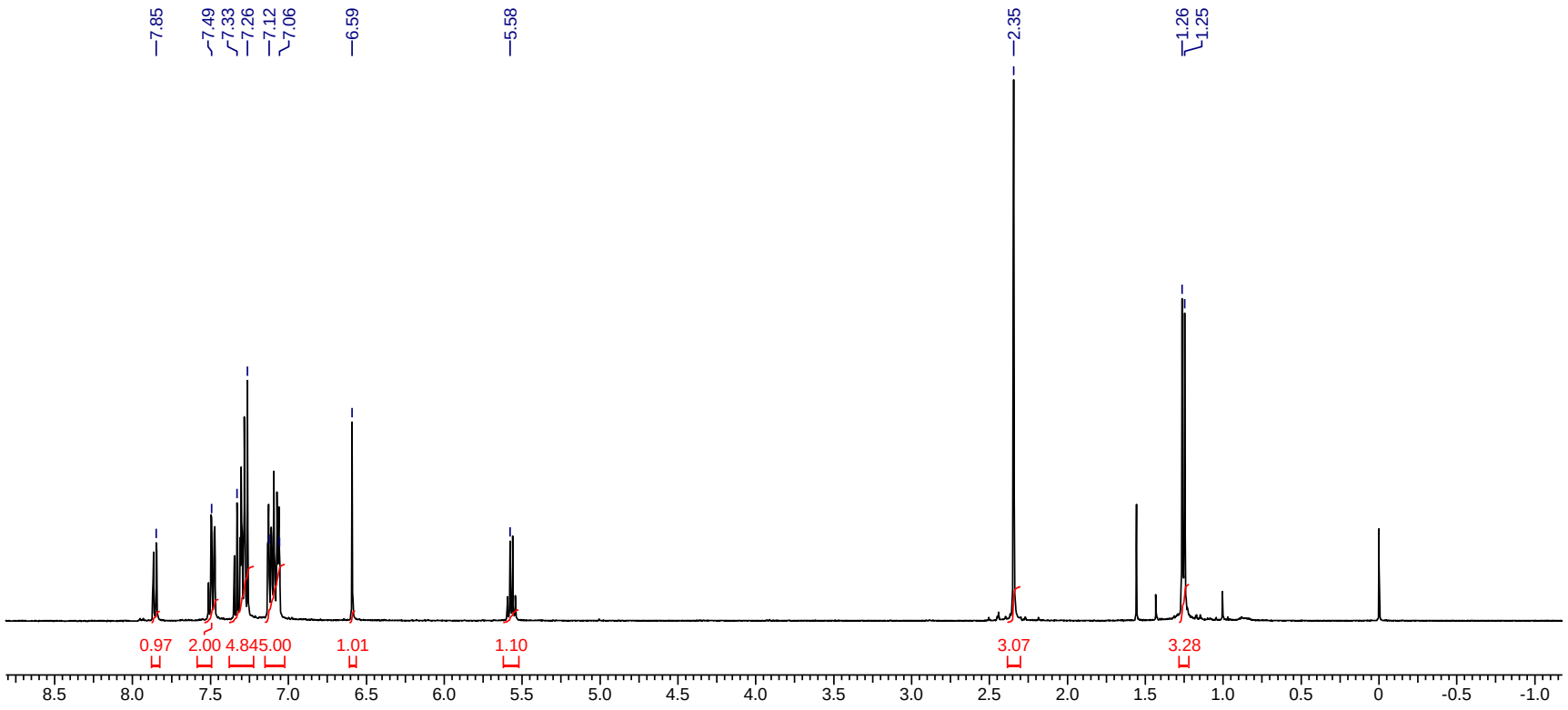
7.85
7.49
7.33
7.26
7.12
7.06
6.59
5.58
2.35
1.26
1.25
0.97
2.00
4.84
5.00
1.01
1.10
3.07
3.28
8.5
8.0
7.5
7.0
6.5
6.0
5.5
5.0
4.5
4.0
3.5
3.0
2.5
2.0
1.5
1.0
0.5
0
-0.5
-1.0

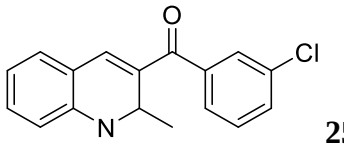
O
Cl
N

25c

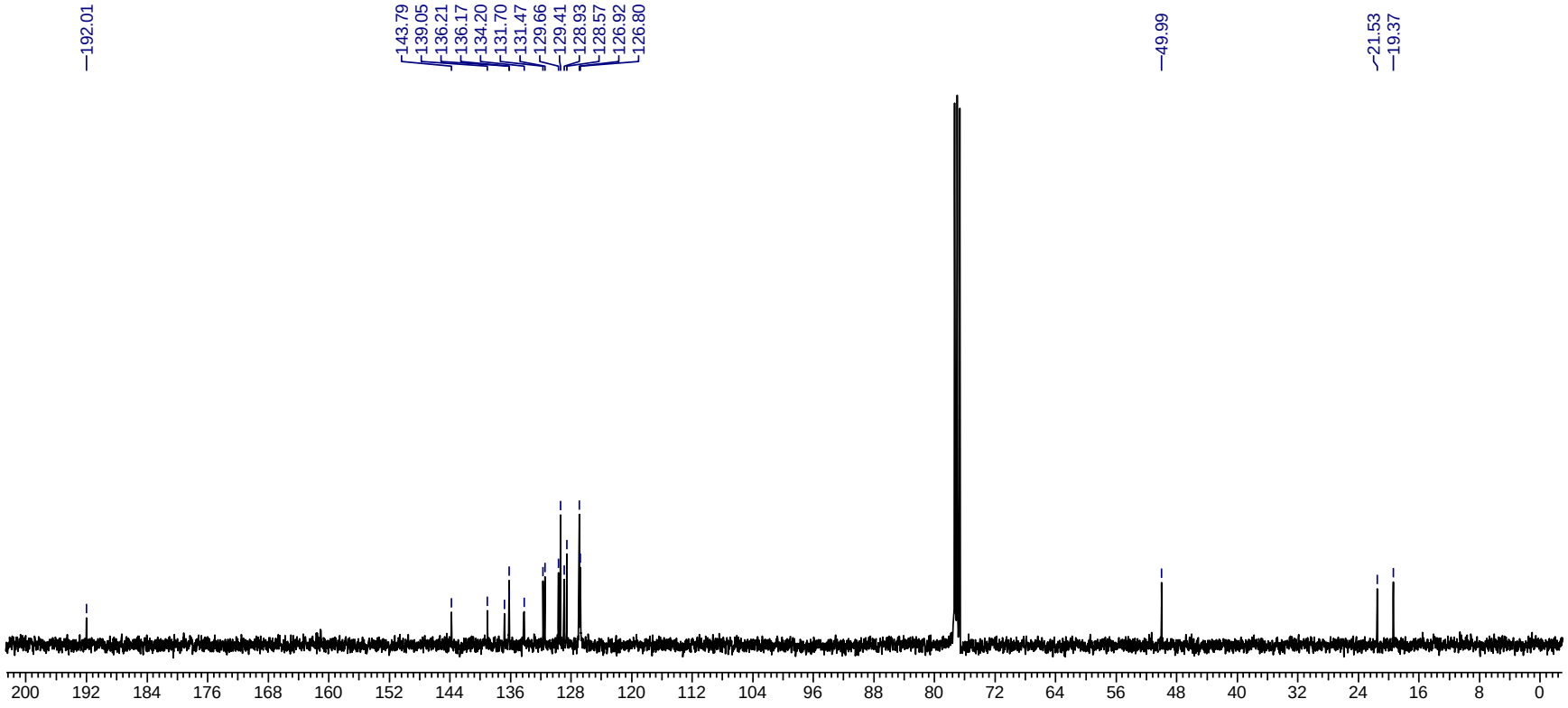
192.01
143.79
139.05
136.21
136.17
134.20
131.70
131.47
129.66
129.41
128.93
128.57
126.92
126.80
49.99
21.53
19.37
200
192
184
176
168
160
152
144
136
128
120
112
104
96
88
80
72
64
56
48
40
32
24
16
8
0

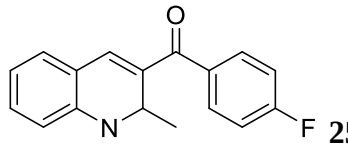
O
N
F

25d

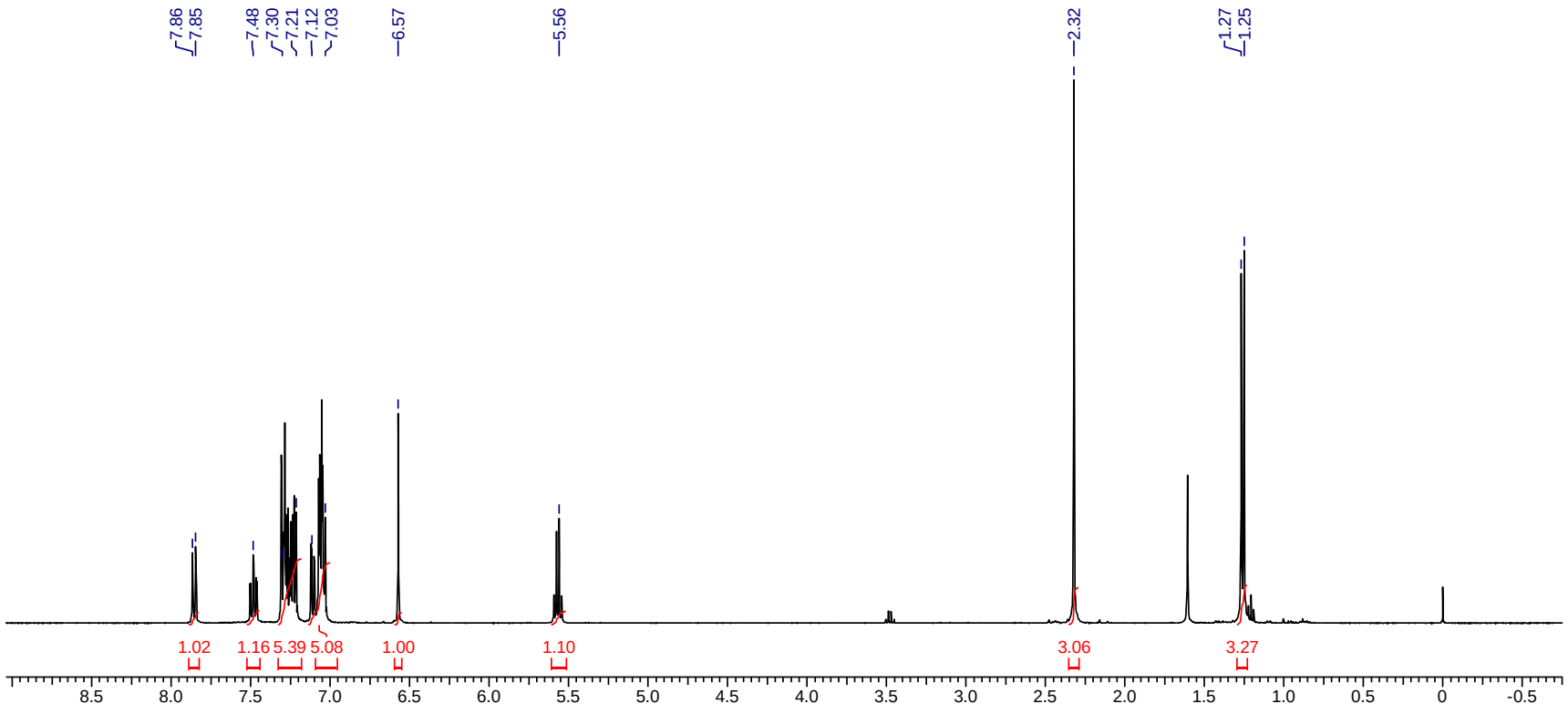
7.86
7.85
7.48
7.30
7.21
7.12
7.03
6.57
5.56
2.32
1.27
1.25
1.02
1.16
5.39
5.08
1.00
1.10
3.06
3.27
8.5
8.0
7.5
7.0
6.5
6.0
5.5
5.0
4.5
4.0
3.5
3.0
2.5
2.0
1.5
1.0
0.5
0
-0.5

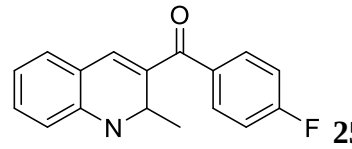
O
N
F

25d

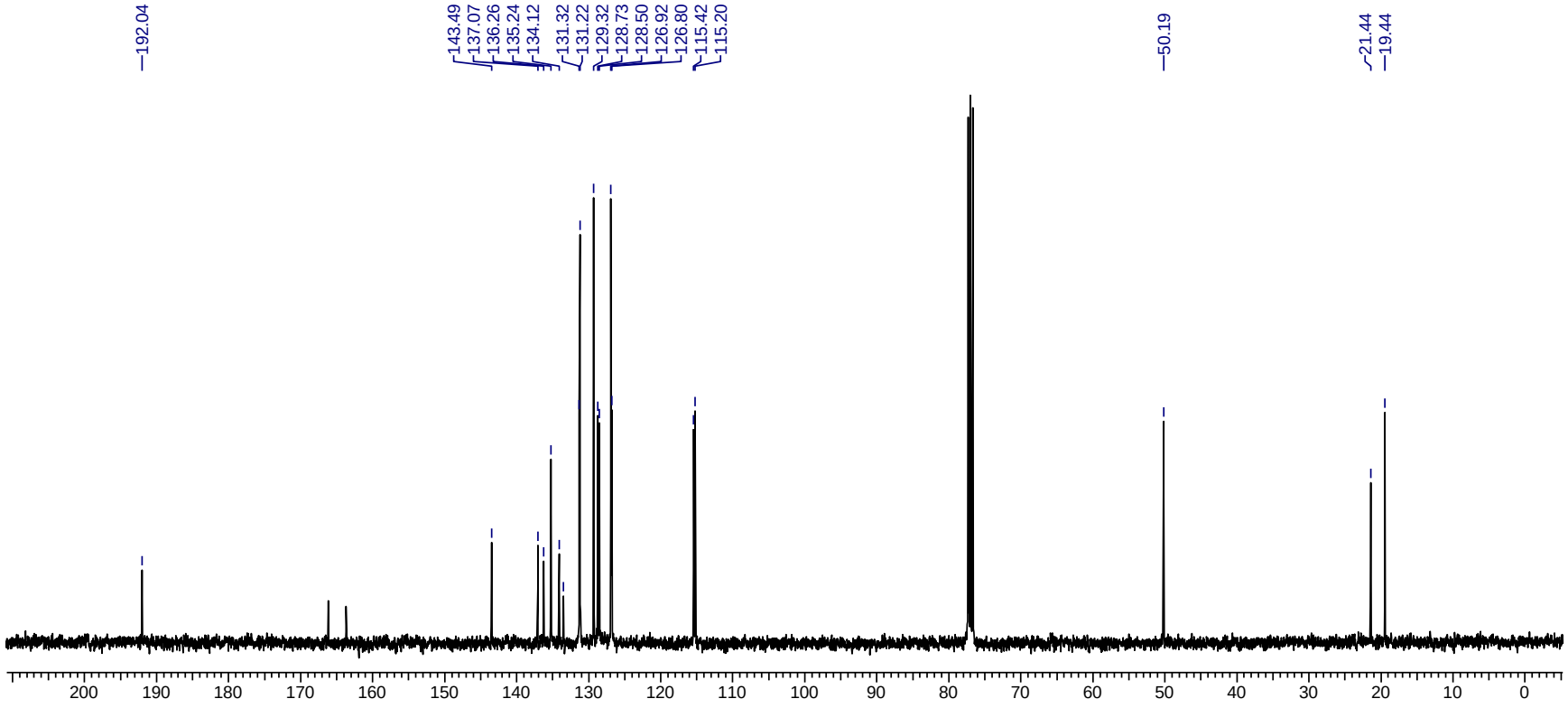
192.04
143.49
137.07
136.26
135.24
134.12
131.32
131.22
129.32
128.73
128.50
126.92
126.80
115.42
115.20
50.19
21.44
19.44
200
190
180
170
160
150
140
130
120
110
100
90
80
70
60
50
40
30
20
10
0

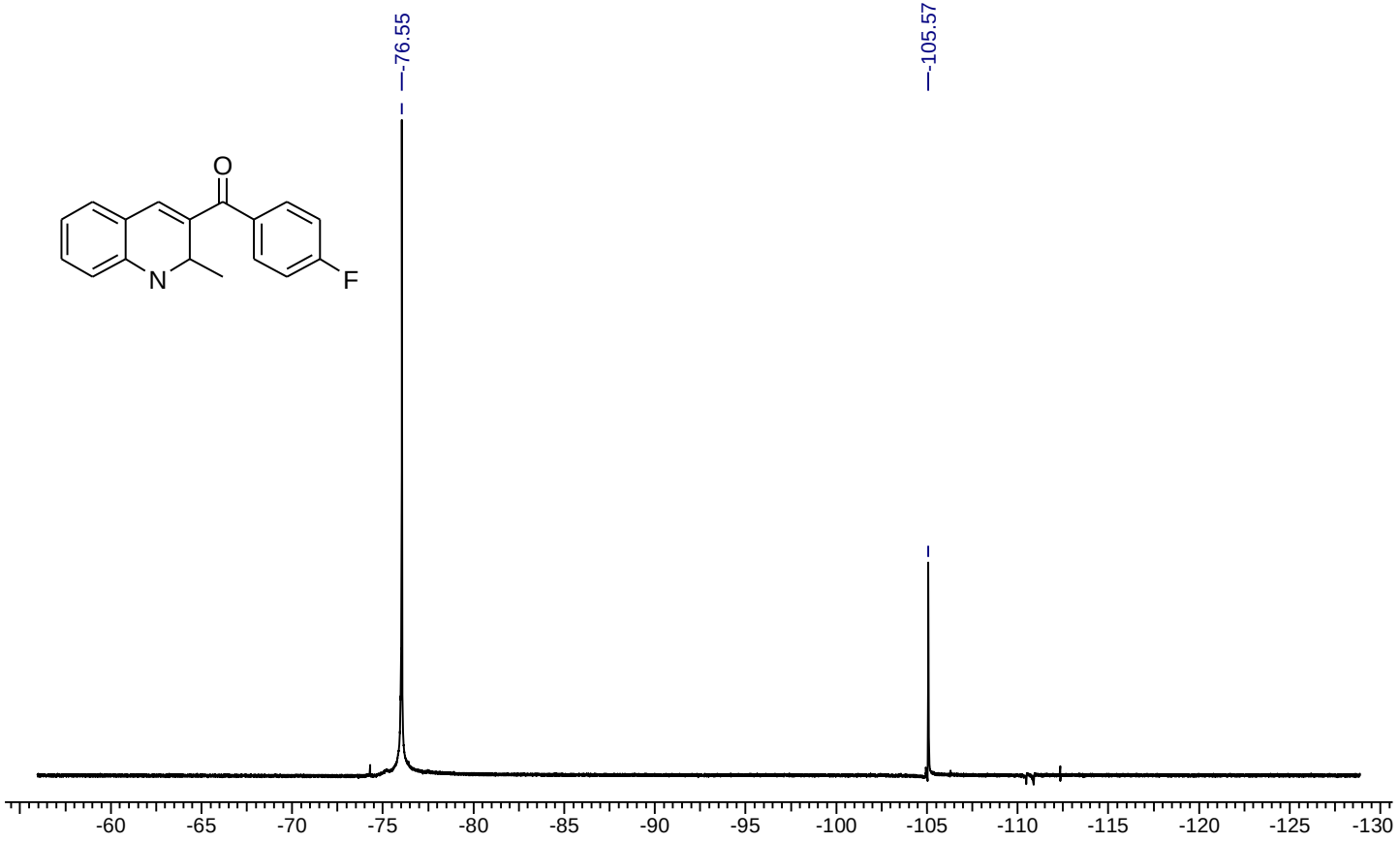
-76.55
-105.57
O
N
F
-60
-65
-70
-75
-80
-85
-90
-95
-100
-105
-110
-115
-120
-125
-130

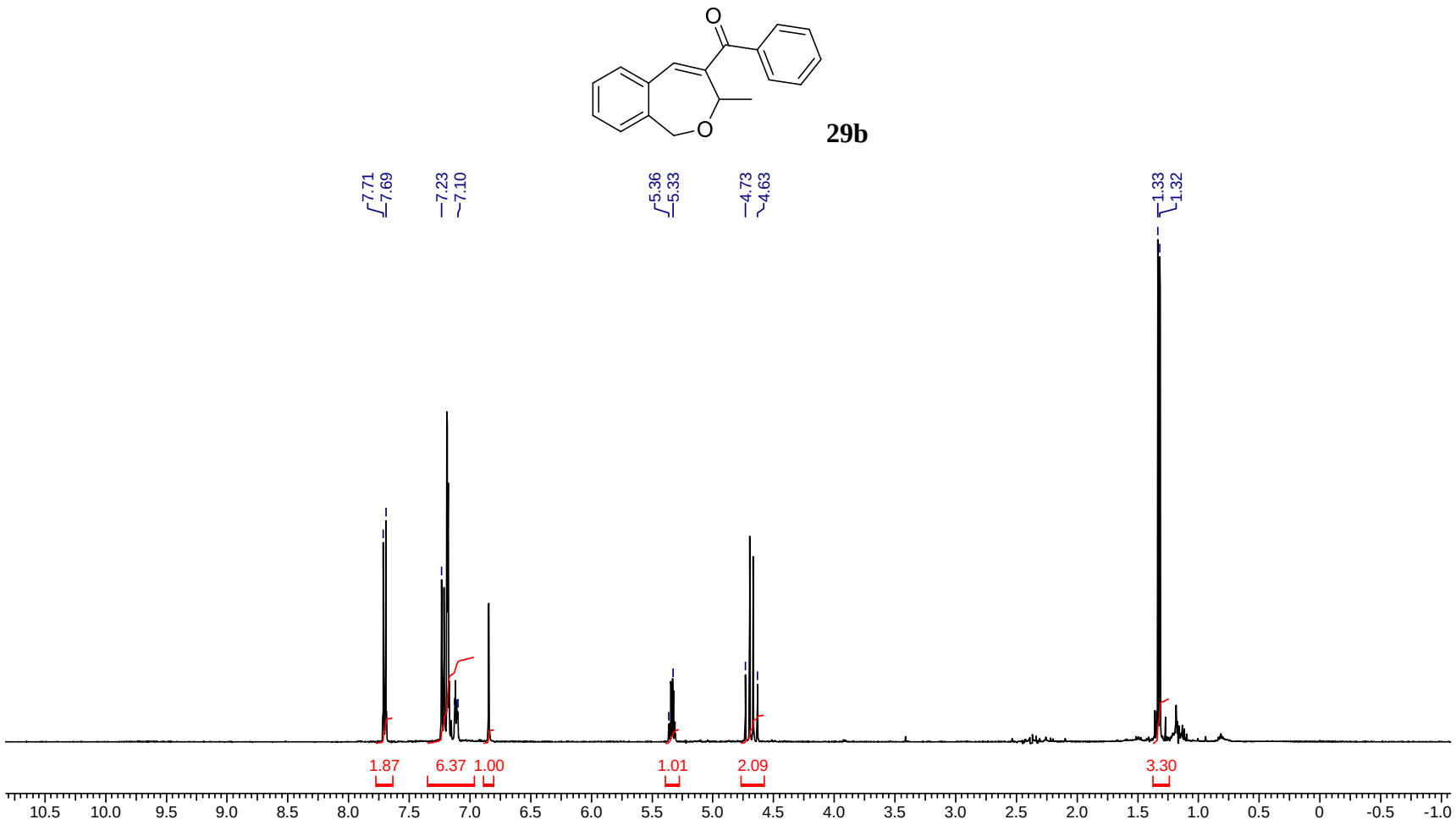
O
O
29b
7.71
7.69
7.23
7.10
5.36
5.33
4.73
4.63
1.33
1.32
1.87
6.37
1.00
1.01
2.09
3.30
10.5
10.0
9.5
9.0
8.5
8.0
7.5
7.0
6.5
6.0
5.5
5.0
4.5
4.0
3.5
3.0
2.5
2.0
1.5
1.0
0.5
0
-0.5
-1.0

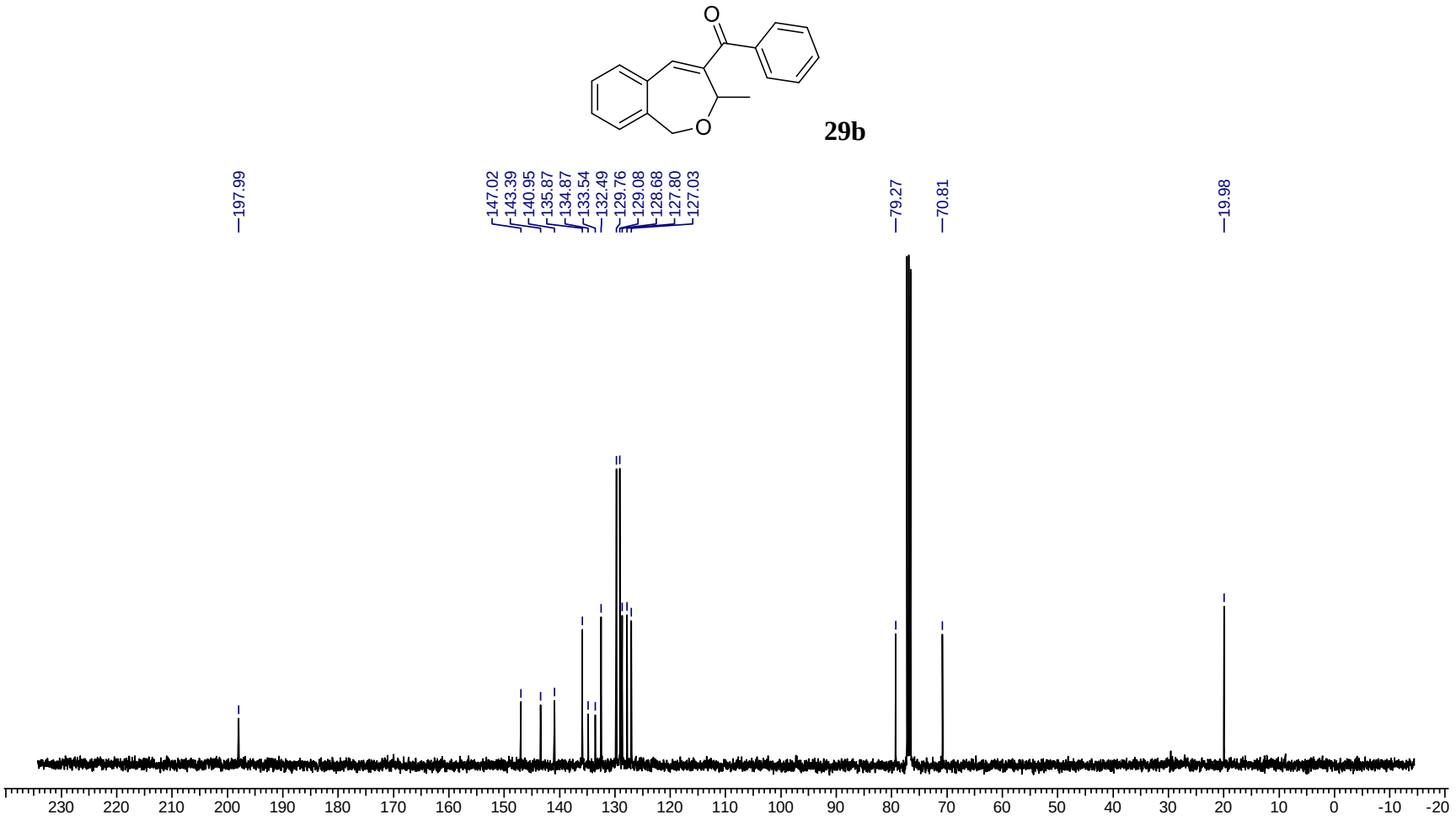
O
O
29b
197.99
147.02
143.39
140.95
135.87
134.87
133.54
132.49
129.76
129.08
128.68
127.80
127.03
79.27
70.81
19.98
230 220 210 200 190 180 170 160 150 140 130 120 110 100 90 80 70 60 50 40 30 20 10 0 -10 -20

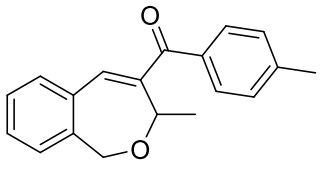
O
O

29c

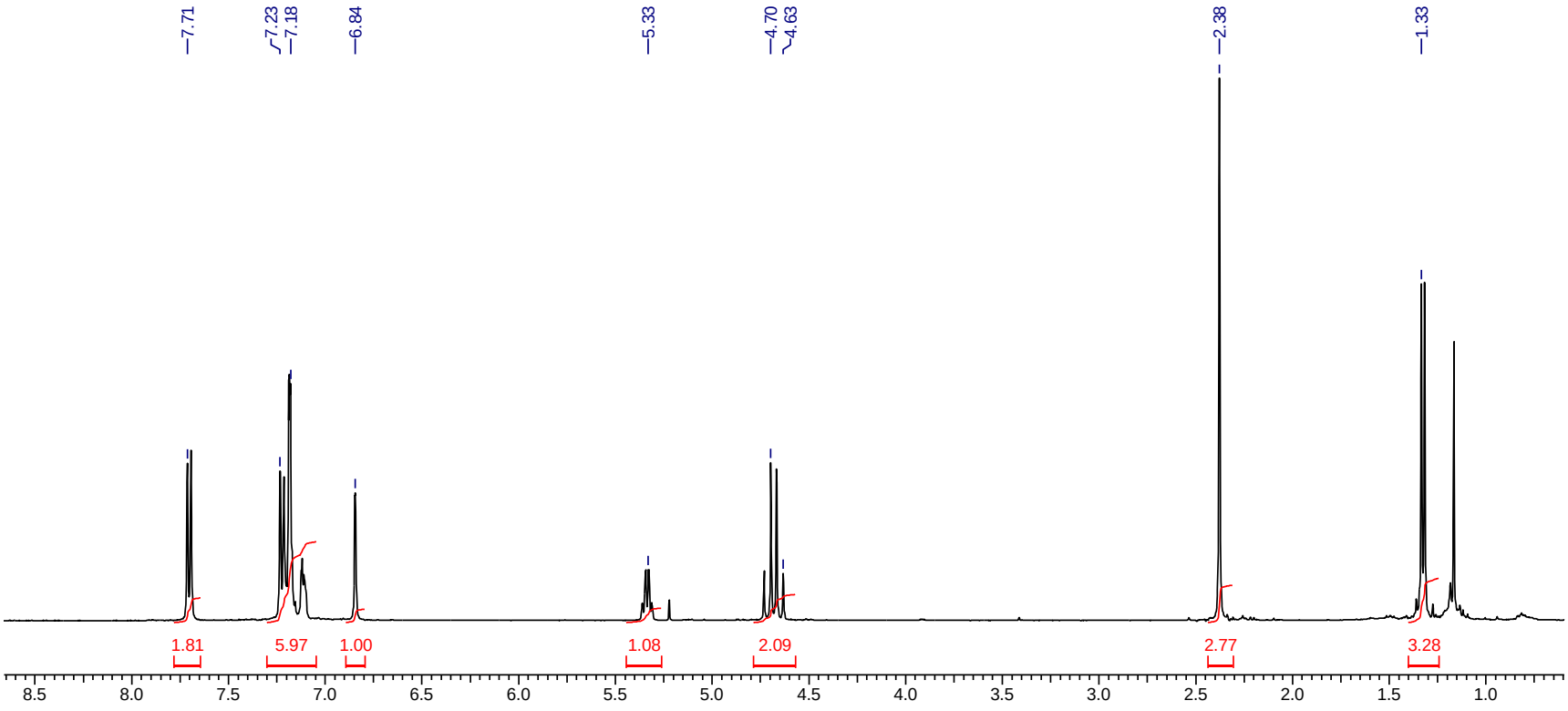
7.71
7.23
7.18
6.84
5.33
4.70
4.63
2.38
1.33
1.81
5.97
1.00
1.08
2.09
2.77
3.28
8.5
8.0
7.5
7.0
6.5
6.0
5.5
5.0
4.5
4.0
3.5
3.0
2.5
2.0
1.5
1.0

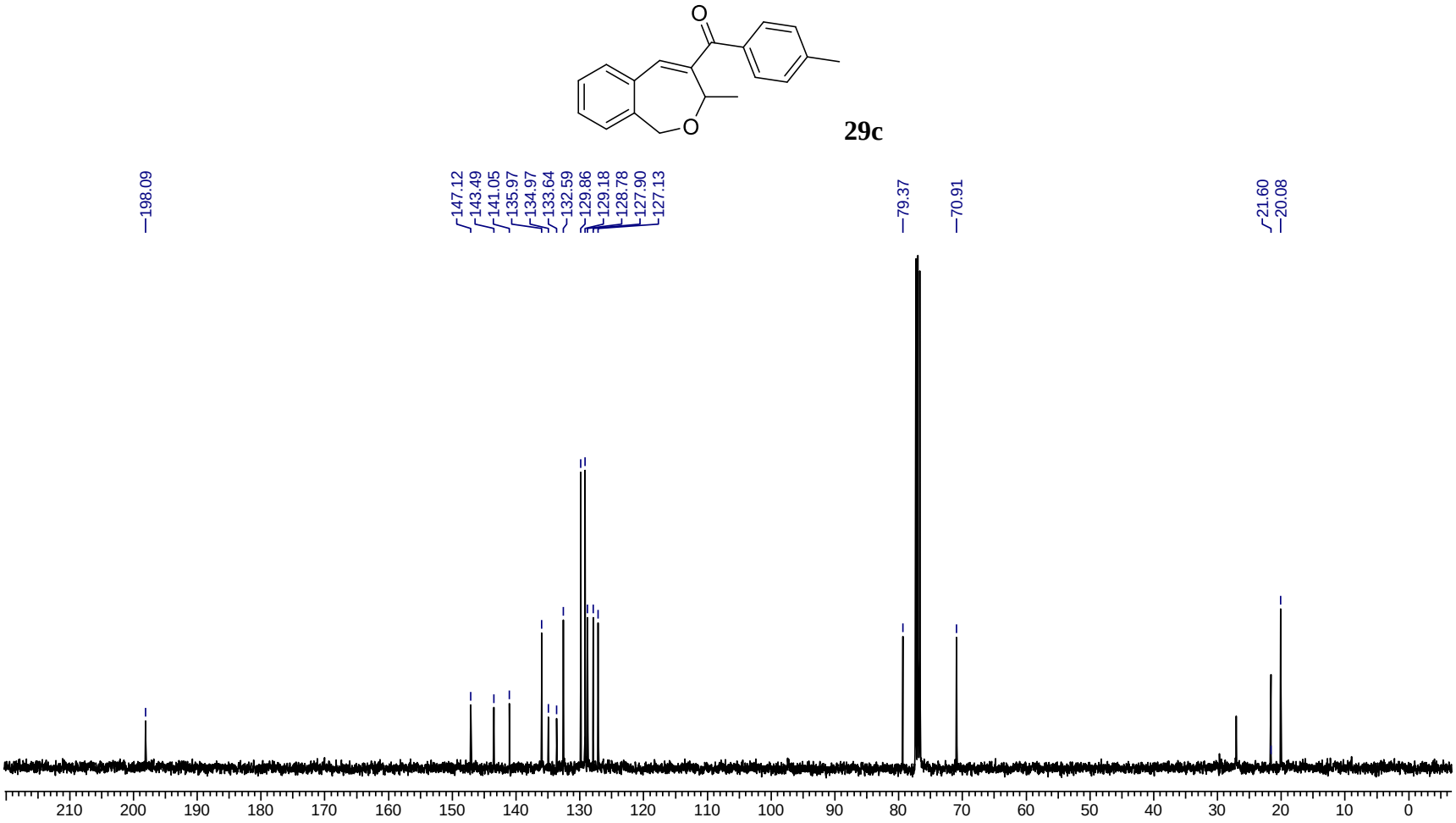
O
O
29c
198.09
147.12
143.49
141.05
135.97
134.97
133.64
132.59
129.86
129.18
128.78
127.90
127.13
79.37
70.91
21.60
20.08
210
200
190
180
170
160
150
140
130
120
110
100
90
80
70
60
50
40
30
20
10
0

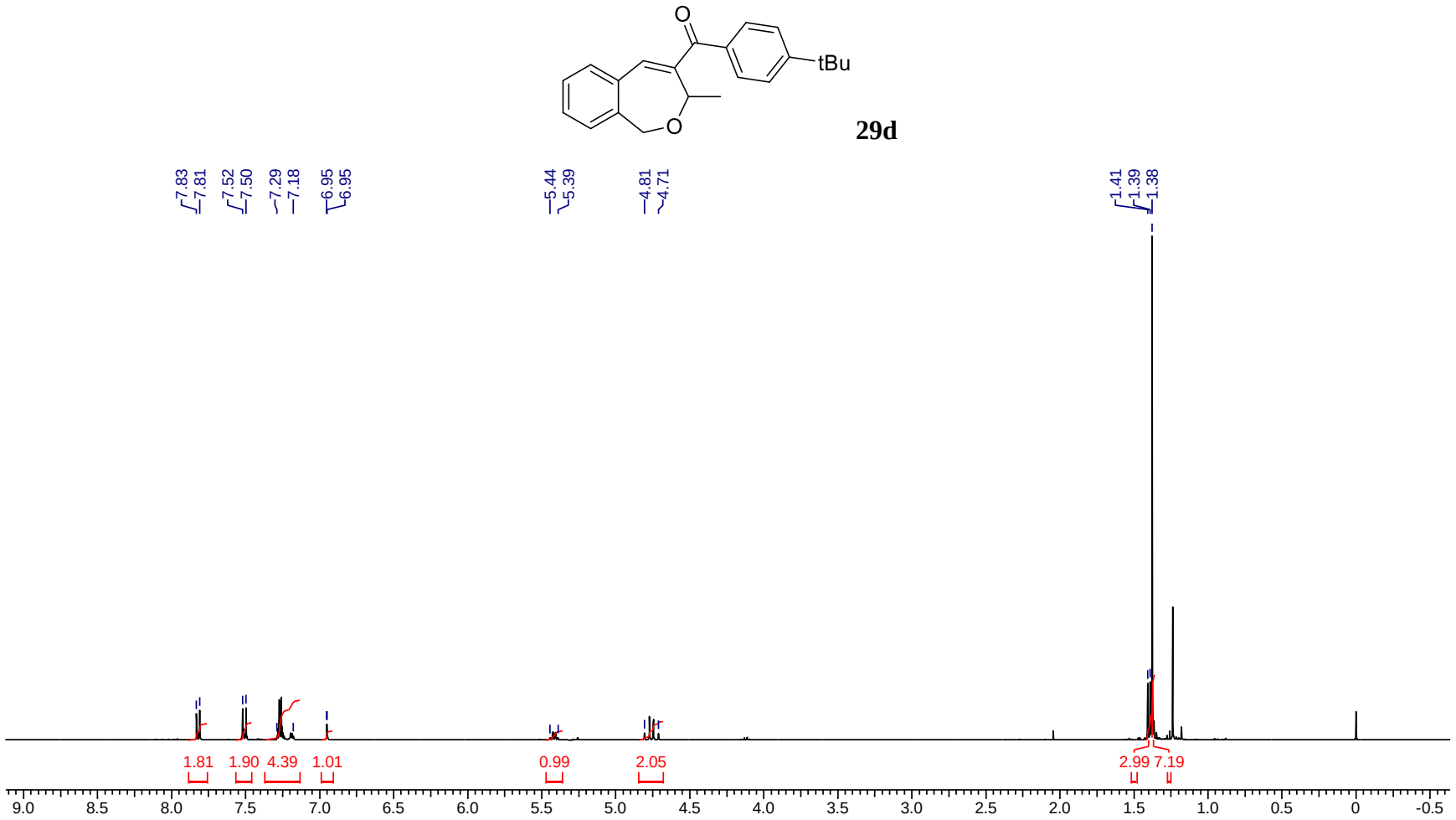
O
tBu
O
29d
7.83
7.81
7.52
7.50
7.29
7.18
6.95
6.95
5.44
5.39
4.81
4.71
1.41
1.39
1.38
1.81
1.90
4.39
1.01
0.99
2.05
2.99
7.19
9.0
8.5
8.0
7.5
7.0
6.5
6.0
5.5
5.0
4.5
4.0
3.5
3.0
2.5
2.0
1.5
1.0
0.5
0
-0.5

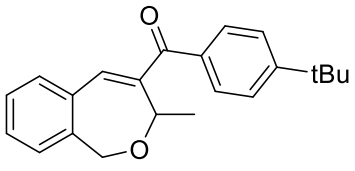
O
tBu
O

29d

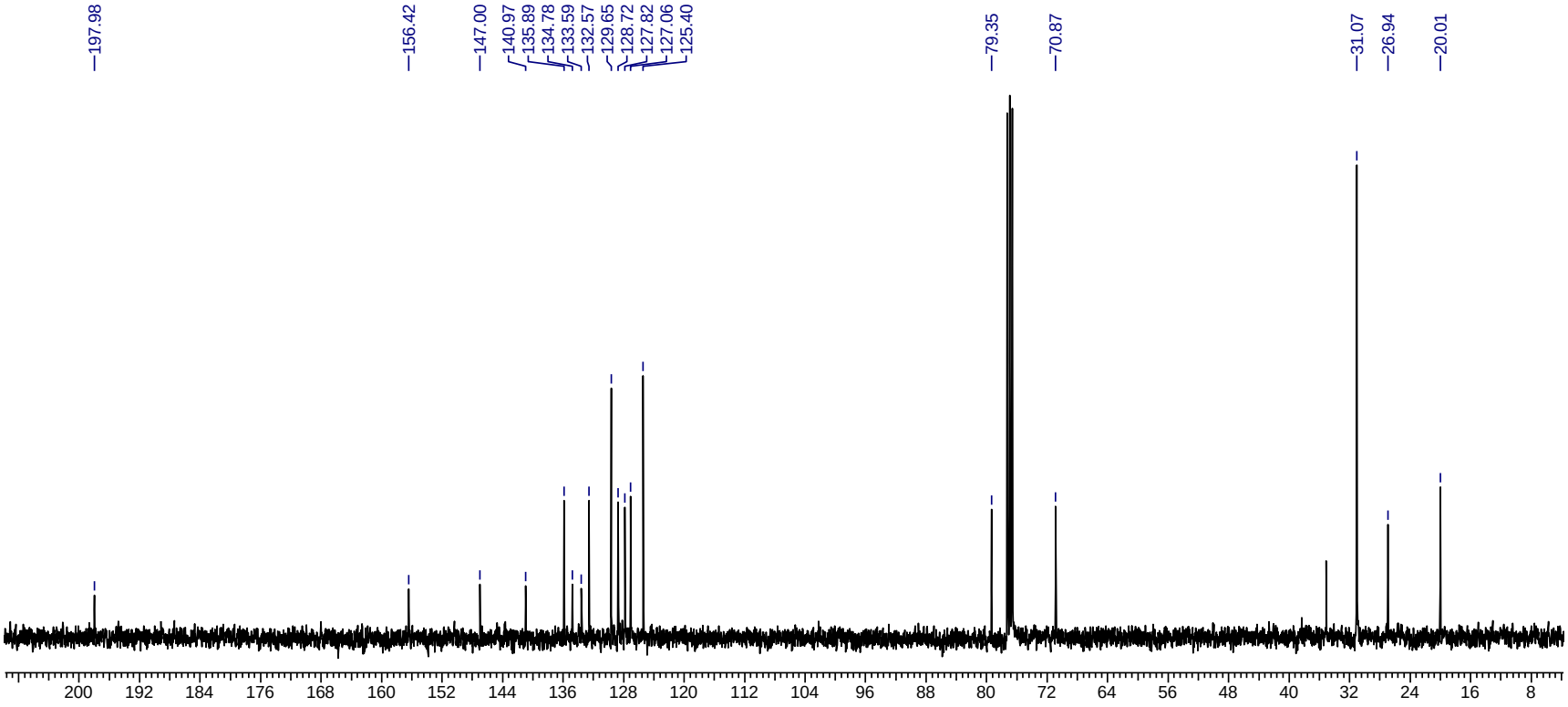
197.98
156.42
147.00
140.97
135.89
134.78
133.59
132.57
129.65
128.72
127.82
127.06
125.40
79.35
70.87
31.07
26.94
20.01
200
192
184
176
168
160
152
144
136
128
120
112
104
96
88
80
72
64
56
48
40
32
24
16
8

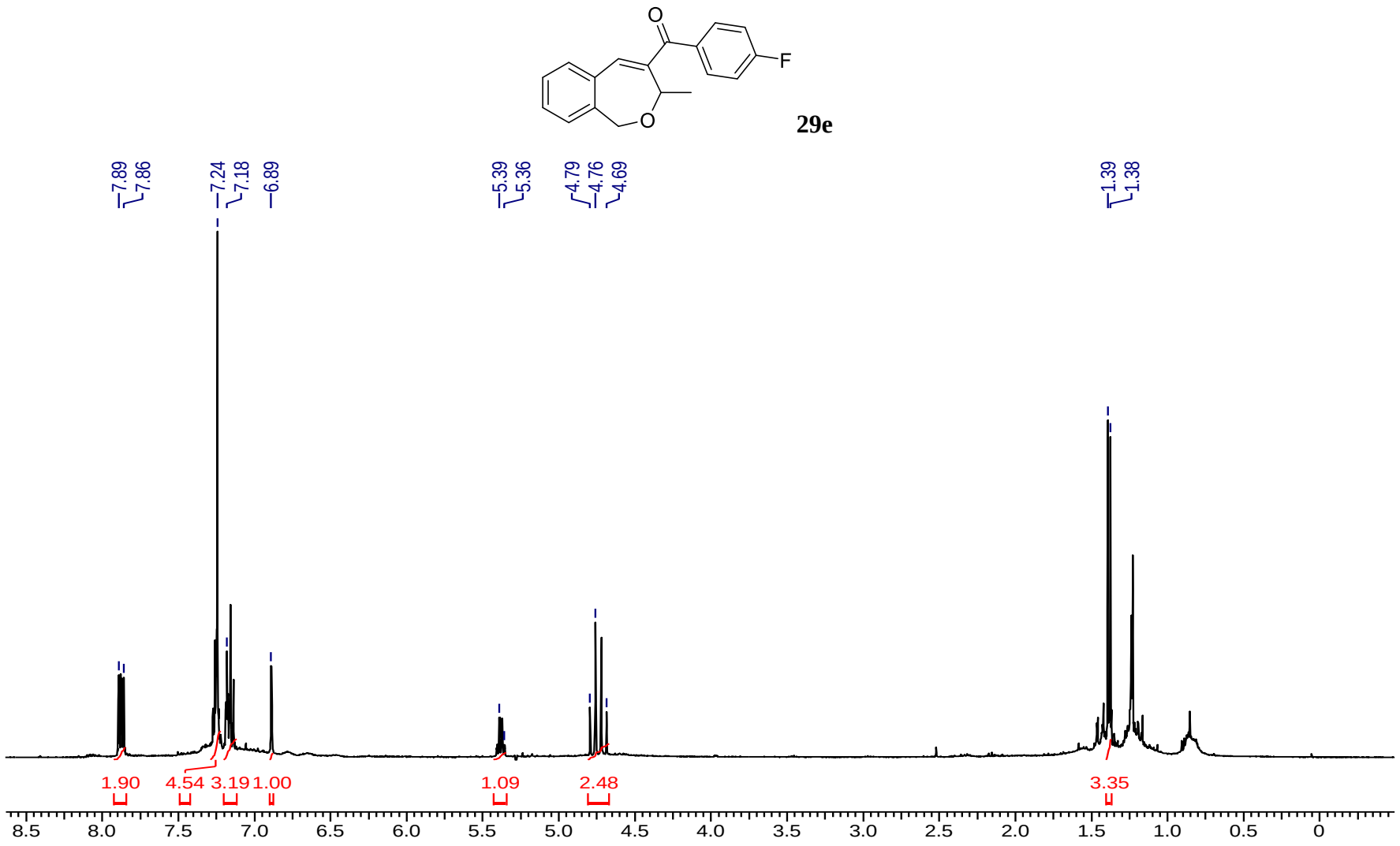
O
F
O
29e
7.89
7.86
7.24
7.18
6.89
5.39
5.36
4.79
4.76
4.69
1.39
1.38
1.90
4.54
3.19
1.00
1.09
2.48
3.35
8.5
8.0
7.5
7.0
6.5
6.0
5.5
5.0
4.5
4.0
3.5
3.0
2.5
2.0
1.5
1.0
0.5
0

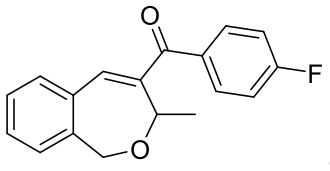
O
F
O

29e

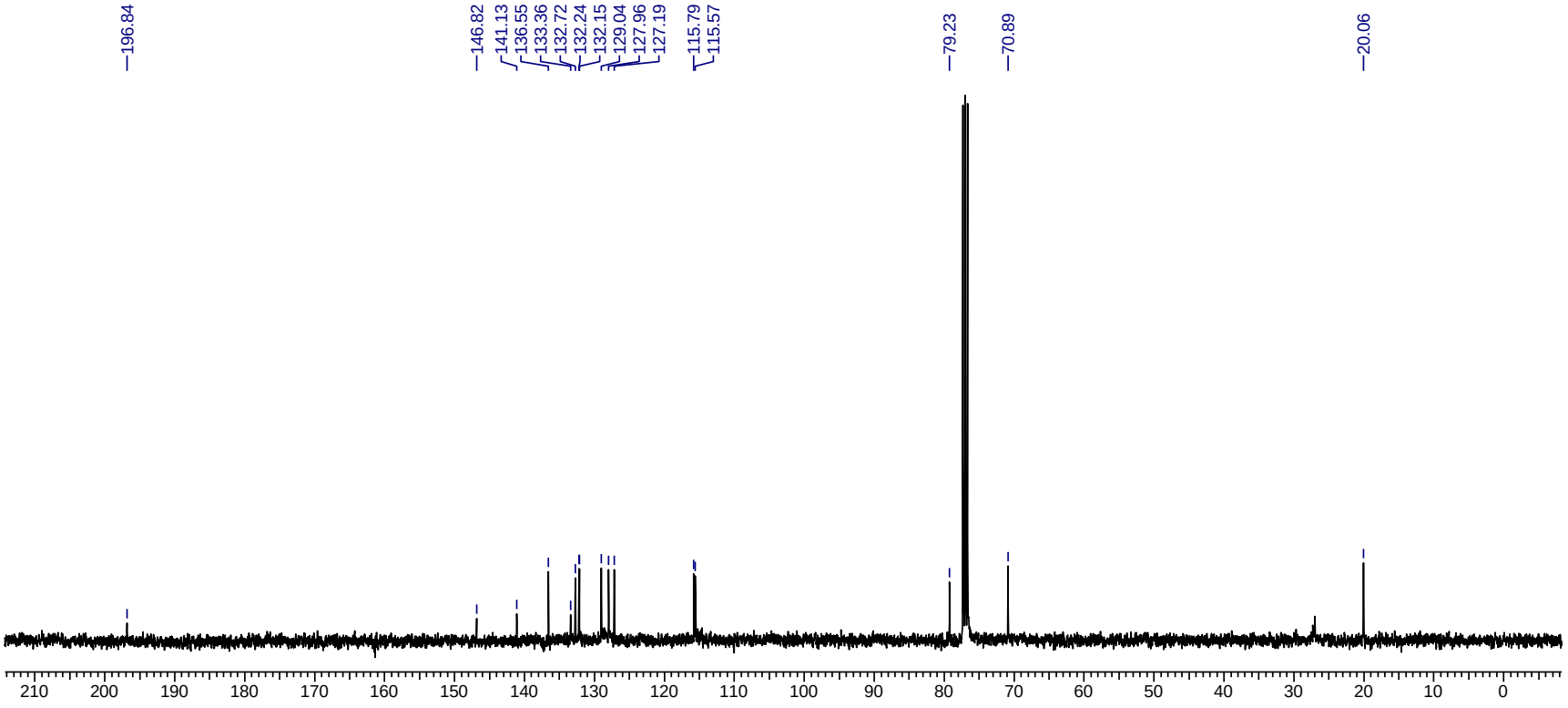
196.84
146.82
141.13
136.55
133.36
132.72
132.24
132.15
129.04
127.96
127.19
115.79
115.57
79.23
70.89
20.06
210
200
190
180
170
160
150
140
130
120
110
100
90
80
70
60
50
40
30
20
10
0

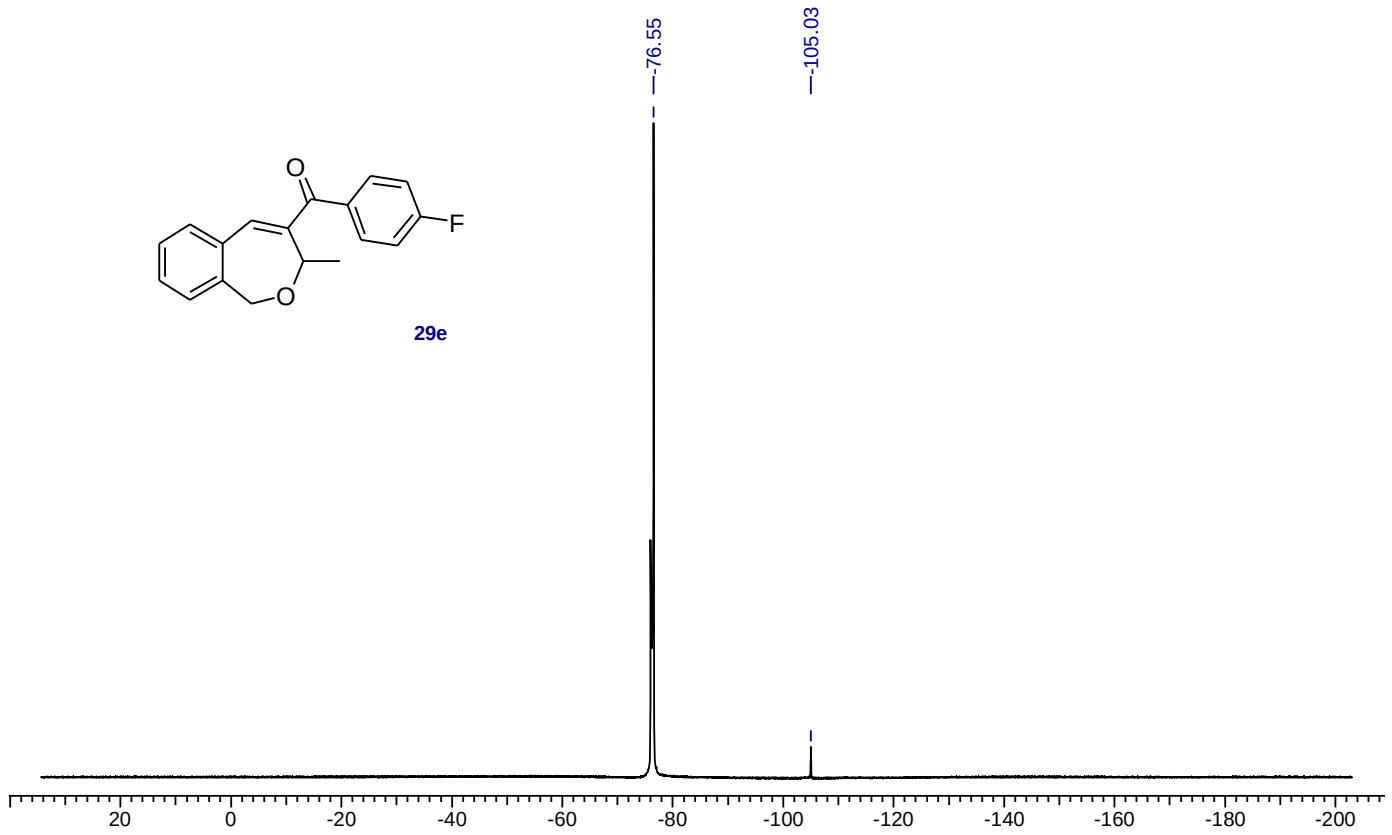
-76.55
-105.03
O
F
O
29e
20
0
-20
-40
-60
-80
-100
-120
-140
-160
-180
-200

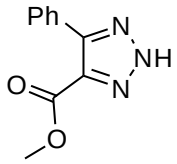
Ph
N
NH
N
O
O

77

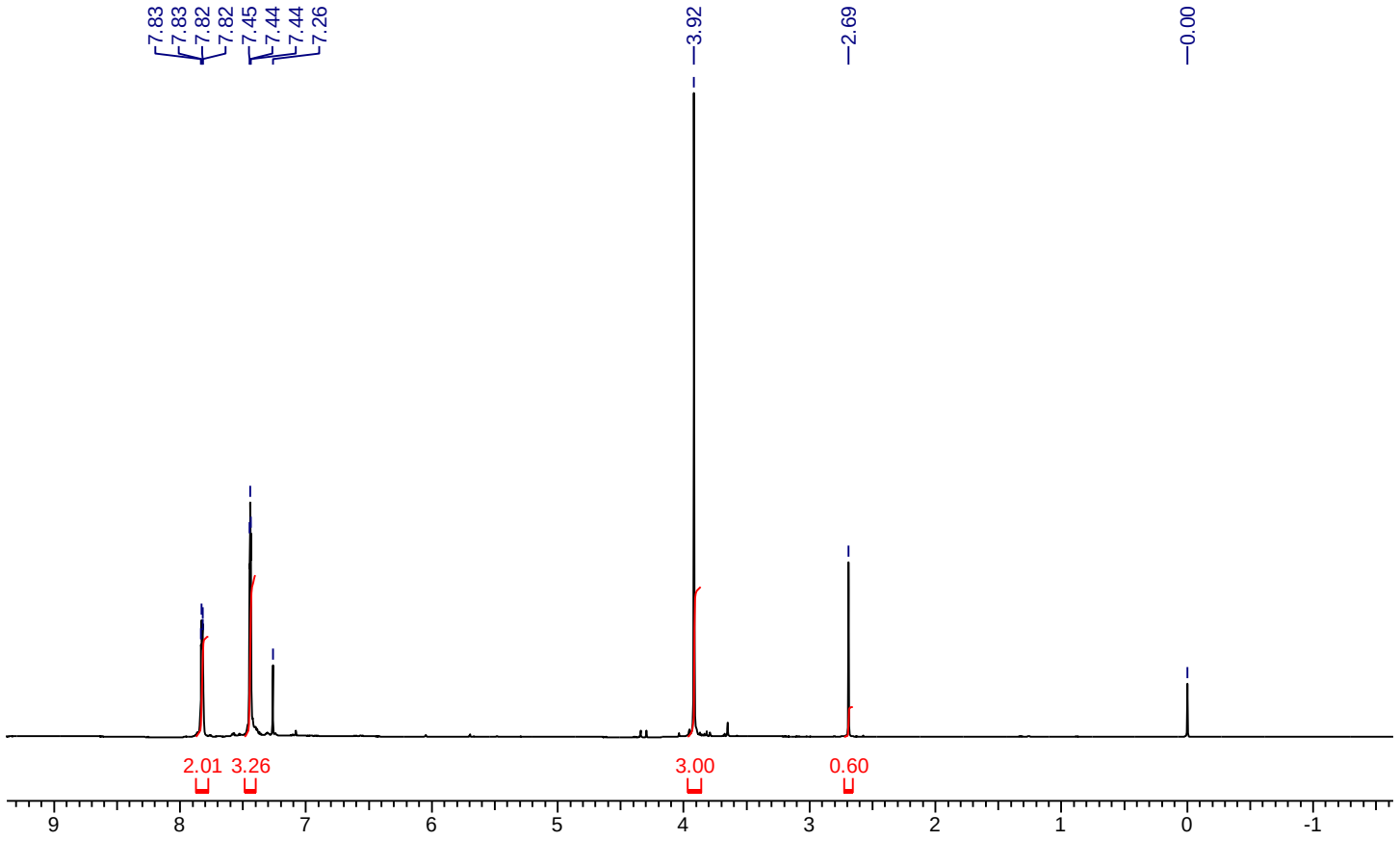
7.83
7.83
7.82
7.82
7.45
7.44
7.44
7.26
3.92
2.69
0.00
2.01
3.26
3.00
0.60
9
8
7
6
5
4
3
2
1
0
-1

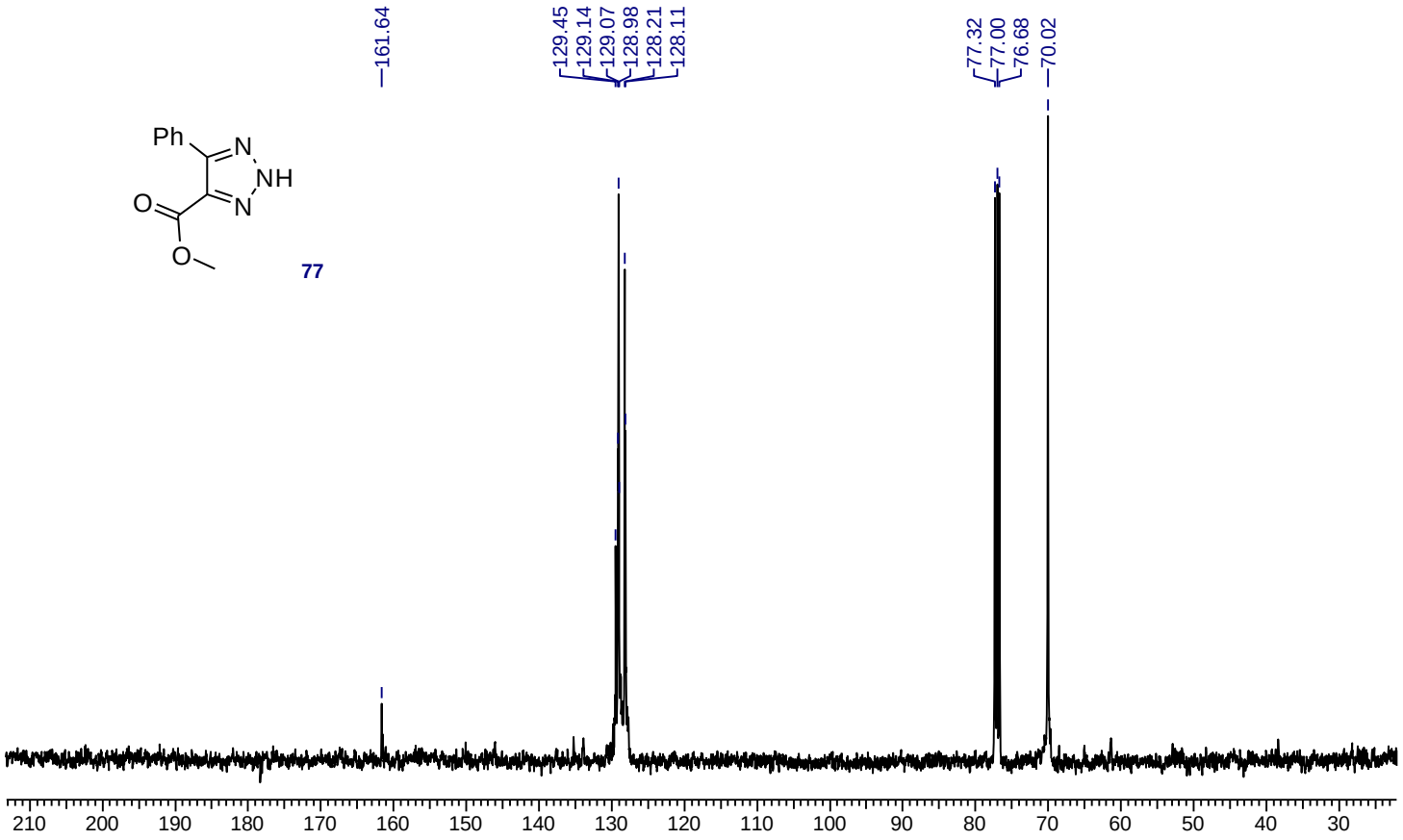
161.64
129.45
129.14
129.07
128.98
128.21
128.11
77.32
77.00
76.68
70.02
Ph
N
NH
N
O
O
77
210
200
190
180
170
160
150
140
130
120
110
100
90
80
70
60
50
40
30

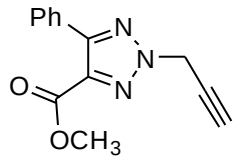
Ph
N
N
N
O
OCH3

79

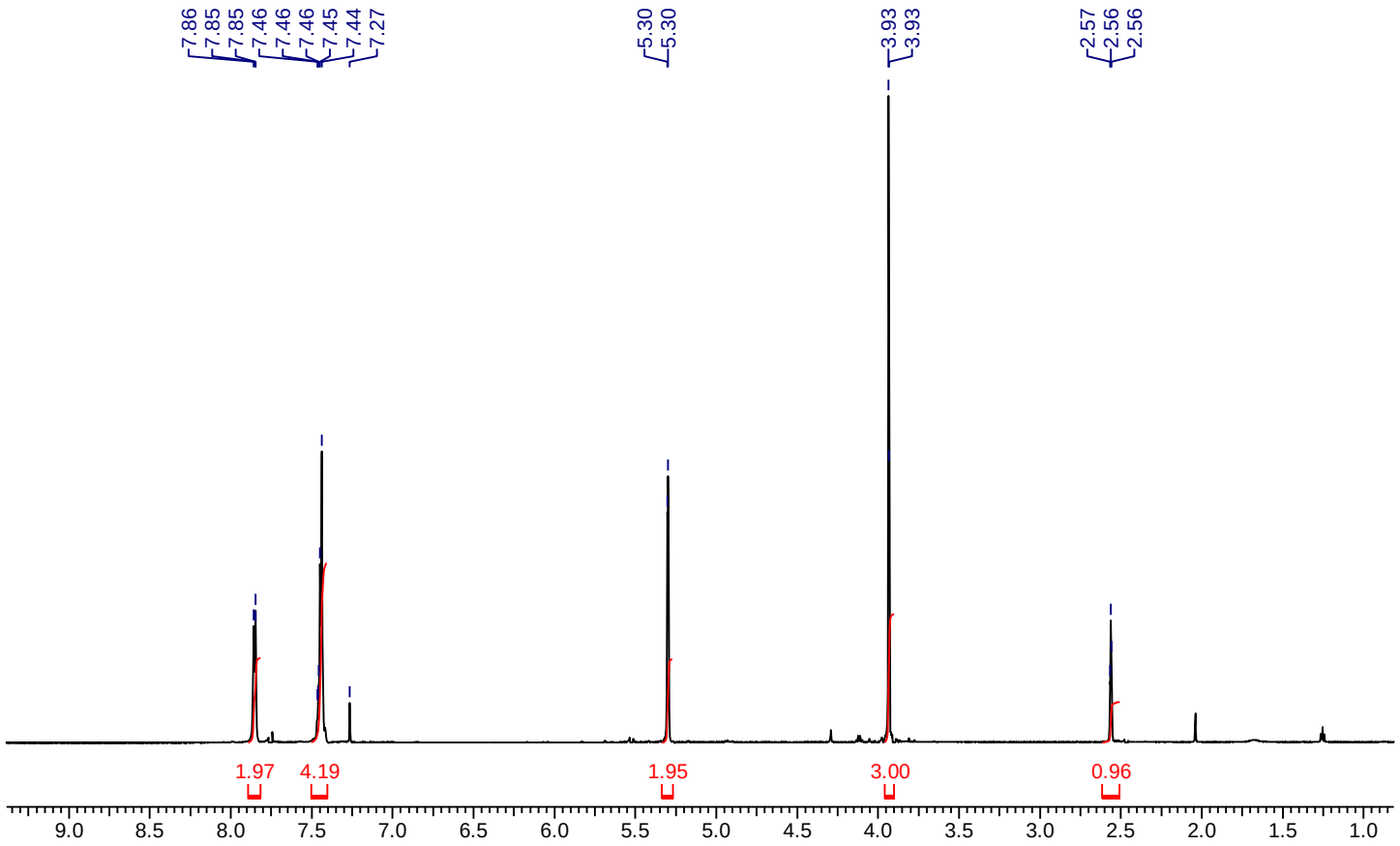
7.86
7.85
7.85
7.46
7.46
7.46
7.45
7.44
7.27
5.30
5.30
3.93
3.93
2.57
2.56
2.56
1.97
4.19
1.95
3.00
0.96
9.0
8.5
8.0
7.5
7.0
6.5
6.0
5.5
5.0
4.5
4.0
3.5
3.0
2.5
2.0
1.5
1.0

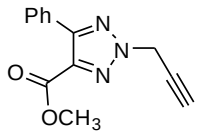
Ph
N
N
N
O
OCH3

79

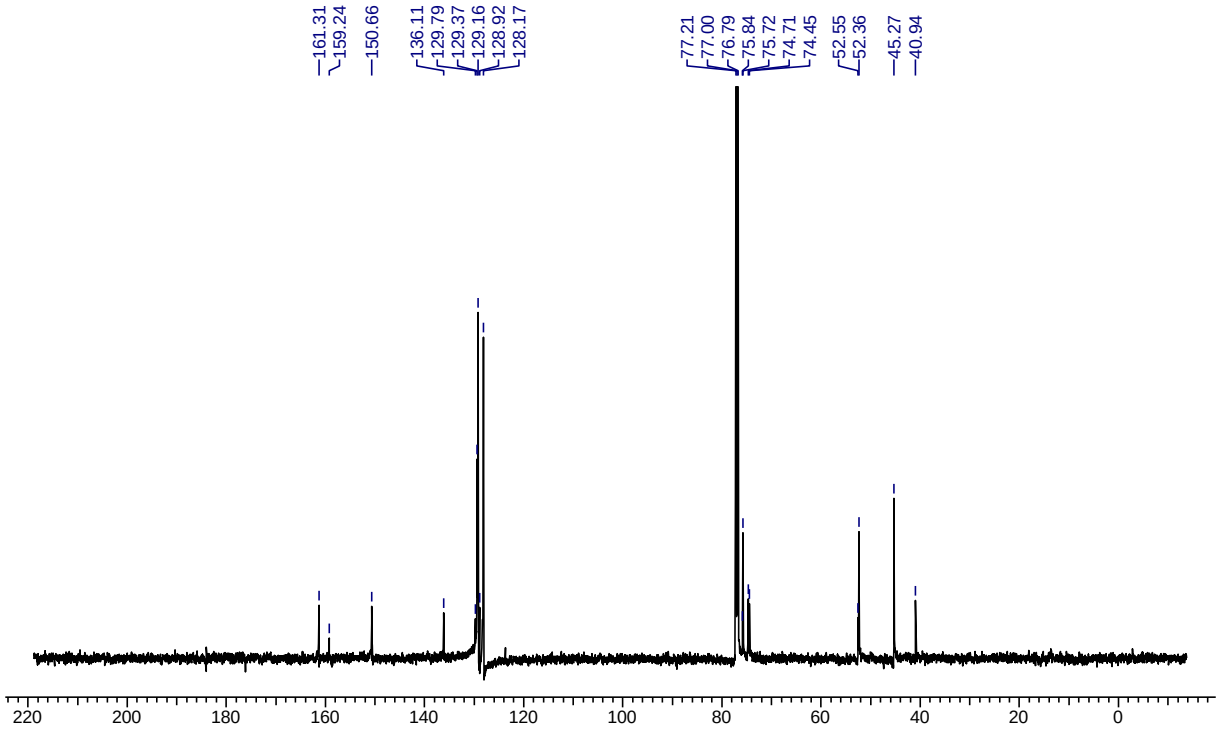
161.31
159.24
150.66
136.11
129.79
129.37
129.16
128.92
128.17
77.21
77.00
76.79
75.84
75.72
74.71
74.45
52.55
52.36
45.27
40.94
220
200
180
160
140
120
100
80
60
40
20
0

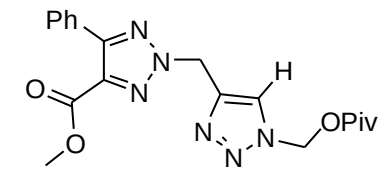
Ph
N
N
N
O
O
H
N
N
N
OPiv

80

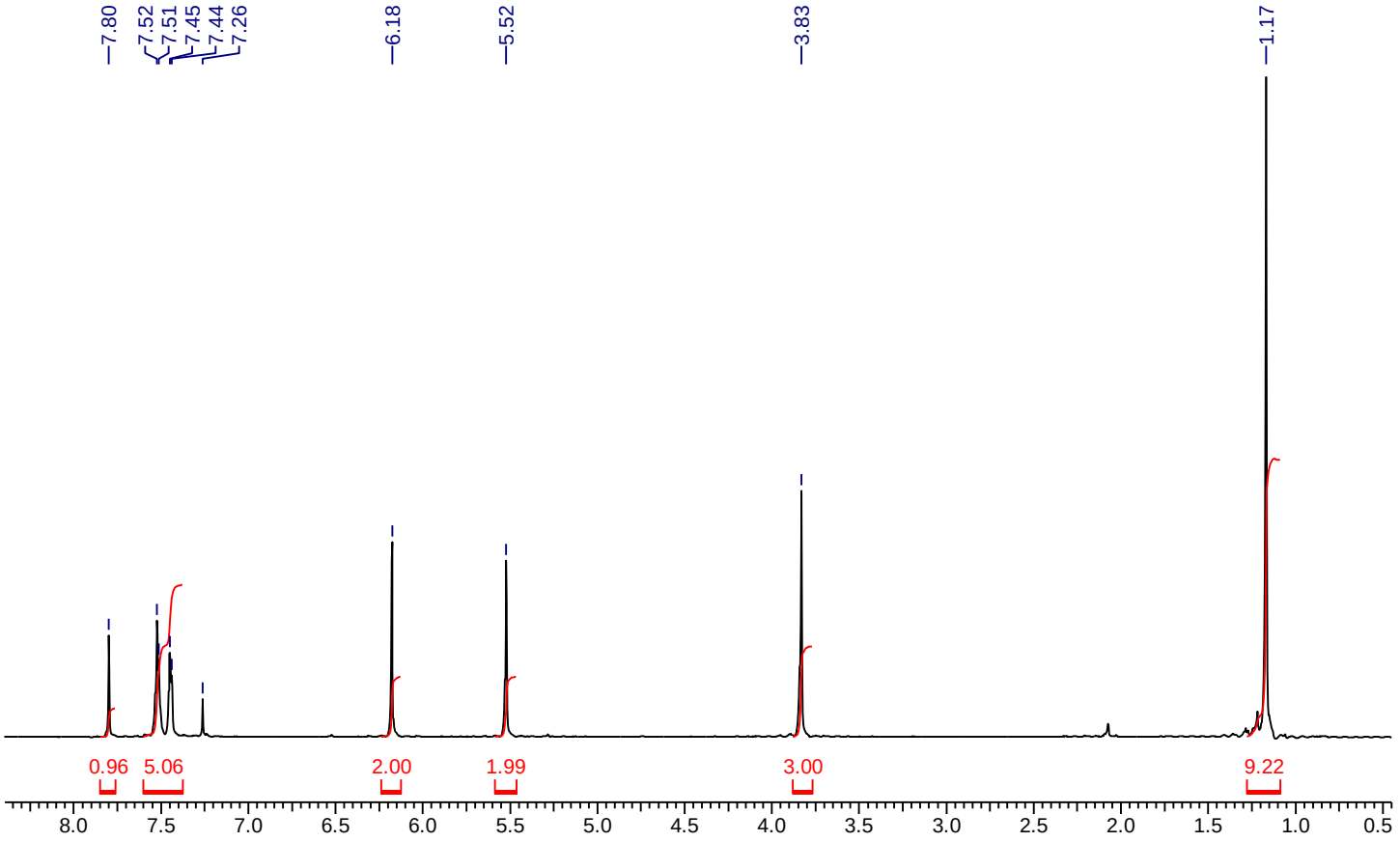
7.80
7.52
7.51
7.45
7.44
7.26
6.18
5.52
3.83
1.17
0.96
5.06
2.00
1.99
3.00
9.22
8.0
7.5
7.0
6.5
6.0
5.5
5.0
4.5
4.0
3.5
3.0
2.5
2.0
1.5
1.0
0.5

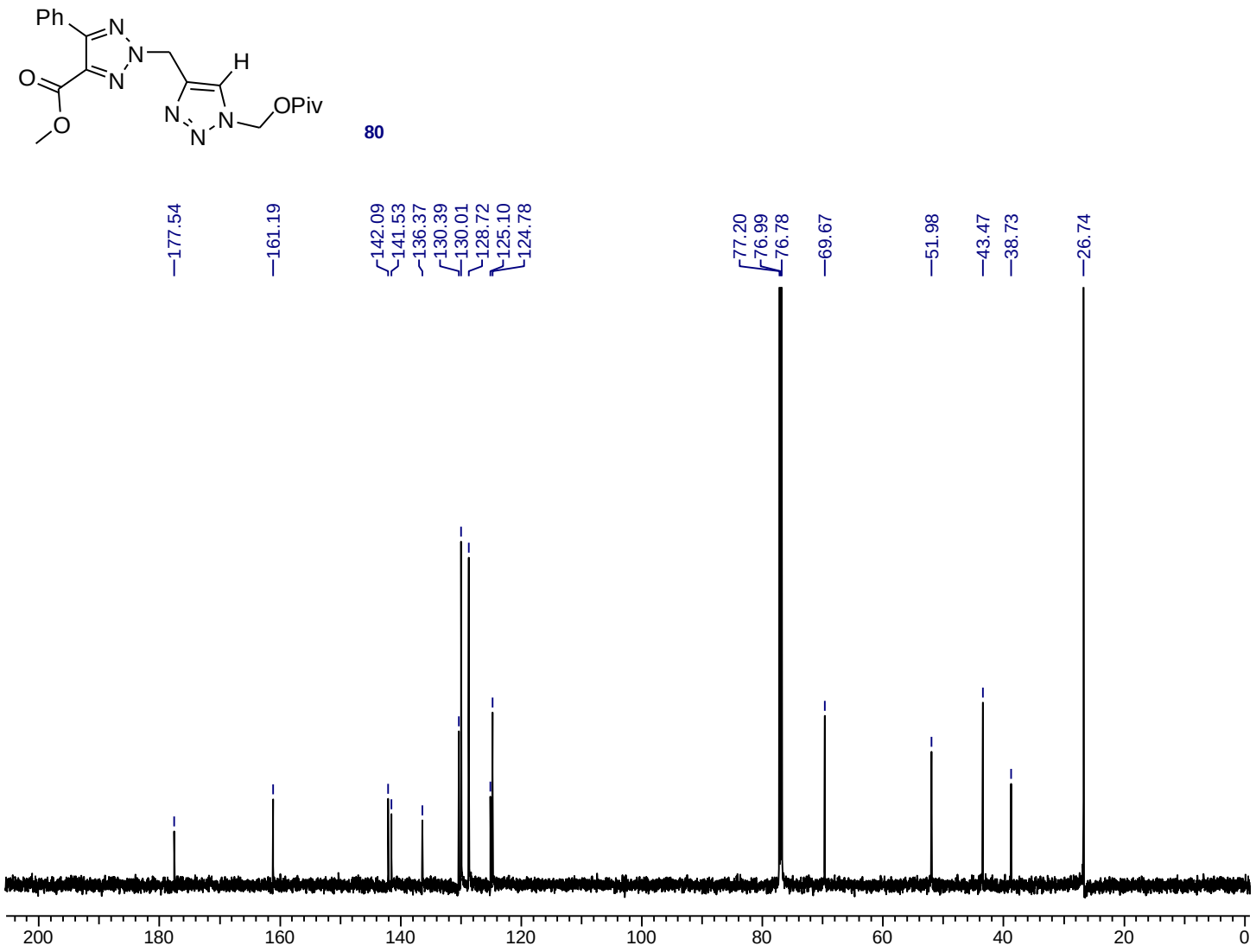
Ph
N
N
N
O
O
H
N
N
N
OPiv
80
177.54
161.19
142.09
141.53
136.37
130.39
130.01
128.72
125.10
124.78
77.20
76.99
76.78
69.67
51.98
43.47
38.73
26.74
200
180
160
140
120
100
80
60
40
20
0

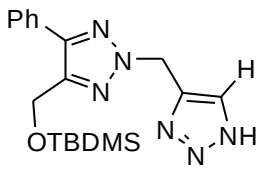
Ph
N
N
N
H
N
NH
N
OTBDMS

82

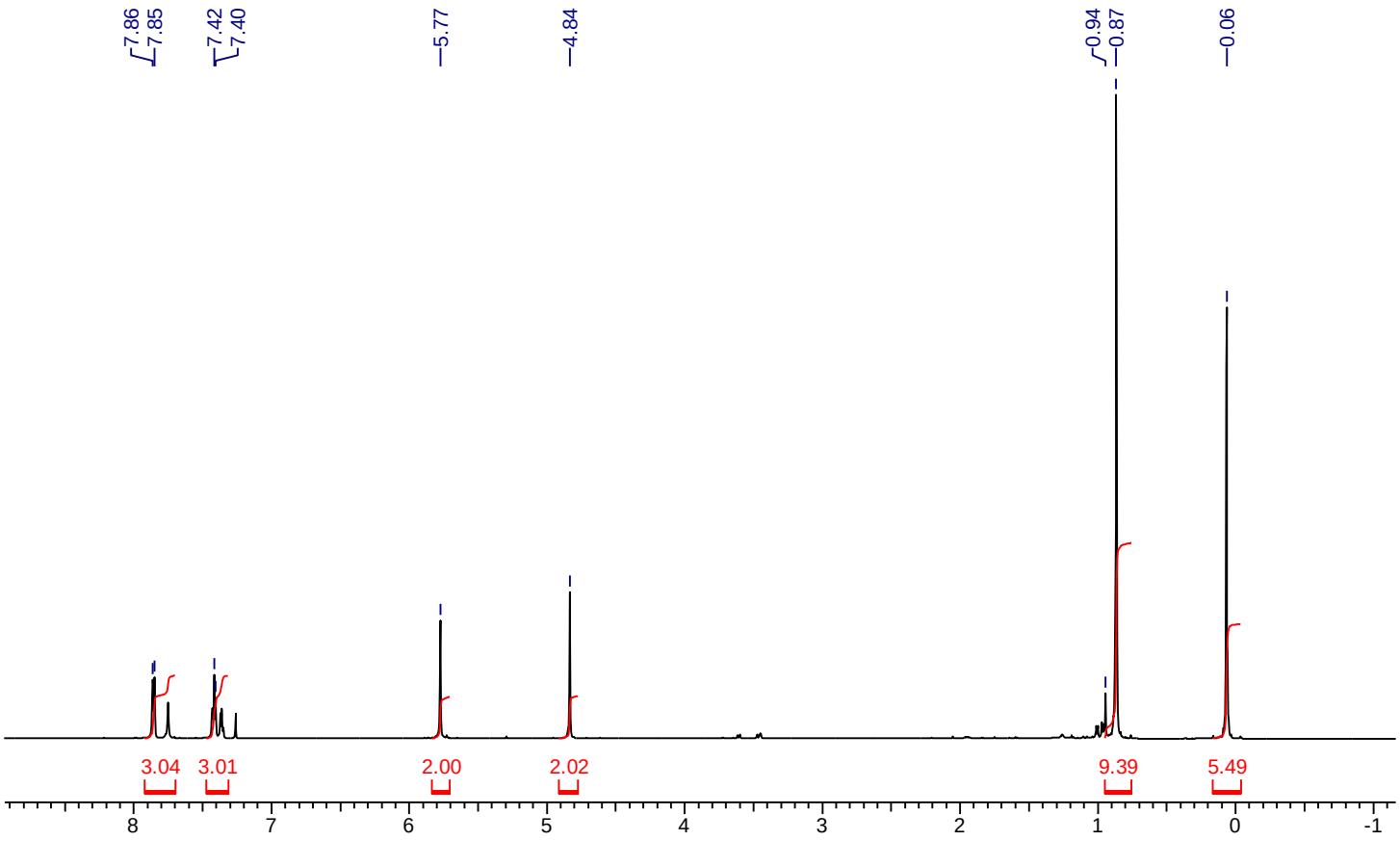
7.86
7.85
7.42
7.40
5.77
4.84
0.94
0.87
0.06
3.04
3.01
2.00
2.02
9.39
5.49
8
7
6
5
4
3
2
1
0
-1

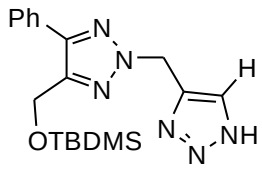
Ph
N
N
N
H
N
NH
N
OTBDMS

82

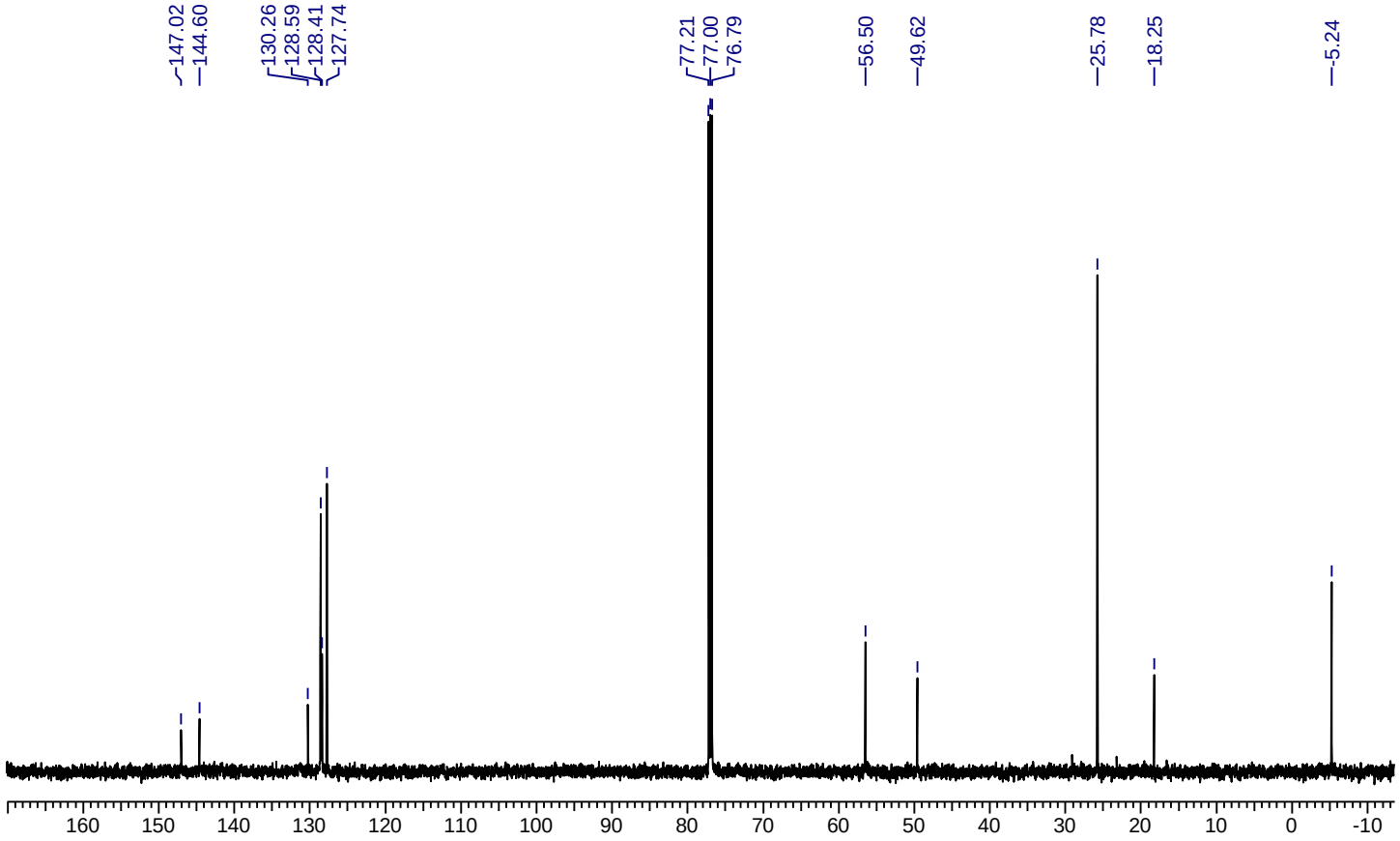
147.02
144.60
130.26
128.59
128.41
127.74
77.21
77.00
76.79
56.50
49.62
25.78
18.25
-5.24
160
150
140
130
120
110
100
90
80
70
60
50
40
30
20
10
0
-10

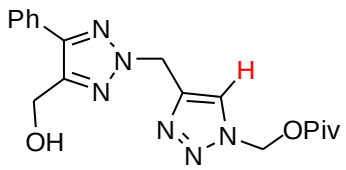
Ph
N
N
N
H
N
N
N
OPiv
OH

84

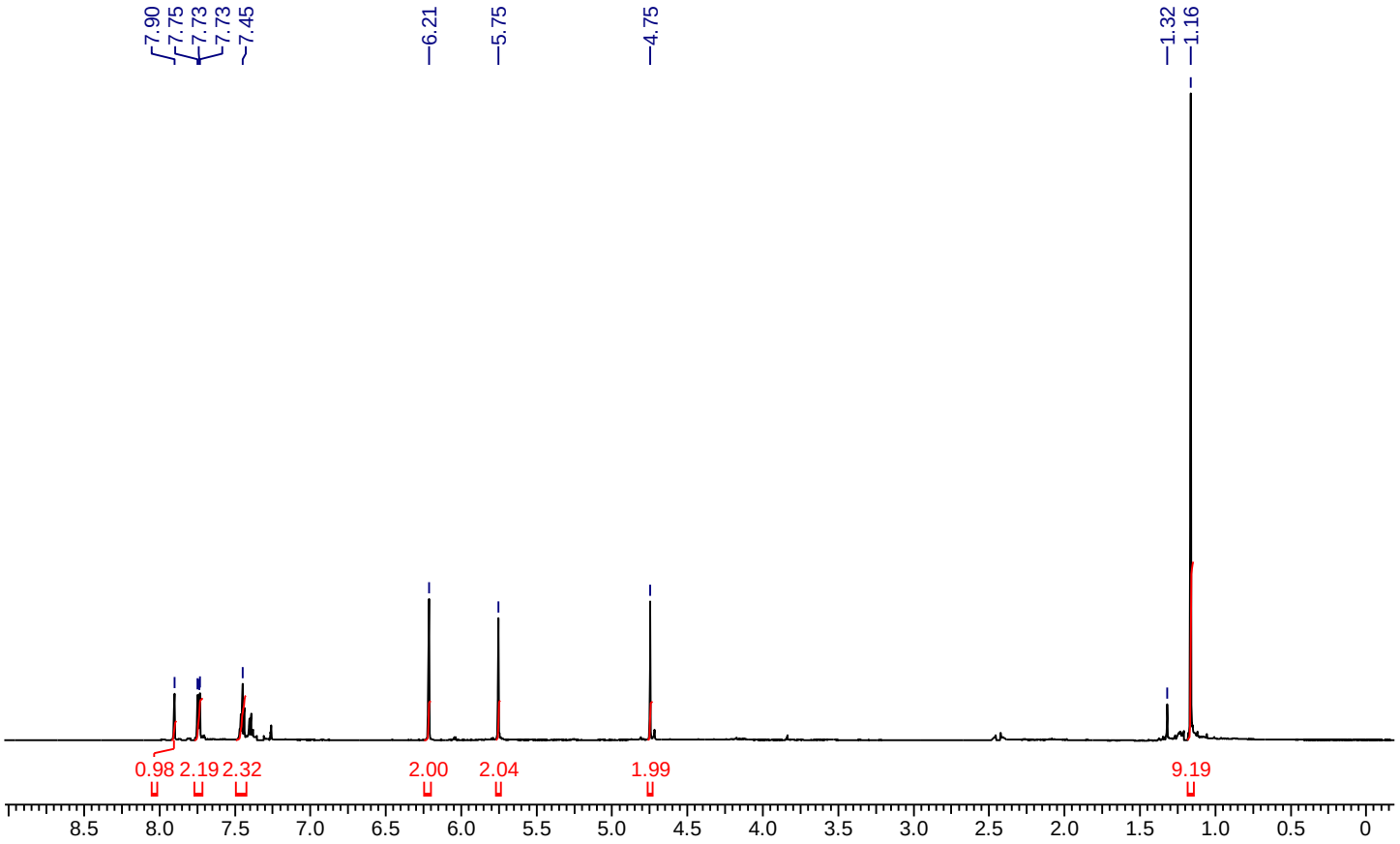
7.90
7.75
7.73
7.73
7.45
6.21
5.75
4.75
1.32
1.16
0.98
2.19
2.32
2.00
2.04
1.99
9.19
8.5
8.0
7.5
7.0
6.5
6.0
5.5
5.0
4.5
4.0
3.5
3.0
2.5
2.0
1.5
1.0
0.5
0

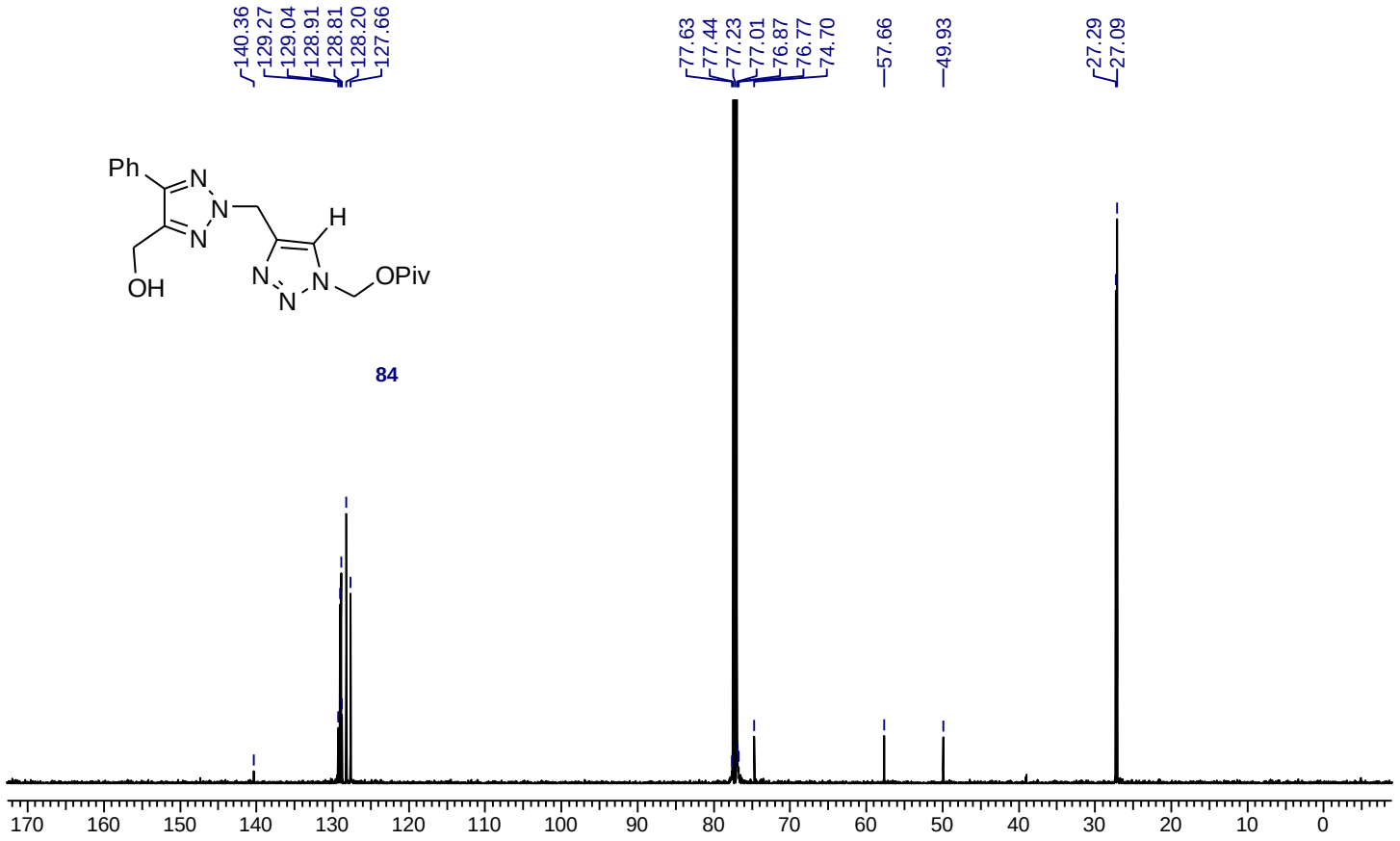
140.36
129.27
129.04
128.91
128.81
128.20
127.66
77.63
77.44
77.23
77.01
76.87
76.77
74.70
57.66
49.93
27.29
27.09
Ph
N
N
N
H
N
N
N
OPiv
OH
84
170
160
150
140
130
120
110
100
90
80
70
60
50
40
30
20
10
0

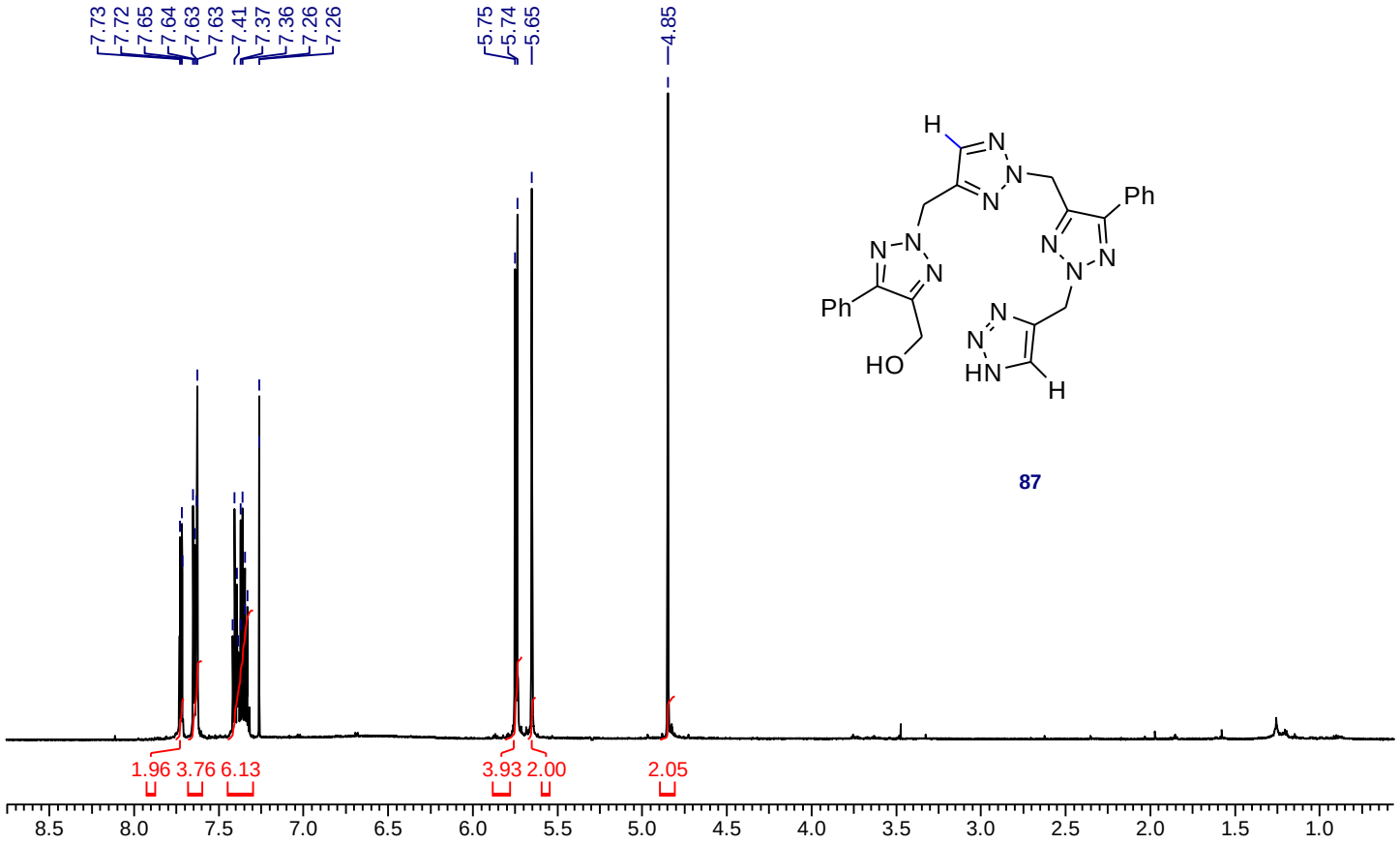
7.73
7.72
7.65
7.64
7.63
7.63
7.41
7.37
7.36
7.26
7.26
5.75
5.74
5.65
4.85
1.96 3.76 6.13
3.93 2.00
2.05
8.5 8.0 7.5 7.0 6.5 6.0 5.5 5.0 4.5 4.0 3.5 3.0 2.5 2.0 1.5 1.0
H
N
N
N
Ph
N
N
N
N
N
Ph
HO
N
N
HN
H

87

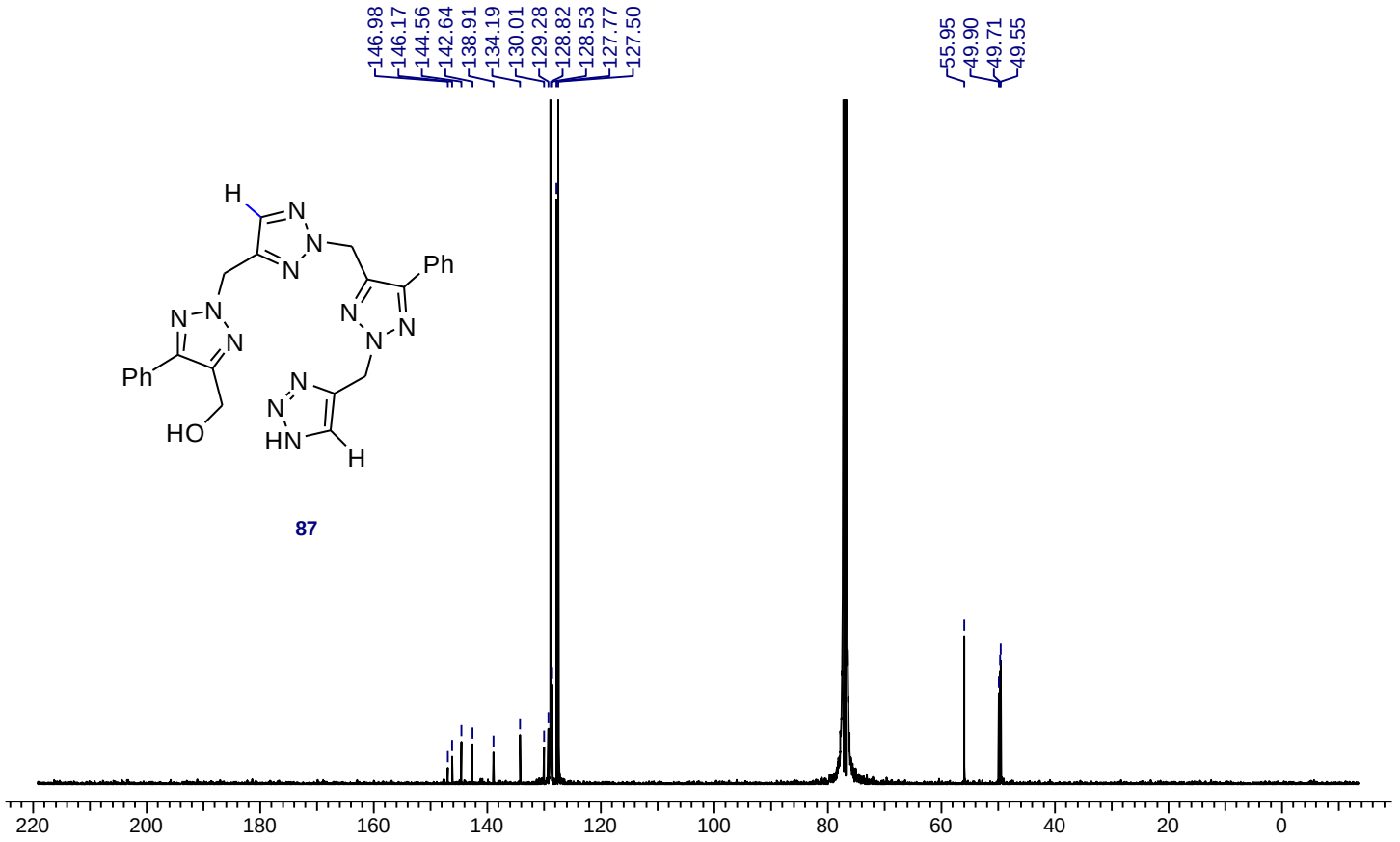
146.98
146.17
144.56
142.64
138.91
134.19
130.01
129.28
128.82
128.53
127.77
127.50
55.95
49.90
49.71
49.55
H
N
N
N
Ph
N
N
N
N
N
Ph
HO
N
N
HN
H
220
200
180
160
140
120
100
80
60
40
20
0

87

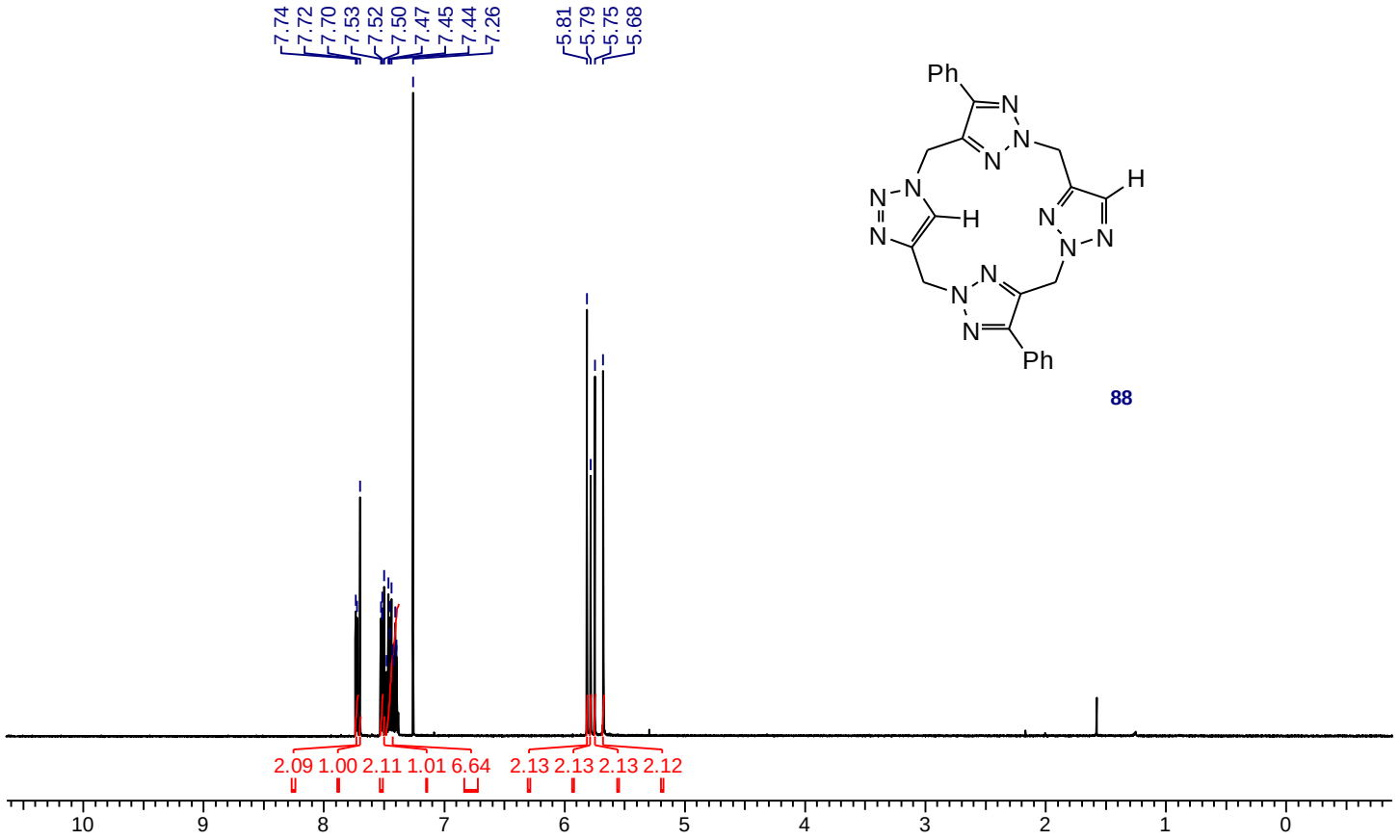
7.74
7.72
7.70
7.53
7.52
7.50
7.47
7.45
7.44
7.26
5.81
5.79
5.75
5.68
2.09 1.00 2.11 1.01 6.64
2.13 2.13 2.13 2.12
10
9
8
7
6
5
4
3
2
1
0
Ph
N
N
N
N
N
H
N
N
H
N
N
N
N
N
Ph
88

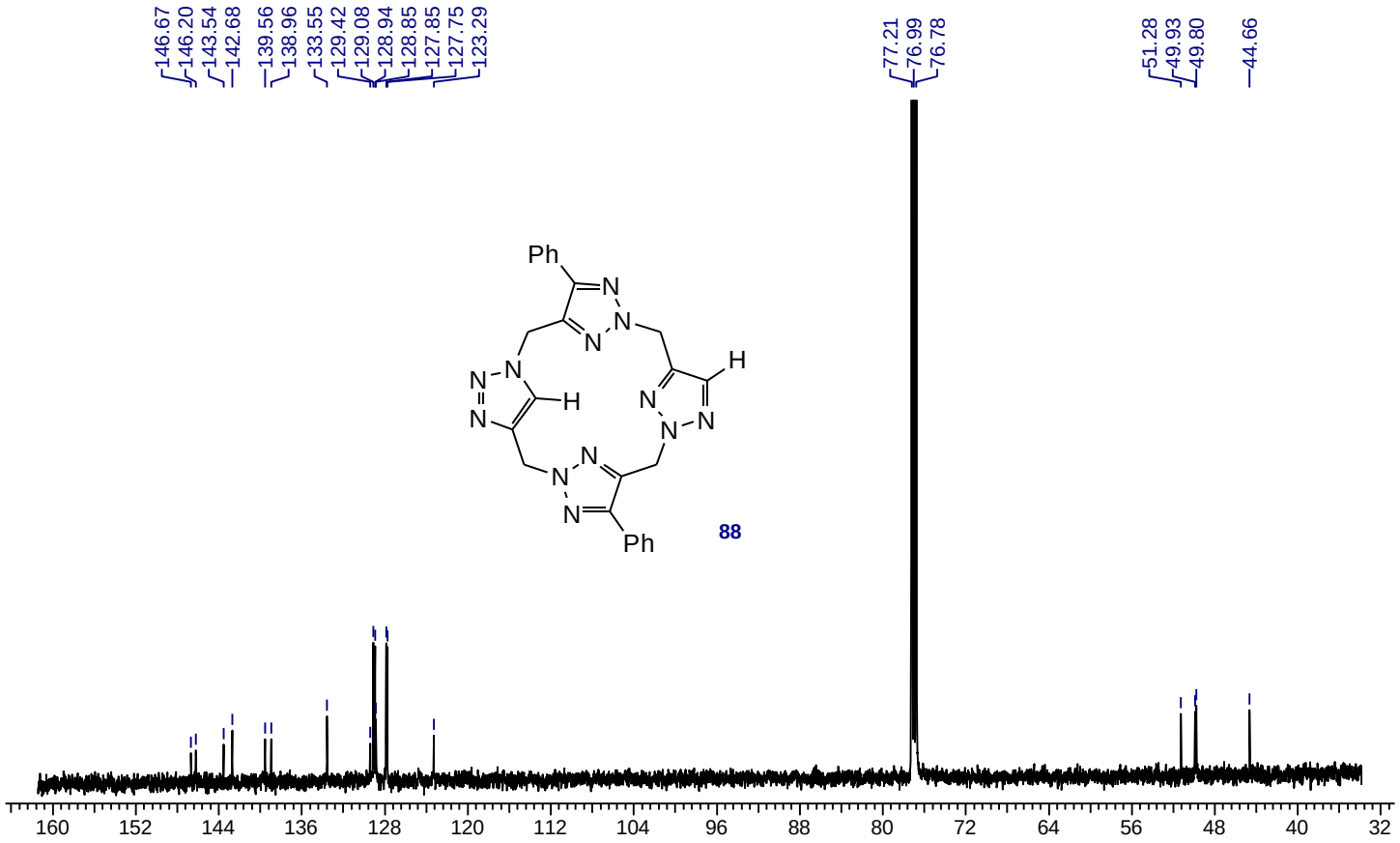
146.67
146.20
143.54
142.68
139.56
138.96
133.55
129.42
129.08
128.94
128.85
127.85
127.75
123.29
77.21
76.99
76.78
51.28
49.93
49.80
44.66
Ph
H
H
Ph
88
160
152
144
136
128
120
112
104
96
88
80
72
64
56
48
40
32

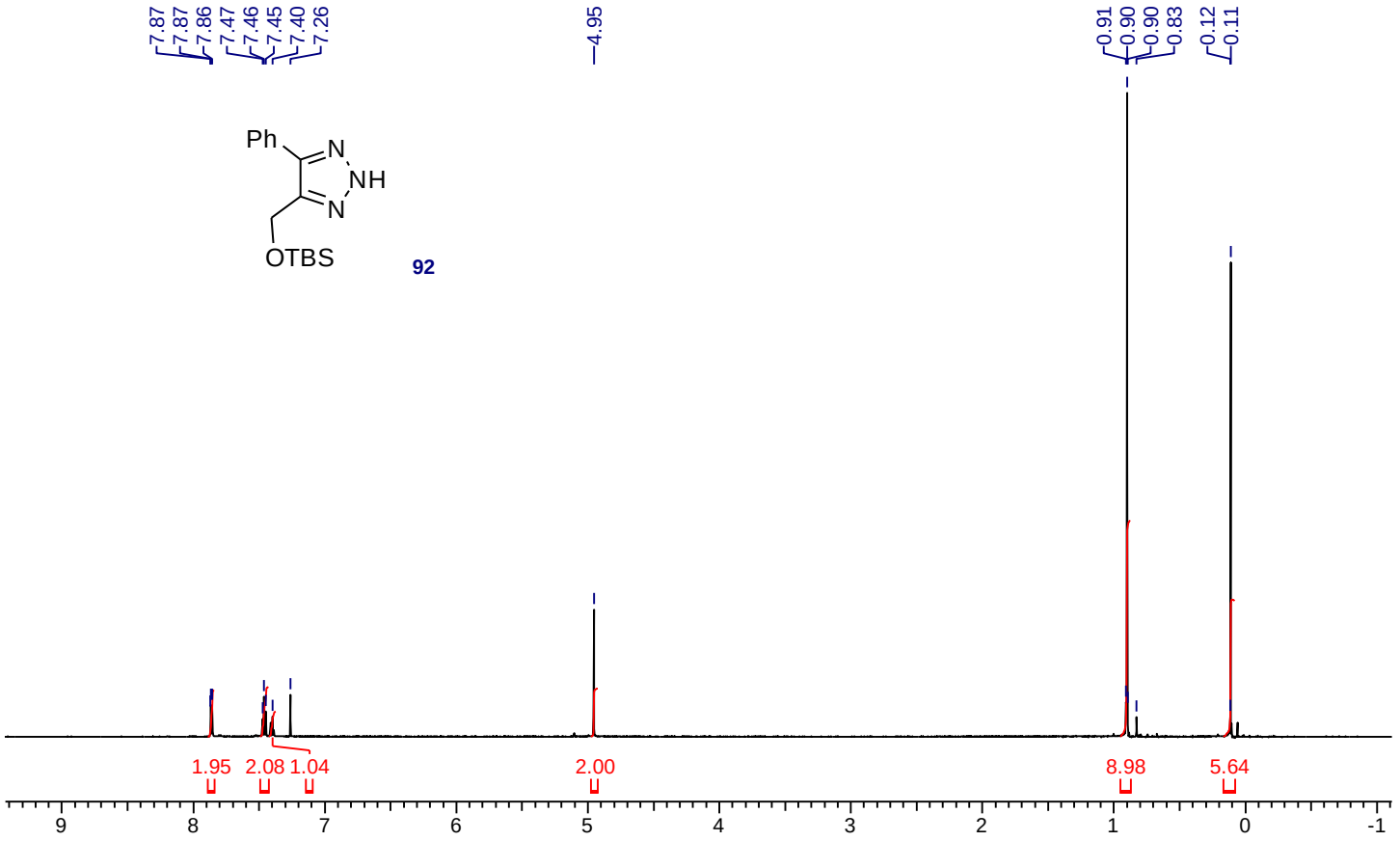
7.87
7.87
7.86
7.47
7.46
7.45
7.40
7.26
4.95
0.91
0.90
0.90
0.83
0.12
0.11
Ph
N
NH
N
OTBS
92
1.95
2.08
1.04
2.00
8.98
5.64
9
8
7
6
5
4
3
2
1
0
-1

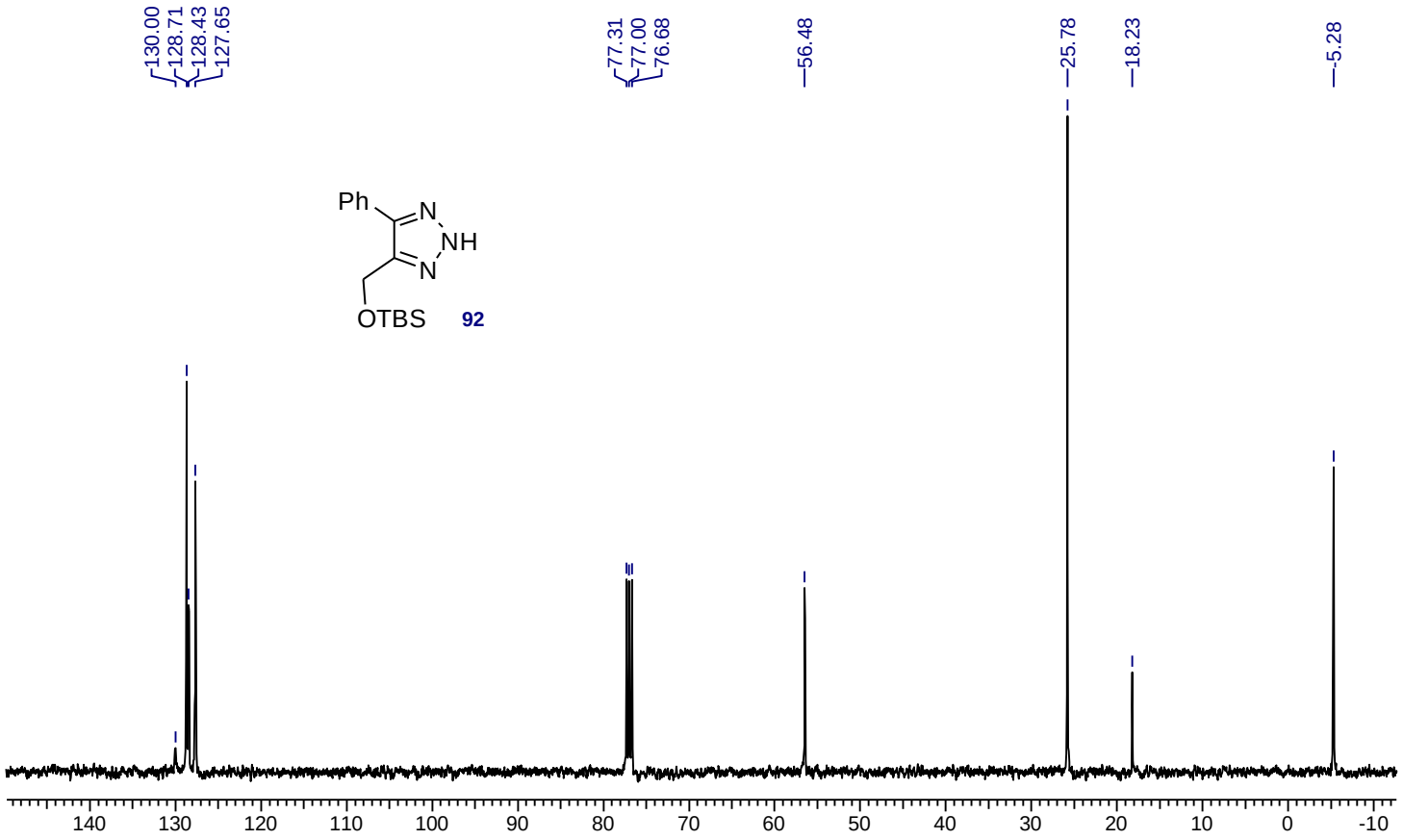
130.00
128.71
128.43
127.65
77.31
77.00
76.68
56.48
25.78
18.23
-5.28
Ph
N
NH
N
OTBS
92
140
130
120
110
100
90
80
70
60
50
40
30
20
10
0
-10

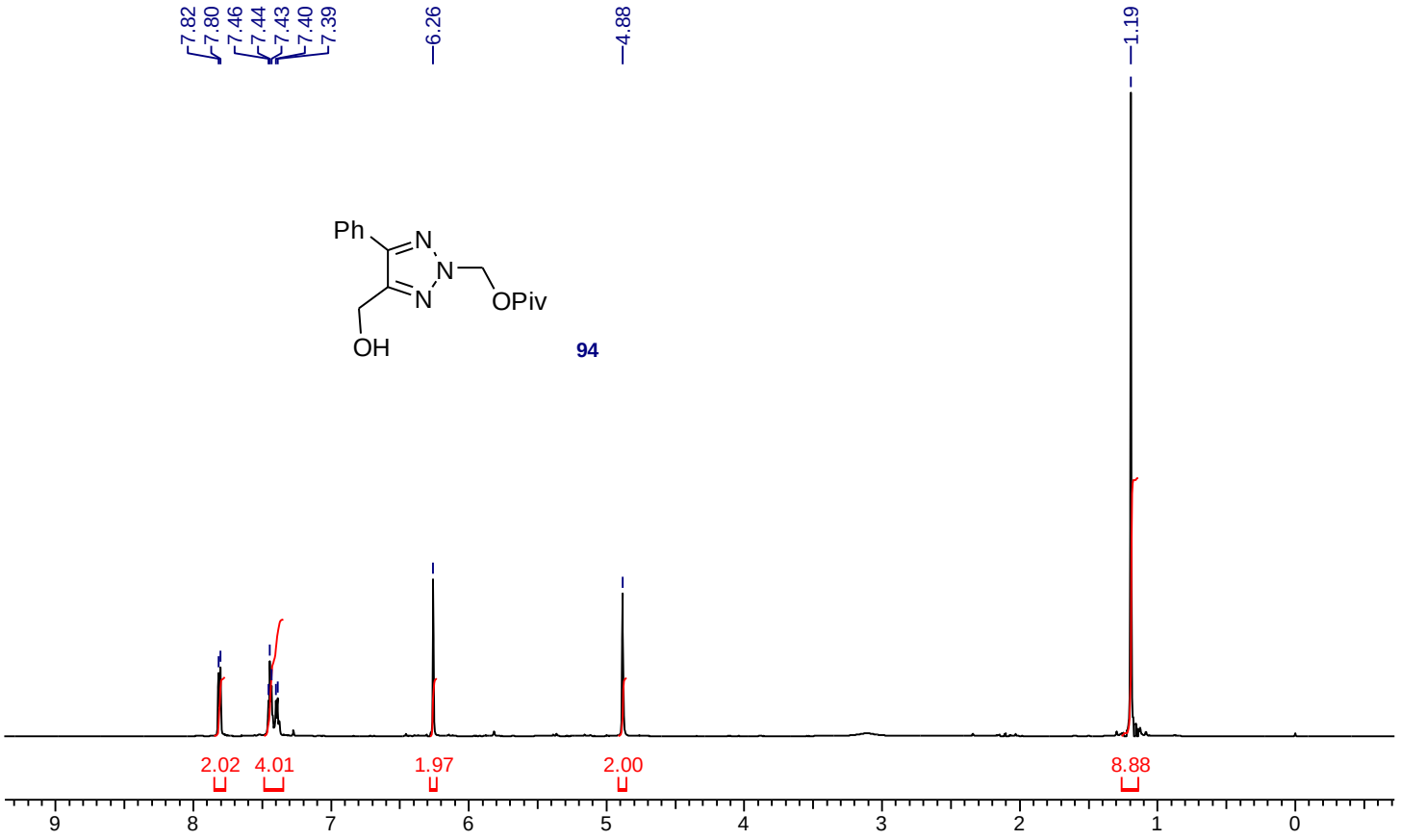
7.82
7.80
7.46
7.44
7.43
7.40
7.39
6.26
4.88
1.19
Ph
N
N
N
OPiv
OH
94
2.02
4.01
1.97
2.00
8.88
9
8
7
6
5
4
3
2
1
0

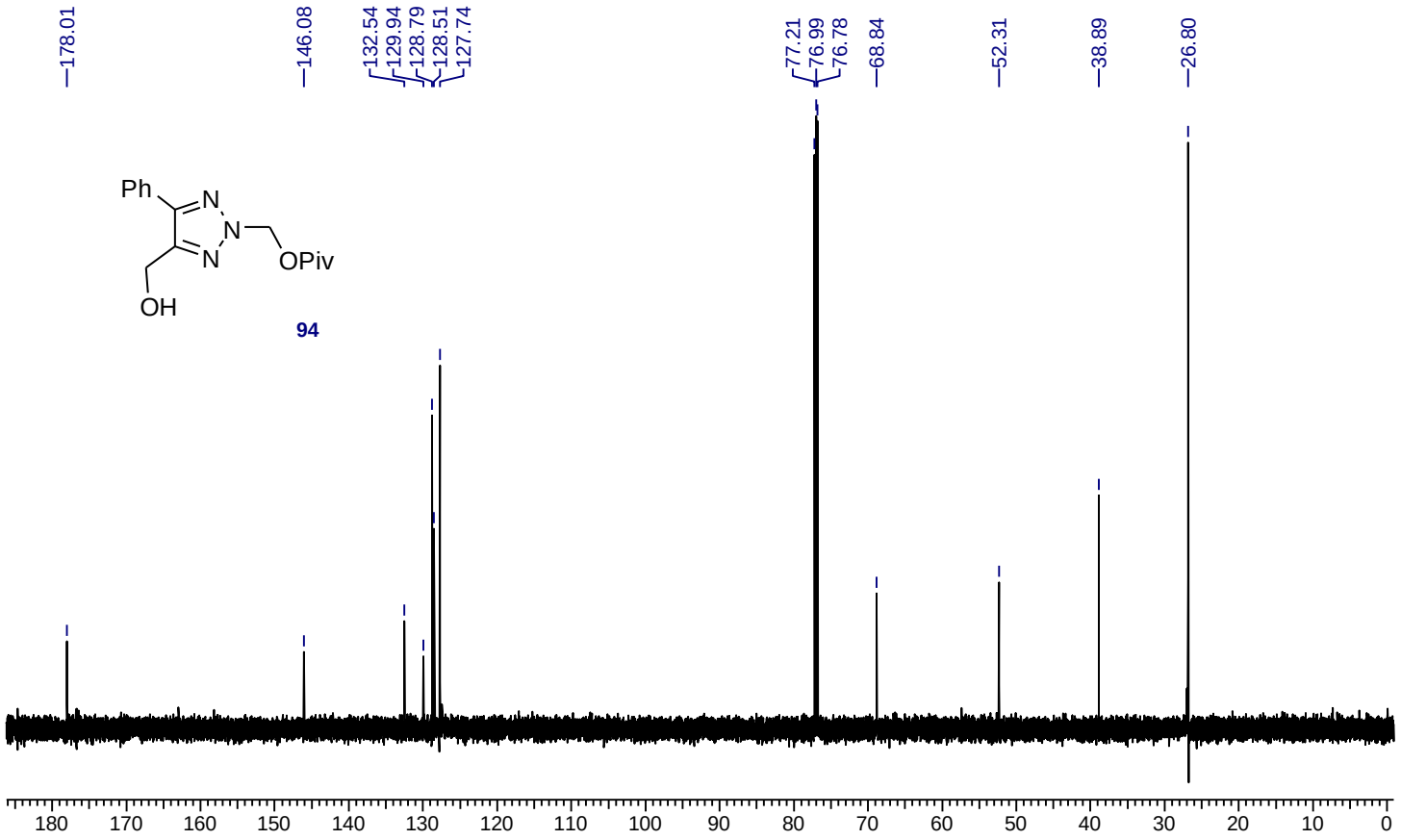
178.01
146.08
132.54
129.94
128.79
128.51
127.74
77.21
76.99
76.78
68.84
52.31
38.89
26.80
Ph
N
N
N
OPiv
OH
94
180
170
160
150
140
130
120
110
100
90
80
70
60
50
40
30
20
10
0

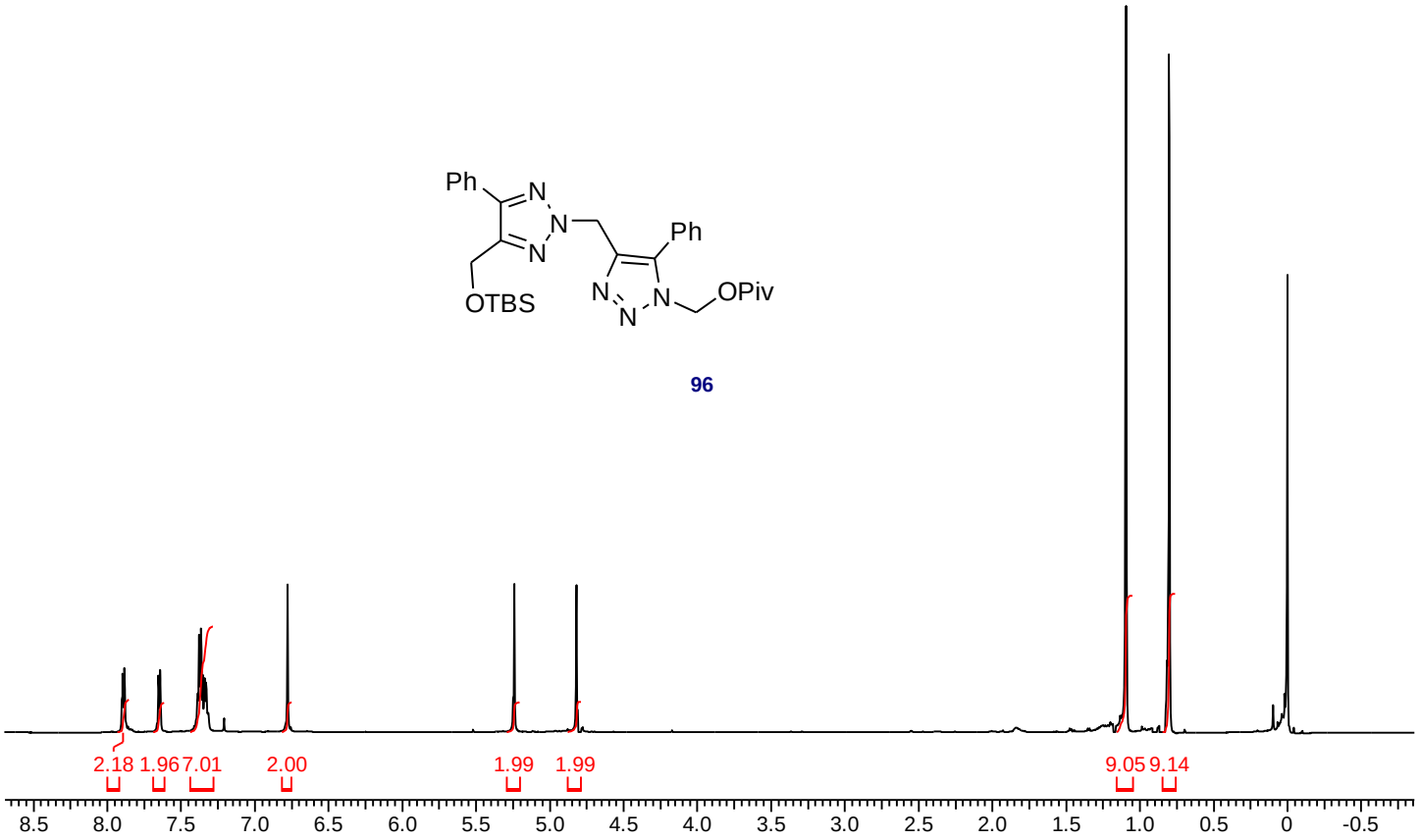
Ph
N
N
N
Ph
N
N
N
OPiv
OTBS
2.18
1.96
7.01
2.00
1.99
1.99
9.05
9.14
8.5
8.0
7.5
7.0
6.5
6.0
5.5
5.0
4.5
4.0
3.5
3.0
2.5
2.0
1.5
1.0
0.5
0
-0.5

96

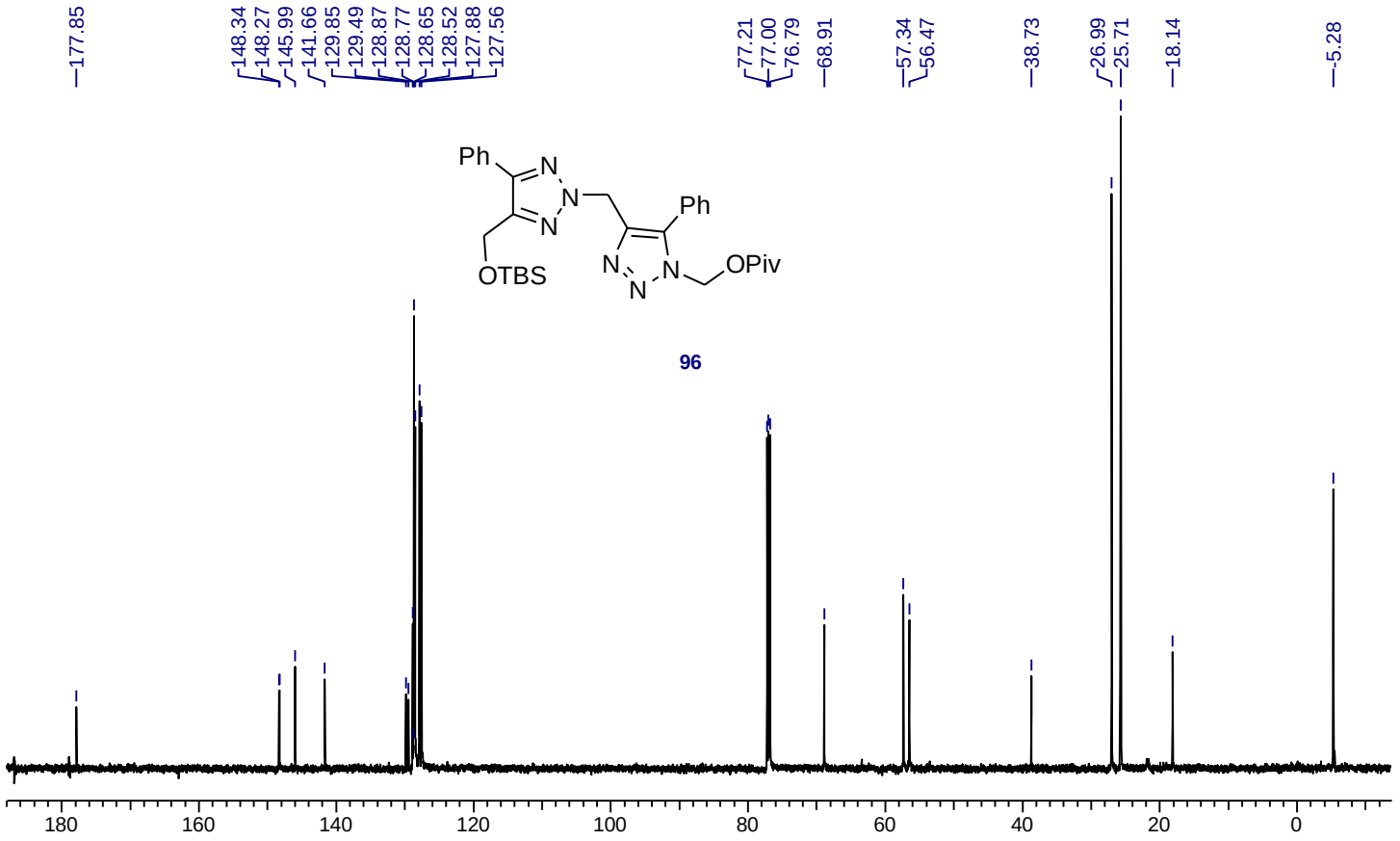
177.85
148.34
148.27
145.99
141.66
129.85
129.49
128.87
128.77
128.65
128.52
127.88
127.56
77.21
77.00
76.79
68.91
57.34
56.47
38.73
26.99
25.71
18.14
-5.28
Ph
N
N
N
Ph
OTBS
N
N
N
OPiv
96
180
160
140
120
100
80
60
40
20
0

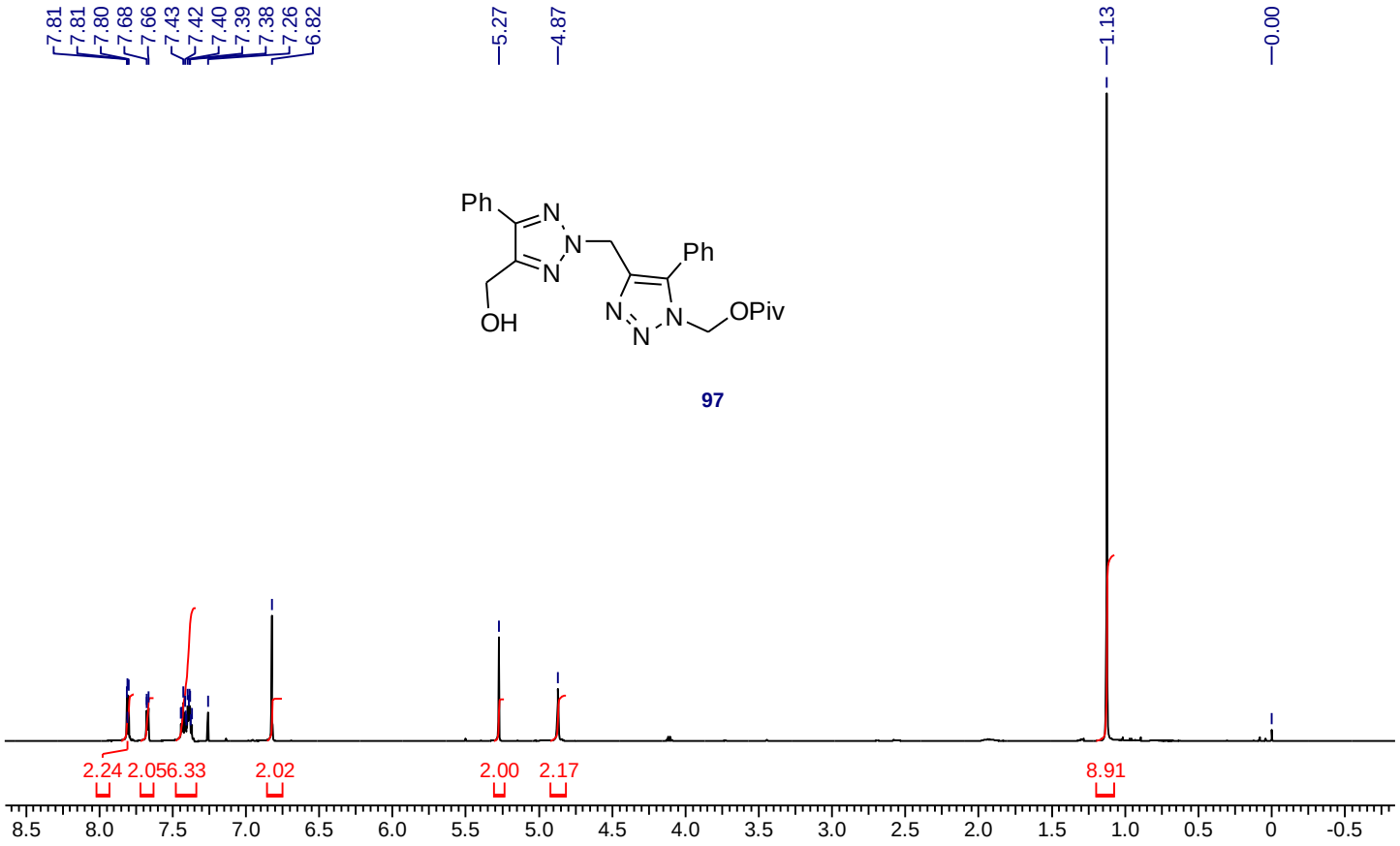
7.81
7.81
7.80
7.68
7.66
7.43
7.42
7.40
7.39
7.38
7.26
6.82
5.27
4.87
1.13
0.00
Ph
N
N
N
Ph
N
N
N
OPiv
OH
97
2.24
2.05
6.33
2.02
2.00
2.17
8.91
8.5
8.0
7.5
7.0
6.5
6.0
5.5
5.0
4.5
4.0
3.5
3.0
2.5
2.0
1.5
1.0
0.5
0
-0.5

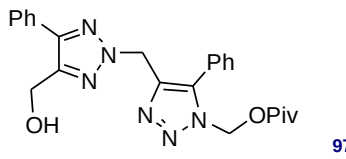
Ph
N
N
N
OH
Ph
N
N
N
OPiv

97

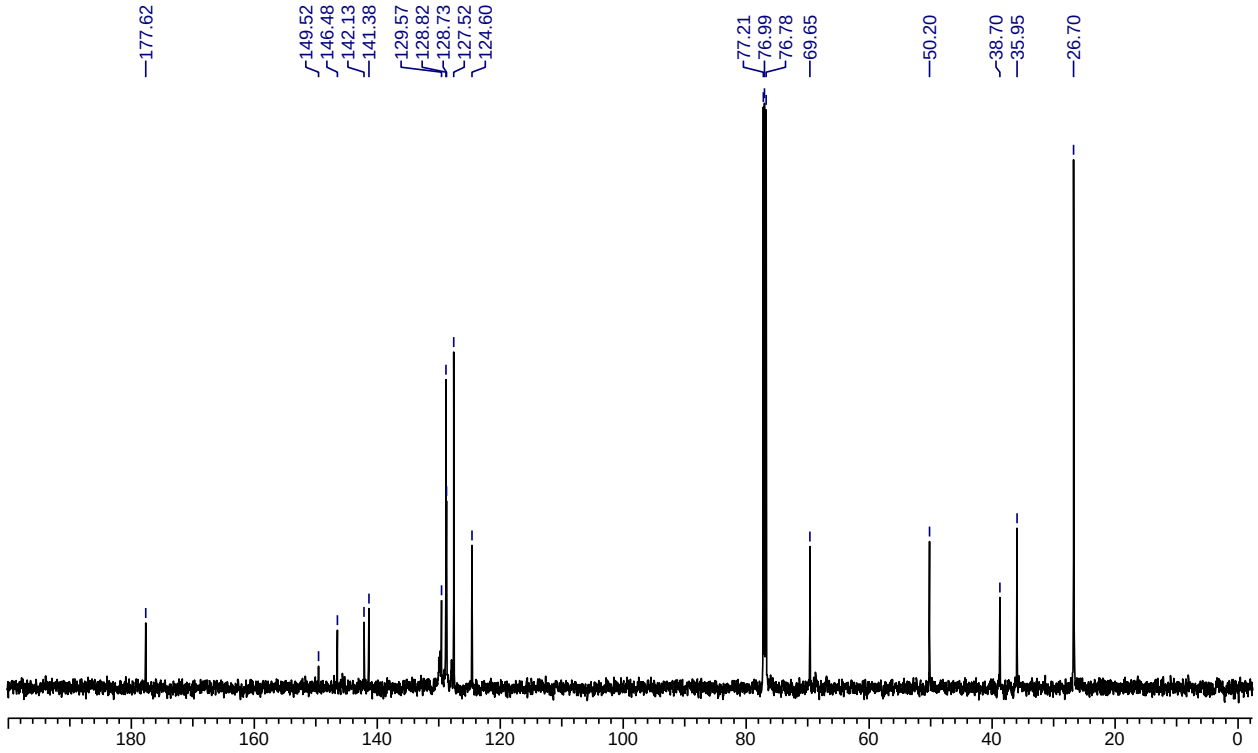
177.62
149.52
146.48
142.13
141.38
129.57
128.82
128.73
127.52
124.60
77.21
76.99
76.78
69.65
50.20
38.70
35.95
26.70
180
160
140
120
100
80
60
40
20
0

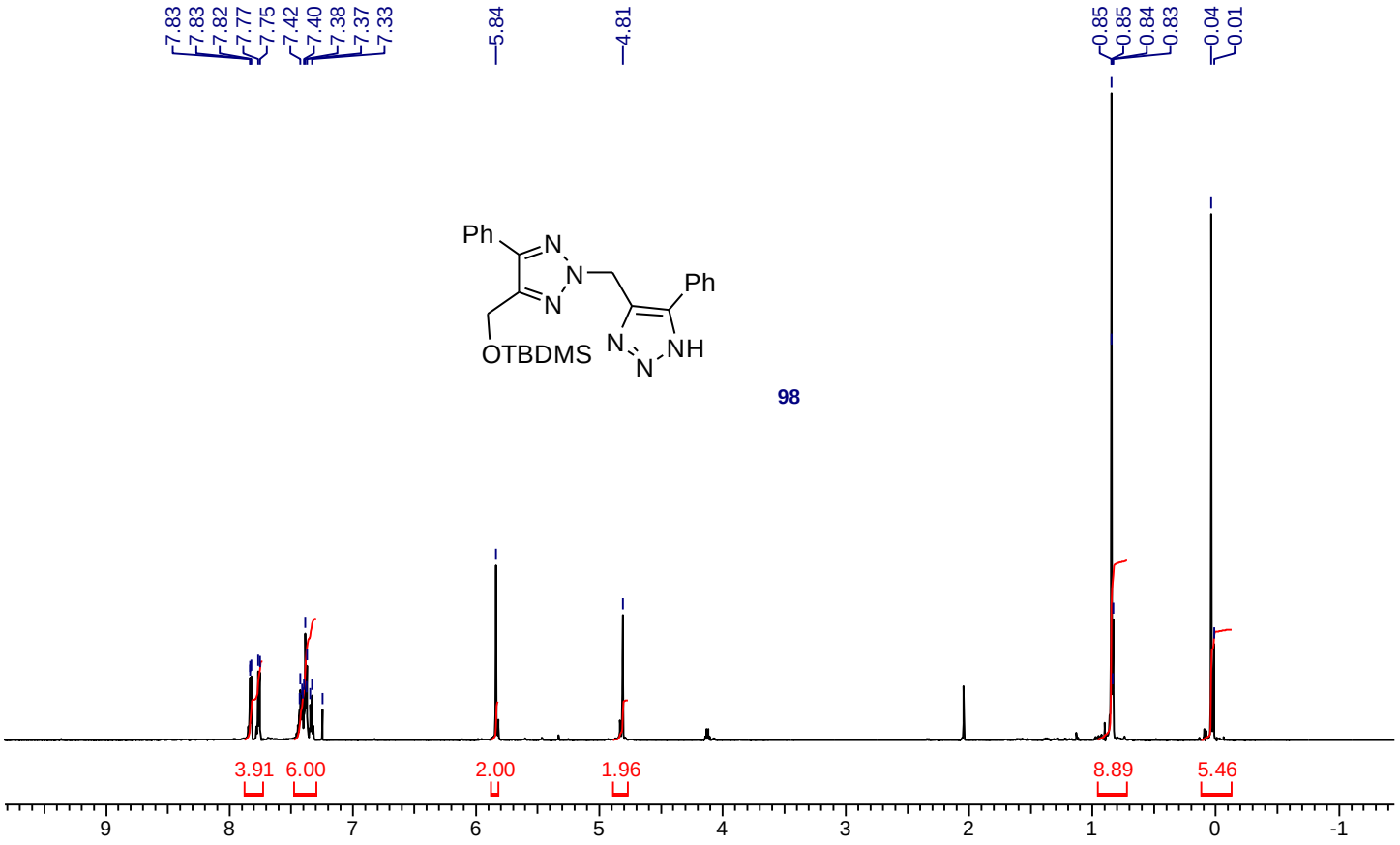
7.83
7.83
7.82
7.77
7.75
7.42
7.40
7.38
7.37
7.33
5.84
4.81
0.85
0.85
0.84
0.83
0.04
0.01
Ph
N
N
N
OTBDMS
N
N
NH
Ph
98
3.91
6.00
2.00
1.96
8.89
5.46
9
8
7
6
5
4
3
2
1
0
-1

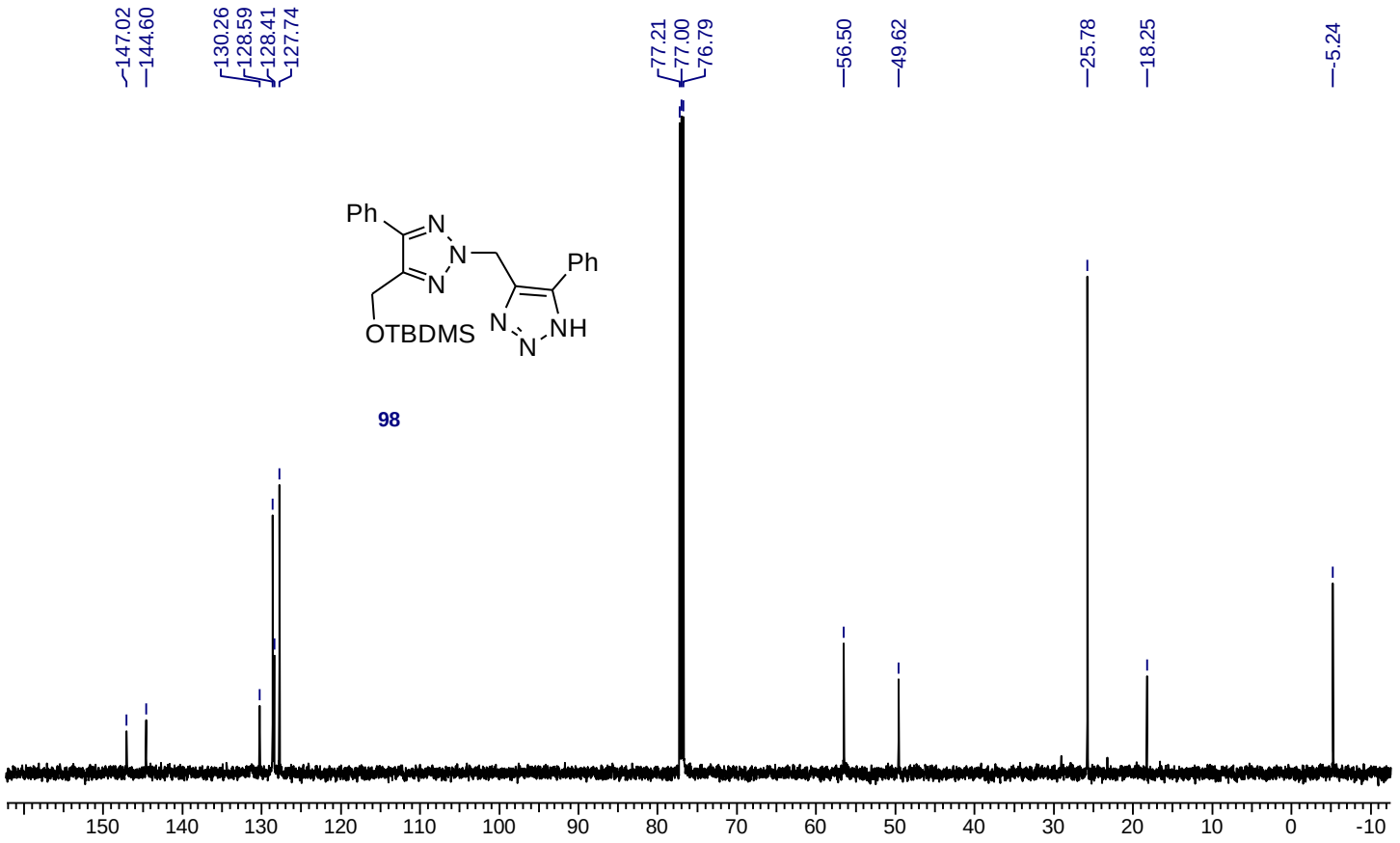
147.02
144.60
130.26
128.59
128.41
127.74
77.21
77.00
76.79
56.50
49.62
25.78
18.25
-5.24
Ph
N
N
N
Ph
N
NH
N
OTBDMS
150
140
130
120
110
100
90
80
70
60
50
40
30
20
10
0
-10

98

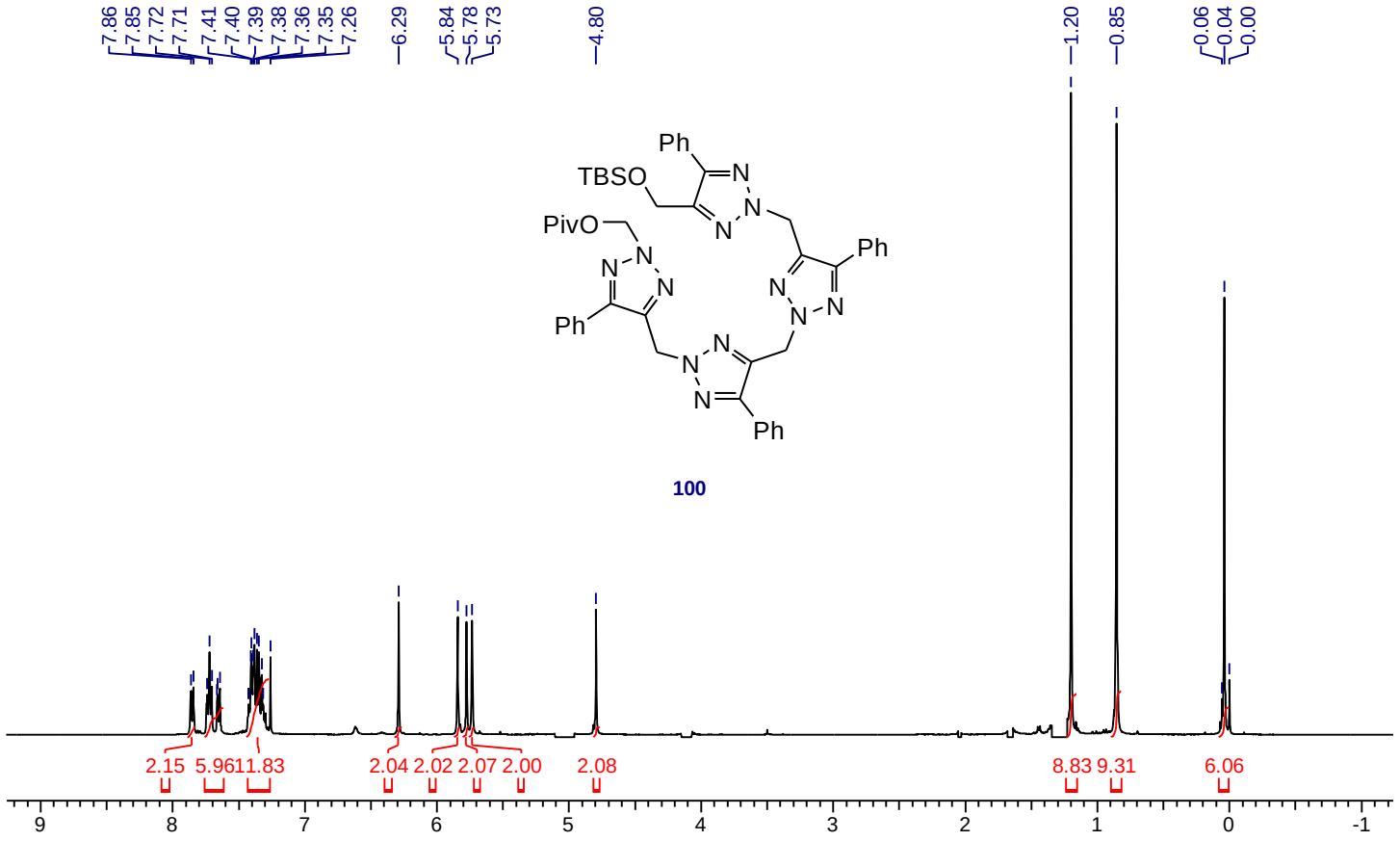
7.86
7.85
7.72
7.71
7.41
7.40
7.39
7.38
7.36
7.35
7.26
6.29
5.84
5.78
5.73
4.80
1.20
0.85
0.06
0.04
0.00
Ph
TBSO
PivO
Ph
Ph
Ph
100
2.15
5.96
11.83
2.04
2.02
2.07
2.00
2.08
8.83
9.31
6.06
9
8
7
6
5
4
3
2
1
0
-1

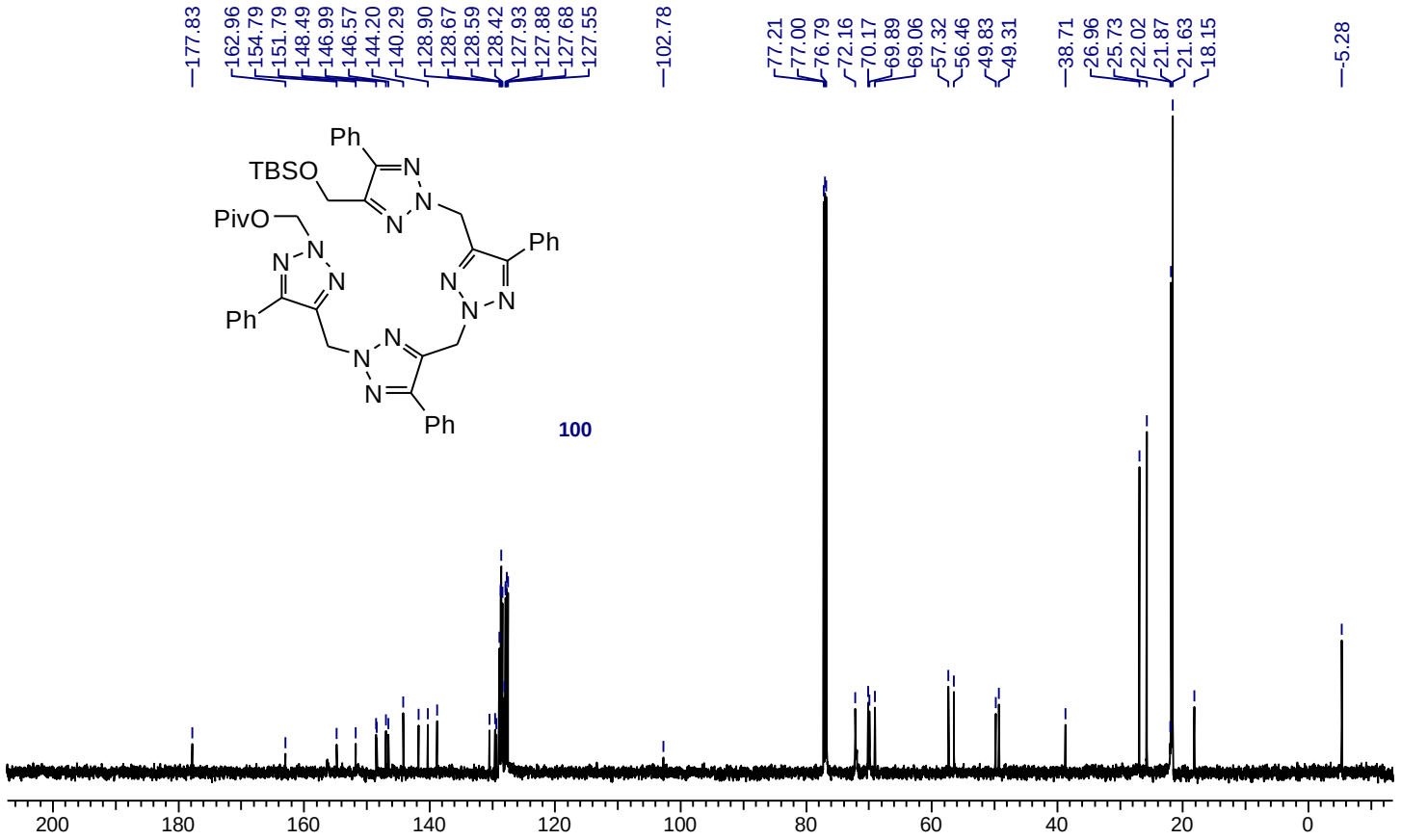
177.83
162.96
154.79
151.79
148.49
146.99
146.57
144.20
140.29
128.90
128.67
128.59
128.42
127.93
127.88
127.68
127.55
102.78
77.21
77.00
76.79
72.16
70.17
69.89
69.06
57.32
56.46
49.83
49.31
38.71
26.96
25.73
22.02
21.87
21.63
18.15
-5.28
Ph
TBSO
PivO
Ph
Ph
Ph
N
100
200
180
160
140
120
100
80
60
40
20
0

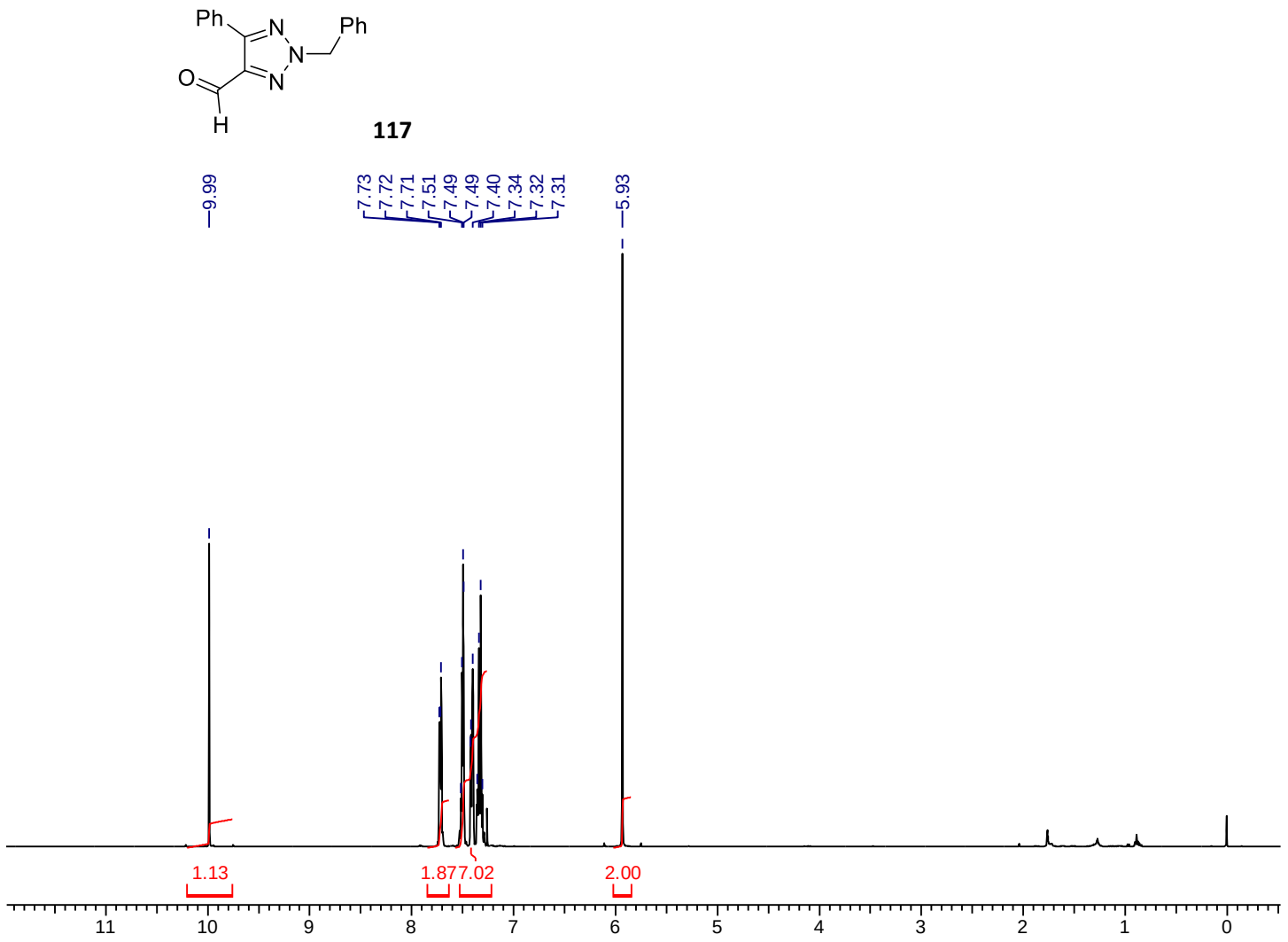
Ph
N
N
N
Ph
O
H
117
9.99
7.73
7.72
7.71
7.51
7.49
7.49
7.40
7.34
7.32
7.31
5.93
1.13
1.87
7.02
2.00
11
10
9
8
7
6
5
4
3
2
1
0

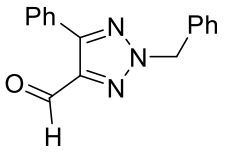
Ph
N
N
Ph
O
N
H

117

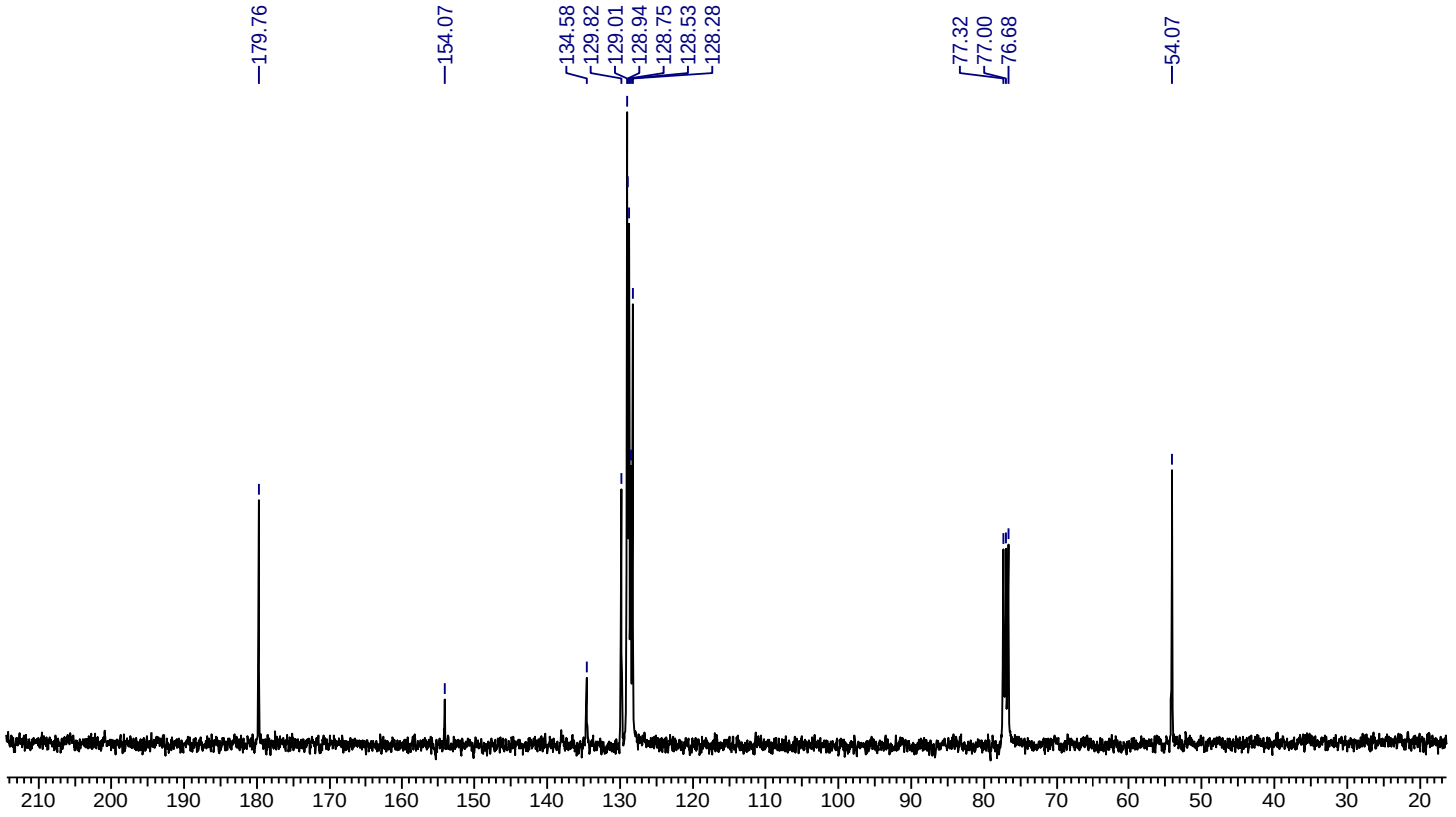
179.76
154.07
134.58
129.82
129.01
128.94
128.75
128.53
128.28
77.32
77.00
76.68
54.07
210
200
190
180
170
160
150
140
130
120
110
100
90
80
70
60
50
40
30
20

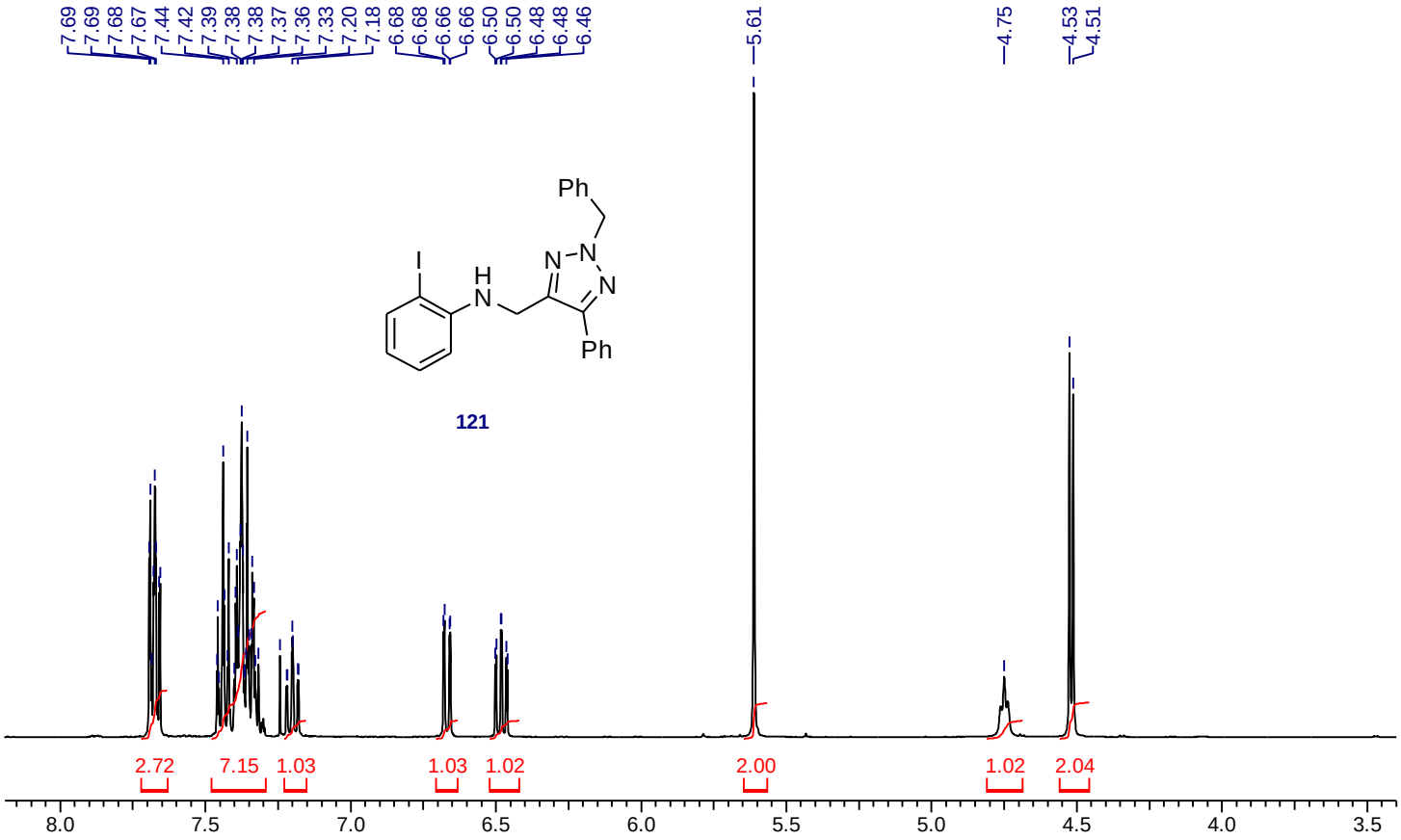
7.69
7.69
7.68
7.67
7.44
7.42
7.39
7.38
7.38
7.37
7.36
7.33
7.20
7.18
6.68
6.68
6.66
6.66
6.50
6.50
6.48
6.48
6.46
5.61
4.75
4.53
4.51
Ph
I
H
N
N
N
N
Ph
121
2.72
7.15
1.03
1.03
1.02
2.00
1.02
2.04
8.0
7.5
7.0
6.5
6.0
5.5
5.0
4.5
4.0
3.5

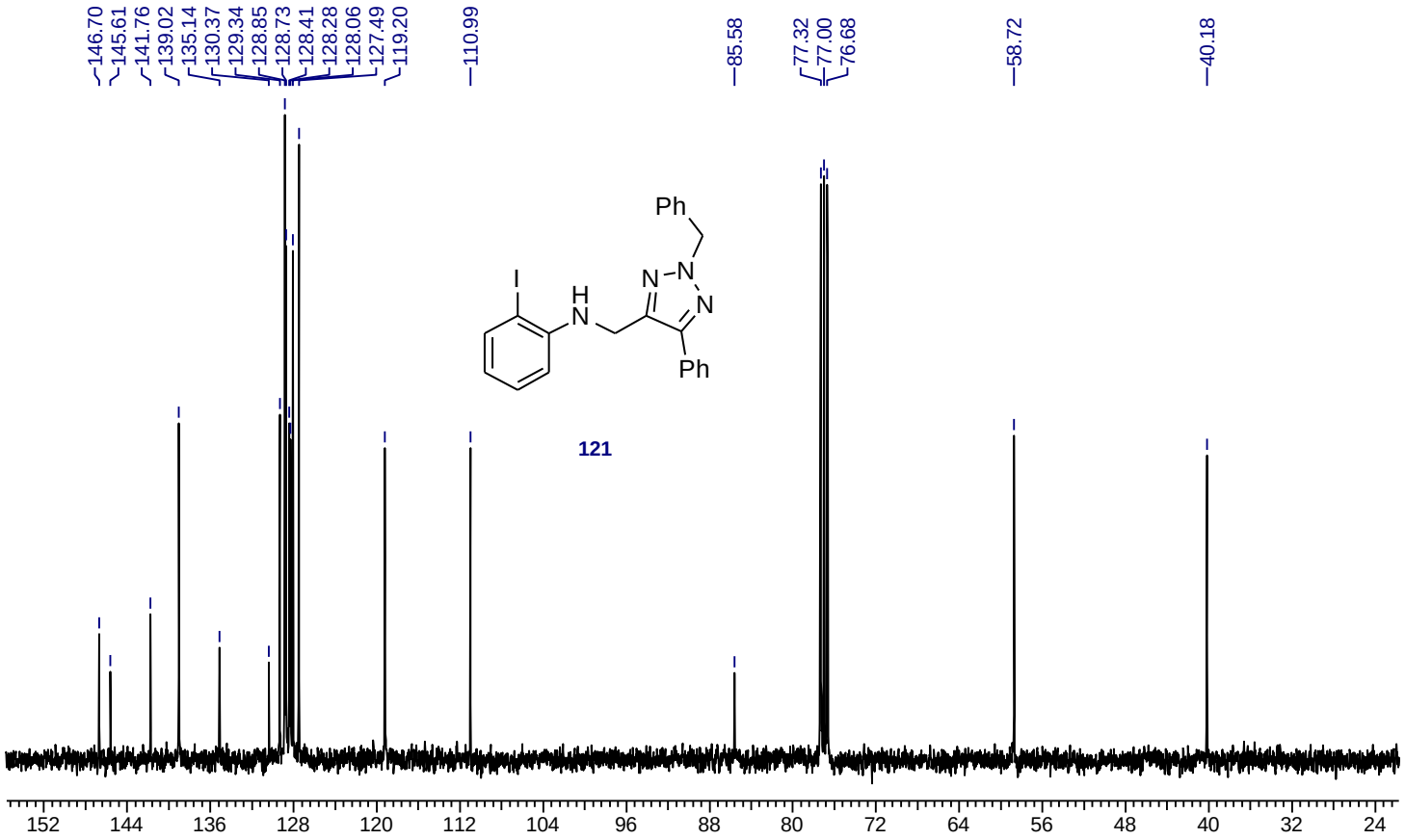
146.70
145.61
141.76
139.02
135.14
130.37
129.34
128.85
128.73
128.41
128.28
128.06
127.49
119.20
110.99
85.58
77.32
77.00
76.68
58.72
40.18
Ph
I
H
N
N
N
N
Ph
121
152
144
136
128
120
112
104
96
88
80
72
64
56
48
40
32
24

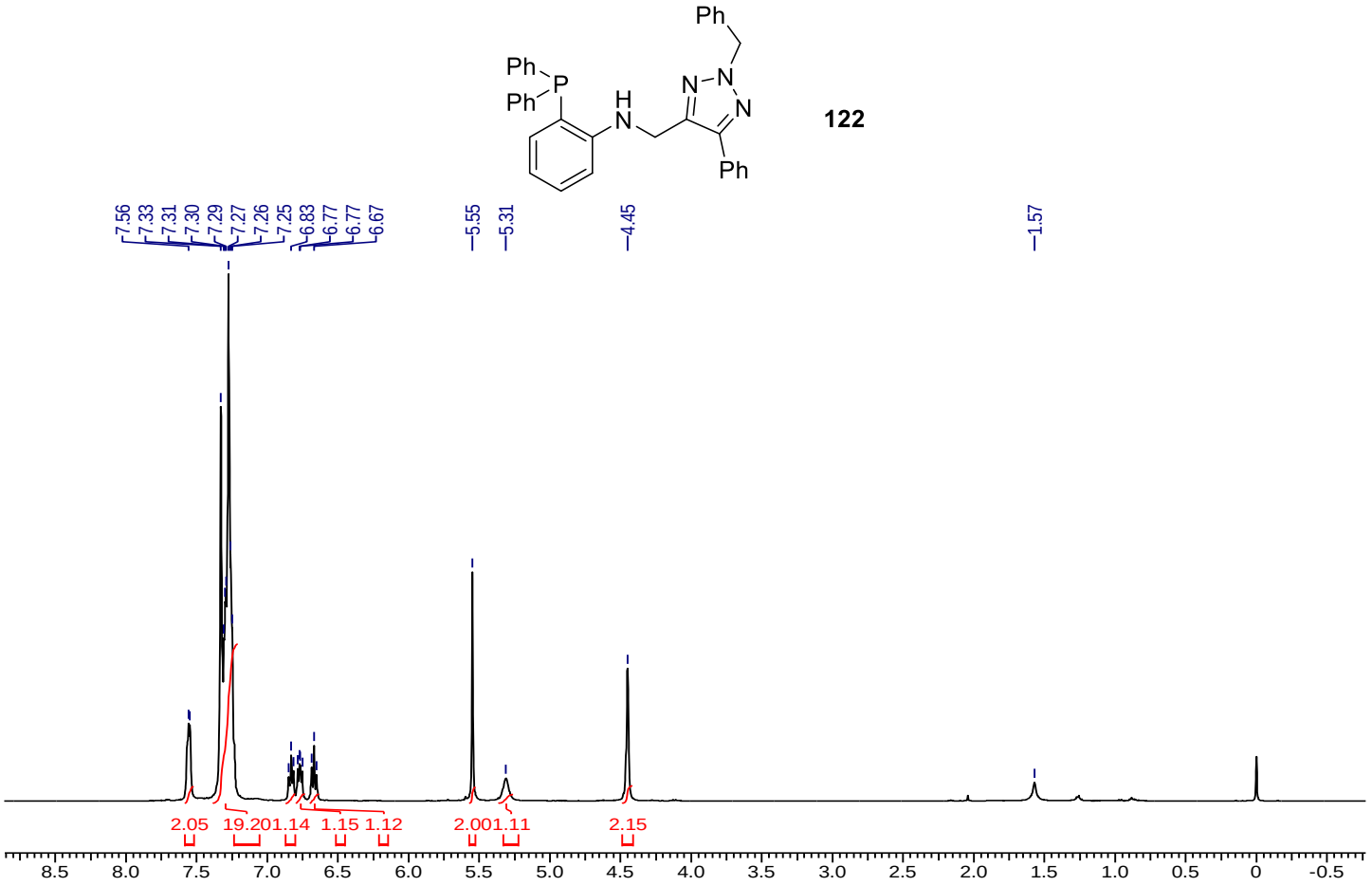
Ph
Ph
P
Ph
H
N
N
N
N
Ph
122
7.56
7.33
7.31
7.30
7.29
7.27
7.26
7.25
6.83
6.77
6.77
6.67
5.55
5.31
4.45
1.57
2.05
19.20
1.14
1.15
1.12
2.00
1.11
2.15
8.5
8.0
7.5
7.0
6.5
6.0
5.5
5.0
4.5
4.0
3.5
3.0
2.5
2.0
1.5
1.0
0.5
0
-0.5

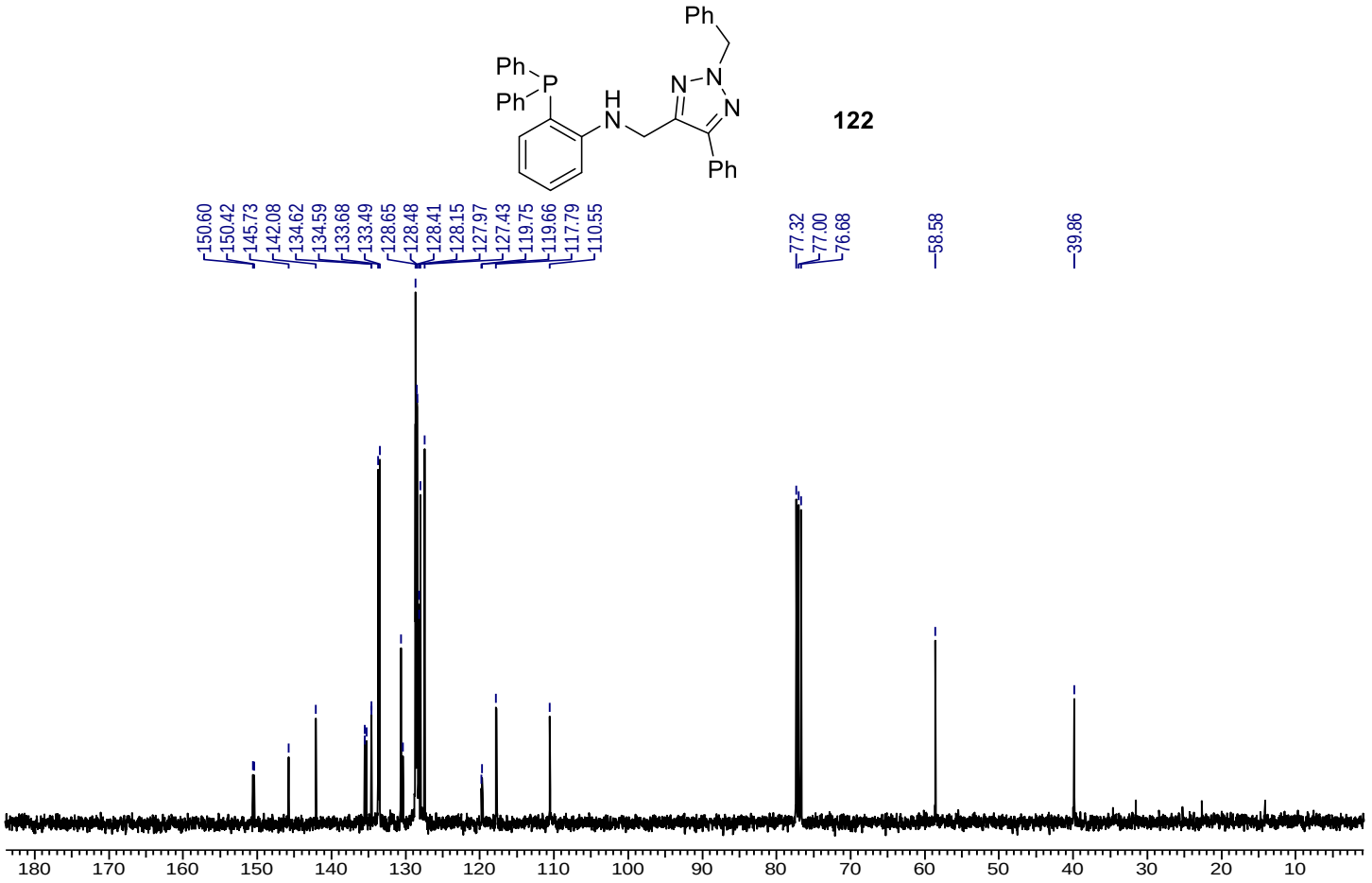
Ph
Ph
P
Ph
H
N
N
N
N
Ph
122
150.60
150.42
145.73
142.08
134.62
134.59
133.68
133.49
128.65
128.48
128.41
128.15
127.97
127.43
119.75
119.66
117.79
110.55
77.32
77.00
76.68
58.58
39.86
180
170
160
150
140
130
120
110
100
90
80
70
60
50
40
30
20
10

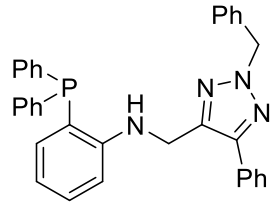

122

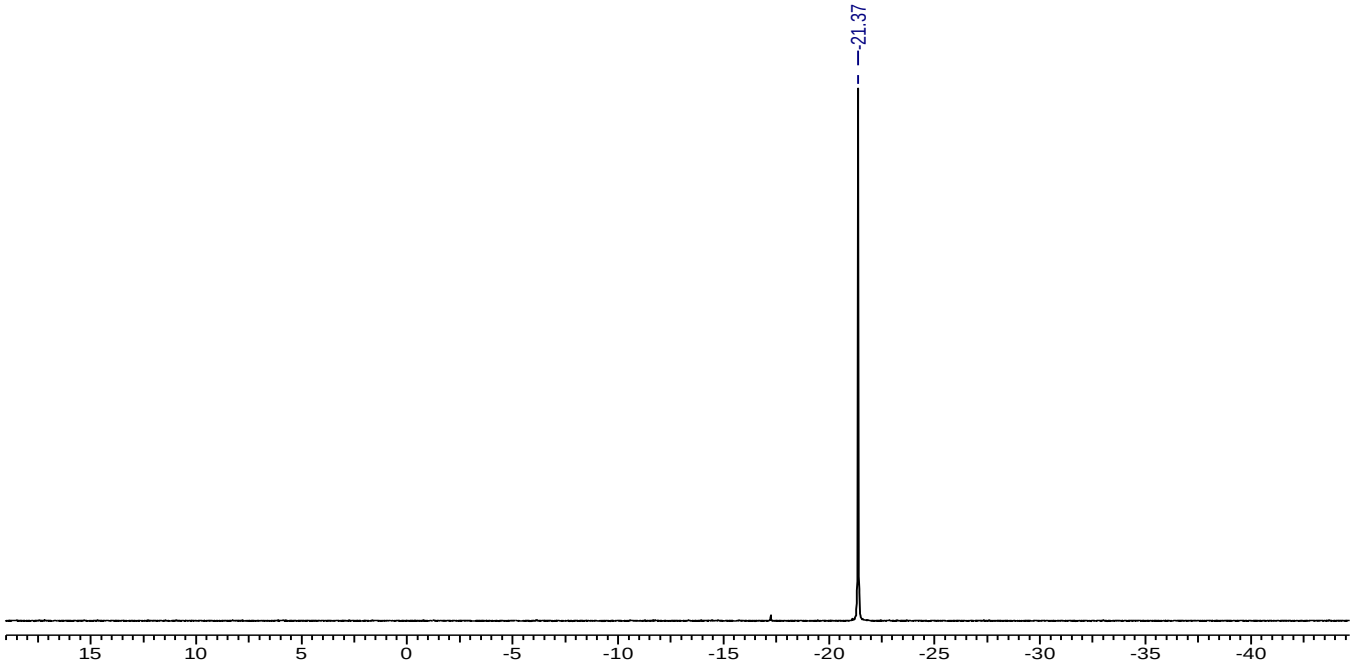

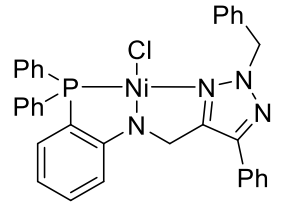
Ph
Cl
Ph
P
Ni
N
N
Ph
N
N
Ph

123

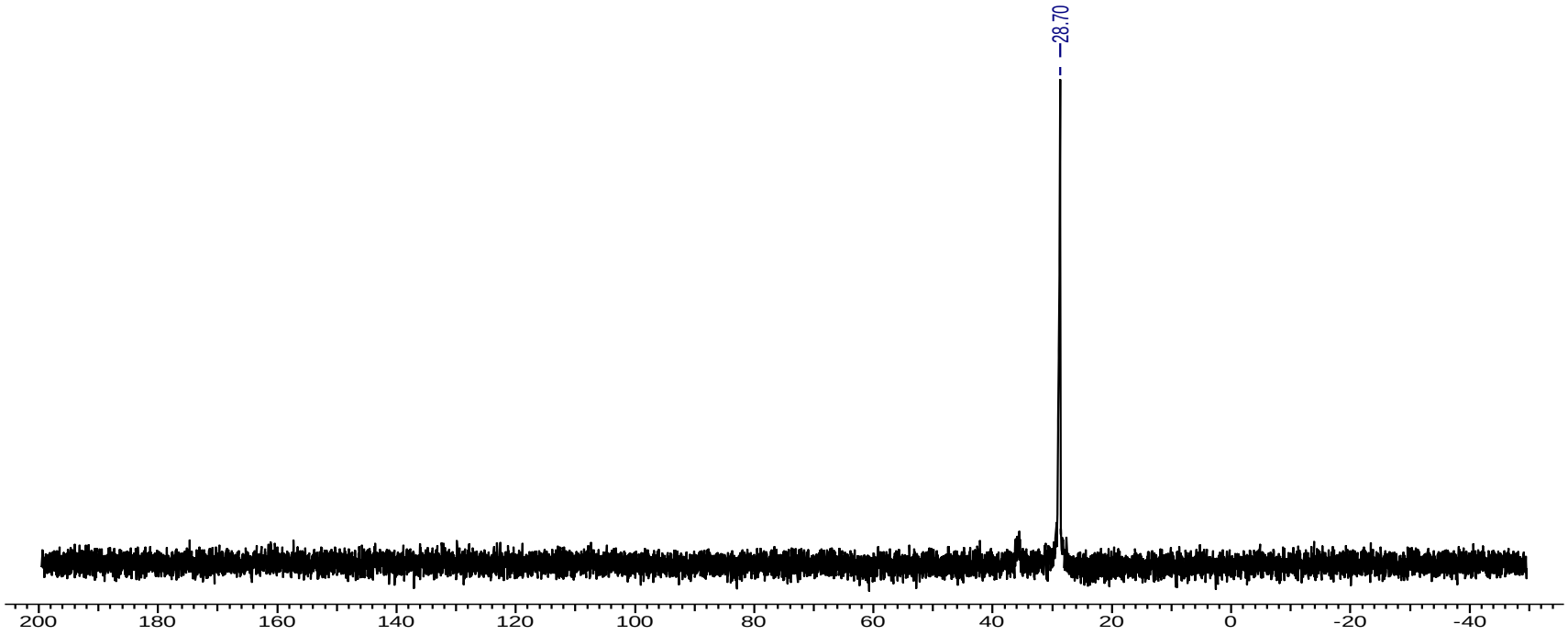
28.70
200
180
160
140
120
100
80
60
40
20
0
-20
-40

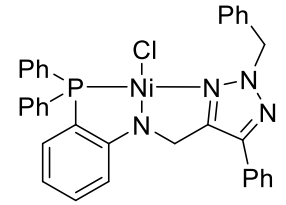
Ph
Cl
Ph
P
Ni
N
N
N
Ph
Ph

123

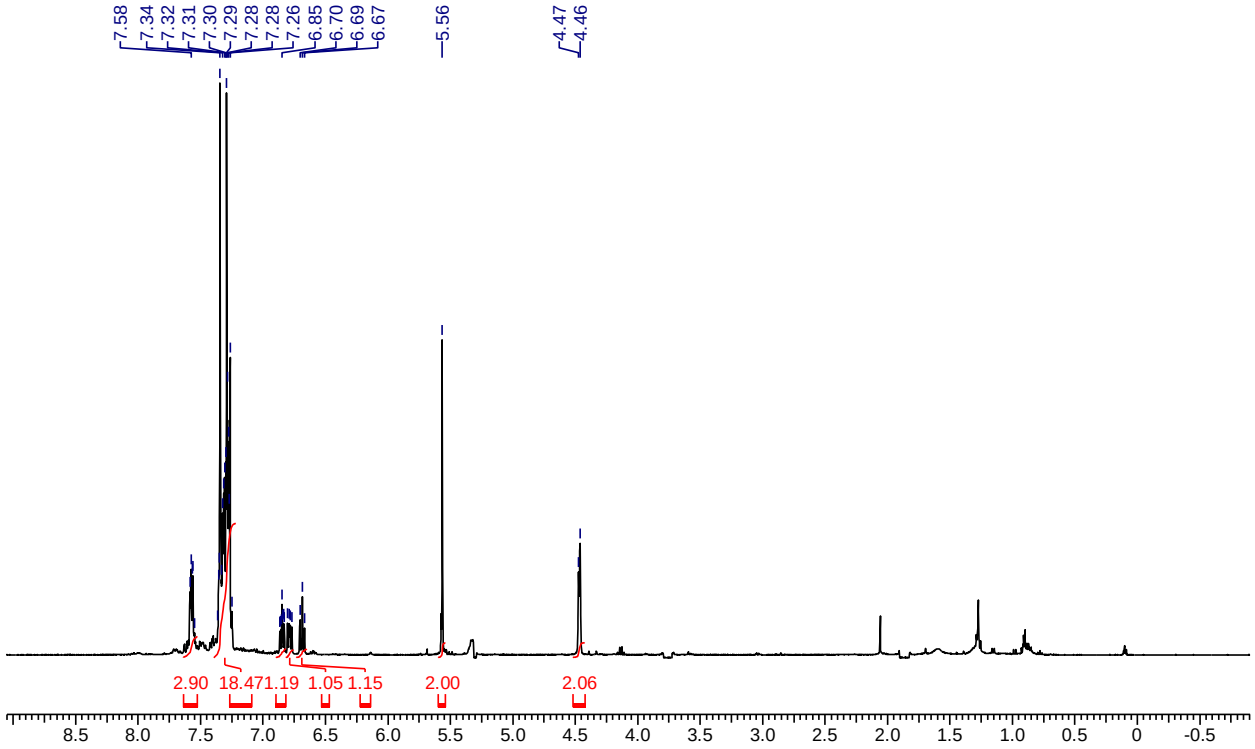
7.58
7.34
7.32
7.31
7.30
7.29
7.28
7.28
7.26
6.85
6.70
6.69
6.67
5.56
4.47
4.46
2.90
18.47
1.19
1.05
1.15
2.00
2.06
8.5
8.0
7.5
7.0
6.5
6.0
5.5
5.0
4.5
4.0
3.5
3.0
2.5
2.0
1.5
1.0
0.5
0
-0.5

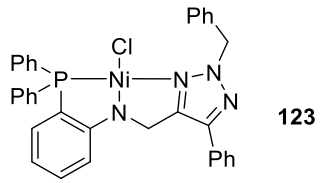
Ph
Cl
Ph
P
Ni
N
N
N
Ph
Ph
N

123

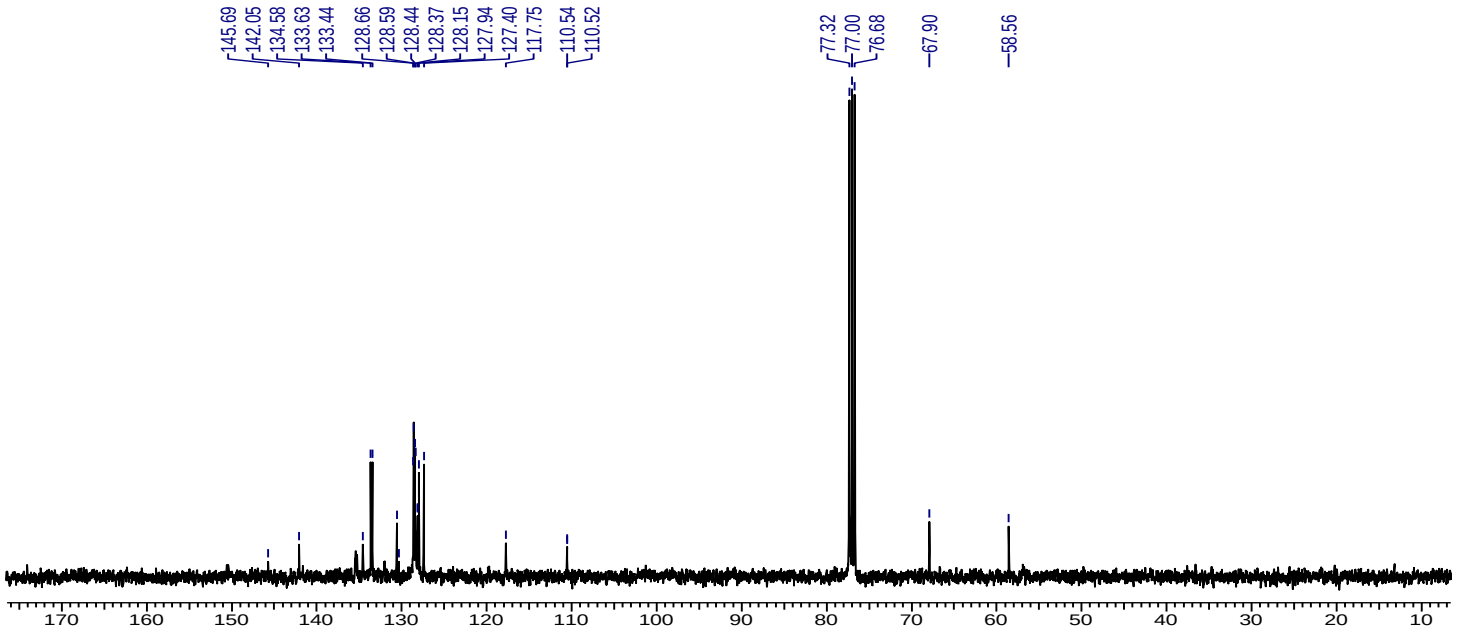
145.69
142.05
134.58
133.63
133.44
128.66
128.59
128.44
128.37
128.15
127.94
127.40
117.75
110.54
110.52
77.32
77.00
76.68
67.90
58.56
170
160
150
140
130
120
110
100
90
80
70
60
50
40
30
20
10

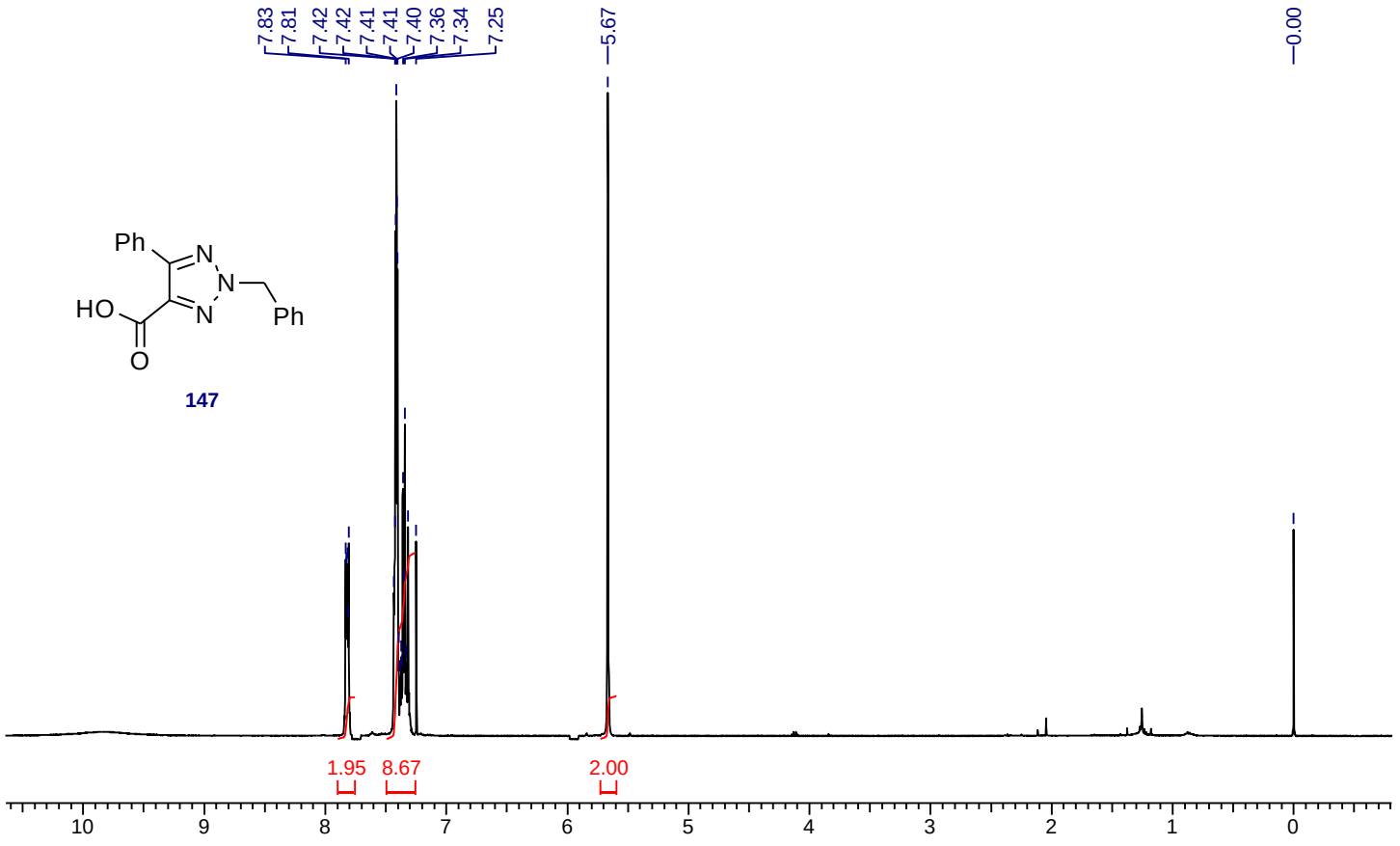
7.83
7.81
7.42
7.42
7.41
7.41
7.40
7.36
7.34
7.25
5.67
0.00
Ph
N
N
N
HO
Ph
O
147
1.95
8.67
2.00
10
9
8
7
6
5
4
3
2
1
0

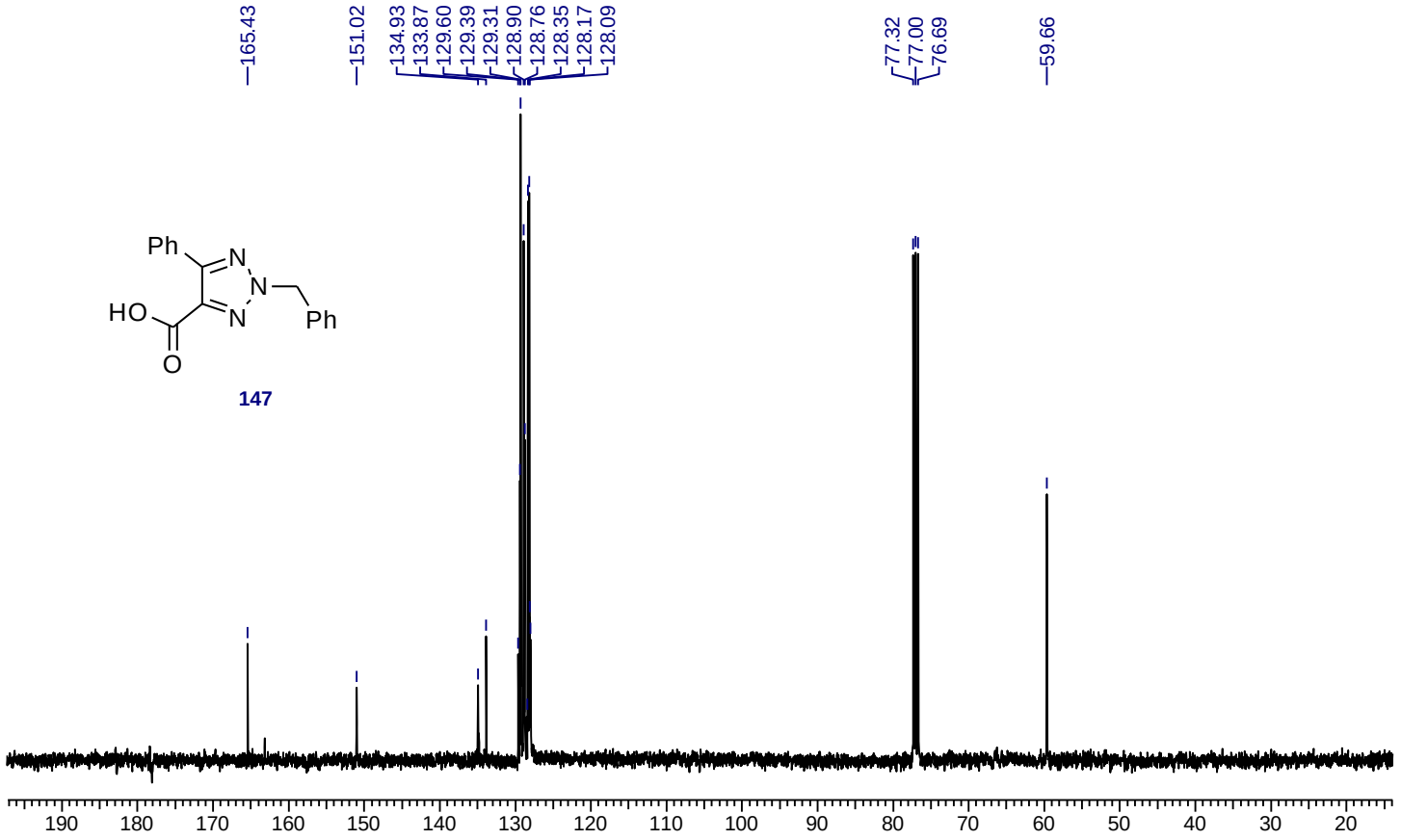
165.43
151.02
134.93
133.87
129.60
129.39
129.31
128.90
128.76
128.35
128.17
128.09
77.32
77.00
76.69
59.66
Ph
N
N
N
HO
Ph
O
147
190
180
170
160
150
140
130
120
110
100
90
80
70
60
50
40
30
20

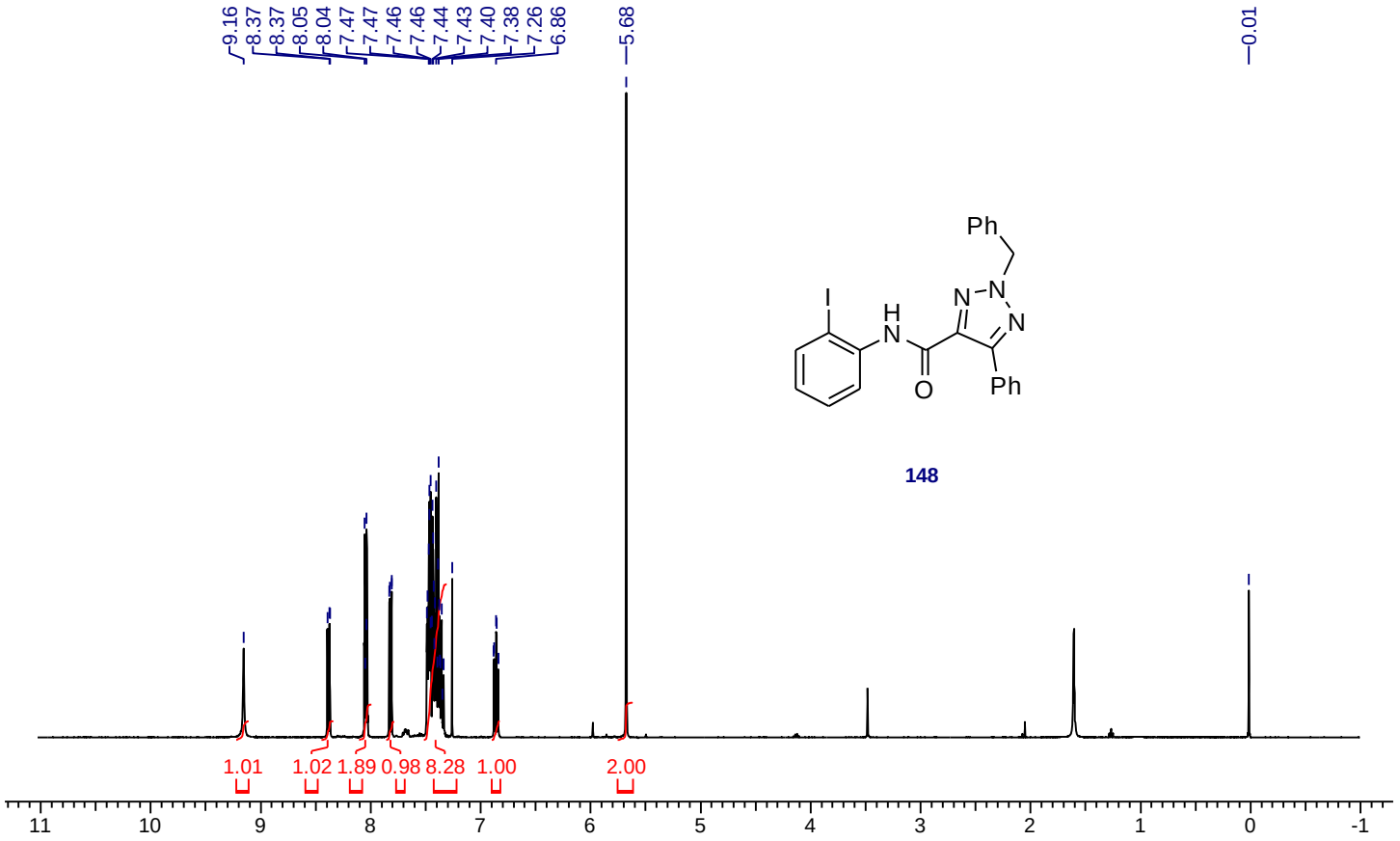
9.16
8.37
8.37
8.05
8.04
7.47
7.47
7.46
7.46
7.44
7.43
7.40
7.38
7.26
6.86
5.68
0.01
1.01
1.02
1.89
0.98
8.28
1.00
2.00
11
10
9
8
7
6
5
4
3
2
1
0
-1
Ph
I
H
N
N
N
N
O
Ph

148

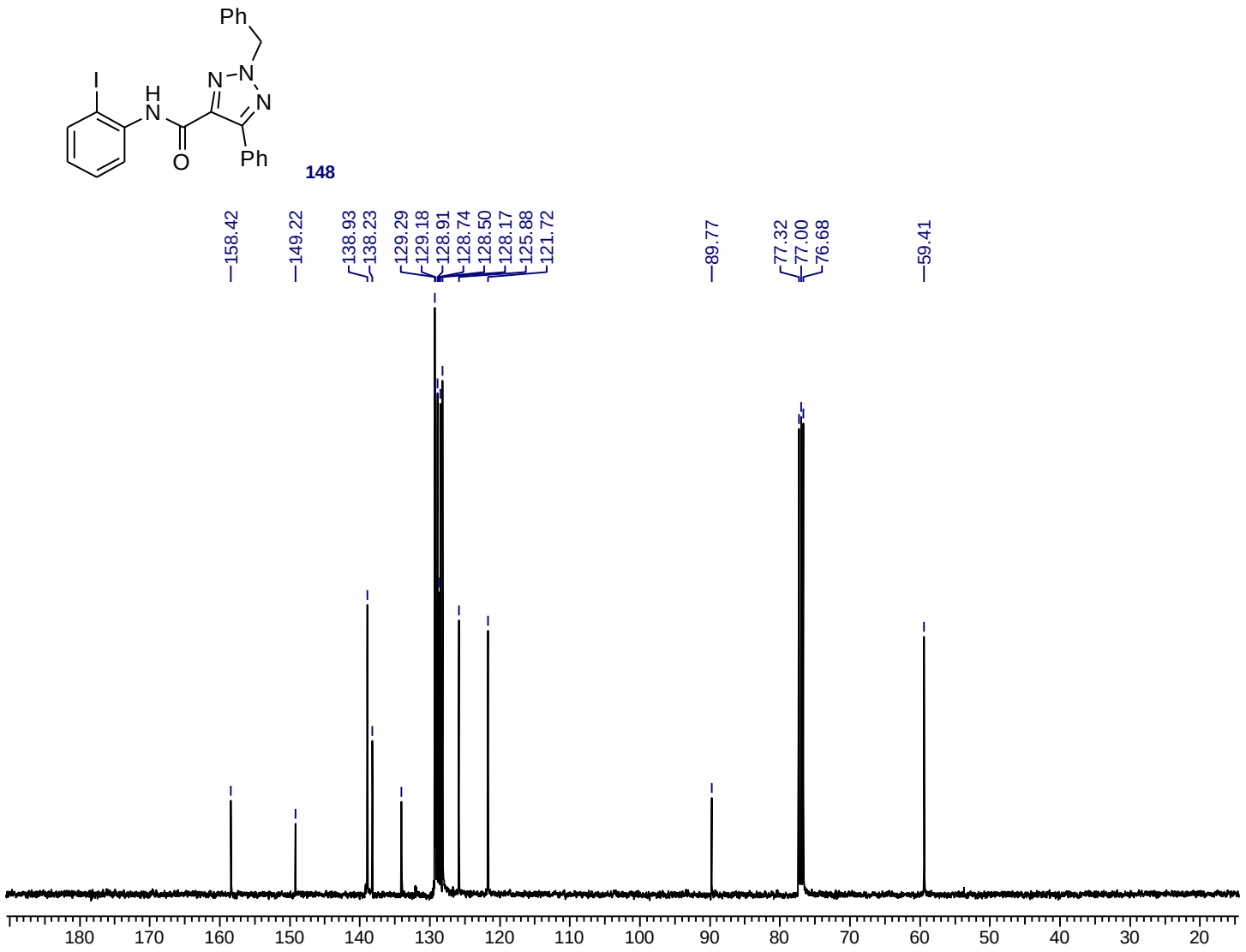
Ph
I
H
N
N
N
N
O
Ph
148
158.42
149.22
138.93
138.23
129.29
129.18
128.91
128.74
128.50
128.17
125.88
121.72
89.77
77.32
77.00
76.68
59.41
180
170
160
150
140
130
120
110
100
90
80
70
60
50
40
30
20

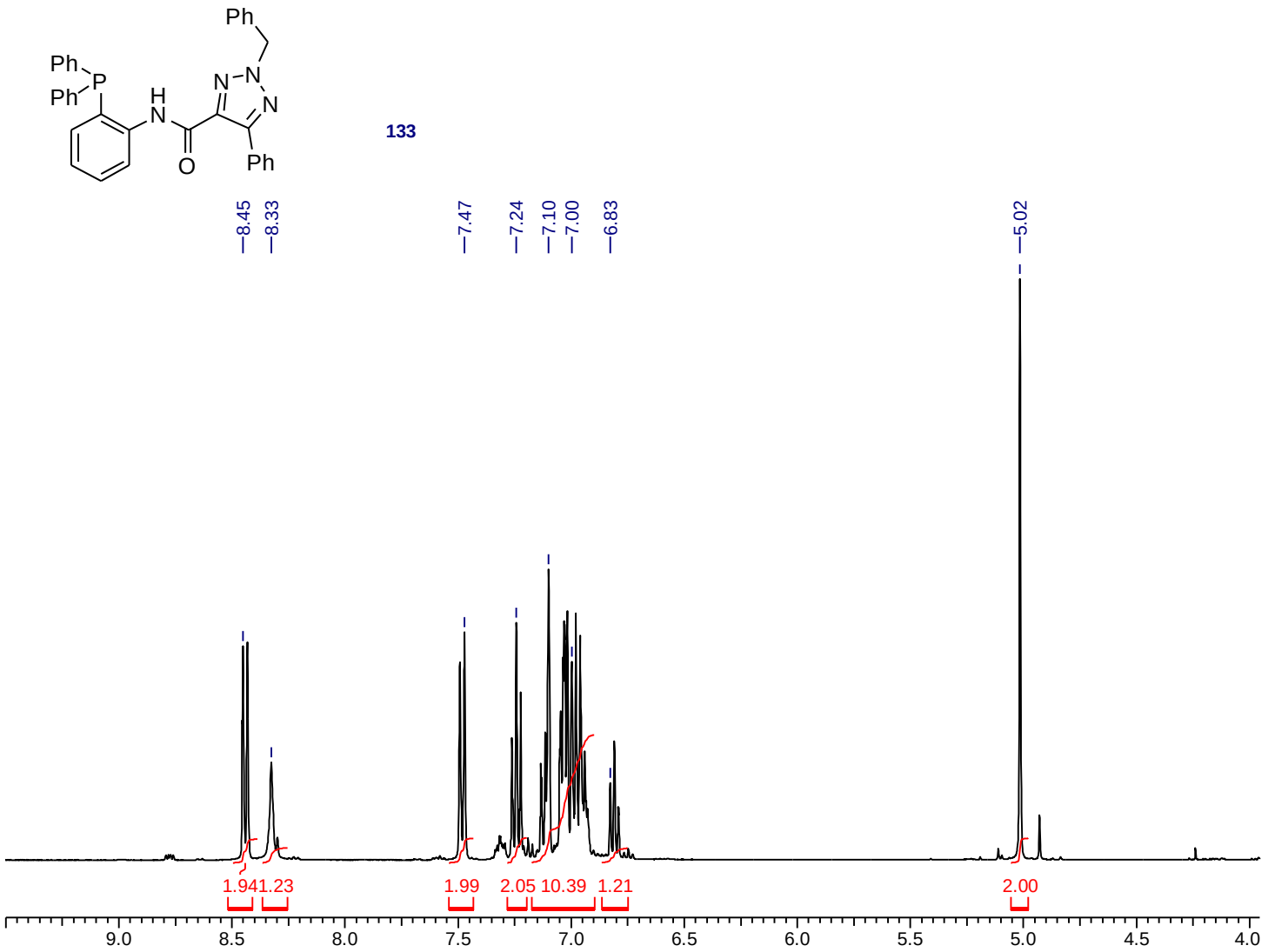
Ph
Ph
P
Ph
H
N
O
N
N
N
Ph
133
8.45
8.33
7.47
7.24
7.10
7.00
6.83
5.02
1.94
1.23
1.99
2.05
10.39
1.21
2.00
9.0
8.5
8.0
7.5
7.0
6.5
6.0
5.5
5.0
4.5
4.0

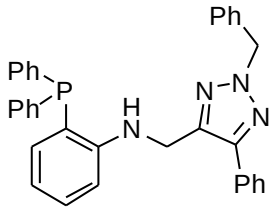
Ph
Ph
P
Ph
H
N
N
N
N
Ph

133

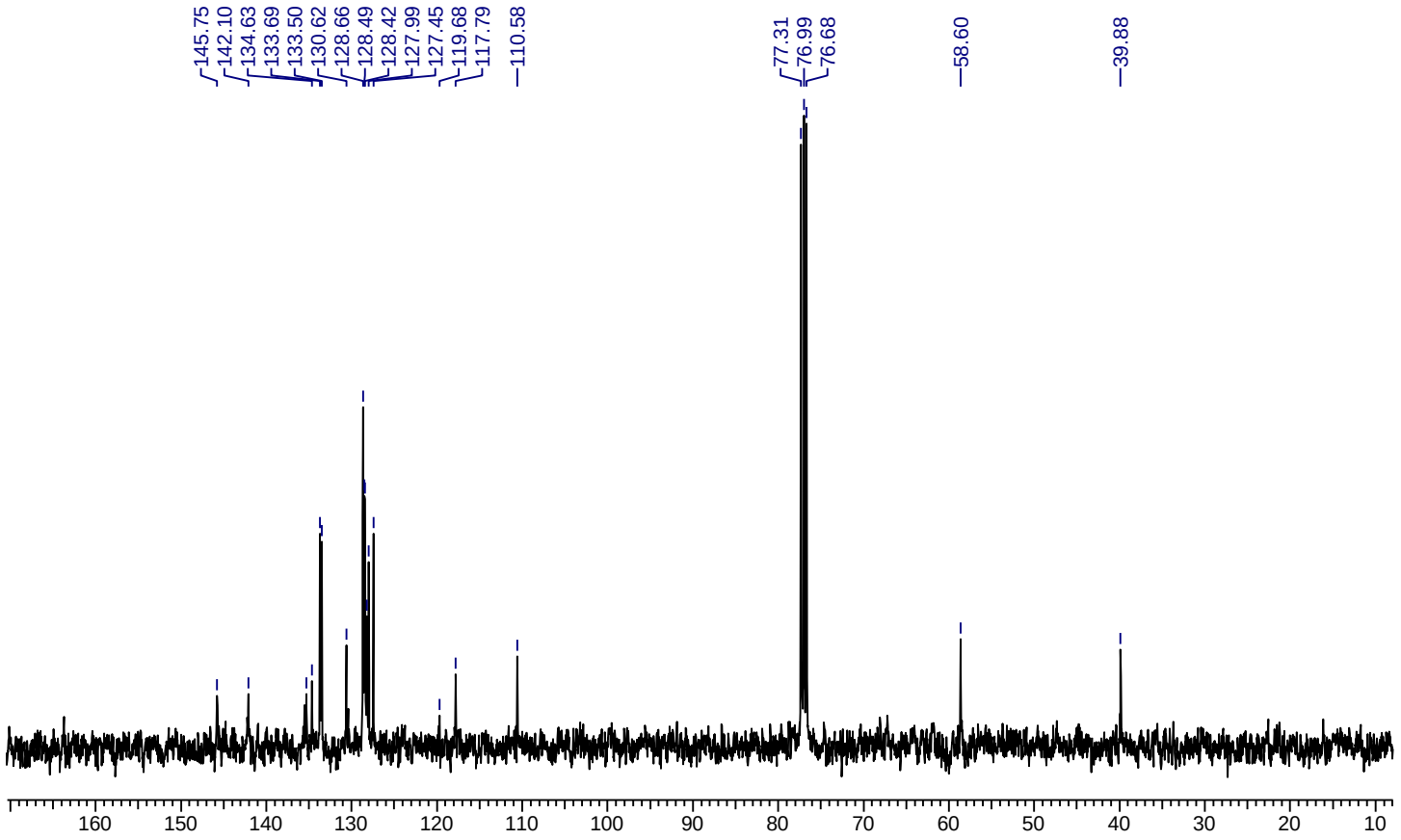
145.75
142.10
134.63
133.69
133.50
130.62
128.66
128.49
128.42
127.99
127.45
119.68
117.79
110.58
77.31
76.99
76.68
58.60
39.88
160
150
140
130
120
110
100
90
80
70
60
50
40
30
20
10

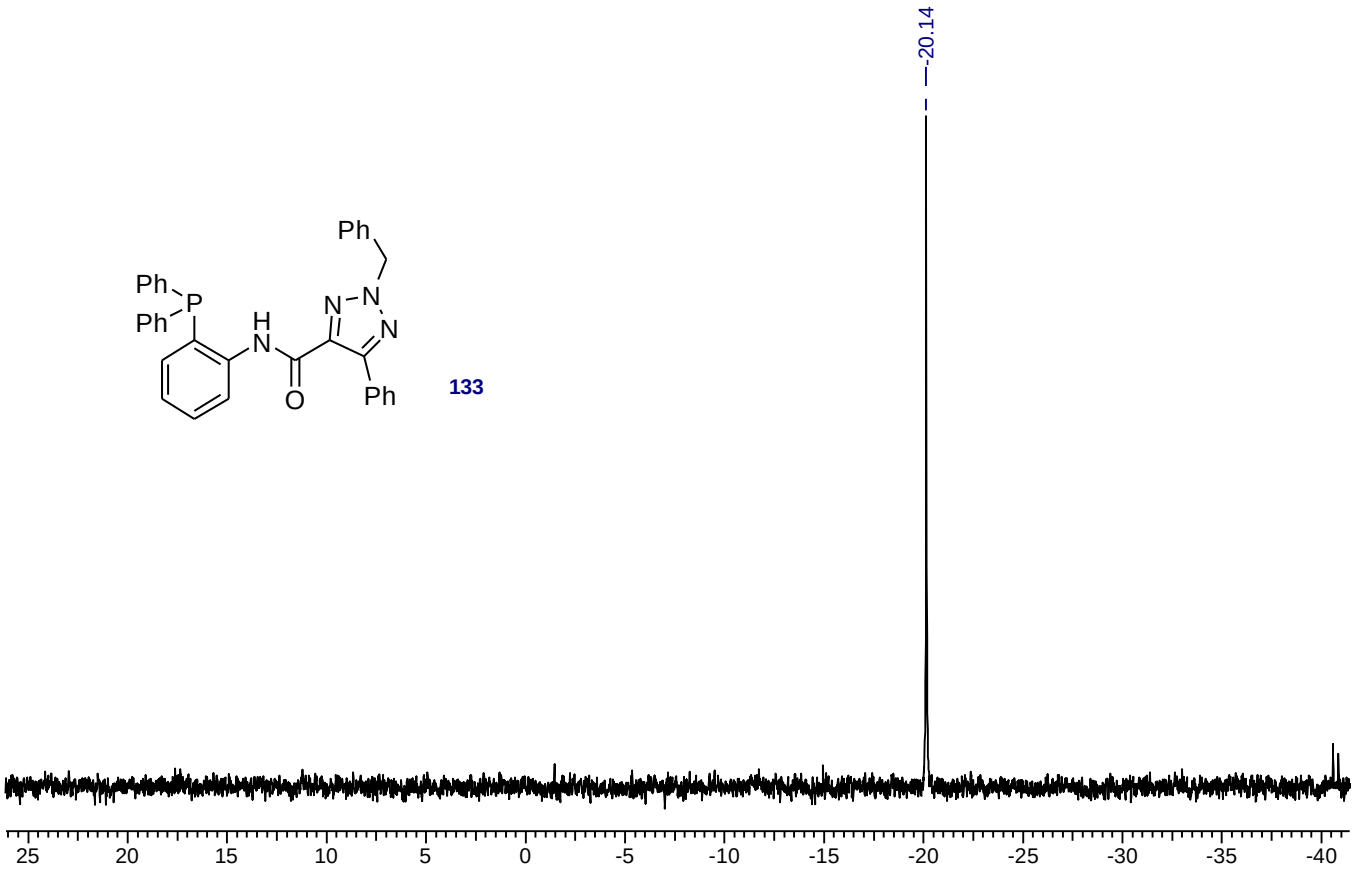
Ph
Ph
P
Ph
H
N
O
N
N
N
Ph
Ph
133
-20.14
25
20
15
10
5
0
-5
-10
-15
-20
-25
-30
-35
-40

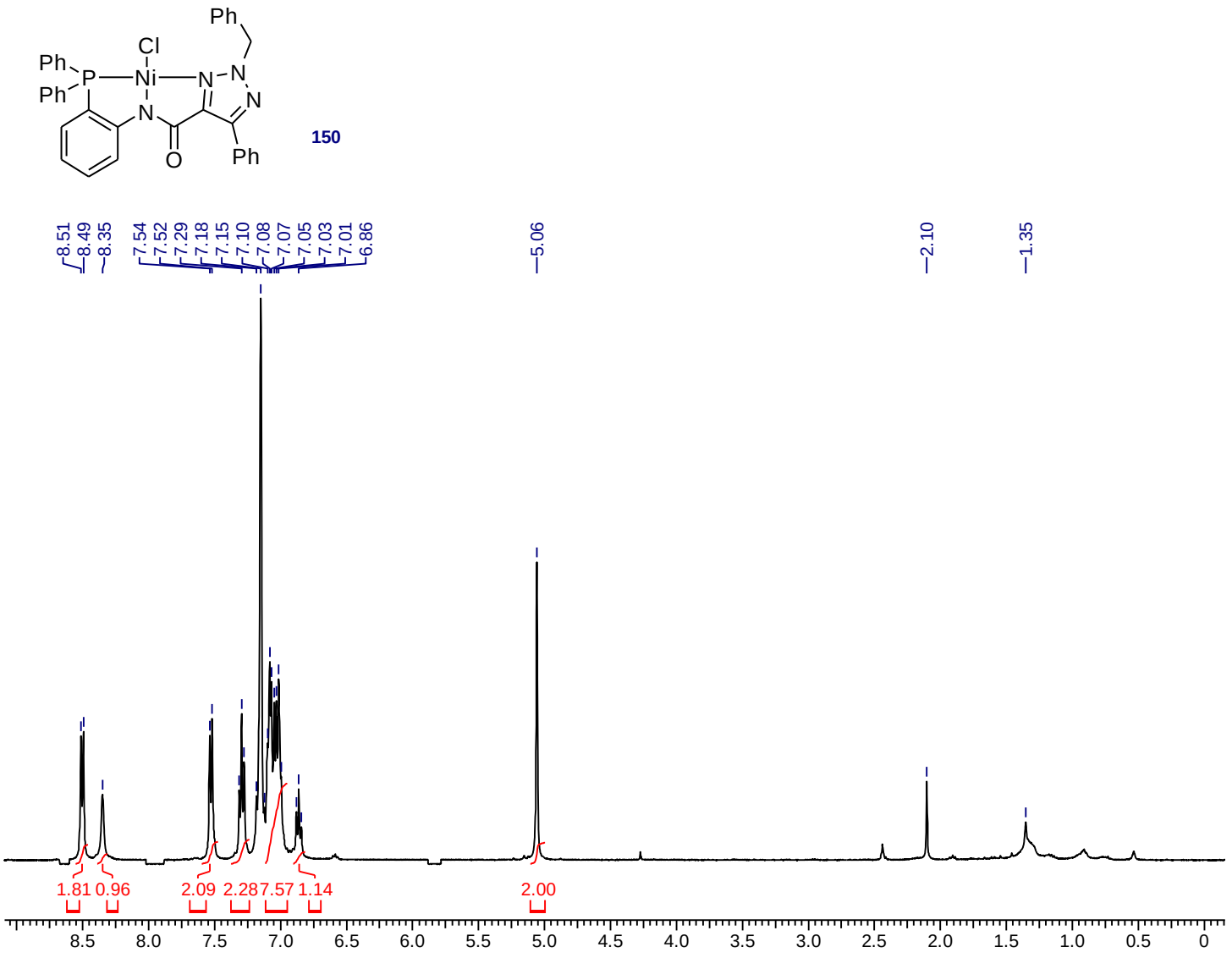
Ph
Cl
Ph
P
Ni
N
N
N
Ph
Ph
N
O
Ph
150
8.51
8.49
8.35
7.54
7.52
7.29
7.18
7.15
7.10
7.08
7.07
7.05
7.03
7.01
6.86
5.06
2.10
1.35
1.81
0.96
2.09
2.28
7.57
1.14
2.00
8.5
8.0
7.5
7.0
6.5
6.0
5.5
5.0
4.5
4.0
3.5
3.0
2.5
2.0
1.5
1.0
0.5
0

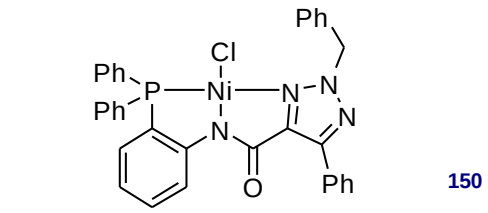
Ph
Cl
Ph
P
Ni
N
N
Ph
N
N
O
Ph

150

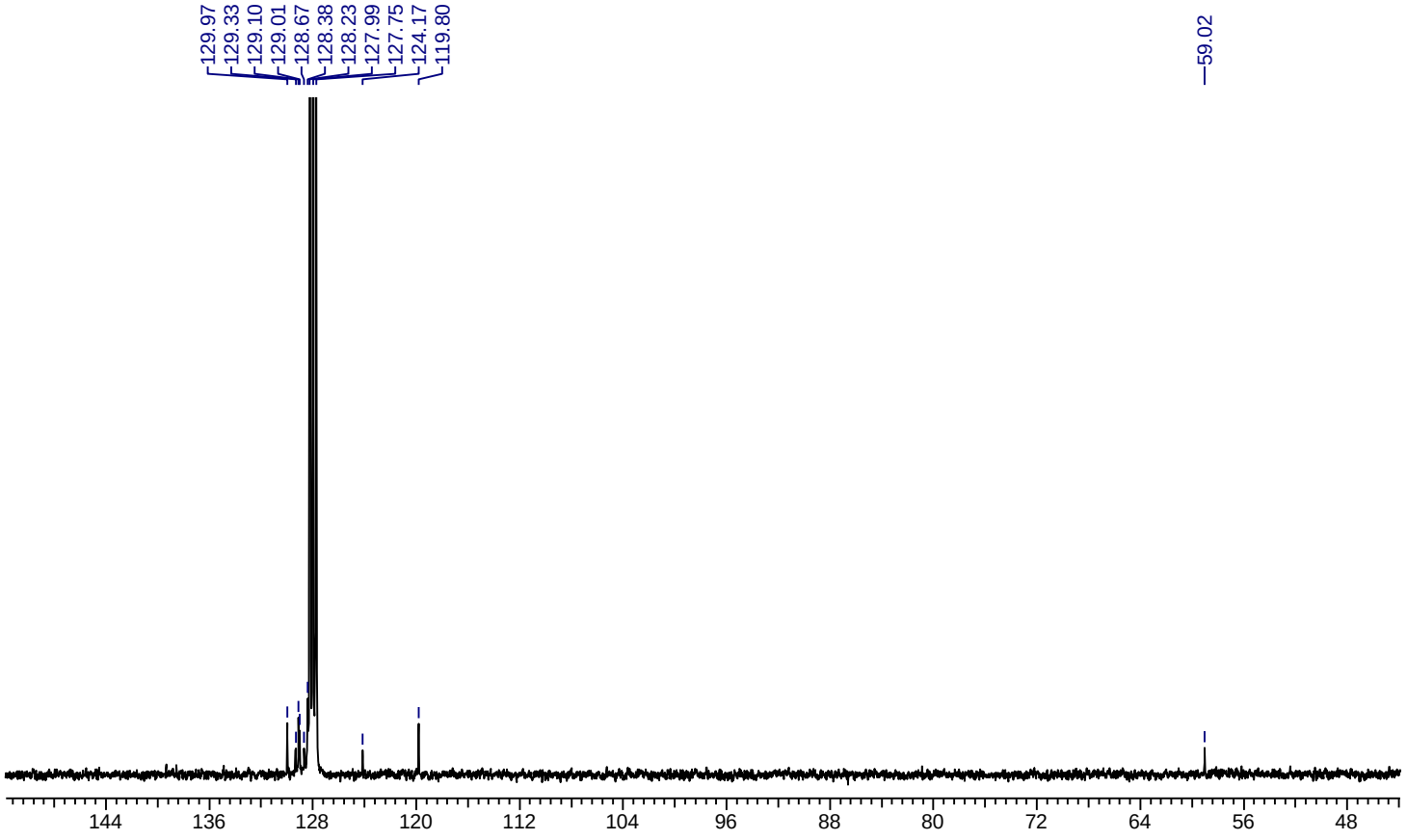
129.97
129.33
129.10
129.01
128.67
128.38
128.23
127.99
127.75
124.17
119.80
59.02
144
136
128
120
112
104
96
88
80
72
64
56
48

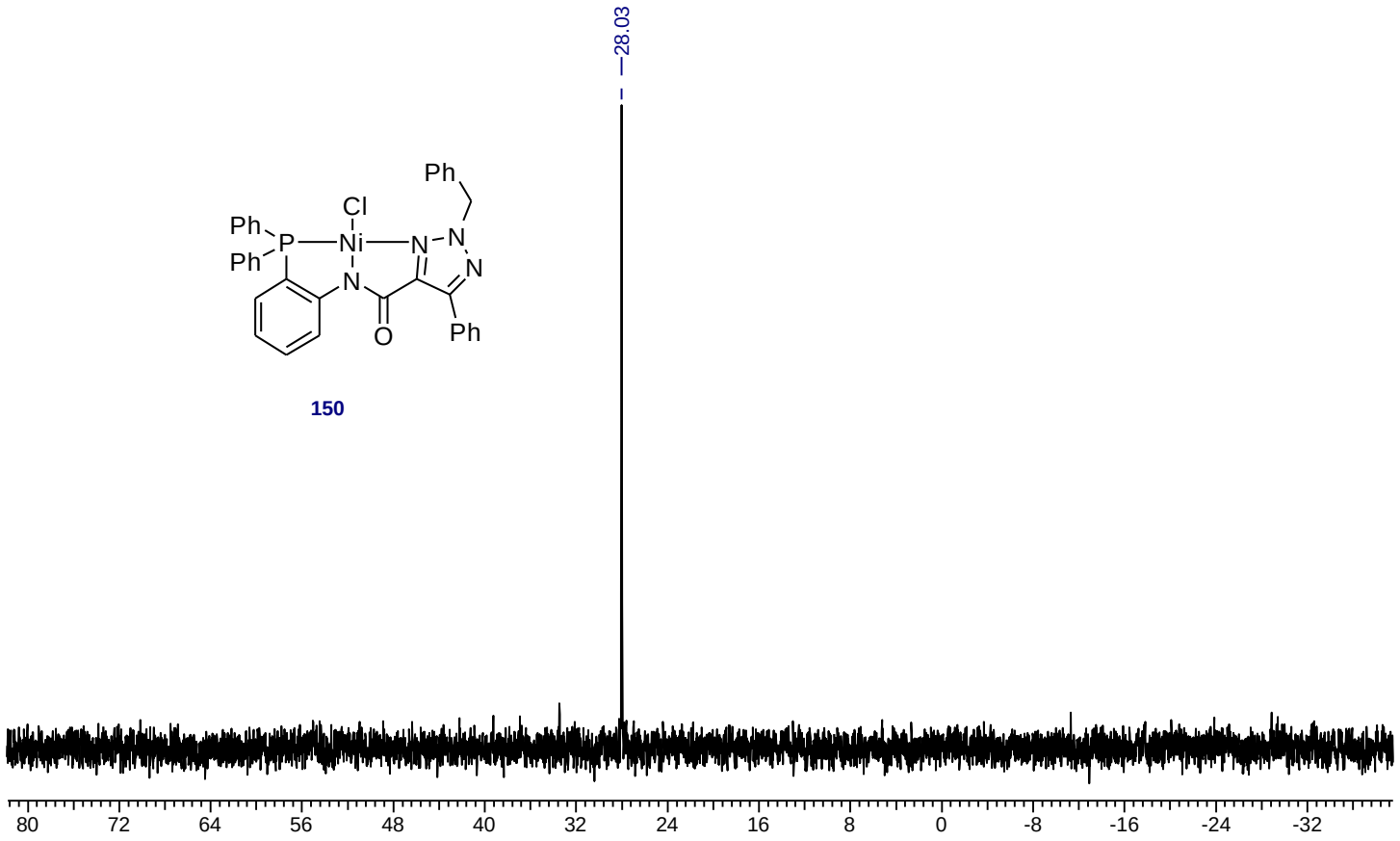

150

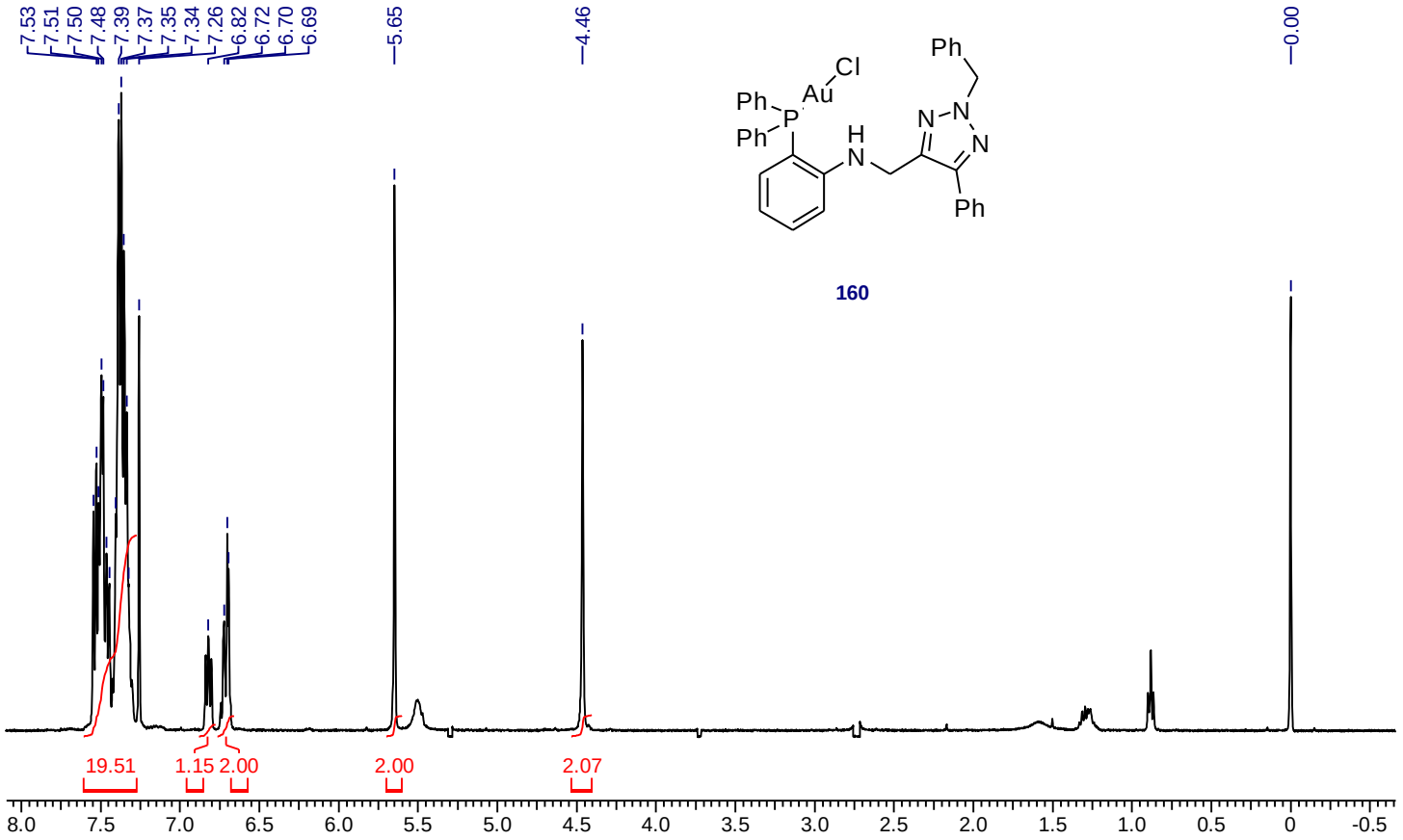
7.53
7.51
7.50
7.48
7.39
7.37
7.35
7.34
7.26
6.82
6.72
6.70
6.69
5.65
4.46
0.00
Ph
Cl
Au
Ph
P
Ph
H
N
N
N
N
Ph
Ph
160
19.51
1.15
2.00
2.00
2.07
8.0
7.5
7.0
6.5
6.0
5.5
5.0
4.5
4.0
3.5
3.0
2.5
2.0
1.5
1.0
0.5
0
-0.5

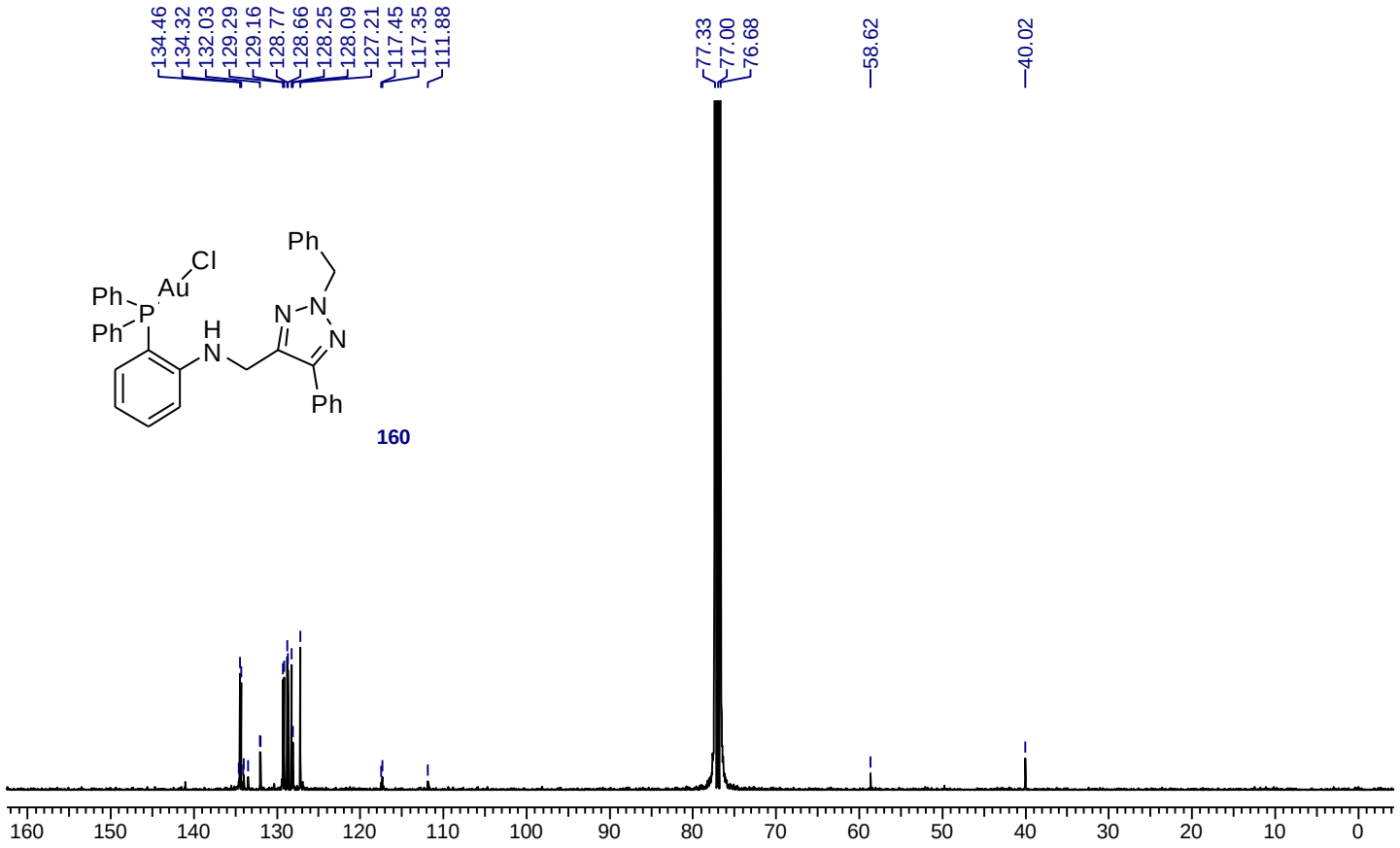
134.46
134.32
132.03
129.29
129.16
128.77
128.66
128.25
128.09
127.21
117.45
117.35
111.88
77.33
77.00
76.68
58.62
40.02
Ph
Cl
Au
Ph
P
Ph
H
N
N
N
N
Ph
160
160
150
140
130
120
110
100
90
80
70
60
50
40
30
20
10
0

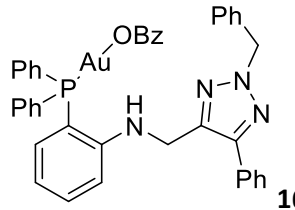

162

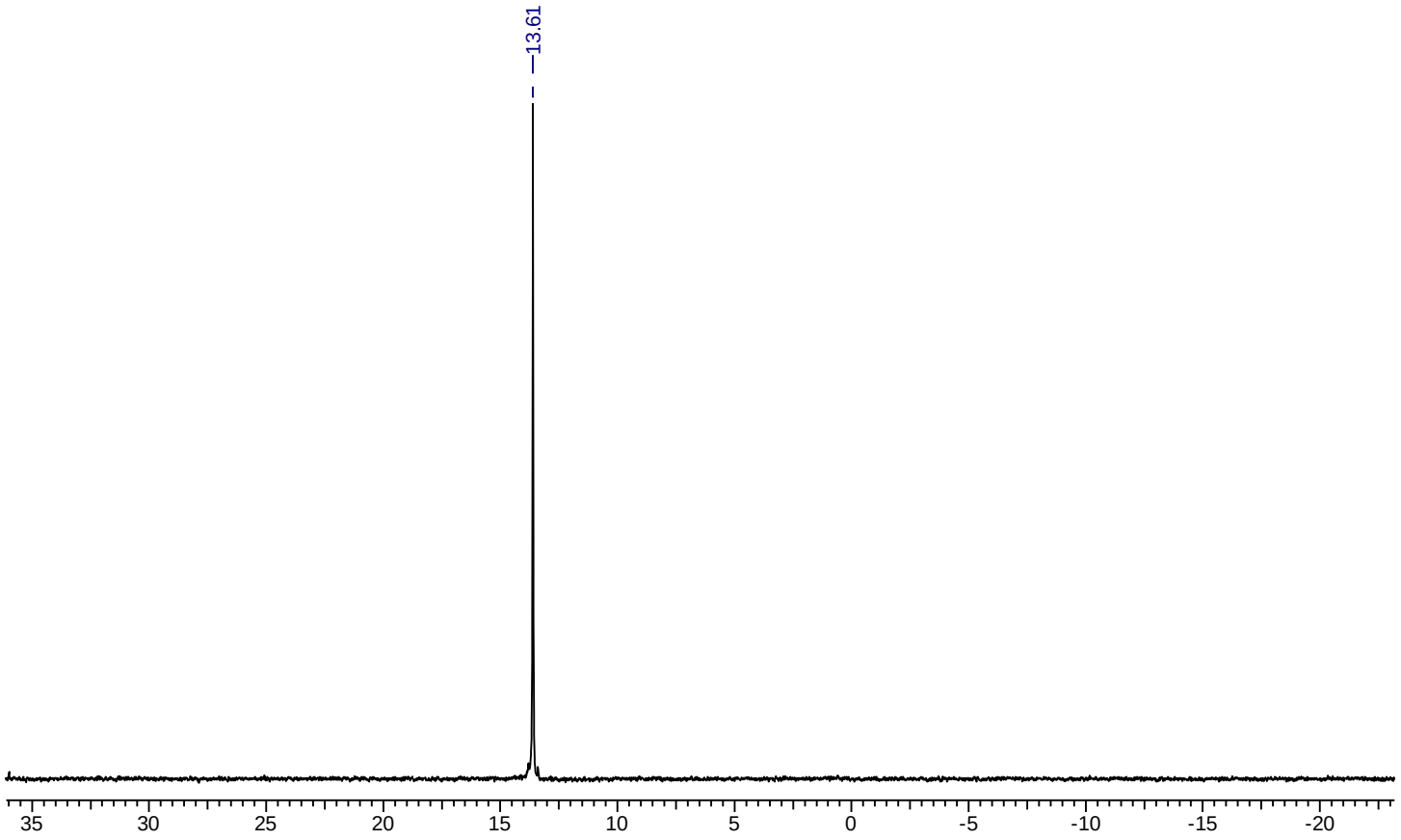

Crystal Structures

Figure 1. Crystal structure of **122**.

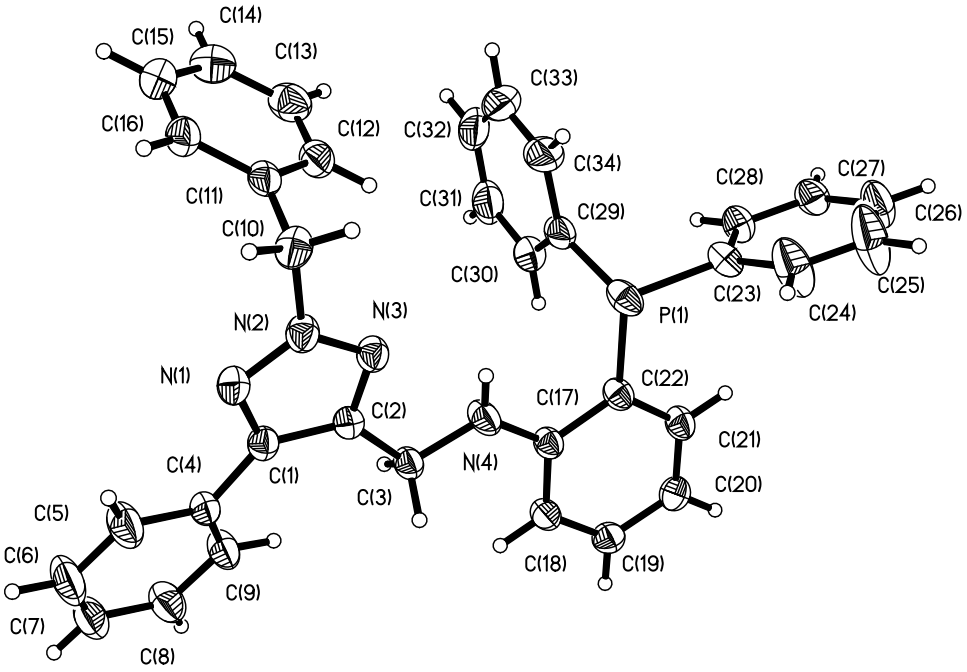

Perspective view of the molecular structure of $C_{34}H_{29}N_4P$ with the atom labeling Scheme provided for the non-hydrogen atoms. The thermal ellipsoids are scaled to enclose 30% probability.

Description of the X-ray Structural Analysis of $C_{34}H_{29}N_4P$

A colorless crystalline fragment of $C_{34}H_{29}N_4P$ was washed with the perfluoropolyether PFO-XR75 (Lancaster) and glued at the end of a glass fiber. The sample was optically aligned on the four-circle of a Siemens P4 diffractometer equipped with a graphite monochromator, a monocap collimator, a Mo Kα radiation source (λ = 0.71073 Å), and a SMART CCD detector held at 5.050 cm from the crystal. Four sets of 20 frames each were collected using the ω scan method and with a 10 s exposure time. Integration of these frames followed by reflection indexing and least-squares refinement produced a crystal orientation matrix for the triclinic crystal lattice.

Data collection consisted of the measurement of a total of 1650 frames in five different runs covering a hemisphere of data. Frame scan parameters are summarized below:

Run	2θ	ω	ϕ	χ	Scan axis	Scan width (°)	Frames (#)	Exposure time (sec.)
1	28	43.00	0.00	280.00	2	-0.3	100	30
2	28	43.00	90.00	280.00	2	-0.3	100	30
3	28	43.00	180.00	280.00	2	-0.3	100	30
4	28	43.00	270.00	280.00	2	-0.3	100	30
5	28	28.00	0.00	30.00	3	0.3	1250	30

The program SMART (version 5.6)[1] was used for diffractometer control, frame scans, indexing, orientation matrix calculations, least-squares refinement of cell parameters, and the data collection. All 1650 crystallographic raw data frames were read by the program SAINT (version 5/6.0)[1] and integrated using 3D profiling algorithms. The resulting data were reduced to produce a total of 10015 reflections and their intensities and estimated standard deviations. An absorption

correction was applied using the SADABS routine available in SAINT.[1] The data were corrected for Lorentz and polarization effects. No evidence of crystal decomposition was observed. Data preparation was carried out by using the program XPREP,[1] which gave 6259 unique reflections (R_{int} = 3.25 %) with indices $-13 \leq h \leq 11$, $-13 \leq k \leq 14$, $-16 \leq l \leq 16$. The triclinic space group was determined to be $P\bar{1}$ (No. 2).

The structure was solved by a combination of direct methods and difference Fourier analysis with the use of SHELXTL 6.1.[2] Idealized positions for the methylene and aromatic hydrogen atoms were included as fixed contributions using a riding model with isotropic temperature factors set at 1.2 times that of the adjacent carbon atom. The residual electron density for the amine hydrogen atom was located and the hydrogen atom position was refined isotropically. Full-matrix least-squares refinement, based upon the minimization of $\Sigma w_i |F_o^2 - F_c^2|^2$, with weighting $w_i^{-1} = [\sigma^2(F_o^2) + (0.0739\ P)^2 + 0.1790\ P]$, where $P = (\text{Max}\ (F_o^2, 0) + 2\ F_c^2)/3$, converged to give final discrepancy indices[3] of R1 = 0.0496, wR2 = 0.1387 for 5073 diffraction data with $I > 2\ \sigma(I)$. The goodness of fit (GOF) value was 1.048.

A correction for secondary extinction was not applied. The maximum and minimum residual electron density peaks in the final difference Fourier map were 0.259 and -0.385 e/Å^3, respectively. The linear absorption coefficient, atomic scattering factors, and anomalous dispersion corrections were calculated from values found in the International Tables of X-ray Crystallography.[4]

References

1. SMART, SAINT and XPREP programs are part of Bruker crystallographic software package for single crystal data collection, reduction and preparation.
2. Sheldrick, G. M., SHELXTL6.1 (2000), Crystallographic software package, Bruker AXS, Inc. Madison, Wisconsin, USA.
3. $R_1 = \sum(||F_o| - |F_c||) / \sum|F_o|$, $wR_2 = [\sum[w(F_o^2 - F_c^2)^2] / \sum[w(F_o^2)^2]]^{1/2}$, $R_{int.} = \sum|F_o^2 - F_o^2(mean)|^2 / \sum[F_o^2]$, and GOF = $[\sum[w(F_o^2 - F_c^2)^2] / (n-p)]^{1/2}$, where n is the number of reflections and p is the total number of parameters which were varied during the last refinement cycle.
4. International Tables for X-ray Crystallography (1974). Vol. IV, p. 55. Birmingham: Kynoch Press. (Present distributor, D. Reidel, Dordrecht.).

Table 1. Crystal data and structure refinement for $C_{34}H_{29}N_4P$.

Identification code	xs50ccd	
Empirical formula	$C_{34}H_{29}N_4P$	
Formula weight	524.58	
Temperature	293(2) K	
Wavelength	0.71073 Å	
Crystal system	triclinic	
Space group	$P\bar{1}$	
Unit cell dimensions	a = 10.219(1) Å	□= 93.222(2)°
	b = 11.226(1) Å	□= 92.138(2)°
	c = 12.737(1) Å	□ = 104.336(2)°
Volume	1411.4(2) $Å^3$	
Z	2	
Density (calculated)	1.234 g/cm^3	
Absorption coefficient	1.27 cm^{-1}	
F(000)	552	
Crystal size	0.56 x 0.52 x 0.40 mm	
Theta range for data collection	1.88 to 27.59°	
Index ranges	$-13 \leq h \leq 11$, $-13 \leq k \leq 14$, $-16 \leq l \leq 16$	
Reflections collected	10015	
Independent reflections	6259 [R(int) = 0.0325]	
Completeness to theta = 27.59°	95.6 %	
Max. and min. transmission	0.951 and 0.932	
Refinement method	Full-matrix least-squares on F^2	
Data / restraints / parameters	6259 / 0 / 356	

Goodness-of-fit on F^2	1.048
Final R indices [I>2sigma(I)]	R1 = 0.0496, wR2 = 0.1387
R indices (all data)	R1 = 0.0595, wR2 = 0.1490
Largest diff. peak and hole	0.259 and -0.385 e/$Å^3$

Table 2. Atomic coordinates (x 10^4) and equivalent isotropic displacement parameters ($Å^2$ x 10^3) for $C_{34}H_{29}N_4P$. U(eq) is defined as one third of the trace of the orthogonalized U_{ij} tensor.

	x	y	z	U(eq)
P(1)	2738(1)	-856(1)	7760(1)	58(1)
N(1)	2039(1)	2784(1)	3876(1)	53(1)
N(2)	1392(1)	1919(1)	4479(1)	53(1)
N(3)	2187(1)	1474(1)	5123(1)	51(1)
N(4)	4196(2)	902(2)	6237(1)	63(1)
C(1)	3354(2)	2894(1)	4124(1)	47(1)
C(2)	3438(1)	2070(1)	4908(1)	46(1)
C(3)	4640(2)	1790(1)	5467(1)	49(1)
C(4)	4389(2)	3805(1)	3612(1)	51(1)
C(5)	4028(2)	4352(2)	2735(2)	82(1)
C(6)	4967(3)	5285(3)	2303(2)	101(1)
C(7)	6272(2)	5679(2)	2722(2)	82(1)
C(8)	6641(2)	5134(2)	3571(2)	74(1)
C(9)	5713(2)	4200(2)	4016(1)	64(1)
C(10)	-64(2)	1688(2)	4592(2)	61(1)

C(11)	-393(1)	2566(1)	5426(1)	52(1)
C(12)	42(2)	2551(2)	6476(1)	64(1)
C(13)	-237(2)	3368(2)	7225(2)	78(1)
C(14)	-926(2)	4223(2)	6949(2)	81(1)
C(15)	-1376(2)	4241(2)	5913(2)	76(1)
C(16)	-1111(2)	3417(2)	5161(1)	64(1)
C(17)	5069(1)	402(1)	6813(1)	46(1)
C(18)	6460(2)	698(1)	6660(1)	52(1)
C(19)	7317(2)	153(2)	7218(1)	54(1)
C(20)	6829(2)	-687(2)	7949(1)	57(1)
C(21)	5464(2)	-969(1)	8128(1)	53(1)
C(22)	4558(1)	-438(1)	7589(1)	47(1)
C(23)	2550(2)	-1977(2)	8773(1)	55(1)
C(24)	2132(3)	-3216(2)	8457(2)	107(1)
C(25)	1974(4)	-4105(2)	9177(2)	137(1)
C(26)	2216(3)	-3768(2)	10236(2)	89(1)
C(27)	2620(2)	-2557(2)	10565(1)	64(1)
C(28)	2800(2)	-1663(2)	9843(1)	57(1)
C(29)	2454(2)	485(2)	8525(1)	64(1)
C(30)	3475(2)	1460(2)	8984(2)	70(1)
C(31)	3156(3)	2410(2)	9592(2)	96(1)
C(32)	1828(5)	2394(3)	9741(2)	121(1)
C(33)	816(4)	1441(4)	9292(3)	131(1)
C(34)	1109(2)	502(3)	8673(2)	95(1)

Table 3. Interatomic distances [Å] and bond angles [°] for $C_{34}H_{29}N_4P$.

P(1)-C(22)	1.827(2)
P(1)-C(23)	1.835(2)
P(1)-C(29)	1.836(2)
N(1)-N(2)	1.332(2)
N(1)-C(1)	1.342(2)
N(2)-N(3)	1.334(2)
N(2)-C(10)	1.460(2)
N(3)-C(2)	1.335(2)
N(4)-C(17)	1.377(2)
N(4)-C(3)	1.442(2)
C(1)-C(2)	1.414(2)
C(1)-C(4)	1.477(2)
C(2)-C(3)	1.505(2)
C(4)-C(9)	1.384(2)
C(4)-C(5)	1.385(2)
C(5)-C(6)	1.388(3)
C(6)-C(7)	1.374(3)
C(7)-C(8)	1.357(3)
C(8)-C(9)	1.391(2)
C(10)-C(11)	1.512(2)
C(11)-C(16)	1.390(2)
C(11)-C(12)	1.395(2)
C(12)-C(13)	1.373(3)

C(13)-C(14)	1.376(3)
C(14)-C(15)	1.384(3)
C(15)-C(16)	1.375(3)
C(17)-C(18)	1.401(2)
C(17)-C(22)	1.428(2)
C(18)-C(19)	1.384(2)
C(19)-C(20)	1.380(2)
C(20)-C(21)	1.383(2)
C(21)-C(22)	1.398(2)
C(23)-C(24)	1.382(3)
C(23)-C(28)	1.386(2)
C(24)-C(25)	1.377(3)
C(25)-C(26)	1.376(3)
C(26)-C(27)	1.356(3)
C(27)-C(28)	1.384(2)
C(29)-C(30)	1.395(3)
C(29)-C(34)	1.399(3)
C(30)-C(31)	1.394(3)
C(31)-C(32)	1.373(5)
C(32)-C(33)	1.370(5)
C(33)-C(34)	1.380(5)

C(22)-P(1)-C(23)	103.23(7)
C(22)-P(1)-C(29)	103.50(7)
C(23)-P(1)-C(29)	100.61(7)

N(2)-N(1)-C(1)	104.32(12)
N(1)-N(2)-N(3)	115.11(12)
N(1)-N(2)-C(10)	121.37(13)
N(3)-N(2)-C(10)	122.12(13)
N(2)-N(3)-C(2)	104.14(12)
C(17)-N(4)-C(3)	123.07(13)
N(1)-C(1)-C(2)	107.81(13)
N(1)-C(1)-C(4)	119.48(13)
C(2)-C(1)-C(4)	132.67(14)
N(3)-C(2)-C(1)	108.60(13)
N(3)-C(2)-C(3)	120.14(12)
C(1)-C(2)-C(3)	131.25(13)
N(4)-C(3)-C(2)	110.11(12)
C(9)-C(4)-C(5)	117.74(16)
C(9)-C(4)-C(1)	122.23(13)
C(5)-C(4)-C(1)	119.91(16)
C(4)-C(5)-C(6)	120.3(2)
C(7)-C(6)-C(5)	121.22(19)
C(8)-C(7)-C(6)	118.89(19)
C(7)-C(8)-C(9)	120.67(19)
C(4)-C(9)-C(8)	121.17(16)
N(2)-C(10)-C(11)	111.45(13)
C(16)-C(11)-C(12)	118.70(16)
C(16)-C(11)-C(10)	120.77(15)
C(12)-C(11)-C(10)	120.52(15)

C(13)-C(12)-C(11)	120.16(17)
C(12)-C(13)-C(14)	120.57(18)
C(13)-C(14)-C(15)	119.96(19)
C(16)-C(15)-C(14)	119.71(19)
C(15)-C(16)-C(11)	120.88(17)
N(4)-C(17)-C(18)	121.59(13)
N(4)-C(17)-C(22)	119.78(13)
C(18)-C(17)-C(22)	118.63(13)
C(19)-C(18)-C(17)	120.86(13)
C(20)-C(19)-C(18)	121.01(14)
C(19)-C(20)-C(21)	118.95(14)
C(20)-C(21)-C(22)	122.22(14)
C(21)-C(22)-C(17)	118.27(13)
C(21)-C(22)-P(1)	123.08(11)
C(17)-C(22)-P(1)	118.49(11)
C(24)-C(23)-C(28)	117.46(16)
C(24)-C(23)-P(1)	118.37(13)
C(28)-C(23)-P(1)	124.17(13)
C(25)-C(24)-C(23)	121.29(19)
C(26)-C(25)-C(24)	120.1(2)
C(27)-C(26)-C(25)	119.65(19)
C(26)-C(27)-C(28)	120.39(16)
C(27)-C(28)-C(23)	121.10(15)
C(30)-C(29)-C(34)	118.3(2)
C(30)-C(29)-P(1)	124.82(13)

C(34)-C(29)-P(1)	116.89(18)
C(31)-C(30)-C(29)	120.5(2)
C(32)-C(31)-C(30)	120.0(3)
C(33)-C(32)-C(31)	120.0(3)
C(32)-C(33)-C(34)	120.9(3)
C(33)-C(34)-C(29)	120.2(3)

Table 4. Anisotropic displacement parameters ($Å^2$ x 10^3) for $C_{34}H_{29}N_4P$. The anisotropic displacement factor exponent takes the form: $-2\pi^2[h^2 a^{*2}U_{11} + ... + 2 h k a^* b^* U_{12}]$.

	U_{11}	U_{22}	U_{33}	U_{23}	U_{13}	U_{12}
P(1)	45(1)	74(1)	48(1)	20(1)	-4(1)	1(1)
N(1)	57(1)	52(1)	53(1)	9(1)	-2(1)	16(1)
N(2)	48(1)	51(1)	61(1)	10(1)	-3(1)	12(1)
N(3)	47(1)	50(1)	56(1)	10(1)	-2(1)	12(1)
N(4)	44(1)	83(1)	66(1)	39(1)	5(1)	14(1)
C(1)	53(1)	46(1)	45(1)	5(1)	1(1)	15(1)
C(2)	47(1)	46(1)	45(1)	6(1)	3(1)	13(1)
C(3)	47(1)	55(1)	49(1)	17(1)	4(1)	13(1)
C(4)	60(1)	50(1)	46(1)	12(1)	8(1)	19(1)
C(5)	69(1)	105(2)	76(1)	46(1)	-1(1)	19(1)
C(6)	93(2)	126(2)	93(2)	73(2)	12(1)	28(2)
C(7)	80(1)	82(1)	84(1)	41(1)	18(1)	13(1)
C(8)	66(1)	78(1)	74(1)	26(1)	6(1)	5(1)
C(9)	63(1)	68(1)	60(1)	26(1)	2(1)	9(1)
C(10)	46(1)	52(1)	82(1)	6(1)	-11(1)	7(1)
C(11)	36(1)	52(1)	66(1)	18(1)	0(1)	3(1)
C(12)	49(1)	73(1)	71(1)	25(1)	0(1)	13(1)
C(13)	68(1)	105(2)	61(1)	16(1)	4(1)	18(1)
C(14)	76(1)	91(1)	76(1)	1(1)	14(1)	21(1)

C(15)	78(1)	76(1)	84(1)	20(1)	13(1)	33(1)
C(16)	61(1)	69(1)	65(1)	21(1)	2(1)	20(1)
C(17)	46(1)	51(1)	43(1)	11(1)	1(1)	11(1)
C(18)	47(1)	55(1)	52(1)	14(1)	6(1)	10(1)
C(19)	45(1)	60(1)	59(1)	7(1)	4(1)	15(1)
C(20)	56(1)	61(1)	59(1)	11(1)	-2(1)	23(1)
C(21)	57(1)	54(1)	49(1)	15(1)	1(1)	13(1)
C(22)	46(1)	51(1)	42(1)	8(1)	-1(1)	7(1)
C(23)	53(1)	59(1)	48(1)	10(1)	4(1)	0(1)
C(24)	179(3)	66(1)	52(1)	3(1)	4(1)	-11(1)
C(25)	256(4)	53(1)	75(1)	7(1)	6(2)	-9(2)
C(26)	132(2)	64(1)	68(1)	25(1)	20(1)	12(1)
C(27)	74(1)	70(1)	47(1)	13(1)	7(1)	15(1)
C(28)	65(1)	54(1)	49(1)	8(1)	0(1)	6(1)
C(29)	54(1)	80(1)	67(1)	38(1)	11(1)	25(1)
C(30)	77(1)	71(1)	69(1)	23(1)	16(1)	28(1)
C(31)	146(2)	75(1)	80(1)	30(1)	29(1)	47(2)
C(32)	187(4)	114(2)	107(2)	63(2)	73(2)	103(2)
C(33)	125(3)	166(3)	152(3)	95(3)	75(2)	104(3)
C(34)	62(1)	127(2)	113(2)	58(2)	24(1)	43(1)

Table 5. Hydrogen atom coordinates (x 10^4) and isotropic displacement parameters ($Å^2$ x 10^3) for $C_{34}H_{29}N_4P$.

	x	y	z	U(eq)
H(1)	3370(20)	687(19)	6272(15)	73(6)
H(3A)	5169	1465	4959	59
H(3B)	5210	2541	5813	59
H(5)	3152	4093	2435	99
H(6)	4708	5649	1718	122
H(7)	6892	6308	2430	98
H(8)	7524	5388	3858	89
H(9)	5986	3835	4594	77
H(10A)	-415	847	4781	73
H(10B)	-503	1780	3924	73
H(12)	521	1986	6668	77
H(13)	43	3344	7925	94
H(14)	-1090	4787	7458	97
H(15)	-1856	4808	5726	91
H(16)	-1415	3430	4465	76
H(18)	6812	1269	6177	62
H(19)	8236	356	7099	65
H(20)	7409	-1057	8315	68
H(21)	5137	-1530	8625	63

H(24)	1955	-3455	7745	128
H(25)	1702	-4935	8948	164
H(26)	2104	-4367	10723	107
H(27)	2777	-2327	11280	77
H(28)	3093	-836	10079	69
H(30)	4375	1475	8884	84
H(31)	3843	3056	9896	115
H(32)	1615	3029	10145	145
H(33)	-81	1428	9407	157
H(34)	410	-122	8354	114

Figure 2. Crystal structure of **123**.

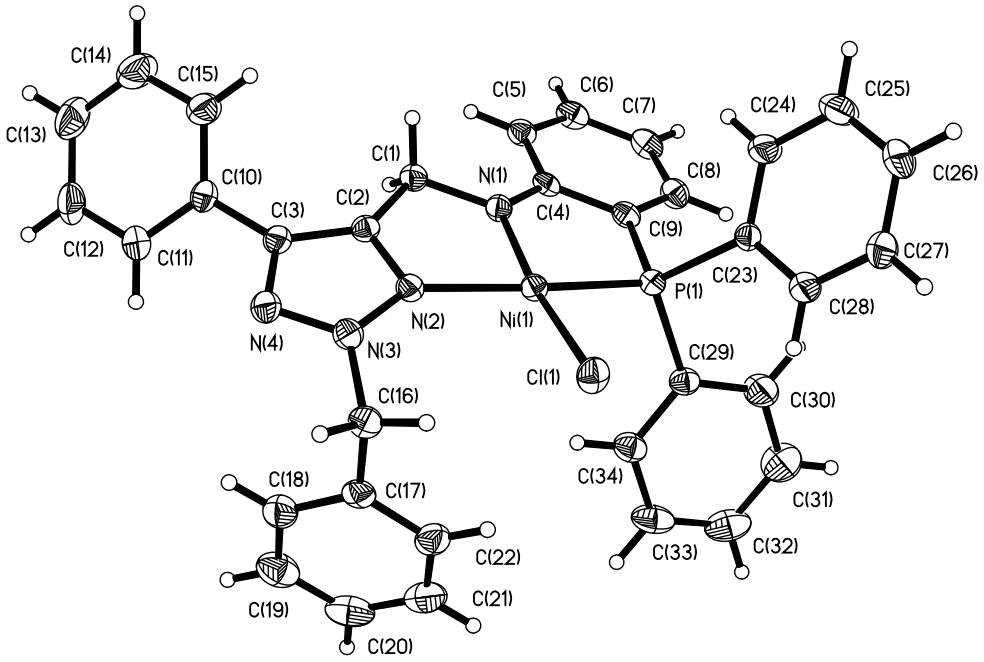

Perspective view of the molecular structure of $NiCl(C_{34}H_{28}PN_4)$ with the atom labeling Scheme provided for the non-hydrogen atoms. The thermal ellipsoids are scaled to enclose 30% probability.

Description of the X-ray Structural Analysis of $NiCl(C_{34}H_{28}PN_4)$

A green crystal of $NiCl(C_{34}H_{28}PN_4)$ was washed with the perfluoropolyether PFO-XR75 (Lancaster) and wedged in a glass capillary. The sample was optically aligned on a Bruker AXS D8 Venture fixed-chi X-ray diffractometer equipped with a Triumph monochromator, a Mo Kα radiation source (λ = 0.71073 Å), and a PHOTON 100 CMOS detector held at 6.00 cm from the crystal. Two sets of 12 frames each were collected using the ω scan method and a 10 s exposure time. Integration of these frames followed by reflection indexing and least-squares refinement produced a crystal orientation matrix for the monoclinic crystal lattice.

Data collection consisted of the measurement of a total of 960 frames in four different runs using omega scans. Frame scan parameters are summarized in Table 6 below:

Table 6. Data collection details for $NiCl(C_{34}H_{28}PN_4)$.

Run	2θ	ω	φ	χ	Scan Width (º)	Frames	Exposure Time (sec)
1	-28.00	-28.00	0.00	54.74	0.50	240	15.00
2	-28.00	-28.00	90.00	54.74	0.50	240	15.00
3	28.00	28.00	180.00	54.74	0.50	240	15.00
4	28.00	28.00	270.00	54.74	0.50	240	15.00

The APEX2 software program (version 2013.10-0)[1] was used for diffractometer control, preliminary frame scans, indexing, orientation matrix calculations, least-squares refinement of cell parameters, and the data collection. The integration of the data using a monoclinic unit cell yielded a total of 27320 reflections to a maximum θ angle of 28.28° (0.75 Å resolution), of which 7091 were independent (average redundancy 3.853, completeness = 99.5%, R_{int} = 2.30%, R_{sig} = 2.08%) and 6033 (85.08%) were greater than $2\sigma(F^2)$. The final cell constants of a = 12.8940(4) Å, b = 25.6807(6) Å, c = 9.0654(2) Å, β = 106.8450(12)°, volume = 2873.00(13) $Å^3$, are based upon the refinement of the XYZ-centroids of 9397 reflections above 20 σ(I) with 6.346° < 2θ < 68.36°. Data were corrected for absorption effects using the multi-scan method (SADABS). The ratio of minimum to maximum apparent transmission was 0.756. The calculated minimum and maximum transmission coefficients (based on crystal size) are 0.705 and 0.834.

The structure was solved by direct methods and difference Fourier analysis using the programs provided by SHELXL-2013.[2] Idealized positions for the hydrogen atoms were included as fixed contributions using a riding model with isotropic temperature factors set at 1.2 times that of the adjacent carbon atom. Full-matrix least-squares refinement, based upon the minimization of $\Sigma w_i |F_o^2 - F_c^2|^2$, with weighting $w_i^{-1} = [\sigma^2(F_o^2) + (0.0326\ P)^2 + 1.9974\ P]$, where $P = (\text{Max}(F_o^2, 0) + 2\ F_c^2)/3$.[2] The final anisotropic full-matrix least-squares refinement on F^2 with 370 variables converged at R1 = 3.75%, for the 6033 data with I>2σ(I) and wR2 = 9.16% for all data. The goodness-of-fit was 1.082.[3]

A correction for secondary extinction was not applied. The largest peak in the final difference electron density synthesis was 0.454 $e^-/Å^3$ and the largest hole was -0.204 $e^-/Å^3$ with an RMS deviation of 0.057 $e^-/Å^3$. The linear absorption coefficient, atomic scattering factors, and

anomalous dispersion corrections were calculated from values found in the International Tables of X-ray Crystallography.[4]

References

1. APEX2 is a Bruker AXS crystallographic software package for single crystal data collection, reduction and preparation.
2. Sheldrick, G. M., SHELXL-2013, Crystallographic software package, Bruker AXS, Inc., Madison, Wisconsin, USA.
3. $R_1 = \sum(||F_o| - |F_c||) / \sum|F_o|$, $wR_2 = [\sum[w(F_o^2 - F_c^2)^2] / \sum[w(F_o^2)^2]]^{1/2}$, $R_{int.} = \sum|F_o^2 - F_o^2(mean)|^2 / \sum[F_o^2]$, and GOF = $[\sum[w(F_o^2 - F_c^2)^2] / (n-p)]^{1/2}$, where n is the number of reflections and p is the total number of parameters which were varied during the last refinement cycle.
4. International Tables for X-ray Crystallography (1974). Vol. IV, p. 55. Birmingham: Kynoch Press. (Present distributor, D. Reidel, Dordrecht.).

Table 7. Crystal data for $NiCl(C_{34}H_{28}PN_4)$.

Identification code	xs2cms	
Chemical formula	$C_{34}H_{28}ClN_4NiP$	
Formula weight	617.73	
Temperature	291(2) K	
Wavelength	0.71073 Å	
Crystal size	0.22 x 0.40 x 0.44 mm	
Crystal system	monoclinic	
Space group	P 2_1/c (No. 14)	
Unit cell dimensions	a = 12.8940(4) Å	α = 90°
	b = 25.6807(6) Å	β = 106.8450(12)°
	c = 9.0654(2) Å	γ = 90°
Volume	2873.00(13) $Å^3$	
Z	4	
Density (calculated)	1.428 g/cm^3	
Absorption coefficient	0.856 mm^{-1}	
F(000)	1280	

Table 8. Data collection and structure refinement for $NiCl(C_{34}H_{28}PN_4)$.

Theta range	3.30 to 28.28°	
Index ranges	$-17 \leq h \leq 9$, $-34 \leq k \leq 34$, $-11 \leq l \leq 12$	
Reflections collected	27320	
Independent reflections	7091 [R(int) = 0.0230]	
Coverage of independent refls	99.5%	
Absorption correction	multi-scan	
Max. and min. transmission	0.834 and 0.705	
Refinement method	Full-matrix least-squares on F^2	
Refinement program	SHELXL-2013 (Sheldrick, 2013)	
Data / restraints / parameters	7091 / 0 / 370	
Goodness-of-fit on F^2	1.082	
Final R indices	6033 data; $I>2\sigma(I)$	R1 = 0.0375, wR2 = 0.0863
	all data	R1 = 0.0468, wR2 = 0.0916
Largest diff. peak and hole	0.454 and -0.204 $e^-/Å^3$	

Table 9. Atomic coordinates and equivalent isotropic atomic displacement parameters ($Å^2$) for $NiCl(C_{34}H_{28}PN_4)$. U(eq) is defined as one third of the trace of the orthogonalized U_{ij} tensor.

	x/a	y/b	z/c	U(eq)
Ni1	0.78573(2)	0.98277(2)	0.53088(3)	0.02953(7)
Cl1	0.95217(4)	0.97081(2)	0.67132(7)	0.04331(13)
P1	0.73752(4)	0.91319(2)	0.62183(6)	0.03014(11)
N1	0.64444(12)	0.98430(6)	0.39970(18)	0.0318(3)
N2	0.79452(13)	0.05162(6)	0.44187(18)	0.0323(3)
N3	0.85768(13)	0.09400(6)	0.4621(2)	0.0368(4)
N4	0.81400(14)	0.13331(7)	0.3712(2)	0.0396(4)
C1	0.61462(16)	0.02659(7)	0.2902(2)	0.0349(4)
C2	0.70574(15)	0.06436(7)	0.3283(2)	0.0312(4)
C3	0.71771(16)	0.11536(8)	0.2844(2)	0.0349(4)
C4	0.56650(14)	0.94981(7)	0.4084(2)	0.0306(4)
C5	0.45713(15)	0.95104(8)	0.3158(2)	0.0374(4)
C6	0.38507(16)	0.91360(8)	0.3345(3)	0.0427(5)
C7	0.41602(17)	0.87408(9)	0.4422(3)	0.0446(5)
C8	0.52184(17)	0.87215(8)	0.5343(3)	0.0411(4)
C9	0.59616(15)	0.90948(7)	0.5179(2)	0.0333(4)
C10	0.64066(17)	0.14870(8)	0.1716(2)	0.0379(4)
C11	0.6231(2)	0.19980(9)	0.2091(3)	0.0540(6)
C12	0.5502(3)	0.23106(10)	0.1041(4)	0.0682(8)
C13	0.4947(3)	0.21151(12)	0.9621(4)	0.0700(8)
C14	0.5111(2)	0.16125(12)	0.9246(3)	0.0701(8)
C15	0.5833(2)	0.12971(10)	0.0295(3)	0.0528(6)
C16	0.95304(15)	0.10174(8)	0.5957(2)	0.0392(4)
C17	0.92026(15)	0.12382(8)	0.7296(2)	0.0379(4)
C18	0.87679(19)	0.17335(10)	0.7222(3)	0.0512(5)
C19	0.8429(2)	0.19259(12)	0.8427(4)	0.0644(7)
C20	0.8524(2)	0.16280(13)	0.9726(3)	0.0664(8)
C21	0.8965(2)	0.11417(12)	0.9821(3)	0.0626(7)
C22	0.93075(19)	0.09452(10)	0.8617(3)	0.0496(5)

	x/a	y/b	z/c	U(eq)
C23	0.79783(15)	0.85211(7)	0.5879(2)	0.0316(4)
C24	0.7505(2)	0.82296(9)	0.4574(3)	0.0520(6)
C25	0.7998(2)	0.77791(11)	0.4268(3)	0.0673(8)
C26	0.8953(2)	0.76132(10)	0.5261(3)	0.0579(6)
C27	0.9437(2)	0.79005(9)	0.6557(3)	0.0518(6)
C28	0.89548(18)	0.83549(8)	0.6859(3)	0.0443(5)
C29	0.75372(16)	0.91574(8)	0.8271(2)	0.0369(4)
C30	0.7425(2)	0.87158(10)	0.9088(3)	0.0586(6)
C31	0.7531(3)	0.87461(13)	0.0648(3)	0.0746(9)
C32	0.7744(2)	0.92172(14)	0.1396(3)	0.0674(8)
C33	0.7857(2)	0.96568(12)	0.0605(3)	0.0600(7)
C34	0.77592(18)	0.96294(9)	0.9041(3)	0.0450(5)

Table 10. Interatomic distances (Å) for NiCl($C_{34}H_{28}PN_4$).

Ni1-N1	1.8652(15)	Ni1-N2	1.9604(16)
Ni1-P1	2.1346(5)	Ni1-Cl1	2.1765(5)
P1-C9	1.7955(19)	P1-C29	1.813(2)
P1-C23	1.8161(19)	N1-C4	1.359(2)
N1-C1	1.446(2)	N2-C2	1.339(2)
N2-N3	1.340(2)	N3-N4	1.322(2)
N3-C16	1.468(2)	N4-C3	1.344(3)
C1-C2	1.485(3)	C2-C3	1.391(3)
C3-C10	1.475(3)	C4-C9	1.408(3)
C4-C5	1.417(3)	C5-C6	1.381(3)
C6-C7	1.385(3)	C7-C8	1.379(3)
C8-C9	1.393(3)	C10-C15	1.376(3)
C10-C11	1.390(3)	C11-C12	1.384(4)
C12-C13	1.374(4)	C13-C14	1.367(4)
C14-C15	1.384(3)	C16-C17	1.507(3)
C17-C18	1.384(3)	C17-C22	1.387(3)
C18-C19	1.380(4)	C19-C20	1.380(4)
C20-C21	1.364(4)	C21-C22	1.386(4)
C23-C28	1.381(3)	C23-C24	1.383(3)
C24-C25	1.387(3)	C25-C26	1.366(4)
C26-C27	1.375(3)	C27-C28	1.386(3)
C29-C30	1.384(3)	C29-C34	1.386(3)
C30-C31	1.383(4)	C31-C32	1.375(4)
C32-C33	1.367(4)	C33-C34	1.388(3)

Table 11. Bond angles (°) for NiCl($C_{34}H_{28}PN_4$).

N1-Ni1-N2	83.16(7)	N1-Ni1-P1	85.64(5)
N2-Ni1-P1	166.42(5)	N1-Ni1-Cl1	172.40(5)
N2-Ni1-Cl1	101.73(5)	P1-Ni1-Cl1	90.23(2)
C9-P1-C29	109.77(9)	C9-P1-C23	106.54(9)
C29-P1-C23	106.13(9)	C9-P1-Ni1	101.92(7)
C29-P1-Ni1	113.98(7)	C23-P1-Ni1	118.07(6)
C4-N1-C1	118.38(15)	C4-N1-Ni1	123.46(13)
C1-N1-Ni1	118.02(12)	C2-N2-N3	104.89(15)
C2-N2-Ni1	113.46(12)	N3-N2-Ni1	141.42(13)
N4-N3-N2	113.77(16)	N4-N3-C16	120.97(16)
N2-N3-C16	123.62(16)	N3-N4-C3	104.91(16)
N1-C1-C2	107.20(15)	N2-C2-C3	108.01(16)
N2-C2-C1	117.49(16)	C3-C2-C1	133.99(17)
N4-C3-C2	108.40(17)	N4-C3-C10	121.92(18)
C2-C3-C10	129.56(18)	N1-C4-C9	117.76(16)
N1-C4-C5	125.22(18)	C9-C4-C5	117.01(17)
C6-C5-C4	120.09(19)	C5-C6-C7	122.00(19)
C8-C7-C6	119.06(19)	C7-C8-C9	120.1(2)
C8-C9-C4	121.75(18)	C8-C9-P1	127.26(16)
C4-C9-P1	110.98(13)	C15-C10-C11	118.8(2)
C15-C10-C3	121.0(2)	C11-C10-C3	120.2(2)
C12-C11-C10	120.4(2)	C13-C12-C11	119.8(3)
C14-C13-C12	120.2(2)	C13-C14-C15	120.2(3)
C10-C15-C14	120.5(2)	N3-C16-C17	110.61(16)
C18-C17-C22	118.5(2)	C18-C17-C16	120.7(2)
C22-C17-C16	120.7(2)	C19-C18-C17	120.5(3)
C20-C19-C18	120.5(3)	C21-C20-C19	119.6(3)
C20-C21-C22	120.4(3)	C21-C22-C17	120.6(2)
C28-C23-C24	118.47(18)	C28-C23-P1	120.87(15)
C24-C23-P1	120.51(15)	C23-C24-C25	120.5(2)
C26-C25-C24	120.5(2)	C25-C26-C27	119.7(2)
C26-C27-C28	120.1(2)	C23-C28-C27	120.7(2)
C30-C29-C34	119.0(2)	C30-C29-P1	121.36(17)

C34-C29-P1	119.61(17)	C31-C30-C29	120.4(2)
C32-C31-C30	120.0(3)	C33-C32-C31	120.3(2)
C32-C33-C34	120.1(2)	C29-C34-C33	120.2(2)

Table 12. Anisotropic atomic displacement parameters ($Å^2$) for $NiCl(C_{34}H_{28}PN_4)$. The anisotropic atomic displacement factor exponent takes the form: $-2\pi^2[h^2 a^{*2} U_{11} + ... + 2 h k a^* b^* U_{12}]$.

	U_{11}	U_{22}	U_{33}	U_{23}	U_{13}	U_{12}
Ni1	0.02686(12)	0.02902(12)	0.03181(13)	-0.00080(9)	0.00705(9)	-0.00008(9)
Cl1	0.0296(2)	0.0439(3)	0.0525(3)	0.0050(2)	0.0055(2)	0.00180(19)
P1	0.0315(2)	0.0284(2)	0.0299(2)	-0.0013(2)	0.0079(2)	-0.0001(17)
N1	0.0288(7)	0.0297(7)	0.0342(8)	0.0004(6)	0.0049(6)	-0.0024(6)
N2	0.0339(8)	0.0308(7)	0.0318(8)	-0.0012(6)	0.0089(6)	-0.0028(6)
N3	0.0354(8)	0.0361(8)	0.0386(9)	0.0004(7)	0.0101(7)	-0.0067(7)
N4	0.0416(9)	0.0388(9)	0.0388(9)	0.0032(7)	0.0123(7)	-0.0069(7)
C1	0.0340(9)	0.0323(9)	0.0346(10)	-0.0010(8)	0.0041(8)	-0.0012(7)
C2	0.0315(8)	0.0331(9)	0.0293(9)	-0.0009(7)	0.0091(7)	0.0012(7)
C3	0.0381(10)	0.0350(9)	0.0316(9)	0.0018(8)	0.0100(8)	-0.0037(8)
C4	0.0298(8)	0.0276(8)	0.0341(9)	-0.0089(7)	0.0091(7)	0.0004(7)
C5	0.0313(9)	0.0377(10)	0.0405(11)	-0.0056(8)	0.0062(8)	-0.0001(8)
C6	0.0287(9)	0.0468(11)	0.0509(12)	-0.0112(10)	0.0089(9)	-0.0033(8)
C7	0.0368(10)	0.0434(11)	0.0576(14)	-0.0099(10)	0.0196(10)	-0.0109(9)
C8	0.0420(11)	0.0374(10)	0.0465(12)	-0.0014(9)	0.0168(9)	-0.0040(8)
C9	0.0304(9)	0.0331(9)	0.0379(10)	-0.0062(8)	0.0124(8)	-0.0033(7)
C10	0.0415(10)	0.0374(10)	0.0372(10)	0.0068(8)	0.0154(8)	-0.0018(8)
C11	0.0715(16)	0.0362(11)	0.0507(14)	0.0049(10)	0.0119(12)	-0.0058(11)
C12	0.093(2)	0.0377(12)	0.0742(19)	0.0152(12)	0.0243(16)	0.0115(13)
C13	0.0737(19)	0.0667(17)	0.0639(17)	0.0240(14)	0.0107(14)	0.0223(15)
C14	0.0740(18)	0.0772(19)	0.0474(14)	0.0049(13)	-0.0009(13)	0.0208(15)

	U_{11}	U_{22}	U_{33}	U_{23}	U_{13}	U_{12}
C15	0.0608(14)	0.0520(13)	0.0412(12)	-0.0002(10)	0.0076(11)	0.0123(11)
C16	0.0285(9)	0.0430(11)	0.0438(11)	-0.0002(9)	0.0067(8)	-0.0074(8)
C17	0.0276(8)	0.0429(10)	0.0397(10)	-0.0036(8)	0.0041(8)	-0.0096(8)
C18	0.0483(12)	0.0482(12)	0.0523(13)	-0.0015(11)	0.0072(10)	-0.0028(10)
C19	0.0492(14)	0.0648(16)	0.0743(19)	-0.0196(14)	0.0102(13)	0.0034(12)
C20	0.0492(14)	0.094(2)	0.0576(16)	-0.0283(15)	0.0190(12)	-0.0201(14)
C21	0.0603(15)	0.0822(19)	0.0420(13)	-0.0031(13)	0.0093(11)	-0.0232(14)
C22	0.0437(12)	0.0546(13)	0.0444(12)	0.0025(10)	0.0030(10)	-0.0072(10)
C23	0.0360(9)	0.0282(8)	0.0312(9)	0.0013(7)	0.0108(7)	0.0016(7)
C24	0.0534(13)	0.0491(13)	0.0427(12)	-0.0103(10)	-0.0031(10)	0.0144(10)
C25	0.0745(18)	0.0575(15)	0.0572(16)	-0.0256(13)	-0.0011(13)	0.0159(13)
C26	0.0651(15)	0.0428(12)	0.0645(16)	-0.0075(11)	0.0164(13)	0.0180(11)
C27	0.0486(12)	0.0448(12)	0.0555(14)	0.0006(10)	0.0050(11)	0.0132(10)
C28	0.0441(11)	0.0404(11)	0.0423(11)	-0.0040(9)	0.0030(9)	0.0050(9)
C29	0.0365(10)	0.0419(10)	0.0334(10)	-0.0038(8)	0.0120(8)	0.0009(8)
C30	0.0858(19)	0.0509(13)	0.0452(13)	-0.0019(11)	0.0288(13)	-0.0096(13)
C31	0.104(2)	0.082(2)	0.0492(15)	0.0075(14)	0.0399(16)	-0.0065(18)
C32	0.0658(17)	0.105(2)	0.0378(13)	-0.0120(14)	0.0253(12)	0.0003(16)
C33	0.0575(15)	0.0760(17)	0.0489(14)	-0.0272(13)	0.0190(12)	-0.0011(13)
C34	0.0455(11)	0.0459(11)	0.0449(12)	-0.0090(9)	0.0151(10)	0.0019(9)

Table 13. Hydrogen atom coordinates and isotropic atomic displacement parameters ($Å^2$) for $NiCl(C_{34}H_{28}PN_4)$.

	x/a	y/b	z/c	U(eq)
H1A	0.5487	0.0432	0.2976	0.042
H1B	0.6022	0.0136	0.1860	0.042
H5	0.4339	-0.0229	0.2424	0.045
H6	0.3136	-0.0850	0.2728	0.051
H7	0.3661	-0.1508	0.4523	0.054
H8	0.5436	-0.1541	0.6074	0.049
H11	0.6606	0.2131	0.3052	0.065
H12	0.5387	0.2652	0.1297	0.082
H13	0.4460	0.2325	-0.1087	0.084
H14	0.4735	0.1482	-0.1718	0.084
H15	0.5932	0.0954	0.0036	0.063
H16A	1.0031	0.1254	0.5682	0.047
H16B	0.9897	0.0687	0.6252	0.047
H18	0.8703	0.1938	0.6354	0.061
H19	0.8135	0.2259	0.8363	0.077
H20	0.8289	0.1758	1.0532	0.08
H21	0.9035	0.0941	1.0698	0.075
H22	0.9611	0.0614	0.8695	0.06
H24	0.6850	-0.1663	0.3897	0.062
H25	0.7677	-0.2411	0.3381	0.081
H26	0.9275	-0.2693	0.5061	0.07
H27	1.0089	-0.2210	0.7234	0.062
H28	0.9292	-0.1450	0.7730	0.053
H30	0.7278	-0.1603	0.8584	0.07
H31	0.7459	-0.1552	1.1191	0.089
H32	0.7812	-0.0763	1.2444	0.081
H33	0.7999	-0.0025	1.1116	0.072
H34	0.7843	-0.0072	0.8509	0.054

Figure 3. Crystal structure of **150**.

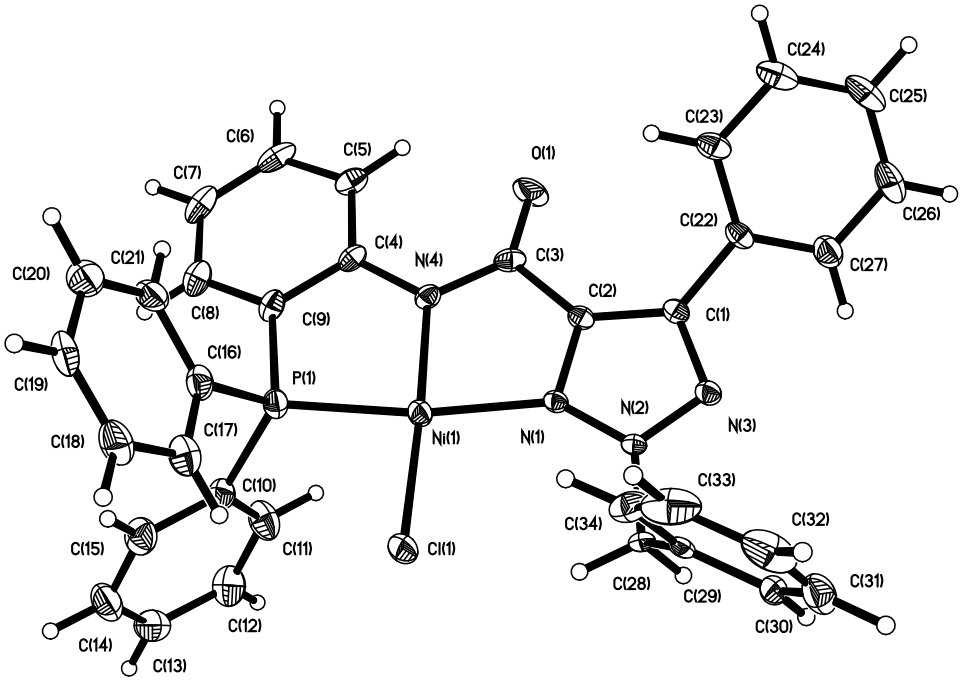

Perspective view of the molecular structure of $[C_{34}H_{26}PON_4]NiCl$ with the atom labeling Scheme for the non-hydrogen atoms. The thermal ellipsoids are scaled to enclose 50% probability.

Description of the X-ray Structural Analysis of $[C_{34}H_{26}PON_4]NiCl$

An irregular orange crystal of $[C_{34}H_{26}PON_4]NiCl$ was covered in a polybutene oil (Sigma-Aldrich) and placed on the end of a MiTeGen loop. The sample was cooled to 100 K with an Oxford Cryostream 700 system and optically aligned on a Bruker AXS D8 Venture fixed-chi X-ray diffractometer equipped with a Triumph monochromator, a Mo Kα radiation source (λ = 0.71073 Å), and a PHOTON 100 CMOS detector. Two sets of 12 frames each were collected using the omega scan method with a 10 s exposure time. Integration of these frames followed by reflection indexing and least-squares refinement produced a crystal orientation matrix for the orthorhombic crystal lattice.

Data collection consisted of the measurement of a total of 372 frames in one run using omega scans with the detector held at 5.00 cm from the crystal. The frame scan parameters are summarized in Table 14 below:

Table 14. Data collection details for $[C_{34}H_{26}PON_4]NiCl$.

Run	2θ	ω	φ	χ	Scan Width (º)	Frames	Exposure Time (sec)
1	17.38	-165.62	16.40	54.79	0.50	372	20.00

The APEX2 software program (version 2014.1-1)[1] was used for diffractometer control, preliminary frame scans, indexing, orientation matrix calculations, least-squares refinement of cell parameters, and the data collection. The frames were integrated with the Bruker SAINT software package using a narrow-frame algorithm. The integration of the data using an orthorhombic unit cell yielded a total of 25263 reflections to a maximum θ angle of 27.50° (0.77 Å resolution), of

which 6321 were independent (average redundancy 3.997, completeness = 99.7%, R_{int} = 3.01%, R_{sig} = 2.89%) and 5284 (83.59%) were greater than $2\sigma(F^2)$. The final cell constants of a = 15.4857(6) Å, b = 17.9197(7) Å, c = 19.8508(8) Å, volume = 5508.6(4) $Å^3$, are based upon the refinement of the XYZ-centroids of 9965 reflections above 20 σ(I) with 6.088° < 2θ < 59.99°. Data were corrected for absorption effects using the multi-scan method (SADABS). The ratio of minimum to maximum apparent transmission was 0.713. The calculated minimum and maximum transmission coefficients (based on crystal size) are 0.619 and 0.888.

The structure was solved by the direct methods and difference Fourier analysis using the programs provided by SHELXL-2014.[2] Idealized positions for the hydrogen atoms were included as fixed contributions using a riding model with isotropic temperature factors set at 1.2 times (methylene and aromatic hydrogens) that of the adjacent carbon atom. Full-matrix least-squares refinement, based upon the minimization of $\Sigma w_i |F_o^2 - F_c^2|^2$, with weighting $w_i^{-1} = [\sigma^2(F_o^2) + (0.0680\ P)^2 + 19.6731\ P]$, where $P = (\text{Max}(F_o^2, 0) + 2\ F_c^2)/3$.[2] The final anisotropic full-matrix least-squares refinement on F^2 with 379 variables converged at R1 = 5.50 %, for the 5284 observed data with $I>2\sigma(I)$ and wR2 = 15.64 % for all data. The goodness-of-fit was 1.081.[3]

A correction for secondary extinction was not applied. The largest peak in the final difference electron density synthesis was 1.614 $e^-/Å^3$ and the largest hole was -0.924 $e^-/Å^3$ with an RMS deviation of 0.110 $e^-/Å^3$. The linear absorption coefficient, atomic scattering factors, and anomalous dispersion corrections were calculated from values found in the International Tables of X-ray Crystallography.[4]

References

1. APEX2 is a Bruker AXS crystallographic software package for single crystal data collection, reduction and preparation.
2. Sheldrick, G. M., SHELXL-2013, Crystallographic software package, Bruker AXS, Inc., Madison, Wisconsin, USA.
3. $R_1 = \sum(||F_o| - |F_c||) / \sum|F_o|$, $wR_2 = [\sum[w(F_o^2 - F_c^2)^2] / \sum[w(F_o^2)^2]]^{1/2}$, $R_{int.} = \sum|F_o^2 - F_o^2(mean)|^2 / \sum[F_o^2]$, and GOF = $[\sum[w(F_o^2 - F_c^2)^2] / (n-p)]^{1/2}$, where n is the number of reflections and p is the total number of parameters which were varied during the last refinement cycle.
4. International Tables for X-ray Crystallography (1974). Vol. IV, p. 55. Birmingham: Kynoch Press. (Present distributor, D. Reidel, Dordrecht.).

Table 15. Crystal data for $[C_{34}H_{26}PON_4]NiCl$.

Identification code	xs42cms	
Empirical formula	$C_{34}H_{26}ClN_4NiOP$	
Emp. formula weight	631.72 g/mol	
Temperature	100(2) K	
Wavelength	0.71073 Å	
Crystal size	0.136 x 0.406 x 0.592 mm	
Crystal system	orthorhombic	
Space group	Pbcn (No. 60)	
Unit cell dimensions	a = 15.4857(6) Å	α = 90°
	b = 17.9197(7) Å	β = 90°
	c = 19.8508(8) Å	γ = 90°
Volume	5508.6(4) $Å^3$	
Z (empirical units)	8	
Density (calculated)	1.523 g/cm^3	
Absorption coefficient	0.897 mm^{-1}	
F(000)	2608	

Table 16. Data collection and structure refinement for $[C_{34}H_{26}PON_4]NiCl$.

Theta range of data used in the structural refinement	2.82 to 27.50°	
Index ranges	$-18 \leq h \leq 20$, $-23 \leq k \leq 17$, $-22 \leq l \leq 25$	
Reflections	25263	
Independent reflections	6321 [R(int) = 0.0301]	
% coverage	99.7%	
Absorption correction	multi-scan	
Max. and min. trans.	0.888 and 0.619	
Refinement method	Full-matrix least-squares on F^2	
Refinement program	SHELXL-2014 (Sheldrick, 2014)	
Data / restraints / parameters	6321 / 0 / 379	
Goodness-of-fit on F^2	1.081	
Final R indices	5284 data; $I>2\sigma(I)$	R1 = 0.0550, wR2 = 0.1471
	all data	R1 = 0.0679, wR2 = 0.1564
Largest diff. peak and hole	1.614 and -0.924 e/Å^3	

Table 17. Atomic coordinates and equivalent isotropic atomic displacement parameters ($Å^2$) for $[C_{34}H_{26}PON_4]NiCl$. U(eq) is defined as one third of the trace of the orthogonalized U_{ij} tensor.

	x/a	y/b	z/c	U(eq)
Ni1	0.75788(3)	0.05931(2)	0.44115(2)	0.01613(13)
Cl1	0.67462(5)	0.01049(5)	0.51665(4)	0.0233(2)
P1	0.65172(5)	0.06235(5)	0.37243(4)	0.01745(19)
O1	0.96542(17)	0.14996(16)	0.35183(13)	0.0283(6)
N1	0.86844(16)	0.06385(15)	0.49236(13)	0.0124(5)
N2	0.90497(17)	0.04695(15)	0.55096(13)	0.0133(5)
N3	0.98374(17)	0.07441(15)	0.55876(13)	0.0150(5)
N4	0.82618(17)	0.10529(15)	0.37201(13)	0.0146(5)
C1	0.0004(2)	0.11182(17)	0.50130(16)	0.0137(6)
C2	0.9281(2)	0.10413(18)	0.45921(16)	0.0137(6)
C3	0.9087(2)	0.12320(18)	0.38789(16)	0.0169(6)
C4	0.7931(2)	0.11418(18)	0.30618(15)	0.0157(6)
C5	0.8380(2)	0.14256(18)	0.25020(17)	0.0193(7)
C6	0.7984(3)	0.14324(19)	0.18766(17)	0.0234(8)
C7	0.7151(3)	0.1165(2)	0.17798(17)	0.0254(8)
C8	0.6691(2)	0.0901(2)	0.23235(17)	0.0236(7)
C9	0.7069(2)	0.0900(2)	0.29629(16)	0.0185(7)
C10	0.5951(2)	0.9757(2)	0.35599(17)	0.0207(7)
C11	0.6448(3)	0.9129(2)	0.3431(2)	0.0307(9)
C12	0.6051(3)	0.8438(2)	0.3314(2)	0.0326(9)

	x/a	y/b	z/c	U(eq)
C13	0.5168(3)	0.8385(2)	0.33116(19)	0.0293(8)
C14	0.4670(3)	0.9014(3)	0.3438(2)	0.0323(9)
C15	0.5055(2)	0.9690(2)	0.3564(2)	0.0281(8)
C16	0.5673(2)	0.1309(2)	0.38862(18)	0.0212(7)
C17	0.5123(2)	0.1212(2)	0.4432(2)	0.0267(8)
C18	0.4451(2)	0.1708(2)	0.4536(2)	0.0294(8)
C19	0.4327(2)	0.2301(2)	0.4117(2)	0.0240(8)
C20	0.4890(2)	0.2416(2)	0.3571(2)	0.0275(8)
C21	0.5561(2)	0.1912(2)	0.3447(2)	0.0248(8)
C22	0.0800(2)	0.15637(18)	0.49601(16)	0.0157(6)
C23	0.0792(2)	0.2245(2)	0.46243(17)	0.0207(7)
C24	0.1510(3)	0.2707(2)	0.46461(19)	0.0268(8)
C25	0.2239(3)	0.2491(2)	0.4986(2)	0.0307(9)
C26	0.2260(2)	0.1803(3)	0.5314(2)	0.0318(9)
C27	0.1541(2)	0.1345(2)	0.53005(19)	0.0237(7)
C28	0.8631(2)	0.00485(18)	0.60560(15)	0.0148(6)
C29	0.84946(19)	0.05500(17)	0.66581(16)	0.0137(6)
C30	0.8926(2)	0.0410(2)	0.72578(17)	0.0194(7)
C31	0.8834(2)	0.0883(2)	0.78010(19)	0.0289(8)
C32	0.8311(3)	0.1504(2)	0.7746(2)	0.0368(10)
C33	0.7872(3)	0.1647(2)	0.7152(2)	0.0364(10)
C34	0.7960(2)	0.1167(2)	0.66082(19)	0.0243(7)

	x/a	y/b	z/c	U(eq)

Table 18. Interatomic distances (Å) for $[C_{34}H_{26}PON_4]NiCl$.

Ni1-N4	1.919(3)	Ni1-N1	1.993(3)
Ni1-P1	2.1370(9)	Ni1-Cl1	2.1619(9)
P1-C9	1.806(3)	P1-C10	1.813(4)
P1-C16	1.823(4)	O1-C3	1.230(4)
N1-N2	1.328(4)	N1-C2	1.345(4)
N2-N3	1.324(4)	N2-C28	1.472(4)
N3-C1	1.348(4)	N4-C3	1.355(4)
N4-C4	1.413(4)	C1-C2	1.403(4)
C1-C22	1.473(4)	C2-C3	1.487(4)
C4-C5	1.407(4)	C4-C9	1.416(5)
C5-C6	1.385(5)	C6-C7	1.390(6)
C7-C8	1.377(5)	C8-C9	1.398(5)
C10-C11	1.389(5)	C10-C15	1.393(5)
C11-C12	1.401(6)	C12-C13	1.371(6)
C13-C14	1.389(6)	C14-C15	1.373(6)
C16-C17	1.390(5)	C16-C21	1.399(5)
C17-C18	1.384(5)	C18-C19	1.363(6)
C19-C20	1.407(6)	C20-C21	1.398(5)
C22-C27	1.388(5)	C22-C23	1.391(5)

C23-C24	1.388(5)	C24-C25	1.371(6)
C25-C26	1.394(6)	C26-C27	1.384(5)
C28-C29	1.510(4)	C29-C34	1.385(5)
C29-C30	1.388(5)	C30-C31	1.379(5)
C31-C32	1.380(6)	C32-C33	1.385(7)
C33-C34	1.387(6)		

Table 19. Bond angles (°) for $[C_{34}H_{26}PON_4]NiCl$.

N4-Ni1-N1	82.75(11)	N4-Ni1-P1	87.50(8)
N1-Ni1-P1	170.24(8)	N4-Ni1-Cl1	176.79(9)
N1-Ni1-Cl1	100.09(8)	P1-Ni1-Cl1	89.66(4)
C9-P1-C10	108.28(16)	C9-P1-C16	107.57(16)
C10-P1-C16	105.17(16)	C9-P1-Ni1	100.21(11)
C10-P1-Ni1	117.74(12)	C16-P1-Ni1	117.15(11)
N2-N1-C2	105.0(3)	N2-N1-Ni1	143.4(2)
C2-N1-Ni1	111.3(2)	N3-N2-N1	114.2(2)
N3-N2-C28	120.7(3)	N1-N2-C28	125.0(3)
N2-N3-C1	105.2(3)	C3-N4-C4	122.1(3)
C3-N4-Ni1	117.1(2)	C4-N4-Ni1	120.7(2)
N3-C1-C2	107.6(3)	N3-C1-C22	119.4(3)
C2-C1-C22	132.7(3)	N1-C2-C1	108.0(3)
N1-C2-C3	116.7(3)	C1-C2-C3	134.9(3)
O1-C3-N4	129.1(3)	O1-C3-C2	119.9(3)
N4-C3-C2	111.0(3)	C5-C4-N4	126.3(3)

C5-C4-C9	117.9(3)	N4-C4-C9	115.8(3)
C6-C5-C4	119.5(3)	C5-C6-C7	122.2(3)
C8-C7-C6	119.4(3)	C7-C8-C9	119.7(4)
C8-C9-C4	121.3(3)	C8-C9-P1	124.2(3)
C4-C9-P1	114.4(2)	C11-C10-C15	118.9(3)
C11-C10-P1	117.3(3)	C15-C10-P1	123.7(3)
C10-C11-C12	120.2(4)	C13-C12-C11	120.1(4)
C12-C13-C14	119.7(4)	C15-C14-C13	120.6(4)
C14-C15-C10	120.5(4)	C17-C16-C21	120.5(3)
C17-C16-P1	119.5(3)	C21-C16-P1	120.0(3)
C18-C17-C16	119.7(4)	C19-C18-C17	121.1(4)
C18-C19-C20	119.7(3)	C21-C20-C19	120.2(4)
C20-C21-C16	118.8(4)	C27-C22-C23	119.3(3)
C27-C22-C1	120.3(3)	C23-C22-C1	120.2(3)
C24-C23-C22	120.1(3)	C25-C24-C23	120.4(4)
C24-C25-C26	120.0(3)	C27-C26-C25	119.8(4)
C26-C27-C22	120.4(4)	N2-C28-C29	109.9(3)
C34-C29-C30	119.5(3)	C34-C29-C28	120.1(3)
C30-C29-C28	120.3(3)	C31-C30-C29	120.7(3)
C30-C31-C32	119.6(4)	C31-C32-C33	120.3(4)
C32-C33-C34	120.0(4)	C29-C34-C33	119.9(4)

Table 20. Anisotropic atomic displacement parameters ($Å^2$) for $[C_{34}H_{26}PON_4]NiCl$. The anisotropic atomic displacement factor exponent takes the form: $-2\pi^2[h^2 a^{*2} U_{11} + ... + 2 h k a^* b^* U_{12}]$.

	U_{11}	U_{22}	U_{33}	U_{23}	U_{13}	U_{12}
Ni1	0.0121(2)	0.0209(2)	0.0154(2)	0.00155(16)	0.00022(15)	-0.0016(2)
Cl1	0.0150(4)	0.0328(5)	0.0222(4)	0.0053(3)	0.0020(3)	-0.0043(3)
P1	0.0137(4)	0.0215(4)	0.0171(4)	-0.0002(3)	-0.0010(3)	0.0005(3)
O1	0.0273(13)	0.0398(16)	0.0178(12)	0.0036(11)	0.0063(10)	-0.0174(12)
N1	0.0108(12)	0.0139(12)	0.0124(12)	0.0007(10)	0.0022(10)	-0.0011(10)
N2	0.0124(12)	0.0152(13)	0.0124(12)	0.0029(10)	0.0019(10)	-0.0026(10)
N3	0.0132(13)	0.0172(13)	0.0145(13)	0.0008(10)	0.0016(10)	-0.0023(10)
N4	0.0161(13)	0.0165(13)	0.0111(12)	0.0019(10)	0.0010(10)	0.0011(10)
C1	0.0123(13)	0.0131(14)	0.0158(14)	-0.0013(12)	0.0024(11)	-0.0003(11)
C2	0.0124(14)	0.0148(15)	0.0140(14)	-0.0004(12)	0.0033(11)	-0.0011(11)
C3	0.0222(16)	0.0156(15)	0.0129(14)	0.0012(12)	0.0047(12)	-0.0012(13)
C4	0.0210(15)	0.0150(15)	0.0112(14)	0.0005(12)	0.0006(12)	0.0049(12)
C5	0.0257(17)	0.0174(16)	0.0148(14)	0.0013(13)	0.0044(13)	0.0047(13)
C6	0.041(2)	0.0151(16)	0.0137(15)	0.0004(12)	0.0050(14)	0.0126(15)
C7	0.037(2)	0.0252(18)	0.0146(16)	-0.0016(14)	-0.0039(14)	0.0149(16)
C8	0.0267(18)	0.0261(18)	0.0181(16)	-0.0025(14)	-0.0048(14)	0.0066(15)
C9	0.0190(16)	0.0228(17)	0.0138(15)	-0.0002(13)	-0.0012(12)	0.0054(13)
C10	0.0192(16)	0.0245(18)	0.0183(16)	0.0001(14)	-0.0035(13)	-0.0021(13)
C11	0.0194(17)	0.033(2)	0.040(2)	-0.0064(18)	-0.0004(16)	0.0022(15)

	U_{11}	U_{22}	U_{33}	U_{23}	U_{13}	U_{12}
C12	0.031(2)	0.034(2)	0.033(2)	-0.0063(18)	-0.0034(17)	0.0055(17)
C13	0.037(2)	0.0287(19)	0.0220(17)	-0.0013(15)	-0.0020(16)	-0.0088(17)
C14	0.0197(17)	0.045(2)	0.032(2)	-0.0003(18)	0.0002(15)	-0.0057(17)
C15	0.0215(17)	0.032(2)	0.0306(19)	0.0004(16)	0.0017(15)	0.0059(16)
C16	0.0184(16)	0.0225(17)	0.0228(17)	-0.0029(14)	-0.0059(13)	-0.0013(13)
C17	0.0192(17)	0.030(2)	0.0306(19)	-0.0035(16)	-0.0014(15)	0.0017(15)
C18	0.0169(17)	0.041(2)	0.030(2)	-0.0051(17)	0.0034(15)	0.0006(16)
C19	0.0144(15)	0.0237(18)	0.0339(19)	-0.0115(15)	-0.0063(14)	0.0025(13)
C20	0.0255(18)	0.0198(17)	0.037(2)	-0.0010(16)	0.0005(16)	0.0013(15)
C21	0.0162(16)	0.0192(17)	0.039(2)	0.0027(15)	0.0027(15)	-0.0006(13)
C22	0.0136(14)	0.0186(16)	0.0149(14)	-0.0039(12)	0.0047(12)	-0.0041(12)
C23	0.0203(16)	0.0215(17)	0.0203(16)	-0.0004(14)	0.0076(13)	-0.0050(14)
C24	0.0298(19)	0.0213(18)	0.0293(19)	-0.0039(15)	0.0111(16)	-0.0093(15)
C25	0.0231(18)	0.032(2)	0.037(2)	-0.0098(17)	0.0100(16)	-0.0144(16)
C26	0.0150(16)	0.042(2)	0.038(2)	-0.0068(19)	-0.0015(15)	-0.0069(16)
C27	0.0178(16)	0.0284(19)	0.0247(17)	0.0001(15)	-0.0002(14)	-0.0040(14)
C28	0.0164(14)	0.0158(15)	0.0123(14)	0.0051(12)	0.0007(12)	-0.0037(12)
C29	0.0091(13)	0.0149(15)	0.0170(15)	0.0033(12)	0.0025(11)	-0.0036(11)
C30	0.0134(14)	0.0267(17)	0.0181(15)	0.0043(14)	-0.0006(12)	-0.0033(13)
C31	0.0235(18)	0.044(2)	0.0195(17)	-0.0052(17)	0.0012(14)	-0.0111(17)
C32	0.042(2)	0.033(2)	0.035(2)	-0.0157(18)	0.0163(19)	-0.0151(19)
C33	0.043(2)	0.0206(19)	0.046(2)	0.0038(18)	0.021(2)	0.0066(17)
C34	0.0247(17)	0.0214(17)	0.0267(18)	0.0074(15)	0.0058(15)	0.0051(14)

Table 21. Hydrogen atom coordinates and isotropic atomic displacement parameters ($Å^2$) for $[C_{34}H_{26}PON_4]NiCl$.

	x/a	y/b	z/c	U(eq)
H5	0.8952	0.1611	0.2552	0.023
H6	0.8292	0.1626	0.1501	0.028
H7	0.6901	0.1165	0.1343	0.031
H8	0.6120	0.0719	0.2264	0.028
H11	0.7060	-0.0833	0.3422	0.037
H12	0.6393	-0.1993	0.3236	0.039
H13	0.4897	-0.2081	0.3224	0.035
H14	0.4059	-0.1024	0.3438	0.039
H15	0.4707	0.0116	0.3654	0.034
H17	0.5209	0.0807	0.4734	0.032
H18	0.4070	0.1633	0.4904	0.035
H19	0.3861	0.2636	0.4194	0.029
H20	0.4815	0.2836	0.3286	0.033
H21	0.5933	0.1978	0.3072	0.03
H23	1.0294	0.2394	0.4380	0.025
H24	1.1497	0.3177	0.4424	0.032
H25	1.2729	0.2809	0.4998	0.037
H26	1.2767	0.1650	0.5545	0.038
H27	1.1555	0.0877	0.5526	0.028
H28A	0.8997	-0.0381	0.6185	0.018

	x/a	y/b	z/c	U(eq)
H28B	0.8068	-0.0147	0.5899	0.018
H30	0.9288	-0.0016	0.7295	0.023
H31	0.9129	0.0782	0.8211	0.035
H32	0.8251	0.1834	0.8117	0.044
H33	0.7511	0.2074	0.7117	0.044
H34	0.7654	0.1261	0.6202	0.029

Table 22. Hydrogen atom coordinates (x 10^4) and isotropic displacement parameters (Å^2 x 10^3) for $C_{34}H_{29}N_4P$.

	x	y	z	U(eq)
H(1)	3370(20)	687(19)	6272(15)	73(6)
H(3A)	5169	1465	4959	59
H(3B)	5210	2541	5813	59
H(5)	3152	4093	2435	99
H(6)	4708	5649	1718	122
H(7)	6892	6308	2430	98
H(8)	7524	5388	3858	89
H(9)	5986	3835	4594	77
H(10A)	-415	847	4781	73
H(10B)	-503	1780	3924	73
H(12)	521	1986	6668	77
H(13)	43	3344	7925	94
H(14)	-1090	4787	7458	97
H(15)	-1856	4808	5726	91
H(16)	-1415	3430	4465	76
H(18)	6812	1269	6177	62
H(19)	8236	356	7099	65
H(20)	7409	-1057	8315	68
H(21)	5137	-1530	8625	63

H(24)	1955	-3455	7745	128
H(25)	1702	-4935	8948	164
H(26)	2104	-4367	10723	107
H(27)	2777	-2327	11280	77
H(28)	3093	-836	10079	69
H(30)	4375	1475	8884	84
H(31)	3843	3056	9896	115
H(32)	1615	3029	10145	145
H(33)	-81	1428	9407	157
H(34)	410	-122	8354	114

Figure 4. Crystal structure of **160**.

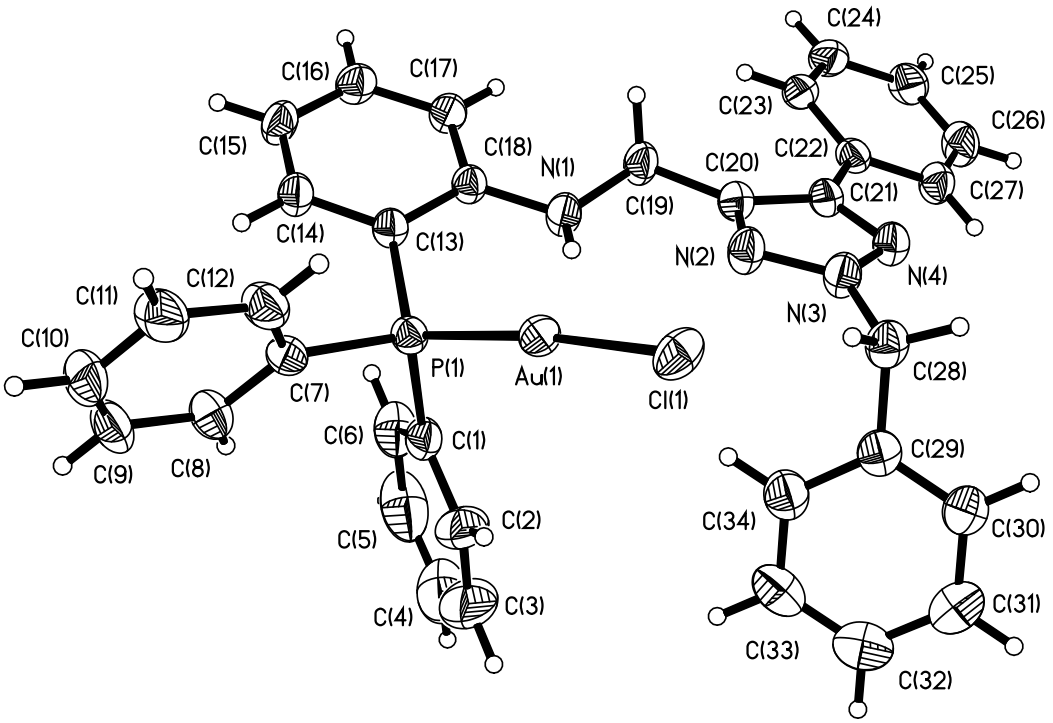

Perspective view of the molecular structure of $C_{34}H_{29}AuClN_4P$ with the atom labeling scheme.

The thermal ellipsoids are scaled to enclose 30% probability.

Description of the X-ray Structural Analysis of $C_{34}H_{29}AuClN_4P.1/2C_5H_{12}$

A colorless crystal of $C_{34}H_{29}AuClN_4P.1/2C_5H_{12}$ was washed with the perfluoropolyether PFO-XR75 (Lancaster) and wedged in a glass capillary. The sample was optically aligned on the four-circle of a Siemens P4 diffractometer equipped with a graphite monochromator, a monocap collimator, a Mo Kα radiation source (λ = 0.71073 Å), and a SMART CCD detector held at 5.050 cm from the crystal. Four sets of 20 frames each were collected using the ω scan method and with a 10 s exposure time. Integration of these frames followed by reflection indexing and least-squares refinement produced a crystal orientation matrix for the triclinic crystal lattice.

Data collection consisted of the measurement of a total of 1650 frames in five different runs covering a hemisphere of data. Frame scan parameters are summarized below:

Run	2θ	ω	ϕ	χ	Scan axis	Scan width (°)	Frames (#)	Exposure time (sec.)
1	28	43.00	0.00	280.00	2	-0.3	100	40
2	28	43.00	90.00	280.00	2	-0.3	100	40
3	28	43.00	180.00	280.00	2	-0.3	100	40
4	28	43.00	270.00	280.00	2	-0.3	100	40
5	28	28.00	0.00	30.00	3	0.3	1250	40

The program SMART (version 5.6)[1] was used for diffractometer control, frame scans, indexing, orientation matrix calculations, least-squares refinement of cell parameters, and the data collection. All 1650 crystallographic raw data frames were read by program SAINT (version 5/6.0)[1] and integrated using 3D profiling algorithms. The resulting data were reduced to produce a total of 11778 reflections and their intensities and estimated standard deviations. An absorption correction

was applied using the SADABS routine available in SAINT.[1] The data were corrected for Lorentz and polarization effects. Data preparation was carried out by using the program XPREP,[1] which gave 7361 unique reflections (R_{int} = 3.81 %) with indices $-13 \leq h \leq 13$, $-15 \leq k \leq 16$, $-15 \leq l \leq 17$. The triclinic space group was determined to be $P\bar{1}$ (No. 2).

The structure was solved by a combination of direct methods and difference Fourier analysis with the use of SHELXTL 6.1.[2] Idealized positions for the aromatic and methylene hydrogen atoms were included as fixed contributions using a riding model with isotropic temperature factors set at 1.2 that of the adjacent carbon atom. The amine hydrogen bound to atom N(1) was refined isotropically. The crystal contained a badly disordered pentane molecule located on an inversion center. The pentane molecule was treated as a diffuse electron density contribution with the aid of the SQUEEZE routine in the program PLATON.[3] Although specific positions for the independent carbon and hydrogen atoms were not determined, the calculated density, absorption coefficient and empirical formula weight reflect their presence within the crystal lattice. Full-matrix least-squares refinement, based upon the minimization of $\Sigma w_i |F_o^2 - F_c^2|^2$, with weighting $w_i^{-1} = [\sigma^2(F_o^2) + (0.0524\ P)^2 + 0.0\ P]$, where $P = (\text{Max}\ (F_o^2, 0) + 2\ F_c^2)/3$, converged to give final discrepancy indices[4] of R1 = 0.0403, wR2 = 0.0967 for 6301diffraction data with $I > 2\ \sigma(I)$. The goodness of fit (GOF) value was 0.993.

A correction for secondary extinction was not applied. The maximum and minimum residual electron density peaks in the final difference Fourier map were 2.464 and -0.885 e/Å^3, respectively. The linear absorption coefficient, atomic scattering factors, and anomalous dispersion corrections were calculated from values found in the International Tables of X-ray Crystallography.[5]

References

1. SMART, SAINT and XPREP programs are part of Bruker crystallographic software package for single crystal data collection, reduction and preparation.
2. Sheldrick, G. M., SHELXTL6.1 (2000), Crystallographic software package, Bruker AXS, Inc. Madison, Wisconsin, USA.
3. PLATON, written by Professor Anthony L. Spek, Bijvoet Centre for Biomolecular Research, Utrecht University. Current versions of PLATON for Windows are available from Professor Louis J. Farrugia, Department of Chemistry, University of Glasgow at www.chem.gla.ac.uk/~louis/software/.
4. $R_1 = \sum(||F_o| - |F_c||) / \sum|F_o|$, $wR_2 = [\sum[w(F_o^2 - F_c^2)^2] / \sum[w(F_o^2)^2]]^{1/2}$, $R_{int.} = \sum|F_o^2 - F_o^2(mean)|^2 / \sum[F_o^2]$, and GOF = $[\sum[w(F_o^2 - F_c^2)^2] / (n-p)]^{1/2}$, where n is the number of reflections and p is the total number of parameters which were varied during the last refinement cycle.
5. International Tables for X-ray Crystallography (1974). Vol. IV, p. 55. Birmingham: Kynoch Press. (Present distributor, D. Reidel, Dordrecht.).

Table 23. Crystal data and structure refinement for $C_{34}H_{29}AuClN_4P\cdot 1/2C_5H_{12}$.

Identification code	xs54plt	
Empirical formula	$C_{34}H_{29}AuClN_4P\cdot 1/2C_5H_{12}$	
Formula weight	793.07	
Temperature	293(2) K	
Wavelength	0.71073 Å	
Crystal system	triclinic	
Space group	$P\bar{1}$	
Unit cell dimensions	a = 10.7328(12) Å	□= 111.710(2)°
	b = 13.0351(15) Å	□= 93.212(2)°
	c = 13.3008(15) Å	□ = 105.216(2)°
Volume	1643.7(3) $Å^3$	
Z	2	
Density (calculated)	1.602 g/cm^3	
Absorption coefficient	46.37 cm^{-1}	
F(000)	786	
Crystal dimensions	0.12 x 0.18 x 0.40 mm	
θ range for data collection	2.22 to 27.55°	
Index ranges	$-13 \le h \le 13$, $-15 \le k \le 16$, $-15 \le l \le 17$	
Reflections collected	11778	
Independent reflections	7361 [R(int) = 0.0381]	
Completeness to θ= 27.55°	97.1 %	
Max. and min. transmission	0.606 and 0.259	
Refinement method	Full-matrix least-squares on F^2	

Data / restraints / parameters	7361 / 0 / 374
Goodness-of-fit on F^2	0.993
Final R indices [$I>2\sigma(I)$]	R1 = 0.0403, wR2 = 0.0967
R indices (all data)	R1 = 0.0483, wR2 = 0.1004
Largest diff. peak and hole	2.464 and -0.885 e/$Å^3$

Table 24. Atomic coordinates (x 10^4) and equivalent isotropic displacement parameters ($Å^2$ x 10^3) for $C_{34}H_{29}AuClN_4P$. U(eq) is defined as one third of the trace of the orthogonalized U_{ij} tensor.

	x	y	z	U(eq)
Au(1)	7776(1)	2608(1)	6732(1)	49(1)
Cl(1)	9152(1)	1875(1)	5627(1)	66(1)
P(1)	6610(1)	3453(1)	7934(1)	44(1)
N(1)	4825(4)	909(3)	6977(4)	59(1)
N(2)	6298(4)	-457(3)	6039(3)	58(1)
N(3)	6877(4)	-1286(3)	5767(3)	57(1)
N(4)	6120(4)	-2316(3)	5686(3)	56(1)
C(1)	7066(6)	3410(4)	9253(4)	59(1)
C(2)	8355(7)	3510(6)	9576(5)	88(2)
C(3)	8727(11)	3522(8)	10605(7)	121(3)
C(4)	7883(14)	3428(8)	11269(6)	126(4)
C(5)	6582(13)	3333(7)	10963(6)	120(4)
C(6)	6159(8)	3312(5)	9950(5)	80(2)
C(7)	7031(4)	4976(3)	8178(3)	49(1)
C(8)	7135(5)	5829(4)	9209(4)	61(1)
C(9)	7405(6)	6981(4)	9358(5)	75(2)
C(10)	7578(6)	7279(4)	8473(5)	78(2)
C(11)	7481(7)	6452(5)	7447(5)	80(2)

C(12)	7211(5)	5287(4)	7304(4)	65(1)
C(13)	4830(4)	2920(3)	7626(3)	45(1)
C(14)	4122(5)	3707(4)	7846(4)	54(1)
C(15)	2770(5)	3349(4)	7701(4)	60(1)
C(16)	2113(5)	2183(4)	7315(4)	58(1)
C(17)	2778(4)	1371(4)	7084(4)	54(1)
C(18)	4158(4)	1718(3)	7212(3)	46(1)
C(19)	4131(5)	-317(4)	6445(5)	59(1)
C(20)	5096(5)	-979(4)	6131(4)	54(1)
C(21)	4990(5)	-2149(3)	5901(3)	49(1)
C(22)	3874(5)	-3127(3)	5885(3)	48(1)
C(23)	2592(5)	-3101(4)	5828(4)	55(1)
C(24)	1588(5)	-4035(4)	5796(4)	64(1)
C(25)	1844(6)	-5029(4)	5800(4)	68(1)
C(26)	3105(6)	-5057(4)	5850(4)	68(1)
C(27)	4142(5)	-4124(4)	5904(4)	59(1)
C(28)	8267(5)	-1048(5)	5710(4)	61(1)
C(29)	9100(5)	-728(4)	6799(4)	58(1)
C(30)	9884(6)	-1381(5)	6913(5)	66(1)
C(31)	10673(7)	-1057(6)	7901(6)	82(2)
C(32)	10645(7)	-97(6)	8797(5)	87(2)
C(33)	9851(7)	546(6)	8703(5)	87(2)
C(34)	9085(6)	229(5)	7710(5)	73(1)

Table 25. Interatomic distances [Å] and bond angles [°] for $C_{34}H_{29}AuClN_4P$.

Au(1)-P(1)	2.232(1)
Au(1)-Cl(1)	2.281(1)
P(1)-C(7)	1.812(4)
P(1)-C(13)	1.818(4)
P(1)-C(1)	1.821(5)
N(1)-C(18)	1.379(5)
N(1)-C(19)	1.445(6)
N(2)-C(20)	1.327(6)
N(2)-N(3)	1.332(5)
N(3)-N(4)	1.336(6)
N(3)-C(28)	1.454(6)
N(4)-C(21)	1.317(6)
C(1)-C(2)	1.383(8)
C(1)-C(6)	1.395(8)
C(2)-C(3)	1.397(10)
C(3)-C(4)	1.314(13)
C(4)-C(5)	1.393(14)
C(5)-C(6)	1.386(11)
C(7)-C(12)	1.373(7)
C(7)-C(8)	1.385(6)
C(8)-C(9)	1.387(7)
C(9)-C(10)	1.377(9)
C(10)-C(11)	1.368(8)

C(11)-C(12)	1.405(7)
C(13)-C(14)	1.388(6)
C(13)-C(18)	1.415(5)
C(14)-C(15)	1.381(7)
C(15)-C(16)	1.375(7)
C(16)-C(17)	1.380(6)
C(17)-C(18)	1.411(6)
C(19)-C(20)	1.498(6)
C(20)-C(21)	1.412(6)
C(21)-C(22)	1.495(6)
C(22)-C(23)	1.383(6)
C(22)-C(27)	1.412(6)
C(23)-C(24)	1.383(7)
C(24)-C(25)	1.395(7)
C(25)-C(26)	1.362(8)
C(26)-C(27)	1.392(7)
C(28)-C(29)	1.511(8)
C(29)-C(30)	1.383(7)
C(29)-C(34)	1.385(7)
C(30)-C(31)	1.378(9)
C(31)-C(32)	1.381(10)
C(32)-C(33)	1.373(10)
C(33)-C(34)	1.374(9)

P(1)-Au(1)-Cl(1)	174.21(4)

C(7)-P(1)-C(13)	105.3(2)
C(7)-P(1)-C(1)	105.9(2)
C(13)-P(1)-C(1)	106.0(2)
C(7)-P(1)-Au(1)	109.3(2)
C(13)-P(1)-Au(1)	119.8(1)
C(1)-P(1)-Au(1)	109.7(2)
C(18)-N(1)-C(19)	120.8(4)
C(20)-N(2)-N(3)	104.4(4)
N(2)-N(3)-N(4)	114.5(4)
N(2)-N(3)-C(28)	122.3(4)
N(4)-N(3)-C(28)	122.7(4)
C(21)-N(4)-N(3)	104.4(3)
C(2)-C(1)-C(6)	119.8(5)
C(2)-C(1)-P(1)	118.5(5)
C(6)-C(1)-P(1)	121.6(5)
C(1)-C(2)-C(3)	119.0(8)
C(4)-C(3)-C(2)	121.9(9)
C(3)-C(4)-C(5)	120.0(7)
C(6)-C(5)-C(4)	120.5(8)
C(5)-C(6)-C(1)	118.7(8)
C(12)-C(7)-C(8)	119.1(4)
C(12)-C(7)-P(1)	118.7(3)
C(8)-C(7)-P(1)	122.2(4)
C(7)-C(8)-C(9)	120.6(5)
C(10)-C(9)-C(8)	119.6(5)

C(11)-C(10)-C(9)	120.8(5)
C(10)-C(11)-C(12)	119.2(6)
C(7)-C(12)-C(11)	120.7(5)
C(14)-C(13)-C(18)	119.6(4)
C(14)-C(13)-P(1)	119.4(3)
C(18)-C(13)-P(1)	120.9(3)
C(15)-C(14)-C(13)	121.6(4)
C(16)-C(15)-C(14)	119.0(4)
C(15)-C(16)-C(17)	121.3(4)
C(16)-C(17)-C(18)	120.5(4)
N(1)-C(18)-C(17)	120.7(4)
N(1)-C(18)-C(13)	121.4(4)
C(17)-C(18)-C(13)	117.9(4)
N(1)-C(19)-C(20)	109.4(4)
N(2)-C(20)-C(21)	108.1(4)
N(2)-C(20)-C(19)	120.6(4)
C(21)-C(20)-C(19)	131.3(5)
N(4)-C(21)-C(20)	108.6(4)
N(4)-C(21)-C(22)	120.1(4)
C(20)-C(21)-C(22)	131.3(4)
C(23)-C(22)-C(27)	119.0(4)
C(23)-C(22)-C(21)	122.6(4)
C(27)-C(22)-C(21)	118.4(4)
C(24)-C(23)-C(22)	120.6(4)
C(23)-C(24)-C(25)	120.7(5)

C(26)-C(25)-C(24)	118.7(5)
C(25)-C(26)-C(27)	122.1(5)
C(26)-C(27)-C(22)	118.9(5)
N(3)-C(28)-C(29)	112.6(4)
C(30)-C(29)-C(34)	118.5(5)
C(30)-C(29)-C(28)	121.2(4)
C(34)-C(29)-C(28)	120.3(5)
C(31)-C(30)-C(29)	120.6(5)
C(30)-C(31)-C(32)	119.8(6)
C(33)-C(32)-C(31)	120.3(6)
C(32)-C(33)-C(34)	119.5(6)
C(33)-C(34)-C(29)	121.3(6)

Table 26. Anisotropic displacement parameters ($Å^2$ x 10^3) for $C_{34}H_{29}AuClN_4P$. The anisotropic displacement factor exponent takes the form: $-2\pi^2[h^2 a^{*2}U_{11} + ... + 2 h k a^* b^* U_{12}]$.

	U_{11}	U_{22}	U_{33}	U_{23}	U_{13}	U_{12}
Au(1)	41(1)	53(1)	53(1)	20(1)	10(1)	16(1)
Cl(1)	55(1)	91(1)	72(1)	41(1)	26(1)	39(1)
P(1)	43(1)	39(1)	47(1)	15(1)	7(1)	11(1)
N(1)	34(2)	37(2)	95(3)	18(2)	5(2)	8(2)
N(2)	51(2)	43(2)	81(3)	24(2)	17(2)	17(2)
N(3)	52(2)	51(2)	70(2)	22(2)	15(2)	21(2)
N(4)	60(2)	47(2)	62(2)	20(2)	13(2)	21(2)
C(1)	78(3)	48(2)	53(2)	19(2)	4(2)	27(2)
C(2)	91(5)	109(5)	66(3)	29(3)	-9(3)	45(4)
C(3)	148(8)	144(7)	78(4)	36(5)	-18(5)	74(6)
C(4)	226(13)	118(6)	63(4)	38(4)	13(6)	97(8)
C(5)	223(12)	93(5)	70(4)	42(4)	56(6)	69(7)
C(6)	120(6)	73(3)	65(3)	34(3)	32(3)	44(4)
C(7)	42(2)	43(2)	55(2)	18(2)	4(2)	5(2)
C(8)	69(3)	50(2)	60(3)	20(2)	16(2)	12(2)
C(9)	74(4)	41(2)	85(4)	8(2)	9(3)	5(2)
C(10)	78(4)	41(2)	104(4)	28(3)	7(3)	6(2)
C(11)	90(5)	57(3)	84(4)	35(3)	-3(3)	2(3)
C(12)	71(3)	49(2)	63(3)	20(2)	1(2)	6(2)
C(13)	45(2)	41(2)	51(2)	18(2)	11(2)	14(2)

C(14)	55(3)	43(2)	65(3)	21(2)	12(2)	18(2)
C(15)	51(3)	59(3)	78(3)	26(2)	15(2)	30(2)
C(16)	42(2)	60(3)	71(3)	26(2)	10(2)	16(2)
C(17)	42(2)	45(2)	71(3)	23(2)	5(2)	10(2)
C(18)	44(2)	40(2)	54(2)	18(2)	10(2)	13(2)
C(19)	50(3)	37(2)	85(3)	20(2)	6(2)	14(2)
C(20)	56(3)	43(2)	59(2)	17(2)	4(2)	17(2)
C(21)	54(3)	37(2)	51(2)	14(2)	5(2)	14(2)
C(22)	56(3)	38(2)	44(2)	13(2)	1(2)	11(2)
C(23)	54(3)	44(2)	60(2)	17(2)	-5(2)	14(2)
C(24)	52(3)	56(3)	73(3)	21(2)	-3(2)	11(2)
C(25)	71(4)	44(2)	77(3)	22(2)	2(3)	5(2)
C(26)	89(4)	45(2)	76(3)	28(2)	12(3)	23(3)
C(27)	64(3)	44(2)	69(3)	22(2)	10(2)	19(2)
C(28)	53(3)	65(3)	68(3)	26(2)	21(2)	21(2)
C(29)	48(3)	58(3)	67(3)	25(2)	19(2)	12(2)
C(30)	65(3)	70(3)	71(3)	32(2)	20(3)	23(3)
C(31)	70(4)	97(4)	100(4)	60(4)	21(3)	28(3)
C(32)	84(4)	95(4)	75(4)	42(3)	6(3)	7(4)
C(33)	91(5)	68(3)	74(4)	12(3)	9(3)	4(3)
C(34)	70(4)	63(3)	80(3)	22(2)	16(3)	20(3)

Table 27. Hydrogen atom coordinates (x 10^4) and isotropic displacement parameters ($Å^2$ x 10^3) for $C_{34}H_{29}AuClN_4P$.

	x	y	z	U(eq)
H(1)	5520(40)	1140(40)	7010(30)	27(10)
H(2)	8966	3569	9115	106
H(3)	9595	3597	10825	145
H(4)	8155	3427	11945	152
H(5)	5992	3282	11442	144
H(6)	5287	3235	9738	97
H(8)	7023	5627	9807	74
H(9)	7467	7549	10051	89
H(10)	7764	8052	8573	93
H(11)	7593	6657	6852	96
H(12)	7153	4721	6611	78
H(14)	4569	4494	8096	64
H(15)	2311	3888	7861	72
H(16)	1202	1937	7209	69
H(17)	2312	588	6841	65
H(19A)	3535	-469	5794	70
H(19B)	3620	-564	6939	70
H(23)	2403	-2450	5811	66
H(24)	733	-4000	5772	76
H(25)	1167	-5660	5768	82

H(26)	3279	-5720	5849	82
H(27)	4997	-4157	5952	71
H(28A)	8542	-418	5471	73
H(28B)	8409	-1728	5167	73
H(30)	9878	-2045	6318	80
H(31)	11222	-1484	7964	98
H(32)	11167	116	9467	104
H(33)	9831	1192	9307	104
H(34)	8547	664	7648	87

Figure 5. Crystal structure of **162**.

Perspective view of the molecular structure of $Au[P(C_6H_5)_2C_6H_4NHCH_2(C_{15}H_{12}N_3)](O_2CC_6H_5)$, **160** with the atom labeling Scheme provided for the non-hydrogen atoms. The thermal ellipsoids are scaled to enclosed 30% probability.

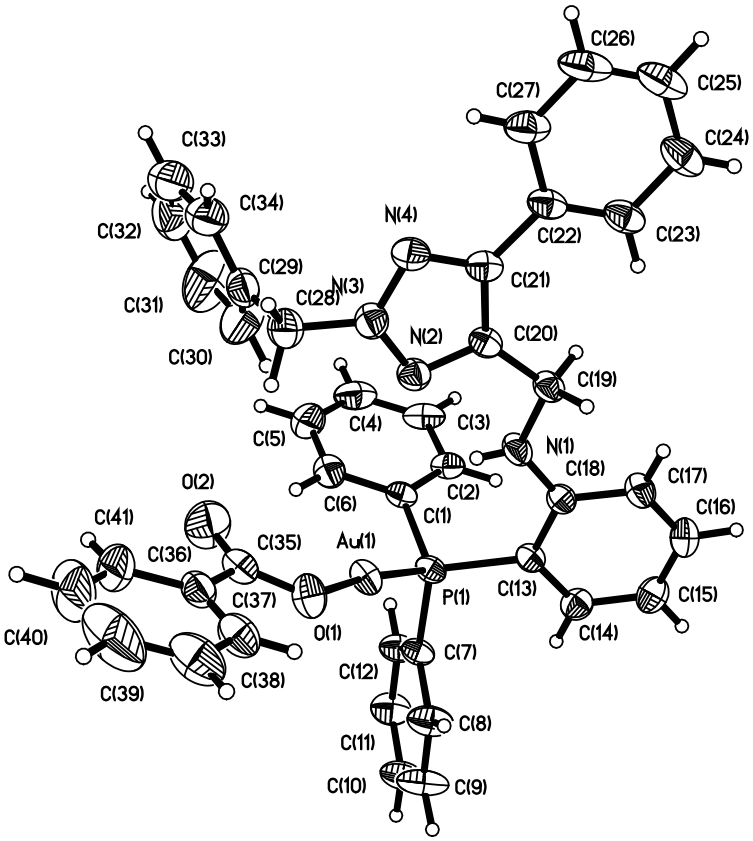

Description of the X-ray Structural Analysis of

$Au[P(C_6H_5)_2C_6H_4NHCH_2(C_{15}H_{12}N_3)](O_2CC_6H_5)\cdot 2H_2O$

A colorless crystal of $Au[P(C_6H_5)_2C_6H_4NHCH_2(C_{15}H_{12}N_3)](O_2CC_6H_5)\cdot 2H_2O$ was washed with the perfluoropolyether PFO-XR75 (Lancaster) and wedged in a glass capillary. The sample was optically aligned on the four-circle of a Siemens P4 diffractometer equipped with a graphite monochromator, a monocap collimator, a Mo Kα radiation source (λ = 0.71073 Å), and a SMART CCD detector held at 5.030 cm from the crystal. Four sets of 20 frames each were collected using the ω scan method and with a 10 s exposure time. Integration of these frames followed by reflection indexing and least-squares refinement produced a crystal orientation matrix for the monoclinic crystal lattice.

Data collection consisted of the measurement of a total of 1650 frames in five different runs covering a hemisphere of data. Frame scan parameters are summarized below:

Run	2θ	ω	ϕ	χ	Scan axis	Scan width (°)	Frames (#)	Exposure time (sec.)
1	28	43.00	0.00	280.00	2	-0.3	100	40
2	28	43.00	90.00	280.00	2	-0.3	100	40
3	28	43.00	180.00	280.00	2	-0.3	100	40
4	28	43.00	270.00	280.00	2	-0.3	100	40
5	28	28.00	0.00	30.00	3	0.3	1250	40

The program SMART (version 5.6)[1] was used for diffractometer control, frame scans, indexing, orientation matrix calculations, least-squares refinement of cell parameters, and the data

collection. All 1650 crystallographic raw data frames were read by the program SAINT (version 5/6.0)[1] and integrated using 3D profiling algorithms. The resulting data were reduced to produce a total of 23666 reflections and their intensities and estimated standard deviations. An absorption correction was applied using the SADABS routine available in SAINT.[1] The data were corrected for Lorentz and polarization effects. No evidence of crystal decomposition was observed. Data preparation was carried out by using the program XPREP,[1] which gave 8101 unique reflections (R_{int} = 4.33 %) with indices $-11 \leq h \leq 14$, $-17 \leq k \leq 17$, $-31 \leq l \leq 32$. The monoclinic space group was determined to be $P2_1/n$, a non-standard setting of $P2_1/c$ (No. 14).

The structure was solved by a combination of direct methods and difference Fourier analysis with the use of SHELXTL 6.1.[2] Idealized positions for the hydrogen atoms were included as fixed contributions using a riding model with isotropic temperature factors set at 1.2 times that of the adjacent carbon atom. The position of the amine proton was refined isotropically. The crystallographic asymmetric unit also contains two independent molecules of water. The presence of water in the lattice was verified by the appearance of a proton NMR resonance at 1.6 ppm in the solution NMR spectrum for a $CDCl_3$ solution prepared by dissolving crystals of the gold compound. The empirical formula weight, density, and linear absorption coefficient were calculated based upon the presence of two water molecules per gold complex. Full-matrix least-squares refinement, based upon the minimization of $\Sigma w_i |F_o^2 - F_c^2|^2$, with weighting $w_i^{-1} = [\sigma^2(F_o^2) + (0.0617\ P)^2 + 1.3664\ P]$, where $P = (\text{Max}(F_o^2, 0) + 2\ F_c^2)/3$, converged to give final discrepancy indices[3] of R1 = 0.0418, wR2 = 0.1103 for 6502 diffraction data with $I > 2\ \sigma(I)$. The goodness of fit (GOF) value was 1.050.

A correction for secondary extinction was not applied. The maximum and minimum residual electron density peaks in the final difference Fourier map were 1.286 and –1.021 e/Å^3,

respectively. The linear absorption coefficient, atomic scattering factors, and anomalous dispersion corrections were calculated from values found in the International Tables of X-ray Crystallography.[4]

References

1. SMART, SAINT and XPREP programs are part of Bruker crystallographic software package for single crystal data collection, reduction and preparation.
2. Sheldrick, G. M., SHELXTL6.1 (2000), Crystallographic software package, Bruker AXS, Inc. Madison, Wisconsin, USA.
3. PLATON, written by Professor Anthony L. Spek, Bijvoet Centre for Biomolecular Research, Utrecht University. Current versions of PLATON for Windows are available from Professor Louis J. Farrugia, Department of Chemistry, University of Glasgow at www.chem.gla.ac.uk/~louis/software/.
4. $R_1 = \sum(||F_o| - |F_c||) / \sum|F_o|$, $wR_2 = [\sum[w(F_o^2 - F_c^2)^2] / \sum[w(F_o^2)^2]]^{1/2}$, $R_{int.} = \sum|F_o^2 - F_o^2(mean)|^2 / \sum[F_o^2]$, and $GOF = [\sum[w(F_o^2 - F_c^2)^2] / (n-p)]^{1/2}$, where n is the number of reflections and p is the total number of parameters which were varied during the last refinement cycle.
5. International Tables for X-ray Crystallography (1974). Vol. IV, p. 55. Birmingham: Kynoch Press. (Present distributor, D. Reidel, Dordrecht.).

Table 28. Crystal data and structure refinement for

$Au[P(C_6H_5)_2C_6H_4NHCH_2(C_{15}H_{12}N_3)](O_2CC_6H_5)\cdot 2H_2O$.

Identification code	xs62ccd	
Empirical formula	$C_{41}H_{38}AuN_4O_4P$	
Formula weight	878.69	
Temperature	293(2) K	
Wavelength	0.71073 Å	
Crystal system	monoclinic	
Space group	$P2_1/n$	
Unit cell dimensions	a = 10.810(1) Å	a= 90°
	b = 13.600(1) Å	b= 96.298(2)°
	c = 24.893(2) Å	g = 90°
Volume	3637.9(5) $Å^3$	
Z	4	
Density (calculated)	1.604 g/cm^3	
Absorption coefficient	41.36 cm^{-1}	
F(000)	1752	
Crystal dimensions	0.14 x 0.24 x 0.42 mm	
θ range for data collection	2.15 to 27.49°	
Index ranges	$-11 \le h \le 14$, $-17 \le k \le 17$, $-31 \le l \le 32$	
Reflections collected	23666	
Independent reflections	8101 [R(int) = 0.0433]	
Completeness to θ = 27.49°	97.1 %	
Max. and min. transmission	0.595 and 0.276	

Refinement method	Full-matrix least-squares on F^2
Data / restraints / parameters	8101 / 0 / 464
Goodness-of-fit on F^2	1.050
Final R indices [$I>2\sigma(I)$]	R1 = 0.0418, wR2 = 0.1103
R indices (all data)	R1 = 0.0544, wR2 = 0.1217
Largest diff. peak and hole	1.286 and -1.021 e/$Å^3$

Table 29. Atomic coordinates (x 10^4) and equivalent isotropic displacement parameters ($Å^2$ x 10^3) for $Au[P(C_6H_5)_2C_6H_4NHCH_2(C_{15}H_{12}N_3)](O_2CC_6H_5)\cdot 2H_2O$. U(eq) is defined as one third of the trace of the orthogonalized U_{ij} tensor.

	x	y	z	U(eq)
Au(1)	4067(1)	6514(1)	1103(1)	53(1)
P(1)	4528(1)	7855(1)	659(1)	45(1)
O(1)	3455(3)	5256(3)	1457(1)	68(1)
O(2)	4747(4)	5458(4)	2190(2)	109(2)
N(1)	5993(4)	6298(3)	88(2)	55(1)
N(2)	6853(3)	4978(3)	834(2)	54(1)
N(3)	7504(3)	4314(3)	1134(2)	59(1)
N(4)	8357(3)	3832(3)	889(2)	60(1)
C(1)	6018(3)	8390(3)	908(2)	48(1)
C(2)	6674(3)	8949(4)	576(2)	55(1)
C(3)	7759(4)	9422(4)	781(3)	71(2)
C(4)	8180(4)	9343(4)	1316(3)	79(2)
C(5)	7557(5)	8786(6)	1649(3)	85(2)
C(6)	6465(5)	8289(5)	1450(2)	69(1)
C(7)	3380(3)	8818(3)	723(2)	48(1)
C(8)	2129(4)	8591(4)	604(3)	75(2)
C(9)	1234(4)	9296(5)	637(3)	91(2)
C(10)	1564(4)	10231(5)	800(3)	80(2)

C(11)	2800(4)	10467(4)	916(3)	71(1)
C(12)	3702(4)	9763(3)	880(2)	59(1)
C(13)	4584(3)	7688(3)	-61(2)	44(1)
C(14)	3926(4)	8324(4)	-425(2)	57(1)
C(15)	3993(5)	8242(4)	-974(2)	65(1)
C(16)	4740(5)	7520(4)	-1164(2)	64(1)
C(17)	5381(4)	6877(4)	-809(2)	58(1)
C(18)	5325(3)	6930(3)	-251(2)	46(1)
C(19)	6739(4)	5528(3)	-103(2)	51(1)
C(20)	7289(3)	4905(3)	355(2)	47(1)
C(21)	8246(3)	4191(3)	393(2)	52(1)
C(22)	9061(4)	3845(3)	-9(2)	55(1)
C(23)	8917(4)	4140(4)	-539(2)	64(1)
C(24)	9700(5)	3785(5)	-903(3)	80(2)
C(25)	10647(5)	3147(5)	-726(4)	89(2)
C(26)	10803(5)	2851(5)	-205(4)	91(2)
C(27)	10025(4)	3190(5)	158(3)	76(2)
C(28)	7413(5)	4205(5)	1706(2)	72(1)
C(29)	8372(5)	4817(5)	2041(2)	70(1)
C(30)	8267(9)	5817(7)	2072(3)	117(3)
C(31)	9184(13)	6387(7)	2370(5)	149(5)
C(32)	10163(8)	5925(9)	2633(3)	118(3)
C(33)	10289(6)	4930(8)	2603(3)	109(3)
C(34)	9406(5)	4393(6)	2303(3)	89(2)
C(35)	3915(4)	5021(4)	1928(2)	61(1)

C(36)	3333(4)	4133(4)	2155(2)	66(1)
C(37)	2449(6)	3591(4)	1846(3)	76(2)
C(38)	1920(7)	2783(6)	2064(4)	111(3)
C(39)	2239(14)	2535(10)	2579(7)	171(6)
C(40)	3095(12)	3026(11)	2892(5)	149(5)
C(41)	3658(7)	3871(7)	2691(3)	107(3)
O(3)	5753(8)	6717(7)	3833(4)	190(5)
O(4)	6301(10)	6671(8)	2776(5)	207(5)

Table 30. Interatomic distances [Å] and bond angles [°] for $Au[P(C_6H_5)_2C_6H_4NHCH_2(C_{15}H_{12}N_3)](O_2CC_6H_5)$.

Au(1)-O(1)	2.066(3)
Au(1)-P(1)	2.217(1)
P(1)-C(13)	1.814(4)
P(1)-C(1)	1.814(4)
P(1)-C(7)	1.823(4)
O(1)-C(35)	1.263(6)
O(2)-C(35)	1.207(6)
N(1)-C(18)	1.357(6)
N(1)-C(19)	1.434(5)
N(2)-N(3)	1.324(5)
N(2)-C(20)	1.332(6)
N(3)-N(4)	1.330(6)
N(3)-C(28)	1.447(7)
N(4)-C(21)	1.322(6)
C(1)-C(2)	1.376(6)
C(1)-C(6)	1.391(7)
C(2)-C(3)	1.385(6)
C(3)-C(4)	1.365(9)
C(4)-C(5)	1.355(10)
C(5)-C(6)	1.402(8)
C(7)-C(12)	1.376(6)

C(7)-C(8)	1.387(6)
C(8)-C(9)	1.371(7)
C(9)-C(10)	1.371(8)
C(10)-C(11)	1.374(7)
C(11)-C(12)	1.377(6)
C(13)-C(14)	1.390(6)
C(13)-C(18)	1.418(5)
C(14)-C(15)	1.381(7)
C(15)-C(16)	1.387(8)
C(16)-C(17)	1.375(7)
C(17)-C(18)	1.398(6)
C(19)-C(20)	1.489(6)
C(20)-C(21)	1.416(6)
C(21)-C(22)	1.479(6)
C(22)-C(23)	1.372(8)
C(22)-C(27)	1.399(7)
C(23)-C(24)	1.393(7)
C(24)-C(25)	1.376(10)
C(25)-C(26)	1.351(10)
C(26)-C(27)	1.379(9)
C(28)-C(29)	1.507(8)
C(29)-C(34)	1.359(8)
C(29)-C(30)	1.368(10)
C(30)-C(31)	1.405(13)
C(31)-C(32)	1.339(14)

C(32)-C(33)	1.363(13)
C(33)-C(34)	1.359(10)
C(35)-C(36)	1.500(8)
C(36)-C(37)	1.373(9)
C(36)-C(41)	1.389(8)
C(37)-C(38)	1.377(9)
C(38)-C(39)	1.333(16)
C(39)-C(40)	1.323(17)
C(40)-C(41)	1.418(15)

O(1)-Au(1)-P(1)	173.5(1)
C(13)-P(1)-C(1)	105.2(2)
C(13)-P(1)-C(7)	105.9(2)
C(1)-P(1)-C(7)	105.6(2)
C(13)-P(1)-Au(1)	115.1(1)
C(1)-P(1)-Au(1)	113.5(2)
C(7)-P(1)-Au(1)	110.8(1)
C(35)-O(1)-Au(1)	119.6(3)
C(18)-N(1)-C(19)	122.5(4)
N(3)-N(2)-C(20)	103.6(3)
N(2)-N(3)-N(4)	115.5(4)
N(2)-N(3)-C(28)	122.3(4)
N(4)-N(3)-C(28)	121.7(4)
C(21)-N(4)-N(3)	104.5(4)
C(2)-C(1)-C(6)	119.4(4)

C(2)-C(1)-P(1)	120.9(4)
C(6)-C(1)-P(1)	119.6(4)
C(1)-C(2)-C(3)	120.5(5)
C(4)-C(3)-C(2)	120.1(5)
C(5)-C(4)-C(3)	120.5(5)
C(4)-C(5)-C(6)	120.6(6)
C(1)-C(6)-C(5)	119.0(6)
C(12)-C(7)-C(8)	118.6(4)
C(12)-C(7)-P(1)	122.9(3)
C(8)-C(7)-P(1)	118.5(4)
C(9)-C(8)-C(7)	120.6(5)
C(10)-C(9)-C(8)	120.3(5)
C(9)-C(10)-C(11)	119.6(5)
C(10)-C(11)-C(12)	120.2(5)
C(7)-C(12)-C(11)	120.7(4)
C(14)-C(13)-C(18)	120.1(4)
C(14)-C(13)-P(1)	119.7(3)
C(18)-C(13)-P(1)	120.1(3)
C(15)-C(14)-C(13)	121.1(5)
C(14)-C(15)-C(16)	119.3(5)
C(17)-C(16)-C(15)	120.2(5)
C(16)-C(17)-C(18)	122.1(4)
N(1)-C(18)-C(17)	120.5(4)
N(1)-C(18)-C(13)	122.3(4)
C(17)-C(18)-C(13)	117.2(4)

N(1)-C(19)-C(20)	110.7(4)
N(2)-C(20)-C(21)	108.6(4)
N(2)-C(20)-C(19)	119.4(3)
C(21)-C(20)-C(19)	131.9(4)
N(4)-C(21)-C(20)	107.8(4)
N(4)-C(21)-C(22)	121.0(4)
C(20)-C(21)-C(22)	131.2(4)
C(23)-C(22)-C(27)	118.2(5)
C(23)-C(22)-C(21)	123.0(4)
C(27)-C(22)-C(21)	118.8(5)
C(22)-C(23)-C(24)	120.8(5)
C(25)-C(24)-C(23)	119.6(7)
C(26)-C(25)-C(24)	120.4(6)
C(25)-C(26)-C(27)	120.5(6)
C(26)-C(27)-C(22)	120.5(7)
N(3)-C(28)-C(29)	111.8(4)
C(34)-C(29)-C(30)	117.6(7)
C(34)-C(29)-C(28)	120.7(6)
C(30)-C(29)-C(28)	121.6(6)
C(29)-C(30)-C(31)	121.4(8)
C(32)-C(31)-C(30)	118.2(9)
C(31)-C(32)-C(33)	121.2(8)
C(34)-C(33)-C(32)	119.7(8)
C(33)-C(34)-C(29)	121.8(8)
O(2)-C(35)-O(1)	124.8(5)

O(2)-C(35)-C(36)	120.7(5)
O(1)-C(35)-C(36)	114.5(4)
C(37)-C(36)-C(41)	119.1(6)
C(37)-C(36)-C(35)	121.1(5)
C(41)-C(36)-C(35)	119.8(6)
C(36)-C(37)-C(38)	120.2(7)
C(39)-C(38)-C(37)	120.3(10)
C(40)-C(39)-C(38)	121.9(10)
C(39)-C(40)-C(41)	120.1(10)
C(36)-C(41)-C(40)	118.3(9)

Table 31. Anisotropic displacement parameters ($Å^2$ x 10^3) for $Au[P(C_6H_5)_2C_6H_4NHCH_2(C_{15}H_{12}N_3)](O_2CC_6H_5)\cdot 2H_2O$. The anisotropic displacement factor exponent takes the form: $-2p^2[h^2 a^{*2}U_{11} + ... + 2 h k a^* b^* U_{12}]$.

	U_{11}	U_{22}	U_{33}	U_{23}	U_{13}	U_{12}
Au(1)	67(1)	41(1)	55(1)	-1(1)	22(1)	-2(1)
P(1)	45(1)	37(1)	54(1)	-4(1)	14(1)	3(1)
O(1)	93(2)	51(2)	61(2)	6(2)	19(2)	-14(2)
O(2)	92(3)	132(5)	101(4)	-13(3)	-2(3)	-43(3)
N(1)	68(2)	52(2)	48(2)	-2(2)	19(2)	17(2)
N(2)	56(2)	51(2)	56(2)	1(2)	9(2)	7(2)
N(3)	68(2)	53(2)	55(2)	4(2)	9(2)	6(2)
N(4)	56(2)	54(2)	72(3)	1(2)	10(2)	6(2)
C(1)	43(2)	46(2)	58(3)	-4(2)	12(2)	7(2)
C(2)	43(2)	53(3)	70(3)	7(2)	9(2)	6(2)
C(3)	42(2)	60(3)	112(5)	5(3)	11(2)	5(2)
C(4)	49(2)	73(4)	113(5)	-23(3)	0(3)	2(2)
C(5)	73(3)	111(5)	69(4)	-16(4)	-7(3)	5(3)
C(6)	64(2)	86(4)	59(3)	-7(3)	10(2)	-1(2)
C(7)	45(2)	37(2)	63(3)	-4(2)	15(2)	5(2)
C(8)	53(2)	53(3)	122(6)	-15(3)	18(3)	-5(2)
C(9)	41(2)	74(4)	160(7)	-11(4)	22(3)	5(2)
C(10)	58(2)	67(4)	118(5)	-6(3)	23(3)	21(2)

C(11)	70(3)	40(3)	102(4)	-10(3)	14(3)	8(2)
C(12)	50(2)	40(2)	86(3)	-9(2)	11(2)	6(2)
C(13)	47(2)	38(2)	49(2)	-2(2)	10(2)	0(2)
C(14)	59(2)	50(3)	60(3)	1(2)	2(2)	5(2)
C(15)	75(3)	60(3)	58(3)	10(2)	-4(2)	1(2)
C(16)	84(3)	64(3)	45(2)	3(2)	7(2)	-6(3)
C(17)	70(2)	52(3)	52(3)	-3(2)	16(2)	5(2)
C(18)	49(2)	43(2)	48(2)	-3(2)	9(2)	1(2)
C(19)	57(2)	46(2)	52(2)	-6(2)	13(2)	9(2)
C(20)	49(2)	38(2)	56(2)	-4(2)	11(2)	1(2)
C(21)	46(2)	39(2)	69(3)	-8(2)	5(2)	-1(2)
C(22)	44(2)	42(2)	79(3)	-20(2)	9(2)	-1(2)
C(23)	55(2)	53(3)	87(4)	-19(3)	18(2)	-3(2)
C(24)	73(3)	74(4)	97(5)	-36(3)	34(3)	-13(3)
C(25)	63(3)	83(4)	129(6)	-42(4)	37(4)	-3(3)
C(26)	53(2)	76(4)	145(7)	-35(4)	15(3)	14(3)
C(27)	55(2)	68(4)	104(5)	-20(3)	2(3)	12(2)
C(28)	77(3)	76(4)	65(3)	14(3)	15(3)	0(3)
C(29)	82(3)	75(4)	55(3)	6(3)	19(2)	5(3)
C(30)	152(7)	94(6)	97(5)	-10(4)	-28(5)	24(5)
C(31)	219(12)	95(7)	119(8)	-32(5)	-36(9)	5(7)
C(32)	117(6)	156(10)	80(5)	-31(6)	12(4)	-30(6)
C(33)	86(4)	136(8)	104(6)	-21(5)	10(4)	12(5)
C(34)	80(3)	96(5)	92(5)	-9(4)	13(3)	11(3)
C(35)	60(2)	62(3)	64(3)	-3(2)	21(2)	2(2)

C(36)	68(2)	72(4)	61(3)	15(3)	24(2)	12(2)
C(37)	87(3)	64(4)	82(4)	7(3)	34(3)	-7(3)
C(38)	118(5)	80(5)	144(7)	15(5)	64(5)	-13(4)
C(39)	211(13)	122(10)	203(14)	83(10)	128(11)	22(9)
C(40)	194(11)	154(12)	108(8)	81(8)	54(8)	55(9)
C(41)	117(5)	133(7)	72(4)	40(5)	14(4)	37(5)
O(3)	161(7)	131(8)	281(14)	-34(6)	43(8)	-25(4)
O(4)	186(8)	230(12)	200(10)	-66(7)	1(7)	-28(6)

Table 32. Hydrogen atom coordinates (x 10^4) and isotropic displacement parameters ($Å^2$ x 10^3) for $Au[P(C_6H_5)_2C_6H_4NHCH_2(C_{15}H_{12}N_3)](O_2CC_6H_5)$.

	x	y	z	U(eq)
H(1N)	5870(40)	6250(40)	370(20)	43(13)
H(2)	6386	9010	211	66
H(3)	8201	9794	553	85
H(4)	8899	9674	1453	95
H(5)	7857	8733	2012	102
H(6)	6047	7898	1678	83
H(8)	1895	7954	502	90
H(9)	400	9139	547	109
H(10)	954	10703	832	96
H(11)	3028	11105	1020	85
H(12)	4536	9927	962	70
H(14)	3432	8812	-297	68
H(15)	3542	8667	-1214	78
H(16)	4808	7471	-1532	77
H(17)	5866	6391	-945	69
H(19A)	7400	5813	-286	61
H(19B)	6229	5123	-360	61
H(23)	8290	4583	-657	77
H(24)	9584	3976	-1264	96

H(25)	11182	2919	-966	107
H(26)	11440	2415	-90	109
H(27)	10143	2982	516	91
H(28A)	7526	3519	1806	87
H(28B)	6588	4402	1783	87
H(30)	7573	6126	1893	141
H(31)	9112	7068	2385	179
H(32)	10768	6289	2840	141
H(33)	10977	4620	2786	130
H(34)	9512	3717	2276	107
H(37)	2207	3770	1490	91
H(38)	1337	2408	1851	133
H(39)	1849	2001	2722	205
H(40)	3327	2816	3244	179
H(41)	4230	4241	2913	128